

Resorufin as an Electron Acceptor in Glucose Oxidase-Catalyzed Oxidation of Glucose

Hatsuo MAEDA,* Shinya MATSU-URA, Toshihisa SENBA, Seiji YAMASAKI, Hitoshi TAKAI, Yuji YAMAUCHI, and Hidenobu OHMORI

Graduate School of Pharmaceutical Sciences, Osaka University, 1–6 Yamada-oka, Suita, Osaka 565–0871, Japan.

Received November 15, 1999; accepted March 16, 2000

Resorufin (1) has been found to act as an electron acceptor in glucose oxidase (GOD)-catalyzed oxidation of glucose. When a 1 : 1 : 1 mixture of solutions of 1 (5.0 μ M), glucose, and GOD (4.0 mg/ml) in phosphate buffer (pH 7.4, 0.1 M) was incubated at 36 °C under aerobic conditions and the reaction was followed by a measurement of changes in fluorescence intensity due to 1, only two types of fluorometric traces were observed: (1) when a glucose solution of less than 0.7 mM was subjected to the enzymatic reaction, no consumption of 1 was observed; (2) the reaction with glucose at more than 1.0 mM always consumed 1, affording a regression fluorometric curve, and yet the obtained fluorometric traces could be almost superimposed on one another with no dependence on the glucose concentration. The reasons for the observed phenomena are discussed.

Key words resorufin; electron acceptor; glucose oxidase; glucose; oxidation; indicator reaction

Molecular oxygen (O_2) acts as an electron acceptor in glucose oxidase (GOD)-catalyzed oxidation of glucose, and is reduced to H_2O_2 .¹⁾ Thus, colorimetry in the visible range as one of the most useful tools for GOD-dependent analyses of glucose has been achieved with color reactions induced by H_2O_2 in the presence of an additional enzyme such as catalase or peroxidase.²⁾ Indicator reactions for colorimetry are recognized as well-designed chemical processes. However, H_2O_2 -independent colorimetry for glucose determination seems worth developing, because such methods would be simpler and more practical than H_2O_2 -dependent colorimetry, and would be free from complications caused by electron donors present in biological fluids.²⁾ Many compounds have been shown to reoxidize the reduced form (GOD_{red}) of GOD in place of O_2 .^{3–8)} However, most of them are employed for GOD-dependent analysis of glucose in cooperation with not a colorimetric but an electrochemical technique. To our knowledge, only phenazine ethosulfate was demonstrated to be a suitable dye for H_2O_2 -independent enzymatic colorimetry of glucose; it functions as the sole electron acceptor instead of O_2 , and is transformed to its reduced form detectable in the visible range.^{6c)}

Resorufin anion (1^-) exhibits strong absorption (λ_{max} 571 nm, ϵ 4–7 $\times 10^4$)^{9,10a,d,f)} and emission (excitation maximum at 563 nm and emission maximum at 587 nm in pH 7.4 buffer)^{10g)} at wavelengths >550 nm, where potential interference in analysis of colored or turbid serum components can be avoided.¹¹⁾ Thus, enzymatic consumption and release of 1^- have been used as indicator reactions for spectrophotometric analyses.^{10–12)} On the other hand, the phenoxazin-3-one skeleton of 1 can be regarded as an analogue of dyes working as an electron acceptor in GOD-catalyzed oxidation of glucose such as Meldola's blue and methylene blue.^{8c)} Taking the spectrophotometric and structural property of 1 into consideration, it is expected that 1 has potential utility not only as an electron acceptor but also as a spectrophotometric indicator for H_2O_2 -independent colorimetry of glucose. However, no study has been done to elucidate this possibility of 1, as far as we are aware. Here, we report that 1 functions as an electron acceptor with a color change in GOD-catalyzed oxi-

dation of glucose under certain conditions. Although it was indicated that the observed behavior of 1 will not find direct application to H_2O_2 -independent enzymatic analysis of glucose, the present results should give a clue for developing novel indicators with 3H-phenoxazin-3-one skeletons for GOD-dependent colorimetry of glucose.

Results and Discussion

Aqueous solution of 1^- (0.3 mM, as sodium salt) was an intense pink color. When aq. GOD (4.0 mg/ml) and aq. glucose (10.0 mM) solutions were added to a solution of 1^- , the color gradually faded and the mixture became colorless after incubation at 36 °C for 10 min (Chart 1). The color of 1^- was not affected by treatment with GOD alone under these conditions. A similar color regression took place on reaction of 1^- with GOD and glucose under anaerobic conditions, and no color change was observed on reaction of 1^- with H_2O_2 . Thus, 1 might be useful as an H_2O_2 -independent indicator in enzymatic analysis of glucose employing only GOD. It should be mentioned here that the bleached mixture returned to its original color when the incubation was continued for more than 30 min under aerobic conditions.

Similar phenomena have been reported on reaction of 1 with NADPH and NADPH-cytochrome reductase at physiological pH, where 1 exists predominantly as 1^- .^{13,14)} In this enzymatic reaction under aerobic conditions, the absorbance at 570 nm due to 1^- decreased markedly within a few min-

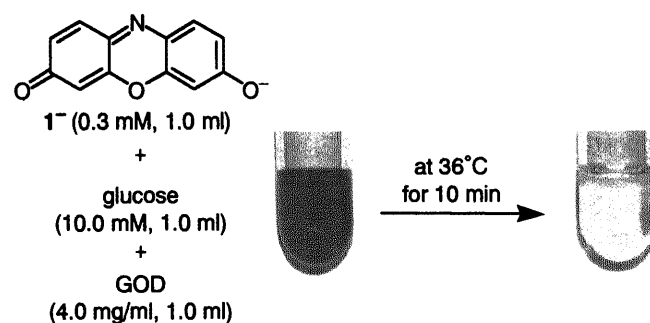


Chart 1

* To whom correspondence should be addressed. e-mail: h-maeda@phs.osaka-u.ac.jp

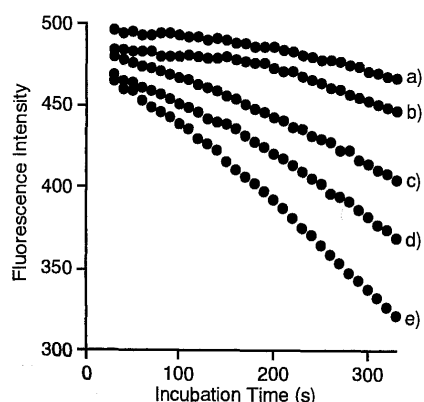


Fig. 1. Effects of Incubation Temperature on Fluorometric Traces Obtained during Incubation of a 1:1:1 Mixture of **1** ($5.0\ \mu\text{M}$), Glucose ($2.0\ \text{mM}$), and GOD ($4.0\ \text{mg/ml}$) for 5.5 min under Aerobic Conditions

Excitation and emission wavelengths: 568 and 582 nm, respectively. Incubation temperature: a, $24\ ^\circ\text{C}$; b, $27\ ^\circ\text{C}$; c, $30\ ^\circ\text{C}$; d, $33\ ^\circ\text{C}$; e, $36\ ^\circ\text{C}$.

utes, and was restored to the original value after incubation for 15 min.¹³⁾ It has been proposed that **1** rather than **1**⁻ serves as an electron acceptor in the enzymatic oxidation of NADPH, being reduced to colorless dihydroresorufin (**2**)^{13,14)} which is reoxidized to **1** by dissolved oxygen (DO) after NADPH is totally consumed.¹³⁾ Thus, a similar reaction mechanism may explain our findings: a catalytic cycle of glucose oxidation with GOD seems to be established in the presence of **1**, while the dye is reduced into **2**. This is the first report to show that **1** functions as an electron acceptor with a color change in GOD-catalyzed oxidation of glucose.

The reaction of **1**, glucose, and GOD was studied in more detail by a fluorometric method. Commercially available **1** seemed to contain some impurities, and hydrolysis of acetyl resorufin purified by recrystallization was recommended as the best way to obtain pure **1**.⁹⁾ A CH_3CN solution of acetyl resorufin ($1.0\ \text{mM}$) was diluted 1000-, 500-, 200-, 100-fold with phosphate buffer (pH 7.4, $0.1\ \text{M}$). By allowing the resulting solution to stand overnight, a solution of **1** (1.0 , 2.0 , 5.0 or $10.0\ \mu\text{M}$) was obtained. It was confirmed by measurement of UV-visible spectra that acetyl resorufin (λ_{max} in CH_3CN , 344 and 435 nm) was totally hydrolyzed to **1** (λ_{max} , 572 nm; ϵ , 7.2×10^4 in phosphate buffer) by standing in phosphate buffer for several hours. Solutions of glucose and GOD were also prepared with the phosphate buffer. Reaction of **1**, glucose, and GOD was initiated by addition of glucose to a mixture of **1** and GOD, where each of the solutions was combined in the same volume, usually $1.0\ \text{ml}$. All fluorometric measurements were carried out with 568 and 582 nm as excitation and emission wavelengths, respectively, and were set in from 30 s after initiation of the enzymatic reaction.

To establish fluorometric conditions useful for analysis of glucose using a color change due to consumption of **1**, effects of the concentrations of **1** and GOD as well as reaction temperature on fluorometric changes in the present enzymatic reaction were examined. Mixtures of **1** ($5.0\ \mu\text{M}$), glucose ($2.0\ \text{mM}$), and GOD ($4.0\ \text{mg/ml}$) were incubated in a fluorometric cell at 24 , 27 , 30 , 33 or $36\ ^\circ\text{C}$ (Fig. 1). Incubation even at $24\ ^\circ\text{C}$ afforded a regression curve, indicating that the enzymatic reaction consumed **1** even at this temperature. However, the clearest change in the fluorometric trace was observed with incubation at $36\ ^\circ\text{C}$. All enzymatic reactions

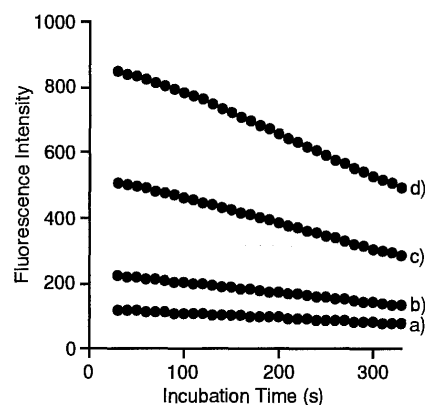


Fig. 2. Effects of Concentration of **1** on Fluorometric Traces Obtained during Incubation of a 1:1:1 Mixture of **1**, Glucose ($2.0\ \text{mM}$), and GOD ($4.0\ \text{mg/ml}$) at $36\ ^\circ\text{C}$ for 5.5 min under Aerobic Conditions

Excitation and emission wavelengths: 568 and 582 nm, respectively. Concentration of **1** in the stock solution: a, $1.0\ \mu\text{M}$; b, $2.0\ \mu\text{M}$; c, $5.0\ \mu\text{M}$; d, $10.0\ \mu\text{M}$.

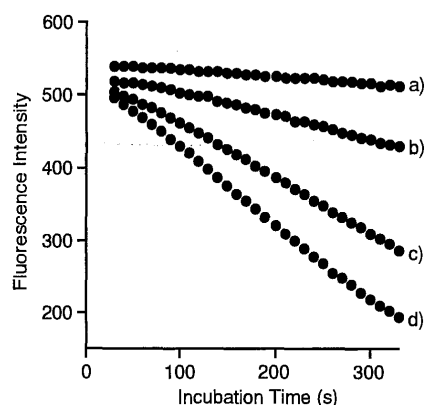


Fig. 3. Effects of Concentration of GOD on Fluorometric Traces Obtained during Incubation of a 1:1:1 Mixture of **1** ($5.0\ \mu\text{M}$), Glucose ($2.0\ \text{mM}$), and GOD at $36\ ^\circ\text{C}$ for 5.5 min under Aerobic Conditions

Excitation and emission wavelengths: 568 and 582 nm, respectively. Concentration of GOD in the stock solution: a, $1.0\ \text{mg/ml}$; b, $2.0\ \text{mg/ml}$; c, $4.0\ \text{mg/ml}$; d, $6.0\ \text{mg/ml}$.

for further examinations were carried out at this temperature.

Figure 2 summarizes the effects of the concentration of **1** on fluorometric changes during the enzymatic reaction with $2.0\ \text{mM}$ glucose and $4.0\ \text{mg/ml}$ GOD. Taking the solubility of **1** in phosphate buffer and detection limit of the fluorometer into consideration, concentrations of **1** between 1 and $10\ \mu\text{M}$ were screened. A regression curve with a larger change in fluorescence intensity was observed as the concentration of **1** was increased. Similarly, the larger changes in fluorescence intensity were observed with higher concentrations of GOD during the enzymatic reaction with $5.0\ \mu\text{M}$ **1** and $2.0\ \text{mM}$ glucose (Fig. 3). These results indicated that a system using $10.0\ \mu\text{M}$ **1** and $6.0\ \text{mg/ml}$ GOD would provide the largest sensitivity in fluorometric detection of glucose under the conditions employed. However, an analysis system with reagents in much smaller amounts would be better, especially as a routine method. A color change reaction with $5.0\ \mu\text{M}$ **1** and $4.0\ \text{mg/ml}$ GOD seemed to be useful for detection of glucose. Accordingly, we attempted to establish a fluorometric method for glucose analysis using the enzymatic reaction with **1** and GOD at these concentrations.

Figure 4 compares fluorometric traces obtained when a mixture of **1** ($5.0\ \mu\text{M}$), GOD ($4.0\ \text{mg/ml}$), and glucose (0.7 or

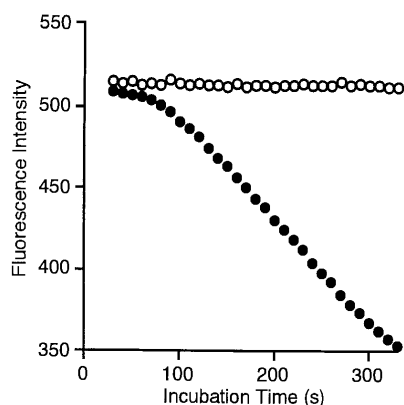


Fig. 4. Effects of Concentration of Glucose on Fluorometric Traces Obtained during Incubation of a 1:1:1 Mixture of **1** ($5.0\ \mu\text{M}$), Glucose, and GOD ($4.0\ \text{mg/ml}$) at 36°C for 5.5 min under Aerobic Conditions

Excitation and emission wavelengths: 568 and 582 nm, respectively. Concentration of glucose in the stock solution: open circles, $0.7\ \text{mM}$; closed circles, $0.8\ \text{mM}$.

$0.8\ \text{mM}$) was incubated at 36°C . In the incubation with $0.7\ \text{mM}$ glucose, no changes were observed in fluorescence intensity, indicating that **1** was not consumed in the enzymatic reaction. The enzymatic reactions with 0.5 and $0.6\ \text{mM}$ glucose afforded essentially the same traces. In contrast with these results, the fluorescence intensity was gradually regressed in the reaction with $0.8\ \text{mM}$ glucose, suggesting that **1** entered the enzymatic reaction and was gradually reduced to the non-fluorometric compound **2**. A regression trace was also obtained when the incubation was performed with 0.9 , 1.0 , 1.1 , 1.2 , 1.5 , 2.0 , or $10.0\ \text{mM}$ glucose, which is not included in Fig. 4 for simplicity. Interestingly, no relationship was observed between glucose concentrations and changes in fluorescence intensity. When glucose at more than $0.8\ \text{mM}$ was subjected to the enzymatic reaction, almost the same traces were afforded in all cases. The regression trace obtained in the reaction with $0.8\ \text{mM}$ glucose was nearly superimposed on that observed even with $10.0\ \text{mM}$ glucose. The results described above indicated that the incubation of a mixture of **1**, glucose, and GOD resulted in only two types of fluorometric behavior depending on whether **1** enters the enzymatic reaction.

Variation in the lower limit of glucose concentration affording a regression curve was recognized when the fluorometric experiments were repeated on different days under essentially the same conditions. The results of several sets of experiments demonstrated that a regression curve was invariably observed when glucose at more than $1.0\ \text{mM}$ was used, while **1** always remained intact in the enzymatic reactions with glucose at less than $0.7\ \text{mM}$. This rule held even when the concentrations of **1** and GOD were changed.

The observed variation in glucose concentration determining whether **1** was reduced through the enzymatic reaction seemed to stem from a daily variation in the amount of DO in the media. In fact, when a mixture of **1** ($5.0\ \mu\text{M}$), glucose (0.5 or $2.0\ \text{mM}$), and GOD ($4.0\ \text{mg/ml}$) was incubated at 36°C under anaerobic conditions, only one type of fluorometric trace was noted as shown in Fig. 5. As mentioned above, incubation with $0.5\ \text{mM}$ glucose under aerobic conditions induced no changes in fluorescence intensity during the enzymatic reaction, while $2.0\ \text{mM}$ glucose invariably allowed the reaction to consume **1**. These results suggested that the

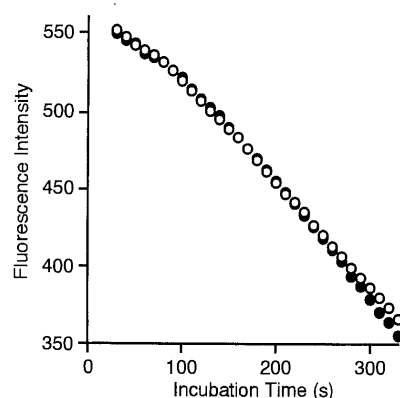


Fig. 5. Effects of Concentration of Glucose on Fluorometric Traces Obtained during Incubation of a 1:1:1 Mixture of **1** ($5.0\ \mu\text{M}$), Glucose, and GOD ($4.0\ \text{mg/ml}$) at 36°C for 5.5 min under Anaerobic Conditions

Excitation and emission wavelengths: 568 and 582 nm, respectively. Concentration of glucose in the stock solution: open circles, $0.5\ \text{mM}$; closed circles, $2.0\ \text{mM}$.

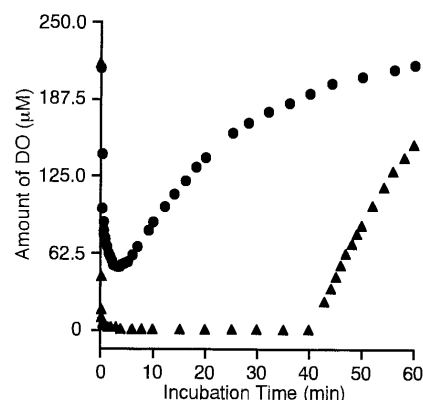


Fig. 6. Changes in Amount of DO during Incubation of a 1:1:1 Mixture of **1** ($5.0\ \mu\text{M}$), Glucose, and GOD ($4.0\ \text{mg/ml}$) at 36°C for 1 h under Aerobic Conditions

Concentration of glucose: circles, $0.5\ \text{mM}$; triangles, $2.0\ \text{mM}$.

amount of DO is a determinant of which fluorometric behaviors are exhibited by the present enzymatic reactions under aerobic conditions.

To evaluate the role of DO, changes in its amount were followed during the incubation of a 1:1:1 mixture of **1** ($5.0\ \mu\text{M}$), glucose (0.5 or $2.0\ \text{mM}$), and GOD ($4.0\ \text{mg/ml}$) at 36°C under aerobic conditions for 1 h. The results are shown in Fig. 6. Regardless of the glucose concentration, DO was rapidly consumed as soon as the enzymatic reaction was initiated, suggesting that GOD-catalyzed oxidation of glucose seems to prefer DO to **1** as an electron acceptor under these conditions. In the reaction with $0.5\ \text{mM}$ glucose, the amount of consumed DO was about $163\ \mu\text{M}$. Note that the glucose concentration in the reaction cell was $167\ \mu\text{M}$ (one third of $0.5\ \text{mM}$) in this case, and glucose had been completely consumed. Thus, no participation of **1** in this enzymatic reaction was observed on the fluorometric trace even after prolonged incubation (Fig. 7). In the enzymatic reaction with $2.0\ \text{mM}$ glucose ($667\ \mu\text{M}$ in the reaction cell) under aerobic conditions, DO was almost totally consumed within 1 min after initiation, the amount being about $220\ \mu\text{M}$. DO level was kept at *ca.* $1\ \mu\text{M}$ and began to gradually rise about 40 min after incubation (Fig. 6). In this case, consumption of **1** began as soon as the enzymatic reaction was initiated as shown in Fig.

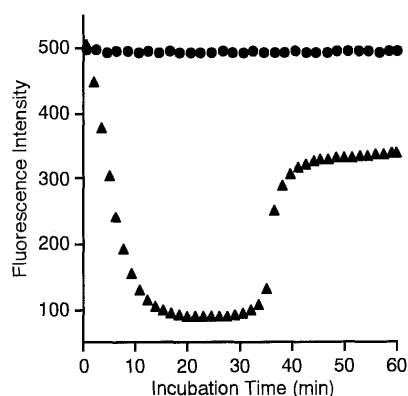


Fig. 7. Fluorometric Traces Obtained during Incubation of a 1:1:1 Mixture of **1** (5.0 μM), Glucose, and GOD (4.0 mg/ml) at 36 $^{\circ}\text{C}$ for 1 h under Aerobic Conditions

Excitation and emission wavelengths: 568 and 582 nm, respectively. Concentration of glucose in the stock solution: circles, 0.5 mM; triangles, 2.0 mM.

7. After about 80% of **1** was consumed, its level remained constant for 20 min then began to gradually increase, reaching another constant value 40 min after initiation of the reaction. It is worthy of note that the results in Figs. 6 and 7 were quite reproducible. The observation supports that the enzymatic reactions transforms **1** into **2**, which is reoxidized into **1** by O_2 supplied from the atmosphere into a fluorometric cell after most glucose is consumed, similar to the reaction of **1**, NADPH, and NADPH-cytochrome reductase mentioned above.^{13,14} Why fluorescence intensity did not recover to the original level in the enzymatic reaction is not clear.

Quantitative elucidation of the efficiency of **1** as an electron acceptor in GOD-catalyzed oxidation of glucose was attempted. The scheme shown in Chart 2 describes the plausible present reaction sequence. Under anaerobic conditions, reactions (3) and (4) can be ignored, allowing quantitative evaluation of reaction (2). However, it was remarkably difficult to carry out the incubation of a mixture of **1**, glucose, and GOD for a longer time under anaerobic conditions. Even when the incubation using carefully deoxygenated buffer solutions of **1**, glucose, and GOD was carried out in a cell room of a fluorometer purged with N_2 gas, a fluorometric trace similar to that obtained for 2.0 mM glucose was afforded, although the period of a first plateau was prolonged. This observation as well as the results in Fig. 7 indicated the following points: (i) under severely deoxygenated conditions, a small amount of O_2 is supplied from the atmosphere to the incubation media, by which reactions (3) and (4) are brought about; (ii) the extent to which reactions (3) and (4) participate in the reaction sequence is similar between the incubations under aerobic and carefully deoxygenated conditions; (iii) the enzymatic reaction under aerobic conditions can realize nearly anaerobic conditions through a rapid consumption of DO in a medium as soon as the incubation is started. Therefore, reaction (2) was semi-quantitatively evaluated from a fluorometric trace obtained by the incubation of a mixture of **1**, glucose, and GOD under aerobic conditions, ignoring a small supply of O_2 from the atmosphere, namely, reactions (3) and (4).

GOD-catalyzed oxidation of glucose is known to follow a ping-pong type mechanism,¹⁶⁾ which is also applicable to the present case. When the whole process shown by reactions (1)

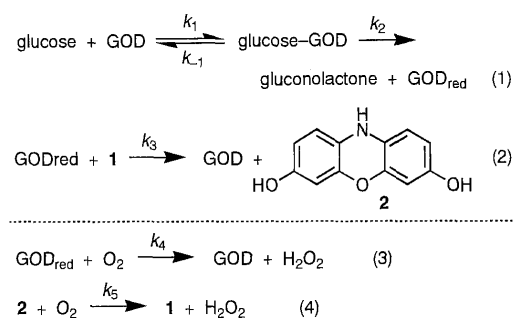


Chart 2

and (2) in Chart 2 is assumed to be in a steady state as suggested by the same types of reactions with other dyes,^{8c)} the total concentration of GOD ($[\text{GOD}_{\text{total}}]$) can be expressed by:

$$[\text{GOD}_{\text{total}}] = [\text{GOD}_{\text{red}}] \{ k_3[\text{1}]/k_2 + 1 + k_3(k_{-1} + k_2)[\text{1}]/k_1 k_2 [\text{glucose}] \} \quad (1)$$

where $[\text{GOD}_{\text{red}}]$, $[\text{glucose}]$ and $[\text{1}]$ are concentrations of GOD_{red} , glucose and **1**, respectively, and k_1 , k_{-1} , k_2 , and k_3 are rate constants of the steps shown in Chart 2. The rate (v) for consumption of **1** is given by:

$$v = k_3[\text{GOD}_{\text{red}}][\text{1}] \quad (2)$$

When Eq. (1) is divided by Eq. (2), v is expressed by:

$$[\text{GOD}_{\text{total}}]/v = 1/k_2 + 1/k_3[\text{1}] + (k_{-1} + k_2)/k_1 k_2 [\text{glucose}] \quad (3)$$

Under the conditions that reaction (1) is much faster than reaction (2) and $[\text{glucose}] \gg [\text{1}]$, Eq. (3) is transformed into:

$$v = -d[\text{1}]/dt = k_3[\text{GOD}_{\text{total}}][\text{1}] \quad (4)$$

Thus, the consumption of **1** obeys pseudo-first order kinetics, being consistent with the results in Figs. 2—5. Accordingly, the apparent rate constant $k_{\text{obs}} = k_3[\text{GOD}_{\text{total}}]$ was estimated from a linear transformation between incubation time (t) and $\ln(I_t - I_{\infty})$: I_t and I_{∞} are fluorescence intensities at t and ∞ sec after incubation, respectively. As I_{∞} , an average fluorescence intensity at a first plateau region from 20 to 30 min after incubation as seen in Fig. 7 was used. Incubation was carried out for a mixture of 5.0 mM glucose, 3.0 mg/ml GOD, and 5.0 μM **1** under essentially the same procedure and conditions as the case in Fig. 7. A linear relationship between t and $\ln(I_t - I_{\infty})$ was observed from 3 to 20 min after incubation, correlation coefficient being 0.998. The slope (k_{obs}) of the correlation line was divided by $[\text{GOD}_{\text{total}}]$, to give $6.6 \times 10^2 \text{ M}^{-1} \text{ s}^{-1}$ as k_3 . Since reaction (4) was ignored, the estimated k_3 is a minimum value.

Similarly, k_4 for O_2 was also estimated to be $1.6 \times 10^5 \text{ M}^{-1} \text{ s}^{-1}$ from k_{obs} obtained by a linear transformation between t and $\ln[\text{O}_2]$, where incubation was carried out with 5.0 mM glucose and 0.03 mg/ml GOD, and was followed by measurement of the DO amount under essentially the same procedure and conditions as those used for Fig. 6. The obtained k_4 for O_2 is not in conflict with the reported value ($10 \times 10^5 \text{ M}^{-1} \text{ s}^{-1}$ at pH 7.4 and 25 $^{\circ}\text{C}$).¹⁷⁾

Under the present conditions, the amount of DO in phosphate buffer lies between 0.22 and 0.28 mM. As a rate constant for reoxidation of GOD_{red} , O_2 possesses more than 200-fold larger value than **1**. These facts clearly demonstrate that **1** does not enter the enzymatic reaction until DO is almost consumed through GOD-catalyzed oxidation of glucose. Ac-

cordingly, it is estimated that the enzymatic reactions with less than 0.66 mM glucose in the stock solution, which corresponds to 0.22 mM in the reaction cell, induce no consumption of **1**, while in GOD-catalyzed oxidation of glucose at more than 0.84 mM, **1** invariably served as an electron acceptor with a change in fluorescence intensity. This estimation is consistent with the observed phenomena in the present enzymatic reaction under aerobic conditions: glucose at less than 0.7 mM induced no change in fluorescence intensity, while glucose at more than 1.0 mM allowed **1** to be reduced to non-fluorescent **2** by GOD_{red}. Thus, the fate of **1** in the enzymatic reaction described here under aerobic conditions was dictated by whether the concentration of glucose added to the reaction cell exceeded the amount of DO.

To evaluate the utility of **1** as an electron acceptor in GOD-catalyzed oxidation of GOD, a kinetic datum for reaction (4) as well as that for reaction (2) is important. This is because the balance between reoxidation of GOD_{red} by a dye and reoxidation of the reduced form of a dye by DO is a determinant of how usefully a dye serves as an indicator in GOD-dependent colorimetry. In this study, the reoxidation of **1** into **2** could not be quantitatively evaluated. Accordingly, using the value of k_3 , only the ability of **1** as an electron acceptor was compared with some other dyes. Rate constants for reoxidation of GOD_{red} by methylene blue, Meldola's blue, and methylene green are reportedly 1.3×10^3 , 1.9×10^4 , and $5.5 \times 10^3 \text{ M}^{-1} \text{ s}^{-1}$, respectively.^{8c)} These values are much larger than k_3 for **1**. From the viewpoint of an electron acceptor, it is unlikely that **1** serves as a better electron acceptor for GOD-catalyzed oxidation of glucose than these dyes.

In conclusion, **1** was shown to act as an electron acceptor in GOD-catalyzed oxidation of glucose, provided that glucose at a concentration of more than 1.0 mM is subjected to the enzymatic reaction. However, the bleaching process through transformation of **1** into **2** exhibited no dependence on glucose concentration. This is ascribed to the relatively small value of the rate constant for **1** to reoxidize GOD_{red}. Although **1** was shown not to be useful as an indicator for GOD-dependent analysis of glucose, the present results have implied that properly designed dyes with 3H-phenoxazin-3-one skeletons will serve as a novel type of electron acceptors applicable to H₂O₂-independent enzymatic analysis of glucose. Further studies are currently underway to explore derivatives of **1** as alternative indicators available for enzymatic analysis of glucose.

Experimental

Reagents and sample solutions Resorufin sodium salt was purchased from Aldrich and used without further purification. GOD from *Aspergillus niger* (EC 1.1.3.4) and glucose were used as supplied. A solution of **1** (1.0, 2.0, 5.0, or 10.0 μM) was prepared as follows: a CH₃CN solution of acetyl resorufin (1.0 mM) was diluted 10-fold with phosphate buffer (0.1 M, pH 7.4; Na₂HPO₄ + NaH₂PO₄); the solution was further diluted 10-, 20-, 50-, or 100-fold with phosphate buffer; the resulting solution was allowed to stand overnight. Acetyl resorufin^{16c,19)} was prepared by reaction of **1** with acetic anhydride in pyridine at room temperature and recrystallized from ethyl acetate.²⁰⁾ All other chemicals were of reagent grade and were used without further purification. Deionized and distilled water was used throughout the present study. CH₃CN was of HPLC grade. All solutions of glucose and GOD were prepared in phosphate buffer (0.1 M, pH 7.4; Na₂HPO₄ + NaH₂PO₄). Glucose solutions were stored overnight to allow equilibration of α - and β -anomers.

Apparatus and procedures All fluorometric measurements were carried out using a JASCO Model FP-750 spectrofluorometer equipped with a

JASCO ETC-272 Peltier thermostatted single cell holder. Each solution of **1**, GOD, and glucose in 1.0 ml was added to a cuvette (10 \times 10 \times 45 mm) in the cell holder in this order with stirring at 500 rpm. Measurement of the fluorescence at excitation and emission wavelengths of 568 and 582 nm, respectively, was started 30 s after addition of glucose solution. For measurements under anaerobic conditions, each solution was added to a cuvette after N₂ gas was passed through for several minutes, and fluorometry was performed under an N₂ atmosphere. A DO level was determined using a Horiba OM-14 DO meter equipped with a Horiba 5420 DO electrode. All measurements of the amount of DO in the reaction mixture were carried out by a procedure similar to that used for the fluorometric measurements except that solutions of **1**, GOD, and glucose were combined in a final volume of 30.0 ml.

Acknowledgment This paper was supported in part by Mitsubishi Chemical Corporation Fund.

References and Notes

- 1) For a review of GOD, see: Wilson R., Turner A. P. F., *Biosens. Bioelectron.*, **7**, 165—185 (1992).
- 2) Michal G., Möllering H., Siedel J., "Methods of Enzymatic Analysis," ed. by Bergmeyer H. U., 3rd ed., VCH, Weinheim, 1983; Vol. 1, pp. 197—232.
- 3) For examples using Fe(CN)₆³⁻ or Ru(CN)₆³⁻ as an electron acceptor, see: a) Schlöpfer P., Mindt W., Racine P., *Clin. Chim. Acta*, **57**, 283—289 (1974); b) Crumbliss A. L., Hill H. A. O., Page D. J., *J. Electroanal. Chem.*, **206**, 327—331 (1986); c) Ikeda S., Yoshioka T., Nankai S., *J. Electrochem. Soc. Jpn (Denki Kagaku)*, **63**, 1145—1147 (1995).
- 4) For examples using ferrocene or its derivative as an electron acceptor, see: a) Cass A. E. G., Davis G., Francis G. D., Hill H. A. O., Aston W. J., Higgins I. J., Plotkin E. V., Scott L. D. L., Turner A. P. F., *Anal. Chem.*, **56**, 667—671 (1984); b) Gründig B., Krabisch C., *Anal. Chim. Acta*, **222**, 75—81 (1989); c) Liaudet E., Battaglini F., Calvo E. J., *J. Electroanal. Chem.*, **293**, 55—68 (1990); d) Hale P. D., Boguslavsky L. I., Inagaki T., Karan H. I., Lee H. S., Skotheim T. A., *Anal. Chem.*, **63**, 677—682 (1991); e) Schuhmann W., Ohara T. J., Schmidt H.-L., Heller A., *J. Am. Chem. Soc.*, **113**, 1394—1397 (1991); f) Yokoyama K., Shibasaki T., Murakami Y., *J. Electrochem. Soc. Jpn (Denki Kagaku)*, **64**, 1221—1227 (1996); g) Liu H., Li H., Sun K., Qin Y., Qi D., *Anal. Chim. Acta*, **358**, 137—144 (1998).
- 5) For examples using benzoquinone as an electron acceptor, see: a) Williams D. L., Doig A. R., Jr., Korosi A., *Anal. Chem.*, **42**, 118—121 (1970); b) Ikeda T., Katasho I., Kamei M., Senda M., *Agric. Biol. Chem.*, **48**, 1969—1976 (1984); c) Wang P., Amarasinghe S., Leddy J., Arnold M., Dordick J. S., *Polymer*, **39**, 123—127 (1998). Also see ref. 3a.
- 6) For examples using phenazine methosulfate or its derivative as an electron acceptor, see: a) Aleksandrovskii Ya. A., Bezhikina L. V., Rodionov Yu. V., *Biokhimiya*, **46**, 708—716 (1981); b) Yokoyama K., Tamiya E., Karube I., *J. Electroanal. Chem.*, **273**, 107—117 (1989); c) Wilsey C. D., Freitag H., Int. Patent WO 9306487 (1993); d) Liu H., Ying T., Sun K., Li H., Qi D., *Anal. Chim. Acta*, **344**, 187—199 (1997).
- 7) For an example using tetrathiafulvalene as an electron acceptor, see: Lei C., Zhang Z., Liu H., Deng J., *J. Electroanal. Chem.*, **419**, 93—98 (1996). Also see ref. 4b.
- 8) For examples using compounds other than in refs. 3—7 as an electron acceptor, see: a) Kuly's J. J., Cenas N. K., *Biochim. Biophys. Acta*, **744**, 57—63 (1983); b) Rishpon J., Rosen-Margalit I., Harth R., Ozer D., Bettelheim A., *J. Electroanal. Chem.*, **307**, 293—298 (1991); c) Kuly's J., Buch-Ramussen T., Bechgaard K., Razumas V., Kazlauskaitė J., Marcinkeviciene J., Christensen J. B., Hansen H. E., *J. Mol. Catal.*, **91**, 407—420 (1994).
- 9) Kitson T. M., *Bioorg. Chem.*, **24**, 331—339 (1996).
- 10) For examples of methods based on enzymatic release of **1**, see: a) Prough R. A., Burke M. D., Mayer R. T., "Methods in Enzymology," ed. by Wood W. A., Academic Press, New York, 1978; Vol. 52, pp. 372—376; b) Simpson D. J., Unkefer C. J., Whaley T. W., Marrone B. L., *J. Org. Chem.*, **56**, 5391—5396 (1991); c) Kasai K., Yamaji N., *Anal. Sci.*, **8**, 161—164 (1992); d) Kitson T. M., Kitson K. E., *Adv. Exp. Med. Biol.*, **414** (Enzymology and Molecular Biology of Carbonyl Metabolism 6), 201—208 (1997); e) Kitson T. M., Kitson K. E., *Biochem. J.*, **322**, 701—708 (1997); f) Hadd A. G., Raymond D. E., Halliwell J. W., Jacobson S. C., Ramsey J. M., *Anal. Chem.*, **69**,

- 3407—3412 (1997); g) Zhou M., Diwu Z., Panchuk-Voloshina N., Haugland R. P., *Anal. Biochem.*, **253**, 162—168 (1997); h) O'Neill R. B., Dillon S. A., Morgan P. M., *Biochem. Soc. Trans.*, **26**, S84 (1998).
- 11) For a brief overview of analytical use of **1**, Herrmann R., *Chimia*, **45**, 317—318 (1991).
- 12) For examples of methods based on enzymatic consumption of **1**, see: a) Brotea F. P., Thibert R. J., *Microchem. J.*, **37**, 368—376 (1988); b) Brotea G. P., Draisey T. F., Thibert R. J., *Microchem. J.*, **39**, 1—9 (1989).
- 13) Dutton D. R., Reed G. A., Parkinson A., *Arch. Biochem. Biophys.*, **268**, 605—616 (1989).
- 14) Balvers W. G., Boersma M. G., Vervoort J., Rietjens I. M. C. M., *Chem. Res. Toxicol.*, **5**, 268—273 (1992).
- 15) In previous studies, ethanol was used as a solvent for recrystallization.^{9,10d} However, recrystallization from ethanol induced partial hydrolysis of the acetyl derivative to **1**. Thus, recrystallization from ethyl acetate seems to be the best way to purify the compound.
- 16) Nakamura S., Ogura Y., *J. Biochem.*, **63**, 308—316 (1968).
- 17) Weibel M. K., Bright H. J., *J. Biol. Chem.*, **246**, 2734—2744 (1971).

Synthesis and Biological Activities of 2-Arachidonoylglycerol, an Endogenous Cannabinoid Receptor Ligand, and Its Metabolically Stable Ether-linked Analogues

Yoshitomo SUHARA,^a Hiroaki TAKAYAMA,^a Shinji NAKANE,^b Tomoyuki MIYASHITA,^b Keizo WAKU,^b and Takayuki SUGIURA^{*,b}

Department of Pharmaceutical Chemistry,^a and Hygienic Chemistry and Nutrition,^b Faculty of Pharmaceutical Sciences, Teikyo University, Sagamiko, Kanagawa 199–0195, Japan. Received November 22, 1999; accepted March 14, 2000

We synthesized 2-arachidonoylglycerol (**1**), an endogenous cannabinoid receptor ligand, and its metabolically stable ether-linked analogues. Compound **1** was synthesized from 1,3-benzylideneglycerol (**6**) and arachidonic acid in the presence of *N,N'*-dicyclohexylcarbodiimide and 4-dimethylaminopyridine followed by treatment with boric acid and trimethyl borate. An ether-linked analogue of 2-arachidonoylglycerol (**2**) was synthesized from **6** and 5,8,11,14-eicosatetraenyl iodide (**9**). The ether-linked analogues of 2-palmitoylglycerol (**4**) and 2-oleoylglycerol (**5**) were synthesized from **6** and hexadecyl iodide (**12**) and 9-octadecenyl iodide (**14**), respectively. We confirmed that **1** stimulates NG108-15 cells to induce rapid transient elevation of the intracellular free Ca^{2+} concentrations through a CB1 receptor-dependent mechanism. Noticeably, **2** exhibited appreciable agonistic activity, although its activity was significantly lower than that of **1**. Compound **2** would be a useful tool in exploring the physiological significance of **1**, because this compound is resistant to hydrolyzing enzymes in contrast to **1**. On the other hand, the ether-linked analogues of either **4** or **5** failed to act as a CB1 receptor agonist. Compounds **4** and **5** would also be valuable as control molecules in experiments where **2** is employed.

Key words cannabinoid; 2-arachidonoylglycerol; anandamide; Δ^9 -tetrahydrocannabinol; monoacylglycerol; ether-linked analogue

Δ^9 -Tetrahydrocannabinol (Δ^9 -THC) is a psychoactive ingredient of marijuana and is known to exhibit a variety of pharmacological activities *in vitro* and *in vivo*.¹⁾ For example, Δ^9 -THC induces euphoria, heightened sensory awareness, altered cognition, inhibition of memory and reduced spontaneous activity. Noticeably, Δ^9 -THC also exerts several beneficial effects such as analgesia, antiemesis, promotion of appetite and immunosuppression in humans and in experimental animals; cannabimimetic molecules without deleterious activities should be of potential value as possible therapeutic drugs.

The mechanism underlying various *in vitro* and *in vivo* actions of cannabinoids remained unclear until the late 1980's. It has long been assumed that the effects of Δ^9 -THC may be due to the membrane perturbation of target tissues and cells. Studies by several investigators in this decade, however, revealed that various cannabinoids including Δ^9 -THC interact with specific receptor sites,²⁾ termed the CB1 receptor (present primarily in the nervous system)³⁾ and the CB2 receptor (present mainly in the immune system),⁴⁾ thereby eliciting the responses.

The discovery of such specific receptor sites for the cannabinoids prompted a search for the endogenous ligand as in the case of opioids. To date, two types of arachidonic acid-containing molecules have been proposed as putative endogenous ligands: *N*-arachidonylethanolamine (anandamide)⁵⁾ and 2-arachidonoylglycerol (**1**).^{6–8)} Recently, we provided evidence that **1** but not anandamide is the endogenous natural ligand for the cannabinoid CB1 receptor.^{9,10)} Compound **1** is a potent full agonist toward the CB1 receptor and exhibits various cannabimimetic activities such as the inhibition of adenylyl cyclase in mouse splenocytes, inhibition of twitch response in mouse vas deferens, modulation of proliferation of mouse lymphocytes, Ca^{2+} transients in NG108-15 cells, inhibition of long-term potentiation in hippocampus

and the induction of hypomotility, hypothermia and analgesia when administered to mice.^{7–13)}

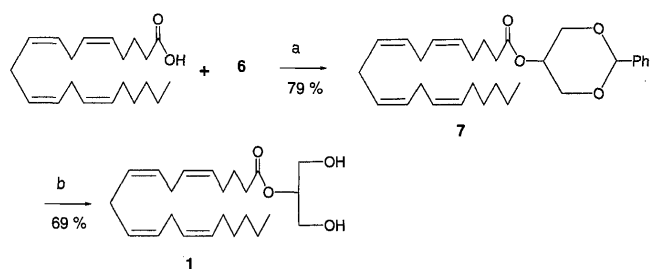
Compound **1** is the natural ligand of the cannabinoid receptor; it seems possible that cannabimimetic compounds without undesirable deleterious properties and therapeutically valuable will be found from among the structural analogues or derivatives of **1**. One important problem concerning **1** as a pharmacological tool or a therapeutic drug is that it is very easily cleaved by hydrolyzing enzymes.^{14,15)} The development of metabolically stable analogues is, therefore, essential. Previously, we¹⁰⁾ and Mechoulam *et al.*¹⁶⁾ developed an ether-linked analogue of 2-arachidonoylglycerol (**2**). This compound exhibited appreciable agonistic activities *in vitro* and *in vivo*.^{10,16)} However, detailed information including the chemical data concerning the synthesis of this novel class of the 2-arachidonoylglycerol analogue has not yet been reported. Furthermore, not much is yet known concerning the chemical synthesis of **1** itself. It is important to provide detailed information concerning chemical synthesis of these compounds in order to develop more potent and valuable analogues of 2-arachidonoylglycerol in the future. It is also necessary to develop an analogue of **2** lacking agonistic activity as a control molecule, because high concentrations of the ether-linked analogues of the monoacylglycerols may also exert nonspecific physiocochemical effects such as detergent effects.

Here, we report the biological activities as well as details of the chemical synthesis of **1**, its ether-linked analogue (**2**) which acts as the CB1 receptor agonist, and the newly developed ether-linked analogues of 2-arachidonoylglycerol (**3**)—(**5**) which lack agonistic activities toward the CB1 receptor.

Results and Discussion

As shown in Chart 1, the synthesis of 2-arachidonoylglycerol (**1**) was carried out from commercially available arachi-

* To whom correspondence should be addressed. e-mail: sugiurat@pharm.teikyo-u.ac.jp



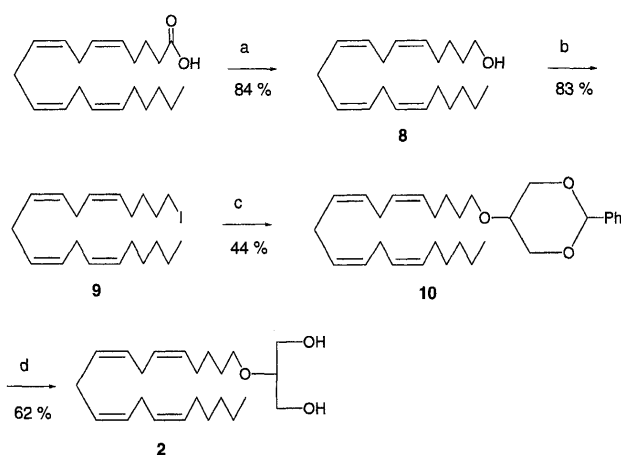
Reagents and conditions: (a) **6**:1, 3-benzylideneglycerol, DCC, DMF; (b) boric acid, trimethyl borate.

Chart 1

donic acid and glycerol. The primary hydroxy groups of glycerol were selectively protected by benzaldehyde using 5-sulfosalicylic acid dihydrate as a catalyst in benzene, and then recrystallized from benzene/hexane to give a secondary alcohol **6** in 17% yield. Esterification of the arachidonic acid with alcohol **6** using 4-dimethylaminopyridine (DMAP) and *N,N*-dicyclohexylcarbodiimide (DCC) in dry toluene at room temperature for 6 h provided ester **7** in 79% yield. Deprotection of the benzylidene group was accomplished by dissolving ester **7** in trimethyl borate at room temperature followed by the addition of boric acid.¹⁷⁾ The reaction mixture was stirred at 100 °C for 30 min, then cooled to room temperature. Chromatography on silica gel gave **1** in 69% yield with 55% conversion. In this process, about 10% of transesterification was observed in **1** by ¹H-NMR, therefore, compound **1** was further purified by borate-impregnated TLC to remove any contaminating 1- or 3-isomer. The purity was confirmed by ¹³C-NMR and MS. Recently, Han and Razdan¹⁸⁾ also reported the chemical synthesis of 2-arachidonoylglycerol, although their method employing triisopropylsilyl chloride as a hydroxy group-protecting reagent was different from our currently described procedure. The advantage in using 1,3-benzylideneglycerol (**6**) for the synthesis of **1** and its analogues is that the coupling products **7**, **10**, **13**, and **15** are detectable under UV lamp (254 nm).

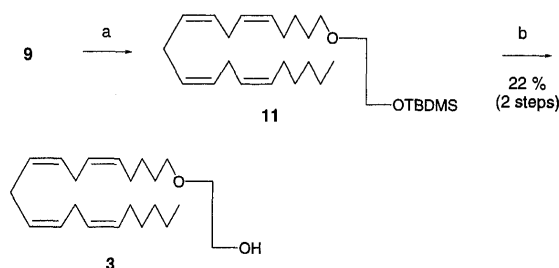
Chart 2 summarizes the synthesis of an ether-linked analog of 2-arachidonoylglycerol, 2-(5,8,11,14-eicosatetraenyl)-glycerol (**2**), which is a metabolically stable cannabinoid receptor ligand. To make an ether bond, arachidonic acid was first converted to an alcohol **8** with lithium aluminum hydride (LiAlH₄) in dry diethyl ether at 0 °C, and then treated with methyltriphenoxyphosphonium iodide in *N,N*-dimethylformamide (DMF) to give the iodo derivative **9** in good yield. 2-(5,8,11,14-Eicosatetraenyl)-1,3-benzylideneglycerol (**10**) was obtained by condensing **9** and **6** using Ag₂O and tetra-*n*-butylammonium iodide (*n*-Bu₄NI) in DMF. After stirring at 90 °C for 6 h in the dark, the coupling product **10** was isolated in 30% yield. Finally, deprotection of the benzylidene group in **10** with boric acid and trimethyl borate gave **2** in 62% yield.

The synthesis of an ether-linked analogue of monoarachidonylethylene glycol (1-eicosatetraenyl-oxyethanol (**3**)) is outlined in Chart 3. The coupling of 5,8,11,14-eicosatetraenyl iodide (**9**) with 3-(*tert*-butyldimethylsilyl)oxyethanol and subsequent removal of the *tert*-butyldimethylsilyl (TBDMS) ether moiety in **11** by treatment with tetrabutylammonium fluoride (TBAF) gave **3** in 22% yield in two steps.



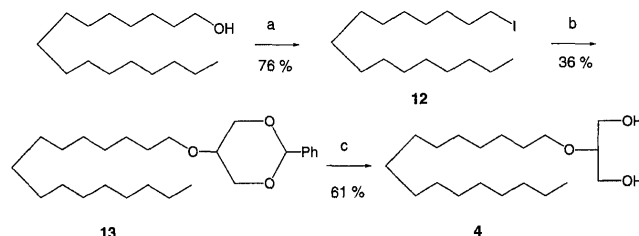
Reagents and conditions: (a) LiAlH₄, ether; (b) CH₃P(OC₆H₅)₃I, DMF; (c) Ag₂O, *n*-Bu₄NI, DMF, **6**, at 90 °C; (d) boric acid, trimethyl borate.

Chart 2



Reagents and conditions: (a) Ag₂O, *n*-Bu₄NI, DMF, 2-(*tert*-butyldimethylsilyl)oxyethanol, at 90 °C; (b) 1M TBAF in THF.

Chart 3



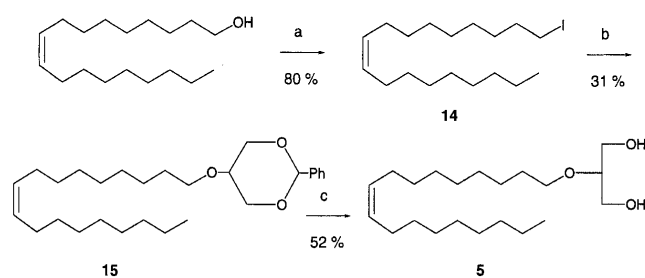
Reagents and conditions: (a) CH₃P(OC₆H₅)₃I, DMF; (b) Ag₂O, *n*-Bu₄NI, DMF, **6**, at 90 °C; (c) boric acid, trimethyl borate.

Chart 4

2-Hexadecylglycerol (**4**) was prepared from commercially available hexadecanol as shown in Chart 4. The alcohol was converted to the iodide **12** using methyltriphenoxyphosphonium iodide in DMF. The coupling of **12** with 1,3-benzylideneglycerol gave **13**, which was then hydrolyzed to give **4** as described for **2**.

2-(9-Octadecenyl)glycerol (**5**) was synthesized from commercially available *cis*-9-octadecen-1-ol as shown in Chart 5. The iodide **14** was obtained in 80% yield using methyltriphenoxyphosphonium iodide in DMF. The coupling of **14** with 1,3-benzylideneglycerol gave **15**, which was then hydrolyzed to give **5** as described for **2**.

Figure 1 shows the effects of **1**, **2** and related compounds **3**–**5** on the intracellular free Ca²⁺ concentrations ([Ca²⁺]_i) in NG108-15 cells which are known to express the cannabi-



Reagents and conditions: (a) $\text{CH}_3\text{P}(\text{OC}_6\text{H}_5)_3$, DMF; (b) Ag_2O , $n\text{-Bu}_4\text{NI}$, DMF, 6, at 90°C ; (c) boric acid, trimethyl borate.

Chart 5

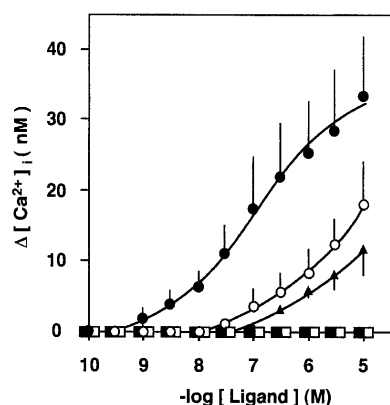


Fig. 1. Comparison of the Activities of 2-Arachidonoylglycerol and Its Ether-linked Analogues in Inducing Rapid Elevation of $[\text{Ca}^{2+}]_i$ in NG108-15 Cells

Effects of 2-arachidonoylglycerol and its ether-linked analogues on $[\text{Ca}^{2+}]_i$ were examined using Fura-2/AM and a CAF-100 Ca^{2+} analyzer. (●), 2-arachidonoylglycerol (1) (2-AG); (○), an ether-linked analogue of 2-arachidonoylglycerol (2) (2-AG ether); (▲), an ether-linked analogue of monoarachidonylethyleneglycol (3); (□), an ether-linked analogue of 2-palmitoylglycerol (4); (■), an ether-linked analogue of 2-oleoylglycerol (5). The mean values \pm S.D. were taken from five determinations.

noid CB1 receptor. Low concentrations of **1** induce rapid transient increases in $[\text{Ca}^{2+}]_i$ in the NG108-15 cells; the response was detectable from as low as 1 nM, reaching a maximum around $10\text{ }\mu\text{M}$. Such a response induced by **1** was blocked by pretreatment of the cells with SR141716A, a cannabinoid CB1 receptor-specific antagonist (data not shown), suggesting that rapid transient increases in $[\text{Ca}^{2+}]_i$ occurred through a CB1 receptor-dependent mechanism. Noticeably, **2** also exhibited appreciable agonistic activity, yet its activity was significantly lower than that of **1**. These observations are in general agreement with the result reported earlier,¹⁰ but appear to be inconsistent with the result of the *in vivo* experiment where **2** exhibited much more potent biological activity than **1**.¹⁶ We also found that an ether-linked analogue of monoarachidonylethyleneglycol (**3**) possesses some weak agonistic activity.

We next examined the activities of the structural analogues of **2** having saturated or monoenoic fatty chains. We found that neither the ether-linked analogue of 2-palmitoylglycerol (**4**) nor the ether-linked analogue of 2-oleoylglycerol (**5**) elicits rapid, transient increases in $[\text{Ca}^{2+}]_i$. It is apparent, therefore, that both **4** and **5** are devoid of appreciable agonistic activity toward the cannabinoid CB1 receptor. Compound **2** is resistant to hydrolyzing enzymes and may exist for a long period *in vitro* or *in vivo* without receiving hydrolysis; thus, in

some cases, it is not clear whether the effects of **2** are mediated only through the cannabinoid receptors or also through other sites of action. To clarify this issue, compounds **4** and **5**, which lack cannabimimetic activity, should be valuable tools.

Despite the increasing attention paid to **1** these days,^{19,20} information concerning it and its structural analogues is still quite limited. Thus, the synthesis of a number of 2-arachidonoylglycerol analogues and evaluation of their biological and pharmacological activities are essential to better understand the physiological significance of **1** and to develop a new class of therapeutic drugs that acts on the cannabinoid receptors in the future.

Experimental

General Methods Melting points were determined using a Yanagimoto hot-stage melting point apparatus and are uncorrected. ^1H -NMR and ^{13}C -NMR spectra were recorded in CDCl_3 on a GSX 400 spectrometer. Chemical shifts are given in ppm (δ) using tetramethylsilane (TMS) as the internal standard. Mass spectra were registered on a JMS SX-102A instrument. Elemental analysis was performed with a Perkin-Elmer 2400 II instrument. Column chromatography was carried out on silica gel 60 (70–230 mesh, Merck) and preparative TLC was run on silica gel 60 F_{254} (Merck). Unless otherwise noted, all reagents were purchased from commercial suppliers and used as received.

1,3-Benzylideneglycerol (6) Glycerol (120 g, 1.30 mol), benzaldehyde (120 g, 1.13 mol), and 5-sulfosalicylic acid dihydrate (1.20 g, $55.0\text{ }\mu\text{mol}$) were dissolved in benzene (120 ml), and the mixture was then refluxed at 120°C overnight with a Dean-Stark apparatus to remove the water. After having cooled to room temperature, the reaction mixture was diluted with diethyl ether (500 ml) and washed with saturated aqueous NaHCO_3 and brine. The organic layer was dried over MgSO_4 followed by filtration and evaporation. The residue was recrystallized from benzene/hexane (20:1) (2 l) to give **6** (41 g, yield 17%) as white needles: mp $79\text{--}81^\circ\text{C}$. ^1H -NMR (CDCl_3) δ : 7.52–7.35 (m, 5H), 5.55 (s, 1H), 4.15 (dd, 4H, $J=11.2$, 19.5 Hz), 3.62 (t, 1H), 3.11 (br s, 1H). ^{13}C -NMR (CDCl_3) δ : 137.8, 129.1, 128.3, 125.8, 101.7, 72.3, 64.0. High resolution (HR)-EI-MS m/z : 180.0785 (Calcd for $\text{C}_{10}\text{H}_{12}\text{O}_3$: 180.0787). *Anal.* Calcd for $\text{C}_{10}\text{H}_{12}\text{O}_3$: C, 66.65; H, 6.71. Found: C, 66.71; H, 6.58.

2-Arachidonoyl-1,3-benzylideneglycerol (7) To a solution of **6** (60 mg, $330\text{ }\mu\text{mol}$) and arachidonic acid (all-*cis*-5,8,11,14-eicosatetraenoic acid) (100 mg, $328\text{ }\mu\text{mol}$) in dry toluene (30 ml) was added DCC (136 mg, $656\text{ }\mu\text{mol}$) and DMAP (12 mg, $99\text{ }\mu\text{mol}$). The reaction mixture was stirred at room temperature for 6 h, then diluted with ethyl acetate (EtOAc) (50 ml). The mixture was washed with water (50 ml) and brine (50 ml), and the organic layer was dried over MgSO_4 and removed. The residue was chromatographed on silica gel (hexane/EtOAc, 3:1, v/v) to give **7** (121 mg, yield 79%) as a colorless oil: ^1H -NMR (CDCl_3) δ : 7.52–7.49 (m, 2H), 7.37–7.26 (m, 3H), 5.56 (s, 1H), 5.40–5.35 (m, 8H), 4.72 (t, 1H, $J=1.6$ Hz), 4.27 (dd, 2H, $J=1.6$, 12.8 Hz), 4.16 (dd, 2H, $J=1.6$, 12.8 Hz), 2.83–2.80 (m, 6H), 2.44 (tt, 2H, $J=5.2$, 7.6 Hz), 2.14 (tt, 2H, $J=6.7$, 7.0 Hz), 2.05 (dd, 2H, $J=6.7$, 13.7 Hz), 1.78–1.74 (m, 2H), 1.36–1.22 (m, 6H), 0.89 (br t, 3H, $J=6.7$ Hz). ^{13}C -NMR (CDCl_3) δ : 173.6, 137.8, 130.5, 129.0, 128.9, 128.6, 128.3, 128.21, 128.15, 127.9, 127.5, 126.0, 101.2, 69.1, 65.8, 33.7, 31.5, 29.3, 27.2, 26.5, 25.6, 24.8, 22.5, 14.0. HR-EI-MS m/z : 466.3096 (Calcd for $\text{C}_{30}\text{H}_{42}\text{O}_4$: 466.3083).

2-Arachidonoylglycerol (1) A suspension of **7** (500 mg, 1.07 mmol) and boric acid (132 mg, 2.13 mmol) in trimethyl borate (5 ml) was refluxed at 100°C for 20 min. After having cooled to room temperature, the reaction mixture was diluted with EtOAc (100 ml) and successively washed with 50 ml of water and brine. The organic layer was dried (MgSO_4), and the solvent was removed. Silica gel column chromatography (hexane/EtOAc, the ratio ranging from 1:1 to 0:1, v/v) of the crude residue provided the product **1** (280 mg, 69%) as a colorless oil. Further, compound **1** (12.0 mg) was purified by borate-impregnated TLC to remove contaminating 1- or 3-isomer. Then, pure **1** (10.7 mg) was obtained in 89% yield as a colorless oil: ^1H -NMR (CDCl_3) δ : (m, 8H), 4.93 (tt, 1H, $J=4.7$, 4.7 Hz), 3.83 (d, 4H, $J=4.6$ Hz), 2.85–2.78 (m, 8H), 2.38 (t, 2H, $J=7.6$ Hz), 2.18–2.03 (m, 4H), 1.73 (tt, 2H, $J=7.3$, 7.3 Hz), 1.40–1.23 (m, 6H), 0.89 (br t, 3H, $J=6.7$ Hz). ^{13}C -NMR (CDCl_3) δ : 173.8, 130.5, 129.0, 128.8, 128.6, 128.3, 128.1, 127.8, 127.5, 75.1, 62.5, 33.7, 31.5, 29.3, 27.2, 26.5, 25.6, 24.8, 22.5, 14.0. HR-EI-

MS m/z : 378.2779 (Calcd for $C_{23}H_{38}O_4$: 378.2770).

5,8,11,14-Eicosatetraenol (8) A solution of arachidonic acid (25 mg, 82 μ mol) in dry diethyl ether (5 ml) was added dropwise to $LiAlH_4$ (30 mg, 791 μ mol) in dry diethyl ether at 0 °C under argon. The reaction mixture was stirred at room temperature for 1 h. EtOAc (0.5 ml) was then added dropwise to the mixture to remove excess $LiAlH_4$ at 0 °C. The mixture was diluted with EtOAc (30 ml), then filtered through Celite. The filtrate was successively washed with 20 ml of water and brine. The organic layer was dried ($MgSO_4$) and removed *in vacuo*. The crude residue was chromatographed on silica gel (hexane:EtOAc, 5:1, v/v) to give **8** (20 mg, 84%) as a colorless oil: 1H -NMR ($CDCl_3$) δ : 5.42–5.33 (m, 8H), 3.65 (t, 2H, $J=6.5$ Hz), 2.86–2.78 (m, 6H), 2.13–2.03 (m, 4H), 1.63–1.56 (m, 2H), 1.48–1.26 (m, 9H), 0.89 (br t, 3H, $J=6.8$ Hz). ^{13}C -NMR ($CDCl_3$) δ : 130.5, 129.9, 128.5, 128.3, 128.1, 127.9, 127.5, 62.8, 32.3, 31.5, 29.3, 27.2, 26.9, 25.7, 25.6, 22.5, 14.0. HR-EI-MS m/z : 290.2621 (Calcd for $C_{20}H_{34}O$: 290.2610).

5,8,11,14-Eicosatetraenyl Iodide (9) To a solution of **8** (100 mg, 328 μ mol) in dry DMF (10 ml) was added methyltriphenoxyposphonium iodide (280 mg, 619 μ mol). The mixture was stirred at room temperature for 20 min under argon. The crude product was purified by flash column chromatography (hexane/EtOAc, 20:1, v/v) to afford **9** (120 mg, 83%) as a colorless oil: 1H -NMR ($CDCl_3$) δ : 5.42–5.33 (m, 8H), 3.19 (t, 2H, $J=6.9$ Hz), 2.86–2.80 (m, 6H), 2.12–2.03 (m, 4H), 1.84 (tt, $J=7.0$, 7.4 Hz, 2H), 1.54–1.27 (m, 8H), 0.89 (br t, 3H, $J=7.1$ Hz). ^{13}C -NMR ($CDCl_3$) δ : 130.5, 129.3, 128.6, 128.4, 128.2, 127.8, 127.5, 33.0, 31.6, 31.5, 30.4, 29.3, 27.2, 26.1, 25.6, 22.6, 14.1. HR-EI-MS m/z : 400.1628 (Calcd for $C_{20}H_{33}I$: 400.1628).

2-(5,8,11,14-Eicosatetraenyl)-1,3-benzylideneglycerol (10) 1,3-Benzylideneglycerol (**6**) (200 mg, 1.11 mmol), Ag_2O (191 mg, 824 μ mol) and n -Bu₄NI (20 mg, 55 μ mol) were added to a stirred solution of iodide **9** (220 mg, 550 μ mol) in DMF (10 ml) at room temperature under argon. The suspension was stirred at 90 °C for 6 h in the dark. After having cooled to room temperature, the mixture was diluted with EtOAc (100 ml) and water (100 ml). The generated silver was removed by filtering through Celite, and the filtrate was successively washed with 100 ml of water and brine. The organic layer was dried over $MgSO_4$ and evaporated to dryness. Column chromatography on silica gel (hexane/EtOAc, 5:1, v/v) of the crude residue gave **10** (109 mg, 44%) as a colorless oil: 1H -NMR ($CDCl_3$) δ : 7.52–7.50 (m, 2H), 7.35–7.32 (m, 3H), 5.55 (s, 1H), 5.41–5.36 (m, 8H), 4.33 (dd, 2H, $J=1.5$, 12.5 Hz), 4.04 (dd, 2H, $J=1.8$, 12.5 Hz), 3.56 (t, 2H, $J=16.7$ Hz), 3.26 (t, 1H, $J=1.5$ Hz), 2.84–2.80 (m, 6H), 2.13–2.03 (m, 4H), 1.70–1.64 (m, 2H), 1.52–1.44 (m, 2H), 1.36–1.26 (m, 6H), 0.89 (br t, 3H, $J=7.0$ Hz). ^{13}C -NMR ($CDCl_3$) δ : 138.2, 130.5, 130.0, 128.8, 128.5, 128.4, 128.1, 128.0, 127.9, 127.6, 126.2, 101.3, 70.7, 69.0, 68.8, 65.8, 31.5, 29.4, 29.3, 27.2, 27.0, 26.2, 25.6, 22.6, 14.0. HR-EI-MS m/z : 452.3293 (Calcd for $C_{30}H_{44}O_3$: 452.3290).

2-(5,8,11,14-Eicosatetraenyl)glycerol (2) Compound **2** was prepared from **10** (420 mg, 929 μ mol) in a manner similar to that for **1**. Column chromatography on silica gel (hexane/EtOAc, 1:2, v/v) gave **2** (210 mg, 62%) as a colorless oil: 1H -NMR ($CDCl_3$) δ : 5.40–5.33 (m, 8H), 3.77 (dt, 2H, $J=4.6$, 5.8 Hz), 3.68 (dt, 2H, $J=4.8$, 5.5 Hz), 3.58 (t, 2H, $J=6.6$ Hz), 3.46 (dt, 1H, $J=4.6$, 4.9 Hz), 2.86–2.80 (m, 6H), 2.13–2.03 (m, 4H), 1.91 (br s, 2H), 1.67–1.58 (m, 2H), 1.48–1.43 (m, 2H), 1.38–1.26 (m, 6H), 0.89 (br t, 3H, $J=6.8$ Hz). ^{13}C -NMR ($CDCl_3$) δ : 130.5, 129.8, 128.6, 128.3, 128.21, 128.15, 127.9, 127.5, 79.6, 70.0, 62.3, 31.5, 29.7, 29.3, 27.2, 27.0, 26.2, 25.6, 22.6, 14.1. HR-EI-MS m/z : 364.2980 (Calcd for $C_{23}H_{40}O_3$: 364.2979).

1-(5,8,11,14-Eicosatetraenyl)oxyethanol (3) To a solution of iodide **9** (180 mg, 435 μ mol) in DMF (5 ml) was added 1-(*tert*-butyldimethylsilyl)oxyethanol (77 mg, 435 μ mol), Ag_2O (151 mg, 652 μ mol) and n -Bu₄NI (16 mg, 43 μ mol) at room temperature. The suspension was stirred at 90 °C for 6 h under argon in the dark. After having cooled to room temperature, the reaction mixture was diluted with EtOAc (30 ml) and water (20 ml) followed by filtration through Celite to remove the generated silver. The filtrate was successively washed with 100 ml of water and brine. The organic layer was dried over $MgSO_4$ then removed *in vacuo*. The crude residue **11** was used in the next step without further purification. Namely, a 1.0 M solution of TBAF in THF (870 μ mol/870 μ l) was added dropwise to crude silyl ether **11** in THF (5 ml) at 0 °C under argon. The reaction mixture was warmed to room temperature and stirred for 1 h. Removal of the solvent and subsequent chromatography on silica gel (hexane/EtOAc, 5:1 to 3:1, v/v) of the residue gave pure **3** (33 mg, 22% in two steps) as a colorless oil: 1H -NMR ($CDCl_3$) δ : 5.42–5.33 (m, 8H), 3.73 (d, 2H, $J=4.0$ Hz), 3.53 (t, 2H, $J=4.0$ Hz), 3.48 (t, 2H, $J=6.5$ Hz), 2.86–2.78 (m, 6H), 2.08 (ddd, 4H, $J=6.7$, 14.3 Hz), 1.97 (br s, 1H), 1.65–1.57 (m, 2H), 1.47–1.26 (m, 8H),

0.89 (br t, 3H, $J=6.9$ Hz). ^{13}C -NMR ($CDCl_3$) δ : 130.5, 129.9, 128.6, 128.4, 128.1, 127.9, 127.6, 71.7, 71.2, 61.9, 31.5, 29.32, 29.29, 27.2, 27.0, 26.1, 25.6, 22.6, 14.1. HR-EI-MS m/z : 334.2864 (Calcd for $C_{22}H_{38}O_2$: 334.2872).

Hexadecyl Iodide (12) Hexadecyl iodide (**12**) was prepared from commercially available hexadecanol (100 mg, 413 μ mol) as described for **9**. Column chromatography on silica gel (hexane/EtOAc, 1:2, v/v) gave **12** (110 mg, 76%) as a colorless oil: 1H -NMR ($CDCl_3$) δ : 3.17 (t, 2H, $J=7.2$ Hz), 1.82 (tt, 2H, $J=7.0$, 7.3 Hz), 1.26 (br s, 26H), 0.88 (br t, 3H, $J=6.8$ Hz). ^{13}C -NMR ($CDCl_3$) δ : 33.6, 31.9, 30.5, 29.69, 29.65, 29.56, 29.43, 29.36, 28.6, 22.7, 14.1. HR-EI-MS m/z : 352.1635 (Calcd for $C_{16}H_{33}I$: 352.1628).

2-Hexadecyl-1,3-benzylideneglycerol (13) 2-Hexadecyl-1,3-benzylideneglycerol (**13**) was prepared from **12** (100 mg, 284 μ mol) as described for **10**. Silica gel column chromatography (hexane/EtOAc, 1:2, v/v) gave **13** (41 mg, 36%) as a white solid: mp 49–51 °C. 1H -NMR ($CDCl_3$) δ : 7.52–7.50 (m, 2H), 7.37–7.26 (m, 3H), 5.54 (s, 1H), 4.33 (d, 2H, $J=11.9$ Hz), 4.04 (d, 2H, $J=11.6$ Hz), 3.54 (t, 2H, $J=6.8$ Hz), 3.25 (br s, 1H), 1.68–1.61 (m, 2H), 1.26 (br s, 26H), 0.89 (br t, 3H, $J=7.0$ Hz). ^{13}C -NMR ($CDCl_3$) δ : 138.2, 128.8, 128.1, 126.2, 101.3, 70.6, 69.05, 68.97, 31.9, 29.8, 29.7, 29.6, 29.5, 29.3, 26.1, 22.7, 14.1. HR-EI-MS m/z : 404.3293 (Calcd for $C_{26}H_{44}O_3$: 404.3291). Anal. Calcd for $C_{26}H_{44}O_3$: C, 77.18; H, 10.96. Found: C, 77.27; H, 11.23.

2-Hexadecylglycerol (4) 2-Hexadecylglycerol (**4**) was prepared from **13** (40 mg, 99 μ mol) in the manner described for **1**. Silica gel column chromatography (hexane/EtOAc, 1:2, v/v) provided **4** (19 mg, 61%) as a white solid: mp 56–58 °C. 1H -NMR ($CDCl_3$) δ : 3.77 (tt, 2H, $J=5.5$, 5.5 Hz), 3.68 (tt, 2H, $J=5.5$, 5.5 Hz), 3.57 (t, 2H, $J=6.7$ Hz), 3.46 (t, 1H, $J=4.8$ Hz), 1.93 (brs, 2H), 1.64–1.54 (m, 2H), 1.26 (br s, 26H), 0.88 (br t, 3H, $J=7.3$ Hz). ^{13}C -NMR ($CDCl_3$) δ : 79.5, 70.2, 62.2, 31.9, 30.0, 29.6, 29.5, 29.4, 29.3, 26.1, 22.6, 14.1. HR-EI-MS m/z : 316.2980 (Calcd for $C_{19}H_{40}O_3$: 316.2979). Anal. Calcd for $C_{19}H_{40}O_3$: C, 72.10; H, 12.74. Found: C 72.66; H, 12.88.

9-Octadecenyl Iodide (14) 9-Octadecenyl iodide (**14**) was prepared from commercially available *cis*-9-octadecen-1-ol (940 mg, 3.50 mmol) as described for **8**. Column chromatography on silica gel (hexane/EtOAc, 1:2, v/v) gave **14** (1060 mg, 80%) as a colorless oil: 1H -NMR ($CDCl_3$) δ : 5.39–5.32 (m, 2H), 3.18 (t, 2H, $J=7.0$ Hz), 2.06–1.99 (m, 4H), 1.82 (dt, 2H, $J=7.1$, 7.1 Hz), 1.40–1.22 (m, 22H), 0.88 (br t, 3H, $J=6.7$ Hz). ^{13}C -NMR ($CDCl_3$) δ : 130.0, 129.7, 33.6, 31.9, 30.5, 29.76, 29.69, 29.5, 29.4, 29.3, 29.2, 28.5, 27.22, 27.16, 22.7, 14.1. HR-EI-MS m/z : 378.1791 (Calcd for $C_{18}H_{35}I$: 378.1783).

2-(9-Octadecenyl)-1,3-benzylideneglycerol (15) 2-(9-Octadecenyl)-1,3-benzylideneglycerol (**15**) was prepared from **14** (910 mg, 2.41 mmol) as described for **10**. Silica gel column chromatography (hexane/EtOAc, 1:2, v/v) gave **15** (321 mg, 31%) as a colorless oil: 1H -NMR ($CDCl_3$) δ : 7.52–7.50 (m, 2H), 7.37–7.29 (m, 3H), 5.55 (s, 1H), 5.38–5.31 (m, 2H), 4.33 (dd, 2H, $J=1.5$, 12.5 Hz), 4.03 (dd, 2H, $J=1.8$, 12.5 Hz), 3.54 (t, 2H, $J=6.7$ Hz), 3.26 (t, 1H, $J=1.8$ Hz), 2.02–1.99 (m, 4H), 1.68–1.60 (m, 2H), 1.30–1.26 (m, 22H), 0.88 (br t, 3H, $J=6.7$ Hz). ^{13}C -NMR ($CDCl_3$) δ : 138.2, 129.9, 129.83, 129.77, 128.8, 128.1, 126.2, 101.3, 70.6, 69.03, 68.95, 65.5, 31.9, 29.8, 29.74, 29.65, 29.59, 29.48, 29.43, 29.29, 29.25, 29.20, 29.1, 27.2, 26.1, 25.9, 22.6, 14.1. HR-EI-MS m/z : 430.3444 (Calcd for $C_{28}H_{46}O_3$: 430.3447).

2-(9-Octadecenyl)glycerol (5) 2-(9-Octadecenyl)glycerol (**5**) was prepared from **15** (270 mg, 626 μ mol) in the same manner described for **1**. Silica gel column chromatography (hexane/EtOAc, 1:2, v/v) provided **5** (112 mg, 52%) as a colorless oil: 1H -NMR ($CDCl_3$) δ : 5.36–5.33 (m, 2H), 3.77 (dt, 2H, $J=5.5$, 5.5 Hz), 3.68 (dt, 2H, $J=5.5$, 5.5 Hz), 3.57 (t, 2H, $J=6.7$ Hz), 3.46 (t, 1H, $J=4.8$ Hz), 2.04–1.99 (m, 4H), 1.93 (br s, 2H), 1.62–1.55 (m, 2H), 1.38–1.24 (m, 22H), 0.88 (br t, 3H, $J=6.9$ Hz). ^{13}C -NMR ($CDCl_3$) δ : 130.0, 129.8, 79.5, 70.2, 62.2, 31.9, 30.1, 29.7, 29.52, 29.47, 29.43, 29.32, 29.25, 27.2, 26.1, 22.7, 14.1. HR-EI-MS m/z : 342.3142 (Calcd for $C_{21}H_{42}O_3$: 342.3134).

Determination of $[Ca^{2+}]_i$ in NG108-15 Cells $[Ca^{2+}]_i$ in neuroblastoma \times glioma hybrid NG108-15 cells was determined using Fura-2/AM in a CAF-100 Ca^{2+} analyzer as previously described.^{9–11)}

Acknowledgments We are grateful to Junko Shimode, Jinko Nonobe and Maroka Kitsukawa for the spectroscopic measurements. This study was supported in part by Grants-in-Aid from the Ministry of Education, Science, Sports and Culture of Japan.

References

- 1) Dewey W. L., *Pharmacological Reviews*, **38**, 151–178 (1986).
- 2) Devane W. A., Dysarz F. A., III, Johnson M. R., Melvin L. S., Howlett

- A. C., *Mol. Pharmacol.*, **34**, 605—613 (1988).
- 3) Matsuda L. A., Lolait S. J., Brownstein M. J., Young A. C., Bonner T. I., *Nature*, **346**, 561—564 (1990).
 - 4) Munro S., Thomas K. L., Abu-Shaar M., *Nature*, **365**, 61—65 (1993).
 - 5) Devane W. A., Hanus L., Breuer A., Pertwee R. G., Stevenson L. A., Griffin G., Gibson D., Mandelbaum A., Etinger A., Mechoulam R., *Science*, **258**, 1946—1949 (1992).
 - 6) Sugiura T., Itoh K., Waku K., Hanahan D.J., *Proc. Jpn. Conf. Biochem. Lipids*, **36**, 71—74 (in Japanese) (1994).
 - 7) Sugiura T., Kondo S., Sukagawa A., Nakane S., Shinoda A., Itoh K., Yamashita A., Waku K., *Biochem. Biophys. Res. Commun.*, **215**, 89—97 (1995).
 - 8) Mechoulam R., Ben-Shabat S., Hanus L., Ligumsky M., Kaminski N. E., Schatz A. R., Gopher A., Almog S., Martin B. R., Compton D. R., Pertwee R. G., Griffin G., Bayewitch M., Barg J., Vogel Z., *Biochem. Pharmacol.*, **50**, 83—90 (1995).
 - 9) Sugiura T., Kodaka T., Kondo S., Nakane S., Kondo H., Waku K., Ishima Y., Watanabe K., Yamamoto I., *J. Biochem.*, **122**, 890—895 (1997).
 - 10) Sugiura T., Kodaka T., Nakane S., Miyashita T., Kondo S., Suhara Y., Takayama H., Waku K., Seki C., Baba N., Ishima Y., *J. Biol. Chem.*, **274**, 2794—2801 (1999).
 - 11) Sugiura T., Kodaka T., Kondo S., Tonegawa T., Nakane S., Kishimoto S., Yamashita A., Waku K., *Biochem. Biophys. Res. Commun.*, **229**, 58—64 (1996).
 - 12) Lee M., Yang K. H., Kaminski N. E., *J. Pharmacol. Exp. Ther.*, **275**, 529—536 (1995).
 - 13) Stella N., Schweitzer P., Piomelli D., *Nature*, **388**, 773—778 (1997).
 - 14) Di Marzo V., Bisogno T., Sugiura T., Melck D., De Petrocellis L., *Biochem. J.*, **331**, 15—19 (1998).
 - 15) Goparaju S. K., Ueda N., Yamaguchi H., Yamamoto S., *FEBS Lett.*, **422**, 69—73 (1998).
 - 16) Mechoulam R., Fride E., Ben-Shabat S., Meiri U., Horowitz M., *Eur. J. Pharmacol.*, **362**, R1—3 (1998).
 - 17) Martin J. B., *J. Am. Chem. Soc.*, **75**, 5482—5483 (1953).
 - 18) Han K., Razdan R. K., *Tetrahedron Lett.*, **40**, 1631—1634 (1999).
 - 19) Di Marzo V., Melck D., Bisogno T., De Petrocellis L., *Trends Neurosci.*, **21**, 521—528 (1998).
 - 20) Di Marzo V., *Biochim. Biophys. Acta*, **1392**, 153—175 (1998).

Autoxidation of Ascorbic Acid Catalyzed by the Copper(II) Bound to L-Histidine Oligopeptides, (His)_iGly and Acetyl-(His)_iGly (*i*=9, 19, 29). Relationship between Catalytic Activity and Coordination Mode

Jun-ichi UEDA,*^a Akira HANAKI,*^{b,1)} Keiichiro HATANO,^c and Terumi NAKAJIMA^d

National Institute of Radiological Sciences,^a Anagawa 4–9–1, Chiba 263–8555, Japan, Faculty of Engineering, Shizuoka University,^b Jyohoku 3, Hamamatsu 432–8011, Japan, Faculty of Pharmaceutical Sciences, Nagoya City University,^c Mizuho-ku, Nagoya 467–8603, Japan, and Suntory Institute for Bioorganic Research,^d Shimamoto-cho, Mishima-gun, Osaka 618–0000, Japan. Received November 25, 1999; accepted April 4, 2000

Spectroscopic and kinetic studies on the autoxidation of ascorbic acid catalyzed by copper complexes of histidine oligopeptides, (His)_iGly (*i*=4, 9, 19, 29), and their acetyl derivatives, Ac-(His)_iGly (*i*=9, 19) have been carried out at pH 4.4 and 25°C under dioxygen. The reaction was monitored at 260 nm using a stopped-flow spectrophotometric technique. The reaction fitted the “Michaelis–Menten” mechanism, and ascorbate was oxidized by the “Ping-Pong” mechanism. The Cu(II) complexed with the oligopeptide (*i*≥9) enhanced the reaction approximately two-fold relative to the aqueous Cu(II). The catalytic activity depends on the molecular weight which is related to the number of histidyl residues and on the coordination mode of the copper-binding site. Results of circular dichroism (CD) experiments revealed the existence of two types of Cu(II). The catalytically active Cu(II), which is accommodated in the imidazole clusters composed of at least six histidyl residues, exhibits *d–d* transition bands at 520 and 630 nm, and is easily dissociable, enhances the autoxidation; Ac-(His)₉Gly is likely to accommodate approximately three active Cu(II) ions. The Cu(II), which is complexed tightly with the terminal H₂N–X–Y–His– moiety, where X and Y denote amino acids, inhibits the autoxidation, and exhibits absorption bands at 480 and 550 nm.

Key words autoxidation; ascorbic acid; copper ion; histidine peptide; circular dichroism; active site

A variety of metalloenzymes, which contain copper ions in the active center, function in electron transfer, *e.g.*, plastocyanin, storage and transport of dioxygen, *e.g.*, hemocyanin, disproportionation of superoxides, *e.g.*, superoxide dismutase, oxygenation, *e.g.*, tyrosinase, and oxidation, *e.g.*, ascorbate oxidase.²⁾ These functions involve primarily electron transfer, and the copper ions, which are located in histidine-rich clusters coordinating with the imidazole nitrogens, comprise the active site.^{3–5)} Recently, X-ray crystallographic studies of metalloenzymes have provided much information on the coordination environment around the active centers.

The copper ion in the oxidase is turned over between the Cu(II) and Cu(I) state during the reaction. The Cu(II) is reduced to Cu(I) by the substrate. The Cu(I) in low molecular-weight complexes, as well as in the oxidase, is able to associate with dioxygen to form an adduct, L–Cu(I)–O₂,⁶⁾ which can either dissociate back to Cu(I)–L and O₂ or disproportionate to the Cu(II) species and superoxide ions; where L denotes a ligand. The oxygen adduct can also react with another Cu(I)–L to form a peroxide, L–Cu(I)–O₂–Cu(I)–L, which subsequently undergoes redox cleavage to form the Cu(II) species and hydrogen peroxide (H₂O₂). In the presence of an appropriate electron donor (reductant) namely ascorbic acid or cysteine, the L–Cu(I)–O₂ is likely to cleave into the Cu(II) species and H₂O₂.⁷⁾ The reductant is likely to donate two electrons to the receptor. Thus, copper complexes are capable of catalyzing autoxidation of ascorbic acid and thiol compounds of biological relevance.^{8–11)}

Addition of metal chelating agents modifies the activities of the catalyst. Generally, metal chelating agents such as EDTA inhibit the autoxidation. In contrast, poly-L-histidine (PLH) which could coordinate with Cu(II) is shown to enhance considerably the autoxidation of ascorbic acid.^{12–14)} We have been studying the importance of histidyl residues

and imidazole clusters in constructing the metal-binding sites.^{15–17)} Results from equilibrium dialysis experiments revealed that PLH complexes contain at least two types of Cu(II), which were classified as either catalytically active or inactive/inhibitory ions.¹⁵⁾ The active Cu(II) readily dissociated from the complexes on addition of NaClO₄ and CH₃COONa.

The PLH synthesized by polymerization methods is composed of a population of histidine oligomers with various molecular weights. Therefore, the interrelation among coordination modes of Cu(II), the molecular weight, and the activity of the catalyst is not well understood. In order to clarify the coordination mode and structure of histidine peptides with Cu(II), we intended to synthesize chemically homogeneous oligopeptides, (His)_iGly (*i*=9, 19, 29), which possess two types of metal-binding sites, one each at the amino terminus and in the imidazole-rich cluster, and their *N*-acetylated derivatives Ac-(His)_iGly (*i*=9, 19), which lack the amino terminal binding site. Results from spectroscopic and kinetic experiments reveal that the Cu(II) with *d–d* transition bands at 520 and 630 nm is catalytically active and that with the bands at 480 and 550 nm is inhibitory.

Experimental

Materials Ultrosyn resin, 9-fluorenylmethoxycarbonylglycine pentafluorophenyl ester (Fmoc-Gly-OPFP) and *N*_α-(9-fluorenylmethoxycarbonyl)-*N*_ω-*tert*-butoxycarbonyl-L-histidine pentafluorophenyl ester (Fmoc-His(Boc)-OPFP) purchased from Pharmacia Co. (Sweden) were used as received. Histidine, glycine, 2-*tert*-butoxycarbonyloxyimino-2-phenylacetone-trile (Boc-ON), trifluoroacetic acid (TFA), *N,N*-dimethylformamide (DMF), and 20% piperidine in DMF were obtained from Kokusan Chemical Co. (Japan). *N*-hydroxybenzotriazole (HOBt), diethyl phosphorocyanidate (DEPC), benzyl alcohol, *p*-toluenesulfonic acid (*p*-TsOH), anisole and acetic anhydride were purchased from Wako Pure Chemical Co. (Japan). 4-Methoxybenzenesulfonyl chloride (MBS-Cl) was purchased from Aldrich Chemical Co. (U.S.A.). HisGly was a product of BACHEM Feinchemikalien

* To whom correspondence should be addressed. e-mail: ueda@nirs.go.jp

AG (Switzerland).

Solid-Phase Synthesis of Histidine Oligopeptides The histidine oligopeptides, (His)_iGly (*i*=9, 19, 29), and their acetyl derivatives, Ac-(His)_iGly (*i*=9, 19), were synthesized by a solid-phase technique on an semi-automatic peptide synthesizer LKB BIOLYNX 4175 (Bromma, Sweden) using Ultrosyn resin. Firstly, Fmoc-His(Boc)-OPFP was coupled to the glycine attached on Ultrosyn resin by HOBT to yield Fmoc-His(Boc)-Gly-resin. Next, the Fmoc at the amino terminus of Fmoc-His(Boc)-Gly-resin was removed with a 20% piperidine in DMF to yield His(Boc)-Gly-resin, which was subsequently coupled to Fmoc-His(Boc)-OPFP affording the Fmoc-His(Boc)-His(Boc)-Gly-resin. The same procedure was repeated until the appropriate Fmoc-[His(Boc)]_{*i*}-Gly-resin was synthesized. Finally, the Fmoc group at the amino terminus of the Fmoc-[His(Boc)]_{*i*}-Gly-resin was removed by a 20% piperidine in DMF to yield [His(Boc)]_{*i*}-Gly-resin. Cleavage and deprotection of the peptide from the resin were achieved by treatment with 95% TFA for 1 h at room temperature. The *N*-acetyl derivatives of [His(Boc)]_{*i*}-Gly were prepared by treatment with 10% acetic anhydride in DMF. The synthesized histidine oligopeptide mixtures were separated and purified by high performance liquid chromatography on the TSKgel SP-2SW column (Tosoh Co., Japan) according to the method described previously.¹⁸⁾

Liquid-Phase Synthesis of Histidine Oligopeptides (His)_iGly was synthesized by a conventional liquid-phase method. Starting materials were Boc-His(MBS)-OH and Gly-OBzl *p*-TsOH, and DEPC was used as a coupling agent. Firstly, Boc-His(MBS)-Gly-OBzl was prepared and subsequently treated with 50% TFA for 50 min affording NH₂-His(MBS)-Gly-OBzl. This was then coupled with Boc-His(MBS)-OH to yield Boc-[His(MBS)]₂-Gly-OBzl. Finally, Boc-[His(MBS)]₄-Gly-OBzl prepared by stepwise coupling was treated with hydrogen fluoride (HF) in the presence of anisole to afford (His)₄Gly. Stepwise procedures are summarized in Chart 1. The peptide was purified according to the method described previously.¹⁸⁾

Procedure for the Measurement of Ascorbate Autoxidation Routinely, the reactions were carried out at 25 °C and pH 4.4 under dioxygen. Solutions of $8.0 \times 10^{-5} \text{ mol dm}^{-3}$ ascorbate and $4.0 \times 10^{-6} \text{ mol dm}^{-3}$ Cu(II) complexes, which were prepared freshly before kinetic runs in 0.02 mol dm⁻³ acetate buffer, were mixed with a UNION MX-7 rapid-mixing apparatus to start the reaction, and subsequent changes in absorbance at 260 nm were monitored on a UNION SM-401 spectrophotometer. Before and during the measurement, the solutions were purged with water-saturated O₂ at 100 ml/min. The activity, v_{obsd} , was obtained from the initial rate of ascorbate consumption. The dead-time of the mixing apparatus was assessed within 1 s.

Circular Dichroism (CD) Measurement Measurements of CD were carried out at room temperature and pH 4.4 in 0.02 mol dm⁻³ acetate buffer, and the concentration of Cu(II) was fixed at $8.1 \times 10^{-5} \text{ mol dm}^{-3}$. The spectrum was recorded from 300 nm to 700 nm on a JASCO J-40 spectropolarimeter. Cell length used here was 5 cm.

Analysis of Kinetic Data The oxidation of ascorbate obeys the "Michaelis-Menten" mechanism and the rate, v_{obsd} , is expressed by Eq. 1:¹⁵⁾

$$v_{\text{obsd}} = v_{\text{max}} / \{1 + (K_m / [\text{AscH}]_0)\} \quad (1)$$

where [AscH]₀ stands for the total concentration of ascorbate. The terms, v_{max} and K_m , are the maximum rate and the "Michaelis-Menten" constant given by Eqs. 2 and 3, respectively;

$$v_{\text{max}} = k_2[\text{Cu}]_0 \quad (2)$$

$$K_m = (k_{-1} + k_2) / k_1 \quad (3)$$

where [Cu]₀ represents the total concentration of copper.

The kinetic parameters, v_{max} and K_m , were calculated from the v_{obsd} -[AscH]₀ plot by a nonlinear least-squares method programmed by one of authors (K. H.).

Results and Discussion

Catalytic Activities Both (His)_iGly and Ac-(His)_iGly (*i*=9, 19) accelerated the copper-catalyzed autoxidation of ascorbic acid. The rate-pH plots showed bell-shaped curves with a maximum around pH 4.4. Subsequently, spectroscopic and kinetic experiments were done at pH 4.4. The systems without Cu(II) lack the catalytic activity.

(1) **Coppers Associated with (His)_iGly:** Plots of the relative rate, v/v_0 , against the concentrations of (His)_iGly (*i*=1, 4,

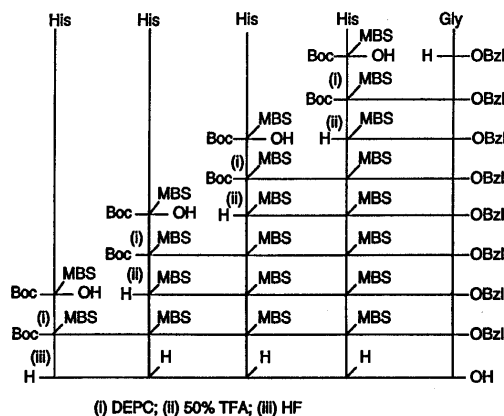


Chart 1. Solution Synthesis of (His)₄Gly

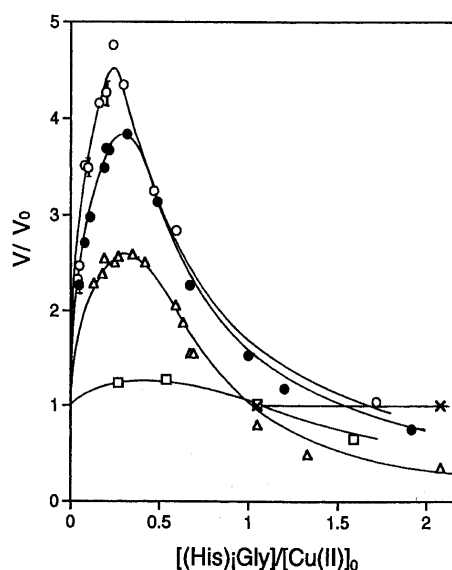


Fig. 1. Plot of the Autoxidation Rate, v/v_0 , against $[(\text{His})_i\text{Gly}]/[\text{Cu(II)}]_0$ at pH 4.4

($\times-\times$): HisGly; ($\square-\square$): (His)₄Gly; ($\triangle-\triangle$): (His)₉Gly; ($\bullet-\bullet$): (His)₁₉Gly; ($\circ-\circ$): (His)₂₉Gly. [Ascorbate] = $8.0 \times 10^{-5} \text{ mol dm}^{-3}$, [Cu(II)] = $4.0 \times 10^{-6} \text{ mol dm}^{-3}$, at 25 °C under O₂. Data are the average of at least three experiments.

9, 19, 29) are shown in Fig. 1, where v_0 denotes the rate in the absence of peptides, [Cu(II)]₀ is fixed at $4.0 \times 10^{-6} \text{ mol dm}^{-3}$, and [(His)_iGly] is varied. The rate depended not only on the concentration but also the molecular weight of the peptides. The Cu(II) complexed with HisGly did not affect the oxidation; the rate was approximately the same as that of aqueous Cu(II). In the pH range from 4 to 5, HisGly forms CuL or CuL₂ species with a histamine-like coordination structure, where L represents the peptide.¹⁹⁾ This suggests that Cu(II) with histamine-like coordination structures neither accelerates nor inhibits the autoxidation. Under optimum conditions, the Cu(II) complexed with (His)₄Gly enhanced the reaction approximately 1.2-fold, but the Cu(II) with (His)₉Gly increased the rate 2.5-fold. Thus, the molecular weight of the peptide, *i.e.*, numbers of serial histidyl residues, contributes to the enhancement of the catalytic activity. When the v/v_0 values exhibited maxima, the peptide would bind enough Cu(II) ions to work efficiently. In terms of maximum v/v_0 , the various (His)_iGly complexes ranked in increasing order as follows;

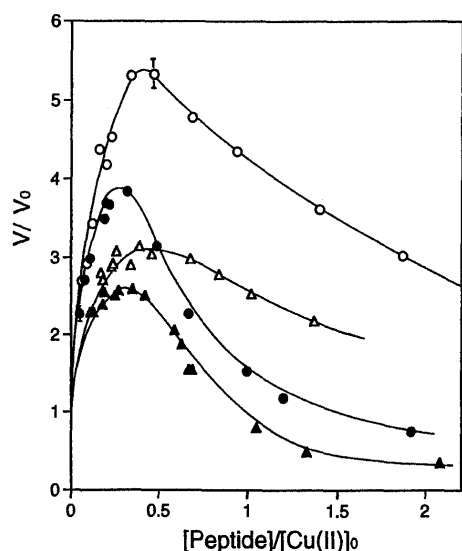


Fig. 2. Plot of the Autoxidation Rate, v/v_0 , against $[Peptide]/[Cu(II)]_0$ at pH 4.4; Effect of *N*-Acetylation

(▲—▲): $(His)_9Gly$; (●—●): $(His)_{19}Gly$; (Δ—Δ): $Ac-(His)_9Gly$; (○—○): $Ac-(His)_{19}Gly$. Conditions are the same as in Fig. 1. Data are the average of at least three experiments.

$(His)_4Gly$ (2) < $(His)_9Gly$ (3) < $(His)_{19}Gly$ (4) < $(His)_{29}Gly$ (6)

where in parentheses are shown approximate numbers of histidyl residues per one molar $Cu(II)$, (number of His -residue)/ $[Cu(II)]$. The greater the molecular weight, the more copper atoms each peptide can accommodate and the more effective the complex becomes.

The v/v_0 decreased as the $[L]/[Cu(II)]_0$ increased over 0.3–0.4, and finally became less than unity. This suggests formation of inactive/inhibitory $Cu(II)$ complexes. The $(His)_iGly$ is considered to have $(i+1)$ donor sets from one terminal amino nitrogen and i imidazole nitrogens. $(His)_iGly$ ($i \geq 9$) primarily coordinates with multi-equivalent $Cu(II)$ forming at least two types of complexes with different coordination modes. Those $Cu(II)$ ions would have opposite functions: one accelerates the autoxidation and the other inhibits it.

(2) Coppers Associated with $Ac-(His)_iGly$: $Ac-(His)_iGly$ lacks the binding site at the amino terminus. Their complexes were catalytically more active than the corresponding $(His)_iGly$ complexes. In Fig. 2 is shown the v/v_0 -plots for $Ac-(His)_iGly$ ($i=9, 19$), along with those for $(His)_iGly$. The v/v_0 for the $Ac-(His)_iGly$ system reached a maximum around $[L]/[Cu(II)]_0=0.5$. As the $[L]/[Cu(II)]_0$ increased, the activity resulted in a rapid drop probably because the active $Cu(II)$ sites on the peptide would be dispersed. However, the $Ac-(His)_iGly$, lacking the $Cu(II)$ site at the amino terminus, did not make the v/v_0 drop below unity. Thus, blocking of the terminal binding site certainly induced enhancement of the reaction system. The v/v_0 for $Ac-(His)_iGly$ complexes was arranged as follows;

$Ac-(His)_9Gly$ (2) < $Ac-(His)_{19}Gly$ (3)

where in parentheses are shown (number of His -residue)/ $[Cu(II)]$. The $(His)_iGly$ could accommodate more than one molar $Cu(II)$, as compared with the corresponding *N*-acetylated peptides. This is probably due to the $Cu(II)$ bound at the amino terminus. Enhancement of the activities

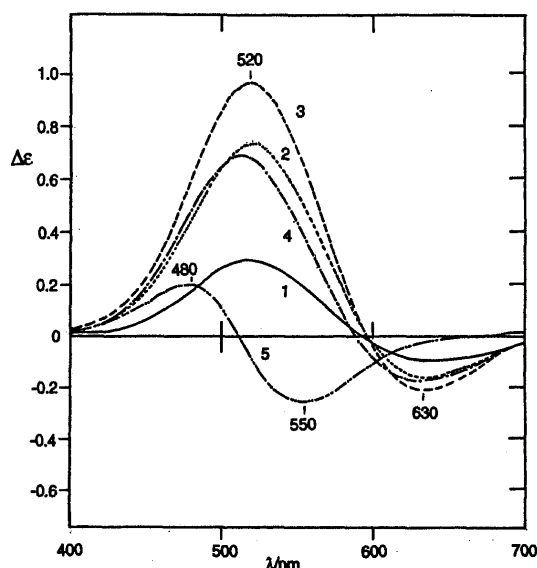


Fig. 3. CD Spectra of the $Cu(II)$ Coordinated with $(His)_{19}Gly$ at pH 4.4

$[(His)_{19}Gly]/[Cu(II)]=0.12$ (1); 0.25 (2); 0.37 (3); 0.62 (4); 1.9 (5). $[Cu(II)]=8.1 \times 10^{-3} \text{ mol dm}^{-3}$ at room temperature.

by *N*-acetylation is as follows:

$Ac-(His)_9Gly/(His)_9Gly=1.4$ and $Ac-(His)_{19}Gly/(His)_{19}Gly=1.2$

Though the increase in the autoxidation rate is related to the increase in the total number of His -residues, the enhancement by *N*-acetylation is not. In other words, the contribution of the inhibitory $Cu(II)$ to the reaction is diminished with the increase in total His -numbers.

Coordination Modes and Structures of the $Cu(II)$ Complexes Circular dichroism has been shown to provide useful information about environments around metal sites.²⁰⁾ Coordination of a transition metal ion with a chiral ligand induces the CD at its $d-d$ transition band, and the λ_{max} depends on the ligand-field strength.²¹⁾ In an attempt to obtain information on the $Cu(II)$ binding sites, measurements of the CD spectra of $Cu(II)$ with $(His)_iGly$ ($i=9, 19, 29$) and $Ac-(His)_iGly$ ($i=9, 19$) were made.

(1) $Cu(II)$ Complexes of $(His)_iGly$: The CD spectra of the $Cu(II)$ with $(His)_{19}Gly$ at various $[L]/[Cu(II)]_0$ ratios from 0.06 to 1.9 are shown in Fig. 3. The spectra at $[L]/[Cu(II)]_0 < 0.4$ exhibited two $d-d$ transition bands; one positive at 520 nm and the other negative at 630 nm, and its intensity increased proportionally to $[L]$, reaching a maximum at $[L]/[Cu(II)]_0=0.37$ ($\Delta\epsilon$; $0.97 \text{ mol}^{-1} \text{ dm}^3 \text{ cm}^{-1}/Cu(II)$ at 520 nm, $-0.21 \text{ mol}^{-1} \text{ dm}^3 \text{ cm}^{-1}/Cu(II)$ at 630 nm). As the $[L]/[Cu(II)]_0$ increased over 0.4, however, the spectrum underwent blue and hypochromic shifts. At $[L]/[Cu(II)]_0=1.9$, the values for λ_{max} were 480 nm ($\Delta\epsilon$; $0.20 \text{ mol}^{-1} \text{ dm}^3 \text{ cm}^{-1}$) and 550 nm ($\Delta\epsilon$; $-0.25 \text{ mol}^{-1} \text{ dm}^3 \text{ cm}^{-1}$). Similar results were obtained for the $(His)_{29}Gly$ complex; λ_{max} ($\Delta\epsilon/\text{mol}^{-1} \text{ dm}^3 \text{ cm}^{-1}/Cu(II)$): 520 nm (0.60), 630 nm (-0.17) at $[L]/[Cu(II)]_0=0.33$, and 480 nm (0.04), 560 nm (-0.03) at $[L]/[Cu(II)]_0=1.74$ (data not shown). On the basis of the CD spectrum, it is clear that the $(His)_{19}Gly$ and $(His)_{29}Gly$ complexes have the same type of coordination mode. The $Cu(II)$ associated with $Cu(II)-(His)_9Gly$ was a little different. The 520/630 nm bands were obscure at low $[L]/[Cu(II)]_0$ ratios below 0.6. But, at $[L]/[Cu(II)]_0 > 0.6$, the CD spectrum exhib-

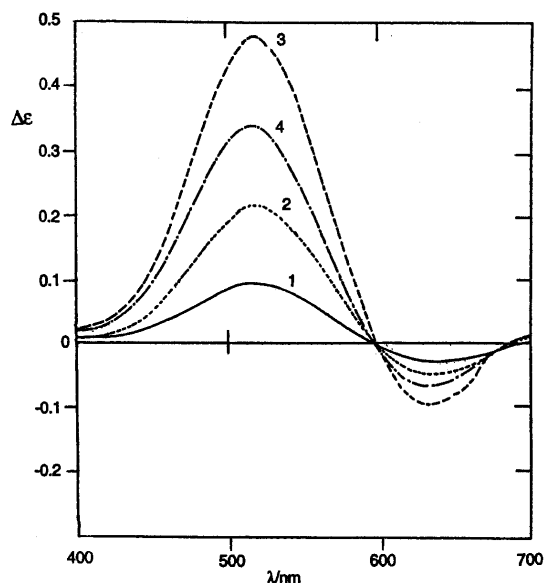


Fig. 4. CD Spectra of Cu(II) Coordinated with Ac-(His)₁₉Gly at pH 4.4
[Ac-(His)₁₉Gly]/[Cu(II)]=0.13 (1); 0.25 (2); 0.63 (3); 1.88 (4). Conditions are the same as in Fig. 3.

ited well-separated *d-d* transition bands at 480 nm ($\Delta\epsilon$; $0.25 \text{ mol}^{-1} \text{ dm}^3 \text{ cm}^{-1}$) and 550 nm ($\Delta\epsilon$; $-0.35 \text{ mol}^{-1} \text{ dm}^3 \text{ cm}^{-1}$) (data not shown). (His)_{*i*}Gly (*i*=9, 19, 29) are likely to form complexes with the same coordination mode as long as the peptides are in excess.

(2) Cu(II) Complexes of Ac-(His)_{*i*}Gly: The Cu(II) in the Ac-(His)_{*i*}Gly (*i*=9, 19) complexes always showed a similar type of CD spectrum exhibiting two *d-d* bands; one positive at 520 nm and the other negative at 630 nm. It did not exhibit the 480/550 nm bands even if the peptide existed in excess in the system. The CD spectra of the Ac-(His)₁₉Gly complexes are shown in Fig. 4, where [L]/[Cu(II)]₀ is changed from 0.13 to 1.88. The intensity of the spectrum, reaching a maximum at [L]/[Cu(II)]₀=0.63, decreased without changing the λ_{max} . The spectral parameters for the Ac-(His)_{*i*}Gly complexes were as follows; λ_{max} ($\Delta\epsilon/\text{mol}^{-1} \text{ dm}^3 \text{ cm}^{-1}/\text{Cu(II)}$): 520 nm (0.68) and 630 nm (-0.36) for Ac-(His)₉Gly complex, 520 nm (0.47) and 630 nm (-0.09) for Ac-(His)₁₉Gly complex. The $\Delta\epsilon$ for the Ac-(His)₉Gly complex is bigger than that of the Ac-(His)₁₉Gly, probably because of steric strain around the Cu(II) sites. Those *N*-acetylated peptides lacking the binding-site at the amino terminal could incorporate Cu(II) in the imidazole cluster to a limit. Thus, the 520/630 nm bands are assignable to the Cu(II) accommodated in the imidazole cluster, and the 480/550 nm bands to that at the amino terminus.

Number of Cu(II) Ions Bound to the Peptides The average number of Cu(II) ions bound to the histidine peptides ($\nu = [\text{Cu}_n\text{L}]/[\text{L}]_0$) could be determined by titration of L with Cu(II) using CD spectroscopy, where [Cu_{*n*}L] stands for the concentration of bound Cu(II). The measurements were carried out at 520 nm; [Cu(II)] was variable and [L] was fixed. The titration curves for Ac-(His)₁₉Gly and (His)₁₉Gly are shown in Figs. 5A and 5B. The maximum binding numbers for Ac-(His)₉Gly and Ac-(His)₁₉Gly were calculated as approximately 2 and 3 mol, respectively. The maximum ν for (His)₁₉Gly and for (His)₂₉Gly are difficult to determine. Since these peptides possess two types of Cu(II) ions having different λ_{max} , the titration curve appeared complicated and inter-

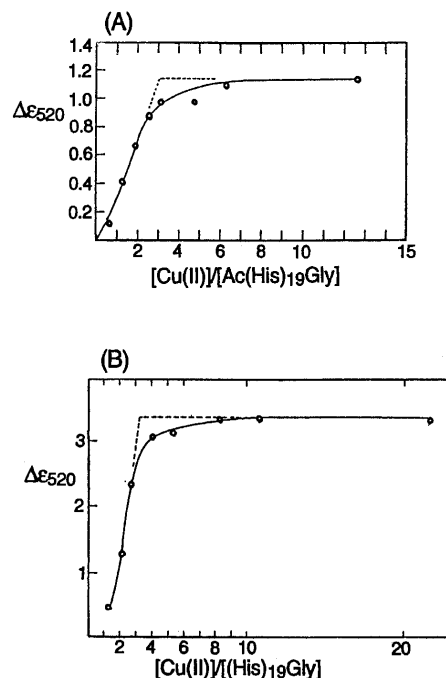
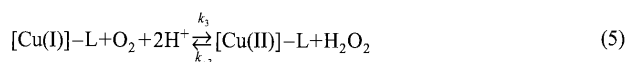
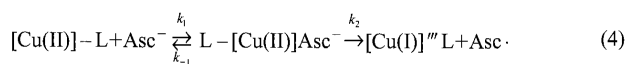


Fig. 5. CD Titration of Ac(His)₁₉Gly (A) and (His)₁₉Gly (B) with Cu(II) at pH 4.4

[Ac(His)₁₉Gly]= $2.6 \times 10^{-5} \text{ mol dm}^{-3}$ and [(His)₁₉Gly]= $3.0 \times 10^{-5} \text{ mol dm}^{-3}$ at room temperature.

sected on the abscissa at [Cu(II)]/[L]₀=1. The maximum ν for (His)_{*i*}Gly (*i*=19, 29) could be estimated as 3—4 mol, in which one molar Cu(II) is bound to the nitrogen at the amino terminus.

Mechanism of the Ascorbate Oxidation The autoxidation of ascorbic acid by the poly-L-histidine (degree of polymerization=*ca.* 50) complexes has been shown to obey the “Michaelis–Menten” mechanism and can be expressed briefly by Eqs. 4 and 5.¹⁵⁾



where L, Asc⁻ and Asc[·] represent ligands, ascorbate, and its free radical, respectively. Double reciprocal plots of the rate against the concentration of the substrates give straight lines. When ascorbate was arranged as the variable substrate and dioxygen as the changing fixed substrate, the family of lines in a reciprocal plot was parallel.¹⁵⁾ This fits the “Ping-Pong” mechanism.²²⁾

Oxidation by the (His)_{*i*}Gly and Ac-(His)_{*i*}Gly complexes appeared a little complicated. In the system with low molecular-weight peptides, such as HisGly and probably (His)₄Gly, the family of lines in a reciprocal plot intersect at a point. This fits the “sequential mechanism”.^{7,22)} Spectroscopic studies have revealed that both (His)_{*i*}Gly and Ac-(His)_{*i*}Gly complexes accommodate multi-equivalent Cu(II) ions. The autoxidation by those Cu(II) complexes occurs primarily by the “Ping-Pong” mechanism. Double reciprocal plots for the systems containing (His)₁₉Gly and Ac-(His)₁₉Gly at an appropriate [L]/[Cu(II)]₀ ratio are shown in Figs. 6A and 6B. However, since the peptide is capable of accommodating different

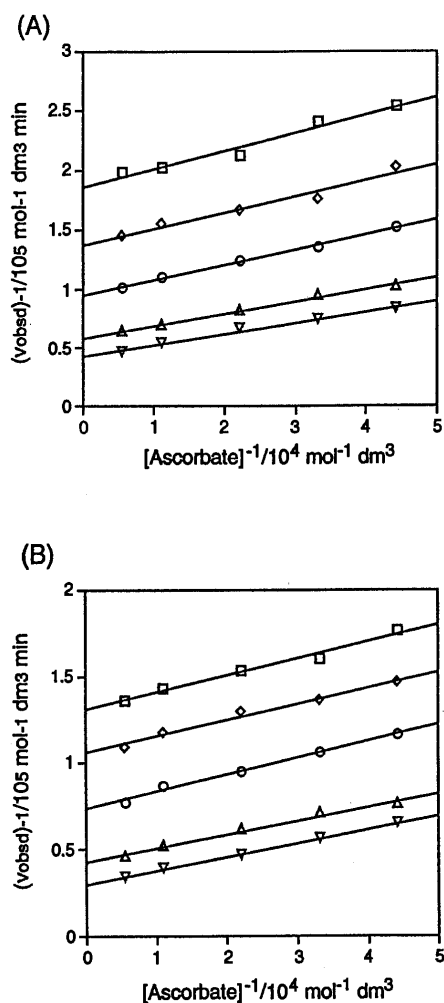
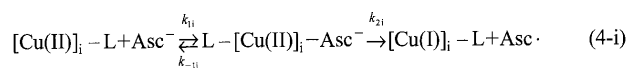
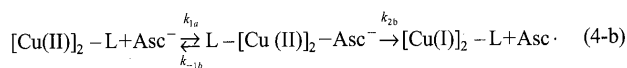
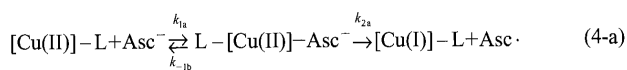


Fig. 6. Double Reciprocal Plot of the v_{obsd} against the Concentration of Ascorbate

Partial pressure of O_2 : (\square — \square) 10%, (\diamond — \diamond) 20%, (\circ — \circ) 40%, (\triangle — \triangle) 70%, (∇ — ∇) 100%. (A) $(\text{His})_{19}\text{Gly}$, $[\text{Cu(II)}] = 4.0 \times 10^{-6} \text{ mol dm}^{-3}$, $[\text{L}]/[\text{Cu(II)}] = 0.68$ and (B) $\text{Ac}-(\text{His})_{19}\text{Gly}$, $[\text{Cu(II)}] = 4.0 \times 10^{-6} \text{ mol dm}^{-3}$, $[\text{L}]/[\text{Cu(II)}] = 0.48$. Data are the average of at least three experiments.

numbers of Cu(II) depending on $[\text{L}]/[\text{Cu(II)}]_0$, the double reciprocal plots are not always straight lines.

The autoxidation can be expressed as a composite reactions (4-a), (4-b), ..., and (4-i).



The reaction was analyzed as a linear combination of two from Eqs. 4-a, 4-b, ..., and 4-i. By the nonlinear least-square method, the $v_{\text{obsd}} - [\text{AscH}]$ plots at various $[\text{L}]/[\text{Cu(II)}]$ were resolved into two main curves and individual K_m and V_{max} values were determined. Typical examples for the system with $(\text{His})_{19}\text{Gly}$ and with $\text{Ac}-(\text{His})_{19}\text{Gly}$ are shown in Figs. 7 and 8, respectively. The plot for $(\text{His})_{19}\text{Gly}$ at $[\text{L}]/[\text{Cu(II)}]_0 = 0.09$ was divided into a straight line and a saturation curve; the former resulted from the reaction by aque-

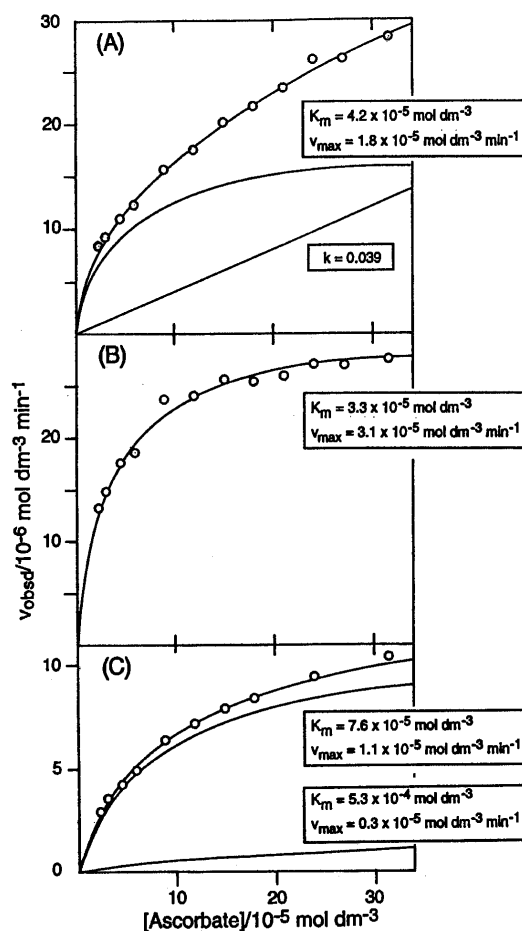


Fig. 7. Resolution of $v_{\text{obsd}} - [\text{AscH}]$ Plot for the $\text{Cu(II)}-(\text{His})_{19}\text{Gly}$ system at pH 4.4

$[\text{Cu(II)}] = 4.0 \times 10^{-6} \text{ mol dm}^{-3}$, (A) $[(\text{His})_{19}\text{Gly}]/[\text{Cu(II)}] = 0.09$; (B) $[(\text{His})_{19}\text{Gly}]/[\text{Cu(II)}] = 0.35$; (C) $[(\text{His})_{19}\text{Gly}]/[\text{Cu(II)}] = 1.18$. Data are the average of at least three experiments.

ous Cu(II) and the latter resulted from the "Michaelis-Menten" mechanism. The rate- $[\text{Asc}^-]$ plot for aqueous Cu(II) was shown to be linear.¹⁵⁾ At $[\text{L}]/[\text{Cu(II)}]_0 = 0.35$, the plot was expressed by a single saturation curve with $K_m = 3.3 \times 10^{-5} \text{ mol dm}^{-3}$ and $v_m = 3.1 \times 10^{-5} \text{ mol dm}^{-3}/\text{min}$, where both the catalytic activity and the CD intensity reached the maximum. The $(\text{His})_{19}\text{Gly}$ could accommodate multi-equivalents Cu(II) , and the contribution of the inhibitory Cu(II) is neglected in the kinetic expression. As the $[\text{L}]/[\text{Cu(II)}]$ ratio increased, the plot could be resolved again into two saturation curves with different parameters. The plot with a smaller v_{max} and bigger K_m is ascribable to the Cu(II) at the amino terminus.

The plots for $\text{Ac}-(\text{His})_{19}\text{Gly}$ were always expressed by a single saturation curve with $K_m = 2.5 - 3.5 \times 10^{-5} \text{ mol dm}^{-3}$ and $v_m = 2.6 - 3.3 \times 10^{-5} \text{ mol dm}^{-3}/\text{min}$, indicating that the reactions obey the "Michaelis-Menten" mechanism.

Conclusion

The catalytic activities of Cu(II) toward the autoxidation of ascorbic acid were enhanced more than two-fold by the complexation with histidine oligopeptide. Not only the molecular weight of the peptide but also the number of serial histidyl residues affects the enhancement. This is supported by the observation that addition of a large excess of Ac-His-NHCH_3

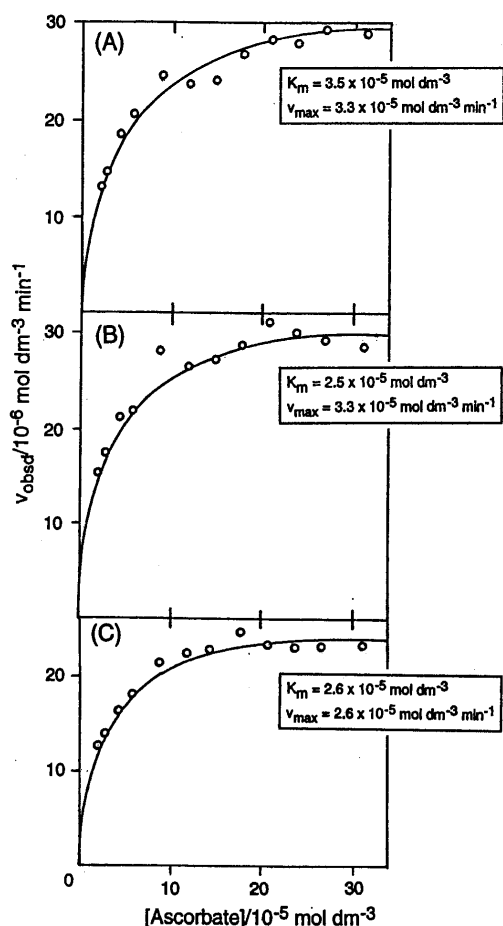


Fig. 8. Resolution of $v_{\text{obsd}}/[\text{AscH}]$ Plot for the Cu(II)-Ac-(His)₁₉Gly System at pH 4.4

[Cu(II)] = $4.0 \times 10^{-6} \text{ mol dm}^{-3}$, (A) [Ac-(His)₁₉Gly]/[Cu(II)] = 0.16; (B) [Ac-(His)₁₉Gly]/[Cu(II)] = 0.32; (C) [Ac-(His)₁₉Gly]/[Cu(II)] = 1.26. Data are the average of at least three experiments.

does not accelerate the autoxidation.¹⁷⁾ The Cu(II) coordinated with the amino terminal peptide fragment; *i.e.*, NH₂-X-Y-His- (X and Y denote amino acid residues), certainly inhibits the reaction. The imidazole cluster constructed with the sequence of -(His)_{*n*}- is necessary for the Cu(II) complex to have high catalytic activity. The minimum number of histidyl residues is five or six. These peptides are likely to coordinate with two Cu(II) ions or more which exhibit two CD bands at 520 and 630 nm and are readily dissociable from the complexes by the addition of NaClO₄ or CH₃COONa.¹⁵⁾

The involvement of free metal ions in *in vivo* oxidation has been questioned because most of these ions are linked to prosthetic groups or are tightly sequestered by specific binding proteins. Experiments with autoxidation by the labile Cu(II) bound to Ac-(His)₁₉Gly suggest the presence of a labile and catalytically active metal in the metalloprotein. Labile Cu(II) bound to an imidazole group, which is Chelex-removable, has been found in ceruloplasmin, and has catalytic activity inducing oxidation of low density lipoprotein.²³⁾

Acknowledgements We thank Dr. T. Ozawa, National Institute of Radiological Sciences, and Prof. A. Odani, Nagoya University, for helpful discussions and advice.

References and Notes

- 1) Present address: National Institute of Radiological Sciences, Anagawa 4-9-1, Chiba 263-8555, Japan.
- 2) Karlin K. D., *Science*, **261**, 701-708 (1993).
- 3) Tainer J. A., Getzoff E. D., Beem K. M., Richardson J. S., Richardson D. C., *J. Mol. Biol.*, **160**, 181-217 (1982).
- 4) Messerschmidt A., Ladenstein R., Huber R., Bolognesi M., Avigliano L., Petruzzelli R., Rossi A., Finazzi-Agro A., *J. Mol. Biol.*, **224**, 179-205 (1992).
- 5) Que L., Jr. (ed.), "Metal Clusters in Proteins," ACS Symposium Series 372, Am. Chem. Soc., Washington, DC, 1988.
- 6) Zuberbühler A. D., "Bioinorganic Chemistry of Copper," ed. by Karlin K. D., Tyeklar Z., Chapman & Hall, London, 1993, p. 264.
- 7) Hanaki A., *Bull. Chem. Soc. Jpn.*, **68**, 831-837 (1995).
- 8) Hanaki A., *Chem. Pharm. Bull.*, **17**, 1964-1966 (1969).
- 9) Gamp H., Zuberbühler A. D., *Metal Ions Biol. Syst.*, **12**, 133-189 (1981).
- 10) Mi L., Zuberbühler A. D., *Helv. Chim. Acta*, **75**, 1547-1556 (1992).
- 11) Jameson R. F., Blackburn N. J., *J. Chem. Soc., Dalton*, **1982**, 9-13.
- 12) Pecht I., Amber M., *Nature (London)*, **207**, 1386-1387 (1965).
- 13) Pecht I., Levitzki A., Amber M., *J. Am. Chem. Soc.*, **89**, 1587-1591 (1967).
- 14) Levitzki A., Pecht I., Berger A., *J. Am. Chem. Soc.*, **94**, 6844-6849 (1972).
- 15) Ueda J., Hanaki A., *Bull. Chem. Soc. Jpn.*, **57**, 3511-3516 (1984).
- 16) Ueda J., Ikota N., Hanaki A., Koga K., *Inorg. Chim. Acta*, **135**, 43-46 (1987).
- 17) Ueda J., Hanaki A., Nakajima T., *Chem. Pharm. Bull.*, **43**, 359-361 (1995).
- 18) Ueda J., Hanaki A., Yasuhara T., Nakajima T., Soufuku S., *Anal. Sci.*, **8**, 487-489 (1992).
- 19) Aiba H., Yokoyama A., Tanaka H., *Bull. Chem. Soc. Jpn.*, **47**, 136-142 (1974).
- 20) Sigel H., Martin R. B., *Chem. Rev.*, **82**, 385-426 (1982).
- 21) Hanaki A., Ikota N., Nomoto K., Yamauchi O., *Nippon Kagaku Kaishi*, **1988**, 578-584.
- 22) W. W. Cleland, *Biochim. Biophys. Acta*, **67**, 104-137 (1963).
- 23) Mukhopadhyay C. K., Mazumder B., Lindley P. F., Fox P. L., *Proc. Natl. Acad. Sci. U.S.A.*, **94**, 11546-11551 (1997).

Mononuclear and Polynuclear Chelates of Picolinoyldithiocarbazate

Tawfik H. RAKHA and Magdy M. BEKHEIT

Chemistry Department, Faculty of Science, Mansoura University, Mansoura, 35516, Egypt.

Received November 26, 1999; accepted March 17, 2000

Mononuclear and polynuclear chelates of potassium picolinoyldithiocarbazate (KHP_cDC) with Mn(II) , Fe(III) , Fe(II) , Co(II) , Ni(II) , Cu(II) , Zn(II) , Cd(II) , Hg(II) , Pd(II) and U(VI)O_2 have been prepared and characterized by chemical and thermal (TG, DTG, DTA) analyses, molar conductivities, spectral (UV-Visible, IR, NMR, ESR) and magnetic moment measurements. The molar conductivities of the complexes lie in the non-electrolyte range whilst KHP_cDC is a 1 : 1 electrolyte. Changes in selected vibrational absorption of the ligand upon coordination indicate that KHP_cDC behaves as monoanionic and coordinates in a bidentate, tridentate and/or bridging tetradentate manner. *Trans*-form structure is proposed for $[\text{Pd}(\text{HP}_c\text{DC})_2] \cdot 2\text{H}_2\text{O}$ and $[\text{Cd}(\text{HP}_c\text{DC})_2]$ complexes on the basis of NMR data. An octahedral structure is proposed for Fe(III) , Fe(II) and Ni(II) complexes, a square-planar structure for Co(II) and Pd(II) complexes and a tetragonally distorted octahedral structure for the Cu(II) chelate on the basis of spectroscopic and magnetic data. The ligand field parameters (B , Dq , β) for the Fe(III) and Ni(II) chelates were calculated. TG, DTG and DTA studies support the different modes of chelation of KHP_cDC . The solid metal acetate chelates have a unique decomposition exotherm profile which can be used as a rapid and sensitive tool for the detection of acetate-containing complexes.

Key words dithiocarbazate; coordination mode; transition metal; spectral; thermal

Coordination compounds containing pyridine moiety, NS and ONS donors are of considerable importance due to the possibility of their dimetallation leading to the formation of compounds having a toxophoric nature.¹⁾ Moreover, they possess bactericidal, fungicidal and antitumor activities.^{2–5)} Dithiocarbazate derivatives containing a heterocyclic moiety as well as metal complexes continue to arouse special interest owing to their anticancer, antituberculosis, antiinflammatory and antiulcer properties.^{6–9)} Great attention is also given to the carcinostatic properties of these compounds which possess some degree of cytotoxic activity¹⁰⁾ against a spectrum of transplanted neoplasm.⁶⁾ The pharmacological properties of such derivatives and their ability to form stable complexes with transition metal ions present in trace amounts in living organisms provided the impetus for this study.^{11–14)} In this paper, potassium picolinoyldithiocarbazate (KHP_cDC) and its metal complexes were prepared and characterized by different studies.¹⁵⁾

Experimental

All chemicals used were of BDH quality (British Drug House Ltd., England) or equivalent quality.

Synthesis of the Ligand Picolinoylhydrazine was prepared as described by Aggarwal and Rao.¹⁶⁾

Potassium picolinoyldithiocarbazate (KHP_cDC) was prepared by stirring a mixture of potassium hydroxide (8.4 g, 0.15 mol) and picolinoylhydrazine (13.7 g, 0.10 mol) in absolute ethanol (50 ml) for about 1 h. Carbon disulphide (11.4 g, 0.15 mol) was then added and the mixture was stirred for an additional 6 h. The resulting yellow crystals of KHP_cDC were removed immediately by filtration, washed with absolute ethanol and dry diethyl ether, recrystallized from absolute ethanol and finally dried in a vacuum desiccator over fused CaCl_2 .

Synthesis of Metal Chelates Complexes $\text{M}(\text{HP}_c\text{DC})_2$ [$\text{M}=\text{Co(II)}$, Ni(II) or Cd(II)], $\text{M}(\text{HP}_c\text{DC})_2 \cdot 2\text{H}_2\text{O}$ [$\text{M}=\text{Cu(II)}$ or Pd(II)] and $[\text{Hg}(\text{HP}_c\text{DC})\text{Cl}(\text{H}_2\text{O})]$ were prepared by adding the metal chloride (1 mmol) in 25 ml bidistilled water to a solution of KHP_cDC (0.50 g, 2 mmol) in 25 ml bidistilled water. The mixture was stirred for 20 min. $[\text{Fe}(\text{HP}_c\text{DC})_2]$ complex was prepared by the same method using (0.28 g, 1 mmol) of ferrous sulphate in 25 ml bidistilled water. $[\text{Fe}(\text{HP}_c\text{DC})_3]$ was obtained using (0.27 g, 1 mmol) of ferric chloride in 25 ml bidistilled water and (0.75 g, 3 mmol) of KHP_cDC in 25 ml bidistilled water.

Complexes $\text{M}(\text{HP}_c\text{DC})(\text{OAc}) \cdot 2\text{H}_2\text{O}$ [$\text{M}=\text{Co(II)}$ or Ni(II)] and $[\text{M}$

$(\text{HP}_c\text{DC})(\text{OAc})(\text{H}_2\text{O})]$ [$\text{M}=\text{Zn(II)}$ or Cd(II)] were prepared by adding KHP_cDC (0.25 g, 1 mmol) in 25 ml bidistilled water to the metal acetate (1 mmol) in 25 ml bidistilled water. The mixture was stirred for 20 min. $[\text{UO}_2(\text{HP}_c\text{DC})(\text{OAc})(\text{H}_2\text{O})]$ complex was prepared by the same method using (0.42 g, 1 mmol) of uranyl acetate in 25 ml of absolute ethanol. $[\text{Mn}(\text{HP}_c\text{DC})(\text{OAc})(\text{H}_2\text{O})_2]$ was prepared from the metal chloride in the presence of (0.82 g, 10 mmol) sodium acetate as a buffering agent.

The resulting solid complexes which formed during stirring were immediately filtered off, washed several times with bidistilled water followed by an aqueous-ethanolic solution and then diethyl ether and finally dried in a vacuum desiccator over fused CaCl_2 .

Analyses and Measurements The metal and halide contents were determined by standard methods.¹⁷⁾ Carbon and hydrogen analyses were performed by the Microanalytical Unit of Mansoura University. IR spectra in the 200–4000 cm^{-1} range were recorded on a Mattson 5000 FTIR spectrometer as KBr discs; electronic spectra in dimethylsulphoxide (DMSO) were obtained using an UV-2-100 Unicam UV/Visible spectrometer. ^1H -NMR spectra in $\text{DMSO}-d_6$ solutions were recorded, using TMS as an internal reference, on a Varian Gemini (200 MHz) spectrometer. ESR spectra were made in the solid state at room temperature, with a JEOL JESRE-XG spectrometer (100 kHz magnetic field modulation) calibrated with 2,2-diphenyl-1-picrylhydrazyl (DPPH), at Tanta University. Magnetic moments at 25 °C were determined using a Gouy balance with $[\text{Hg}(\text{Co}(\text{SCN})_4)]$ as calibrant. TG, DTG and DTA measurements were made in a N_2 atmosphere between 20–1000 °C, using a Shimadzu thermogravimetric analyser TGA-50 with $\alpha\text{-Al}_2\text{O}_3$ as a reference. Molar conductivities (Λ_m) for 10^{-3}M , solutions in DMSO at 25 °C were measured using a Tacussel conductivity bridge type CD6NG. Molecular weight measurements for all complexes were made by Rast's method¹⁸⁾ using camphor as a solvent.

Results and Discussion

Stoichiometries, colours, melting points, partial elemental analyses, molar conductivities and magnetic moments of the metal chelates of KHP_cDC are given in Table 1. The complexes are stable in air, insoluble in most organic solvents, but readily soluble in dimethylformamide (DMF) and DMSO. The molar conductivities of the complexes in DMSO at 25 °C are in the 4–20 $\text{ohm}^{-1} \cdot \text{cm}^2 \cdot \text{mol}^{-1}$ range indicating their non-electrolytic nature,¹⁹⁾ but KHP_cDC shows a value (48 $\text{ohm}^{-1} \cdot \text{cm}^2 \cdot \text{mol}^{-1}$) corresponding to a 1 : 1 electrolyte. Molecular weight determinations suggest a polymeric nature for the complexes $[\text{M}(\text{HP}_c\text{DC})(\text{OAc})(\text{H}_2\text{O})]$ [$\text{M}=\text{Zn(II)}$, Cd(II) or U(VI)O_2].

* To whom correspondence should be addressed. e-mail: sinfac@mum.mans.eun.eg

Table 1. Physical Properties and Analytical Data for KHP_cDC and Its Metal Complexes

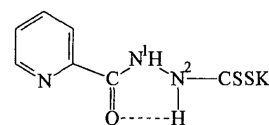
Compound	Colour	mp (°C)	Found (Calcd) (%)				Λ_m (ohm ⁻¹ ·cm ² ·mol ⁻¹)	μ_{eff} (B.M.)
			C	H	M	X		
KHP _c DC	Yellow	265	33.3 (33.4)	2.5 2.4	15.4 15.6	—	48	—
[Mn(HP _c DC)(OAc)(H ₂ O) ₂]	Brownish yellow	>300	30.0 (29.8)	3.7 3.6	15.1 15.2	—	18	5.84
[Co(HP _c DC)(OAc)]·2H ₂ O	Dark brown	>300	29.6 (29.5)	3.6 3.6	16.0 16.1	—	16	3.08
[Ni(HP _c DC)(OAc)(H ₂ O) ₂]	Brown	>300	29.4 (29.5)	3.7 3.6	16.2 16.0	—	7	2.38
[Pd(HP _c DC) ₂]·2H ₂ O	Orange	>300	29.9 (29.7)	2.7 2.8	18.6 18.8	—	4	Diam.
[Hg(HP _c DC)Cl(H ₂ O)]	Yellow	280	17.7 (18.0)	1.6 1.7	43.3 43.0	7.7 7.6	6	Diam.
[Fe(HP _c DC) ₃]	Reddish brown	>300	36.6 (36.4)	2.4 2.6	8.0 8.1	—	20	5.74
[Co(HP _c DC) ₂]	Brown	>300	34.7 (34.8)	2.6 2.5	12.4 12.2	—	11	2.76
[Cu(HP _c DC) ₂ (H ₂ O) ₂]	Greenish black	217	31.8 (32.1)	3.0 3.1	12.2 12.1	—	6	1.82
[Fe(HP _c DC) ₂]	Brown	>300	34.9 (35.0)	2.3 2.5	11.8 11.6	—	18	5.16
[Ni(HP _c DC) ₂]	Reddish brown	>300	35.0 (34.8)	2.5 2.5	11.9 12.1	—	10	2.18
[Cd(HP _c DC) ₂]	Yellow	>300	31.5 (31.3)	2.1 2.3	20.9 20.9	—	7	Diam.
[Zn(HP _c DC)(OAc)(H ₂ O)]	Yellow	>300	30.7 (30.5)	3.3 3.1	18.1 18.4	—	12	Diam.
[Cd(HP _c DC)(OAc)(H ₂ O)]	Yellow	>300	26.3 (26.9)	2.9 2.8	28.2 28.0	—	10	Diam.
[UO ₂ (HP _c DC)(OAc)(H ₂ O)]	Deep brown	>300	19.1 (19.3)	1.9 2.0	42.9 42.6	—	8	Diam.

Table 2. Selected IR Band Positions (cm⁻¹) in the Spectra of KHP_cDC and Its Metal Complexes

Compound	$\nu(\text{N}^1\text{H})$	$\nu(\text{C}=\text{O})$	$\nu(\text{C}=\text{N})$ pyridine	Pyridine ring breathing mode	$\nu_{\text{as}}(\text{CSS})$	$\nu(\text{N}-\text{N})$	$\nu(\text{M}-\text{O})$	$\nu(\text{M}-\text{N})$	$\nu(\text{M}-\text{S})$
KHP _c DC	3170	1652	1590	994	1090, 1120	1035	—	—	—
[Mn(HP _c DC)(OAc)(H ₂ O) ₂]	3120	1655	1585	986	1091, 1125	1055	485	405	385
[Co(HP _c DC)(OAc)]·2H ₂ O	3138	1650	1589	992	1106, 1130	1060	515	425	380
[Ni(HP _c DC)(OAc)(H ₂ O) ₂]	3125	1655	1588	996	1098, 1120	1055	510	425	380
[Pd(HP _c DC) ₂]·2H ₂ O	3145	1680	1590	994	1090, 1116	1052	—	430	390
[Hg(HP _c DC)Cl(H ₂ O)]	3133	1670	1592	996	1081, 1112	1056	565 ^{a)}	405	385
[Fe(HP _c DC) ₃]	3232	1646	1582	988	1095	1050	—	—	390
[Co(HP _c DC) ₂]	3225	1650	1592	986	1102	1052	—	—	375
[Cu(HP _c DC) ₂ (H ₂ O) ₂]	3223	1654	1588	992	1092	1050	580 ^{a)}	—	370
[Fe(HP _c DC) ₂]	3115	1650	1600	1022	1099, 1117	1060	—	420	385
[Ni(HP _c DC) ₂]	3135	1648	1602	1010	1090, 1115	1060	—	425	365
[Cd(HP _c DC) ₂]	3138	1655	1602	1016	1092, 1125	1062	—	405	370
[Zn(HP _c DC)(OAc)(H ₂ O)]	3115	1630	1611	1025	1092, 1125	1065	500	410	365
[Cd(HP _c DC)(OAc)(H ₂ O)]	3110	1635	1606	1015	1095, 1128	1066	510	425	375
[UO ₂ (HP _c DC)(OAc)(H ₂ O)]	3111	1638	1607	1030	1098, 1118	1069	520	415	380

a) Assigned to the metal-oxygen stretching vibration of coordinated water.

IR and NMR Spectral Studies The significant IR bands of KHP_cDC and its metal complexes are summarized in Table 2. The IR spectrum of KHP_cDC exhibits a strong split band at *ca.* 1100 cm⁻¹ (1090, 1120) assigned to $\nu_{\text{as}}(\text{CSS})$.¹³⁾ The two bands at 3300 and 3170 cm⁻¹ are attributed to $\nu(\text{N}^2\text{H})$ and $\nu(\text{N}^1\text{H})$ modes, respectively.²⁰⁾ The strong band at 1652 cm⁻¹ is assigned to $\nu(\text{C}=\text{O})$. The bands observed at 1590 and 994 cm⁻¹ are assigned to pyridine ring $\nu(\text{C}=\text{N})$ and pyridine ring breathing mode, respectively.²¹⁾ Also, the medium intensity band at 1035 cm⁻¹ is attributed to the

Fig. 1. Structure of the Ligand (KHP_cDC)

$\nu(\text{N}-\text{N})$ vibration.¹³⁾ Two weak, broad bands at *ca.* 2075 and *ca.* 1950 cm⁻¹ are assigned to the stretching and bending vibrations of (N-H...O), suggesting the presence of intramolecular hydrogen bonding¹³⁾ (Fig. 1).

Table 3. ^1H -NMR Spectral Data of KHP_cDC and Some of Its Diamagnetic Complexes

Compound	^1H Chemical shift (δ) in ppm				
	$\text{N}^1\text{-H}$	$\text{N}^2\text{-H}$	Pyridine (H)	H_2O (Coord.)	$\text{CH}_3\text{-C}$
KHP_cDC	10.40	8.85	7.45—8.60	—	—
$[\text{Pd}(\text{HP}_c\text{DC})_2] \cdot 2\text{H}_2\text{O}$	10.05	9.15	7.60—8.65	—	—
$[\text{Cd}(\text{HP}_c\text{DC})_2]$	10.25	9.20	7.55—8.65	—	—
$[\text{Cd}(\text{HP}_c\text{DC})(\text{OAc})(\text{H}_2\text{O})]$	10.15	9.10	7.90—8.85	4.45	2.45
$[\text{Zn}(\text{HP}_c\text{DC})(\text{OAc})(\text{H}_2\text{O})]$	10.10	9.15	7.80—8.75	4.40	2.55

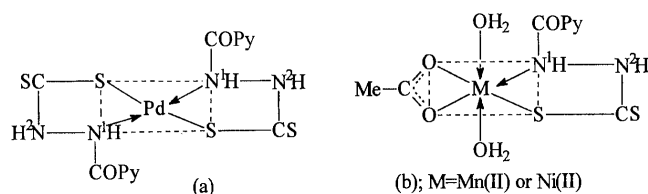


Fig. 2

^1H -NMR spectral data of KHP_cDC and some of its diamagnetic complexes are depicted in Table 3. The NMR spectrum of KHP_cDC in $\text{DMSO}-d_6$ shows two signals at 10.40 and 8.85 ppm (*i.e.*, down-field of TMS), which disappear upon adding D_2O . These two signals are assigned to the N^1H and N^2H protons,¹²⁾ respectively.

KHP_cDC coordinates in monoanionic bidentate NS fashion *via* the nitrogen atom of the N^1H group and the sulphur atom of the SK group, with displacement of potassium ion from the CSSK group; forming a five-membered ring including the metal atom as shown in Fig. 2. This behaviour is found in the complexes having the formulae $\text{M}(\text{HP}_c\text{DC})(\text{OAc}) \cdot 2\text{H}_2\text{O}$ [$\text{M}=\text{Mn}(\text{II})$, $\text{Co}(\text{II})$ or $\text{Ni}(\text{II})$], $[\text{Pd}(\text{HP}_c\text{DC})_2] \cdot 2\text{H}_2\text{O}$ and $[\text{Hg}(\text{HP}_c\text{DC})\text{Cl}(\text{H}_2\text{O})]$. This complexation mode is supported by: (i) the shift to lower wave number of N^1H vibration band; (ii) the appearance of a strong split band near 1100 cm^{-1} , indicating monodentate sulphur chelation^{12,22)}; (iii) the bands assignable to $\nu(\text{C}=\text{O})$ and pyridine ring $\nu(\text{C}=\text{N})$ remain more or less at the same positions, indicating that these groups do not take part in coordination and (iv) the appearance of new bands in the $430\text{--}405$ and $390\text{--}380\text{ cm}^{-1}$ regions assignable to $\nu(\text{M}-\text{N})$ ²³⁾ and $\nu(\text{M}-\text{S})$,²⁴⁾ respectively. In addition, the acetate complexes exhibit two new bands at *ca.* 1560 and *ca.* 1445 cm^{-1} attributable to $\nu_{\text{as}}(\text{C}-\text{O})$ and $\nu_{\text{s}}(\text{C}-\text{O})$ vibrations of the acetate group.²⁵⁾ The difference (*ca.* 115 cm^{-1}) between these two bands indicates the bidentate bonding mode of the acetate group. Moreover, the NMR spectrum of the diamagnetic $\text{Pd}(\text{II})$ complex displays the two signals attributable to the two protons of N^1H and N^2H groups at 10.05 and 9.15 ppm, indicating that NH 's do not deprotonate on complexation. As expected for this complex, *cis*- and *trans*-isomers are possible, the presence of one resonance for each signal suggesting *trans*-configuration^{26,27)} as shown in Fig. 2a.

Also, KHP_cDC behaves as monoanionic bidentate SS ligand coordinating through the CSS group as shown in Fig. 3. This behaviour is found in $[\text{Fe}(\text{HP}_c\text{DC})_3]$, $[\text{Co}(\text{HP}_c\text{DC})_2]$ and $[\text{Cu}(\text{HP}_c\text{DC})_2(\text{H}_2\text{O})_2]$ complexes. Evidence for SS bonding in these complexes is provided by the N^1H stretching frequencies. In KHP_cDC , the $\nu(\text{N}^1\text{H})$ is observed at 3170 cm^{-1} . If NS bonding occurs, the N^1H stretching frequencies in the

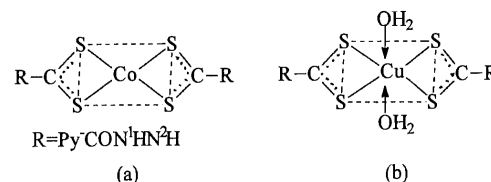


Fig. 3

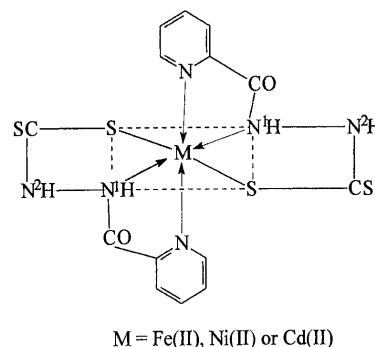


Fig. 4

metal complexes should occur at lower frequencies than in the free ligand, but as Table 2 shows, in these metal chelates $\nu(\text{N}^1\text{H})$ is shifted to higher frequencies ($3232\text{--}3223\text{ cm}^{-1}$). Further evidence of disulphur chelation is given by the appearance of a single strong band¹³⁾ at *ca.* 1100 cm^{-1} . Also, new bands appear in the $390\text{--}370\text{ cm}^{-1}$ region assignable to $\nu(\text{M}-\text{S})$.²⁴⁾ However, the bands due to $\nu(\text{C}=\text{O})$ and $\nu(\text{C}=\text{N})$ (pyridine) remain more or less at the same positions, indicating that these groups play no part in the coordination.

In $[\text{Cu}(\text{HP}_c\text{DC})_2(\text{H}_2\text{O})_2]$ and $[\text{M}(\text{HP}_c\text{DC})(\text{OAc})(\text{H}_2\text{O})_2]$ [$\text{M}=\text{Mn}(\text{II})$ or $\text{Ni}(\text{II})$] complexes, the two water molecules exist either in the *cis*- or *trans*-form but the observation of a medium unsplit band in the $580\text{--}600\text{ cm}^{-1}$ range is assigned to the metal-oxygen stretching vibration,^{25,28)} suggesting the existence of *trans*-form rather than the *cis*-form as shown in Figs. 2b, 3b.

KHP_cDC can also function as a monoanionic tridentate NNS ligand coordinating through the azomethine nitrogen of the pyridine ring, the nitrogen atom of N^1H group and the sulphur atom of the SK group, with displacement of the potassium ion from the CSSK group, forming four five-membered rings including the metal atom. This chelation mode (Fig. 4) which is found in $[\text{M}(\text{HP}_c\text{DC})_2]$ [$\text{M}=\text{Fe}(\text{II})$, $\text{Ni}(\text{II})$ or $\text{Cd}(\text{II})$] is supported by: (i) the shift to higher wave number of the pyridine ring $\nu(\text{C}=\text{N})$ and pyridine ring breathing mode²¹⁾; (ii) the shift to lower wave number of the N^1H vibration band; (iii) the appearance of a strong split band at *ca.* 1110 cm^{-1} ascribed to $\nu_{\text{as}}(\text{CSS})$,¹³⁾ indicat-

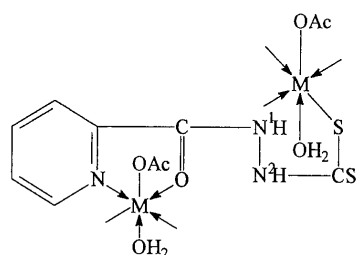
M = Zn(II), Cd(II) or U(VI)O₂

Fig. 5

ing monodentate sulphur chelation^{12,22)} and (iv) the band attributable to the carbonyl group remains unaltered, indicating that this group plays no part in the coordination. Moreover, the NMR spectrum of Cd(II) chelate shows two signals at 10.25 and 9.20 ppm assignable to the two protons of N¹H and N²H groups, and the presence of one resonance for each signal suggests the *trans*-isomer form.^{26,27)}

Finally, in [M(HP_cDC)(OAc)(H₂O)] [M = Zn(II), Cd(II) or U(VI)O₂], KHP_cDC coordinates in monoanionic bridging tetradentate NONS fashion *via* the carbonyl oxygen and the azomethine nitrogen of the pyridine ring from one end, and the sulphur atom of the SK group and the nitrogen atom of the N¹H group on the other, with displacement of the potassium ion from the CSSK group. Geometrical factors prevent the coordination of all the donors to a single metal ion, which must, therefore, act as a bridging unit between two metal centers, giving a polymeric structure.²⁹⁾ This chelation mode as in Fig. 5 is confirmed by the following evidence: (i) the shift of both $\nu(\text{C}=\text{O})$ and $\nu(\text{N}^1\text{H})$ to lower wave numbers; (ii) the appearance of a strong split band near 1100 cm⁻¹, assignable to $\nu_{\text{as}}(\text{CSS})$, indicating monodentate sulphur chelation^{12,22)}; (iii) the significant shift to higher wave numbers of pyridine ring $\nu(\text{C}=\text{N})$ and pyridine ring breathing mode²¹⁾ and (iv) the shift to higher wave number of $\nu(\text{N}-\text{N})$. The molecular weight values (1780, 2000 and 2780) of the Zn(II), Cd(II) and U(VI)O₂ chelates, respectively, confirm their polymeric nature. In addition, the NMR spectra of Zn(II) and Cd(II) chelates indicate that the NH groups do not deprotonate on chelation.

The uranyl chelate exhibits three bands at 922, 885 and 263 cm⁻¹, assigned to ν_3 , ν_1 and ν_4 vibrations, respectively, of the dioxouranium ion.²⁹⁾ The force constant (F) for bonding sites of the (U=O) vibration is calculated by the method of McGlynn *et al.*³⁰⁾; the F_{uo} value is 7.017 mdyn Å⁻¹. The U–O bond distance is calculated with the help of the equation: $R_{\text{u-o}} = 1.08 F^{-1/3} + 1.17$.

The U–O bond distance is 1.73 Å and falls in the usual region as reported earlier.²⁹⁾

The new bands observed in the chelates at 520–485, 430–405, 390–365 and 285 cm⁻¹ are tentatively assigned to $\nu(\text{M}-\text{O})$,²⁹⁾ $\nu(\text{M}-\text{N})$,²³⁾ $\nu(\text{M}-\text{S})$ ²⁴⁾ and $\nu(\text{Hg}-\text{Cl})$,²⁴⁾ respectively.

The presence of water within the coordination sphere in the hydrated chelates is supported by the presence of bands in the 3440–3390, 1625–1605 sh and 980–955 w cm⁻¹ ranges in the spectra of the chelates due to OH stretching, HOH deformation and H₂O rocking.²⁵⁾

Magnetic, Electronic and ESR Spectral Studies The magnetic moments of the metal chelates are depicted in

Table 1.

The electronic spectrum of [Cu(HP_cDC)₂(H₂O)₂] chelate exhibits one broad band at 16949 cm⁻¹ with a shoulder at 14493 cm⁻¹ assigned to ${}^2\text{B}_{1g} \rightarrow {}^2\text{E}_g$ and ${}^2\text{B}_{1g} \rightarrow {}^2\text{A}_{1g}$ transitions, respectively, in a tetragonally distorted octahedral geometry around copper(II)³¹⁾ ion. The magnetic moment value (1.82 B.M.) of the Cu(II) chelate is consistent with the presence of one unpaired electron which rules out the possibility of spin–spin interaction in the crystalline state and excludes a polymeric structure.

In order to obtain further information about the stereochemistry and to determine the magnetic interaction in [Cu(HP_cDC)₂(H₂O)₂], the X-band ESR spectrum in the solid state was recorded at room temperature. The spectrum is typical of those reported for axial type copper(II) complexes,^{32,33)} with two g -values; $g_{\parallel} = 2.279$ and $g_{\perp} = 2.053$ giving $g_{\text{av}} = 2.128$. It is clear that $g_{\text{av}} = (g_{\parallel} + 2g_{\perp})/3 > g_{\perp} > 2.040$, characteristic of axial symmetry, with planar arrangement of the two ligand molecules around copper(II), and the two water molecules occupying the axial positions as shown in Fig. 3. The g -values suggest a tetragonally distorted octahedral geometry³³⁾ for the chelate, in agreement with the electronic spectral data; $g_{\parallel} > g_{\perp} > g_e$ (free electron spin) indicating a $d_{x^2-y^2}$ ground state. In axial symmetry, the g -values are correlated with the expression³⁴⁾ $G = (g_{\parallel} - 2)/(g_{\perp} - 2)$ which reflects the spin-exchange interaction between copper(II) centers in the solid polycrystalline complexes. According to Hathaway and Billig,³⁵⁾ if the axial symmetry parameter $G > 4$ the spin-exchange interaction is negligible whereas if $G < 4$ a considerable spin-exchange interaction is indicated. In the present study, the calculated G -value for the copper(II) chelate is 5.26, indicating the absence of spin-exchange interaction between copper(II) ions. In conclusion, magnetic, electronic and ESR spectral data as well as the molecular weight measurement inferred the monomeric structure of [Cu(HP_cDC)₂(H₂O)₂] complex.

The magnetic moments (2.76–3.08 B.M.) for the cobalt(II) complexes, [Co(HP_cDC)₂] and [Co(HP_cDC)(OAc)]·2H₂O, fall in the range reported for square-planar and/or low-spin octahedral structures. The presence of a characteristic band in the 21739–21978 cm⁻¹ range with a comparatively high molecular extinction coefficient ($\epsilon = 225\text{--}260 \text{ l}\cdot\text{mol}^{-1}\cdot\text{cm}^{-1}$) supports the square-planar structure around the cobalt(II) ion.¹²⁾

The electronic spectra of the nickel(II) chelates display two bands in the 15748–16529 and 25316–26667 cm⁻¹ ranges, assignable to the ${}^3\text{A}_{2g} \rightarrow {}^3\text{T}_{1g}(\text{F})$ (ν_2) and ${}^3\text{A}_{2g} \rightarrow {}^3\text{T}_{1g}(\text{P})$ (ν_3) transitions,³⁶⁾ respectively. The calculated values of ligand field parameters: B (803 cm⁻¹), β (0.77), $10 Dq$ (10390 cm⁻¹) and ν_2/ν_1 (1.59) for [Ni(HP_cDC)(OAc)(H₂O)₂]; B (753 cm⁻¹), β (0.72), $10 Dq$ (9930 cm⁻¹) and ν_2/ν_1 (1.59) for [Ni(HP_cDC)₂] lie in the range reported for an octahedral environment around nickel(II) ion.³⁷⁾ Also, the values of ϵ for ν_2 ($10\text{--}14 \text{ l}\cdot\text{mol}^{-1}\cdot\text{cm}^{-1}$) and μ_{eff} (2.18–2.38 B.M.) are consistent with octahedral geometry.³⁶⁾

The electronic spectrum of [Pd(HP_cDC)₂]·2H₂O shows a band at 21739 cm⁻¹, which is assigned to the ${}^1\text{A}_{1g} \rightarrow {}^1\text{B}_{1g}$ transition with an ϵ value of $84 \text{ l}\cdot\text{mol}^{-1}\cdot\text{cm}^{-1}$ in a planar configuration.¹⁹⁾ Also, the high-energy band at 28090 cm⁻¹ may be attributed to a charge transfer phenomenon.

The electronic spectrum of [Fe(HP_cDC)₃] shows three

Table 4. Thermal Behaviour of the $M(\text{HP}_c\text{DC})(\text{OAc}) \cdot 2\text{H}_2\text{O}$ and $[\text{Cu}(\text{HP}_c\text{DC})_2(\text{H}_2\text{O})_2]$ Complexes

Compound (Molecular weight)	Temp. range (°C)	Decomposition product loss (Formula weight)		Weight % Found (Calcd)
$[\text{Mn}(\text{HP}_c\text{DC})(\text{OAc})(\text{H}_2\text{O})_2]$ (362.292)	150—225	$2\text{H}_2\text{O}$	(36.032)	10.0 (9.9)
	225—325	$\text{C}_5\text{H}_4\text{N}(\text{Py})$	(78.094)	21.3 (21.6)
	325—405	$\text{C}_2\text{H}_3\text{O}_2(\text{AcO})$	(59.046)	16.4 (16.3)
	405—690	CONHNHCS	(102.116)	28.0 (28.2)
	>690	Residue; MnS	(87.004)	24.2 (24.0)
$[\text{Ni}(\text{HP}_c\text{DC})(\text{OAc})(\text{H}_2\text{O})_2]$ (366.062)	145—255	$2\text{H}_2\text{O}$	(36.032)	10.0 (9.8)
	255—375	$\text{C}_5\text{H}_4\text{N}(\text{Py})$	(78.094)	21.2 (21.3)
	375—430	$\text{C}_2\text{H}_3\text{O}_2(\text{AcO})$	(59.046)	16.3 (16.1)
	430—730	CONHNHCS	(102.116)	27.6 (27.9)
	>730	Residue; NiS	(90.774)	24.9 (24.8)
$[\text{Co}(\text{HP}_c\text{DC})(\text{OAc})] \cdot 2\text{H}_2\text{O}$ (366.282)	80—155	$2\text{H}_2\text{O}$	(36.032)	9.6 (9.8)
	205—362	$\text{C}_5\text{H}_4\text{N}(\text{Py})$	(78.094)	21.5 (21.3)
	362—420	$\text{C}_2\text{H}_3\text{O}_2(\text{OAc})$	(59.046)	16.2 (16.1)
	420—860	CONHNHCS	(102.116)	27.7 (27.9)
	>860	Residue; CoS	(90.994)	25.0 (24.8)
$[\text{Cu}(\text{HP}_c\text{DC})_2(\text{H}_2\text{O})_2]$ (524.120)	190—250	$2\text{H}_2\text{O}$	(36.032)	7.1 (6.9)
	250—320	$2\text{C}_5\text{H}_4\text{N}(\text{Py})$	(156.188)	29.6 (29.8)
	320—870	$\text{CONHNHCS} + \text{CONHNHCS}$	(236.296)	45.3 (45.1)
	>870	Residue, CuS	(95.604)	18.1 (18.2)

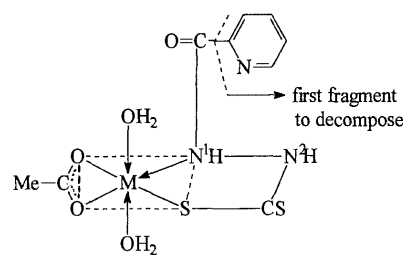
bands at 15385, 23810 and 29240 cm^{-1} assignable to ${}^6\text{A}_{1g} \rightarrow {}^4\text{T}_{1g}(\text{G})$, ${}^6\text{A}_{1g} \rightarrow {}^4\text{T}_{2g}(\text{G})$ and ${}^6\text{A}_{1g} \rightarrow {}^4\text{T}_{2g}(\text{D})$ transitions,³⁶⁾ respectively. The magnetic moment value (5.74 B.M.) for this complex indicates that it is of high-spin octahedral type. Also, the calculated B (641 cm^{-1}), β (0.67) and $10 Dq$ (7050 cm^{-1}) values together with the comparatively low molecular extinction coefficient (ϵ) for ν_2 ($0.41 \cdot \text{mol}^{-1} \cdot \text{cm}^{-1}$) supports the octahedral geometry.³⁶⁾ On the other hand, $[\text{Fe}(\text{HP}_c\text{DC})_2]$ has a magnetic moment of 5.16 B.M. and an ϵ value for ν_2 ($31 \cdot \text{mol}^{-1} \cdot \text{cm}^{-1}$) indicating an octahedral high-spin arrangement with a ${}^5\text{T}_{2g}$ ground state. The absorption spectrum is consistent with those previously observed in high-spin octahedral iron(II) complexes.^{36,38)}

The μ_{eff} value (5.84 B.M.) of $[\text{Mn}(\text{HP}_c\text{DC})(\text{OAc})(\text{H}_2\text{O})_2]$ is as expected for high-spin $3d^5$ systems. The electronic spectrum displays very weak absorption bands which are not of much help in deciding the transition.²⁹⁾

Finally, the UV spectrum of the $[\text{UO}_2(\text{HP}_c\text{DC})(\text{OAc})(\text{H}_2\text{O})]$ shows two bands at 21277 and 26596 cm^{-1} assignable to ${}^1\Sigma_g^+ \rightarrow {}^2\Pi_u$ transition of dioxouranium(VI)²⁰⁾ and charge transfer probably $n \rightarrow \pi^*$, respectively.

Thermal Studies The thermal behaviour of $[\text{M}(\text{HP}_c\text{DC})(\text{OAc})(\text{H}_2\text{O})_2]$ [$\text{M} = \text{Mn}(\text{II})$ or $\text{Ni}(\text{II})$], $[\text{Co}(\text{HP}_c\text{DC})(\text{OAc})] \cdot 2\text{H}_2\text{O}$ and $[\text{Cu}(\text{HP}_c\text{DC})_2(\text{H}_2\text{O})_2]$ has been studied under an atmosphere of N_2 . The stage of decomposition, temperature range, decomposition product lost as well as the found and calculated weight loss percentages are depicted in Table 4.

$[\text{M}(\text{HP}_c\text{DC})(\text{OAc})(\text{H}_2\text{O})_2]$ complexes are thermally stable up to 145°C , above which point four main decomposition steps are observed. $[\text{Mn}(\text{HP}_c\text{DC})(\text{OAc})(\text{H}_2\text{O})_2]$ shows an endothermic DTA peak at 205°C accompanied by 10.0% weight loss in the TG curve, which can be correlated with elimination of two molecules of water. This relatively high temperature suggests that water is coordinated. In the second step, the strong endotherm at 300°C is most probably ascribable to the partial decomposition of the complex and release of the loosely bound pyridyl nucleus¹³⁾ as shown in Fig. 6, displaying 21.3% weight loss in the TG curve. Also, in the third step, the strong exotherm at 372°C and its connecting

Fig. 6. Decomposition Pathways of the $[\text{M}(\text{HP}_c\text{DC})(\text{OAc})(\text{H}_2\text{O})_2]$

shoulder at 390°C in the DTA curve (16.4% weight loss) seems to be correlated with the loss of the acetate portion.^{39,40)} Over the $405\text{--}690^\circ\text{C}$ range (fourth step), the DTA curve displays a series of exothermic effects at 505, 565 and 660°C (28.0% weight loss) attributed to complete decomposition of the remaining portion of the organic molecule, along with rupture of the chelate bond, leaving MnS as residue comprising 24.2% of the initial mass of the complex.

For $[\text{Co}(\text{HP}_c\text{DC})(\text{OAc})] \cdot 2\text{H}_2\text{O}$, the following phenomena occur: (i) an endothermic DTA peak at 135°C accompanied by 9.6% weight loss, which can be ascribed to the elimination of the two water molecules of crystallization; (ii) loss of the loosely bound pyridyl nucleus¹³⁾ accompanied by 21.5% weight loss and an endotherm at 345°C ; (iii) strong exotherm at 390°C and its connecting shoulder at 410°C correlates with release of the acetate portion; (iv) a series of exotherms in the $420\text{--}860^\circ\text{C}$ range leaves behind CoS comprising 25.0%.

$[\text{Cu}(\text{HP}_c\text{DC})_2(\text{H}_2\text{O})_2]$ is thermally stable up to 190°C , above which temperature the TG, DTG and DTA curves display the following phenomena: (i) an endotherm at 217°C corresponding to melting of the solid complex¹²⁾; (ii) a broad endothermic peak at 235°C attributed to elimination of the two coordinating water molecules; (iii) release of two pyridyl nuclei accompanied by an endotherm at 275°C ; (iv) a series of exothermic effects at 500, 615, 670 and 740°C ascribed to complete decomposition of the complex, leaving CuS as a final residue representing 18.1%.

Thermal analyses of the studied solid complexes support the different modes of coordination between KHP₄DC and the central metal ions. Also, DTA data can be used as a rapid and sensitive tool for the detection of acetate-containing complexes.

From the above discussion it is worth mentioning that the pyridine-ring azomethine group takes part in chelation, forming a stable five-membered ring including the metal atom. In contrast, in our previous study¹³ on potassium nicotinoyldithiocarbamate this group played no part in the complexation, probably due to the geometrical factors which prevent the coordination of (CN)_{py}.

References

- 1) Crim J. A., Petering H. G., *Cancer Res.*, **27**, 1278—1285 (1967).
- 2) Mandal N. K., Sinha R., Banerjee K. P., *J. Indian Chem. Soc.*, **63**, 221—222 (1986).
- 3) Petering H. G., Buskirk H. H., Crim J. A., *Cancer Res.*, **27**, 1115—1121 (1967).
- 4) Buu-Hoi N. P., Loc T. B., Xuong N. D., *Bull. Chim. Soc. (Fr)*, 694—697 (1955).
- 5) Campbell M. J. M., *Coord. Chem. Rev.*, **15**, 279—319 (1975).
- 6) Ali M. A., Livingstone S. E., *Coord. Chem. Rev.*, **13**, 101—132 (1974).
- 7) Williams D. R., *Chem. Rev.*, **72**, 203—213 (1972).
- 8) Boyle E., Freeman P. C., Gouldie A. C., Mangon F. R., Thomson M., *J. Pharm. Pharmacol.*, **28**, 865—868 (1976).
- 9) Foye W. O., Duvall R. N., *J. Am. Pharm. Assoc.*, **47**, 285—288 (1958).
- 10) Das M., Livingstone S. E., *Brit. J. Cancer*, **37**, 463—466 (1978).
- 11) Ahuja I. S., Singh R., Rai C. P., *Transition Met. Chem.*, **2**, 257—260 (1977).
- 12) Rakha T. H., *Transition Met. Chem.*, **23**, 101—103 (1998).
- 13) Rakha T. H., *Synth. React. Inorg. Met.-Org. Chem.*, **30**, 205—224 (2000).
- 14) Ali M. A., Edwards A. A., Tuah J., *Transition Met. Chem.*, **23**, 41—44 (1998).
- 15) Rakha T. H., *Transition Met. Chem.*, **24**, 659—665 (1999).
- 16) Aggarwal R. C., Rao T. R., *J. Inorg. Nucl. Chem.*, **40**, 1177—1178 (1978).
- 17) Vogel A. I., "A Textbook of Quantitative Inorganic Analysis," Longmans, London, 1978.
- 18) Mann S. G., Caunders B. C., "Practical Organic Chemistry," Longmans, London, 1960.
- 19) Geary W. J., *Coord. Chem. Rev.*, **7**, 81—122 (1971).
- 20) Rakha T. H., Nawar N., Abu El-Reash G. M., *Synth. React. Inorg. Met.-Org. Chem.*, **26**, 1705—1718 (1996).
- 21) Maurya R. C., Mishra D. D., Jaiswal S. K., Dubey J., *Synth. React. Inorg. Met.-Org. Chem.*, **25**, 521—535 (1995).
- 22) Sharma R. R., Singh B., Kapoor R. N., *Transition Met. Chem.*, **12**, 431—432 (1987).
- 23) Beecroft B., Campbell M. J., Grzeskowiak R., *J. Inorg. Nucl. Chem.*, **36**, 55—59 (1974).
- 24) Ferraro J. R., "Low Frequency Vibrations of Inorganic and Coordination Compounds," Plenum Press, New York, 1971.
- 25) Nakamoto K., "Infrared Spectra of Inorganic and Coordination Compounds," Wiley, New York, 1970.
- 26) Basuli F., Peng S. M., Bhattacharya S., *Inorg. Chem.*, **36**, 5645—5647 (1997).
- 27) Mostafa S. I., *Transition Met. Chem.*, **23**, 397—401 (1998).
- 28) Shallaby A. M., Soliman M. S., El-Shazly R. M., Mostafa M. M., *Synth. React. Inorg. Met.-Org. Chem.*, **18**, 807—821 (1988).
- 29) Khalifa M. E., Rakha T. H., Bekheit M. M., *Synth. React. Inorg. Met.-Org. Chem.*, **26**, 1149—1161 (1996).
- 30) McGlynn S. P., Smith J. K., Neely W. C., *J. Chem. Phys.*, **35**, 105—116 (1961).
- 31) Campbell M. J., Grzeskowiak R., *J. Chem. Soc.*, **1967**, 396—401.
- 32) El-Shazly M. F., El-Dissouky A., Salem T. M., Osman M. M., *Inorg. Chim. Acta*, **40**, 1—6 (1980).
- 33) El-Sonbati A. Z., El-Bindary A. A., *New Polym. Mater.*, **5**, 51—60 (1996).
- 34) Procter I. M., Hathaway B. J., Nicholls P., *J. Chem. Soc. A*, **1968**, 1678—1684.
- 35) Hathaway B. J., Billig D. E., *Coord. Chem. Rev.*, **5**, 143—207 (1970).
- 36) Lever A. B. P., "Inorganic Electronic Spectroscopy," 2nd ed., Elsevier, Amsterdam, 1984.
- 37) Sacconi L., *Coord. Chem. Rev.*, **1**, 192—204 (1966).
- 38) Pandey G. S., Nigam P. C., Agarwala U., *Indian J. Chem.*, **15A**, 537—541 (1977).
- 39) Rakha T. H., Ibrahim K. M., Khalifa M. I., *Thermochim. Acta*, **144**, 53—63 (1989).
- 40) Rakha T. H., Bekheit M. M., El-Agez M. M., *Synth. React. Inorg. Met.-Org. Chem.*, **29**, 449—472 (1999).

Synthesis, Conformation, and Chemical Properties of New Mini Parallel Double-Stranded Peptides Conjugated with –Phe–Phe– and –Phe–Phe–X– Sequences

Shigeki KOBAYASHI,^{*,a} Hiroki KOBAYASHI,^a Takatoshi YAMAGUCHI,^a Miharuru NISHIDA,^a Kentaro YAMAGUCHI,^b Masaaki KURIHARA,^c Naoki MIYATA,^c and Akira TANAKA^{*,a}

Department of Analytical Chemistry of Medicines, Showa Pharmaceutical University,^a 3–3165 Higashi-Tamagawagakuen, Machida, Tokyo 194–8543, Japan, Chemical Analysis Center, Chiba University,^b 1–33 Yayoicho, Inage-ku, Chiba 263–8522, Japan, and Division of Organic Chemistry, National Institute of Health Sciences,^c 1–18–1 Kamiyoga, Setagaya-ku, Tokyo 158–8501, Japan. Received December 6, 1999; accepted March 4, 2000

To investigate the chemical conformations and functions of the –Phe–Phe–Val– or –Phe–Phe– sequences contained in the Alzheimer's disease related β -amyloid peptide, a series of mini parallel double-stranded peptides conjugated with two peptide residues to one spacer were designed and prepared. The structure of the compounds was elucidated by circular dichroism (CD) spectrum and NMR two dimensional (2D) nuclear Overhauser enhancement and exchange spectroscopy (NOESY) measurements. The structure of 1,2-ethano-bis(L-Phe–L-Phe–L-Leu), 1,12-dodecano-bis(L-Phe–L-Phe–L-Leu), 1,12-dodecano-bis(L-Phe–L-Phe–L-Val), and 1,12-dodecano (D-Phe–D-Phe–D-Leu) conjugated with L-Leu and L-Val residues show a β -turn-like nucleation. The dihedral angles ($\theta=+75^\circ$, $+180^\circ$, $\omega=+90^\circ$, $\phi=-87^\circ$, $\psi=+180^\circ$) obtained from experimental coupling constant (J) data, *etc.* support that 1,12-dodecano-bis(L-Phe–L-Phe) adopts β -turn mimic nucleation. The 1,12-dodecano-bis(L-Leu–L-Leu–L-Phe), 1,12-dodecano-bis(L-Ile–L-Phe–L-Leu), and 1,12-dodecano-bis(L-Phe–L-Val–L-Leu), *etc.* adopt most probably a random structure by CD studies.

It was found by titration spectrum that an inclusion complex of 1:1 ratio (association constant; $K_a=1.0\times 10^4\text{ M}^{-1}$) is formed between 1,12-dodecano-bis(L-Phe–L-Phe–L-Leu) and azobenzene (guest, $[L_0]=1.758\times 10^{-5}\text{ M}^{-1}$). Moreover, the stability of the complexes was increased in order of 1,12-dodecano-bis(L-Phe–L-Phe–L-Leu)·azobenzene>1,12-dodecano-bis(L-Phe–L-Phe–L-Val)·azobenzene>1,12-dodecano-bis(L-Phe–L-Val–L-Leu)·azobenzene. The data show that X–Phe–L-Phe–L-spacer(S)–L-Phe–L-Phe–X (X=amino acids; S=1,2-ethano- and 1,12-dodecano-) plays an important role as a binding site of the artificial receptor. The hydrophobic interaction of the four Phe's in the two strands is a very interesting issue in the physiological action of proteins as well as the conformation of the backbone of X–L-Phe–L-Phe–spacer(S)–L-Phe–L-Phe–X.

Key words double-stranded peptide; β -turn mimetics; β -amyloid peptide; binding affinity; artificial receptor; downfield shift

Much attention has been paid by chemists to the mechanisms of β -sheet folding and the functions of β -sheet structures found in peptides and proteins. However, their functions are poorly understood yet in comparison with α -helical structures.¹⁾ The heptad repeat unit –Pro–X–X– segment found in gene regulatory proteins,²⁾ the –Phe–Phe–Val– sequence contained in Alzheimer's disease related β -amyloid peptide,³⁾ the two β -strands of the DNA recognition motif of the *met* repressor protein dimer,⁴⁾ and the repeat unit –Pro–Val–Orn–Leu–D-Phe– found in antibacterial gramicidins S,⁵⁾ *etc.* are given as examples of β -turn and antiparallel β -sheet structures in living body. The type II' β -turn conformation adopted by the –Pro–X–X– segment can stabilize a β -turn conformation, and the –Pro–Val–Orn–Leu–D-Phe– sequence of gramicidins S adopts a stable antiparallel β -sheet structure. To clarify the chemical stability, functions, and stereochemistry of β -turn (or β -hairpin) and antiparallel β -sheet structures, recently, the design and synthesis of peptides have been reported by a number of research groups.⁶⁾ The model compounds which mimic β -sheet and β -turn structures have been shown to adopt β -hairpin structures in aqueous solution, and that hydrogen bonding can stabilize β -turn structures.

This paper deals with the stereochemistry and chemical properties of the –Phe–Phe–Val– sequence contained in Alzheimer's disease related β -amyloid peptide, since the conformation, stability, and biological role of its hydrophobic se-

quence are poorly understood. First, we investigated the conformation and stability of parallel double-stranded peptides which consist of two parallel strands of –Phe–Phe–Val– conjugated by a mini loop. The conformation change was studied in the cases of the replacement of –Phe–Phe–Val– in –Phe–Phe–Leu– and of –Phe–Phe–Val– in –Phe–Phe–, *etc.* The design and synthesis of double-stranded peptides, *e.g.* 1,2-ethano-bis(AA)s and 1,12-dodecano-bis(AA)s (AA=amino acids) 1–3, were studied as a model of simple mini parallel β -turn-like peptide mimetics, as shown in Chart 1. Compounds 1–3 contain a parallel double-stranded peptide sequence conjugated with a spacer, such as an ethano- or dodecano-group in geometrical symmetry, and changes in the tertiary conformation can be expected from species of the amino acid residues or spacers. The conformation of parallel double-stranded peptides was analyzed by using both experimental and computational approaches. Studies by ¹H-NMR titrations, nuclear Overhauser effects (NOE), and circular dichroism (CD) spectrum measurements revealed the structure of the parallel 1,2-ethano-bis(L-Phe–L-Phe) and 1,12-dodecano-bis(L-Phe–L-Phe), *etc.* which mediate a β -turn sheet nucleation.

The CD spectra of the 1,2-ethano-bis(L-Phe–L-Phe–L-Leu), 1,12-dodecano-bis(L-Phe–L-Phe–L-Leu), and 1,12-dodecano-bis(L-Phe–L-Phe–L-Val) conjugated L-Leu and L-Val residues show β -sheet nucleation. On the other hand, it is clear that the conformation of 1,12-dodecano-bis(L-Leu–L-Leu–L-Phe)

* To whom correspondence should be addressed. e-mail: kobayasi@ac.shoyaku.ac.jp

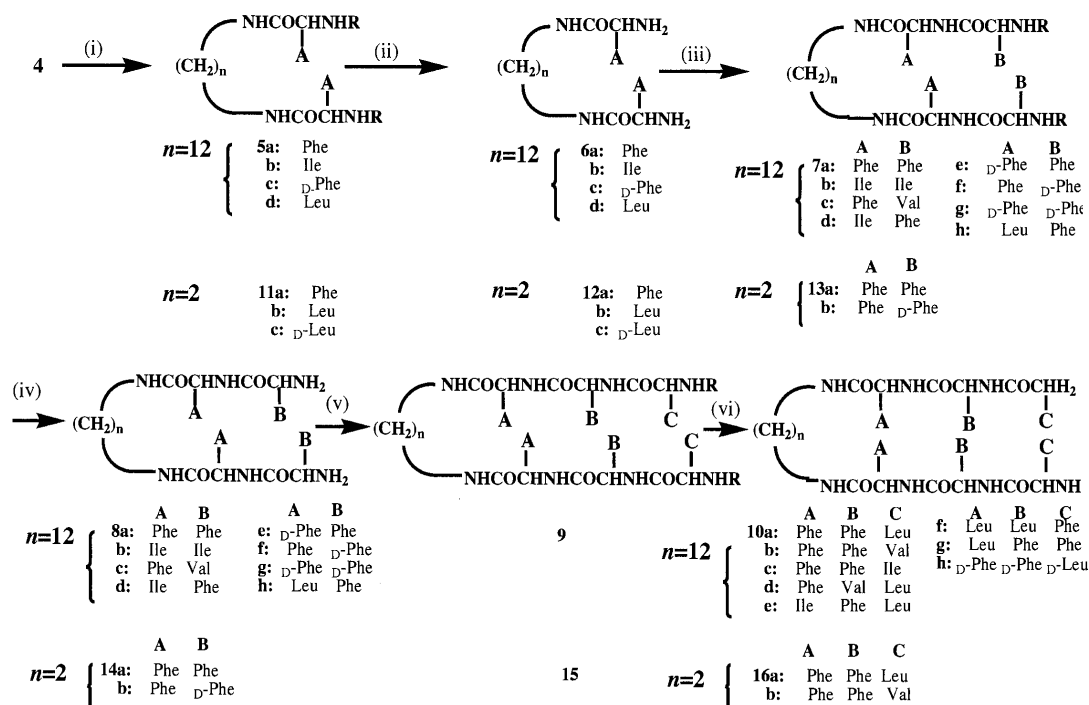


Chart 1. Pathway for the Synthesis of Mini Parallel Double-Stranded Peptides Corresponding to Peptides 1–3

(i) CDI, ZAOH, dry CHCl_3 , (ii) 5% Pd/C, H_2 , DMF/CH₃OH (or TFA at 4 °C). (iii) CDI, ZBOH, dry CHCl_3 (or DEPC, ZBOH, TEA, DMF). (iv) 5% Pd/C, H_2 , DMF/CH₃OH (or TFA). (v) CDI, ZCOH, dry CHCl_3 (or DEPC, ZCOH, TEA, DMF). (vi) 5% Pd/C, H_2 , DMF/CH₃OH (or TFA at 4 °C). Where A–C represent the corresponding amino acid residues.

and 1,12-dodecano-bis(L-Ile–L-Phe–L-Leu), *etc.* probably adopts a random structure by CD spectrum and two dimensional (2D) nuclear Overhauser enhancement and exchange spectroscopy (NOESY) experiments. We show four dihedral angles (ω , ϕ , ψ , θ) obtained from the data of NMR NOEs, $^3J_{\text{C}\alpha\text{H},\text{NH}}$ coupling constants and molecular mechanics (MM2)⁷⁾ calculation. The average dihedral angles at $\omega = -70^\circ$, $\phi = -89^\circ$, $\psi = +115^\circ$, and $\theta = +75^\circ$ (and $+180^\circ$) support that the backbone of 1,12-dodecano-bis(L-Phe–L-Phe) is a nucleation mediated β -turn sheet. The $^{-1}\text{Phe}-^2\text{Phe}$ -residues on parallel double-stranded act as a hydrophobic connector to stabilize a turn conformation mediated β -sheet nucleation. The data for the binding affinity (K_a) between ligand and double-stranded peptides also indicate that the X–Phe–L-Phe–L-spacer(S)–L-Phe–L-Phe–X (X = Val, Ile, Leu; S = ethano-, dodecano-) adopt the β -turn sheet structure and that the compounds are useful artificial receptor models. It seems that the synthesis of X–Phe–L-Phe–L-spacer(S)–L-Phe–L-Phe–X conjugated spacer to the –Phe–Phe–Val– sequence contained in Alzheimer's disease related β -amyloid peptide can contribute to the development of useful agents for elucidating the structures and chemical functions of –Phe–Phe–Val– and –Phe–Phe– analogues, *etc.*

Results and Discussion

Synthesis of Double-Stranded Peptides and Assignment of Chemical Shifts Three different types of C_2 symmetrical double-stranded peptides 1–3 were synthesized. The syntheses of 1,2-ethano-bis(peptide) and 1,12-dodecano-bis(peptide) 1–3 conjugated with a spacer such as ethylenediamine or 1,12-dodecanodiamine(4) at the C-terminal of the amino acid residues were carried out by stepwise condensation followed by coupling of carbobenzoxy protected-L-

amino acid (CbzPheOH, Cbz = carbobenzoxy) with the spacer, as shown in Chart 1. The couplings were carried out by the C-activating method using *N,N'*-carbonyldiimidazole (CDI)⁸⁾ in dry chloroform (or the diethyl phosphorocyanidate (DEPC) method⁹⁾ in dry dimethylformamide (DMF)). By coupling Cbz-L-LeuOH and 8a using CDI, we obtained the 1,12-dodecano-bis(L-Phe–L-Phe–L-LeuCbz) 9a. The target 10a (1,12-dodecano-bis(L-Phe–L-Phe–L-Leu)) was obtained by controlled hydrogenation over Pd/C mild catalytic deprotection of 9a in DMF/MeOH in an overall yield of 58.5%. To form a different configuration in these compounds, the D-Phe residue was introduced, and 6c and 8e were obtained as the enantiomer and diastereomer for 6a and 8a, respectively. The *tert*-butoxycarbonyl group (=Boc) was used for N protection of D-Phe and removed with trifluoroacetic acid (TFA) to produce 1,2-ethano-bis(L-Phe–D-Phe), 1,12-dodecano-bis(D-Phe–D-Phe), and 1,2-ethano-bis(L-Phe–L-Phe–L-Leu), *etc.*

All free bases were purified in an overall yield of 40–60% after recrystallization and by silica gel column chromatography or by reverse-phase high performance liquid chromatography (RP-HPLC), and characterized by ^1H - and ^{13}C -NMR, IR spectrometry, FAB mass spectrometry, and/or elemental analysis. The purity of these double-stranded peptides was checked by thin layer chromatography (TLC) or analytical RP-HPLC. The samples were dissolved in MeOH and loaded on a 5×150 mm Octadecylsilane (ODS) C18 column, and were eluted with 90% acetonitrile containing 0.05% TFA at room temperature. In order to demonstrate the effect of the secondary structure formation of parallel double-stranded peptides, we synthesized single-stranded peptides 17a, 18a, and 19a, as shown in Chart 2. The synthesis was performed by stepwise reactions of, for example, lauryl-

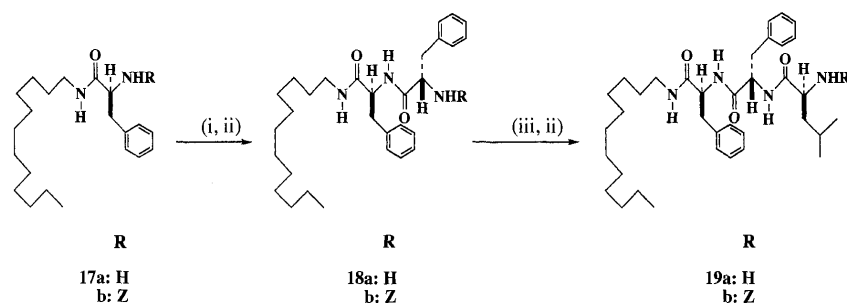


Chart 2. Pathway of the Synthesis of Single-Stranded Peptides Conjugated with a Spacer

(i) CDI, ZPheOH, dry CHCl_3 , (ii) 5% Pd/C, H_2 , CH_3OH , (iii) CDI, ZLeuOH, dry CHCl_3 .

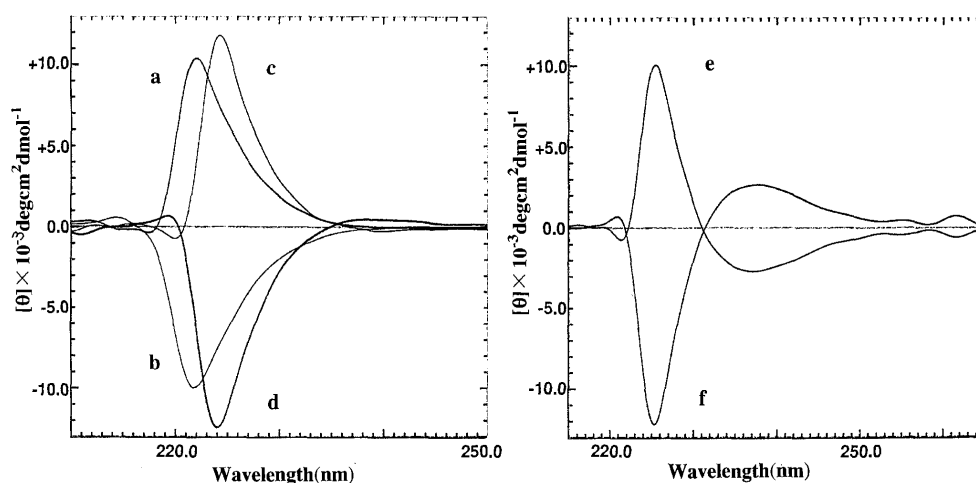


Fig. 1. CD Spectra for Mirror Images of Double-Stranded Peptides, **6a**, **6c**, **8a**, **8g**, **10a** and **10h**

Double-stranded peptides concentration, **6a** (1.05×10^{-3} M) (a), **6c** (1.21×10^{-3} M) (b), **8a** (6.91×10^{-4} M) (c), **8g** (7.28×10^{-4} M) (d), **10a** (5.52×10^{-4} M) (e) and **10h** (5.23×10^{-4} M) (f) in 85 % methanol at 22 °C, x-axis, nm; y-axis, molar ellipticity $[\theta]$.

amine with the corresponding amino acid residue employing CDI C-activation to produce a single-stranded peptide **19a** in a total yield of 40%.

The ^{13}C signals of 1,12-dodecano-bis(peptide) could be assigned by ^1H - ^1H 2D correlated spectroscopy (COSY), ^{13}C - ^1H COSY, and distortionless enhancement by polarization transfer (DEPT) technique, and by comparison with the spectra of the constituent amino acids. The structural assignments of 1,2-ethano-bis(L-Phe-L-Phe-L-Leu) **16a** (a) and 1,12-dodecano-bis(L-Leu-L-Leu-L-Phe) **10f** (b) were made on the basis of chemical shifts and C-H COSY spectra measured by 500 MHz NMR in a 5 mm solution. The corresponding chemical shifts of the Phe² β - and Phe³ β -protons (βH s) of **10f** and **16a** appeared at 2.72 and 3.08 ppm, at 2.78 and 2.98 ppm, respectively. The individual shifting of Phe² βH and Phe³ βH suggests that the structure of the aromatic side chain has a rigid conformation in the intra-molecule. The ^{13}C signal of the α carbons of the key compounds, **6a** and **8a**, appeared at 56.48 ppm, and at 54.33 and 56.27 ppm, respectively. Further, the ^{13}C signals of the α carbons of **10a** were observed at 53.43, 54.13, and 54.25 ppm at higher field than the signal of **6a** and **8a**. The two C $^{\alpha}\text{H}$ signals of 1,12-dodecano-bis(D-Phe-L-Phe) **8e** were observed at 53.85 and 56.20 ppm, while the signals of the diastereomer **8f** appeared at 54.37 and 54.58 ppm in $\text{CDCl}_3/\text{DMSO}-d_6$ (0.5/0.2 v/v%). The NMR data clearly show that the double-stranded peptides have different ensemble average conformations.

CD Spectrum Studies The secondary structure of 1,2-

ethano-bis(L-Phe-L-Phe-L-X) (X=Leu, Val, and without), 1,12-dodecano-bis(L-Phe-L-Phe-L-X) (X=Leu, Ile, Val, and without), and 1,12-dodecano-bis(L-Phe-L-Val-L-Leu), etc. were examined by CD spectrometry under the same conditions in 85% methanol solution. The spectra showed the profile of the two CD spectrum types, class I and II. At CD profile of class I, the negative first Cotton effect in **10a**–**c** was observed at 237 nm, and the positive second Cotton effect which showed a large value of molar ellipticity ($[\theta] = 1 \times 10^{-4} \text{ deg cm}^2 \text{ dmol}^{-1}$), was measured at 205 nm, indicating a β -sheet or type II turn structure.¹⁰ The CD spectra observed for the two enantiomers, **6a** and **6c**, **8a** and **8c** show the mirror image, and they are stereochemically pure. 1,12-Dodecano-bis(L-Phe-L-Phe-L-Leu) **10a** and **10h** are enantiomers. In fact, these CD spectra show the mirror image, as shown in Fig. 1.

The CD profiles of the 1,2-ethano-bis(L-Phe-L-Phe-L-Leu) **16a** and 1,12-dodecano-bis(L-Phe-L-Phe-L-Leu) **10a** are very similar to a β -sheet or type II turn-like conformation of literature data.¹¹ Moreover, the CD profiles of **10b**, **c**, **10h**, and **16a** (class I) were also consistent with a β -sheet mimic conformation. However, the CD profile of 1,12-dodecano-bis(L-Phe-L-Val-L-Leu) **10d** when a -L-Phe is replaced with a -L-Val is different from that of **10a**, and adopts a random conformation. In addition, the replacement of the tripeptide residue -L-Phe-L-Phe-L-Leu with -L-Leu-L-Leu-L-Phe affords **10f** and exhibits a random conformation, as shown in Fig. 2. This finding suggests that the aromatic interaction be-

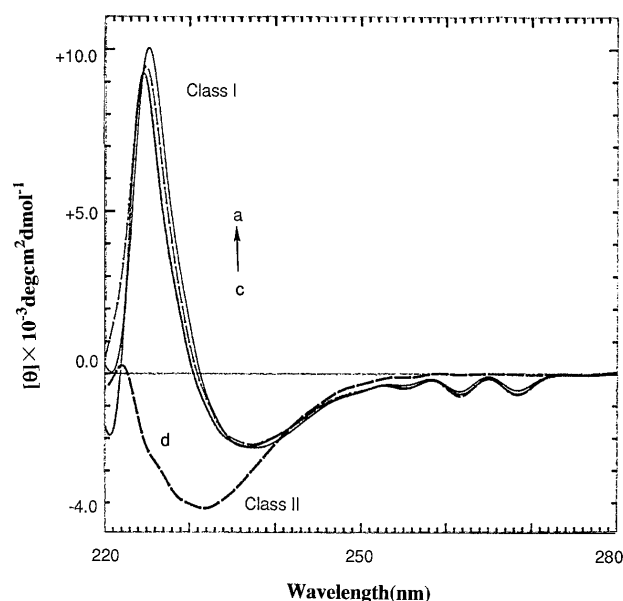


Fig. 2. Profile of CD Spectra for 1,12-Dodecano-bis(peptide)s, **10a–c** (a–c) and **10f** (d)

1,12-Dodecano-bis(peptide) concentration, **10a** (3.94×10^{-4} M), **10b** (5.86×10^{-4} M), **10c** (3.62×10^{-4} M), and **10f** (8.06×10^{-4} M) in 85% methanol solution at 22 °C, x-axis, nm; y-axis, molar ellipticity $[\theta]$.

tween the C-terminal Phe on both strands is a primary factor to form β -sheet-like nucleation. The relationship between conformation and sequence of amino acid residues of double-stranded peptides **2** and **3** is summarized in Table 1. Accordingly, the X-L-Phe-L-Phe-spacer(Y)-L-Phe-L-Phe-X (X=amino acids and Y=1,2-ethano- and 1,12-dodecano-, etc) is an important domain of mimetic mediator for β -sheet nucleation.

The depth at 237 nm of CD spectra of double-stranded peptides **6a**, **8a**, and **10a–c** increases in order of -L-Phe<-L-Phe-L-Phe<-L-Phe-L-Phe-L-Ile<-L-Phe-L-Phe-L-Val<-L-Phe-L-Phe-L-Leu (Fig. 2). This order of the depth is equal to the order of mediation of β -sheet mimetic nucleation. Especially, sequences such as -L-Phe-X and -L-Phe-L-Phe-X favor a β -sheet mimic nucleation in double-stranded peptides. To further investigate the β -sheet mimic nucleation, the CD spectra of 1,2-ethano-bis(L-Phe-L-Phe-L-Leu) were measured, as shown in Fig. 3. As the CD profile of 1,2-ethano-bis(L-Phe-L-Phe-L-Leu) is similar to the profile of 1,12-dodecano-bis(L-Phe-L-Phe-L-Leu), the structure also adopts β -sheet mimic conformation. The depth at 238 nm of CD spectra of 1,2-ethano-bis(peptide)s **12a**, **14a**, and **16a** also increases in order of L-Phe-L-Phe-L-Leu<L-Phe<-L-Phe-L-Phe. The -Phe-L-Phe-L-CONHCH₂CH₂NHCO-L-

Table 1. Relationship between Types of CD Spectrum Profiles and Amino Acid Sequences of Synthesized 1,12-Dodecano-bis (A–B–C)

Class I ^{a)} compound	Amino acid residue			Class II ^{a)} compound	Amino acid residue		
	A	B	C		A	B	C
8a	Phe	Phe	—	8b	Ile	Ile	—
8c	Phe	Val	—	8d	Ile	Phe	—
10a	Phe	Phe	Leu	10d	Phe	Val	Leu
10b	Phe	Phe	Val	10e	Ile	Phe	Leu
10c	Phe	Phe	Ile	10f	Leu	Leu	Phe
19a^{b)}	Phe	Phe	Leu	10g	Leu	Phe	Phe

a) Type of CD spectrum profile. b) Single-stranded tripeptide.

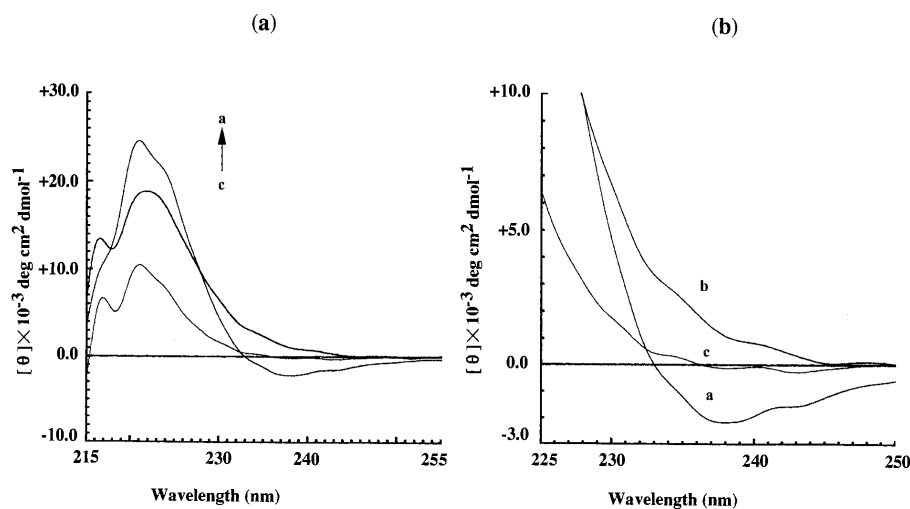
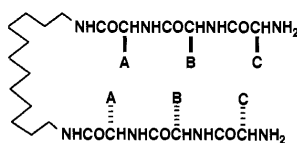


Fig. 3. Profile of CD Spectra for 1,2-Ethano-bis(peptide)s, **12a**, **14a**, and **16a**

1,2-Ethano-bis(peptide) concentration, **12a** (3.94×10^{-4} M) (c), **14a** (5.86×10^{-4} M), and **16a** (8.06×10^{-4} M) in 85% methanol solution at 22 °C, x-axis, nm; y-axis, molar ellipticity $[\theta]$.

Phe-L-Phe- domain also adopts a β -sheet or type II β -turn mimic nucleation. From these results, the sequences of -Phe-Phe-X (X=Leu, Ile, Val, *etc.*) are a useful probe for the design of β -sheet mimetic nucleation of double-stranded peptides. Thus we clarified the relationship between the conformation and amino acid residues in a double-stranded peptide. The X-L-Phe-L-Phe-spacer(Y)-L-Phe-L-Phe-X (X=Val, Ile, Leu, *etc.*; Y=1,2-ethano-, 1,12-dodecano-) forms a stable conformation for the hydrophobic interaction

and intramolecular hydrogen bonding in both strands.

¹H-NMR of Double-Stranded Peptides In CDCl₃/DMSO-*d*₆ (0.7/0.0 v/v%) (295 K) in the ¹H-NMR, the chemical shifts of amide -NH^a- and amide -NH^b- of 1,2-ethano-bis(L-Phe-L-Phe) **14a** appear at 6.23 and 7.77 ppm. From a ratio-dependent change of solution in the changed ratio range from CDCl₃/DMSO-*d*₆ (0.7/0.0 v/v%) to CDCl₃/DMSO-*d*₆ (0.5/0.2 v/v%), these resonances shifted to 7.68 and 7.89 ppm, respectively, as shown in Fig. 4. The difference (δ ppm) of chemical shifts of the amide protons and α protons (α H) is summarized in Table 2. The large downfield shifting (δ = -1.45 ppm) of the amide proton, -NH^a-, in **14a** indicates that the amide proton favors a hydrogen-bond structure in DMSO-*d*₆, but the amide proton favors no hydrogen-bond structure in CDCl₃. In contrast, the chemical shift of the amide proton, -NH^b-, indicates that a hydrogen-bond is formed in both CDCl₃ and DMSO-*d*₆. The downfield shifting of these amide protons of **8a** and **16a** also indicates that the compounds favor the conformation of the β -sheet mimetics.¹²⁾ An interesting observation in Table 2 is that the downfield shift (-0.20 ppm) for amide proton -NH^bCO- of the diastereomer **8e** decreases by the addition of DMSO-*d*₆ in CDCl₃ (0.5/0.2 v/v%). This indicates that the amide proton -NH^bCO- of **8e** strongly forms hydrogen bonding in CDCl₃.

The three amide protons, -NH^{a,b, and c}- in **16a** were observed at δ 7.67, 7.94, and 8.03 in CDCl₃/DMSO-*d*₆ solution (0.5/0.5 v/v%), respectively, and the large downfield shift of

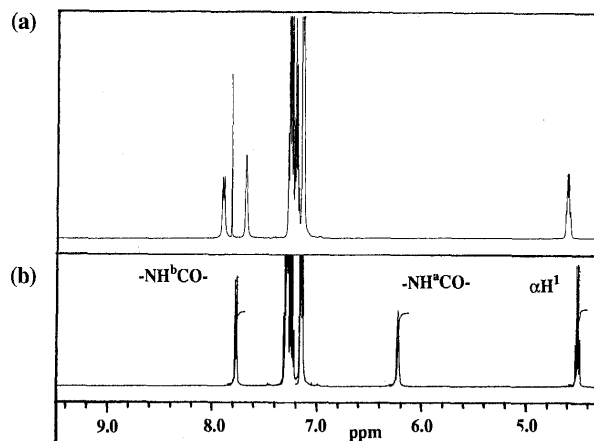


Fig. 4. Downfield Shifts of Amide, -NHCO-, Protons Chemical Shifts for 1,2-Ethano-bis(L-Phe-L-Phe) **14a** Obtained from 500 MHz Spectra in DMSO-*d*₆/CDCl₃ (Volume Ratio=0.2/0.5) (a) and in CDCl₃ (b)

Table 2. Solvent Shifts of Amide Protons, α -Protons, and β -Protons for Double-Stranded Peptides **8a**, **8e**, **8f**, **14a**, and **14b** in Solution

	Solvent	-NH ^a CO- δ (ppm)	-NH ^b CO- δ (ppm)	Phe ¹ C α H δ (ppm)	Phe ² C α H δ (ppm)	Phe ² C β H δ (ppm)
8a	CDCl ₃	6.21	7.88	4.62	3.55	2.56
	CDCl ₃ /DMSO- <i>d</i> ₆ ^{a)}	7.61	8.90	4.50	4.09	2.94
	Δ ppm	-1.40	-1.02	-0.12	-0.54	-0.38
8e	CDCl ₃	5.88	7.75	4.54	3.54	2.66
	CDCl ₃ /DMSO- <i>d</i> ₆ ^{a)}	7.45	7.95	4.61	3.49	2.58
	Δ ppm	-1.57	-0.20	-0.07	+0.05	+0.06
8f	CDCl ₃ ^{b)}	7.20	8.16	4.57	3.96	2.78
	CDCl ₃ /DMSO- <i>d</i> ₆ ^{a)}	7.78	8.73	4.59	4.05	2.72
	Δ ppm	-0.58	-0.57	-0.02	-0.09	+0.06
14a	CDCl ₃	6.23	7.77	4.50	3.61	2.44
	CDCl ₃ /DMSO- <i>d</i> ₆ ^{a)}	7.68	7.89	4.58	3.52	2.42
	Δ ppm	-1.45	-0.12	-0.08	+0.09	+0.02
14b	CDCl ₃	6.22	7.72	4.46	3.52	2.66
	CDCl ₃ /DMSO- <i>d</i> ₆ ^{a)}	7.80	8.79	4.53	3.94	2.67
	Δ ppm	-1.58	-1.07	-0.07	-0.42	-0.01

a) Conditions: CDCl₃/DMSO-*d*₆=0.5/0.2. b) In the presence of 2.0% DMSO-*d*₆.

Table 3. Solvent Shifts of Amide Protons and α -Protons for Double-Stranded Peptides **10a**, **10g**, and **16a** in Solution

		-NH ^a CO- δ (ppm)	-NH ^b CO- δ (ppm)	-NH ^c CO- δ (ppm)	AA ¹ C α H δ (ppm)	AA ² C α H δ (ppm)	AA ³ C α H δ (ppm)
10a	CDCl ₃	6.08	6.59	7.82	4.58	4.58	4.58
	CDCl ₃ /DMSO- <i>d</i> ₆ ^{a)}	7.23	7.71	7.89	4.57	4.57	4.57
	Δ ppm	-1.15	-1.12	-0.07	+0.01	+0.01	+0.01
10g	CDCl ₃ ^{b)}	7.15	7.76	8.68	4.36	4.66	4.07
	CDCl ₃ /DMSO- <i>d</i> ₆ ^{a)}	7.38	8.07	8.86	4.44	4.71	4.17
	Δ ppm	-0.23	-0.31	-0.18	-0.08	-0.05	-0.10
16a	CDCl ₃ /DMSO- <i>d</i> ₆ ^{c)}	7.67	7.94	8.03	4.47	4.58	3.17
	DMSO- <i>d</i> ₆	7.93	8.06	8.25	4.43	4.54	3.18
	Δ ppm	-0.26	-0.12	-0.22	+0.04	+0.04	-0.01

a) Conditions: CDCl₃/DMSO-*d*₆=0.5/0.2. b) In the presence of DMSO-*d*₆ (3.8 %). c) Conditions: CDCl₃/DMSO-*d*₆=0.5/0.5.

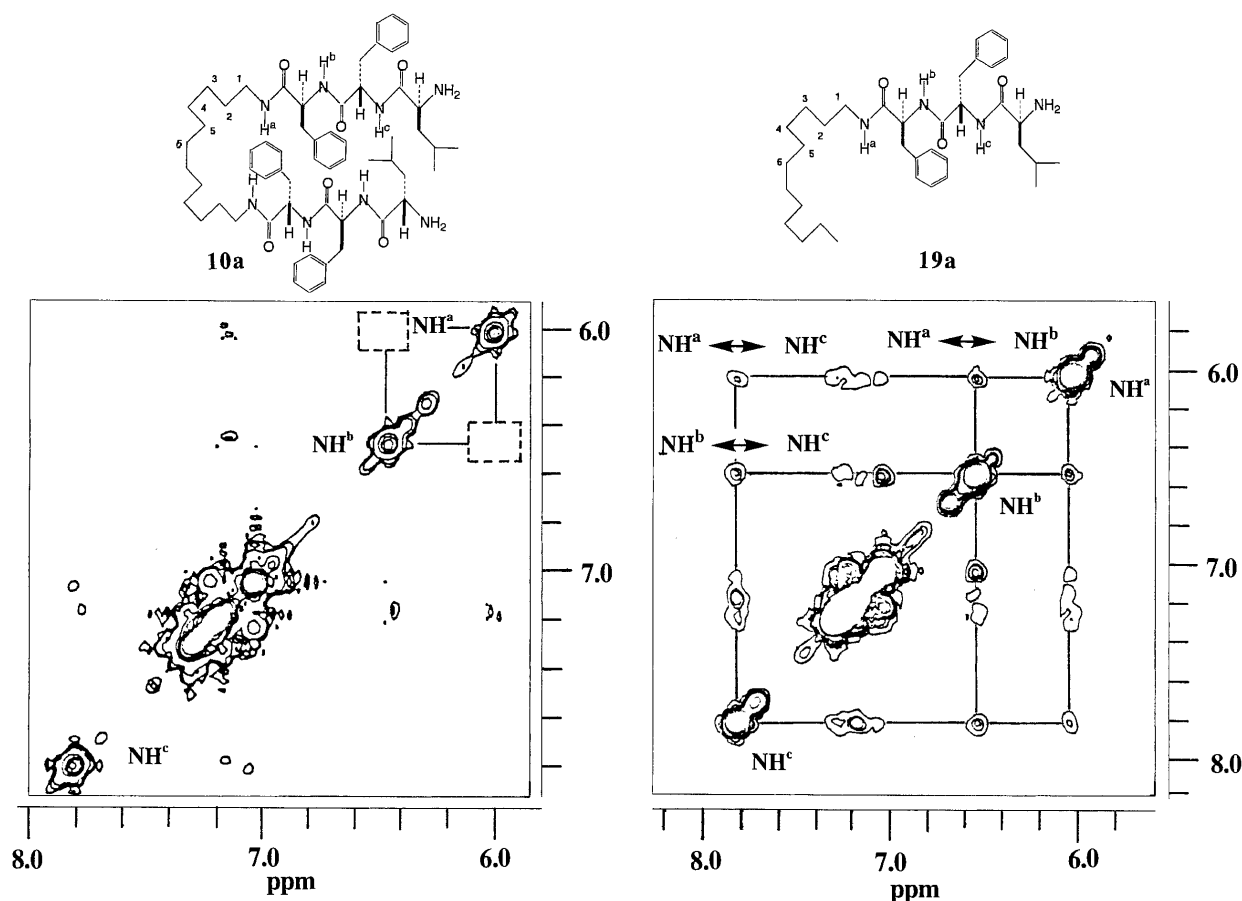


Fig. 5. NOE Cross Peaks in Amide NH Region of 500 MHz NOESY Spectra of Double-Stranded Peptide **10a** (Left) in CDCl_3 and Single-Stranded Peptide **19a** (Right) in CDCl_3

Empty boxes show absent $\text{NH}^a\text{--NH}^b$ NOE cross peaks. Conditions: 22 °C, 6.8 mm, and 500 msec mixing time.

amide proton, $\text{--NH}^a\text{CO--}$, as summarized in Table 3, indicates the formation of a hydrogen bond between the amide protons of both strands. Such downfield shift of the amide proton, $\text{--NH}^a\text{CO--}$, also was observed in 1,12-dodecano-bis(L-Phe-L-Phe-L-Leu) **10a** and 1,12-dodecano-bis(L-Phe-L-Phe-L-Val) **10b**, and these observations support that **10a** and **10b** are an important probe for formation of a double-stranded β -turn structure.

The assignments of the NOE cross coupling between the backbone --NHCO-- and C^αH of **8a**, **10a**, **10f**, **14a**, **16a**, **18a**, and **19a**, etc. were achieved by using 500 MHz NOESY (and/or rotating frame nuclear Overhauser and exchange spectroscopy (ROESY)) technique at a mixing time of 500 msec in CDCl_3 or $\text{CDCl}_3/\text{DMSO-}d_6$ (0.5/0.2 or 0.5/0.5 v/v%) solutions. The 1,12-dodecano-bis(L-Phe-L-Phe-L-LeuH) **10a** adopts the β -sheet mimic nucleation in solution, because no NOE cross peaks were observed between the three amides $\text{--NH}^{a,b,c}\text{CO--}$ and C^αH s, as shown in Fig. 5 (left). The coupling constants of $^3J_{\text{NH}^i, \text{C}^\alpha\text{H}^i} = 8.4$ Hz of Phe¹ (and Phe^{1'}) and $^3J_{\text{NH}^{i+1}, \text{C}^\alpha\text{H}^{i+1}} = 7.4$ Hz of Phe² (and Phe^{2'}) also support that the conformation of **10a** adopts the nucleation mediated β -sheet mimetics in CDCl_3 . In contrast, in the NOE cross peaks of 1,12-dodecano-bis(L-Leu-L-Leu-L-Phe) **10f**, the lack of observed NOE cross peaks between the three amide protons ($\text{--NH}^{a,b,c}\text{CO--}$) and the three $\text{C}^\alpha\text{H}^{1,2,\text{and } 3}$ at $\text{C}^{\alpha 1, 2, \text{and } 3}$ (α carbons^{1, 2, and 3}) supports that **10f** is a random conformation. Moreover, the large $^3J_{\text{NH}^c, \text{C}^\alpha\text{H}^2} = 9.3$ Hz and $^3J_{\text{NH}^b, \text{C}^\alpha\text{H}^1} = 8.4$ Hz coupling constants are also acceptable val-

ues for a random structure.¹³) This observation is consistent with the result from the CD studies.

On the other hand, the $d_{\alpha\text{N}}$ NOE cross peaks between $\alpha\text{H}^1 \leftrightarrow \text{--NH}^a\text{CO--}$, $\alpha\text{H}^1 \leftrightarrow \text{--NH}^b\text{CO--}$, and $\alpha\text{H}^2 \leftrightarrow \text{--NH}^b\text{CO--}$ in **19a** were observed and the d_{NN} NOE strong cross peaks of $\text{--NH}^a\text{CO--} \leftrightarrow \text{--NH}^b\text{CO--}$ also were observed as shown in Fig. 5 (right). This data suggests that the structure of **19a** is α -helix or 3_{10} helix¹⁴) mimic nucleation. As the double-stranded peptide **10a** and **19a** have the same sequence residue, $\text{--L-Phe-L-Phe-L-Leu}$ (N terminus), the pattern of NOE cross peaks should be similar; however, the pattern of NOE cross peaks is dissimilar (left in Fig. 5). The NOE data clearly support that the double-stranded peptide **10a** has a very different time average conformation from the single-stranded peptide **19a**. The strong d_{NN} connectivities show that the peptide chains of **19a** mediate α -helical mimic nucleation. Therefore, the reason why **10a** is different from the conformation in spite of the same sequence is derived from the parallel double-strand effect by the dodecano spacer. This behavior of NOE cross peaks of **10a** is most likely a result of the interaction of the one strand with the other strand in the double-stranded peptides. As expected, the structures of double-stranded peptides are influenced by an intramolecular interaction between the two strands.

The NOE cross peaks are present in between Phe¹ aH and *o*-protons of Phe² side chain on 1,12-dodecano-bis(L-Phe-D-Phe) **8f**. The observation of NOE cross peaks between dodecano-spacer protons and aromatic protons of Phe in **8a** and

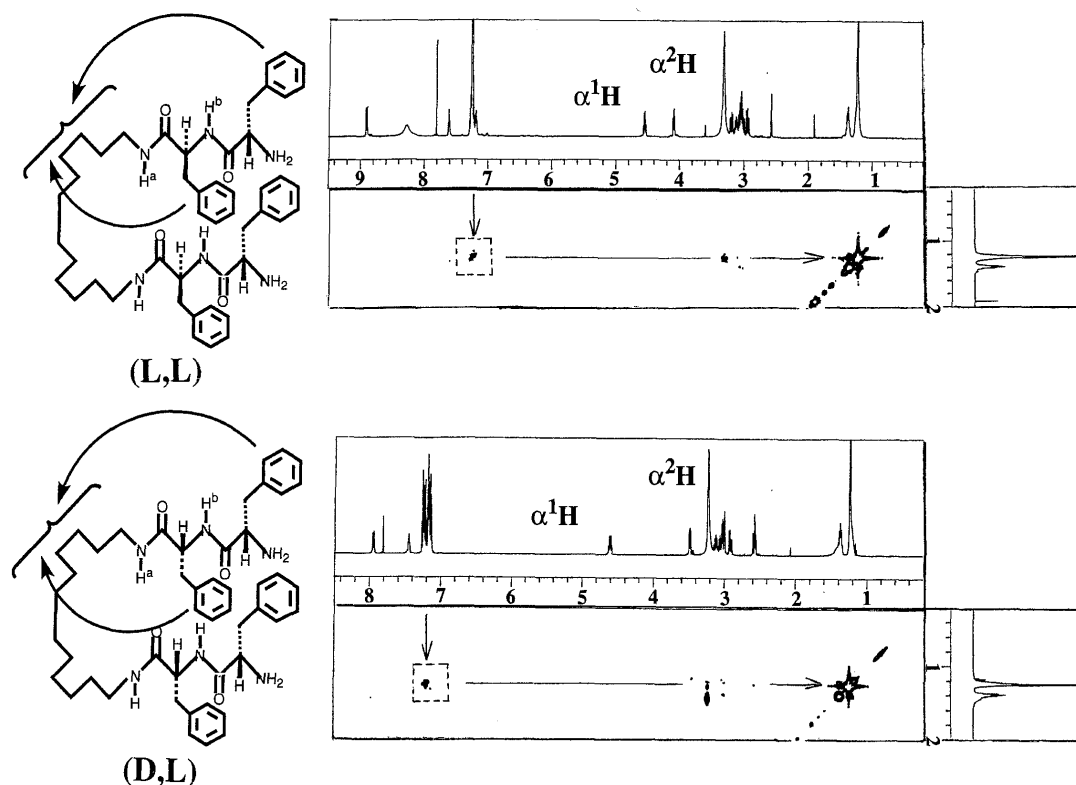


Fig. 6. NOE Cross Peaks in Aromatic Protons–Spacer Protons Region of 500 MHz NOESY Spectra of Double-Stranded Peptides **8a** (a) and **8e** (b). Boxes show aromatic protons–spacer protons NOE cross peaks. Conditions: 22 °C, 10.0 mm, and 500 msec mixing time.

8e confirms the folded structure, as shown in Fig. 6, because the cross peaks suggest that the conformation adopts a more β -turn-like-structure than the linear structure. As an interesting long-range NOE cross peak is also observed between Phe¹ αH and amido proton $-NH^cCO-$ in 1,2-ethano-bis(L-Phe–L-Phe–L-Leu) **16a**, it suggests that **16a** is a folded conformation. Similar NOE cross peaks in the NOESY spectra also could be obtained in **10a**, **10b**, **10g**, **16a**, and **16b**, *etc.* so that the distance between the protons of spacer and the aromatic protons of Phe side chain (and protons of Me groups in Leu) is within 3.5 Å for double-stranded peptides in DMSO- d_6 /CDCl₃ solution. In addition, the low $J_{NH\alpha,CH_2}$ coupling constants ($=5.2$ – 5.5 Hz) with the spacer's proton ($-C^1H_2-$) of the amido proton, $-NH^aCO-$, also support a β -turn-like-conformation at $-C^2H_2-C^1H_2-NH-CO-$ (dihedral angle; $\omega=-70^\circ$) of each strand folded structure for **8a**, **8e**, **10b**, and **10f**, *etc.* In the NMR of **10a** in CDCl₃, the selective upfield shifts of *o*-hydrogen ($\delta=7.02$ ppm) of the Phe side chain are originate from a strong interaction such as anisotropy effect and suggest that the *o*-hydrogen interacts with the other Phe with edge-to-face geometry.

Conformations, Dihedral Angle (θ), and Energy Calculations The energy calculations were performed by use of the MM2 method⁷⁾ to obtain the low-energy conformational geometry of the mini parallel double-stranded peptides. For conformers of 1,2-ethano-bis(L-Phe–L-Phe) **14a** and 1,12-dodecano-bis(L-Phe–L-Phe) **8a**, four dihedral angles ϕ ($CO-NH-C^\alpha H-CO$), ψ ($NH-C^\alpha H-CO-NH$), ω ($CO-NH-CH_2-CH_2$), and θ ($\angle NH^a-C^1-C^2-NH^a$ or $\angle C^5-C^6-C^7-C^8$) were considered, and the calculations were performed with under constraints for the dihedral angles, θ (from 0 to 180°–195° rotation) and ψ . The J values measured by NMR were translated to the dihedral angles, ϕ and ω , by

using the Karplus equation^{15,16)} and the resulting data are summarized in Tables 4 and 5. The low-energy conformers of **8a** and **14a** match the conformation proposed from experimental results (NOEs, $J_{NH,\alpha H}$ and $J_{C^1,NH}$) so that the β -turn-like-conformer is better than the linear conformer.

The average dihedral angles, ϕ and ω , of **14a** were determined from coupling constants, $J_{NHb,\alpha H1}=7.6$ Hz and $J_{NH\alpha,CH_2}=4.4$ Hz (**16a**) in CDCl₃/DMSO- d_6 solution. Compound **14a** has average dihedral angles of $\phi=-87^\circ$ and $\omega=+90^\circ$.¹⁷⁾ The dihedral angles ($\omega=-90^\circ$, $\phi=-87^\circ$, $\psi=+180^\circ$) indicate a β -turn-like structure. The minimized steric energy of **14a** is -28.4 kcal/mol at $\theta=-15^\circ$, and the steric energy at $\theta=+180^\circ$ is -21.6 kcal/mol, and the most probable conformers ($\omega=+90^\circ$, $\phi=-87^\circ$, $\psi=+180^\circ$, $\theta=-15^\circ$, form *a*) of **14a** are presented in Fig. 7. The steric energy for the β -turn-like structure is lower than that of α -helical mimic structure at dihedral angles ($\omega=+90^\circ$, $\phi=-47^\circ$, $\psi=-57^\circ$) in CDCl₃/DMSO- d_6 solution. The dihedral angle ($\omega=+90^\circ$) of 1,2-ethano-bis(D-Leu) observed by ¹H-NMR almost coincided with the value ($\omega=+95^\circ$) obtained by X-ray crystallography.¹⁷⁾ These findings support that **14a** favors a β -turn-like structure.

The dihedral angles, ϕ and ω , of **8a** were determined from coupling constants, $J_{NHb,\alpha H1}=7.6$ Hz and $J_{NH\alpha,CH_2}=5.4$ Hz. The geometries of the conformer were minimized under constraints for backbone dihedral angles, $\phi=-89^\circ$, $\psi=+180^\circ$, $\omega=-70^\circ$ obtained by the experiments. Under the constraint, particularly, we calculated the low-energy conformers of **8a** varied for dihedral angle, θ , from 0 to 210°, as plots of θ dependence energy in Fig. 8. The low-energy conformers $\theta=+75^\circ$ ($\Delta E=-3.8$ kcal/mol) and 180° ($\Delta E=-7.9$ kcal/mol) obtained at $\psi=+180^\circ$ which are more stable than the conformers at $\psi=+115^\circ$. The structure of **8a** was as-

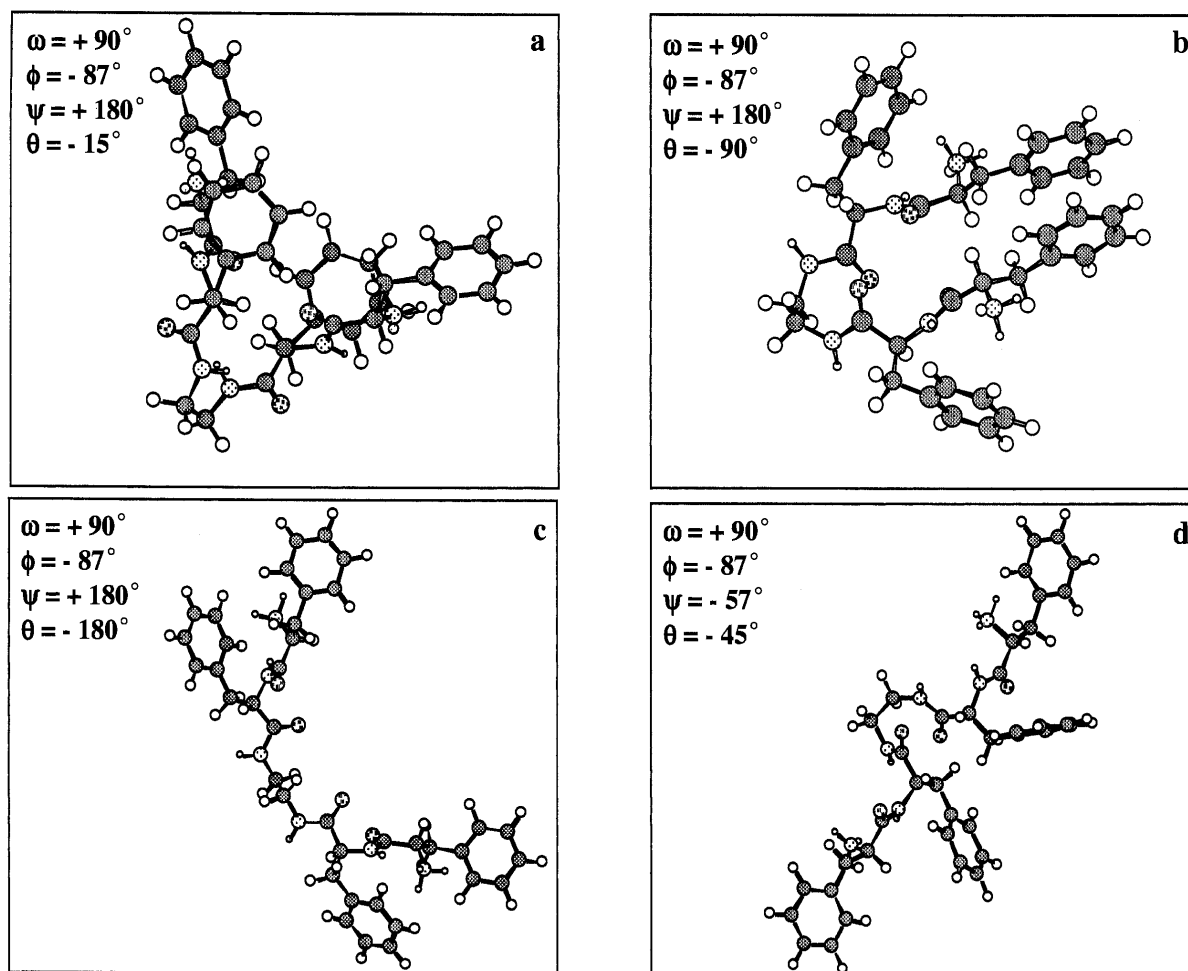


Fig. 7. Cylindrical Bonds Representation of Proposed Most Stable Conformers of 1,2-Ethano-bis(L-Phe-L-Phe) **14a**

The calculation is performed for **14a**, based on the NOE connectivities and observed coupling constant (J Hz). The conformer a is the most stable at dihedral angle $\theta = -15^\circ$ and a–c adopt a nucleation mediate by a β -turn-like structure. The energy minimized conformer d ($\theta = -45^\circ$) calculated under constraints for dihedral angle ($\omega = +90^\circ$, $\phi = -47^\circ$, and $\psi = -57^\circ$), and adopts a α -helix-like structure.

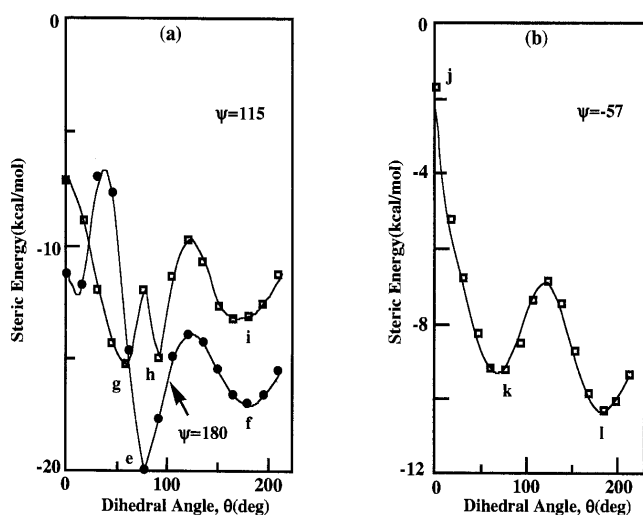


Fig. 8. Steric Energies for 1,12-Dodecano-bis(L-Phe-L-Phe) **8a** as Calculated Using MM2 as a Function of Dihedral Angle (θ)

Energy was calculated under constraint using the corresponding dihedral angles, $\omega = -70^\circ$, $\phi = -89^\circ$, and $\psi = +115^\circ$ (and $\psi = +180^\circ$) (a), and $\omega = -70^\circ$, $\phi = -47^\circ$, and $\psi = -57^\circ$ (b), determined from the observed $^3J_{\alpha N}$ (Hz). The (a) and (b) introduced **8a** in a turn β -strand and a turn α -strand conformation, respectively.

signed to a spiral β -turn-like structure ($\phi = -89^\circ$, $\psi = +180^\circ$, $\theta = +75^\circ$ or 180°). The results are satisfied with the Ramachandran angles. The most probable conformers ($\omega = -70^\circ$, $\phi = -89^\circ$, $\psi = +180^\circ$, $\theta = +75^\circ$, form e) of **8a** are presented in Fig. 9. Here, if **8a** is a structure mediated α -helical mimic nucleation, the compound has average dihedral angles of $\phi = -47^\circ$ and $\psi = -57^\circ$. Figure 9b shows the plot of θ dependence of energy. If **8a** is a nucleation mediated α -helical mimic structure, the low energy conformers are energetically more unstable than that of the β -turn structure. The coupling constant ($J_{\text{NHb}, \alpha\text{H1}}$) should provide *ca.* 3.9 Hz.¹⁸⁾ In summary, the structure of parallel double-stranded peptides **8a** and **10a** (not shown here), *etc.* nucleates a parallel β -turn-like conformation and two low-energy conformers are generated under constraints at dihedral angles $\phi = -89^\circ$ and $\psi = +180^\circ$ rotation (Fig. 9).

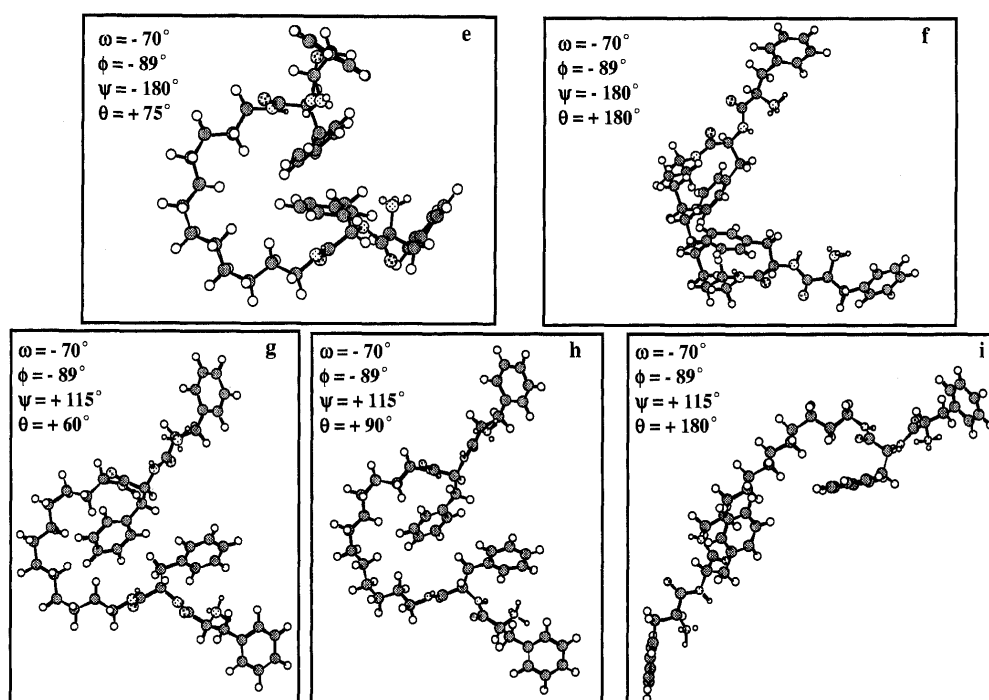
Binding Affinity In order to investigate the chemical properties of double-stranded peptides, which form a β -turn-like conformation, binding studies were performed by UV-visible optical titration under Baba–Nagakura type conditions ($[L_0] < [H_i]$) to determine the association constants K_a (M^{-1}).¹⁹⁾ The method of titration is provided in the experimental section.

$$[H_i][H_j] \times (A_j - A_i) \times K_a = [H_i] \times (A_0 - A_i) \times [H_j] \times (A_i - A_0) \quad (1)$$

Table 4. Minimum Energy and Corresponding Dihedral Angles (θ , ω , ψ , ϕ) of **14a** Determined from Experimental Coupling Constants Values (J) and Calculations

Compounds ^{a)}	$-\text{CH}_2-\text{CH}_2-\text{NH}-\text{CO}-$ ω	$-\text{NH}-\text{CO}-\text{CH}-\text{NH}-$ ψ_1	$-\text{CO}-\text{CH}-\text{NH}-\text{CO}-$ ϕ_1	$-\text{NH}-\text{CO}-\text{CH}-\text{NH}-$ ψ_2	$-\text{CH}_2-\text{CH}_2-\text{CH}_2-\text{CH}_2-$ θ	Steric energy (kcal/mol)
Turn β -sheet mimetics						
14a a	+90	+180	-87	+31.5 ^{b)}	-15	-28.40
b	+90	+180	-87	+44.2 ^{b)}	-90	-23.16
c	+90	+180	-87	+36.6 ^{b)}	-180	-21.58
Turn α -helical mimetics						
14a d	+90	-57	-87	-47	-45	-27.19

a) See Fig. 7 for description of backbone dihedral angles (θ) and structures of the double-stranded peptides. b) Calculated values.

Fig. 9. Cylindrical Bonds Representation of Proposed Most Stable Conformers of 1,12-Dodecano-bis(L-Phe-L-Phe) **8a**

The calculation is performed for **8a**, based on the NOE connectivities and observed coupling constants (J Hz). From Fig. 8a, the e and f are the most probable conformations ($\theta = +75^\circ$ and $+180^\circ$) and adopt a β -turn-like structure. The $\psi = +115^\circ$ of conformers g, h, and i is chosen to reflect typical dihedral angle ψ for β -sheet structure to compare e and f with g, h, and i conformers.

Table 5. Minimum Energy and Corresponding Dihedral Angles (θ , ω , ψ , ϕ) of **8a** Determined from Experimental Coupling Constants Values (J) and Calculations

Compounds ^{a)}	$-\text{CH}_2-\text{CH}_2-\text{NH}-\text{CO}-$ ω	$-\text{NH}-\text{CO}-\text{CH}-\text{NH}-$ ψ_1	$-\text{CO}-\text{CH}-\text{NH}-\text{CO}-$ ϕ_1	$-\text{NH}-\text{CO}-\text{CH}-\text{NH}-$ ψ_2	$-\text{CH}_2-\text{CH}_2-\text{CH}_2-\text{CH}_2-$ θ	Steric energy (kcal/mol)
Turn β -sheet mimetics						
8a e	-70	-180	-89	+24.4/+43.8 ^{b)}	+75	-19.94
f	-70	-180	-89	+27.4/+45.6 ^{b)}	+180	-17.00
g	-70	+115	-89	+31.1/+34.8 ^{b)}	+60	-15.19
h	-70	+115	-89	+31/+34.8 ^{b)}	+90	-15.00
i	-70	+115	-89	+31.2/+44.9 ^{b)}	+180	-13.16
Turn α -helical mimetics						
8a j	-70	-57	-47	-47	+0	-1.72
k	-70	-57	-47	-47	+75	-9.22
l	-70	-57	-47	-47	+180	-10.32

a) See Figs. 8 and 9 for description of backbone dihedral angles (θ) and structures of the double-stranded peptides. b) Calculated values.

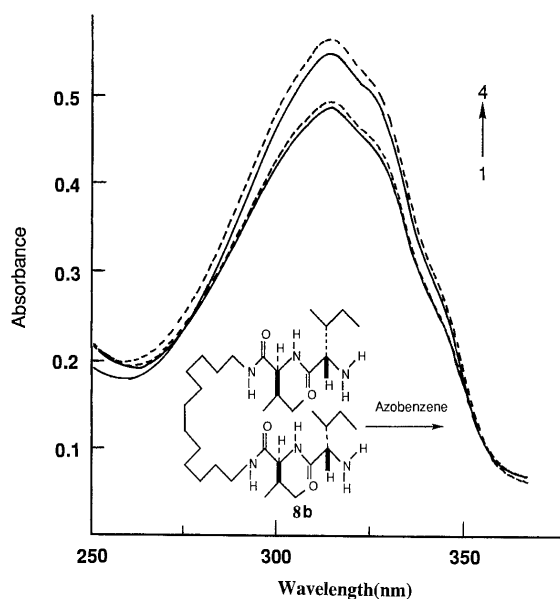


Fig. 10. Electronic Absorption Titration to Determine the Association Constant of Complex between **8b** and Azobenzene in Methanol at $T=295$ K

In titration, $[L_0]$ is 2.11×10^{-5} M, and $[H_i]$ are the following from spectrum 1 to spectrum 4: 0.00, 0.998, 9.89, and 59.9×10^{-5} M.

Table 6. Association Constants K_a (M^{-1}) and Free Energy of Formation ΔG of 1,12-Dodecano-bis(peptide)-Guest Molecular Complex in Methanol Solution

Compound	CD type	Guest	K_a ($\times 10^4$)	$-\Delta G$ (kcal/mol)	T (K)
8a	Class I	Azobenzene	0.96	5.4	298
8b	Class II	Azobenzene	1.2	5.5	295
8a	Class I	Pyrene	3.5	6.2	298
8b	Class II	Pyrene	0.29	4.7	298
10a	Class I	Azobenzene	1.0	5.5	297
10b	Class I	Azobenzene	0.81	5.3	295
10c	Class II	Azobenzene	0.028	3.3	295
10a	Class I	PHA	0.13	4.2	296
10d	Class II	PHA	0.048	3.6	296

$$-\Delta G = RT \times \ln K_a \quad (2)$$

In Eq. 1, A_0 , A_i , and A_j are the absorbance of the guest (substrate) when molar concentration of the host (dodecano double strand peptide) is $[L_0]$, $[H_i]$, and $[H_j]$, respectively. The values of a free energy of formation, $-\Delta G$ (kcal/mol), of the host-guest complex were calculated by Eq. 2. The guests, azobenzene, pyrene, or *N*-phenyl-1-naphthylamine (PHA) were used in all cases to determine K_a , since there is non-overlapping absorption with that of Phe.

As seen in a typical titration curve of Fig. 10, the titration spectrum with 1,12-dodecano-bis(L-Ile-L-Ile) **8b** and azobenzene (guest, $[L_0]=2.11 \times 10^{-5} M^{-1}$) was consistent with formation of a 1:1 inclusion complex with an isosbestic point at about 280 and 360 nm. The K_a was estimated to be 1.2×10^4 (M^{-1}) $[(1.22+1.24+1.03)/3 \times 10^4]$ as the mean value of the apparent K_i obtained from the absorbance (A_i) at 310, 320, and 330 nm in methanol. The $-\Delta G$ of **8a** pyrene complex ($=6.2$ kcal/mol) is 1.5 kcal/mol larger than that of **8b**·pyrene complex ($=4.7$ kcal/mol). The increase in its binding energy means that the hydrophobicity of the binding site in dodecano double-stranded peptides is increased by the side chain on the Phe residue. When the replacement of a

Table 7. Association Constants K_a (M^{-1}) and Free Energy of Formation ΔG of 1,2-Ethano-bis(peptide)-Guest Molecular Complex in Methanol Solution

Compound	CD type	Guest	K_a ($\times 10^4$)	$-\Delta G$ (kcal/mol)	T (K)
14a	—	Azobenzene	0.348	4.8	297
14b	—	Azobenzene	0.83	5.3	297
16a	Class I	Azobenzene	0.165	4.3	297

single residue (from Phe to Ile) in **10a** is afforded, the intensity of the binding constant is higher than that of **10e**. In fact, the stability of inclusion complex formation increased in order of **10a**·azobenzene > **10b**·azobenzene > **10d**·azobenzene. The thermodynamic data for the binding complex are summarized in Table 6. For understanding structure-function relationship based on the order, we studied the binding with the double-strand peptides of PHA. A similar result, for instance, was obtained from the complex formation by interaction with **10a** and **10d** of PHA. The results showed that the stability increases in order of **10a**·PHA > **10d**·PHA. We examined how the substrates fit into the size and conformation of the binding site. Table 7 shows that the diastereoselectivity of 1,2-ethano-bis(L-Phe-L-Phe) **14a** and 1,2-ethano-bis(L-Phe-D-Phe) **14b** for substrate (azobenzene) was observed, and $-\Delta G$ energy for inclusion complex, 1,2-ethano-bis(L-Phe-D-Phe)·azobenzene, increases about 0.5 kcal/mol compared with 1,2-ethano-bis(L-Phe-L-Phe)·azobenzene complex.

By including the substrate in the binding site, the peptide mimetic system gave binding constants that are different by several kilocalories by changing the amino acid of the host, as shown in Table 6. The intensity change in the binding energy indicates that the binding site of class I type in double strand peptides is strongly lipophilic, compared to the class II type. According to the hydrophobic parameter value (π) of several amino acids reported by Akamatsu and Fujita^{11c)} replacement of a single residue -Ile-Ile from **8b** to -Phe-Phe **8a** increases the sum of the hydrophobic parameter from 3.62 to 3.90. Consequently, the thermodynamic data demonstrate the importance of the hydrophobic parameter on the double-stranded peptides. Interestingly, the **6a**·chalcone complex with an electron withdrawing group in the intermolecule, of **6a** increases the $-\Delta G$ ($=6.9$ kcal/mol), depending on the effect of π - π stacking based on the charge transfer between chalcone and side chain on the residue. The best hosts (=the artificial receptors) for binding with the substrate are observed with Class I CD type of the double-stranded peptides and probably resulted from fit orientation of substrate within binding site of -L-Phe-L-Phe-L-X (X=amino acid) from NMR studies as described in the previous section. Our results show that the double-stranded peptides of class I CD type bind with substrate stronger than those of class II CD type.

Conclusion

In this work, double-stranded peptides, X^3 -L-Phe²-L-Phe¹-spacer(S)-L-Phe¹-L-Phe²-X³ (X=amino acids; S=ethano- and dodecano-) were designed and synthesized to clarify the chemical function of the -Phe-Phe-Val- sequence (and analogs) contained in Alzheimer's disease related β -

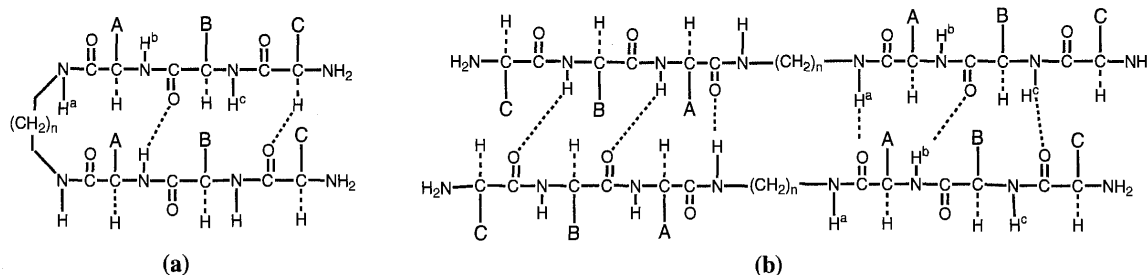


Fig. 11. Structure of Double-Stranded Peptides

(a) Intramolecular folding structure. (b) Interstranded dimer by hydrogen-bonding. Where A—C represent the corresponding amino acid residues.

amyloid peptide. The ^1H -NMR and CD studies indicate that the double-stranded peptides are a chemical skeleton mediated β -turn sheet mimetic structure. However, the other double-stranded peptide, $\text{Phe}^3\text{-L-Leu}^2\text{-L-Leu}^1\text{-(S)-Leu}^1\text{-L-Leu}^2\text{-L-Phe}^3$ (S=dodecano-), *etc.* mediates a turn random-form nucleation. The difference in the two conformations indicates that the hydrophobic interactions between Phe^1 and Phe^2 of each strand are promoted by the formation of the parallel β -turn sheet mimetics. From computational chemical (energy potential diagram) and experimental results, the results can be summarized as follows.

(i) The turn-structure and -conformation of double-stranded peptides also were confirmed by the thermodynamic data for the inclusion of substrate.

(ii) The CD profiles of $\text{X}^3\text{-L-Phe}^2\text{-L-Phe}^1\text{-spacer(S)-L-Phe}^1\text{-L-Phe}^2\text{-X}^3$ were consistent with literature data of a β -turn sheet mimic conformation.

(iii) The β -sheet conformation was characterized by $J_{\text{NHb}, \alpha\text{H1}}$ value in the range from 7 to 9 Hz.

(iv) The geometry based on NOESY, $J_{\text{NHb}, \alpha\text{H1}}$ values, and computational calculation of 1,12-dodecano-bis(L-Phe¹-L-Phe²) has the average dihedral angles at $\omega = -70^\circ$, $\phi = -89^\circ$, $\psi = +115^\circ$, $\theta = +75^\circ$ (and $+180^\circ$) and adopts a structure mediated parallel β -turn sheet-like conformation in solution.

(v) The selective downfield shift of the amide protons on double-stranded peptide also suggests the possibility of β -turn sheet and hydrogen bonding interaction, as shown in Fig. 11.

(vi) The presence of a low-concentration of $d_{\text{NHb}, \alpha\text{H1}}$ and $d_{\text{Phe}, \text{spacer}}$ supports an intrastranded hydrogen bonding (a) in a double-stranded peptide, but not the interstranded hydrogen bonding between dimer (b), as shown in Fig. 11.

The chemical and biological functions of -Phe-Phe-Val- or -Phe-Phe- sequences contained in Alzheimer's disease related β -amyloid peptide are not known yet, however our results support that the sequences play an important role to replace the conformation to β -sheet structure. The double-stranded peptides should prove to be very useful compounds in medicinal chemistry. Further study of these and related double-stranded peptides should continue to provide insight on the origins of turn β -sheet and biological activities.

Experimental

Materials Melting points were taken on a Yanako (MP-21) apparatus and are uncorrected. IR spectra were recorded with a JASCO A-100 spectrophotometer and UV-visible spectra with a JASCO U-best 30 spectrophotometer. ^1H - and ^{13}C -NMR spectra were recorded with a JNM GX-270 (270 MHz), α -500 (500 MHz), or Valian GEMINI 300 (300 MHz) spectrometer with TMS (tetramethylsilane) as an internal standard. FAB mass spec-

tral data were recorded with a JEOL JMS-HX110 spectrometer, and relevant data are tabulated as m/z . TLC was performed using Silica gel 60 F_{254} (Merck) plates and the following solvent systems: $\text{CHCl}_3\text{-MeOH}$ (20:1) (A) and $\text{CHCl}_3\text{-MeOH}$ (10:1) (B). The peptides were detected on the TLC plates using iodine vapor or UV absorption. Silica gel column chromatography was performed on Wako gel C-200 (100 mesh) or Merck Silica gel 60N (100 mesh). Analytical RP-HPLC was carried out on a TOSO CCPD system equipped with a Tskgel (ODS-120T) column. Elemental analyses were done as by Yanako HCN coder (MT-3). All UV-vis and CD spectra used commercial solvents of the highest available purity for spectroscopy.

Typical Synthesis. Typical Synthesis of the 1,12-Dodecano-bis(L-PheZ) (5a) CDI (3.98 g, 22.0 mmol) was added to a solution of Z-L-PheOH (6.20 g, 21.0 mmol) in dry CHCl_3 (50 ml). After stirring for 1.5 h at room temperature, 1,12-dodecanodiamine **4** (2.0 g, 10.0 mmol) was added to the stirred solution, then stirred overnight. This solution was evaporated to dryness. After addition of aq. MeOH, the solid was collected, and washed with aq. MeOH, 5% citric acid, 5% NaHCO_3 , and water, and dried *in vacuo*. The resulting product, **5a**, a colorless solid was obtained in 97.0% yield, and the crude product (3.5 g) was purified by column chromatography on silica gel (45 g) eluted with CHCl_3 and 3% MeOH/ CHCl_3 (stepwise elution); mp 157—158 °C (from aq. MeOH); R_f (A): 0.59; FAB-MS m/z 764 ($M^+ + 1$).

1,12-Dodecano-bis(L-Phe-L-Phe-L-ValBoc) (9b) To a magnetically stirred solution of 1,12-dodecano-bis(L-Phe-L-Phe) **8a** (1.65 g, 2.1 mmol), Boc-L-ValOH (0.934 g, 4.3 mmol), and triethylamine (TEA) (0.62 ml) in dry DMF (20 ml) was added DEPC (0.86 g, 5.3 mmol) at 4 °C. The resulting solution was stirred at 4 °C for 1 h and then at room temperature overnight. The solution was poured into ice/water, and the precipitate was collected by filtration, washed with 5% citric acid, 5% NaHCO_3 , and water, and dried to give colorless crystals of **9b**: 81.0% yield, and the product was purified by column chromatography on silica gel (45.0 g) eluted with CHCl_3 and 3% MeOH/ CHCl_3 (stepwise elution); mp 198—200 °C; R_f (A): 0.36; HR-FAB-MS (nitrobenzyl alcohol) m/z 1188 ($M^+ + 1$); Found 1187.7490, Calcd for $\text{C}_{68}\text{H}_{99}\text{N}_8\text{O}_{10}$ 1187.7485.

The following compounds, **5a**—**9h** were prepared from the corresponding Z(or Boc)-protected amino acid similarly to the above described method. 1,12-Dodecano-bis(L-IleZ) **5b**: 85.0% yield; mp 142—143 °C (from ether/MeOH); R_f (A) 0.24. 1,12-Dodecano-bis(D-PheBoc) **5c**: 91.0% yield; mp 125—127 °C (from ether/MeOH); R_f (A) 0.76; FAB-MS (nitrobenzyl alcohol) m/z 696 ($M^+ + 1$). 1,12-Dodecano-bis(L-LeuZ) **5d**: 95.7% yield; mp 97—99 °C; R_f (A) 0.87; FAB-MS (nitrobenzyl alcohol) m/z 696 ($M^+ + 1$). 1,12-Dodecano-bis(L-Phe-L-PheZ) **7a**: 96.5% yield; mp 201—202 °C (from MeOH); R_f (A) 0.49; FAB-MS (nitrobenzyl alcohol) m/z 1058 ($M^+ + 1$). 1,12-Dodecano-bis(L-Ile-L-IleZ) **7b**: 89.0% yield; mp 180—183 °C (from MeOH); R_f (A) 0.45; FAB-MS (nitrobenzyl alcohol) m/z 946 ($M^+ + 1$). 1,12-Dodecano-bis(L-Phe-L-ValBoc) **7c**: 98.5% yield; mp 145—147 °C; R_f (A) 0.55; HR-FAB-MS (nitrobenzyl alcohol) m/z 894 ($M^+ + 1$); Found 893.6116, Calcd for $\text{C}_{50}\text{H}_{81}\text{N}_6\text{O}_8$ 893.6118. 1,12-Dodecano-bis(L-Ile-L-PheZ) **7d**: 95.6% yield; mp 205—206 °C; R_f (A) 0.67; FAB-MS (nitrobenzyl alcohol) m/z 990 ($M^+ + 1$). 1,12-Dodecano-bis(D-Phe-L-PheBoc) **7e**: 83.1% yield; mp 178—180 °C; R_f (A) 0.76; HR-FAB-MS (nitrobenzyl alcohol) m/z 990 ($M^+ + 1$); Found 989.6118, Calcd for $\text{C}_{58}\text{H}_{81}\text{N}_6\text{O}_8$ 989.6116. 1,12-Dodecano-bis(L-Phe-D-PheZ) **7f**: 86.7% yield; mp 182—184 °C; R_f (A) 0.32; HR-FAB-MS (nitrobenzyl alcohol) m/z 1058 ($M^+ + 1$); Found 1057.5809, Calcd for $\text{C}_{64}\text{H}_{77}\text{N}_6\text{O}_8$ 1057.5803. 1,12-Dodecano-bis(D-Phe-D-PheBoc) **7g**: 83.0% yield; mp 186—187 °C; R_f (A) 0.47; FAB-MS (nitrobenzyl alcohol) m/z 990 ($M^+ + 1$). 1,12-Dodecano-bis(L-Leu-L-PheZ) **7h**: 92.3% yield; mp 231—232 °C; R_f (A) 0.67; FAB-MS (nitrobenzyl alcohol) m/z 990 ($M^+ + 1$). 1,12-Dodecano-bis(L-Phe-L-Phe-L-

LeuZ) **9a**: 91.8% yield; mp 206—208 °C (from ether/MeOH); *Rf* (A) 0.23; FAB-MS (nitrobenzyl alcohol) *m/z* 1284 ($M^+ + 1$). 1,12-Dodecano-bis(L-Phe-L-Phe-L-IleZ) **9c**: 90% yield; mp 207—210 °C (from MeOH); *Rf* (B) 0.57. 1,12-Dodecano-bis(L-Phe-L-Val-L-LeuBoc) **9d**: 85.2% yield; mp 234—236 °C (from MeOH); *Rf* (A) 0.41; HR-FAB-MS (nitrobenzyl alcohol) *m/z* 1120 ($M^+ + 1$); mass found 1119.7828, Calcd for $C_{62}H_{103}N_8O_{10}$ 1119.7800. 1,12-Dodecano-bis(L-Ile-L-Phe-L-LeuZ) **9e**: 83.0% yield; mp 195—198 °C (from MeOH); *Rf* (A) 0.48; FAB-MS (nitrobenzyl alcohol) *m/z* 1216 ($M^+ + 1$). 1,12-Dodecano-bis(L-Leu-L-Leu-L-PheZ) **9f**: 87.9% yield; mp 193—195 °C (from MeOH); *Rf* (A) 0.26; FAB-MS *m/z* 1216 ($M^+ + 1$). 1,12-Dodecano-bis(L-Leu-L-Phe-L-PheBoc) **9g**: 85.5% yield; mp 175—177 °C (from MeOH); *Rf* (B) 0.81; HR-FAB-MS (nitrobenzyl alcohol) *m/z* 1216 ($M^+ + 1$); Found 1215.7792, Calcd for $C_{70}H_{103}N_8O_{10}$ 1215.7796. 1,12-Dodecano-bis(D-Phe-D-Phe-D-LeuZ) **9h**: 91.0% yield; mp 205—207 °C; *Rf* (A) 0.55; HR-FAB-MS (nitrobenzyl alcohol) *m/z* 1284 ($M^+ + 1$); Found 1284.7579, Calcd for $C_{70}H_{100}N_8O_{10}$ 1284.7566.

Synthesis of the 1,2-Ethano-bis(L-(or D)-amino acid), 1,2-Ethano-bis(L-Phe-L-Phe-L-ValBoc) 15b To a magnetically stirred solution of 1,2-ethano-bis(L-Phe-L-Phe) **14a** (0.49 g, 0.76 mmol), Boc-L-ValOH (0.35 g, 1.6 mmol), and TEA (0.2 ml) in dry DMF (10 ml) was added DEPC (0.35 g, 2.2 mmol) at 4 °C. The resulting solution was stirred at 4 °C for 1 h and then at room temperature overnight. The solution was poured into ice/water, and then the precipitates were collected, washed with 5% citric acid, 5% $NaHCO_3$, and water, and dried *in vacuo*: 87.0% yield. The crude material obtained was purified on a silica gel (50 g) column chromatography eluting with $CHCl_3$ and 3% MeOH/ $CHCl_3$ (stepwise elution) to give 1,2-ethano-bis(L-Phe-L-Phe-L-ValBoc) **15b** as a colorless crystals: mp 263—265 °C; TLC *Rf* (A) 0.38; HR-FAB-MS (nitrobenzyl alcohol) *m/z* 1048 ($M^+ + 1$); Found 1047.5923, Calcd for $C_{58}H_{79}N_8O_{10}$ 1047.5919.

The following compounds, **11a—15a** were prepared from the corresponding Z(or Boc)-protected amino acid similarly to the above described method. 1,2-Ethano-bis(L-PheBoc) **11a**: 96.4% yield; mp 195—197 °C; *Rf* (A) 0.35. 1,2-Ethano-bis(L-LeuZ) **11b**: 95.8% yield; mp 190—192 °C; *Rf* (A) 0.40. 1,2-Ethano-bis(D-LeuZ) **11c**: 87.6% yield; mp 191—193 °C; *Rf* (A) 0.42. 1,2-Ethano-bis(L-Phe-L-PheBoc) **13a**: 97.9% yield; mp 225—227 °C; *Rf* (A) 0.33; HR-FAB-MS (nitrobenzyl alcohol) *m/z* 850 ($M^+ + 1$); Found 849.4521, Calcd for $C_{48}H_{61}N_4O_8$ 849.4556. 1,2-Ethano-bis(L-Phe-D-PheBoc) **13b**: 95.5% yield; mp 230—232 °C; *Rf* (A) 0.25; FAB-MS (nitrobenzyl alcohol) *m/z* 850 ($M^+ + 1$). 1,2-Ethano-bis(L-Phe-L-Phe-L-LeuBoc) **15a**: 73.0% yield; mp 248—250 °C; *Rf* (A) 0.48; HR-FAB-MS (nitrobenzyl alcohol) *m/z* 1076 ($M^+ + 1$); Found 1075.6207, Calcd for $C_{60}H_{83}N_8O_{10}$ 1075.6230.

Synthesis of the Lauryl-L-(or D)-amino Acids The following compounds, **17b** were prepared from the corresponding Z-protected amino acid with similarly to the above described method. Lauryl-L-Phe-L-Phe **17b**: 83.0% yield; mp 113—114 °C (from ether/MeOH); *Rf* (A) 0.81; FAB-MS (nitrobenzyl alcohol) *m/z* 467 ($M^+ + 1$).

The following compounds, **18b, 19b** were prepared from the corresponding Z-protected amino acid with similarly to the above described method. Lauryl-L-Phe-L-Phe **18b**: 93.5% yield; mp 134—134 °C (from MeOH); *Rf* (A) 0.73; HR-FAB-MS (nitrobenzyl alcohol) *m/z* 614 ($M^+ + 1$); mass found 614.3951, Calcd for $C_{38}H_{52}N_2O_4$ 614.3961. Lauryl-L-Phe-L-Phe-L-LeuZ **19b**: 85.7% yield; mp 170—173 °C (from ether/ $CHCl_3$); *Rf* (A) 0.64; HR-FAB-MS (nitrobenzyl alcohol) *m/z* 727 ($M^+ + 1$); Found 727.4794, Calcd for $C_{44}H_{63}N_4O_5$ 727.4801.

Deprotection. Synthesis of the 1,12-Dodecano-bis(L-Phe) (6a) 5a (3.80 g, 4.98 mmol) was dissolved, by heating on a water bath, in MeOH/DMF (120 ml/30 ml). A slurry consisting of 5% Pd/C (0.75 g) was added, and the mixture was shaken in a hydrogen atmosphere. The catalyst was removed by filtration, and the filtrate and washings were combined and evaporated. The residue crystallized with water in an ice bath, to afford **6a** (2.61 g, 87.8%) of colorless crystals: *Rf* (A) 0.23; mp 116—117 °C (from ether/ $CHCl_3$). $[\alpha]_D^{25} + 22.8$ ($c = 0.264$, MeOH). 1H -NMR (signal assignments from the spectra of H-H COSY at 500 MHz, $CDCl_3$) δ 1.19—1.28 (m, 10H, $-(CH_2)_5 \times 5$), 2.58—2.81 (dd, 1H, $J = 9.0$, 13.6 Hz, $Phe^C H$), 3.19—3.37 (m, 3H, $-C^1 H_2-$ and $Phe^C H$), 3.53—3.67 (dd, 1H, $J = 4.4$, 9.5 Hz, $Phe^C H$), 7.24 (br s, 1H, $-NHCO-$), 7.24—7.25 (m, 5H, Ar-H). ^{13}C -NMR (signal assignments from the spectra of C-H COSY at 500 MHz, $CDCl_3$) ppm 26.95 (C3), 29.24 (C4, 5, 6), 29.53 (C2), 39.10 (C1), 41.16 ($Phe^C H$), 56.48 ($Phe^C H$), 126.70 (p), 128.58 (o), 129.22 (m), 138.03 (t), 173.90 ($-NHCO-$). IR (KBr) cm^{-1} : 3270, 1640; HR-MS *m/z*: Found 494.3606. Calcd for $C_{30}H_{46}N_4O_2$ 494.3618.

The following compounds, **6a—10h** were prepared from the corresponding Z(or Boc)-protected amino acid with similarly to the above described

method. 1,12-Dodecano-bis(L-Phe) **6a**: 97.0% yield; mp 116—117 °C (from ether/ $CHCl_3$); *Rf* (A) 0.23. 1,12-Dodecano-bis(L-Ile) **6b**: 92.0% yield; mp 83—84 °C (from MeOH); *Rf* (A) 0.23. 1,12-Dodecano-bis(D-Phe) **6c**: 94.7% yield; mp 115—116 °C (from ether/MeOH); *Rf* (A) 0.20. 1,12-Dodecano-bis(L-Leu) **6d**: 87.0% yield; mp 95—97 °C (from hexane/ $CHCl_3$); *Rf* (A) 0.14. 1,12-Dodecano-bis(L-Phe-L-Phe) **8a**: 82.8% yield; mp 120—122 °C (from MeCN); *Rf* (B) 0.49. 1,12-Dodecano-bis(L-Ile-L-Ile) **8b**: 89.3% yield; mp 122—124 °C (from ether/ $CHCl_3$); *Rf* (A) 0.23. 1,12-Dodecano-bis(L-Phe-L-Val) **8c**: 90.5% yield; mp 144—146 °C (from ether/ $CHCl_3$); *Rf* (B) 0.43. 1,12-Dodecano-bis(L-Ile-L-Phe) **8d**: 87.0% yield; mp 125—126 °C (from ether/MeOH); *Rf* (B) 0.46. 1,12-Dodecano-bis(D-Phe-L-Phe) **8e**: 73.8% yield; mp 102—104 °C (from ether/MeOH); *Rf* (B) 0.41. 1,12-Dodecano-bis(L-Phe-D-Phe) **8f**: 75.0% yield; mp 115—116 °C (from ether/ $CHCl_3$); *Rf* (B) 0.42. 1,12-Dodecano-bis(D-Phe-D-Phe) **8g**: 74.7% yield; mp 128—129 °C (from MeCN); *Rf* (B) 0.50. 1,12-Dodecano-bis(L-Leu-L-Phe) **8h**: 76.0% yield; mp 68—70 °C (from MeCN); *Rf* (B) 0.48. 1,12-Dodecano-bis(L-Phe-L-Phe-L-Leu) **10a**: 71.8% yield; mp 186—188 °C (from ether/ $CHCl_3$); *Rf* (B) 0.30. 1,12-Dodecano-bis(L-Phe-L-Phe-L-Val) **10b**: 81.0% yield; mp 215—217 °C (from ether/ $CHCl_3$); *Rf* (B) 0.27. 1,12-Dodecano-bis(L-Phe-L-Phe-L-Ile) **10c**: 79.5% yield; mp 127—129 °C (ether/ $CHCl_3$); *Rf* (A) 0.23. 1,12-Dodecano-bis(L-Phe-L-Val-L-Leu) **10d**: 86.5% yield; mp 214—217 °C (from MeOH/ $CHCl_3$ /ether); *Rf* (B) 0.31. 1,12-Dodecano-bis(L-Ile-L-Phe-L-Leu) **10e**: 91.8% yield; mp 161—163 °C (from ether/ $CHCl_3$); $[\alpha]_D^{25} - 19.1$ ($c = 0.300$, MeOH); *Rf* (B) 0.30. 1,12-Dodecano-bis(L-Leu-L-Leu-L-Phe) **10f**: 90.5% yield; mp 104—106 °C (from MeOH); *Rf* (B) 0.54. 1,12-dodecano-bis(L-Leu-L-Phe-L-Phe) **10g**: 93.5% yield; mp 210—213 °C (dec.) (from ether/MeOH); *Rf* (B) = 0.54. 1,12-Dodecano-bis(D-Phe-D-Phe-D-Leu) **10h**: 66.3% yield; mp 188—190 °C (from ether/ $CHCl_3$); *Rf* (B) 0.32; FAB-MS (nitrobenzyl alcohol) *m/z* 1016 ($M^+ + 1$).

Synthesis of 1,12-Dodecano-bis(D-Phe-D-Phe) (8g) To N_α -Boc protected **7g** (2.00 g, 1.9 mmol) anhydrous TFA (12 ml) was added dropwise over a period of 0.5 min. The mixture was stirred at 4 °C for 80 min, and then was poured into ice/water, and adjusted to pH 7—8 with 5% $NaHCO_3$ and 1 M NaOH. The resulting solid was collected, washed with water, and dried *in vacuo*: 74.7% yield. The product was purified with silica gel (35 g) column chromatography eluting with $CHCl_3$ and 3% MeOH/ $CHCl_3$ (stepwise elution) to give **8g** as colorless crystals: mp 128—129 °C (from ether/MeOH); TLC *Rf* (B) 0.50. 1H -NMR (signal assignments from the spectra of H-H COSY at 500 Mz, $CDCl_3$ /DMSO- d_6) δ 1.21—1.37 (m, 10H, $-(CH_2)_5 \times 5$), 2.58 (dd, 1H, $J = 8.9$, 13.2 Hz, $Phe^C H$), 2.91 (dd, 1H, $J = 7.6$, 13.4 Hz, $Phe^1 C^H$), 3.02 (dd, $J = 5.2$, 12.8 Hz, $Phe^2 C^H$), 3.06—3.12 (m, 3H, $-C^1 H_2-$, $Phe^1 C^H$), 3.49 (dd, 1H, $J = 4.3$, 9.2 Hz, $Phe^2 C^H$), 4.61 (dd, 1H, $J = 7.6$, 14.3 Hz, $Phe^1 C^H$), 7.14—7.31 (m, 10H, Ar-H), 7.45 (t, 1H, $J = 5.2$ Hz, $-NH^bCO-$), 7.95 (d, 1H, $J = 8.2$ Hz, nNH^bCO-). ^{13}C -NMR ($CDCl_3$ /DMSO- d_6) ppm 26.65 (C3), 29.05 (C6), 29.14 (C4), 29.28 (C2, 5), 38.09 (C1), 38.20 ($Phe^1 C^H$), 39.07 ($Phe^2 C^H$), 54.50 ($Phe^2 C^H$), 54.78 ($Phe^1 C^H$), 126.38 (p), 126.90 (p'), 128.11 (o), 128.41 (o'), 129.30 (m), 129.47 (m'), 135.62 (t), 137.34 (t'), 169.55 ($-NH^bCO-$), 170.37 ($-NH^bCO-$); IR (KBr) 3270, 1630 cm^{-1} ; FAB-MS (nitrobenzyl alcohol) *m/z* 790 ($M^+ + 1$).

1,12-Dodecano-bis(L-Ile) (**6b**): Colorless solid; $[\alpha]_D^{25} + 10.4$ ($c = 0.156$, MeOH); 1H -NMR ($CDCl_3$) δ 0.88 (t, 3H, $J = 7.0$ Hz, $Ile^C H_3$), 0.94 (d, 3H, $J = 7.0$ Hz, $Ile^C H_2$), 1.20—1.40 (m, 10H, $-(CH_2)_5 \times 5$), 1.40—1.56 (m, 2H, $Ile^C H_2$), 1.88—2.04 (m, 1H, $Ile^C H$), 3.15—1.33 (m, 3H, $Ile^C H$, $-C^1 H_2-$), 7.24 (br, 1H, $-NHCO-$); ^{13}C -NMR ($CDCl_3$) ppm 11.92 ($Ile^C H$), 16.26 ($Ile^C H$), 23.78 (C3), 27.01 ($Ile^C H$), 29.29 (C6), 29.53 (C4, C5), 29.71 (C2), 38.04 ($Ile^C H$), 39.04 (C1), 60.00 ($Ile^C H$), 174.07 ($-NHCO-$); IR (KBr) 3270, 1630 cm^{-1} .

1,12-Dodecano-bis(L-Phe-L-Phe) (**8a**): Colorless solid; $[\alpha]_D^{25} + 5.5$ ($c = 0.319$, MeOH); 1H -NMR (signal assignments from the spectra of H-H COSY at 500 Mz, $CDCl_3$) δ 1.21—1.37 (m, 10H, $-(CH_2)_5 \times 5$), 2.56 (dd, 1H, $J = 9.5$, 14.0 Hz, $Phe^2 C^H$), 3.03—3.21 (m, 4H, $-C^1 H_2-$, $Phe^1 C^H$, $Phe^2 C^H$), 3.55 (dd, 1H, $J = 4.0$, 9.5 Hz, $Phe^2 C^H$), 4.62 (dd, 1H, $J = 7.8$, 15.7 Hz, $Phe^1 C^H$), 6.21 (t, 1H, $J = 5.4$ Hz, $-NH^bCO-$), 7.14—7.33 (m, 10H, Ar-H), 7.88 (d, 1H, $J = 8.4$ Hz, $-NH^bCO-$); ^{13}C -NMR (signal assignments from the spectra of C-H COSY at 500 Mz, $CDCl_3$) ppm 26.77 (C3), 29.19 (C6), 29.28 (C4), 29.41 (C5), 29.47 (C2), 38.36 (C1), 39.49 ($Phe^1 C^H$), 40.71 ($Phe^2 C^H$), 54.33 ($Phe^2 C^H$), 56.27 ($Phe^1 C^H$), 126.87 (p , p'), 128.52 (o'), 128.72 (o), 129.23 (m'), 129.34 (m), 136.91 (t'), 137.56 (t), 170.63 ($-NH^bCO-$), 174.50 ($-NH^bCO-$); IR (KBr) 3280, 1635 cm^{-1} ; FAB-MS (nitrobenzyl alcohol) *m/z* 789 ($M^+ + 1$). Anal. Calcd for $C_{48}H_{64}N_6O_4 \cdot 1/2 H_2O$ (798.0838): C, 72.24; H, 8.21; N, 10.53. Found: C, 72.46; H, 8.14; N, 10.48.

1,12-Dodecano-bis(L-Ile-L-Ile) (**8b**): Colorless solid; $[\alpha]_D^{25} - 22.4$ ($c =$

0.154, MeOH); $^1\text{H-NMR}$ (CDCl_3) δ 0.88—0.99 (overlap, 12H, $\text{CH}_3 \times 4$), 1.25—1.54 (m, 14H, $-(\text{CH}_2)_5$), 1.90—1.98 (m, 2H, $\text{Ile}^1 \text{C}^\beta\text{H}$, $\text{Ile}^2 \text{C}^\beta\text{H}$), 3.15—3.28 (m, 3H, $-\text{C}^1\text{H}_2-$, $\text{Ile}^2 \text{C}^\alpha\text{H}$), 4.17 (dd, 1H, $J=6.8$, 9.0 Hz, $\text{Ile}^1 \text{C}^\alpha\text{H}$), 6.40 (m, 1H, $-\text{NH}^b\text{CO}-$), 7.88 (d, 1H, $J=9.0$ Hz, $-\text{NH}^b\text{CO}-$); $^{13}\text{C-NMR}$ (CDCl_3) ppm 11.09 ($\text{Ile}^1 \text{Me}$), 11.92 ($\text{Ile}^2 \text{Me}$), 15.62 ($\text{Ile}^1 \text{Me}$), 16.14 ($\text{Ile}^2 \text{Me}$), 23.95 (C3, 4, 5, 6), 25.01 ($\text{Ile}^1 \text{C}^\gamma$), 26.95 ($\text{Ile}^2 \text{C}^\gamma$), 29.30 (C2), 36.75 ($\text{Ile}^1 \text{C}^\beta$), 38.16 (C1), 39.45 ($\text{Ile}^2 \text{C}^\beta$), 57.59 ($\text{Ile}^1 \text{C}^\alpha$), 60.00 ($\text{Ile}^2 \text{C}^\alpha$), 171.26 ($-\text{NH}^b\text{CO}-$), 174.54 ($-\text{NH}^b\text{CO}-$); IR (KBr) 3270, 1630 cm^{-1} ; FAB-MS (nitrobenzyl-alcohol) m/z 654 ($\text{M}^+ + 1$).

1,12-Dodecano-bis(L-Phe-L-Val) (**8c**): Colorless solid; $^1\text{H-NMR}$ ($\text{CDCl}_3/\text{DMSO-}d_6$) δ 0.67 (d, 3H, $J=6.8$ Hz, Val CH_3), 0.86 (d, 3H, $J=6.8$ Hz, Val CH_3), 1.18—1.38 (m, 10H, $-(\text{CH}_2)_5$), 2.03 (m, 1H, Val C^βH), 2.92 (dd, 1H, $J=8.3$, 13.7 Hz, Phe C^βH), 3.06—3.15 (m, 4H, $-\text{C}^1\text{H}_2-$ and Phe C^βH), 3.15—3.25 (m, 1H, Val C^αH), 4.63 (dd, 1H, $J=8.3$, 14.4 Hz, Phe C^αH), 7.10—7.25 (m, 5H, Ar-H), 7.53 (m, 1H, $-\text{NH}^b\text{CO}-$), 8.02 (d, 1H, $J=8.3$ Hz, $-\text{NH}^b\text{CO}-$); $^{13}\text{C-NMR}$ ($\text{DMSO-}d_6/\text{CDCl}_3$) ppm 16.33 (Val CH_3), 19.39 (Val CH_3), 26.61 (C3), 29.01 (Val C^β), 29.12 (C4, 5, 6), 29.23 (C2), 30.80 (C1), 38.43 (Phe C^β), 38.99 (Val C^β), 53.76 (Val C^α), 59.82 (Phe C^α), 126.32 (p), 128.05 (o), 129.18 (m), 137.29 (i), 170.80 ($-\text{NH}^b\text{CO}-$), 173.64 ($-\text{NH}^b\text{CO}-$); IR (KBr) 3280, 1630 cm^{-1} .

1,12-Dodecano-bis(L-Ile-L-Phe) (**8d**): Colorless solid; $[\alpha]_D^{25}$ -30.2 ($c=0.344$, MeOH); $^1\text{H-NMR}$ (CDCl_3) δ 0.87—0.94 (m, 6H, Ile Me $\times 2$), 1.24—1.04 (m, 14H, $-(\text{CH}_2)_5 \times 7$), 3.63 (m, 1H, Phe C^αH), 4.16 (dd, 1H, $J=8.3$, 14.0 Hz, Ile C^αH), 6.25 (t, 1H, $J=5.3$ Hz, $-\text{NH}^b\text{CO}-$), 7.24—7.26 (m, 5H, Ar-H), 7.86 (d, 1H, $J=9.0$ Hz, $-\text{NH}^b\text{CO}-$); $^{13}\text{C-NMR}$ (CDCl_3) ppm 11.21 (Ile Me), 15.61 (Ile Me), 25.01 (Ile C^γ), 29.41 (C4, 5, and 6), 33.99 (C2), 36.87 (C1), 39.51 (Ile C^β), 41.04 (Phe C^β), 56.48 (Phe C^α), 57.77 (Ile C^α), 126.81 (p), 128.59 (o), 129.28 (m), 137.67 (i), 171.08 ($-\text{NH}^b\text{CO}-$), 174.37 ($-\text{NH}^b\text{CO}-$); IR (KBr) 3260, 1630 cm^{-1} ; HR-FAB-MS m/z [M^+ , $\text{C}_{42}\text{H}_{68}\text{N}_6\text{O}_4$] Calcd 720.5301, Found 720.5346. Anal. Calcd for $\text{C}_{42}\text{H}_{68}\text{N}_6\text{O}_4 \cdot 1/2\text{H}_2\text{O}$: C, 69.10; H, 9.53; N, 11.51. Found: C, 69.33; H, 9.28; N, 11.50.

1,12-Dodecano-bis(D-Phe-L-Phe) (**8e**): Colorless solid; $^1\text{H-NMR}$ (signal assignments from the spectra of H-H COSY at 500 Mz, $\text{CDCl}_3/\text{DMSO-}d_6$) δ 1.21—1.37 (m, 10H, $-(\text{CH}_2)_5 \times 5$), 2.58 (dd, 1H, $J=8.9$, 13.2 Hz, Phe² C^βH), 2.91 (dd, 1H, $J=7.6$, 13.4 Hz, Phe¹ C^βH), 3.02 (dd, $J=5.2$, 12.8 Hz, Phe² C^βH), 3.06—3.12 (m, 3H, $-\text{C}^1\text{H}_2-$, Phe¹ C^βH), 3.49 (dd, 1H, $J=4.3$, 9.2 Hz, Phe² C^αH), 4.61 (dd, 1H, $J=7.6$, 14.3 Hz, Phe¹ C^αH), 7.14—7.31 (m, 10H, Ar-H), 7.45 (t, 1H, $J=5.2$ Hz, $-\text{NH}^b\text{CO}-$), 7.95 (d, 1H, $J=8.2$ Hz, $-\text{NH}^b\text{CO}-$); $^{13}\text{C-NMR}$ ($\text{CDCl}_3/\text{DMSO-}d_6$) ppm 26.62 (C3), 29.02 (C6), 29.11 (C4), 29.25 (C5), 29.28 (C2), 38.32 (C1), 38.98 (Phe¹ C^β), 40.94 (Phe² C^β), 53.85 (Phe² C^α), 56.20 (Phe¹ C^α), 126.26 (p), 126.32 (p'), 128.02 (o), 128.21 (o'), 129.15 (m), 129.22 (m'), 137.26 (i), 138.18 (i'), 170.65 ($-\text{NH}^b\text{CO}-$), 174.02 ($-\text{NH}^b\text{CO}-$); IR (KBr) 3280, 1630 cm^{-1} ; FAB-MS (nitrobenzyl alcohol) m/z 790 ($\text{M}^+ + 1$).

1,12-Dodecano-bis(L-Phe-D-Phe) (**8f**): Colorless solid; $^1\text{H-NMR}$ (signal assignments from the spectra of HOM spin decoupling at 500 Mz, $\text{CDCl}_3/\text{DMSO-}d_6$) δ 1.20—1.40 (m, 10H, $-(\text{CH}_2)_5 \times 5$), 2.72 (dd, 1H, $J=7.6$, 14.0 Hz, Phe² C^βH), 2.83 (dd, 1H, $J=9.5$, 13.7 Hz, Phe¹ C^βH), 2.92 (dd, $J=5.5$, 14.0 Hz, Phe² C^βH), 3.06—3.14 (m, 3H, $-\text{C}^1\text{H}_2-$, Phe¹ C^βH), 4.05 (dd, 1H, $J=5.5$, 7.3 Hz, Phe² C^αH), 4.59 (dd, 1H, $J=5.0$, 8.9 Hz, Phe¹ C^αH), 7.14—7.31 (m, 10H, Ar-H), 7.78 (br, 1H, $-\text{NH}^b\text{CO}-$), 8.73 (d, 1H, $J=8.5$ Hz, $-\text{NH}^b\text{CO}-$); $^{13}\text{C-NMR}$ ($\text{CDCl}_3/\text{DMSO-}d_6$) ppm 26.63 (C3), 29.03 (C6), 29.15 (C4), 29.26 (C2, 5), 37.88 (C1), 38.20 (Phe¹ C^β), 39.10 (Phe² C^β), 54.37 (Phe² C^α), 54.58 (Phe¹ C^α), 126.43 (p), 126.88 (p'), 128.08 (o), 128.37 (o'), 129.27 (m), 129.44 (m'), 135.41 (i), 137.47 (i'), 169.38 ($-\text{NH}^b\text{CO}-$), 170.54 ($-\text{NH}^b\text{CO}-$); IR (KBr) 3280, 1630 cm^{-1} ; FAB-MS (nitrobenzyl alcohol) m/z 790 ($\text{M}^+ + 1$).

1,12-Dodecano-bis(L-Phe-L-Phe-L-Leu) (**10a**): Colorless solid; $[\alpha]_D^{25}$ -22.4 ($c=0.078$, MeOH); $^1\text{H-NMR}$ (signal assignments from the spectra of H-H COSY at 500 Mz, CDCl_3) δ 0.86 (d, 3H, $J=10.4$ Hz, Leu Me), 0.88 (d, 3H, $J=10.4$ Hz, Leu Me), 1.11—1.36 (m, 10H, $-(\text{CH}_2)_5 \times 5$), 1.50—1.58 (m, 1H, Leu C^γH), 2.85—3.04 (m, 2H, Phe² C^βH), 3.06—3.19 (m, 7H, $-\text{C}^1\text{H}_2-$, Leu C^βH , Phe¹ C^βH , Phe² C^βH), 4.58 (m, 3H, $J=7.4$, 8.4 Hz, Leu C^αH , Phe¹ C^αH , Phe² C^αH), 6.08 (brs, 1H, $-\text{NH}^b\text{CO}-$), 6.59 (d, 1H, $J=8.4$ Hz, $-\text{NH}^b\text{CO}-$), 7.04—7.31 (m, 10H, Ar-H), 7.82 (d, 1H, $J=7.4$ Hz, $-\text{NH}^b\text{CO}-$); $^{13}\text{C-NMR}$ (signal assignments from the spectra of C-H COSY at 500 Mz, CDCl_3) ppm 21.48 (Leu Me), 23.25 (Leu Me), 24.83 (C3), 26.83 (Leu C^γ), 29.24 (C4, 5, 6), 29.47 (C2), 37.52 (C1), 37.87 (Leu C^β), 39.69 (Phe¹ C^β), 43.80 (Phe² C^β), 53.43 (Leu C^α), 54.13 (Phe² C^α), 54.25 (Phe¹ C^α), 126.70 (p), 127.00 (p'), 128.46 (o), 128.58 (o'), 129.28 (m), 129.40 (m'), 136.56 (i), 136.79 (i'), 170.14 ($-\text{NH}^b\text{CO}-$), 170.73 ($-\text{NH}^b\text{CO}-$), 176.13 ($-\text{NH}^b\text{CO}-$); IR (KBr) 3280, 1630 cm^{-1} ; FAB-MS (nitrobenzyl alcohol) m/z 1016 ($\text{M}^+ + 1$). Anal. Calcd for $\text{C}_{66}\text{H}_{86}\text{N}_8\text{O}_6 \cdot 1/2\text{H}_2\text{O}$: C, 70.35;

H, 8.56; N, 10.94. Found: C, 70.61; H, 8.49; N, 11.00.

1,12-Dodecano-bis(L-Phe-L-Phe-L-Val) (**10b**): Colorless solid; $^1\text{H-NMR}$ ($\text{CDCl}_3/\text{DMSO-}d_6$) δ 0.86 (d, 3H, $J=6.7$ Hz, Val Me), 0.90 (d, 3H, $J=7.0$ Hz, Val Me), 1.15—1.35 (m, 10H, $-(\text{CH}_2)_5 \times 5$), 2.11 (m, 1H, Val C^βH), 2.88—2.96 (m, 1H, Phe² C^βH), 3.01—3.28 (m, 5H, $-\text{C}^1\text{H}_2-$, Phe¹ C^βH , Phe² C^βH), 3.58 (d, 1H, $J=5.2$ Hz, Val C^αH), 4.52—4.67 (m, 2H, Phe¹ C^αH , Phe² C^αH), 7.14—7.26 (m, 10H, Ar-H), 7.96 (d, 1H, $J=8.2$ Hz, $-\text{NH}^b\text{CO}-$), 8.57 (d, 1H, $J=7.9$ Hz, $-\text{NH}^b\text{CO}-$); $^{13}\text{C-NMR}$ ($\text{CDCl}_3/\text{DMSO-}d_6$) ppm 16.03 (Val Me), 19.43 (Val Me), 26.71 (C3), 29.12 (C4, 5, 6), 29.34 (C2), 30.71 (Val C^β), 37.75 (C1), 39.10 (Phe¹, Phe² C^β), 54.01 (Val C^α), 56.24 (Phe² C^α), 60.06 (Phe¹ C^α), 126.40 (p), 128.11 (o), 128.22 (o'), 129.10 (m), 129.22 (m'), 136.85 (i), 137.15 (i'), 170.26 ($-\text{NH}^b\text{CO}-$), 170.61 ($-\text{NH}^b\text{CO}-$), 174.66 ($-\text{NH}^b\text{CO}-$); IR (KBr) 3270, 1630 cm^{-1} ; FAB-MS (nitrobenzyl alcohol) m/z 988 ($\text{M}^+ + 1$).

1,12-Dodecano-bis(L-Phe-L-Val-L-Leu) (**10d**): Colorless solid; $[\alpha]_D^{25}$ -27.3 ($c=0.172$, MeOH); $^1\text{H-NMR}$ ($\text{CDCl}_3/\text{DMSO-}d_6$) δ 0.78 (d, 3H, $J=6.7$ Hz, Val Me), 0.83 (d, 3H, $J=6.7$ Hz, Val Me), 0.93 (t, 6H, $J=6.7$ Hz, Leu Me $\times 2$), 1.18—1.41 (m, 10H, $-(\text{CH}_2)_5 \times 5$), 1.55 (m, 2H, Val C^βH), 1.75 (m, 1H, Leu C^γH), 2.03 (m, 1H, Val C^βH), 2.91 (dd, 1H, $J=8.5$, 14.0 Hz, Phe C^βH), $-(\text{CH}_2)_2 \times 2$, 3.05—3.15 (overlap, 3H, $-\text{C}^1\text{H}_2-$, Phe C^βH), 3.44 (dd, 1H, $J=4.8$, 9.4 Hz, Leu C^αH), 4.16 (dd, 1H, $J=6.7$, 8.5 Hz, Val C^αH), 4.60 (dd, 1H, $J=8.5$, 14.3 Hz, Phe C^αH), 7.18—7.23 (m, 5H, Ar-H), 7.38 (t, 1H, $J=5.5$ Hz, $-\text{NH}^b\text{CO}-$), 7.76 (d, 1H, $J=8.5$ Hz, $-\text{NH}^b\text{CO}-$), 8.01 (d, 1H, $J=8.5$ Hz, $-\text{NH}^b\text{CO}-$); $^{13}\text{C-NMR}$ ($\text{CDCl}_3/\text{DMSO-}d_6$) ppm 17.76 (Ile Me), 19.19 (Ile Me), 21.48 (Leu Me), 23.23 (Leu Me), 24.34 (Leu C^γ), 26.62 (C3), 29.02 (C4), 29.06 (C5), 29.23 (C6), 29.28 (C2), 30.47 (Val C^β), 37.73 (C1), 39.09 (Leu C^β), 43.18 (Phe C^β), 53.04 (Leu C^α), 54.09 (Phe C^α), 58.09 (Val C^α), 126.26 (p), 128.03 (o), 129.15 (m), 137.44 (Ar-C), 170.62 ($-\text{NH}^b\text{CO}-$), 170.84 ($-\text{NH}^b\text{CO}-$), 174.70 ($-\text{NH}^b\text{CO}-$); IR (KBr) 3280, 1630 cm^{-1} ; FAB-MS (nitrobenzyl alcohol) m/z 920 ($\text{M}^+ + 1$).

1,12-Dodecano-bis(L-Leu-L-Leu-L-Phe) (**10f**): Colorless solid; $[\alpha]_D^{25}$ -44.0 ($c=0.217$, MeOH); $^1\text{H-NMR}$ (CDCl_3) δ 0.87—0.92 (overlap, 12H, Leu Me $\times 4$), 1.20—1.30 (m, 10H, $-(\text{CH}_2)_5 \times 5$), 1.52—1.74 (m, 6H, Leu $\text{C}^\gamma\text{H}_2 \times 2$, Leu $\text{C}^\beta\text{H} \times 2$), 2.74 (dd, 1H, $J=9.2$, 13.7 Hz, Phe C^βH), 3.18—3.22 (m, 3H, $-\text{C}^1\text{H}_2-$, Phe C^βH), 3.64 (dd, 1H, $J=4.0$, 9.2 Hz, Phe C^αH), 4.39—4.47 (overlap, 2H, Leu¹ C^αH , Leu² C^αH), 6.58 (t, 1H, $J=5.5$ Hz, $-\text{NH}^b\text{CO}-$), 6.96 (d, 1H, $J=8.4$ Hz, $-\text{NH}^b\text{CO}-$), 7.19—7.31 (m, 5H, Ar-H), 7.78 (d, 1H, $J=9.3$ Hz, $-\text{NH}^b\text{CO}-$); $^{13}\text{C-NMR}$ (CDCl_3) ppm 22.02 (Leu Me), 22.19 (Leu Me), 22.87 (Leu Me), 22.98 (Leu Me), 24.81 (Leu C^γ), 24.86 (Leu C^γ), 26.83 (C3), 29.15, 29.35, 29.41 (C2), 39.59 (C1), 40.74 (Leu $\text{C}^\beta \times 2$, 40.82 (Phe C^β), 51.85 (Leu¹ C^α), 51.89 (Leu² C^α), 56.18 (Phe¹ C^α), 126.90 (p), 128.72 (o), 129.32 (m), 137.48 (i), 171.60 ($-\text{NH}^b\text{CO}-$), 172.16 ($-\text{NH}^b\text{CO}-$), 174.70 ($-\text{NH}^b\text{CO}-$); IR (KBr) 3260, 1630 cm^{-1} ; FAB-MS (nitrobenzyl alcohol) m/z 948 ($\text{M}^+ + 1$).

1,12-Dodecano-bis(L-Leu-L-Phe-L-Phe) (**10g**): Colorless solid; $^1\text{H-NMR}$ ($\text{CDCl}_3/\text{DMSO-}d_6$) δ 0.89 (d, 3H, $J=6.4$ Hz, Leu Me), 0.93 (d, 3H, $J=6.4$ Hz, Leu Me), 1.53 (m, 2H, Leu $\text{C}^\beta\text{H} \times 2$), 1.64 (m, 1H, Leu C^γH), 2.93 (dd, 1H, $J=8.8$, 14.3 Hz, Phe² C^βH), 2.98 (dd, 1H, $J=8.8$, 14.3 Hz, Phe³ C^βH), 3.07 (dd, 2H, $J=6.4$, 13.4 Hz, $-\text{C}^1\text{H}_2-$), 3.11 (dd, 1H, $J=5.5$, 13.7 Hz, Phe² C^βH), 3.20 (dd, 1H, $J=5.2$, 14.3 Hz, Phe³ C^βH), 4.07 (dd, 1H, $J=5.0$, 8.0 Hz, Phe³ C^αH), 4.36 (ddd, 1H, $J=5.8$, 8.24, 14.6 Hz, Phe¹ C^αH), 4.66 (ddd, 1H, $J=5.8$, 8.24, 13.7 Hz, Phe² C^αH), 7.17—7.28 (m, 10H, Ar-H), 7.38 (t, 1H, $J=5.5$ Hz, $-\text{NH}^b\text{CO}-$), 8.07 (t, 1H, $J=8.2$ Hz, $-\text{NH}^b\text{CO}-$), 8.86 (t, 1H, $J=8.2$ Hz, $-\text{NH}^b\text{CO}-$); $^{13}\text{C-NMR}$ ($\text{CDCl}_3/\text{DMSO-}d_6$) ppm 21.87 (Leu Me), 22.97 (Leu Me), 24.46 (C3), 26.63 (Leu C^γ), 29.02 (C4), 29.18 (C5), 29.26 (C2, 6), 37.18 (Leu¹ C^β), 37.76 (C1), 39.03 (Phe² C^β), 41.26 (Phe³ C^β), 51.72 (Leu¹ C^α), 53.89 (Phe² C^α), 54.92 (Phe³ C^α), 126.41 (p), 127.14 (p'), 128.14 (o), 128.50 (o'), 129.33 (m), 129.57 (m'), 134.77 (i), 137.23 (i'), 168.25 ($-\text{NH}^b\text{CO}-$), 170.25 ($-\text{NH}^b\text{CO}-$), 171.76 ($-\text{NH}^b\text{CO}-$); FAB-MS (nitrobenzyl alcohol) m/z 1016 ($\text{M}^+ + 1$).

1,2-Ethano-bis(L-Phe) **12a**: 93.0% yield; mp 116—118 °C (from ether/MeOH); R_f (B) 0.26. 1,2-Ethano-bis(L-Leu) **12b**: 96.7% yield; oil; R_f (B) 0.26. 1,2-Ethano-bis(D-Leu) **12c**: 89.8% yield; mp 97—98 °C; R_f (B) 0.22. 1,2-Ethano-bis(L-Phe-L-Phe) **14a**: 98.0% yield; mp 206—208 °C; R_f (B) 0.44. 1,2-Ethano-bis(L-Phe-D-Phe) **14b**: 95.0% yield; mp 203—206 °C; R_f (B) 0.21. 1,2-Ethano-bis(L-Phe-L-Phe-L-Leu) **16a**: 95.0% yield; mp 249—250 °C (from MeOH); R_f (B) 0.48. 1,2-Ethano-bis(L-Phe-L-Phe-L-Val) **16b**: 94.7% yield; mp 249—251 °C (from MeOH); TLC R_f (B) 0.33.

Synthesis of 1,2-Ethano-bis(L-Phe-L-Phe-L-Val) (16b) To N_α -Boc protected **15b** (0.732 g, mmol) anhydrous TFA (6 ml) was added dropwise over a period of 0.5 min. The mixture was stirred at 4 °C for 60 min, and then was poured into ice/water, and adjusted to pH 7 with 5% NaHCO_3 . The resulting solid was collected, washed with water, and dried *in vacuo*: 94.7% yield. The product was purified with silica gel (50 g) column chromatogra-

phy eluting with 2% MeOH/CHCl₃ and 10% MeOH/CHCl₃ (stepwise elution) to give **16b** as a colorless crystals; mp 249–251 °C (from MeOH); TLC *R_f* (B) 0.33; ¹H-NMR (CDCl₃/DMSO-*d*₆) δ 0.586 (d, 3H, *J*=6.7 Hz, Val Me), 0.777 (d, 3H, *J*=6.7 Hz, Val Me), 1.90 (m, 1H, Val C^βH), 2.81 (dd, 1H, *J*=5.0, 13.7 Hz, Phe² C^βH), 2.88 (dd, 1H, *J*=8.6, 13.7 Hz, Phe¹ C^βH), 2.99 (d, 2H, *J*=4.9 Hz, Phe C^βH), 3.02 (dd, 1H, *J*=5.5, 9.0 Hz, Val C^αH), 3.08 (m, 2H, –C¹H₂–), 4.48 (ddd, 1H, *J*=5.5, 8.3, 8.3 Hz, Phe² C^αH), 4.59 (m, 1H, Phe¹ C^αH), 7.13–7.25 (m, 10H, Ar-H), 7.73 (brs, 1H, –NH²CO–), 7.96 (brs, 1H, –NH²CO–), 8.07 (d, 1H, *J*=8.2 Hz, –NH²CO–); ¹³C-NMR (CDCl₃/DMSO-*d*₆) ppm 16.76 (Val Me), 19.80 (Val Me), 31.19 (Val C^β), 38.03 (C1), 38.80 (Phe C^β), 39.19–41.24 (Leu and Phe C^β, overlap with DMSO-*d*₆), 53.97 (Val C^α), 54.58 (Phe² C^α), 60.37 (Phe¹ C^α), 126.58 (p), 128.35 (o), 129.56 (m), 137.75 (i), 137.93 (i'), 171.21 (–NH²CO–), 171.30 (–NH²CO–), 174.70 (–NH²CO–); FAB-MS (nitrobenzyl alcohol) *m/z* 848 (M⁺ + 1).

1,2-Ethano-bis(L-Phe-L-Phe) (**14a**): Colorless solid; ¹H-NMR (CDCl₃) δ 2.44 (dd, 1H, *J*=9.5, 13.7 Hz, Phe² C^βH), 2.98 (dd, 1H, *J*=7.3, 13.6 Hz, –C¹H₂–), 3.05 (dd, 1H, *J*=7.3, 13.4 Hz, –C¹H₂–), 3.08 (m, 1H, Phe¹ C^βH), 3.10 (dd, 1H, *J*=3.7, 13.7 Hz, Phe² C^βH), 3.19 (m, 1H, Phe¹ C^βH), 3.61 (dd, 1H, *J*=3.7, 9.6 Hz, Phe² C^αH), 4.50 (ddd, 1H, *J*=7.6, 7.8, 7.8 Hz, Phe¹ C^αH), 6.23 (brs, 1H, –NH²CO–), 7.14–7.17, 7.28–7.32 (m, 10H, Ar-H), 7.77 (d, 1H, *J*=8.2 Hz, –NH²CO–); ¹³C-NMR (CDCl₃) ppm 38.1 (C1), 39.4 (Phe¹ C^β), 40.7 (Phe² C^β), 54.2 (Phe² C^α), 56.4 (Phe¹ C^α), 126.9 (p), 127.1 (p), 128.7 (o), 129.4 (m), 136.8 (i) and 137.6 (i'), 171.6 (–NH²CO–), 174.7 (–NH²CO–); FAB-MS (nitrobenzyl alcohol) *m/z* 650 (M⁺ + 1).

1,2-Ethano-bis(L-Phe-D-Phe) (**14b**): Colorless solid; ¹H-NMR (CDCl₃/DMSO-*d*₆=0.5/0.2) δ 2.67 (dd, 1H, *J*=7.9, 14.0 Hz, Phe² C^βH), 2.83 (dd, 1H, *J*=9.5, 13.7 Hz, Phe¹ C^βH), 2.90 (dd, 1H, *J*=5.5, 13.7 Hz, Phe² C^βH), 3.09 (dd, 1H, *J*=5.2, 13.7 Hz, Phe¹ C^βH), 3.20 (m, 2H, –C¹H₂–), 3.94 (dd, 1H, *J*=6.1, 7.3 Hz, Phe² C^αH), 4.53 (ddd, 1H, *J*=5.2, 8.0, 8.9 Hz, Phe¹ C^αH), 6.99–7.02 (m, 2H, *o*-protons), 7.16–7.24 (m, 4H, Ar-H), 7.94 (m, 1H, –NH²CO–), 8.79 (d, 1H, *J*=8.0 Hz, –NH²CO–); FAB-MS (nitrobenzyl alcohol) *m/z* 650 (M⁺ + 1).

1,2-Ethano-bis(L-Phe-L-Phe-L-Leu) (**16a**): Colorless solid; ¹H-NMR (CDCl₃/DMSO-*d*₆) δ 0.788 (d, 3H, *J*=6.7 Hz, Leu Me), 0.824 (d, 3H, *J*=6.7 Hz, Leu Me), 1.11 (ddd, 1H, *J*=5.3, 8.9, 13.8 Hz, Leu C^βH), 1.27 (ddd, 1H, *J*=5.0, 8.6, 13.6 Hz, Leu C^βH), 1.58 (m, 1H, Leu C^γH), 2.78 (dd, 1H, *J*=8.6, 13.7 Hz, Phe² C^βH), 2.84 (dd, 1H, *J*=8.9, 13.7 Hz, Phe¹ C^βH), 2.98 (dd, 2H, *J*=5.0, 13.6 Hz, Phe¹, Phe² C^βH), 3.03 (m, 2H, –C¹H₂–), 3.18 (dd, 1H, *J*=5.2, 9.2 Hz, Leu C^αH), 4.43 (ddd, 1H, *J*=5.8, 8.2, 8.2 Hz, Phe¹ C^αH), 4.54 (m, 1H, Phe² C^αH), 7.13–7.27 (m, 10H, Ar-H), 7.93 (t, 1H, *J*=4.4 Hz, –NH²CO–), 8.06 (brs, 1H, –NH²CO–), 8.25 (d, 1H, *J*=8.2 Hz, –NH²CO–); ¹³C-NMR (CDCl₃/DMSO-*d*₆) ppm 21.5, 23.1 (Leu Me), 23.7 (Leu C^γ), 37.6 (Phe C^β), 37.6 (Phe C^β), 38.0 (C1), 43.2 (Leu C^β), 52.6 (Leu C^α), 54.0 (Phe¹, Phe² C^α), 126.1 (p), 126.2 (p), 127.8 (o), 128.0 (o), 129.1 (m), 129.2 (m), 137.3 (i), 137.58 (i'), 170.5 (–NH²CO–), 170.7 (–NH²CO–), 174.1 (–NH²CO–); FAB-MS (nitrobenzyl alcohol) *m/z* 898 (M⁺ + Na).

The following single-stranded peptides, **17a**–**19a** were prepared from deprotection (Pd/C–H₂ or TFA) of the corresponding Z(or Boc)-protected amino acid similarly to the above described method. Lauryl-L-Phe **17a**: 88.2% yield; mp 51–52 °C (from hexane); *R_f* (B) 0.49. Lauryl-L-Phe-L-PheH (**18a**): 85.0% yield; mp 99–100 °C (from hexane/CHCl₃); *R_f* (B) 0.64. Lauryl-L-Phe-L-Phe-L-Leu (**19a**): 67.7% yield; mp 139–140 °C (from hexane/CHCl₃); *R_f* (B) 0.50.

Synthesis of the Lauryl-L-Phe-L-PheNH₂ (**18a**): Colorless solid; ¹H-NMR (CDCl₃) δ 0.88 (t, 3H, *J*=6.8 Hz, Me), 1.25–1.39 (m, 10H, –(CH₂)₁₀–), 2.49 (dd, 1H, *J*=9.3, 13.7 Hz, Phe² C^βH), 2.95–3.06 (m, 1H, Phe¹ C^βH), 3.10–3.19 (m, 1H, Phe¹ C^βH), 3.10–3.19 (m, 1H, Phe² C^βH), 3.10–3.19 (m, 2H, C¹H), 3.57 (dd, 1H, *J*=3.9, 9.3 Hz, Phe² C^αH), 4.56 (dd, 1H, *J*=8.3, 15.6 Hz, Phe¹ C^αH), 5.89 (brs, 1H, –NH²CO–), 7.14–7.34 (m, 10H, Ar-H), 7.83 (d, 1H, *J*=8.3 Hz, –NH²CO–); ¹³C-NMR (CDCl₃) ppm 14.13 (Me), 22.69 (C10, 11), 26.80 (C9), 29.25 (C8), 29.32 (C7), 29.35 (C6), 29.52 (C5), 29.60 (C4), 29.66 (C3), 31.92 (C2), 38.18 (C1), 39.51 (Phe¹ C^β), 40.72 (Phe² C^β), 54.46 (Phe² C^α), 56.28 (Phe¹ C^α), 126.89 (p), 128.58 (o), 128.73 (m), 136.97, 137.58 (Ar-C), 170.54 (–NH²CO–), 174.49 (–NH²CO–); FAB-MS (nitrobenzyl alcohol) *m/z* 480 (M⁺ + 1).

Lauryl-L-Phe-L-Phe-L-LeuNH₂ (**19a**): Colorless solid; ¹H-NMR (CDCl₃) δ 0.85 (d, 3H, *J*=6.4 Hz, Leu Me), 0.88 (m, 3H, Me), 0.89 (d, 3H, *J*=6.4 Hz, Leu Me), 1.16–1.34 (m, 20H, –(CH₂)₁₀–), 1.53 (m, 1H, Leu C^γH), 2.87 (dd, 1H, *J*=7.0, 13.7 Hz, Phe² C^βH), 3.01–3.20 (overlap, 7H, Phe¹ C^βH, Phe² C^βH, Leu C^βH, –C¹H₂–), 4.47–4.62 (overlap, 3H, Phe¹ C^αH, Phe² C^αH, Leu C^αH), 5.92 (br, 1H, –NH²CO–), 6.37 (d, 1H, *J*=8.2 Hz, –NH²CO–), 7.02–7.33 (m, 10H, Ar-H), 7.80 (d, 1H, *J*=7.3 Hz, –NH²CO–); ¹³C-NMR (CDCl₃) ppm 14.13 (Me), 21.24 (Leu Me), 22.69 (Leu Me), 23.27

(C10, 11), 24.71 (C9), 26.82 (Leu C^γ), 29.22 (C8), 29.31 (C7), 29.35 (C6), 29.56 (C5), 29.64 (C4), 29.67 (C3), 31.92 (C2), 37.10 (Phe¹ C^β), 37.59 (C1), 39.64 (Phe² C^β), 43.41 (Leu C^β), 53.14 (Leu C^α), 53.76 (Phe² C^α), 54.29 (Phe¹ C^α), 126.77 (p), 127.13 (p), 128.50 (o), 128.70 (o), 129.28 (m), 129.40 (m), 136.39 (i), 136.62 (i'), 170.00 (–NH²CO–), 170.54 (–NH²CO–), 176.31 (–NH²CO–); FAB-MS (nitrobenzyl alcohol) *m/z* 593 (M⁺ + 1).

CD Measurements The CD spectra of **8a**–**d**–**10a**–**h** and **19a** were measured on a JASCO J-720 spectrophotometer. Measurements were made in a 1 cm path length in 85% methanol, circular quartz cell at ambient temperature. The CD spectra are shown in Figs. 3–5 with molar ellipticity, [θ], versus wavelength, λ(nm).

¹H-NMR Titrations All ¹H-NMR titration were run at 296 K. ¹H-NMR spectra were taken for each tube and δ values were calculated by subtracting the chemical shift (δ_x) of interest in the spectrum of the mixtures from two α protons (–Phe¹ C^αH, –Phe² C^αH) and two-three amido protons (δ₀) (–NH²CO–, –NH²CO–, or –NH²CO–) in the spectrum of double-stranded peptides **8a**, **8e**, **8f**, **10a**, **10g**, **14a**, **14b**, and **16a** in CDCl₃. In 2 separate NMR tubes 9.0 mg of **8a** and 1.0/0 and 0.5 ml/0.2 ml of the mixture solution of CDCl₃ and DMSO-*d*₆ were added. Concentration ranges for the NMR titrations are as follows: (a) In **8a**, [8a]=1.63×10^{–2} M. (b) In **8e** and **8f**, [8e, f]=1.60×10^{–2} M. (c) In **10a**, **14a**–**b**, and **16a**, [10a], [14a–b], [16a]=1.0–1.27×10^{–2} M.

Binding Studies UV data were collected on a JASCO U-best 30 spectrophotometer in a 10 mm quartz cell in methanol. The value of association constant (*K_a*) was the average of the mean values obtained in the evaluation of the three individual λ (nm). The concentrations of double-stranded peptides, **8a**, **8b**, **10a**, and **10c**, varied as follows: In **8a** and pyrene, [pyrene]=6.625×10^{–6} M. [8a]=0.0, 0.496, 0.992, 1.98, 3.97, 5.96, 7.94 (×10^{–4} M). In **8b** and azobenzene, [azobenzene]=2.11×10^{–5} M. [8b]=0.0, 0.998, 9.98, 59.9 (×10^{–5} M). In **10a** and azobenzene, [azobenzene]=1.758×10^{–5} M. [8b]=0.0, 0.129, 0.259, 0.648, 1.29, 1.943 (×10^{–3} M). In **10c** and PHA, [PHA]=8.05×10^{–5} M, [10c]=0.0, 0.955, 1.91, 3.82, 9.55, 19.09 (×10^{–4} M). In **14a** and azobenzene, [azobenzene]=2.857×10^{–5} M, [14a]=0.0, 0.868, 3.47, 8.68, 13.02 (×10^{–4} M). In **16a** and azobenzene, [azobenzene]=2.857×10^{–5} M, [16a]=0.0, 0.135, 2.70, 8.10, 13.50 (×10^{–4} M).

Energy Calculation The energy calculations were performed by using the CS software with MM2 to determine a minimum energy conformation (local minimum) of mini double-stranded peptides, and by assuming fixed dihedral angle (∠C5–C6–C7–C8, θ (degree)) in dodecano spacer.

Acknowledgements This work was supported by a part of Special Coordination Funds from the Science and Technology Agency(Japan).

References and Notes

- 1) a) Mutter M., *Angew. Chem. Int. Ed. Engl.*, **24**, 639–653 (1985); b) Sibanda B. L., Blundel T. L., Thornton J. M., *J. Mol. Biol.*, **206**, 759–777 (1989); c) Creighton T. E., "Proteins: Structures and Molecular Principle," 2nd ed., Freeman W. H. and Co., New York, 1993; d) Ramirez-Alvarado M., Kortemme T., Blanco F. J., Serrano L., *Bioorg. Med. Chem.*, **7**, 93–103 (1999).
- 2) a) Suzuki M., *J. Mol. Biol.*, **207**, 61–84 (1990); b) Harding M. M., *J. Med. Chem.*, **35**, 4658–4664 (1992).
- 3) a) Barrow C. J., Yasuda A., Kenny P. T., Zagorski M. G., *J. Mol. Biol.*, **225**, 1075–1093 (1992); b) Sticht H., Bayer P., Willbold D., Dammes S., Hilbich C., Beyreuther K., Frank R. W., Rosch P., *Eur. J. Biochem.*, **233**, 293–298 (1995).
- 4) a) Somers W. S., Philips S. E. V., *Nature (London)* **359**, 387–393 (1992); b) Maynard A. J., Searle M. S., *Chem. Commun.*, **1997**, 1297–1298.
- 5) Ovchinnikov Y. A., Ivanov V. T., *Tetrahedron*, **31**, 2177–2209 (1975).
- 6) a) Hopkins R. B., Hamilton A. D., *J. Chem. Soc., Chem. Commun.*, **1987**, 171–173; b) Diaz H., Tsang K. Y., Choo D., Espina J. R., Kelly J. W., *J. Am. Chem. Soc.*, **118**, 3790–3791 (1996); c) Nowick J. S., Holmes D. L., Mackin G., Noronha G., Shaka A. J., Smith E. M., *ibid.*, **118**, 2764–2765 (1996); d) Austin R. E., Maplestone R. A., Sefler A. M., Liu K., Hruzewicz W. N., Liu C. W., Cho H. S., Wemmer D. E., Bartlett P. A., *ibid.*, **119**, 6461–6472 (1997); e) Raghothama S. R., Awasthi S. K., Balaram P., *J. Chem. Soc., Perkin Trans. 2*, **1998**, 137–143.
- 7) The steric energy calculations were performed using the CS Chem 3D pro with MM2 force field. Allinger N. L., *J. Comput. Chem.*, **14**, 755–768 (1993).
- 8) Anderson G. W., Paul R., *J. Am. Chem. Soc.*, **80**, 4423 (1958).
- 9) Takuma S., Hamada Y., Shioiri T., *Chem. Pharm. Bull.*, **30**, 3147–

- 3153 (1982).
- 10) a) Bandekar J., Evans D. J., Krimm S., Leach S. J., Lee S., McQuie J. R., Minasian E., Nemethy E., Pottle M. S., Scheraga H. A., Stimson E. R., Woody R. W., *Int. J. Pept. Protein Res.*, **19**, 187—205 (1982); b) Woody R. W., *Meth. Enzymol.*, **246**, 34—71 (1995).
- 11) a) Blout E. R., Schmier I., Simmons N. S., *J. Am. Chem. Soc.*, **84**, 3193—3194 (1962); b) Bush C. A., Sarkar S. K., Kopple K. D., *Biochemistry*, **17**, 4951—4954 (1978); c) Akamatsu M., Fujita T., *J. Pharm. Sci.*, **81**, 164—173 (1992).
- 12) Raghothama S., Chaddha M., Balaram P., *J. Phys. Chem.*, **100**, 19666—19671 (1996).
- 13) Bour P., *J. Phys. Chem. A*, **103**, 5099—5104 (1999).
- 14) Sheinerman F. B. and Brooks C. L., *J. Am. Chem. Soc.*, **117**, 10098—10103 (1995).
- 15) Hoch J. C., Dodson C. M., Karplus M., *Biochemistry*, **24**, 3831—3841 (1985).
- 16) The corresponding ϕ - and ω -angles (degree) were calculated from the equation $^3J_{\alpha N} = 6.4 \cos \theta - 1.4 \cos \theta + 1.9$ ($\theta = \phi - 60$).¹⁵⁾
- 17) 1,2-Ethano-bis(p-Leu) gave crystals suitable for X-ray analysis. Crystallographic analysis; cell constants and an orientation matrix for data collection corresponded to a primitive orthorhombic cell with dimensions: $a = 11.375 \text{ \AA}$, $b = 15.857 \text{ \AA}$, $c = 9.761 \text{ \AA}$, and $V = 1760.6400 \text{ \AA}^3$.
- 18) Wuthrich K., "NMR of Proteins and Nucleic Acids," John Wiley and Sons, New York, 1986.
- 19) Nagakura S., *J. Am. Chem. Soc.*, **76**, 3070—3073 (1954).

Synthesis of Diaryl-Substituted Imidazo[1,2-*a*]pyridines Designed as Potential Aromatase Inhibitors

Cécile ENGUEHARD,^a Jean-Louis RENOU,^a Hassan ALLOUCHI,^b Jean-Michel LEGER,^c and Alain GUEIFFIER^{*,a}

Laboratoire de Chimie Thérapeutique, UFR des Sciences Pharmaceutiques,^a 31 Av Monge, 37200 Tours, France, Laboratoire de Chimie Physique, UFR des Sciences Pharmaceutiques,^b 31 Av Monge, 37200 Tours, France, and Laboratoire de Chimie Physique et Radiocristallographie, Université Bordeaux II,^c Place de la Victoire, 33000 Bordeaux, France. Received December 13, 1999; accepted March 6, 2000

From a pharmacophore model of bicyclic heterocycles as aromatase inhibitors we have designed three series of imidazo[1,2-*a*]pyridine derivatives. The synthesis and the spectroscopy determination of various compounds are reported. The crystal data of one of these compounds (10b) was obtained. The aromatase inhibition potency was evaluated *in vitro* and no activity was found.

Key words non-steroidal P450 aromatase inhibitors; imidazo[1,2-*a*]pyridine; synthesis; crystal structure

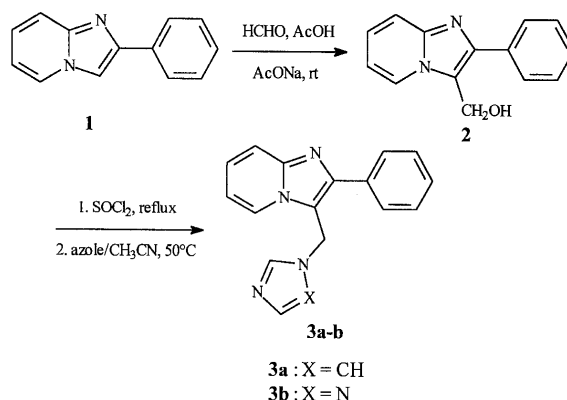
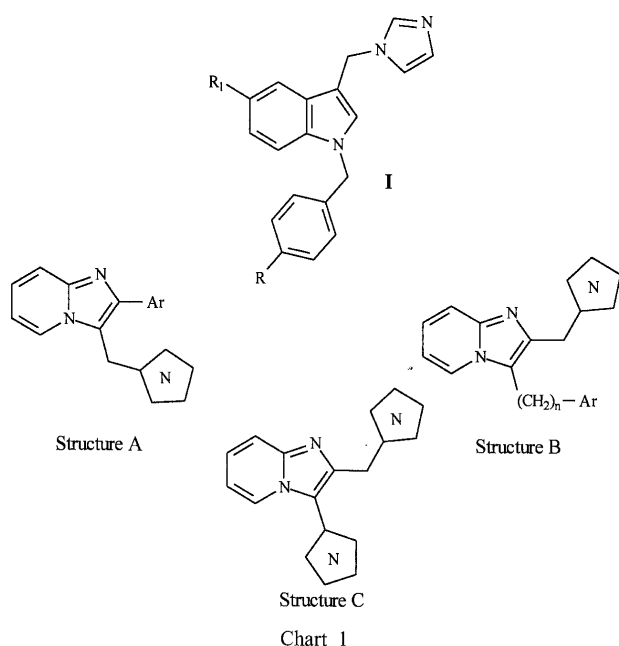
As part of our studies concerning the chemistry of imidazo[1,2-*a*]pyridine structures,¹⁾ we are developing now a program for the design and the preparation of compounds as potential inhibitors of cytochrome P450 aromatase. Non-steroidal aromatase inhibitors are known to prevent estrogen biosynthesis and their implication in the treatment of estrogen dependent diseases such as breast cancer is increasing.²⁾ The present study was based on the pharmacophore model designed by Rault's group³⁾ to fit the catalytic site of the human enzyme. This model consisted of a bicyclic skeleton bearing an azine group for interacting with the heme iron atom and an aryl group that is known to favour this interaction by occupying the extra-hydrophobic pocket located in the active site. Concomitantly, a series of 3-(azol-1-ylmethyl)-1*H*-indoles I revealed potent *in vitro* P450 aromatase inhibition (Chart 1).⁴⁾ These results led us to investigate the aromatase inhibition properties of new aryl-substituted imidazo[1,2-*a*]pyridine derivatives following the structural requirements of the pharmacophore model. The azole fragment was alternatively introduced on the 2- and 3-positions of the

imidazo[1,2-*a*]pyridine leading to structures A and B. A di-heteroaryl compound (structure C) was also included in this study.

Results and Discussion

The 3-hydroxymethylation of 2-phenylimidazo[1,2-*a*]pyridine **1**⁵⁾ was easily achieved using reaction with formaldehyde and sodium acetate in acetic acid media according to our previously described procedure.⁶⁾ The transformation of the expected alcohol **2** into the azolyl compounds **3a–b** was carried out through a treatment with refluxing thionyl chloride, followed by attack of the intermediary chloro derivative with imidazole or triazole in acetonitrile at 50 °C for 48 h (Chart 2). The structure of the imidazolyl compound **3a** was easily demonstrated from NMR spectra. In the case of triazole derivative the 1 and 4 regioisomers could be formed. Usually the N-4 isomer gives a single signal in ¹H- and ¹³C-NMR while the N-1 derivative gives two signals for H-3'/C-3' and H-5'/C-5'.⁷⁾ The ¹H-NMR spectrum of **3b** in CDCl₃ presented a singlet at δ 8.05 for H-3' and H-5' while C-3' and C-5' resonate at δ 152.3 and 142.4. The ambiguity was solved by performing the ¹H-NMR spectrum in DMSO-*d*₆ that gave two singlets at δ 8.02 and 8.87 confirming **3b** to be the N-1 isomer.

Our second investigation was to incorporate the aryl group on the 3-position followed by the introduction of an imidazole ring on the 2-position to provide the geometric isomers.



* To whom correspondence should be addressed. e-mail: gueiffier@univ-tours.fr

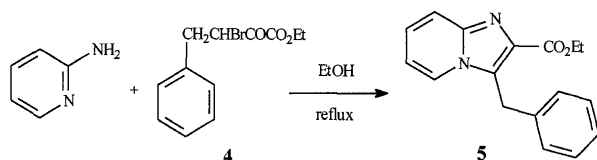


Chart 3

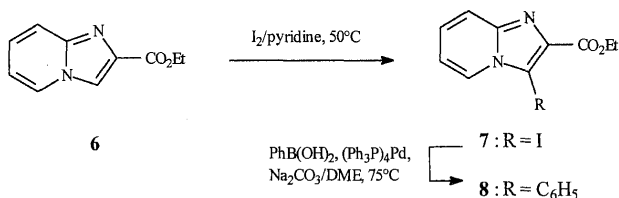


Chart 4

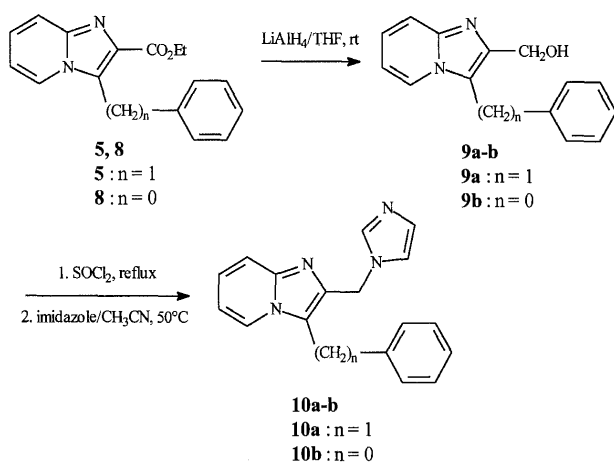


Chart 5

Commercially available ethyl 2-oxo-4-phenylbutyrate was readily brominated to give the α -bromocarbonyl intermediate **4** which was condensed as previously described⁵⁾ with 2-aminopyridine to yield **5** (Chart 3). Synthesis of the lesser homologue **8** through the same synthetic pathway was difficult due to the troublesome access to the ethyl 2-oxo-3-phenylpropanoate. Recently 3-arylation of imidazo[1,2-*a*]pyridine was achieved using Stille conditions⁸⁾ while we have studied the palladium catalyzed Suzuki-type cross coupling reaction.⁹⁾ We chose our strategy to introduce the 3-phenyl ring starting from the appropriate iodo intermediate **7** (Chart 4). This compound was obtained from ethyl imidazo[1,2-*a*]pyridine-2-carboxylate **6** using iodine in pyridine¹⁰⁾ in 46% yield. ¹³C-NMR spectrum of **7** was characterized by the C-3 signal high field shielding to 68 ppm. Suzuki reaction was performed using phenylboronic acid in the presence of sodium carbonate in DME at 75 °C for 0.5 h to give **8** (91% yield).⁹⁾

The ester function of **5** and **8** was reduced using lithium aluminium hydride in tetrahydrofuran at room temperature for 1 h (Chart 5). Proof of the structure was found in ¹H-NMR spectra. Depending on the CDCl₃ solution concentration, a variation of 0.4 ppm could be observed for the H-8 signal due to the formation of a hydrogen bond between the hydroxyl group and the N-1 atom. The substitution of the expected alcohols **9a–b** into the 2-(imidazol-1-ylmethyl)imidazo[1,2-*a*]pyridines **10a–b** was carried out using the syn-

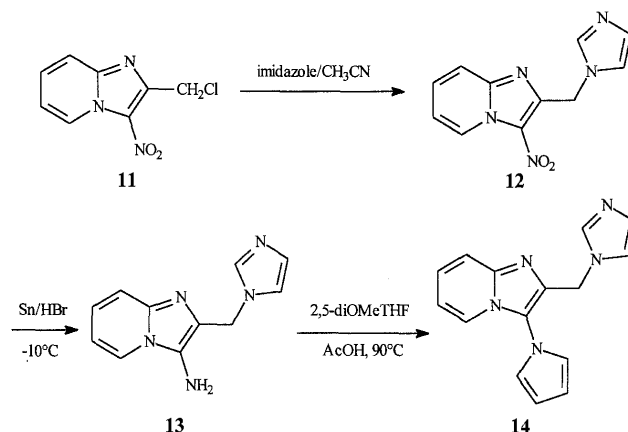


Chart 6

thetic pathway reported for **3a–b**.

Finally, in order to prepare diheteroaryl derivatives, we have changed the phenyl ring of **10b** to a pyrrole fragment (Chart 6). The 2-chloromethyl-3-nitroimidazo[1,2-*a*]pyridine **11**¹¹⁾ was first substituted with imidazole in acetonitrile and then reduced with tin in hydrobromic acid media.¹²⁾ The expected aminoderivative **13** was then involved in a Clauson-Kaas reaction,¹³⁾ using 2,5-dimethoxytetrahydrofuran in acetic acid but 2-(imidazol-1-ylmethyl)-3-(pyrrol-1-yl)imidazo[1,2-*a*]pyridine **14** was obtained in only poor yield.

With a view to further developing the structure–activity relationship study, we were then interested in the crystallographic data for one of the synthesized compounds. Our studies were focused on derivatives of structure B and a crystal of compound **10b** was obtained.

Crystal Structure The fractional coordinates and the equivalent thermal factors (U_{eq}) are listed in Table 1. The thermal ellipsoid representation and the labelling of non-hydrogen atoms of both conformations for one molecule is presented in Fig. 1.¹⁴⁾ The bond lengths and bond angles are given in Tables 2 and 3 respectively and agree quite well with the literature.¹⁵⁾ The interesting torsion angles which entirely define the molecule conformation are reported in Table 4.

The imidazo[1,2-*a*]pyridine ring $\sigma 1$ (atoms N1 to C8A), imidazole ring $\sigma 2$ (atoms N1' to C5'), and phenyl ring $\sigma 3$ (atoms C1'' to C6'') are planar with the dihedral angles reported in Table 5.

The packing of the molecule is shown in Fig. 2. There are numerous weak van der Waals interactions so the crystal cohesion is assumed through several hydrogen bonds (Fig. 3). The molecule I is involved in the following hydrogen bond between the OH group and N atoms (Table 6).

Conclusion

The present paper deals with the synthesis of 2,3-disubstituted imidazo[1,2-*a*]pyridine derivatives as potential aromatase inhibitors. On the basis of a pharmacophore model three types of structures were designed. From the synthesized compounds the crystal data obtained from **10b** was studied. Unfortunately the spatial structure showed the compound does not fit well with the proposed pharmacophore. This result was ascertained by determining the inhibition of the enzyme *in vitro* which showed that these compounds are inactive. Despite this fact, the crystal data of **10b** serve as a start

Table 1a. Atomic Coordinates and Equivalent U_{eq} Factors for Molecule I

	x/a	y/b	z/c	U_{eq}
O1	0.3666 (2)	0.0436 (2)	0.3202 (1)	0.0644 (4)
O2	0.5978 (2)	0.9606 (2)	0.2151 (1)	0.0725 (5)
O3	0.9144 (3)	0.9796 (2)	0.1802 (1)	0.0879 (6)
O4	0.0474 (3)	0.0788 (4)	0.2964 (1)	0.1246 (10)
N1	0.4676 (2)	0.2940 (2)	0.8292 (1)	0.0472 (4)
C2	0.5885 (2)	0.3468 (2)	0.8503 (1)	0.0426 (4)
C3	0.5548 (2)	0.4823 (2)	0.8639 (1)	0.0400 (4)
N4	0.4052 (2)	0.5148 (2)	0.8498 (1)	0.0400 (4)
C5	0.3096 (2)	0.6343 (2)	0.8562 (1)	0.0492 (5)
C6	0.1651 (2)	0.6365 (2)	0.8424 (1)	0.0574 (5)
C7	0.1117 (2)	0.5183 (2)	0.8222 (1)	0.0571 (5)
C8	0.2049 (2)	0.4002 (2)	0.8157 (1)	0.0532 (5)
C8A	0.3565 (2)	0.3970 (2)	0.8297 (1)	0.0433 (4)
C9	0.7338 (2)	0.2573 (2)	0.8577 (1)	0.0499 (5)
N1'	0.7382 (2)	0.1868 (2)	0.9323 (1)	0.0441 (4)
C2'	0.8617 (2)	0.1544 (2)	0.9671 (1)	0.0566 (5)
N3'	0.8291 (2)	0.0922 (2)	1.0336 (1)	0.0592 (5)
C4'	0.6761 (2)	0.0844 (2)	1.0410 (1)	0.0552 (5)
C5'	0.6190 (2)	0.1418 (2)	0.9798 (1)	0.0542 (5)
C1''	0.6426 (2)	0.5805 (2)	0.8900 (1)	0.0415 (4)
C2''	0.7155 (2)	0.5397 (2)	0.9518 (1)	0.0516 (5)
C3''	0.7976 (3)	0.6311 (3)	0.9772 (1)	0.0626 (6)
C4''	0.8061 (3)	0.7645 (3)	0.9424 (1)	0.0630 (6)
C5''	0.7349 (3)	0.8059 (2)	0.8809 (1)	0.0575 (5)
C6''	0.6545 (2)	0.7146 (2)	0.8547 (1)	0.0490 (5)

Table 1b. Atomic Coordinates and Equivalent U_{eq} Factors for Molecule II

	x/a	y/b	z/c	U_{eq}
N1	0.5664 (2)	0.6846 (2)	0.6751 (1)	0.0448 (4)
C2	0.4397 (2)	0.6437 (2)	0.6529 (1)	0.0406 (4)
C3	0.4616 (2)	0.5092 (2)	0.6373 (1)	0.0389 (4)
N4	0.6091 (2)	0.4643 (2)	0.6515 (1)	0.0387 (3)
C5	0.6940 (2)	0.3391 (2)	0.6447 (1)	0.0463 (5)
C6	0.8388 (2)	0.3246 (2)	0.6596 (1)	0.0544 (5)
C7	0.9033 (2)	0.4356 (2)	0.6812 (1)	0.0562 (5)
C8	0.8207 (2)	0.5589 (2)	0.6883 (1)	0.0508 (5)
C8A	0.6686 (2)	0.5745 (2)	0.6735 (1)	0.0417 (4)
C9	0.2988 (2)	0.7410 (2)	0.6508 (1)	0.0510 (5)
N1'	0.2817 (2)	0.8125 (2)	0.5774 (1)	0.0440 (4)
C2'	0.3900 (2)	0.8526 (2)	0.5239 (1)	0.0507 (5)
N3'	0.3333 (2)	0.9123 (2)	0.4648 (1)	0.0527 (4)
C4'	0.1807 (2)	0.9089 (2)	0.4819 (1)	0.0557 (5)
C5'	0.1465 (2)	0.8486 (2)	0.5506 (1)	0.0571 (5)
C1''	0.3650 (2)	0.4226 (2)	0.6078 (1)	0.0398 (4)
C2''	0.3422 (2)	0.2879 (2)	0.6396 (1)	0.0503 (5)
C3''	0.2546 (3)	0.2074 (2)	0.6100 (1)	0.0618 (6)
C4''	0.1865 (3)	0.2607 (3)	0.5487 (1)	0.0658 (6)
C5''	0.2054 (2)	0.3949 (3)	0.5176 (1)	0.0613 (6)
C6''	0.2946 (2)	0.4752 (2)	0.5464 (1)	0.0493 (5)

point in the design of further derivatives.

Experimental

Melting points were determined on a Kofler block and are uncorrected. ^1H -NMR and ^{13}C -NMR spectra were recorded on a Brüker DPX 200 MHz (50 MHz for ^{13}C). Splitting patterns have been designated as follows: s=singlet; bs=broad singlet; d=doublet; t=triplet; q=quartet; dd=doublet; m=multiplet. Analyses indicated by the symbols of the elements were within $\pm 0.5\%$ of the theoretical values. The organic solutions were dried over anhydrous calcium chloride. Previously reported imidazo[1,2-*a*]pyridines synthesized by the described procedure were: 2-phenylimidazo[1,2-*a*]pyridine (1),¹⁶ [2-phenylimidazo[1,2-*a*]pyridin-3-yl]methanol (2),⁶ ethyl imidazo[1,2-*a*]pyridine-2-carboxylate (6),¹⁷ 2-chloromethyl-3-nitroimidazo[1,2-*a*]pyridine (11).¹¹ Possible inversion of two values in the NMR spectra is expressed by an asterisk.

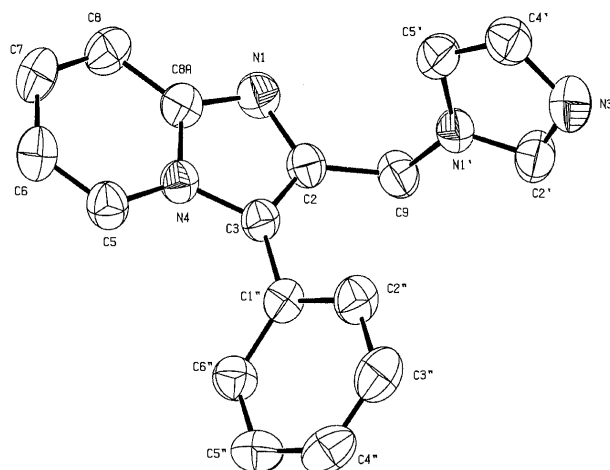
Fig. 1. Ellipsoid Representation (Probability 50%) of One Molecule and Atomic Labelling of **10b**

Table 2. Bond Lengths (Å) and Standard-Deviations in Parenthesis

	Molecule I	Molecule II
N1—C8A	1.333 (2)	1.332 (2)
N1—C2	1.370 (2)	1.372 (2)
C2—C3	1.374 (3)	1.369 (3)
C2—C9	1.495 (3)	1.493 (3)
C3—N4	1.392 (2)	1.391 (2)
C3—C1''	1.470 (3)	1.473 (3)
N4—C5	1.377 (2)	1.377 (2)
N4—C8A	1.385 (2)	1.382 (2)
C5—C6	1.347 (3)	1.347 (3)
C6—C7	1.408 (3)	1.408 (3)
C7—C8	1.355 (3)	1.354 (3)
C8—C8A	1.409 (3)	1.410 (3)
C9—N1'	1.468 (2)	1.468 (2)
N1'—C2'	1.342 (2)	1.339 (3)
N1'—C5'	1.358 (3)	1.363 (2)
C2'—N3'	1.313 (3)	1.313 (3)
N3'—C4'	1.363 (3)	1.358 (3)
C4'—C5'	1.341 (3)	1.343 (3)
C1''—C6''	1.389 (3)	1.390 (3)
C1''—C2''	1.391 (3)	1.393 (3)
C2''—C3''	1.381 (3)	1.378 (3)
C3''—C4''	1.377 (3)	1.381 (3)
C4''—C5''	1.378 (3)	1.375 (3)
C5''—C6''	1.378 (3)	1.379 (3)

Ethyl 3-Bromo-2-oxo-4-phenylbutyrate (4) To a solution of ethyl 2-oxo-4-phenylbutyrate (5 g, 24.2 mmol) in chloroform (30 ml) was added dropwise bromine (1.24 ml, 24.2 mmol). After stirring for 1 h at room temperature, the reaction mixture was washed with water (3×20 ml), dried and concentrated *in vacuo* to give a translucent oil (87%); ^1H -NMR (CDCl_3) δ : 7.44–7.32 (5H, m, Ph); 5.36 (1H, m, CH); 4.45 (2H, q, $J=7.1$ Hz, CH_2); 3.62 (1H, m, AB system, CH_2); 3.33 (1H, m, AB system, CH_2); 1.46 (3H, t, CH_3); *Anal.* Calcd for $\text{C}_{12}\text{H}_{13}\text{BrO}_3$: C, 50.55; H, 4.60. Found: C, 50.21; H, 4.72.

Ethyl 3-Benzylimidazo[1,2-*a*]pyridine-2-carboxylate (5) A solution of 2-aminopyridine (0.66 g, 7.0 mmol) and ethyl 3-bromo-2-oxo-4-phenylbutyrate (2.4 g, 8.4 mmol) was refluxed in ethanol (50 ml) for 4 h. After cooling, the solution was concentrated *in vacuo*, poured into water and made alkaline with sodium carbonate. The aqueous layer was extracted with dichloromethane. The combined and dried organic phases were evaporated to dryness and the residue chromatographed on neutral alumina eluting with dichloromethane to give colorless crystals (51%); mp 88 °C; ^1H -NMR (CDCl_3) δ : 7.85 (1H, d, $J_{\text{H-5 H-6}}=6.8$ Hz, H-5); 7.72 (1H, d, $J_{\text{H-7 H-8}}=9.0$ Hz, H-8); 7.31–7.23 (6H, m, Ph, H-7); 6.81 (1H, t, $J_{\text{H-6 H-7}}=6.8$ Hz, H-6); 4.79 (2H, s, CH_2); 4.57 (2H, q, $J=7.1$ Hz, CH_2); 1.50 (3H, t, CH_3); ^{13}C -NMR

Table 3. Bond Angles (°) and Standard-Deviations in Parenthesis

	Molecule I	Molecule II
C8A-N1-C2	105.42 (15)	105.35 (15)
N1-C2-C3	111.93 (16)	111.83 (16)
N1-C2-C9	120.16 (17)	128.14 (18)
C3-C2-C9	127.88 (18)	119.98 (17)
C2-C3-N4	104.54 (16)	104.72 (15)
C2-C3-C1''	132.44 (17)	132.14 (16)
N4-C3-C1''	122.99 (16)	123.05 (16)
C5-N4-C8A	121.80 (16)	121.58 (16)
C5-N4-C3	130.74 (16)	131.08 (16)
C8A-N4-C3	107.38 (15)	107.31 (14)
C6-C5-N4	118.94 (19)	118.99 (18)
C5-C6-C7	120.7 (2)	120.79 (19)
C8-C7-C6	120.77 (19)	120.73 (19)
C7-C8-C8A	118.97 (19)	118.81 (19)
N1-C8A-N4	110.72 (16)	110.78 (16)
N1-C8A-C8	130.46 (18)	130.10 (18)
N4-C8A-C8	118.79 (17)	119.09 (17)
N1'-C9-C2	111.76 (16)	112.91 (16)
C2'-N1'-C5'	106.30 (17)	106.48 (16)
C2'-N1'-C9	126.56 (17)	128.67 (16)
C5'-N1'-C9	127.15 (16)	124.84 (17)
N3'-C2'-N1'	112.36 (19)	112.16 (18)
C2'-N3'-C4'	104.28 (18)	104.63 (17)
C5'-C4'-N3'	110.67 (19)	110.70 (18)
C4'-C5'-N1'	106.39 (18)	106.03 (19)
C6''-C1''-C2''	118.49 (18)	118.30 (18)
C6''-C1''-C3	121.79 (17)	121.74 (17)
C2''-C1''-C3	119.73 (17)	119.96 (17)
C3''-C2''-C1''	120.4 (2)	120.8 (2)
C4''-C3''-C2''	120.4 (2)	120.2 (2)
C3''-C4''-C5''	119.7 (2)	119.7 (2)
C4''-C5''-C6''	120.1 (2)	120.3 (2)
C5''-C6''-C1''	120.84 (19)	120.7 (2)

Table 4. Significant Torsion Angles (°) with Standard Deviations in Parenthesis

	Molecule I	Molecule II
N1-C2-C9-N1'	-91.8 (2)	98.9 (2)
C2-C9-N1'-C2'	-147.1 (2)	-32.8 (2)
C2-C3-C1''-C6''	130.8 (2)	47.9 (3)

Table 5. Table of Dihedral Angles (°) with Standard Deviations in Parenthesis

	Molecule I	Molecule II
ϕ_2/ϕ_1	81.48 (7)	83.68 (6)
ϕ_3/ϕ_1	52.06 (6)	50.93 (6)
ϕ_3/ϕ_2	55.49 (9)	58.47 (9)

(CDCl₃) δ : 164.8 (CO), 144.8 (C-8a), 136.9 (C-2), 133.8 (Ph-1), 129.5 (Ph-2,6), 128.7 (C-3), 128.6 (Ph-3,5), 127.5 (Ph-4*), 126.3 (C-7*), 124.4 (C-5), 119.7 (C-8), 114.1 (C-6), 61.7 (CH₂), 30.1 (CH₂), 15.1 (CH₃); *Anal.* Calcd for C₁₇H₁₆N₂O₂: C, 72.84; H, 5.75; N, 9.99. Found: C, 72.58; H, 5.69; N, 10.20.

Ethyl 3-Iodoimidazo[1,2-a]pyridine-2-carboxylate (7) To a solution of **6** (3 g, 15.8 mmol) in pyridine (10 ml) was added iodine (6 g, 23.6 mmol). The reaction mixture was heated at 50 °C for 5 h and then poured into water (20 ml). The aqueous solution was extracted with dichloromethane. The combined organic extracts were washed with water (3×20 ml), dried and evaporated to dryness. The residual material was purified by column chromatography (neutral alumina, dichloromethane as eluant) to give brown

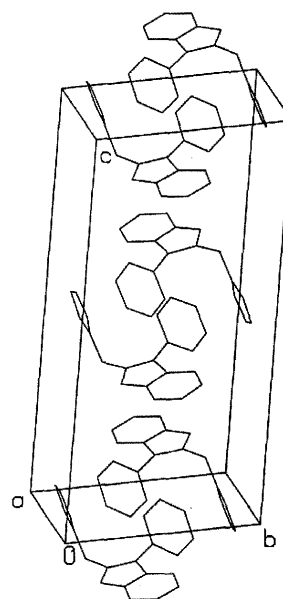
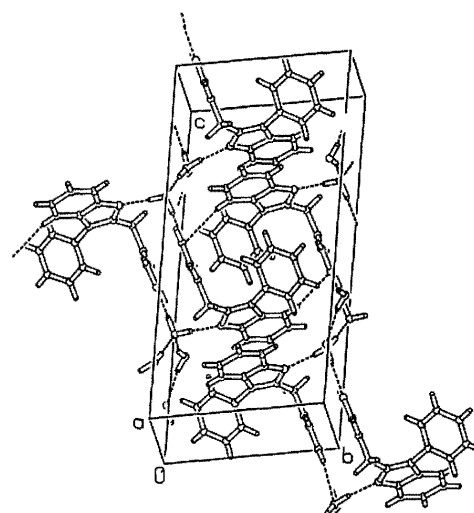
Fig. 2. Packing Representation of **10b**Fig. 3. Packing Representation of **10b**

Table 6. Table of Hydrogen Bond

D-H...A	D-H-A (°)	d(D...A) (Å)	Symmetry
O1-H1A_I...N1_II	179.70	2.795	$[-x+1, -y+1, -z+1]$
O1-H1B_I...N3'_II	168.50	2.814	$[x, y-1, z]$
O2-H2A_I...N1_I	171.25	2.862	$[-x+1, -y+1, -z+1]$
O2-H2B_I...O1_I	173.13	2.777	$[x, y+1, z]$
O3-H3A_I...O2_I	161.48	2.830	
O3-H3B_I...N3'_I	163.84	2.971	$[x, y+1, z-1]$
O4-H4A_I...O3_I	162.81	2.926	$[x-1, y-1, z]$
O4-H4B_I...O1_I	161.39	2.920	

crystals (46%); mp 144 °C; ¹H-NMR (CDCl₃) δ : 8.31 (1H, dt, $J_{H-5, H-6}$ = 6.9 Hz, $J_{H-5, H-7}$ = 1.1 Hz, H-5); 7.72 (1H, dt, $J_{H-7, H-8}$ = 9.2 Hz, $J_{H-6, H-8}$ = 1.1 Hz, H-8); 7.38 (1H, ddd, $J_{H-6, H-7}$ = 6.9 Hz, H-7); 7.05 (1H, td, H-6); 4.54 (2H, q, J = 7.1 Hz, CH₂); 1.51 (3H, t, CH₃); ¹³C-NMR (CDCl₃) δ : 163.1 (CO), 148.2 (C-8a), 138.5 (C-2), 127.5 (C-5, C-7), 119.6 (C-8), 115.1 (C-6), 68.5 (C-3), 61.9 (CH₂), 14.8 (CH₃); *Anal.* Calcd for C₁₀H₉IN₂O₂: C, 38.00; H, 2.87; N, 8.86. Found: C, 38.33; H, 2.91; N, 8.81.

Ethyl 3-Phenylimidazo[1,2-a]pyridine-2-carboxylate (8) To a solution of **7** (0.3 g, 0.95 mmol) in DME (7.6 ml) was added tetrakis(triphenylphosphine)palladium (55 mg, 0.048 mmol), phenylboronic acid (127 mg, 1.05

mmol) and a solution of sodium carbonate (201 mg, 1.90 mmol) in water (3.8 ml). The reaction mixture was heated for 0.5 h at 75 °C with vigorous stirring under nitrogen atmosphere. After **7** was consumed, the solution was concentrated *in vacuo* and the residue diluted in water (100 ml). After extraction with dichloromethane, the dried organic layers were evaporated to dryness. The oily residue was purified by column chromatography (silica gel eluting with dichloromethane) (91%); mp 96 °C (lit.¹⁸) mp 88–90 °C; ¹³C-NMR (CDCl₃) δ: 163.8 (CO), 144.7 (C-8a), 133.4 (C-2), 131.0 (Ph-1,2,6), 129.8 (Ph-4), 129.2 (Ph-3,5), 128.5 (C-3), 126.6 (C-7), 124.4 (C-5), 119.4 (C-8), 114.1 (C-6), 61.3 (CH₂), 14.7 (CH₃).

General Procedure for (Imidazo[1,2-*a*]pyridin-2-yl)methanol Derivatives To a stirred solution of **5** or **8** (6 mmol) in THF (15 ml) was added a suspension of lithium aluminium hydride (12 mmol) in THF (5 ml). After 1 h, water (20 ml) was added dropwise and then the reaction media filtered off. The filtrate was extracted with dichloromethane and the dried organic layers were evaporated to dryness to give white crystals.

(3-Benzylimidazo[1,2-*a*]pyridin-2-yl)methanol (**9a**): Colorless crystals (81%); mp 163 °C; ¹H-NMR (CDCl₃) δ: 7.94 (1H, d, *J*_{H-7 H-8} = 8.8 Hz, H-8); 7.70 (1H, d, *J*_{H-5 H-6} = 6.8 Hz, H-5); 7.25–7.20 (4H, m, Ph, H-7); 7.05 (2H, dd, *J* = 7.2 Hz, *J* = 3.4 Hz, Ph-2,6); 6.72 (1H, t, *J*_{H-6 H-7} = 6.8 Hz, H-6); 4.99 (2H, s, CH₂); 4.81 (1H, s, OH); 4.25 (2H, s, CH₂); ¹³C-NMR (CDCl₃) δ: 144.0 (C-8a, C-2), 137.0 (Ph-1), 129.3 (Ph-2,6), 128.4 (Ph-3,5), 127.3 (Ph-4), 124.9 (C-7), 123.9 (C-5), 119.0 (C-3), 117.8 (C-8), 112.7 (C-6), 57.5 (CH₂), 29.5 (CH₂); *Anal.* Calcd for C₁₅H₁₄N₂O: C, 75.61; H, 5.92; N, 11.76. Found: C, 75.89; H, 5.97; N, 11.94.

(3-Phenylimidazo[1,2-*a*]pyridin-2-yl)methanol (**9b**): Colorless crystals (75%); mp 66 °C (dec.); ¹H-NMR (CDCl₃) δ: 8.18 (1H, d, *J*_{H-5 H-6} = 6.8 Hz, H-5); 7.67 (1H, d, *J*_{H-7 H-8} = 9 Hz, H-8); 7.70–7.44 (5H, m, Ph); 7.21 (1H, dd, *J*_{H-6 H-7} = 6.8 Hz, H-7); 6.77 (1H, t, H-6); 6.60 (1H, bs, OH); 4.89 (2H, s, CH₂); ¹³C-NMR (CDCl₃) δ: 145.2 (C-8a*), 144.3 (C-2*), 130.1 (Ph-2,6), 129.6 (Ph-3,5), 129.0 (Ph-1*), 128.9 (Ph-4*), 125.4 (C-7), 123.9 (C-5), 122.9 (C-3), 117.8 (C-8), 113.0 (C-6), 57.2 (CH₂); *Anal.* Calcd for C₁₄H₁₂N₂O: C, 74.98; H, 5.39; N, 12.49. Found: C, 74.59; H, 5.33; N, 12.72.

General Procedure for Arylmethylimidazo[1,2-*a*]pyridine Derivatives A solution of imidazo[1,2-*a*]pyridinylmethanol derivative **2** or **9a–b** (6 mmol) in thionyl chloride (20 ml) was refluxed for 2 h. After evaporation to dryness, the chloro derivative was washed with petroleum ether (2 × 50 ml), poured into acetonitrile (20 ml) and imidazole or triazole (13.2 mmol) was added. After 48 h of stirring at 50 °C, the solution was concentrated *in vacuo* and the residue diluted in water (20 ml). The solution was extracted with dichloromethane, the dried organic layers evaporated to dryness and the residue was chromatographed on neutral alumina eluting with dichloromethane.

3-(1*H*-Imidazol-1-ylmethyl)-2-phenylimidazo[1,2-*a*]pyridine (**3a**): Colorless crystals (13%); mp 139 °C; ¹H-NMR (CDCl₃) δ: 7.79–7.73 (4H, m, Ph, H-5); 7.59 (1H, bs, Im-2); 7.57–7.42 (3H, m, Ph, H-8); 7.32 (1H, ddd, *J*_{H-7 H-8} = 8.8 Hz, *J*_{H-6 H-7} = 6.8 Hz, *J*_{H-5 H-7} = 1.1 Hz, H-7); 7.15 (1H, bs, Im-4); 6.93 (1H, bs, Im-5); 6.89 (1H, td, *J*_{H-5 H-6} = 6.8 Hz, *J*_{H-6 H-8} = 1.1 Hz, H-6); 5.61 (2H, s, CH₂); ¹³C-NMR (CDCl₃) δ: 146.7 (C-2), 145.7 (C-8a), 136.3 (Im-2), 133.3 (Ph-1), 130.4 (Im-4), 129.0 (Ph-2,6*), 128.6 (Ph-4), 128.4 (Ph-3,5*), 125.7 (C-7), 122.9 (C-5), 118.1 (Im-5), 118.0 (C-8), 113.4 (C-6), 112.6 (C-3), 40.8 (CH₂); *Anal.* Calcd for C₁₇H₁₄N₄: C, 74.43; H, 5.14; N, 20.42. Found: C, 74.58; H, 5.18; N, 20.22.

3-(1*H*-1,2,4-Triazol-1-ylmethyl)-2-phenylimidazo[1,2-*a*]pyridine (**3b**): Colorless crystals (31%); mp 132 °C; ¹H-NMR (CDCl₃) δ: 8.24 (1H, d, *J*_{H-5 H-6} = 6.8 Hz, H-5); 8.05 (2H, s, Tr-3,5); 7.79–7.75 (3H, m, Ph); 7.59–7.48 (3H, m, Ph, H-8); 7.37 (1H, ddd, *J*_{H-7 H-8} = 8.9 Hz, *J*_{H-6 H-7} = 6.8 Hz, *J*_{H-5 H-7} = 1.2 Hz, H-7); 6.95 (1H, td, *J*_{H-6 H-8} = 1.1 Hz, H-6); 5.82 (2H, s, CH₂); ¹H-NMR (DMSO-*d*₆) δ: 8.87 (1H, s, Tr-5); 8.61 (1H, d, *J*_{H-5 H-6} = 6.6 Hz, H-5); 8.02 (1H, s, Tr-3); 7.95 (2H, d, Ph); 7.69 (1H, d, *J*_{H-7 H-8} = 8.8 Hz, H-8); 7.56–7.35 (4H, m, Ph, H-7); 7.04 (1H, t, *J*_{H-6 H-7} = 6.6 Hz, H-6); 5.97 (2H, s, CH₂); ¹³C-NMR (CDCl₃) δ: 152.7 (Tr-3), 147.1 (C-2), 146.2 (C-8a), 142.9 (Tr-5), 133.7 (Ph-1), 129.4 (Ph-2,6*), 129.1 (Ph-4), 129.0 (Ph-3,5*), 126.4 (C-7), 124.2 (C-5), 118.3 (C-8), 113.7 (C-6), 113.1 (C-3), 43.9 (CH₂); *Anal.* Calcd for C₁₆H₁₃N₅: C, 69.80; H, 4.76; N, 25.44. Found: C, 69.45; H, 4.77; N, 25.78.

3-Benzyl-2-(1*H*-imidazol-1-ylmethyl)imidazo[1,2-*a*]pyridine (**10a**): Colorless crystals (13%); mp 128 °C; ¹H-NMR (CDCl₃) δ: 7.74 (1H, dt, *J*_{H-5 H-6} = 6.8 Hz, *J*_{H-5 H-7} = 1.2 Hz, H-5); 7.64 (1H, dt, *J*_{H-7 H-8} = 9.1 Hz, *J*_{H-6 H-8} = 1.2 Hz, H-8); 7.60 (1H, bs, Im-2); 7.36–7.26 (3H, m, Ph); 7.23 (1H, ddd, *J*_{H-6 H-7} = 6.8 Hz, H-7); 7.05–7.00 (4H, m, Ph, Im-4,5); 6.77 (1H, td, H-6); 5.31 (2H, s, CH₂); 4.29 (2H, s, CH₂); ¹³C-NMR (CDCl₃) δ: 145.2 (C-8a), 139.3 (C-2), 137.5 (Im-2), 136.3 (Ph-1), 130.0 (Im-4), 129.5 (Ph-2,6), 128.2 (Ph-3,5), 127.6 (Ph-4), 125.1 (C-7), 124.0 (C-5), 120.0 (C-3), 119.6 (Im-5),

118.2 (C-8), 113.0 (C-6), 44.6 (CH₂), 29.4 (CH₂); *Anal.* Calcd for C₁₈H₁₆N₄: C, 74.98; H, 5.59; N, 19.43. Found: C, 74.58; H, 5.61; N, 19.01.

2-(1*H*-Imidazol-1-ylmethyl)-3-phenylimidazo[1,2-*a*]pyridine (**10b**): Colorless crystals (20%); mp 143 °C; ¹H-NMR (CDCl₃) δ: 8.06 (1H, d, *J*_{H-5 H-6} = 6.8 Hz, H-5); 7.68 (1H, d, *J*_{H-7 H-8} = 9.0 Hz, H-8); 7.61–7.53 (4H, m, Ph, Im-2); 7.42–7.37 (2H, m, Ph); 7.28 (1H, ddd, *J*_{H-6 H-7} = 6.8 Hz, *J*_{H-5 H-7} = 1.3 Hz, H-7); 7.03 (2H, m, Im-4,5); 6.83 (1H, td, *J*_{H-6 H-8} = 1.1 Hz, H-6); 5.25 (2H, s, CH₂); ¹³C-NMR (CDCl₃) δ: 145.2 (C-8a), 138.9 (C-2), 137.4 (Im-2), 130.3 (Ph-2,6), 130.0 (Ph-3,5), 129.8 (Ph-1), 129.6 (Im-4), 128.2 (Ph-4), 125.8 (C-7), 124.1 (C-5), 123.8 (C-3), 119.5 (Im-5), 118.2 (C-8), 113.3 (C-6), 44.5 (CH₂); *Anal.* Calcd for C₁₇H₁₄N₄: C, 74.43; H, 5.14; N, 20.42. Found: C, 74.65; H, 4.98; N, 20.17.

2-(1*H*-Imidazol-1-ylmethyl)-3-nitroimidazo[1,2-*a*]pyridine (**12**): A solution of 2-chloromethyl-3-nitroimidazo[1,2-*a*]pyridine **11**¹¹) (3 g, 14.2 mmol) and imidazole (2.1 g, 30.8 mmol) in acetonitrile (15 ml) was stirred at 50 °C for 24 h. After removal of the solvent *in vacuo*, the reaction mixture was diluted in water (50 ml) and extracted with dichloromethane (2 × 50 ml). The dried organic layers were evaporated to dryness and the oily residue triturated in diethyl ether to give a brown solid (43%); mp 180 °C; ¹H-NMR (CDCl₃) δ: 9.46 (1H, d, *J*_{H-5 H-6} = 6.9 Hz, H-5); 7.85 (1H, d, *J*_{H-7 H-8} = 9.0 Hz, H-8); 7.78 (1H, bs, Im-2); 7.72 (1H, ddd, *J*_{H-6 H-7} = 6.9 Hz, *J*_{H-5 H-7} = 1.3 Hz, H-7); 7.37 (1H, td, *J*_{H-6 H-8} = 1.1 Hz, H-6); 7.19 (1H, bs, Im-4); 7.10 (1H, bs, Im-5); 5.73 (2H, s, CH₂); ¹³C-NMR (CDCl₃) δ: 147.0 (C-8a*), 145.0 (C-2*), 137.9 (Im-2), 131.3 (C-7), 129.5 (C-3), 128.9 (Im-4), 127.7 (C-5), 119.8 (Im-5), 118.6 (C-8); 117.3 (C-6), 45.1 (CH₂); *Anal.* Calcd for C₁₁H₉N₅O₂: C, 54.32; H, 3.73; N, 28.79. Found: C, 54.65; H, 3.78; N, 28.67.

3-Amino-2-(1*H*-imidazol-1-ylmethyl)imidazo[1,2-*a*]pyridine (**13**): To 48% hydrobromic acid (12 ml) cooled at –10 °C was added portionwise tin powder (1.5 g, 12.6 mmol) and then **12** (1.2 g, 5.2 mmol) keeping the temperature below –5 °C. After stirring at 0 °C for 1 h, the reaction mixture was stirred at room temperature for 2 h. The solution was made basic with sodium carbonate and the water removed *in vacuo*. The residue was chromatographed on neutral alumina eluting with dichloromethane–methanol (90:10 v/v) to give a brown solid (63%); mp 127–130 °C (dec); ¹H-NMR (DMSO-*d*₆) δ: 8.08 (1H, d, *J*_{H-5 H-6} = 7.0 Hz, H-5); 7.74 (1H, bs, Im-2); 7.35 (1H, d, *J*_{H-7 H-8} = 9.0 Hz, H-8); 7.20 (1H, bs, Im-4); 7.04 (1H, m, H-7); 6.87 (1H, bs, Im-5); 6.84 (1H, t, *J*_{H-6 H-7} = 7.0 Hz, H-6); 5.27 (4H, s, CH₂, NH₂).

2-(1*H*-Imidazol-1-ylmethyl)-3-(pyrrol-1-yl)imidazo[1,2-*a*]pyridine (**14**): A mixture of **13** (0.75 g, 3.5 mmol) and dimethoxytetrahydrofuran (0.46 ml, 3.5 mmol) in acetic acid (20 ml) was heated at 90 °C for 2 h. After removal of the solvent *in vacuo*, the residue was triturated in diethyl ether (75 ml). After filtration, the filtrate was dried over magnesium sulfate and evaporated to dryness. The residue was chromatographed on neutral alumina eluting with dichloromethane to give **14** as white crystals (13%); mp 153 °C; ¹H-NMR (CDCl₃) δ: 7.65 (1H, dt, *J*_{H-7 H-8} = 9.0 Hz, *J*_{H-6 H-8} = 1.1 Hz, H-8); 7.61 (1H, dt, *J*_{H-5 H-6} = 6.2 Hz, *J*_{H-5 H-7} = 1.1 Hz, H-5); 7.51 (1H, bs, Im-2); 7.32 (1H, ddd, *J*_{H-6 H-7} = 6.2 Hz, H-7); 7.04 (1H, bs, Im-4); 6.99 (1H, bs, Im-5); 6.88 (1H, td, H-6); 6.77 (2H, t, *J* = 2.1 Hz, Py-2,5); 6.52 (2H, t, Py-3,4); 5.18 (2H, s, CH₂); ¹³C-NMR (CDCl₃) δ: 142.8 (C-8a), 137.6 (Im-2), 136.3 (C-2), 130.0 (Im-4), 126.4 (C-7), 123.4 (Py-2,5), 122.9 (C-5), 120.7 (C-3), 119.6 (Im-5), 118.4 (C-8), 113.9 (C-6), 112.1 (Py-3,4), 43.4 (CH₂); *Anal.* Calcd for C₁₅H₁₃N₅: C, 68.43; H, 4.98; N, 26.60. Found: C, 68.32; H, 4.93; N, 26.22.

X-Ray Diffraction of Compound 10b Colorless crystals of compound **10b** were grown by slow evaporation of an ethanol solution at 293 K. The crystal used for X-ray measurement was lamellar, with dimensions: 0.2 × 0.2 × 0.08 mm. The studied compound, C₁₇H₁₄N₄·2H₂O, *M*_r = 310.4 crystallizes in the triclinic system, space group P-1 (*Z* = 2), two independent molecules per asymmetric unit. The unit cell parameters were obtained by least-squares fit of the setting angles of 25 reflections and are as follows: *a* = 8.924(1), *b* = 9.752(1), *c* = 18.645(3) Å, *α* = 82.15(1), *β* = 82.07(1) and *γ* = 83.81(1)° with a cell volume of 1585.5(4) Å³. The calculated density equal to 1.30 g·cm^{–3}. The linear absorption coefficient is *μ* = 0.717 mm^{–1} for the CuKα radiation.

The diffracted intensities were collected with a CAD-4 Enraf-Nonius diffractometer equipped with a graphite monochromator for *θ*_{max} = 65°: 0 ≤ *h* ≤ 10, –11 ≤ *k* ≤ 11, –21 ≤ *l* ≤ 21 and an *ω*–2*θ* scan. Two standard reflections (3 0 –10, 0 –5 –10) were used to monitor the data collection and detect any decrease of intensity; the crystal absorption correction was performed using the *Ψ* scan technique.¹⁹ There were 5316 independent reflections of which 4898 were considered as observed (*I* > 2σ(*I*) and *R*_{int} = 0.012).

The crystal structure was solved and refined using the SHELX97 program.²⁰ Scattering factors were taken from the International Tables for Crystallography.²¹ The hydrogen atoms were introduced in their theoretical

positions and allowed to ride with the atoms to which they are attached. The final reliability factors are: $R=0.051$, $wR=0.127$ and the goodness of fit was equal to $s=1.22$. The weight was equal to: $w=1/[\sigma^2(F_o^2)+(0.0421P)^2+0.6335P]$ where $P=(F_o^2+2F_c^2)/3$. The minimum and maximum residual densities were equal to -0.17 and $0.21 \text{ e } \text{\AA}^{-3}$ respectively; $(\Delta/\sigma)_{\text{max}}=0.04$.

Acknowledgements We thank C. Nativelle, P. Sourdain, S. Moslemi and G.-E. Seralini for the pharmacological evaluation.

References and Notes

- See, for example, Gueiffier A., Lhassani M., Elhakmaoui A., Snoeck R., Andrei G., Chavignon O., Teulade J.-C., Kerbal A., Essassi E. M., Debouzy J.-C., Witvrouw M., Blache Y., Balzarini J., de Clerq E., Chapat J.-P., *J. Med. Chem.*, **39**, 2856—2859 (1996).
- Brodie A., Lu Q., Long B., *J. Steroid. Biochem. Mol. Biol.*, **69**, 205—210 (1999).
- Auvray P., Moslemi S., Sourdain P., Galopin S., Seralini G.-E., Enguehard C., Dallemagne P., Bureau R., Sonnet P., Rault S., *Eur. J. Med. Chem.*, **33**, 451—462 (1998); Sonnet P., Dallemagne P., Guillon J., Enguehard C., Stiebing S., Tanguy J., Bureau R., Rault S., Auvray P., Moslemi S., Sourdain P., Seralini G.-E., *Bioorg. Med. Chem. Lett.*, **8**, 1041—1044 (1998); Sonnet P., Dallemagne P., Guillon J., Enguehard C., Stiebing S., Tanguy J., Bureau R., Rault S., Auvray P., Moslemi S., Sourdain P., Seralini G.-E., *Bioorg. Med. Chem.*, in press.
- Le Borgne M., Marchand P., Duflos M., Delevoye-Seiller B., Piessard-Robert S., Le Baut G., Hartmann R. W., Palzer M., *Arch. Pharm. Pharm. Med. Chem.*, **330**, 141—145 (1997); Le Borgne M., Marchand P., Delevoye-Seiller B., Robert J.-M., Le Baut G., Hartmann R. W., Palzer M., *Bioorg. Med. Chem. Lett.*, **9**, 333—336 (1999).
- Kaye J. A., Parris G. L., Burlant W. J., *J. Am. Chem. Soc.*, **75**, 746—748 (1953).
- Gueiffier A., Mavel S., Lhassani M., Elhakmaoui A., Snoeck R., Andrei G., Chavignon O., Teulade J.-C., Witvrouw M., Balzarini J., de Clerq E., Chapat J.-P., *J. Med. Chem.*, **41**, 5108—5112 (1998).
- Wadsworth H. J., Jenkins S. M., Orlek B. S., Cassidy F., Clark M. S., Brown F., Riley G. J., Graves D., Hawkins J., Naylor C. B., *J. Med. Chem.*, **35**, 1280—1290 (1992); Miles R. W., Samano V., Robins M. J., *J. Org. Chem.*, **60**, 7066—7069 (1995).
- Kawai Y., Satoh S., Yamasaki H., Kayakiri N., Yoshihara K., Oku T., P.C.T. WO 96/34866; Badger A., Bender P., Esser K., Griswold D., Nabil H., Lee J., Votta B., Simon P., P.C.T. WO 91/00092.
- Enguehard C., Collot V., Renou J.-L., Hervet M., Rault S., Gueiffier A., *J. Org. Chem.*, **2000**, submitted.
- Saldabol N. O., Giller S. A., *Chem. Heterocycl. Compd.*, **12**, 1155—1162 (1976).
- Vanille P., Madadi N., Roubaud C., Maldonado J., Crozet M. P., *Tetrahedron*, **47**, 5173—5184 (1991).
- Gueiffier A., Milhavet J.-C., Blache Y., Chavignon O., Teulade J.-C., Madesclaire M., Viols H., Dauphin G., Chapat J.-P., *Chem. Pharm. Bull.*, **38**, 2352—2356 (1990).
- Dallemagne P., Sonnet P., Enguehard C., Rault S., *J. Heterocyclic Chem.*, **33**, 1689—1694 (1996).
- Spek A. L.: Platon 99, Program for Drawing Crystal and Molecular Diagrams, 1999, Univ. of Utrecht, Netherlands.
- Allen F. H., Kennard O., Watson D. G., Brammer L., Orpen A. G., Taylor R., *J. Chem. Soc. Perkin Trans 2*, **12**, S1—S19 (1987).
- Teulade J.-C., Bonnet P.-A., Rieu J.-N., Viols H., Chapat J.-P., Grassy G., Carpy A., *J. Chem. Res. Miniprint*, **1986**, 1842—1874.
- Lombardino J. G., *J. Org. Chem.*, **30**, 2403—2407 (1965).
- Mamedov V. A., Nuretdinov I. A., Sibgatullina F. G., *Bull. Acad. Sci. USSR Div. Chem. Sci.*, **39**, 2380—2382 (1990).
- North A. C. T., Phillips D. C., Matthews F. S., *Acta Cryst. A24*, **1968**, 351—359.
- Sheldrick G. M. (1997) Program for the determination and the refinement of crystal structures, Univ. Göttingen, Germany.
- International Tables for X-Ray Crystallography, Kynoch Press, Birmingham, 1974, Vol. IV.

PEC Films Prepared from Chitosan–Alginate Coacervates

Xiaoliang YAN,^a Eugene KHOR,^b and Lee-Yong LIM^{*a}

Departments of Pharmacy^a and Chemistry,^b National University of Singapore, 10 Kent Ridge Crescent, Singapore 119260.

Received December 13, 1999; accepted March 6, 2000

Chitosan–alginate polyelectrolyte complex (PEC) have been prepared *in situ* in beads and microspheres. This study examines the preparation of suitable chitosan–alginate coacervates for casting into homogeneous PEC films for potential applications in packaging, controlled release systems and wound dressings. Coacervation between chitosan and alginate was rapid, but the rate may be controlled with the addition of water miscible organic solvents. Compared with ethanol and PEG200, acetone was the more promising solvent moderator. Suspensions of fine, uniformly dispersed coacervates were produced by a dropwise addition of 0.25% w/v chitosan solution (solvent: 1 : 1 v/v of 2% acetic acid and acetone) into 0.25% w/v sodium alginate solution in water under rapid agitation. The PEC films were transparent and flexible. They exhibited high permeability to water vapor, but resisted complete dissolution in 0.1 M HCl, distilled water and pH 7.4 phosphate buffer solution. Microscopic heterogeneity in the films could be reduced by immersion in aqueous media, but this was accompanied by modifications in the thickness, permeability and mechanical property of the films.

Key words chitosan–alginate PEC films; coacervation; morphology; permeability; water sorption; mechanical properties

Chitosan is the deacetylated product of chitin, a polysaccharide found in abundance in nature, primarily in crustacean shells. It is water soluble at low pH due to the protonation of the glucosamine moieties. Alginate is a polysaccharide derived from brown seaweed and comprises blocks of guluronic and mannuronic acids. Some salts of alginates, e.g. sodium alginate, are soluble in water. Both polymers are biocompatible and edible, and have been widely studied in the formulation of biomedical^{1–3} and agricultural products.^{4,5}

Whilst the water solubility of the polymers is an advantage in eliminating the use of noxious solvents during processing, it limits the use of the polymers as packaging materials, carriers in controlled release drug delivery systems and as biomaterials. In recent years, the development of polyelectrolyte complexes (PEC) involving chitosan and alginate has gained impetus.^{1,5–12} The PEC has been shown to be water insoluble and proven more effective in limiting the release of encapsulated materials compared to either polymer alone.^{1,7} Such complex formation is expected to result mainly from electrostatic interactions between the amino groups in chitosan and the carboxyl groups in alginate. However, the reaction between chitosan and alginate has been reported to be independent of the pH and ionic strength of the media,^{11,12} leading Mireles *et al.*¹² to postulate that hydrogen bonding and other intramolecular interactions may predominate in the complex formation process.

The preparation of chitosan–alginate PEC to date has involved mainly beads and microsphere systems.^{1,5–10} These systems were heterogeneous, comprising the PEC membrane encapsulating a chitosan or alginate core. In most cases, the extent of reaction is not known or controlled. PEC involving chitosan with other polymers have been reported,^{13–17} and some have been cast into films.^{15–17} The demonstration of film forming capability is important as it widens the applications of the PEC to include membrane products that can be used for packaging, dialysis, coating and wound dressings. The objectives of this study were to examine the feasibility of preparing homogeneous PEC films from chitosan–alginate coacervates, and to characterize the films as a function of processing parameters.

Experimental

Materials Chitosan (Tokyo Kasei Kogyo Company Ltd., Tokyo, Japan) was purified and further deacetylated by refluxing twice with 40% w/v sodium hydroxide in the presence of NaBH₄, intermitted by washing with copious amounts of water. The polymer was then dissolved in 3% v/v acetic acid, regenerated with 1 M sodium hydroxide, washed with distilled water and freeze-dried. Viscosity average molecular weight, M_v , of the purified chitosan, measured by solution viscometry (Cannon Ubbelohde, 30 °C, 0.2 M CH₃COOH/0.1 M CH₃COONa solvent, $K=6.6\times10^{-3}$, $a=0.88$),¹⁸ was $8.60(\pm0.64)\times10^5$ ($n=5$) while its degree of deacetylation, determined by the first derivative UV spectrophotometric method,¹⁹ was $95.7\pm0.2\%$ ($n=5$). Sodium alginate (Lot #2445310L, BDH Ltd., Poole, England) was used as received. It has an intrinsic viscosity of 3.23, which may be approximated to a M_v of 1.04×10^5 (Cannon Ubbelohde, 25 °C, 0.1 M NaCl solvent, $K=6.9\times10^{-6}$, $a=1.13$).²⁰ All other chemicals and reagents were of analytical grade.

Preparation of Films Chitosan solutions (0.0625 to 0.5% w/v) were prepared by adding acetone, ethanol or PEG 200 (0 to 50% v/v) to filtered solutions of the polymer in 2% v/v aqueous acetic acid. Twenty-five milliliters of the solution were added dropwise to 25 ml of sodium alginate (0.0625 to 0.5% w/v) in water. Coacervation was effected under vigorous manual agitation for 20 min. Selected suspensions were cast into polyethylene petri dishes (Sterilin, UK, internal ϕ 85 mm) and allowed to dry overnight at ambient temperature (25 °C).

Processing of Films Dried chitosan–alginate PEC films were immersed for 1 h in distilled water, 0.1 M NaOH, 0.1 M HCl or by sequential immersion for 1 h in 0.1 M NaOH followed by 1 h in 0.1 M HCl. The films were then retrieved with care, washed with distilled water until the washings were neutral to litmus, and dried for 10 h in an oven at 60 °C.

Characterization of Films The PEC films were stored in desiccators at ambient temperature, and measured for weight (Mettler-Toledo) and thickness (Mitutoyo thickness gauge). Surface morphology was observed under a light microscope (LM) (Leica 520804 microscope, Nikon FM2 camera, 200 \times magnification) and a scanning electron microscope (SEM) (JEOL JSM-T220A, 15 kV and 200 \times magnification, Mamiya camera). Film samples were coated with gold-platinum (Ion sputter JFC-1100, 5 min) for the SEM observations.

To determine film permeability to water vapor, film samples of 40 mm diameter were mounted on plastic cups with the help of water impermeable sealant to give test areas of 7.07×10^{-4} m². Each plastic cup contained weighed amounts (5–6 g) of silica gel previously activated at 200 °C for 1 h. At prescribed time intervals, the cups were weighed to determine the amount of water vapor transmitted through the films. The experiments were conducted in triplicates at controlled temperature and relative humidity (Contherm environmental chamber). Control experiments comprised using empty cups sealed with the PEC films, as well as using aluminum foil to seal cups containing the silica gel. In both controls, there were negligible changes in cup weight with time, suggesting that the extent of water vapor sorption by

* To whom correspondence should be addressed. e-mail: phalimly@nus.edu.sg

the PEC films, and water permeability through the plastic cup *per se*, were negligible.

The water sorption capabilities of the PEC films in distilled water, 0.1 M HCl and pH 7.4 phosphate buffer solutions were measured. Triplicate film samples of 30 mm diameter were stored in desiccators to constant weight before immersion in 100 ml of test media at $37.0 \pm 0.1^\circ\text{C}$. At periodic intervals, the films were retrieved from the media, blotted with filter paper and weighed immediately. The extent of water sorption is given as the ratio of weight at time t (W_t) and original weight (W_0) of the films.

Mechanical properties of the films ($n=5$) were determined at 25°C and 50% relative humidity using a tensile tester (Instron 4502). Film samples (70×10 mm) were held at a grip distance of 50 mm and subjected to a strain rate of 1.0 mm/min.

Two milligrams of film were mixed with 200 mg KBr and pressed at 13 tons for 3 min to give sample disks for IR spectroscopic (Jasco FTIR) measurements. Disks were similarly prepared using isolated chitosan–alginate coacervates, alginic acid, chitosan acetate films and purified chitosan instead of the PEC films. The coacervates were obtained from mixing 0.25% w/v chitosan and alginate solutions, and were retrieved by filtration, washed with water, processed as described for the PEC films and freeze-dried. Alginic acid was precipitated by adding 30 ml of 0.1 M HCl to 25 ml of the 0.25% w/v sodium alginate solution, and was recovered by filtration, washed with water and freeze-dried. The chitosan acetate film was prepared by casting 50 ml of 0.25% w/v chitosan solution in 2% v/v acetic acid.

Results and Discussion

Coacervation between Chitosan and Alginate Chitosan has pK_a of 6.5,²¹⁾ while alginate has pK_a values of 3.4 to 4.4.²²⁾ Chitosan and alginate solutions in this study had initial pHs of about 4.15 and 6.84 respectively. Under these circumstances, the amino groups in chitosan and the carboxyl groups in alginate are largely ionized, and coacervation would arise primarily from electrostatic attraction, although hydrogen bonding and hydrophobic interactions have been implicated.¹²⁾

When the chitosan and alginate solutions were mixed by dropwise addition of one solution into the other, capsules were obtained. Rapid coacervation induced the formation of a dense interphasic PEC membrane that separated the polymer solutions and prevented further reaction. Although this technology was commonly employed to prepare beads and microspheres^{5–10)} of chitosan (or alginate) encapsulated by chitosan–alginate PEC membrane, it was not suitable for the production of coacervates for casting into films. Suspensions of the capsules gave rise to heterogeneous films comprising demarcated capsules dispersed in sodium alginate matrix. To prepare coacervates for casting into homogeneous films, the rate of reaction between the two polymers must be sufficiently slow to prevent the formation of interphasic membranes, so that the reaction may be allowed to proceed to completion.

Addition of a water miscible organic solvent (acetone, ethanol or PEG200) into the chitosan solution was effective in slowing the rate of coacervation. The efficiency of the solvent moderators in producing homogeneous precipitation was in the order of acetone > ethanol > PEG200. In solvents of lower polarity, chitosan assumes less extended conformations, which restricts the reaction between the two polyelectrolytes. The rate and extent of coacervation would be determined by the accessibility of reactive groups as the polymers undergo conformational changes in solution.

It was more effective to add the solvent moderator to the chitosan, rather than the alginate, solution because of the latter's poor solubility in the mixed solvents. Other formulation parameters investigated were the concentrations of polymers

(0.0625 to 0.5% w/v) and solvent moderators (10 to 50% v/v), the rate of addition of one polymer solution to the other and the rate of stirring during mixing. Optimal suspensions of fine, uniformly dispersed coacervates were prepared by dropwise addition of 25 ml chitosan solution (0.25% w/v in a 1:1 v/v solvent mixture of 2% v/v water acetic acid and acetone) to 25 ml sodium alginate solution (0.25% w/v in water) under vigorous agitation. These suspensions were used to cast the chitosan–alginate PEC films for this study.

The IR spectrum of the isolated chitosan–alginate coacervates showed a broad band at 1607 cm^{-1} , a shoulder at 1520 cm^{-1} ($\delta_{\text{N-H}}$), and another band at 1400 cm^{-1} ($\delta_{\text{O-H}}$) (Fig. 1a). It had a fingerprint region, 1000 to 1400 cm^{-1} , typical of cellulosic polymers. Coacervates that had been processed with aqueous HCl, whether alone or sequential to NaOH immersion, gave rise to 3 prominent bands at 1750 cm^{-1} , 1635 cm^{-1} and 1520 cm^{-1} . These bands may be attributed to the protonation of residual amino groups (1520 cm^{-1}), and the conversion of the PEC to alginic acid, the 1750 cm^{-1} and 1635 cm^{-1} bands corresponding to the carboxyl and carboxylate carbonyl groups, respectively, of alginic acid (Fig. 1c). On the other hand, when the coacervates were processed with aqueous NaOH, the IR spectrum became poorly resolved, and resembled that for purified chitosan (Fig. 1c). The basic medium may cause the PEC to dissociate into soluble sodium alginate and chitosan precipitate. The latter was retained by filtration and therefore detected in the IR spectrum.

Chitosan–Alginate PEC Films Figures 2 and 3 show the LM and SEM photographs of PEC films prepared from suspensions of the chitosan–alginate coacervates. The surface of unprocessed film (Fig. 2) was undulating, comprising uniformly distributed nodule-like elevations. Mean film thickness was $48.2\text{ }\mu\text{m}$. Processing the PEC films in aqueous NaOH and HCl removed most of the nodules. The films were intact upon retrieval but, due to loss of film matrix ($25.08 \pm 2.45\%$ and $26.42 \pm 1.33\%$ ($n=8$), respectively), became thinner on drying. Film thickness is given in Table 1. Sequential immersion of the PEC films in NaOH followed by HCl also removed the nodules. These films were the thinnest (Table 1), although the weight loss ($29.22 \pm 1.02\%$) was only slightly higher than those processed in NaOH or HCl alone. Extensive film expansion in the aqueous HCl may have given rise to the thinner films.

IR spectra for the chitosan–alginate PEC films are shown in Fig. 1b. Unprocessed films gave a spectrum that was poorly resolved, showing a broad band spanning from 1500 to 1700 cm^{-1} . Immersion of the films in aqueous media reduced their thickness, which improved the resolution of the IR spectra. Processing with aqueous NaOH alone did not significantly change the IR spectrum of the PEC films. Processing the films with HCl, whether alone or sequential to NaOH treatment, produced an additional band at 1520 cm^{-1} , which may be attributed to the protonation of residual amino groups in the films. Unlike the coacervates, acid processing of the films did not produce a prominent IR band at 1750 cm^{-1} . The apparent absence of alginic acid in the PEC films may be explained by its removal during repeated washings of the films during processing. On the other hand, alginic acid would be retained in the coacervates because they were retrieved by filtration after processing.

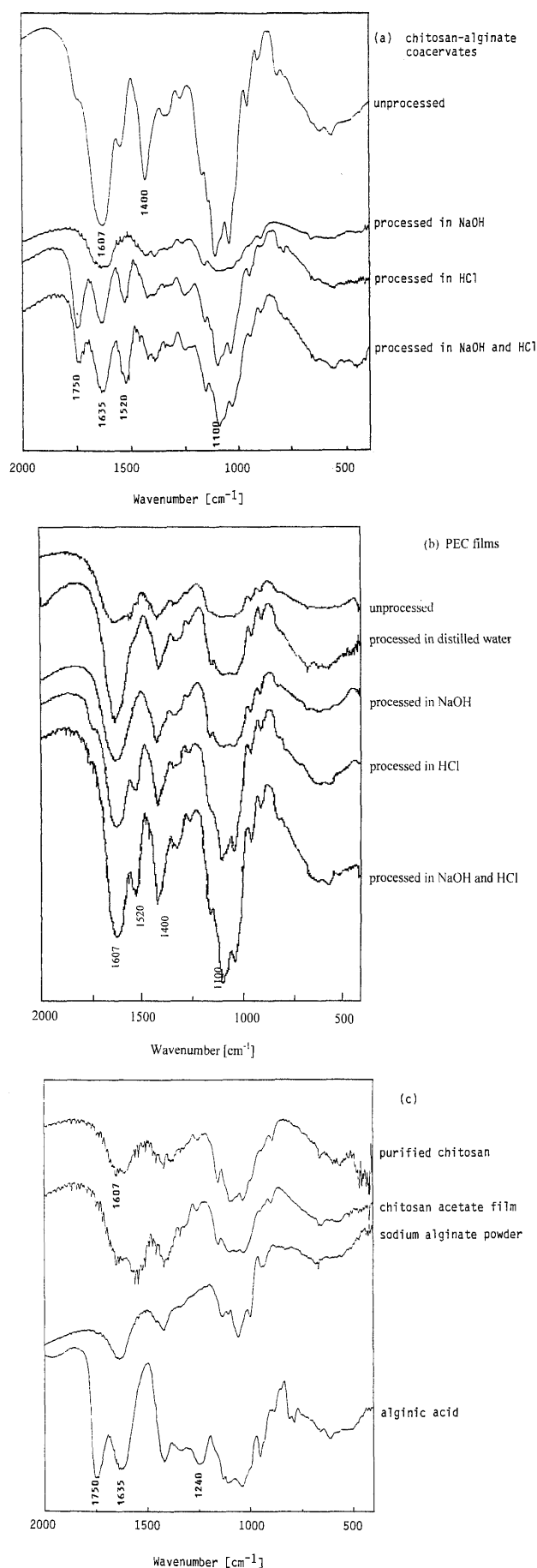


Fig. 1. IR Spectra of (a) Isolated Chitosan-Alginate Coacervates; (b) Chitosan-Alginate PEC Films; (c) Alginate Acid, Sodium Alginate, Chitosan Acetate Film and Purified Chitosan

As mass loss was similar regardless of the nature of processing medium used, we conducted further experiments by processing the PEC films in a similar manner using 0.1 M aqueous acetic acid, distilled water and pH 7.4 phosphate buffer solutions. Weight losses recorded for the films were $25.48 \pm 0.46\%$ ($n=3$), $22.93 \pm 0.75\%$ ($n=3$) and 20.1% ($n=1$) respectively. Compared to the unprocessed film, the film processed with distilled water had a similar but better resolved IR spectrum (Fig. 1b) because it was thinner (Table 1). These results suggest that the loss of film matrix was relatively independent of the nature of the aqueous media, and may be attributed to the removal of non-reacted molecules and unstable PEC from the films during processing and washings. It is pertinent to recognize that the films comprised significant amounts of stable PEC that were not solubilized by distilled water, aqueous acids or bases.

The stability of the PEC is a function of the number of binding sites between adjacent chitosan and alginate molecules. Chitosan molecules in this study had high molecular weight, about 8 times higher than that for the alginate, and are not expected to have extended conformations in the mixed solvent. Since the coacervation reaction is time-dependent, it would continue in the suspensions even as they were cast and allowed to dry into films. For this reason, the films should contain more stable PEC and less residual reactive groups than the isolated coacervates. Although quantitative analysis of residual reactive groups was not carried out, chitosan and alginate should bind in the ratio of 1:1 monomeric unit, equivalent to 1:1.5 by weight of chitosan:alginate, if reaction were carried out to completion.¹¹⁾

The permeability of the chitosan-alginate PEC films to water vapor (Table 1) was relatively high, comparable to cellophane and polyvinyl alcohol films.²³⁾ Thickness and area of the films available for water vapor transmission were considered when calculating the film permeability. Film permeability was reduced after processing with aqueous media, with HCl having a greater effect than NaOH. The film permeability was in the order of unprocessed films > films processed in aqueous NaOH > films processed in distilled water > films processed in aqueous HCl > films processed in both NaOH and HCl. The poorer permeability of processed films could be associated with greater homogeneity in film composition, which allowed for closer molecular chain packing in the films. Rearrangement of polymer chains was probably more extensive in films processed with aqueous HCl because of film expansion in this medium.

While the permeability of the processed films was relatively unchanged, the unprocessed film had lower permeability when the temperature was increased from 25 °C to 32 °C. Enhanced chain mobility at higher temperature may have reduced the porosity of the unprocessed film through molecular rearrangement; but for the already dense processed films, such molecular arrangement would not significantly affect the film porosity. Raising the RH from 50% to 80% also lowered the permeability of the unprocessed film, probably through a mechanism similar to that seen at elevated temperature, while the acid- and base-processed films showed slightly higher permeability to water vapor. The latter may be attributed to a hydration effect.

The capacity of the PEC films for water sorption in different liquid media is shown in Fig. 4. In many instances, the

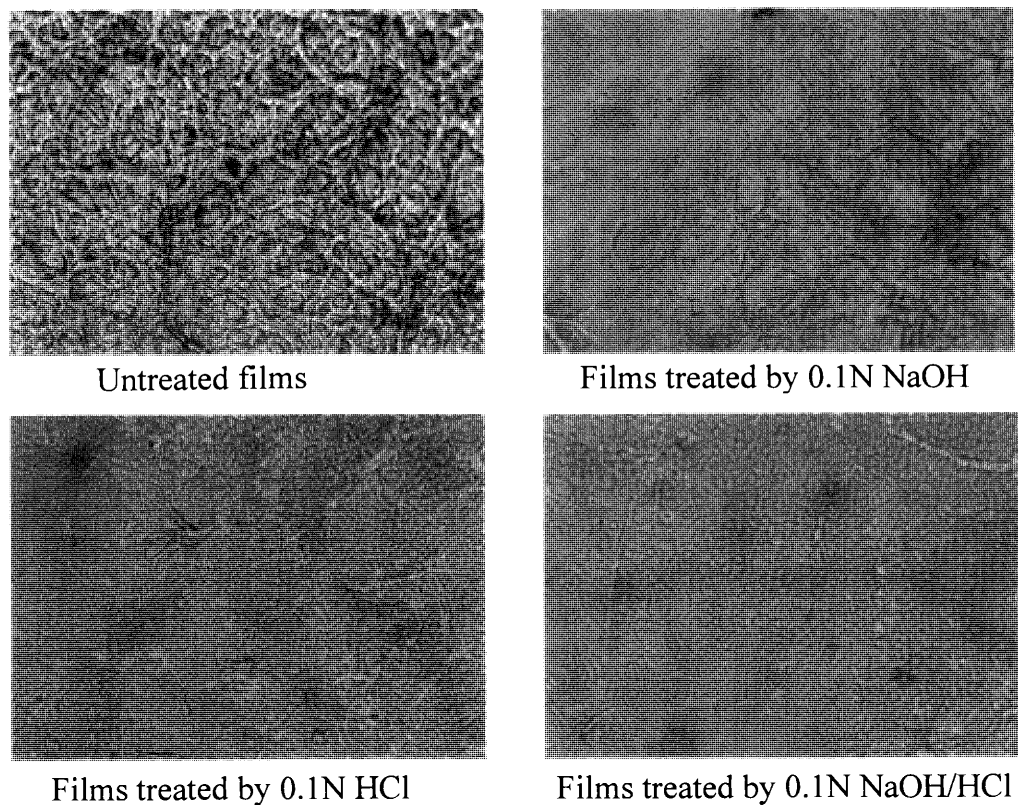


Fig. 2. Morphology of Chitosan-Alginate PEC Films as Observed under a Light Microscope

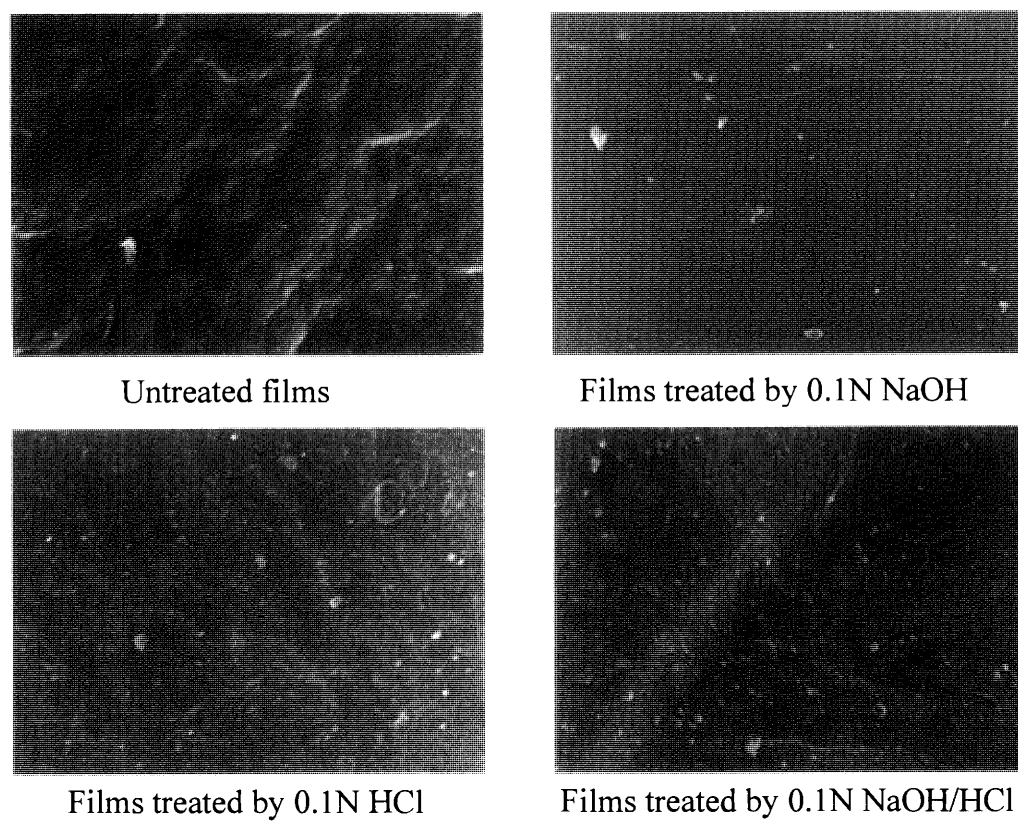


Fig. 3. Surface Morphology of Chitosan-Alginate PEC Films as Observed under a Scanning Electron Microscope

Table 1. Permeability ($\text{g} \cdot \text{mm} \cdot \text{m}^{-2} \cdot 24 \text{ h}^{-1} \cdot \text{mmHg}^{-1}$) and Mechanical Properties of Chitosan–Alginate PEC Films

Processing medium	Thickness (μm) ($n=5$)	Permeability to water vapour ($n=3$)			Mechanical properties ($n=5$)		
		RH 50%, 25 °C	RH 80%, 25 °C	RH 50%, 32 °C	Young's modulus (MPa)	Tensile strength (MPa)	Strain at break (%)
Unprocessed	48.2 ± 7.3	6.21 ± 0.12	5.78 ± 0.32	4.08 ± 0.12	450.91 ± 123.77	4.53 ± 0.83	8.41 ± 1.84
Distilled water	31.9 ± 4.7	3.29 ± 0.06	—	—	—	—	—
0.1 M NaOH	29.6 ± 3.6	3.69 ± 0.14	4.03 ± 0.29	3.89 ± 0.12	1338.22 ± 101.91	12.34 ± 1.20	7.75 ± 1.85
0.1 M HCl	19.1 ± 0.6	2.49 ± 0.05	2.81 ± 0.09	2.37 ± 0.06	918.34 ± 146.38	7.53 ± 1.88	2.46 ± 0.57
0.1 M NaOH, and 0.1 M HCl	17.6 ± 0.9	2.07 ± 0.03	2.19 ± 0.08	2.21 ± 0.10	752.76 ± 48.19	4.49 ± 0.76	2.32 ± 0.20

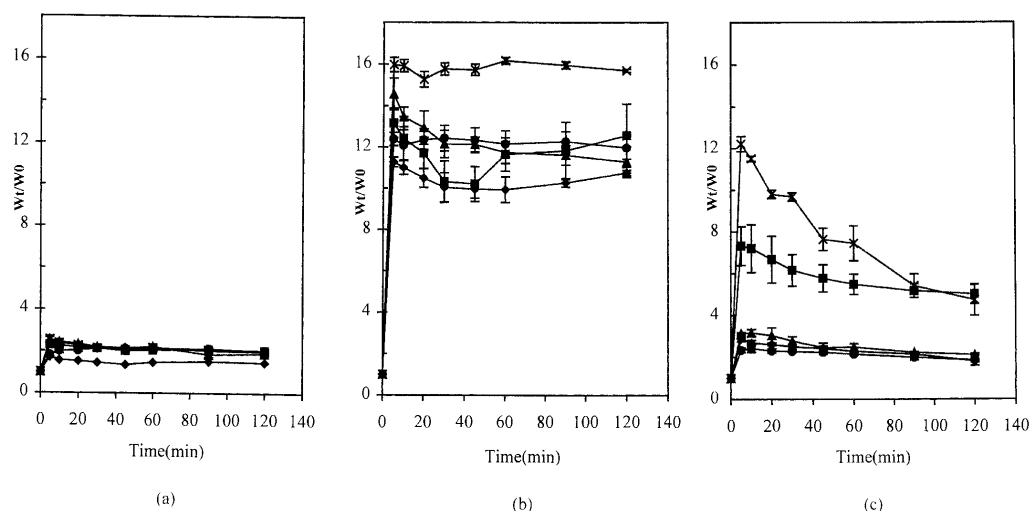


Fig. 4. Water Uptake by PEC Films as Measured by the Extent of Weight Change in (a) pH 7.4 Phosphate Buffer Solutions, (b) 0.1 M HCl and (c) Distilled Water

Symbols: \blacklozenge , unprocessed films; \bullet , processed with distilled water; \blacktriangle , processed with aqueous NaOH; \blacksquare , processed with aqueous HCl; \times , processed with aqueous NaOH and HCl.

films showed rapid weight gain in the first 5 min, followed by gradual weight loss to reach equilibrium level at about 20 min. The weight loss, which was substantial for the thin processed films, may be attributed to solubilization of film matrix. However, it is perplexing that such weight loss was not apparent in the very thin NaOH/HCl processed film when placed in 0.1 M HCl.

All films showed poor water uptakes in the pH 7.4 phosphate buffer solution (Fig. 4a), while relatively large amounts of water were absorbed, particularly for processed films, in 0.1 M HCl (Fig. 4b). This difference is related to medium pH, since the ionic strengths of 0.1 M HCl and the pH 7.4 phosphate buffer solutions were similar (0.1 M and 0.0895 M). In the acid medium, protonation followed by the repelling action of residual amino groups in the PEC films caused film expansion, which facilitated water sorption. PEC films processed in both aqueous NaOH and HCl showed higher water sorption because they were thin films.

Disparate water sorption capabilities were observed in distilled water (Fig. 4c). Unprocessed films and films processed in distilled water or aqueous NaOH had similarly small weight gains, while films processed in aqueous HCl showed higher water uptakes. These results may be accounted for by the presence of protonated amino groups in those films pre-processed in aqueous HCl. In this medium, thin films processed in both NaOH and HCl again showed the highest water uptake in the first few minutes.

The mechanical properties of the PEC films are given in Table 1. The unprocessed film had a moderate Young's modulus and relatively low tensile strength and percent elongation at break point. Processing in NaOH significantly improved the mechanical properties of the films in terms of the Young's modulus and tensile strength, but not the elongation at break point. The enhanced strength may be attributed to the neutralization of charges at residual amino groups, which confer mechanical strength reminiscent of the chitosan film.²⁴ Tensile strength and Young's modulus were also improved, although more modestly, by processing in HCl, or in both NaOH and HCl. In this case, tensile strength may have been acquired from improved chain packing in the relatively more homogeneous films. However, these films were less ductile when compared to the unprocessed film.

Conclusion

Coherent PEC films can be prepared by casting aqueous suspensions of chitosan–alginate coacervates. The PEC films were flexible, porous and hydrophilic, yet resistant to dissolution in water, aqueous acids and bases. Despite gross homogeneity, microscopic heterogeneity was observed in the film morphology. These can be removed by processing with aqueous HCl or NaOH, which also modify the physicochemical properties of the films. Further refinements in the formulation and method of preparation, as well as mechanistic studies, are currently being investigated.

Acknowledgments This study was supported by a National University of Singapore Grant (RP 3982326).

References

- 1) Filipovic-Grcic J., Maysinger D., Zorc B., Jalsenjak I., *Int. J. Pharm.*, **116**, 39—44 (1995).
- 2) Aiedeh K., Gianasi E., Orienti I., Zecchi V., *J. Microencapsulation*, **14**, 567—576 (1997).
- 3) Lloyd L. L., Kennedy J. F., Methacanon P., Paterson M., Knill C. J., *Carbohydr. Polym.*, **37**, 315—322 (1998).
- 4) Ghaouth A. E., Arul J., Asselin A. "Advances in Chitin and Chitosan," ed. by Brine C. J., Sandford P. A., Zikakis J. P., Elsevier Applied Science, 1992, pp. 440—452.
- 5) Tay L. F., Khoh L. K., Loh C. S., Khor E., *Biotechnol. Bioeng.*, **42**, 449—454 (1993).
- 6) Liu L. S., Liu S. Q., Ng S. Y., Froix M., Ohno T., Heller J., *J. Control. Release*, **43**, 65—74 (1997).
- 7) Alexakis T., Boadi D. K., Quong D., Groboillot A., O'Neill I., Poncellet D., Neufeld R. J., *Appl. Biochem. Biotechnol.*, **50**, 93—106 (1995).
- 8) Murata Y., Maeda T., Miyamoto E., Kawashima S., *Int. J. Pharm.*, **96**, 139—145 (1993).
- 9) Knorr D., Daly M., *Process Biochem.*, **23**, 48—50 (1988).
- 10) Lee K. Y., Park W. H., Ha W. S., *J. Appl. Polym. Sci.*, **63**, 425—432 (1997).
- 11) Takahashi T., Takayama K., Machida Y., Nagai T., *Int. J. Pharm.*, **61**, 35—41 (1990).
- 12) Mireles C., Martino M., Bouzas J., Torres J. A., "Advances in Chitin and Chitosan," ed. by Brine C. J., Sandford P. A., Zikakis J. P., Elsevier Applied Science, 1992, pp. 506—515.
- 13) Hugerth A., Caram-Lelham N., Sundelof L. O., *Carbohydr. Polym.*, **34**, 149—156 (1997).
- 14) RemunianLopez C., Bodmeier R., *Int. J. Pharm.*, **135**, 63—72 (1996).
- 15) Thacharodi D., Rao K. P., *Int. J. Pharm.*, **120**, 115—118 (1995).
- 16) Yao K. D., Liu J., Cheng G. X., Lu X. D., Tu H. L., Da Silva J. A. L., *J. Appl. Polym. Sci.*, **60**, 279—283 (1996).
- 17) Nam S. Y., Lee Y. M., *J. Memb. Sci.*, **135**, 161—171 (1997).
- 18) Wang W., Bo S., Li S., Qin W., *Int. J. Biol. Macromol.*, **13**, 281—285 (1991).
- 19) Tan S. C., Khor E., Tan T. K., Wong S. K., *Talanta*, **45**, 713—719 (1998).
- 20) Martinsen A., Skjåk-Bræk G., Smidsrød O., *Carbohydr. Polym.*, **15**, 171—193 (1991).
- 21) Roberts G. A. F., *Chitin Chemistry*, Macmillan: London, 1992, Chapter 5.
- 22) King A. H., "Food Hydrocolloids," Vol. II, ed. by Glicksman M., CRC Press, Boca Raton, 1983, pp. 134.
- 23) *Plastics Design Library*, "Permeability and Other Film Properties of Plastics and Elastomers," William Andrew Inc., 1995, pp. iii.
- 24) Lim L. Y., Khor E., Koo O., *J. Biomed. Mater. Res.*, **43**, 282—290 (1998).

Formation of Spherical Micelles by the Novel Platelet Activating Factor Receptor Antagonist, E5880

Teruko NOMURA,* Yasuyuki ASAI, Naokazu MURAHASHI, and Kiyoshi IWAMOTO

Formulation Research Laboratory, Kawashima, Eisai Co., Ltd., Takehaya-machi, Kawashima-cho, Hashima-gun, Gifu 501-6195, Japan. Received December 13, 1999; accepted March 17, 2000

E5880, a novel platelet activating factor receptor antagonist, was dispersed in water for the preparation of injectable formulation and the physicochemical properties of the micelles were characterized. The critical concentration for formation of micelles was 0.12 mM. Using the area per molecule results, the critical packing parameter was calculated and showed that the structure was composed of spherical micelles and the number of the molecules per micelle was 88. The diameter of a micelle was 8.1 nm. The fluidity and micropolarity around the hydrocarbon region of the micelles were evaluated and compared to the surfactants, stearyltrimethylammonium chloride and cetyltrimethylammonium chloride.

Key words surface tension; micelle; structure; fluidity; micropolarity

Platelet activating factor (PAF) exhibits a variety of biological activities including activation of platelets¹⁾ and neutrophils,²⁾ bronchoconstriction,³⁾ hypermeability in peripheral vein,⁴⁾ hypotension⁵⁾ and cardiac dysfunction.⁶⁾ Because these biological activities of PAF are extremely potent, it is generally accepted that PAF is a mediator of inflammation⁷⁾ and plays important roles in the pathology of thrombosis, asthma or hypotension in shock.^{8–10)} Consequently, it is expected that specific PAF receptor antagonists may be beneficial for the treatment of these diseases, and many efforts to develop potent and specific PAF antagonists have been made.

E5880, a newly synthesized PAF antagonist (Fig. 1), is more potent in PAF receptor binding than in PAF.¹¹⁾ This compound is amphiphilic and is believed to form the micelles in aqueous media. For the treatment of the above diseases, an injectable formulation would be extremely useful, and to develop such a formulation, an understanding of the characteristics of the physicochemical properties of E5880 and its micelles is important.

In this study, to learn the behavior of E5880 micelles in water, critical micelle concentration was determined by the measurement of surface tension. From this, surface density was calculated and a surface pressure-molecular area curve was obtained. The lateral interaction between the molecules was also evaluated, and the fluidity and micropolarity around the hydrocarbon region of the micelles were determined using fluorescence techniques. These features were compared with the surfactants, stearyltrimethylammonium chloride (STAC), which has the same length of hydrocarbon chains (C₁₈) as E5880 and cetyltrimethylammonium chloride (CTAC), which has fewer carbon number (C₁₆) than either E5880 or STAC.

Experimental

Materials E5880 was obtained from Eisai Chemical Co., Ltd. (Ibaraki, Japan). Stearyltrimethylammonium chloride (STAC) was purchased from Tokyo-kasei Co., Ltd. (Tokyo, Japan). 1,6-Diphenyl-1,3,5-hexatriene (DPH) and cetyltrimethylammonium chloride (CTAC) were purchased from Wako Pure Chemical Industries Ltd. (Osaka, Japan). Nile red (NR) was purchased from Lambda Co., Ltd. (Graz, Austria).

Surface Tension Measurement To determine the critical concentration for formation of micelles and interaction between the molecules, the surface tension of aqueous E5880, STAC, and CTAC solutions was measured as a function of concentration of these lipids.¹²⁾ The measurement was performed

by Whilhelmy's plate method using a surface tensiometer (Model CBVP-A3, Kyowa Kaimenkagaku Co., Ltd., Tokyo) at 25 °C.

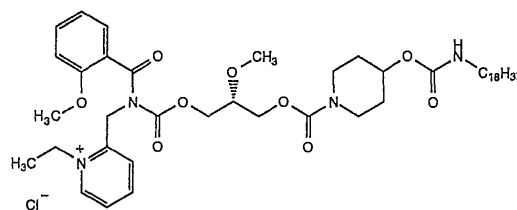
Determination of Size of the Micelles The size distribution of E5880, STAC, and CTAC micelles (concentration: 10 mM) was determined by the dynamic light scattering (DLS) technique using a laser particle analyzer equipped with an Ar laser (Model DLS-7000DL, Otsuka Electronics Co., Ltd., Osaka) at 25 °C. The data were analyzed by histogram method¹³⁾ and weight-averaged size of the micelles was evaluated.

Fluidity of Hydrocarbon Region in the Micelles The fluidity of hydrocarbon region in E5880, STAC and CTAC micelles was determined at 25 °C using a fluorescence polarization technique (probe; DPH) as reported by Iwamoto *et al.* (1982).¹⁴⁾ DPH was added at 0.1 mol% of total lipids. The excitation and emission wavelengths used were 360 nm and 428 nm, respectively.

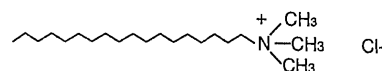
Fluorescence polarization *P* is calculated by

$$P = \frac{I_{VV} - GI_{VH}}{I_{VV} + GI_{VH}} \quad (1)$$

(a)



(b)



(c)

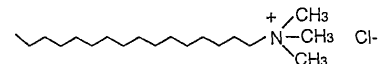


Fig. 1. Chemical Structures; (a) Novel Platelet Activating Factor Receptor Antagonist, E5880, (b) STAC, (c) CTAC

* To whom correspondence should be addressed. e-mail: t4-nomura@nnc.eisai.co.jp

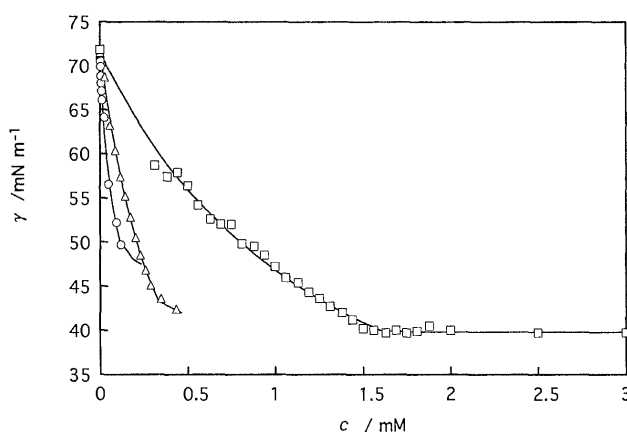


Fig. 2. Surface Tension versus Concentration Curves of the E5880, STAC and CTAC Aqueous Solution at 25 °C
(○) E5880, (△) STAC, (□) CTAC.

where I is the fluorescence intensity, and the subscripts refer to the plane of polarization of the excitation and emission beams (V=vertical, H=horizontal). $G (=I_{HV}/I_{HH})$ is the grating correction factor.

Determination of the Micropolarity around NR in the Micelles The micropolarity of hydrocarbon regions in E5880, STAC and CTAC micelles was determined using a fluorescence technique (probe: NR). NR exhibits a strong environment-dependent blue shift, a high quantum yield and low fluorescence in water.^{16,17} The fluorescence spectra were measured using a fluorescence spectrophotometer (model F-4500, Hitachi Co., Ltd., Tokyo) excited at 549 nm at 25 °C. The micropolarity of NR incorporated into the micelles was evaluated using the wavelength of maximum intensity of emission. Twenty-eight hundredths mg of NR was dissolved in 8.8 ml of acetone (0.1 mM). Five microliters of each solution was then diluted with 5 ml of 10 mM of aqueous E5880, STAC and CTAC solutions, methanol, ethanol, propanol, isopropanol, butanol, isopentyl alcohol, acetone, tetrahydrofuran and acetonitrile, respectively. The wavelengths at the maximum fluorescence intensity of each solution were plotted against the polarity of each solvent.¹⁸ The micropolarity around the probe was determined using this standard curve.

Results and Discussion

Surface Tension Figure 2 shows the surface tension γ vs. concentration c curves of the three lipids, aqueous E5880, STAC and CTAC solution. The γ value decreased with increasing molarity c , and it passed through a break point at the molarity corresponding to critical micelle concentration (cmc). The cmc values of E5880, STAC and CTAC were 0.12, 0.33 and 1.6 mM, respectively. The cmc values of STAC and CTAC were similar to those reported.^{19,20}

Surface Density and Surface Pressure vs. Molecular Area Curve Surface density Γ is calculated from the slope of the γ - c curve using the following equation;¹²⁾

$$\Gamma = -(c/iRT)(\partial\gamma/\partial c)_{T,p} \quad (2)$$

Here, T is temperature and R is the gas constant, and i means the number of ions from electrolytes. The surface density vs. concentration curves are shown in Fig. 3. The Γ value increases with increasing concentration of c and approaches the saturated surface densities Γ_s at cmc.

The surface pressure is expressed by

$$\pi = \gamma_0 - \gamma \quad (3)$$

and surface area per lipid molecules A is calculated by

$$A = 1/N_A \Gamma \quad (4)$$

where N_A is Avogadro's number. Figure 4 shows the surface

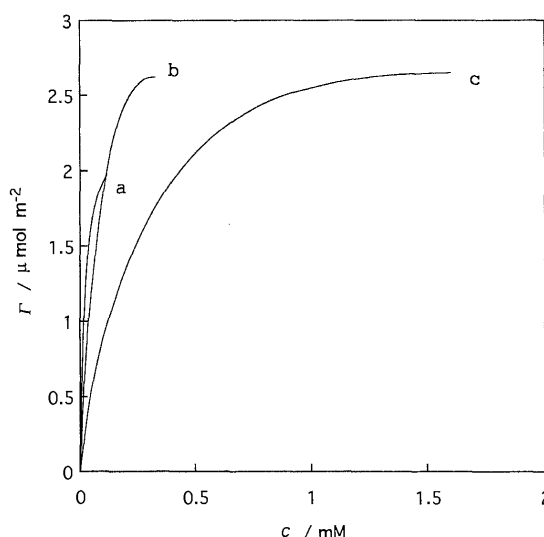


Fig. 3. Surface Density versus Concentration Curves of the E5880, STAC and CTAC Aqueous Solution at 25 °C
(a) E5880, (b) STAC, (c) CTAC.

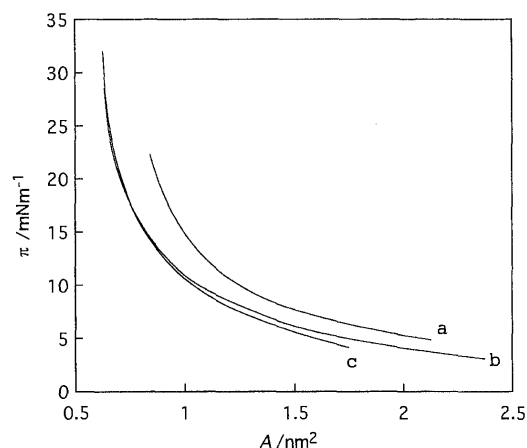


Fig. 4. Surface Pressure versus Molecular Area Curves of E5880, STAC and CTAC Aqueous Solution at 25 °C
(a) E5880, (b) STAC, (c) CTAC.

pressure vs. molecular area (π - A) curves. The limiting areas for E5880, STAC and CTAC were 0.840, 0.633 and 0.627 nm², respectively. The molecular structure of the head group of E5880 is larger than those of STAC and CTAC, therefore the limiting area of E5880 is largest among the three lipids.

Lateral Interaction between the Lipid Molecules A theory for equilibrium between the monolayer and the solution has been developed by Lucassen-Reynders²¹⁾ using the chemical potential.²²⁾ The adsorption isotherms of the lipids were evaluated by the equation:

$$\ln\{(1/c) \cdot [\theta/(1-\theta)]\} = 2\omega\theta + \ln K \quad (5)$$

The fraction of the interface, θ , is equal to Γ/Γ_s . K and ω are parameters showing the magnitude of adsorption and the lateral interaction in the monolayer, respectively. The attractive and repulsive interactions are represented by negative and positive values of the ω parameter, respectively. When the ω values exceeds 2, a phase separation occurs in the monolayer.

Figure 5 illustrates the relationship between θ and

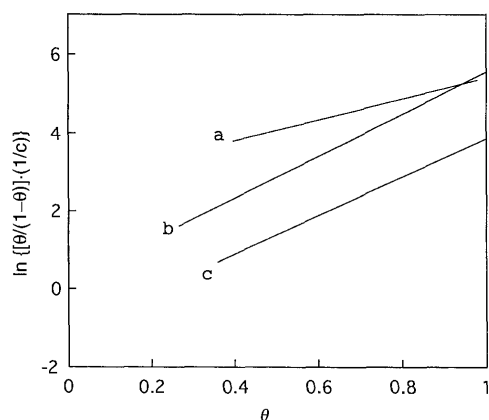


Fig. 5. Relationship between the θ and $\ln\{[\theta/(1-\theta)] \cdot (1/c)\}$ for Evaluation of Lateral Interaction Parameters of Lipids

(a) E5880, (b) STAC, (c) CTAC.

Table 1. Lateral Interaction Parameter K and ω Values of E5880, STAC and CTAC

	K (l/mol)	ω (RT)
E5880	15.6	1.33
STAC	1.19	2.70
CTAC	0.333	2.49

$\ln\{[\theta/(1-\theta)] \cdot (1/c)\}$ for evaluation of lateral interaction parameters of lipids. The K and ω values are summarized in Table 1. The adsorption magnitude of E5880 was the smallest among the lipids. These results indicate that there is attractive interaction between the molecules.

Critical Packing Parameters for the Micelles The critical packing parameters²³⁾ for E5880, STAC and CTAC were calculated based on the area per molecule results (Fig. 4), the volume of the hydrophobic part and the length of the alkyl chain. For the formation of the closed lamellar bilayer structures the effective cross-section of the hydrocarbon moiety must be lower than that of the hydrophilic head-group region. This assumption can be confirmed by an estimation of the critical packing parameter according to the formula;

$$x = v/a \cdot l \quad (6)$$

where v is the volume of the hydrophobic part, a the area of the hydrophilic head group and l the length of the alkyl chain. When $v/a \cdot l < 1/3$ spherical micelles form, $1/3 < v/a \cdot l < 1/2$ tubular micelles form, $1/2 < v/a \cdot l < 1$ vesicles form and $1 < v/a \cdot l$ hexagonal H_{II} structures form. The volume of the hydrocarbon domain (v) and the length of hydrocarbon (l) were calculated using the following equations;

$$v = (27.4 + 26.9n) \times 10^{-3} \text{ (nm}^3\text{)} \quad (7)$$

$$l = 0.15 + 0.1265n \text{ (nm)} \quad (8)$$

where n represents the number of carbons for hydrocarbon chains. For E5880, $v = 0.5116 \text{ nm}^3$, $l = 2.427 \text{ nm}$, $a = 0.843 \text{ nm}^2$. For STAC, $v = 0.5116 \text{ nm}^3$, $l = 2.427 \text{ nm}$, $a = 0.633 \text{ nm}^2$. For CTAC, $v = 0.627 \text{ nm}^3$, $l = 2.174 \text{ nm}$, $a = 0.627 \text{ nm}^2$. The x values for E5880, STAC and CTAC were 0.25, 0.33 and 0.33, respectively. Therefore, it is believed that these three lipids form spherical inverted micelles. The radius (R) and the

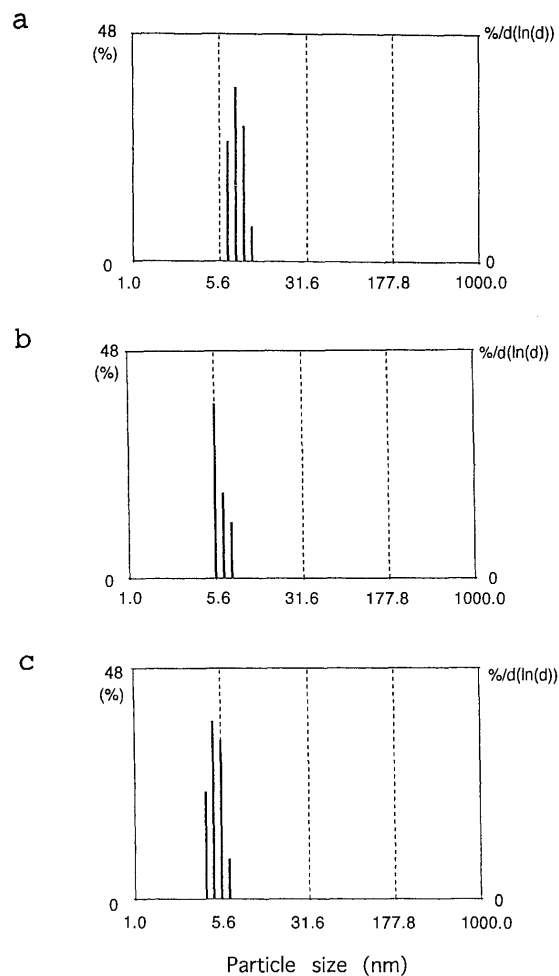


Fig. 6. Histogram of Distribution of Weight-averaged Size of Micelles by the DLS Techniques

(a) E5880: $8.1 \pm 2.3 \text{ nm}$ (mean \pm S.D.), (b) STAC: $6.3 \pm 2.2 \text{ nm}$ (mean \pm S.D.), (c) CTAC: $5.1 \pm 1.3 \text{ nm}$ (mean \pm S.D.).

number of molecules in the micelles (N) were calculated by the following equations:²⁴⁾

$$R = 3v/a \text{ (nm)} \quad (9)$$

and

$$N = 4\pi R^2/a \quad (10)$$

For E5880, $R = 1.82 \text{ nm}$ and $N = 88$. For STAC, $R = 4.65 \text{ nm}$ and $N = 117$. For CTAC, $R = 3.00 \text{ nm}$ and $N = 95$. The N value for CTAC was reported to be $102^{25)}$ and our results were similar to the reported value.

Determination of the Size of the Micelles Figure 6 represents the DLS histograms of the micelles. The weight-averaged diameters for E5880, STAC and CTAC were 8.1, 6.3 and 5.1 nm, respectively. These values were good agreement with the ones calculated using the critical packing parameters.

Fluidity of the Hydrocarbon Regions of the Micelles The fluidity of the micelles was determined by the fluorescence polarization method using DPH as a hydrophobic probe. The polarization of E5880, STAC and CTAC micelles at 25°C was 0.316, 0.105 and 0.098, respectively, indicating that the hydrocarbon region in E5880 micelles is the most rigid and those of STAC and CTAC micelles are similar. The molecular area of the head group of E5880 was largest

among the three lipids. The difference in the order parameter is caused by difference in the structure of the head group of the lipids.

Micropolarity around NR in the Micelles The micropolarity around NR in the micelles was determined, as were the emission maxima of NR embedded in the micelles. It has been reported that the fluorescence characteristics of NR depend on the micropolarity around the probe and which is located in a hydrophobic region in the micelles.^{16,17} Therefore, the emission maxima of NR in the micelles is believed to provide information on the micropolarity around the hydrocarbon chains. Figure 7 shows the relationship between solvent polarity and emission maximum of NR at 25 °C. The emission maxima of E5880, STAC and CTAC micelles were 621, 636 and 636 nm, respectively, indicating that the micropolarity around the probe in the micelles is similar to that of isobutanol, methanol and methanol, respectively. This indicates that the hydrocarbon regions around NR in STAC and CTAC micelles are more hydrated than that of E5880 micelles.

Conclusions

The physicochemical characteristics of E5880 micelles in water were determined and are summarized in Table 2. The cmc of E5880 at 25 °C was 0.12 mM. Using the area/mole-

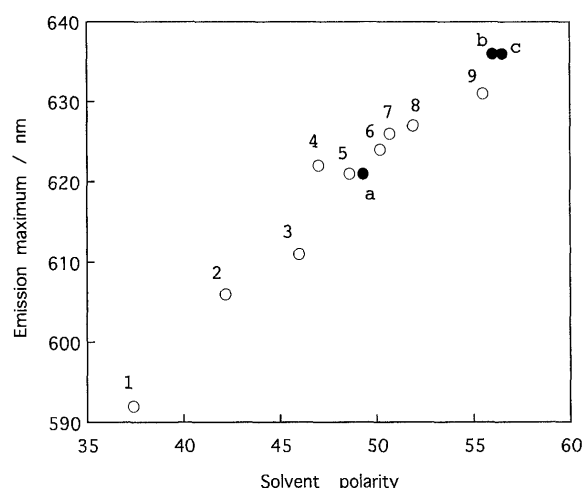


Fig. 7. Relationship between Solvent Polarity and Emission Maximum of NR (0.1 mM) at 25 °C

(1) Tetrahydrofuran, (2) acetone, (3) acetonitrile, (4) isopentyl alcohol, (5) isopropanol, (6) butanol, (7) propanol, (8) ethanol, (9) methanol.

cule results, the structure of the micelles was spherical and the number of molecules per micelle was calculated to be 88. There is an attractive interaction between E5880 molecules. The hydrocarbon region in the micelle was more rigid and less hydrated than those of STAC and CTAC.

References

- Benveniste J., Hansen P. M., Conchreane C. O., *J. Exp. Med.*, **136**, 1356—1377 (1972).
- Shaw J. O., Pinckard R. N., Ferrigini K. S., McManus L. M., Hanahan D. J., *J. Immunol.*, **127**, 1250—1255 (1981).
- Vergafigit B. B., Lefort J., Chignard M., Benveniste J., *Eur. J. Pharmacol.*, **65**, 185—192 (1980).
- Humphrey D. M., McManus L. M., Satouchi K., Hanahan D. J., Pinckard R. N., *Lab. Invest.*, **46**, 422—427 (1982).
- Blank M. L., Synder F., Byers L. W., Brooks B., Muirhead E. E., *Biochem. Biophys. Res. Commun.*, **90**, 1194—1200 (1979).
- Bessin P., Bonnet J., Apfel D., Soulaard C., Desgroux L., Pelas I., Benveniste J., *Eur. J. Pharmacol.*, **86**, 403—413 (1983).
- Sacki S., Masugi F., Ogihara T., Otsuka A., Kumahara Y., Watanabe K., Tamura K., Akashi A., Kumagai A., *Life Sci.*, **37**, 325—329 (1985).
- Ohishi S., Yamaki K., Hayashi M., Tsushima S., Nomura H., *Chem. Pharm. Bull.*, **34**, 4896—4898 (1986).
- Imura Y., Terashita Z., Nishikawa K., *Life Sci.*, **39**, 111—117 (1986).
- Takizawa H., Ishii A., Suzuki S., Shiga J., Miyamoto T., *Int. Arch. Allergy Appl. Immunol.*, **86**, 375—382 (1988).
- Nagaoka J., Harada K., Kimura A., Kobayashi S., Murakami M., Yoshimura T., Yamada K., Asano O., Katayama K., Yamatsu I., *Arzneimittel Forschung Drug Reseach*, **41**, 719—724 (1991).
- Motomura K., Iwanaga S., Aratono M., Matuura R., *J. Colloid Interface Sci.*, **86**, 151 (1982).
- Gulari E., Gulari E., Tsunashima Y., Chu E., *J. Chem. Phys.*, **70**, 3695—3972 (1979).
- Iwamoto K., Sunamoto J., Inoue K., Endo T., Nojima S., *Biochim. Biophys. Acta*, **691**, 44—51 (1982).
- Kawato S., Kinosita K., Ikegami A., *Biochemistry*, **16**, 2319—2324 (1977).
- Greenspan P., Fowler S. D., *J. Lipid Res.*, **26**, 781—789 (1985).
- Sackett D. L., Wolff J., *Anal. Biochem.*, **167**, 228—234 (1987).
- Dimorth K., Reichardt C., *Liebig. Ann.*, **661**, 1—37 (1963).
- Meguro K., Kondo T., Ino T., Nojima S., *Biochim. Biophys. Acta*, **691**, 44—51 (1986).
- Rosen M. J., "Surfactants and Interfacial Phenomena," Wiley-Interscience, 1978.
- Lucassen-Reynders E. H., *J. Phys. Chem.*, **70**, 1777—1785 (1966).
- Handa T., Saito H., Kakce A., Tanaka K., Miyajima K., *Biochemistry*, **31**, 1415—1420 (1992).
- Israelachvili J. N., Mitchell D. J., Ninham B. W., *Biochim. Biophys. Acta*, **470**, 185—201 (1977).
- Israelachvili J. N., Marceja S., Horm R. G., *Q. Rev. Biophys.*, **13**, 121—200 (1980).
- Malliaris A., Binana-Limbelew W., Zana R., *J. Colloid Interface Sci.*, **110**, 114—120 (1986).

Table 2. Physicochemical Characteristics of E5880, STAC and CTAC

	E5880	STAC	CTAC
cmc (mM)	0.12	0.33 0.29 (25 °C) ¹⁹	1.6 1.3 (30 °C) ²⁰
Saturated surface density: Γ_s ($\mu\text{mol}/\text{m}^2$)	2.0	2.6	2.7
Area/molecule (nm^2)	0.843	0.633	0.627
Critical packing parameter	0.25	0.33	0.33
Shape of micelle	Spherical micelle	Spherical micelle	Spherical micelle
Aggregation number	88	117	95 102 ²⁵
Size of micelle (nm)	8.1	6.3	5.1
Emission maximum (nm)	621	636	636
Micropolarity (comparable to organic solvent)	Isopropanol	Methanol	Methanol
Polarization (P)	0.316	0.105	0.098

The Shell Dissolution of Various Empty Hard Capsules

Irene CHIWELE,^a Brian E. JONES,^b and Fridrun PODCZEK^{*,a}

Department of Pharmaceutics, The School of Pharmacy, University of London,^a 29/39 Brunswick Square, London WC1N 1AX, U.K., and Shionogi Qualicaps, S.A.,^b Calle de la Granja, 49, 28108 Alcobendas, Spain.

Received December 20, 1999; accepted March 14, 2000

The shell dissolution properties of gelatine, gelatine/polyethylene glycol (PEG) and hydroxypropyl methylcellulose (HPMC) capsules were studied as a function of temperature, dissolution medium, and after different storage conditions. In any dissolution medium with a pH below or equal to 5.8, HPMC capsule shells dissolved rapidly, and there was no difference in the time in which dissolution occurred in the tested temperature interval of 10 to 55 °C. Gelatine and gelatine/PEG capsule shells, generally, did not dissolve at temperatures below 30 °C. The shell dissolution time of all capsules tested was prolonged and more variable in mixed phosphate buffer pH=6.8. The addition of enzymes (pepsin, pancreatin) to any dissolution medium was found not to enhance the differences between the different types of capsules investigated. In practical terms, the results indicated that capsule formulations should not be taken with drinks from the carbonated Cola-type. Gelatine containing capsules should preferably be administered with a warm drink, whereas HPMC capsules could be given with cold or warm drinks. The latter type of capsules should also be preferred for preparations to be taken in the fasted state. A short storage of gelatine containing capsules under hot humid tropical conditions appeared not to alter the dissolution properties of the shells, and changes in disintegration times and dissolution times of formulations filled in such capsules might be a reflection of changes of the powders incorporated rather than of the capsule shells. However, a short storage of HPMC capsules under such conditions appeared to influence the capsule shell matrix.

Key words gelatine capsules; hydroxypropyl methylcellulose capsules; shell dissolution; two-piece hard shell capsules

Lehuby first patented the two-piece hard shell capsule in 1846. These capsules were made from starch or tapioca, sweetened with some sucrose and coloured with 'fish silver.' Several additions to the patent followed, describing the use of various materials and mixtures including gelatine. Gelatine has been the material of choice for the manufacture of hard shell capsules for a long time. Gelatine is a material widely used in food industry. It is readily soluble in biological fluids at body temperature and is a good film forming material. Its suitability for producing capsules is related to its ability to form a thermally reversible gel. However, some properties of gelatine films are disadvantageous for their use as a capsule shell material. For example, gelatine capsule shells exposed to low relative humidity of the storage air become brittle, which also occurs when they are filled with formulations containing hygroscopic materials. It was found that exposure to tropical conditions, with high relative humidity above about 60–70%, increased the minimum temperature for dissolution of gelatine films from 31 °C to over 50 °C and even up to more than 97 °C.¹⁾ Cross-linking between gelatine proteins due to the presence of aldehyde groups in the filling material can also reduce the solubility of the capsule shells.^{2,3)} Hence, it appears beneficial to be able to use different materials for manufacturing two-piece hard shell capsules. To make the process economic such capsule shells should be manufactured on similar machines, as used for gelatine capsules, and they should have the same performance on conventional filling equipment.

Several materials have been tested in the last decades to replace fully or modify gelatine as the capsule shell material. These attempts often either failed due to difficulties in large-scale manufacture, because the capsules could not be used on conventional filling machines, or the capsules had *in vivo*-solubility problems. However, two new varieties of capsule shells, which were developed in Japan, fulfil all the require-

ments for two-piece hard shell capsules in terms of their manufacture and filling properties:

(1) Five percent of polyethylene glycol (PEG; molecular weight 4000) has been added to the gelatine. These 'gelatine/PEG'—capsules show a minimised brittleness when exposed to air of low relative humidity during storage.⁴⁾ They can also advantageously be used for filling of hygroscopic formulations.

(2) Hydroxypropyl methylcellulose (HPMC) was used as major film forming agent. Carrageenan and potassium chloride were added in small quantities to lower the thermal gelation temperature of HPMC and to promote gelation, respectively.⁵⁾ These 'HPMC' capsules should show no incompatibilities with most filling materials or powders, as the only incompatibility currently known for HPMC is the interaction with some oxidising agents.⁶⁾

On a laboratory scale, cross-linked dextran has been successfully used to form two-piece hard shell capsules by the usual dipping procedure.⁷⁾ Such capsules could be used for the delivery of drugs to the colon without the need to coat them with a polymer film. Experience of their large-scale manufacture, however, is currently not available.

The aim of this work was to compare the shell dissolution properties of ordinary gelatine hard capsules with gelatine/PEG and HPMC capsules in different dissolution media, independent of their capsule content, at different temperatures and after different storage conditions in order to evaluate their suitability as a solid oral dosage form.

Experimental

White opaque two-piece capsule shells made from gelatine, HPMC and gelatine/PEG (Shionogi Qualicaps, S.A., Alcobendas, Madrid, Spain) of size 0 and 3 were used in this study. Water, produced by a combination of demineralisation and reverse osmosis was freshly made over night. Pancreatin (pig pancreas), pepsin A powder (biochemical grade), anhydrous disodiumhydrogen orthophosphate, potassium-dihydrogenorthophosphate, sodium

* To whom correspondence should be addressed. e-mail: podczek@cua.ulsop.ac.uk

chloride and 5 M hydrochloric acid were obtained from Merck (BDH, Poole, U.K.). Sodium taurocholate hydrate (97%) was purchased from Avocado Research Chemicals Ltd. (Heysham, U.K.).

The following dissolution media were prepared according to British Pharmacopoeia (1998, see Appendices XIIB-A187 and IA-A46): 1) 0.1 M hydrochloric acid, pH=1.0; 2) mixed phosphate buffer, pH=6.8; 3) artificial gastric juice. Artificial intestinal juice was prepared from mixed phosphate buffer by adding 0.5 g sodium taurocholate hydrate and 10.0 g pancreatin per final volume of 1000 ml. Solutions containing enzymes, *i.e.* artificial gastric and intestinal juice, were freshly prepared every day.

The determination of the shell dissolution time of the hard capsules followed a method described by Boymond⁸⁾ as modified by Jones and Cole.⁹⁾ In each capsule shell, a steel ball bearing (non-corrodable grade) was placed, and the capsules were closed to their specified closed joined length. For size 0 capsules, the diameter of the ball bearings used was 6.344 mm, and for size 3, steel ball bearings with a diameter of 4.990 mm were used. Special metal holders in the form of a strip of stainless steel were suspended across 800 ml glass beakers. The holders contained holes, through which the capsule body could pass, but not the cap. The holes were spaced 5 mm apart. The liquid level in the glass beaker was kept so that the liquid surface touched the lower surface of the metal holders, but did not cover the top surface. The glass beakers were placed in a water bath (Grants Instruments, type SB 20, Barrington, Cambridge, U.K.) providing thermostatic control of temperature of $\pm 0.5^\circ\text{C}$. The liquid inside the glass beakers was stirred at 37 rpm (Heidolph Laboratory Stirrer, type 12ZR1, Germany). The paddle was kept 1 cm above the base of the glass beakers, and 5 mm from the metal holders. The end point of capsule shell dissolution was defined as the time when the steel ball bearing was released from the capsule body and hit the base of the glass beaker. Results are the mean and standard deviation of ten capsules, tested with five units at a time. In those experiments, where the capsule shells did not release any of the steel ball bearings during 120 min, only 5 capsules were studied, and the experiment was terminated at this point.

Capsules were stored either under ambient room conditions ($19 \pm 1^\circ\text{C}$, 35–40% relative humidity of the air), or under conditions defined as 'tropical' ($37 \pm 0.5^\circ\text{C}$, 75% relative humidity of the storage air¹⁰⁾). To achieve the latter, a desiccator containing a saturated solution of sodium chloride was placed into an incubator set at 37°C (B & T Unitemp, U.K.).

Analysis of Variance (ANOVA) was performed using SPSS 9.0 (SPSS, Woking, U.K.).

Results and Discussion

Water is commonly used as dissolution medium in major Pharmacopoeias. It is also recommended as a drink to patients when taking a solid oral dosage form. In this case, 150 ml is usually recommended. In the current experiments the temperature range was between 10° and 55°C , and a $\sqrt{2}$ geometric progression of test temperatures from room temperature (19°C) upwards was used. The lowest value of 10°C was chosen to represent the taking of the dosage form with a cold drink. In preliminary experiments, placing a 200 ml beaker filled with 150 ml water of 10°C in a 37°C thermostatically controlled water bath had shown that it can take up to 7 min, before temperature equilibrium is achieved, depending on the rate of movement of the outer water mantle. Such a comparatively long time span could influence the initial *in vivo* shell dissolution and consequently the release and dissolution of the capsule formulations. The upper temperature limit of 55°C corresponded to the average drinking temperature of coffee or tea, as determined on such drinks from 10 volunteers using a thermometer.

The end point determination of the disintegration of hard capsules filled with, for example, powders or granules, as described in the major Pharmacopoeias is problematic. It is often not possible to separate the disintegration time of the powder plug from the time for the capsule shell to release the plug. The latter depends on the shell dissolution properties, but is strongly overlaid by the properties of the filling mater-

ial.¹¹⁾ For example, some materials cause swelling of the powder plug on contact with moisture, which will cause opening of the two-piece capsule. In such cases, some of the plug is exposed early to the disintegration liquid, while some parts of the plug may be entrapped at the ends of the capsule shell. The ideal test method would determine the shell dissolution time and the disintegration time of the powder plug separately. As this cannot be achieved with the standard pharmacopoeial disintegration test, in this paper a method was sought, which removes the influence of the filling materials on the dissolution of the capsule shells. Steel ball bearings as filling material ensure that the capsule body remains suspended in the disintegration liquid, but do not dissolve, swell or alter their physical state in any other way. Hence, there is no influence of the filling material on the shell dissolution time. Dissolution of the capsule shell normally starts at the ends of the capsule. Tiny holes may be formed, which continually grow. The size of the ball bearings was chosen to match approximately the inner diameter of the capsule body. For the ball bearing to fall free requires a considerable growth of the dissolved area of the capsule shell, but at some point before this occurs, the capsule body can no longer support its weight and the ball bearing will drop out of the capsule. The authors believe that this test is a method, which is able to distinguish between shell dissolution times of capsules of different materials when tested under different conditions.

The shell dissolution times obtained for capsules of size 0, stored at ambient room conditions, are compared in Fig. 1a. Only HPMC capsules dissolved at the lower temperatures of 10° and 19°C , and their shell dissolution time appeared not to be influenced to any great extent when increasing the temperature up to the upper test limit employed. Gelatine and gelatine/PEG capsules, however, showed strong temperature dependence. Rapid shell dissolution only occurred at temperatures above 30°C . At temperatures below 25°C these capsules swelled and formed leather-like sacks (see Fig. 6), which did not release the ball bearings, unless the capsule cap separated from the capsule body. Modern capsules, however, have strong locking mechanisms between the two shell parts, preventing such opening. Similar trends were observed for all types of capsules using capsule size 3 (Fig. 1b). For HPMC capsules, the shell dissolution times were similar to those obtained for size 0 capsules up to a temperature of 30°C . From 37°C onwards, however, the shell dissolution times were significantly longer for capsules of size 3 (ANOVA, $p < 0.05$). This indicates a tendency of the material to form viscous gels at higher temperatures, which, in these cases, would not affect dosage form dissolution to a larger extent. Although some significant differences in shell dissolution time were also found for gelatine and gelatine/PEG at high temperatures, they were not systematically in one direction. Hence, they may only represent the larger variability of dissolution of these types of capsule shells.

In Fig. 2a, the relationships between shell dissolution time and temperature are illustrated for capsule size 0 using 0.1 M hydrochloric acid as the dissolution medium. The shell dissolution times for HPMC were not different from those obtained in water. For gelatine and gelatine/PEG capsules, however, the shell dissolution was found to be slower at 30°C . Melting and dissolution properties can be altered by pH, de-

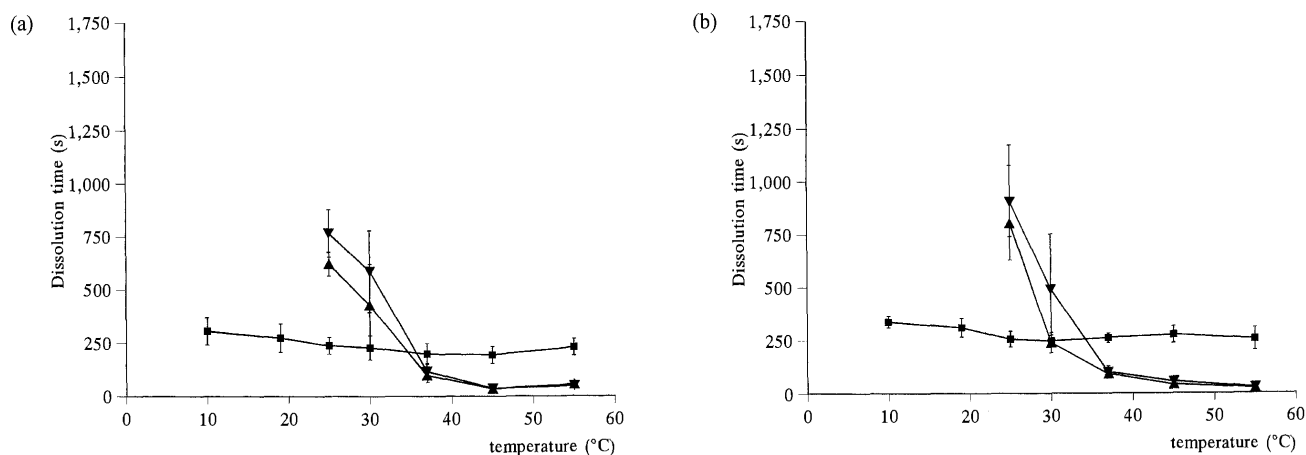


Fig. 1. Shell Dissolution Times of Two-Piece Hard Shell Capsules Size 0 (1a) and Size 3 (1b) in Water as a Function of the Temperature of the Dissolution Medium after Storage under Ambient Room Conditions

■, HPMC capsules; ▲, gelatine capsules; ▼, capsule shells made from a mixture of gelatine and PEG.

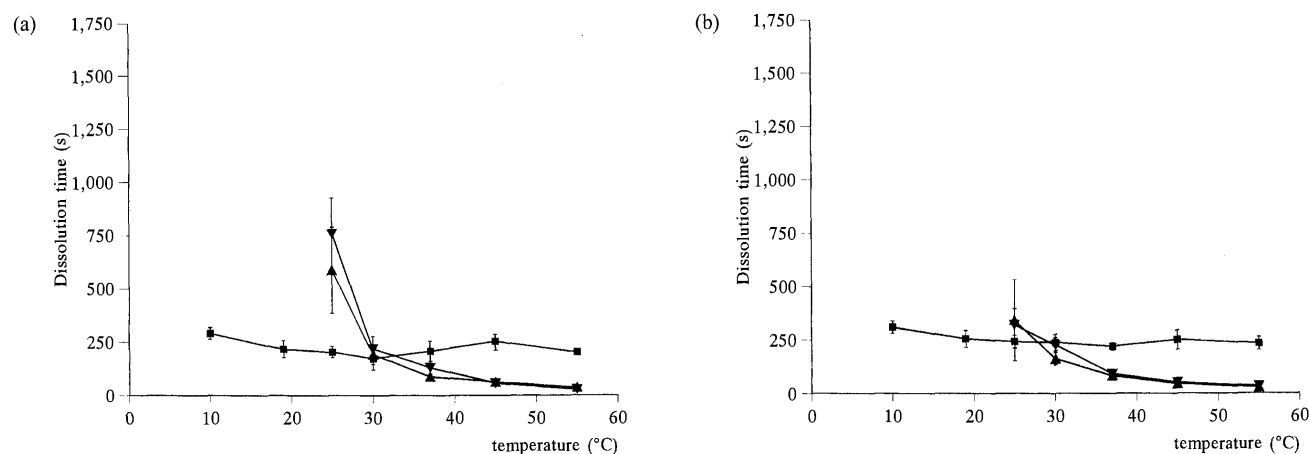


Fig. 2. Shell Dissolution Times of Two-Piece Hard Shell Capsules Size 0 (2a) and Size 3 (2b) in 0.1 M Hydrochloric Acid as a Function of the Temperature of the Dissolution Medium after Storage under Ambient Room Conditions

■, HPMC capsules; ▲, gelatine capsules; ▼, capsule shells made from a mixture of gelatine and PEG.

pending on the origin of the gelatine.¹⁾ The shell dissolution time of HPMC capsules size 3 was generally longer than for size 0 capsules (Fig. 2b), and, except for 10 °C, this difference was significant (ANOVA, $p < 0.05$). For gelatine and gelatine/PEG capsules, however, a tendency for the shell dissolution time to become shorter with the smaller capsule size was observed.

The shell dissolution time of HPMC capsules was significantly increased in mixed phosphate buffer (Fig. 3a; ANOVA, $p < 0.05$). Also, between 20° and 45 °C the shell dissolution time gradually increased, and the dissolution process became more variable. Above 45 °C, HPMC capsules dissolved only slowly *i.e.* it took about 1 h 20 min for size 0 and 1 h for size 3 capsules (Fig. 3b) to dissolve. This could be due to a distortion of the gel point by the pH of the buffer to a higher temperature. At low temperatures, HPMC capsules of size 0 dissolved more rapidly than size 3 capsules, but at a higher temperature the differences in dissolution time were mainly not significant (ANOVA). The pH of the mixed phosphate buffer has also significantly altered the shell dissolution properties of gelatine and gelatine/PEG capsules at temperatures below 37 °C, while at 37 °C and above shell dissolution was similar to that observed in water and 0.1 M

hydrochloric acid. The dependence of dissolution of gelatine capsule shells on pH was previously proposed to have caused great variability of tetracycline absorption in humans,¹²⁾ which gives some support to the findings reported here. Another reason could be the greater relative ionic strength of the mixed phosphate buffer. An increase in ionic strength of the dissolution medium was reported previously to prolong considerably the disintegration time of hard gelatine capsules, filled with lactose.¹³⁾ However, both Elliott's and Hüttenrauch's observations were made at 37 °C, whereas in this paper the effect of pH and ionic strength applies only to temperatures below 37 °C. This might be due to slight differences in the manufacture of gelatine capsules in 1971/72 from today.

From the results shown in Figs. 1–3 some practical conclusions can be drawn. First, neither type of capsules should be taken with drinks such as a carbonated Cola-type drink to avoid slow down of the dissolution of the capsule shell, because these drinks contain considerable amounts of phosphates. Also, the pH dependence of the shell dissolution process suggests that gelatine or gelatine/PEG hard shells should not be used for preparations, which require the patient to take the capsules in the fasted state *i.e.* without intake of

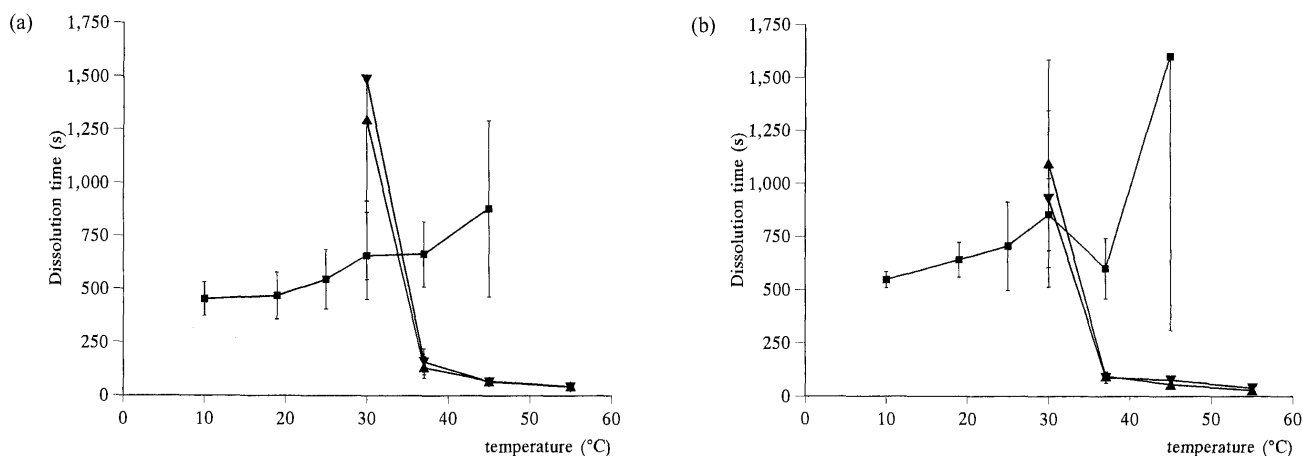


Fig. 3. Shell Dissolution Times of Two-Piece Hard Shell Capsules Size 0 (3a) and Size 3 (3b) in Mixed Phosphate Buffer (British Pharmacopoeia, Values for HPMC at 55 °C Not Included; Size 0: 4694 ± 1061 s; Size 3: 3289 ± 316 s) as a Function of the Temperature of the Dissolution Medium after Storage under Ambient Room Conditions

■, HPMC capsules; ▲, gelatine capsules; ▼, capsule shells made from a mixture of gelatine and PEG.

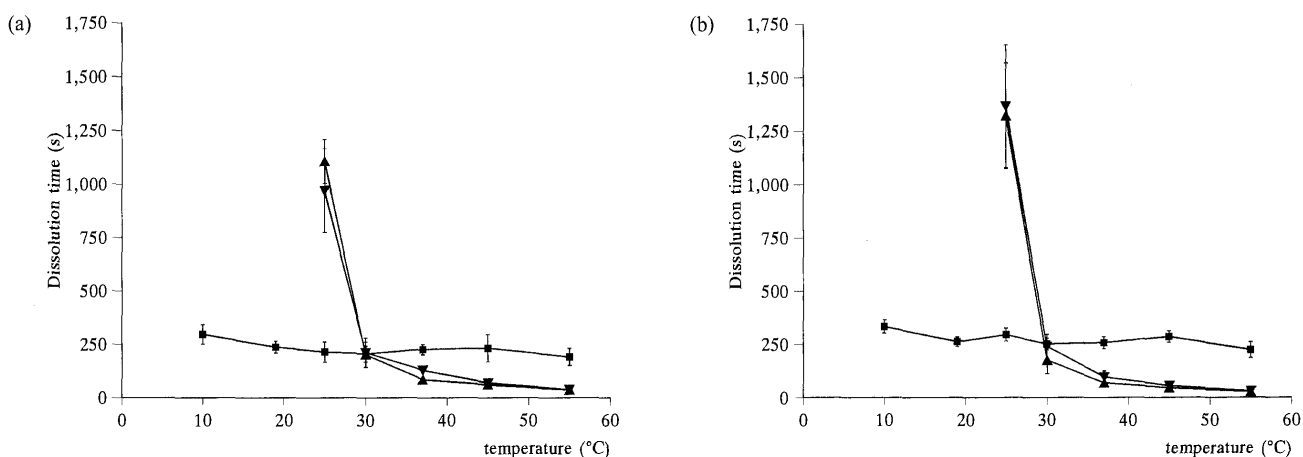


Fig. 4. Shell Dissolution Times of Two-Piece Hard Shell Capsules Size 0 (4a) and Size 3 (4b) in Artificial Gastric Juice (British Pharmacopoeia) as a Function of the Temperature of the Dissolution Medium after Storage under Ambient Room Conditions

■, HPMC capsules; ▲, gelatine capsules; ▼, capsule shells made from a mixture of gelatine and PEG.

food, unless given with a warm drink. Care should be taken with HPMC capsules and hot drinks, but with a cold drink shell dissolution problems could be overcome. Secondly, for gelatine and gelatine/PEG capsules a warm drink such as coffee or tea could promote drug release, whereas a cold drink should be avoided. As long as the pH of the drink is below or equal to that of demineralised water (pH=5.8 in these experiments), HPMC capsules can be taken with any form of drink.

Courts¹⁴ reported that the rate of peptic hydrolysis of gelatine by pepsin was comparatively slow, yet was three times faster than a thermal degradation at 37 °C. However, the results for artificial gastric juice (Figs. 4a,b) were similar to those obtained using 0.1 M hydrochloric acid. The shell dissolution of gelatine containing capsules in artificial gastric juice is therefore not related to the presence of the enzyme. This also applies to HPMC capsules. It is consistent with findings reported by Shiu *et al.*¹⁵ These authors compared dissolution media containing enzymes with enzyme-free media with respect to the drug release profiles from ordinary gelatine capsules in comparison to cross-linked gelatine capsules. Advantage was gained from the addition of enzymes

only for the cross-linked capsules.

The addition of pancreatin and bile salts to mixed phosphate buffer reduced the shell dissolution time of the gelatine and gelatine/PEG shells slightly, but there was still no dissolution below 30 °C (Figs. 5a,b). Courts¹⁴ did not study pancreatin, but some of its components, namely trypsin and chymotrypsin. These enzymes were found to cause heavy proteolysis of alkali-processed ox-bone gelatine. One reason for the absence of effect in this study could be that the dissolution process is the rate limiting process, and consequently enzymatic degradation, although occurring, did not play a significant role. The addition of pancreatin and bile salts changed the shell dissolution properties of HPMC capsules to a limited extent. However, the shell dissolution times were sometimes below and sometimes above those found in mixed phosphate buffer solution. These variations were also not consistent for capsule sizes 0 and 3, and hence, the deviations might reflect the variability of the dissolution process only; they appear not to be enzyme related.

The storage under tropical humid conditions (37 °C and 75% relative humidity of the storage air) for 24 h resulted in a softening and stickiness of all capsules when still warm.

However, after removing them from the storage chamber, they were allowed to cool down for 15 min in a closed 20 ml polyethylene bottle. After that time, they had regained their firmness, and stickiness was minimal. As before, for HPMC capsules the shell dissolution values in artificial gastric juice were consistently longer for size 3 capsules (Fig. 7b) compared to size 0 shells (Fig. 7a), and the difference was in almost all cases statistically significant (ANOVA, $p < 0.05$). The shell dissolution times for HPMC capsules, which had been stored under tropical conditions, in artificial intestinal juice (Figs. 8a, b) were significantly reduced for temperatures between 10 ° and 30 °C (ANOVA, $p < 0.05$). Above 37 °C, however, shell dissolution times were increased, and at 55 °C these capsules did not dissolve during a time span of two hours. During the storage the HPMC capsules took up moisture, which could have led to a hydration of the capsule shell walls. Water penetration through the hydrated material might be slower and thus the capsule shells would not dissolve readily. The change in dissolution behaviour observed for HPMC capsule shells appears to be in contrast to findings reported by Matsuura and Yamamoto,⁵ who used a similar humidity to store antibiotic filled HPMC capsules and did not

report any changes in capsule disintegration. They employed longer storage times and used a storage temperature of 60 °C, higher than normally used in such trials in Europe. The discrepancy between the two findings can only be explained by the deficiencies of the standard disintegration test applied as discussed above.

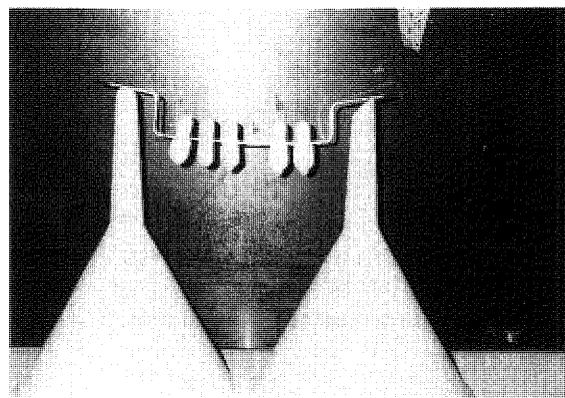


Fig. 6. Gelatine Capsules after Exposure to Water of 19 °C as Dissolution Medium

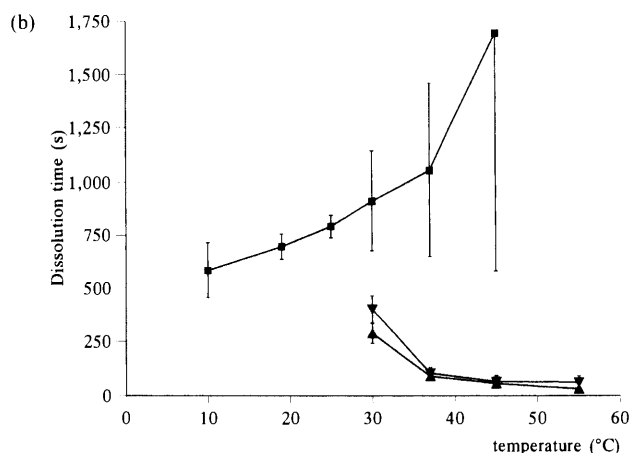
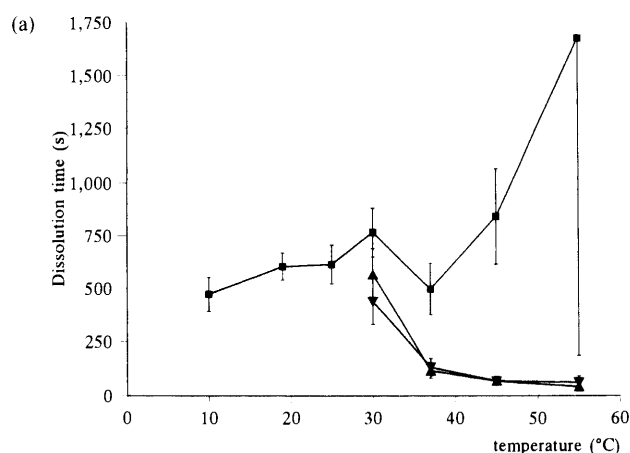


Fig. 5. Shell Dissolution Times of Two-Piece Hard Shell Capsules Size 0 (5a) and Size 3 (5b) in Artificial Intestinal Juice (Boymond *et al.*⁸) as a Function of the Temperature of the Dissolution Medium after Storage under Ambient Room Conditions

■, HPMC capsules; ▲, gelatine capsules; ▼, capsule shells made from a mixture of gelatine and PEG.

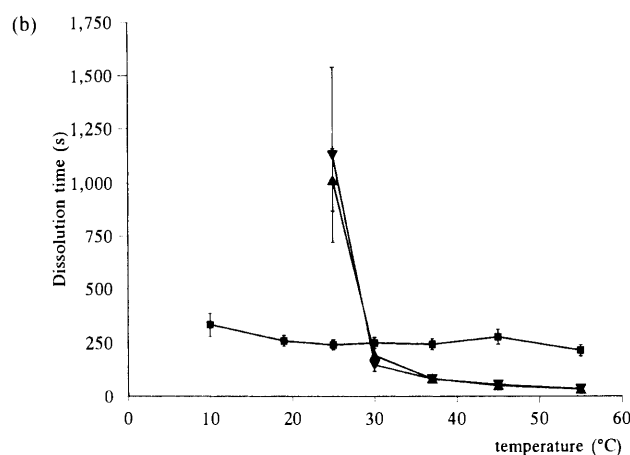
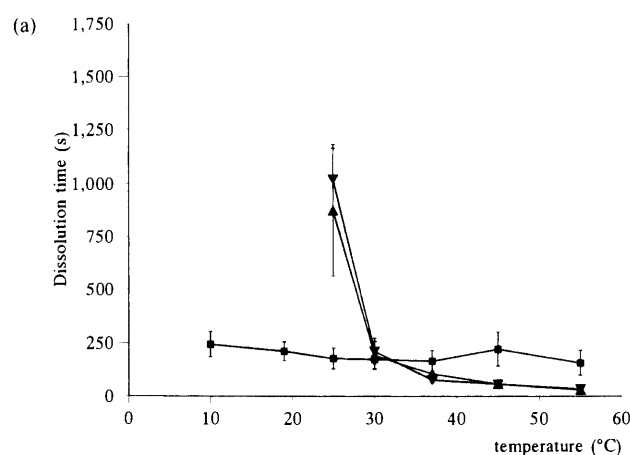


Fig. 7. Shell Dissolution Times of Two-Piece Hard Shell Capsules Size 0 (7a) and Size 3 (7b) in Artificial Gastric Juice (British Pharmacopoeia) as a Function of the Temperature of the Dissolution Medium after Storage of the Capsules at 75% Relative Humidity and 37 °C for 24 h

■, HPMC capsules; ▲, gelatine capsules; ▼, capsule shells made from a mixture of gelatine and PEG.

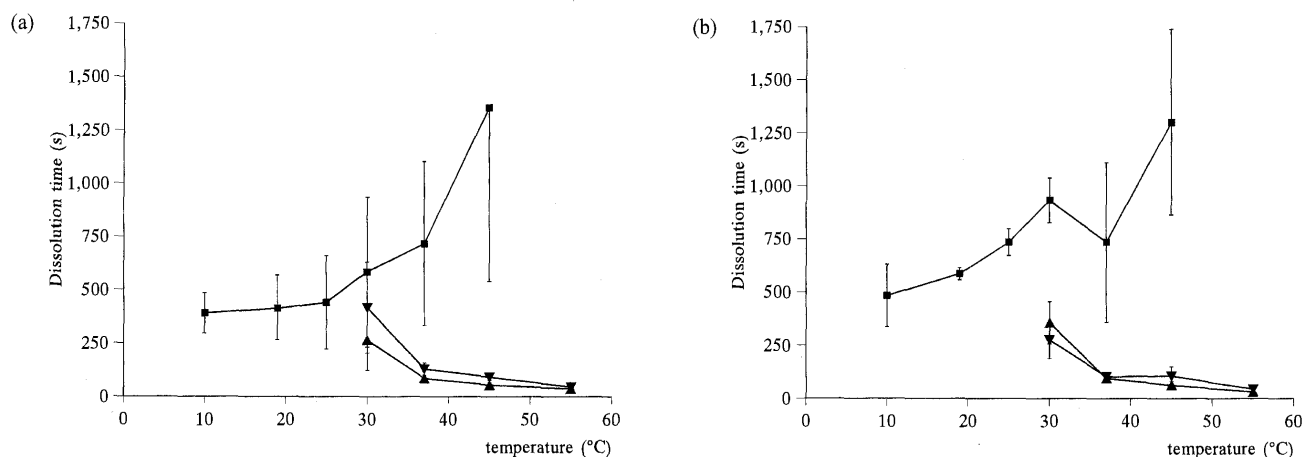


Fig. 8. Shell Dissolution Times of Two-Piece Hard Shell Capsules Size 0 (7a) and Size 3 (7b) in Artificial Intestinal Juice (Boymond *et al.*⁸) as a Function of the Temperature of the Dissolution Medium after Storage of the Capsules at 75% Relative Humidity and 37 °C for 24 h

■, HPMC capsules; ▲, gelatine capsules; ▼, capsule shells made from a mixture of gelatine and PEG.

Conclusions

In any dissolution medium with a pH below or equal to 5.8, HPMC capsules dissolve rapidly and the shell dissolution is independent of temperature between 10° and 55 °C. Gelatine containing capsule shells, however, do not dissolve at temperatures below 30 °C in such dissolution media, and their shell dissolution times are dependent upon temperature. Mixed phosphate buffer appears not to be a suitable dissolution liquid to test the dissolution of capsule shells, because shell dissolution is more variable and prolonged. The addition of enzymes to any dissolution medium does not enhance the differences between the different types of capsules. In practical terms, the results indicated that capsule formulations should not be taken with drinks from the carbonated Cola-type, because these drinks contain a considerable amount of phosphates. Gelatine containing capsules should preferably be administered with a warm drink, whereas HPMC capsules could be given with cold or warm drinks. The latter type of capsules should also be preferred for preparations to be taken in the fasted state *i.e.* without intake of food. A short storage period of gelatine containing capsules under hot humid tropical conditions appears not to alter the dissolution properties of the shells, and changes in disintegration times and dissolution times of formulations filled in such capsules might be a reflection of changes of the powders incorporated rather than of the capsules. However, a short storage period of HPMC capsules under such condi-

tions appears to influence the capsule shell matrix, and hence, care should be taken when this type of capsules is exposed to hot and humid tropical conditions.

Acknowledgements The capsule shells used in this study were a gift from Shionogi Qualicaps, S.A., Alcobendas, Madrid (Spain).

References

- 1) Jones R. T., "Hard Capsules. Development and Technology," ed. by Ridgway K., The Pharmaceutical Press, London, 1987, pp. 31—48.
- 2) Carstensen J. T., Rhodes C. T., *Drug Dev. Ind. Pharm.*, **19**, 2709—2712 (1993).
- 3) Digenes G. A., Gold T. B., Shah V. P., *J. Pharm. Sci.*, **83**, 915—921 (1994).
- 4) Ogura T., Furuya Y., Matsuura S., *Pharm. Technol. Eur.*, **10**(11), 32—42 (1998).
- 5) Matsuura S., Yamamoto T., *Yakuzaigaku*, **53**, 135—140 (1993).
- 6) Harwood R. J., Johnson J. L., "Handbook of Pharmaceutical Excipients," 2nd ed., ed. by Wade A., Weller P. J., The Pharmaceutical Press, London, 1994, pp. 229—232.
- 7) Brondsted H., Andersen C., Hovgaard L., *J. Controlled Release*, **53**, 7—13 (1998).
- 8) Boymond P., Sfiris J., Amacker P., *Pharm. Ind.*, **28**, 836—842 (1966).
- 9) Jones B. E., Cole W. V. J., *J. Pharm. Pharmacol.*, **23**, 438—443 (1971).
- 10) Matthews B. R., *Drug Dev. Ind. Pharm.*, **25**, 831—856 (1999).
- 11) Jones B. E., *Acta Pharm. Suec.*, **9**, 261—263 (1972).
- 12) Elliott G. R., *J. Pharm. Sci.*, **13**, 459 (1972).
- 13) Hüttenrauch R., *Pharmazie*, **26**, 107—108 (1971).
- 14) Courts A., *Biochem. J.*, **59**, 382—386 (1955).
- 15) Shiu G. K., Wang J.-T., Worsley W. N., Cole E. T., Madit N., *Pharm. Res.*, **14**, Suppl. S-718 (1997).

Difference Spatial Distribution Function Analysis of Aqueous Solutions.

III.¹⁾ Hydration Structures of Alcohol and Ether Solutions Having Straight Chain and Branched Alkyl Groups

Toshiyuki HATA and Yukio ONO*

Faculty of Pharmacy and Pharmaceutical Sciences, Fukuyama University, Sanzo, Gakuen-cho, Fukuyama, Hiroshima 729–0292, Japan. Received December 20, 1999; accepted April 25, 2000

Spatial distribution functions (SDFs), $g_{OO}(x,y,z)$ and $g_{OH}(x,y,z)$, obtained from Monte Carlo simulations at 298 K were applied to characterize the anisotropic structure of infinitely dilute aqueous solutions of alcohols and ethers having straight chain and branched alkyl groups. In spite of the different size and shape of the hydrophobic groups, the spatial orientation of the hydrogen-bonded water molecules was found to be of linear type with a triple layer structure in the hydrogen acceptor (HA) region and a double layer structure in the hydrogen donor (HD) region. The volumes and the coordination number (CN) in the HA region were essentially identical for all alcohol and ether solutions, but the volumes for the isopropyl alcohol (IPA) and isopropyl methyl ether (IPE) solutions were greater than those for the other solutions. In the hydrophobic hydration (HH) region, these values increased with increasing size and shape of hydrophobic groups, except in the case of IPA and IPE solutions. These results indicated that the hydration structures around the isopropyl group in alcohol and ether solutions differed from those in other solutions. From the results of the difference SDF (DSDF), $\Delta g_{OO}(x,y,z)$, between SDFs $g_{OO}(x,y,z)$ for the two states, it was apparent that the distribution of hydration water molecules in the HA region for ether solution was characterized by the increase of the distribution in the direction of lone pair electrons on the oxygen atom of the solute molecule with increasing hydrophobicity.

Key words Monte Carlo simulation; alcohol and ether solution; spatial distribution function; difference spatial distribution function; hydration structural change; branched alkyl group

In recent years, numerous researchers have theoretically investigated hydration structures of liquid and aqueous solutions using Monte Carlo (MC) and molecular dynamics (MD) methods, e.g. ref. 2. Although liquid structures can be experimentally determined by either X-ray³⁾ or neutron diffraction,⁴⁾ the structures of aqueous solutions are very difficult to determine by these methods. Therefore, MC and MD methods⁵⁾ are often used, since they can theoretically examine the structure and physicochemical properties of both liquid and aqueous solutions.

An important application of molecular simulation is the investigation of the hydration structures and the solvent effects of bioactive molecules and drugs in aqueous solution.⁶⁾ In a previous paper,¹⁾ we reported that the spatial distribution function (SDF) $g_{OO}(x,y,z)$ obtained from MC simulations accurately characterized the anisotropic hydration structure in alcohol and ether solutions as a simple amphoteric compound. And we found that the difference SDF (DSDF) $\Delta g_{OO}(x,y,z)$ could effectively evaluate the effects of the steric bulk of hydrophobic groups in the solutions.

The molecular structure and the effect of the steric bulk of hydrophobic groups are considered to be very important for the analysis of hydration structure. In particular, *tert*-butyl alcohol (TBA) has hydrophobic groups with the highest steric bulk among all butyl alcohols, but it is freely miscible with water. TBA is well known to exhibit anomalous thermodynamic behavior, and Nakanishi *et al.*⁷⁾ have analyzed the hydration structure of this solution using the radial distribution function (RDF) results obtained from MC simulation.

In this investigation, we analyze hydration structures and the effects of the steric bulk of hydrophobic groups on their respective aqueous solutions of alcohols and ethers having propyl and butyl groups as straight chain alkyl groups and isopropyl and *tert*-butyl groups as branched alkyl groups.

The molecules employed in this investigation are propyl alcohol (PA), isopropyl alcohol (IPA), butyl alcohol (BA), *tert*-butyl alcohol (TBA), and their corresponding methyl ethers (MPE, IPE, BME, and TBE) (Chart 1). Infinitely dilute aqueous solutions of these alcohols and ethers are hereafter referred to as their respective alcohol and ether solutions.

The anisotropic hydration structures and structural changes around alcohols and ethers having straight chain and branched alkyl groups were analyzed using the SDF $g_{OO}(x,y,z)$ obtained from MC simulation. Our results further indicated that these distributions of SDF $g_{OO}(x,y,z)$ could be evaluated from the binding energies (BE). Finally, it was shown that the effects of the steric bulks of the straight chain and branched hydrophobic groups could be characterized by the DSDF $\Delta g_{OO}(x,y,z)$ between the SDFs for two alcohol or two ether solutions.

Computational Procedure

Monte Carlo Simulation For all systems, MC simulations were carried out for one alcohol or ether molecule and 215 water molecules in a cube with a cell length of 18.63 Å within the Metropolis scheme⁸⁾ in the NVT ensemble at 298 K. The molar volume obtained using a liquid water den-

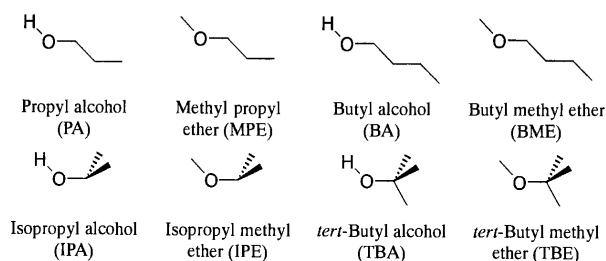


Chart 1. Molecular Geometries

* To whom correspondence should be addressed. e-mail: ono@fupharm.fukuyama-u.ac.jp

sity of 1.0 g cm^{-3} was $18.015 \text{ cm}^3 \cdot \text{mol}^{-1}$.

As in our previous paper,¹⁾ SPC potential⁹⁾ and TIPS potential¹⁰⁾ functions were employed to represent the intermolecular interactions for water, and for alcohol and ether, respectively. These potential functions (SPC and TIPS) were obtained from the sum of the Coulomb and Lennard-Jones terms, respectively. Interatomic distances and bond angles for water, alcohol, and ether molecules were taken from the values reported by Berendsen *et al.*⁹⁾ and Jorgensen.¹⁰⁾ The dihedral angles for each of $\text{C}_{\text{Me}}-\text{C}_{\alpha}-\text{O}-\text{H}$ (IPA) and $\text{C}_{\text{Me}}-\text{C}_{\alpha}-\text{O}-\text{C}_{\text{Me}}$ (IPE) were -60° and 60° . The dihedral angles for each of $\text{C}_{\text{Me}}-\text{C}_{\alpha}-\text{O}-\text{H}$ (TBA) and $\text{C}_{\text{Me}}-\text{C}_{\alpha}-\text{O}-\text{C}_{\text{Me}}$ (TBE) with three equivalent methyl groups were -60° , 60° and 180° . These geometries were fixed in the MC simulation. In the SDF calculations, the O atom and O- C_{α} bond lie on the origin of the coordinate and on the x-axis, respectively. And the respective three atoms of $\text{C}_{\alpha}-\text{O}-\text{H}$ and $\text{C}_{\alpha}-\text{O}-\text{C}_{\text{Me}}$ lie on the x-y plane. After excluding the first 750000 configurations, we employed the subsequent 7500000 configurations to obtain the statistical average in the MC simulations.

Difference Spatial Distribution Function Bosio *et al.*¹¹⁾ reported that the temperature dependence of the hydration structure can be analyzed by the difference radial distribution function (DRDF) for heavy water obtained from X-ray diffraction at various temperatures. They indicated that the network structure of the hydration water decreases with rising temperature. In our previous paper,¹⁾ we proposed a new DSDF method for examining the effect of hydrophobic groups. In the case of alcohol and ether solutions having a straight chain and branched alkyl groups, the DSDF is obtained as the difference between the SDFs for two states calculated by the MC simulation. For example, the DSDF $\Delta g_{\text{OO}}(x, y, z)$ for TBA and IPA solutions is determined as follows.

$$\Delta g_{\text{OO}}(x, y, z) = g_{\text{OO}}(x, y, z)_{\text{TBA}} - g_{\text{OO}}(x, y, z)_{\text{IPA}}$$

Binding Energy Decomposition The binding energy (BE)¹²⁾ is determined as the sum of all spatial cells of the coefficient products obtained from the volume and coordination number (CN), the SDF $g_{\text{OO}}(x, y, z)$, and the averaged potential energies $\langle E(x, y, z) \rangle$ between the solute and solvent molecules at a certain point in a cubic cell. The SDF $g_{\text{OO}}(x, y, z) = 2.1$ is visualized as the high distribution of the first hydration shell, because this SDF value is more than twice that for the bulk state ($g_{\text{OO}}(x, y, z) = 1.0$). In this shell, the distribution of the hydration water molecules around the solute can be divided into hydrogen acceptor (HA), hydrogen donor (HD), and hydrophobic hydration (HH) regions. First, the HA region is defined as the distribution in the vicinity of the lone pair electrons on the oxygen atom of the solute. Second, the HD region corresponds to the distribution in the direction of the H atom of the hydroxyl group. Third, the HH region is classified as the distribution in the neighborhood of the hydrophobic group of the solute. Applying the linked list clustering technique,¹³⁾ we found that the regions of the high density distributions of SDF $g_{\text{OO}}(x, y, z)$ for oxygen (solute)-oxygen (water) pairs could be classified into the above three regions. Therefore, the $\langle \text{BE} \rangle_{\text{sum}}$ could be separated into three constituent BEs as follows.

$$\langle \text{BE} \rangle_{\text{sum}} = \langle \text{BE} \rangle_{\text{HA}} + \langle \text{BE} \rangle_{\text{HD}} + \langle \text{BE} \rangle_{\text{HH}}$$

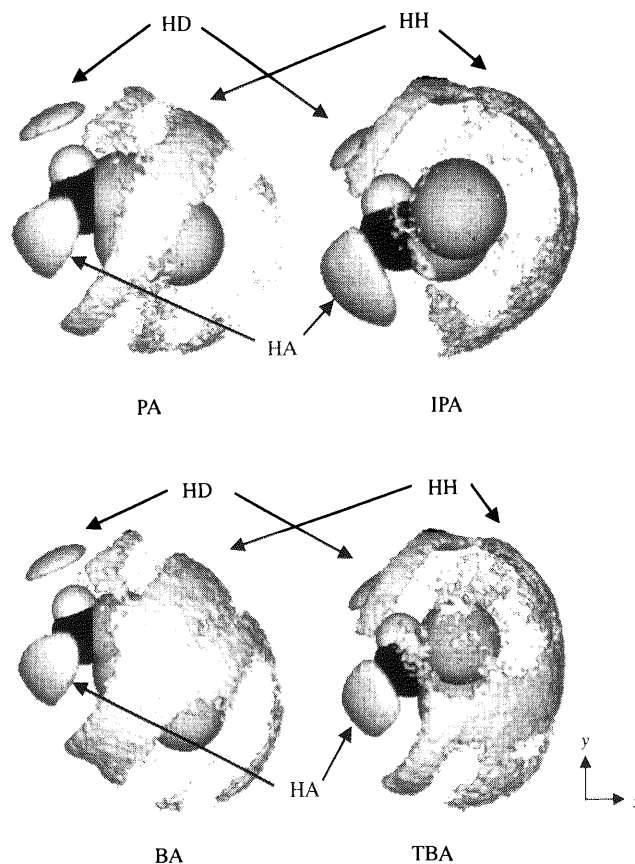


Fig. 1. Isosurface of Oxygen (Solute)-Oxygen (Water) SDF $g_{\text{OO}}(x, y, z) = 2.1$ Viewed Down the z-Axis for Alcohol Solutions

Results and Discussion

Hydration Structure The anisotropic hydration structures of the hydration water molecules around alcohol or ether could be visualized by SDF $g_{\text{OO}}(x, y, z)$ using the graphic display technique. With regard to the PA, IPA, BA, and TBA solutions, Fig. 1 shows the distributions of SDF $g_{\text{OO}}(x, y, z) = 2.1$ between solute and water molecules as obtained from MC simulation at 298 K. As shown in Fig. 1, the high distribution of SDF $g_{\text{OO}}(x, y, z)$ for the hydration water molecules surrounding alcohol could be classified into the HA, HD, and HH regions.

In the HA region, it is apparent that the high distribution in PA, BA, and TBA solutions spread out in the direction of lone pair electrons on the oxygen atom of alcohol, whereas the HA region in the IPA solution is wider than that in other alcohol solutions. This result supports the idea that the number of hydration water molecules excluded by the hydrophobic group of IPA is less than the number excluded by the hydrophobic groups of PA, BA, or TBA, and that the HA region in IPA solution is spread over a wider region in the central vicinity of the lone-pair electrons on the oxygen atom of alcohol.

Figure 2 shows the distributions of SDF $g_{\text{OO}}(x, y, z) = 2.1$ for the MPE, IPE, BME, and TBE solutions. The high distribution of SDF $g_{\text{OO}}(x, y, z)$ for the hydration water molecules around ether can be classified into the HA and HH regions. From these results in the HA region, it should be noted that the high distribution regions of SDF $g_{\text{OO}}(x, y, z)$ in ether solutions narrow less noticeably than those in alcohol solutions, but that the individual patterns of these distributions are

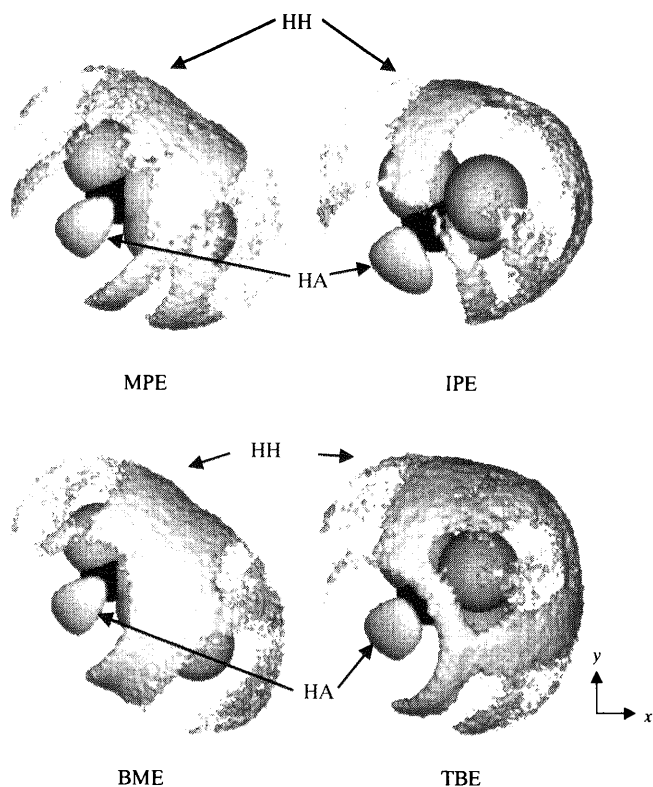


Fig. 2. Isosurface of Oxygen (Solute)-Oxygen (Water) SDF $g_{OO}(x,y,z) = 2.1$ Viewed Down the z -Axis for Ether Solutions

practically identical to those in the corresponding alcohol solutions.

Figure 3 shows the superposition of the oxygen-oxygen and oxygen-hydrogen SDFs, $g_{OO}(x,y,z)$ and $g_{OH}(x,y,z)$ for PA, IPA, BA, and TBA solutions. In the HA region, the maximum distributions of the hydrogen, oxygen, and hydrogen atoms in hydration water molecules occur at distances of approximately 1.8, 2.8, and 3.3 Å, respectively, from the oxygen atom of the alcohol or ether molecules, and these distribution distances are equal in all alcohol and ether solutions¹⁾ regardless of the kind of hydrophobic groups. These findings indicate that the hydration structures of both alcohol and ether solutions are formed by a triple layer structure composed of maximum distribution in the HA region, but that the distribution volume in ether solutions is smaller than that in alcohol solutions (see next section). In the HD region for PA, IPA, BA, and TBA solutions, the maximum distributions of oxygen and hydrogen atoms of water molecules occur at distances of approximately 1.9 and 2.4 Å from the hydrogen atom of the hydroxyl group of the solute, respectively. Therefore, it is evident that the double layer structure is composed of maximum distribution in the HD region. This result is in good agreement with that for the linear type reported by Okazaki *et al.*¹⁴⁾ in methanol solution. These findings clearly suggest that the main spatial orientation of the hydration water molecules around the oxygen and hydrogen atoms of all alcohol molecules in the HA and HD regions is of pronounced linear type. Moreover, these results are very consistent with our previously reported results for methanol and ethanol solutions.^{1a)}

Effect of the Hydrophobic Group A chief determining factor of the hydration structure in aqueous solutions is con-

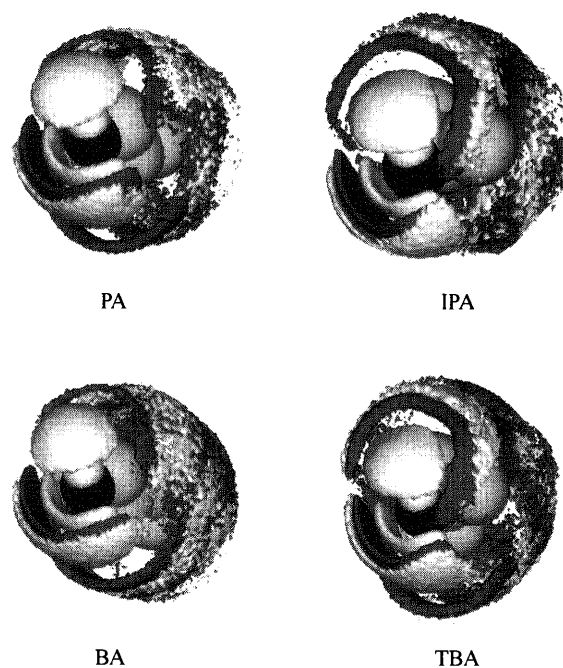


Fig. 3. Superposition Representation of Oxygen (Solute)-Oxygen (Water) and Oxygen (Solute)-Hydrogen (Water) SDF for Alcohol Solutions at 298 K

The bright area shows the increase of oxygen-hydrogen distribution at $g_{OH}(x,y,z) = 1.6$, and the dark area shows the decrease of oxygen-oxygen distribution at $g_{OO}(x,y,z) = 2.1$.

sidered to be the size and shape of the hydrophobic group. Moreover, the contour maps of the BE for alcohol or ether solutions can be effectively used to elucidate the effect of the steric bulk of the hydrophobic groups on the distribution of hydration water molecules in each region.

(a) Effect of the Straight Chain Alkyl Group As shown in Fig. 1, the distributions of hydration water molecules around the hydrophobic group in alcohol solutions spread over the slender band structure along hydrophobic groups. The maximum distributions are especially localized in the central area between the two methyl groups of a hydrophobic group. Moreover, the distribution of water molecules obtained from ether solutions is essentially identical to the distribution obtained using alcohol solutions (Fig. 2).

Applying the linked clustering technique,¹³⁾ we find that the distributions of SDF $g_{OO}(x,y,z) \geq 2.1$ in alcohol solutions can be classified into three regions: HA, HD, and HH. Table 1 shows the values of the volume, CN, and BE ($\langle BE \rangle_x$) for each region. As shown in Table 1, all values in the HD region in the PA and BA solutions are identical to those in the methanol and ethanol solutions.^{1b)} In the HA region, however, the volume (7.6 Å³) in methanol solution^{1b)} is greater than those (7.0, 7.0, and 7.2 Å³) in the ethanol,^{1b)} PA, and BA solutions, respectively, whereas the CN values (1.08, 1.09, and 1.10) in the latter solutions are greater than that (0.99) in the methanol solution. Except in the case of the methanol solution, the volume and CN values were constant, irrespective of the difference in the chain lengths of the alkyl groups. The volume (7.2 Å³) in the dimethyl ether (DME) solution^{1b)} was greater than the volumes (6.7, 6.6, and 6.8 Å³) in the ethyl methyl ether (EME),^{1b)} MPE, and BME solutions (Table 2), respectively. The CN values (1.09, 1.40, and 1.42) in the latter solutions were greater than that (1.02) in the former solution. The volumes in the ether solutions were much smaller

Table 1. Results of Volume, CN, and Binding Energy Decomposition for Alcohol Solutions in $g_{OO}(x, y, z) \leq 2.1$ Region at 298 K

	Volume	CN	$\langle BE \rangle_x$	Volume	CN	$\langle BE \rangle_x$
	PA			IPA		
HA	7.0	1.09	-20.05	7.8	1.09	-19.64
HD	3.1	0.65	-9.39	2.7	0.73	-11.50
HH	24.3	1.82	-3.69	24.7	1.86	-3.87
Sum	34.3	3.56	-33.13	35.2	3.68	-35.01
Total			-82.58			-83.04
	BA			TBA		
HA	7.2	1.10	-19.96	6.8	1.14	-21.99
HD	3.2	0.66	-9.63	2.8	0.73	-11.72
HH	43.2	3.30	-7.52	45.2	3.52	-7.44
Sum	54.6	5.06	-37.11	54.8	5.39	-41.15
Total			-88.99			-93.09

Units for volumes and $\langle BE \rangle_x$ are \AA^3 and kJ mol^{-1} , respectively. Subscript x on $\langle BE \rangle_x$ indicates HA, HD, HH, Sum, and Total. Total values are obtained from the entire cubic cell.

Table 2. Results of Volume, CN, and Binding Energy Decomposition for Ether Solutions in $g_{OO}(x, y, z) \geq 2.1$ Region at 298 K

	Volume	CN	$\langle BE \rangle_x$	Volume	CN	$\langle BE \rangle_x$
	MPE			IPE		
HA	6.6	1.40	-32.53	7.1	1.34	-31.46
HH	44.4	3.40	-8.24	39.9	3.06	-7.52
Sum	51.0	4.80	-40.77	47.0	4.40	-38.98
Total			-98.60			-96.38
	BME			TBE		
HA	6.8	1.42	-33.87	6.2	1.44	-35.67
HH	58.6	4.56	-11.20	59.4	4.68	-11.51
Sum	65.4	5.98	-45.07	65.6	6.12	-47.18
Total			-107.14			-109.16

Units for volumes and $\langle BE \rangle_x$ are \AA^3 and kJ mol^{-1} , respectively. Subscript x on $\langle BE \rangle_x$ indicates HA, HD, HH, Sum, and Total. Total values are obtained from the entire cubic cell.

than those in the alcohol solutions, whereas the CN values of the ether solutions were much greater.

The binding energy $\langle BE \rangle_{\text{HA}}$ ($-17.94 \text{ kJ mol}^{-1}$) in the methanol solution^{1a)} was greater than those (-19.81 , -20.05 , and $-19.96 \text{ kJ mol}^{-1}$) in the ethanol,^{1a)} PA, and BA solutions (Table 1), respectively. Moreover, the $\langle BE \rangle_{\text{HA}}$ ($-17.94 \text{ kJ mol}^{-1}$) in the DME solution^{1b)} was also appreciably greater than those (-19.80 , -32.53 , and $-33.87 \text{ kJ mol}^{-1}$) in the EME,^{1b)} MPE, and BME solutions (Table 2), respectively. These results indicate that the chain length of alkyl groups does not affect the value of $\langle BE \rangle_{\text{HA}}$ in other alcohol solutions (except in the case of the methanol solution), whereas the value of $\langle BE \rangle_{\text{HA}}$ in ether solutions becomes smaller with increasing chain length of alkyl groups. The decrease of $\langle BE \rangle_{\text{HA}}$ in alcohol and ether solutions is not influenced by the decrease of the volume, because the distribution density of hydration water molecules in these solutions increases in the HA region relative to the distribution density in alcohol solutions. In the HH region, the volume and the CN and $\langle BE \rangle_{\text{HH}}$ values in the alcohol and ether solutions increased and stabilized with increasing chain length of the hydrophobic alkyl groups. Moreover, the results of Sum (in Tables 1 and 2) for the first hydration shell in alcohol and ether solutions coincide also with the above results in the HH region.

Figures 4 and 5 show the contour maps of the BE on the

x - y plane of $z=0.075 \text{ \AA}$ in the alcohol and ether solutions, respectively. As observed in our previous paper,¹⁾ the distribution density of the hydration water molecules increased with the growth of the stable BE region depicted in the contour maps (Figs. 4 and 5). In both alcohol and ether having straight chain alkyl groups, the distributions of water molecules in the HA region estimated by these contour maps agreed with the distributions obtained from SDF (Figs. 1 and 2) in these solutions. On the other hand, the area of unstable BE in the HH region was spread over the inside of stable BE region around the hydrophobic group. This indicates that the distribution density of the hydration water molecules increased with increasing lability of the BE. This feature was in agreement with the slender band distribution in the HH region shown in Figs. 1 and 2.

(b) Effect of the Branched Alkyl Group In the HA region, the volume (7.8 \AA^3) in the IPA solution was greater than that (7.0 \AA^3) in the PA solution, and the CN (1.09) in the former was identical with that (1.09) in the latter, as shown in Fig. 1 and Table 1. In the HD region, the volume (2.7 \AA^3) in the IPA solution was smaller than that (3.1 \AA^3) in the PA solution, and the CN (0.73) in the former was greater than that (0.65) in the latter. On the basis of the results described above, we may conclude that, in the HA region, the $\langle BE \rangle_{\text{HA}}$ ($-19.64 \text{ kJ mol}^{-1}$) of the IPA solution was slightly more unstable than that ($-20.05 \text{ kJ mol}^{-1}$) of the PA solution, whereas in the HD region, the $\langle BE \rangle_{\text{HD}}$ ($-11.50 \text{ kJ mol}^{-1}$) of the former was much more stable than that ($-9.39 \text{ kJ mol}^{-1}$) of the latter. It is clear that the difference in this stability in the HD region was due to the CN value induced by the branched alkyl group.

The respective volumes (6.8 and 2.8 \AA^3) in the HA and HD regions in the TBA solution were smaller than the corresponding values (7.2 and 3.2 \AA^3) in the BA solution. The respective CN values (1.14 and 0.73) in the former were greater than the corresponding values (1.10 and 0.66) in the latter. We may therefore conclude that the $\langle BE \rangle_{\text{HA}}$ ($-21.99 \text{ kJ mol}^{-1}$) and $\langle BE \rangle_{\text{HD}}$ ($-11.72 \text{ kJ mol}^{-1}$) values in the TBA solution were much more stable than the corresponding values (-19.96 and $-9.63 \text{ kJ mol}^{-1}$) in the BA solution.

In the HH region shown in Table 1, the volumes and the CN values in the IPA and TBA solutions were slightly greater than the respective values in the PA and BA solutions. The results concerning $\langle BE \rangle_{\text{HH}}$ in the HH region show that neither the IPA nor the TBA solution was affected by the steric bulk of the branched alkyl group. The behaviors of the volume and the CN values in the HA and HD regions in ether solutions were essentially identical to those in the alcohol solutions. As shown in Table 2, however, both the volume (39.9 \AA^3) and the CN (3.06) in the IPE solution were considerably smaller than the corresponding values (44.4 \AA^3 and 3.40) in the MPE solution. The $\langle BE \rangle_{\text{HH}}$ ($-7.52 \text{ kJ mol}^{-1}$) of the former was more unstable than that ($-8.24 \text{ kJ mol}^{-1}$) of the latter. As compared with the $\langle BE \rangle_{\text{HH}}$ of the BME solution, that ($-11.51 \text{ kJ mol}^{-1}$) of the TBE solution was slightly more stable.

Moreover, the results of Sum (in Tables 1 and 2) for the water molecules of the first hydration shell show that both the volumes (35.2 and 54.8 \AA^3) and the CN values (3.68 and 5.39) in the IPA and TBA solutions were greater than those

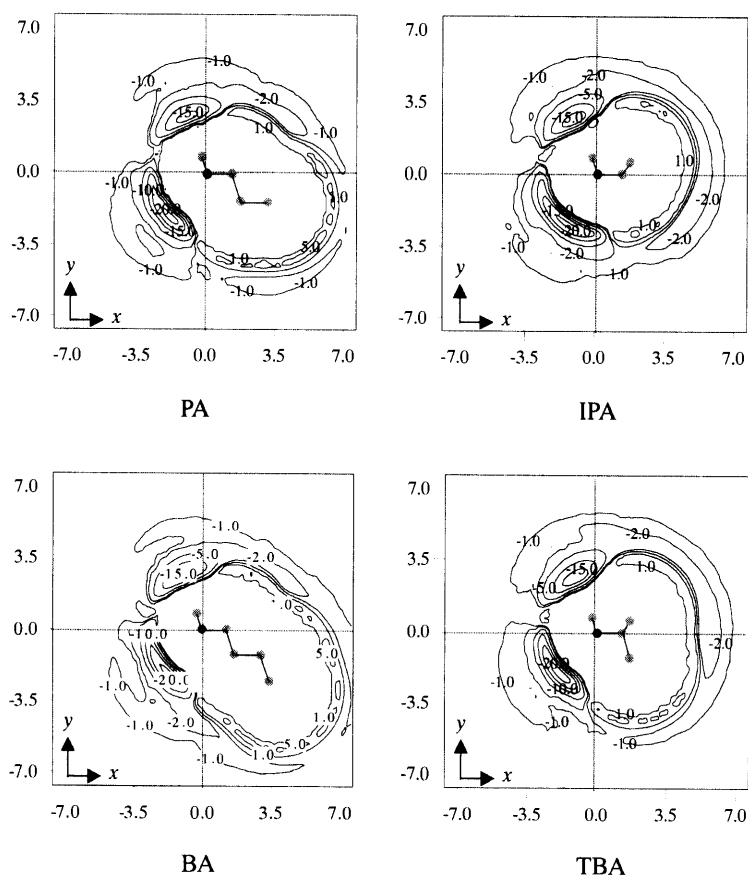


Fig. 4. Contour Maps of Binding Energies for Alcohol Solutions at the x - y Plane of $z=0.075$ Å and 298 K

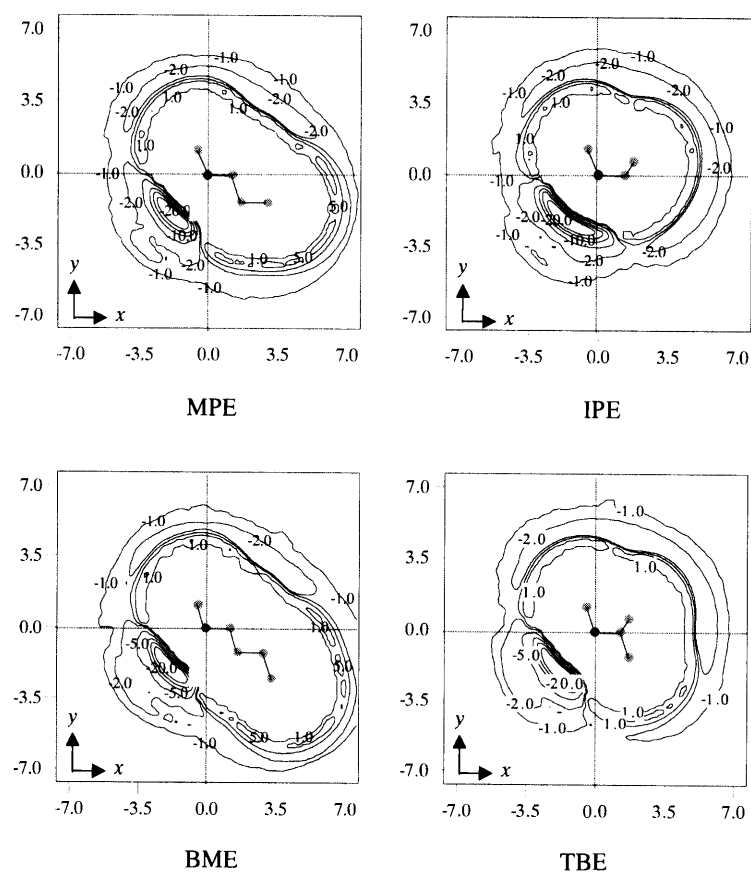


Fig. 5. Contour Maps of Binding Energies for Ether Solutions at the x - y Plane of $z=0.075$ Å and 298 K

in the corresponding PA and BA solutions. And the BE (-35.01 and -41.15 kJ mol $^{-1}$) of the IPA and TBA solutions were more stable than those of the corresponding PA and BA solutions. On the other hand, both the volume (65.6 Å 3) and the CN value (6.12) in the TBE solution were essentially greater than those (65.4 Å 3 and 5.98) in the BME solution, and the BE (-47.18 kJ mol $^{-1}$) of the former was much more stable than that (-45.07 kJ mol $^{-1}$) of the latter. In contrast to our results for the TBE and BME solutions, both the volume (47.0 Å 3) and the CN value (4.40) in the IPE solution were smaller than those (51.0 Å 3 and 4.80) in the MPE solution. The BE (-40.77 kJ mol $^{-1}$) of the latter was much more stable than that (-38.98 kJ mol $^{-1}$) of the former. Taken together, these results, except in the case of the IPE solutions, show that the CN of water molecules in the first hydration shell in the alcohol and ether solutions generally increased with increasing volume, while the CN of that shell increased with increasing length of the straight chain alkyl groups and extending bulk of the branched alkyl groups. The resulting BE in that shell was extremely stable.

The distributions of hydration water molecules in each region were also determined by the contour maps of infinitely dilute aqueous solutions of alcohol and ether having branched alkyl groups. The results showed that the distributions of water molecules in the HA region as estimated using the contour maps of the IPA, TBA, IPE, and TBE solutions were in very close agreement with the respective distributions obtained from SDF (Figs. 1 and 2). It was apparent that the stable BE area (*ca.* -15.0 kJ mol $^{-1}$) in the HA region in the IPA and IPE solutions was appreciably spread out to as far as the sides of the HH region compared with the corresponding areas for the other alcohol and ether solutions. Based on the results, it is clear that the volume in the HA region of the IPA and IPE solutions was greater than those in the other alcohol and ether solutions (Tables 1 and 2).

Evaluation of the Difference Hydration Enthalpy We previously reported that the order of the differences in the hydration enthalpy, $\Delta\Delta H_h^0$, could be easily evaluated by the difference in the total BE and in the BE for the domain of the respective first hydration shell in alcohol and ether solutions.¹⁾ From the values shown in Tables 1 and 2, as well as those from our previous paper,¹⁾ we calculated the differences of hydration enthalpy of PA-ethanol, BA-PA, TBA-BA, and IPA-PA from the differences of their total BE. The resulting $\Delta\Delta H_h^0$, -7.73 (PA-ethanol), -6.41 (BA-PA), -4.10 kJ mol $^{-1}$ (TBA-BA), and -0.46 (IPA-PA) calculated here were in fair agreement with the corresponding $\Delta\Delta H_h^0$, -4.98 , -3.63 , -2.73 , and -0.85 kJ mol $^{-1}$, observed previously.¹⁵⁾ Moreover, the calculated $\Delta\Delta H_h^0$ values obtained from the domain of SDF $g_{OO}(x,y,z) \geq 2.1$ for the first hydration shell were -1.49 , -3.98 , -4.04 , and -1.88 kJ mol $^{-1}$, respectively. However, the corresponding values obtained in the present study were considerably smaller than the observed values. Experimental results for $\Delta\Delta H_h^0$ in ether solution have not yet been reported. From the values shown in Table 2, we calculated $\Delta\Delta H_h^0$ from the difference of the total BE and the domain of SDF $g_{OO}(x,y,z) \geq 2.1$ for the first hydration shell as -26.88 (MPE-EME), -8.54 (BME-MPE), 2.22 (IPE-MPE), and -2.02 (TBE-BME) kJ mol $^{-1}$, and -3.51 (MPE-EME), -2.91 (BME-MPE), 0.72 (IPE-MPE), and -0.31 (TBE-BME) kJ mol $^{-1}$, respectively.

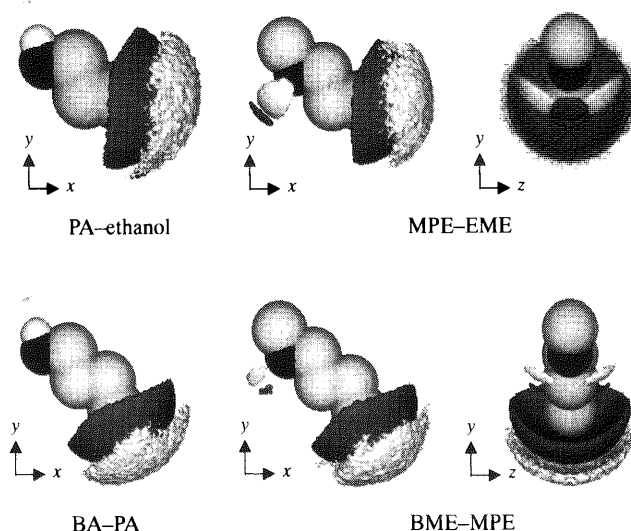


Fig. 6. Isosurface of Difference Oxygen-Oxygen SDF between Aqueous Solutions of Alcohols or Ethers Having Straight Chain Group

Left and center columns are viewed down the z -axis, and right column is viewed down the x -axis. The bright area shows the increase of oxygen-oxygen distribution at $\Delta g_{OO}(x,y,z) = +1.0$, and the dark area shows the decrease of oxygen-oxygen distribution at $\Delta g_{OO}(x,y,z) = -1.0$.

We might conclude that these results highly overestimate the effect of the steric bulk of the hydrophobic alkyl groups. However, it is important to note the coincidence between the calculated $\Delta\Delta H_h^0$ values in this work and the observed values for IPA-PA and TBA-BA of the alkyl groups having the same number of carbon atoms. Based on these results and those of our previous paper,¹⁾ it seems reasonable to conclude that the differences of the hydration enthalpy, $\Delta\Delta H_h^0$, obtained from MC simulation are useful for the evaluation of the order $\Delta\Delta H_h^0$ in alcohol and ether solutions.

DSDF Analysis of Hydration Structure The DSDF analysis proposed in our previous paper¹⁾ is most useful in cases in which the distribution of water molecules in each region is influenced by the differences of the hydrophobic groups. Figures 6 and 7 show an isosurface of DSDF $g_{OO}(x,y,z) = \pm 1.0$ obtained from SDFs of alcohol and ether solutions having straight chain and branched alkyl groups, respectively.

In Figure 6, the DSDFs for PA-ethanol and BA-PA show no difference in the distribution change of hydration water molecules in the HA and HD regions. In the HH region, the distribution change of hydration water molecules surrounding the alkyl group shows a hemispheric decrease, and the decreased area is encircled by an increased distribution area. Moreover, the DSDFs for MPE-EME and BME-MPE are actually identical to those for the corresponding alcohols. However, as seen by viewing in Fig. 6, there is a clear increase in the distribution in the HA region in the direction of lone pair electrons on the oxygen atom of ether.

In IPA-ethanol, as shown in Fig. 7, the distribution change of hydration water molecules around the two methyl groups of IPA shows a hemispheric decrease, and the decreased area is encircled by an increased distribution area just as in the alcohol and ether solutions in Fig. 6. On the other hand, the distribution change of hydration water around the methyl group of ethanol is reverse behavior in the comparison with that of IPA. However, the distribution change for TBA-IPA is

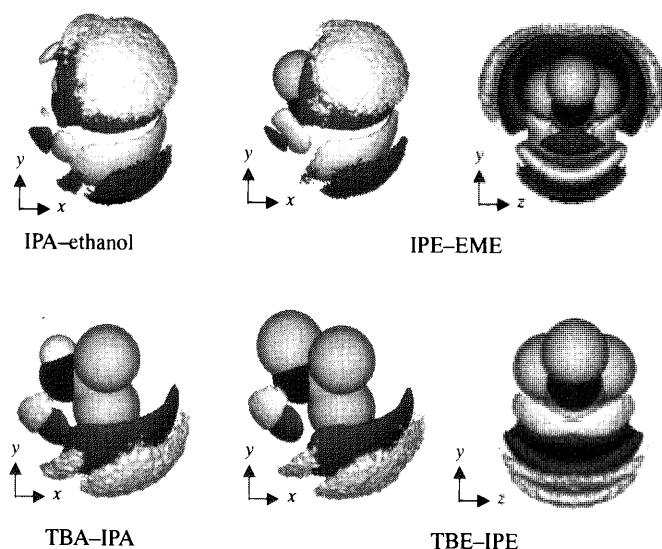


Fig. 7. Isosurface of Difference Oxygen-Oxygen SDF between Aqueous Solutions of Alcohols or Ethers Having Branched Alkyl Group

Left and center columns are viewed down the z -axis, and right column is viewed down the x -axis. The bright area shows the increase of oxygen-oxygen distribution at $\Delta g_{OO}(x,y,z) = +1.0$, and the dark area shows the decrease of oxygen-oxygen distribution at $\Delta g_{OO}(x,y,z) = -1.0$.

similar to that of PA-ethanol and BA-PA in the HH region. In the HA region, the increased distribution of the hydration water molecules for IPA-ethanol appears on the side of the HH region, because this distribution is influenced by the steric bulk of the ethyl group. The increased TBA-IPA area appears on the opposite side of the HD region. In the HD region, the increased area for IPA-ethanol is recognized on the reverse side of the HH region, and its decreased area is observed on the side of the HH region. These results are confirmed by the contour map of the BE in the HD region for the ethanol and IPA solutions. On the other hand, Fig. 7 shows that there was no difference in the distribution of hydration water molecules between the TBA and IPA solutions in the HD region.

With respect to the HA region for IPE-EME and TBE-IPE, the decreased distribution of hydration water molecules in the former was observed in the central region between lone pair electrons on the oxygen atom of ether. In TBE-IPE, on the other hand, the increased distribution area exists in the region of the direction of lone pair electrons on the oxygen atom of ether as viewed down the x -axis in Fig. 7. However, the distribution change in the HH region is essentially identical with those for IPA-ethanol and TBA-IPA.

Conclusion

In this investigation, we analyzed the hydration structure and the effects of the steric bulk of the hydrophobic group in alcohols and ethers having straight chain and branched alkyl groups using the SDF $g_{OO}(x,y,z)$, and DSDF $\Delta g_{OO}(x,y,z)$, respectively.

From the results of the SDF $g_{OO}(x,y,z)$ for eight kinds of alcohol and ether solutions at 298 K, it became apparent that, irrespective of the type of hydrophobic group, the hydration water molecules are essentially distributed in the HA, HD,

and HH regions in alcohol solutions, and in the HA and HH regions in ether solutions. The spatial orientations of the hydrogen-bonded water molecules in all alcohol and ether solutions are clearly of the linear type, and these distributions show a triple layer structure in the HA region and a double layer structure in the HD region.

The anisotropic hydration structures of all ether solutions in the HA and HH regions obtained from the SDF $g_{OO}(x,y,z)$ were essentially identical with those of all alcohol solutions.

In terms of the results of the DSDF $\Delta g_{OO}(x,y,z)$ obtained from the SDFs $g_{OO}(x,y,z)$ for the two ether solutions, it is noteworthy that the increased distributions of hydration water in the HA region spread over the area of the direction of lone pair electrons on the O atom of the solute. However, the increased distribution in the HA region was not observed for alcohol solutions.

Moreover, it is apparent that the difference in the hydration enthalpy $\Delta\Delta H_h^0$ obtained from the total BE and domain of SDF $g_{OO}(x,y,z) \geq 2.1$ is useful for the evaluation of the order of $\Delta\Delta H_h^0$ in alcohol and ether solutions.

In order to investigate the hydration structure in more detail, we are currently examining similar MC simulations for infinitely dilute aqueous solutions of ethylene glycol having two hydrophilic groups. The distribution of SDF $g_{OO}(x,y,z)$ obtained from these MC simulations should help to clarify the hydration structural change through the process of the conformational change of ethylene glycol.

References

- 1) a) Hata T., Ono Y., *Chem. Pharm. Bull.*, **47**, 615–620 (1999); b) *Idem, ibid.*, **48**, 16–20 (2000).
- 2) a) Svishchev I. M., Kusalik P. G., *J. Chem. Phys.*, **99**, 3049–3058 (1993); b) Kusalik P. G., Svishchev I. M., *Science*, **265**, 1219–1221 (1994); c) Svishchev I. M., Kusalik P. G., *J. Chem. Phys.*, **100**, 5165–5171 (1994); d) Liu Q., Brady J. W., *J. Am. Chem. Soc.*, **118**, 12276–12286 (1996); e) Laaksonen A., Kusalik P. G., Svishchev I. M., *J. Phys. Chem. A*, **101**, 5910–5918 (1997).
- 3) Narten A. H., Danford M. D., Lery H. A., *Discuss. Faraday Soc.*, **43**, 97–107 (1967).
- 4) a) Soper A. K., Phillips M. G., *Chem. Phys.*, **107**, 47–60 (1986); b) Soper A. K., *J. Chem. Phys.*, **101**, 6888–6901 (1994).
- 5) Allen M. P., Tildesley D. J., "Computer Simulation of Liquids," Oxford University Press, New York, 1987.
- 6) a) Clementi E., Gorongiu G., *J. Chem. Phys.*, **72**, 3979–3992 (1980); b) Gorongiu G., Clementi E., *Biopolymers*, **20**, 551–571 (1981); c) *Idem, ibid.*, **20**, 2427–2483 (1981).
- 7) Nakanishi K., Ikari K., Okazaki S., Touhara H., *J. Chem. Phys.*, **80**, 1656–1670 (1984).
- 8) Metropolis N., Rosenbluth A. W., Rosenbluth M. N., Teller A. H., Teller E., *J. Chem. Phys.*, **21**, 1087–1092 (1953).
- 9) Berendsen H. J. C., Grigera J. R., Straatsma T. P., *J. Phys. Chem.*, **91**, 6269–6271 (1987).
- 10) Jorgensen W. L., *J. Am. Chem. Soc.*, **103**, 335–340 (1981).
- 11) Bosio L., Chen S.-H., Teixeira J., *Phys. Rev. A*, **27**, 1468–1475 (1983).
- 12) Ben-Naim, "Water and Aqueous Solutions, Introduction to a Molecular Theory," Chapter 5, Plenum Press, 1974.
- 13) Osawa E., Gotō H., Hata T., Derety E., *J. Mol. Struct. (Theochem.)*, **398–399**, 229–236 (1987).
- 14) Okazaki S., Nakanishi K., Touhara H., *J. Chem. Phys.*, **78**, 454–469 (1983).
- 15) Franks F., "Water—a Comprehensive Treatise," Vol. 2, ed. by Franks F., Plenum Press, New York, 1972, Chapter 5.

Synthesis and Anti-platelet, Anti-inflammatory and Anti-allergic Activities of Methoxyisoflavanquinone and Related Compounds

Chiung-Yun CHANG,^a Li-Jiau HUANG,^a Jih-Pyang WANG,^{a,b} Che-Ming TENG,^c Sheng-Chih CHEN,^a and Sheng-Chu KUO^{*,a}

Graduate Institute of Pharmaceutical Chemistry, China Medical College,^a 91 Hsueh Shin Road, Taichung, Taiwan, R.O.C., Department of Education and Research, Taichung Veterans General Hospital,^b Taichung, Taiwan, R.O.C., and Pharmacological Institute, College of Medicine, National Taiwan University,^c Taipei, Taiwan, R.O.C.

Received December 24, 1999; accepted April 2, 2000

In a continuation of our search for novel anti-platelet agents, isoflavone quinone and isoflavanquinone were selected as lead compounds and the synthesis of their methoxy derivatives was carried out. Among them, the 4'- and 7-methoxy derivatives were successfully prepared, whereas the attempt to obtain 3'-methoxy derivatives resulted in their isomers, 3'-methoxyflavone quinone and 3'-methoxyflavanquinone, instead.

After screening for their anti-platelet, anti-inflammatory and anti-allergic activities, a preliminary structure-activity relationship was established.

Compounds 6c, 7a–c, 8c and 9a–c were found to exhibit significant activities. In particular, compound 7c demonstrated very potent anti-platelet, anti-inflammatory and anti-allergic activities and was then recommended for further pharmacological investigation.

Key words methoxyisoflavanquinone; methoxyflavanquinone; anti-platelet activity; anti-inflammatory activity; anti-allergic activity; structure-activity relationship

In a previous paper,¹⁾ we synthesized isoflavanquinone (A) and its related compounds and discovered that both compound A and isoflavone quinone (B) exhibited potent biological activities.

For this reason, we selected both A and B as lead compounds and then synthesized their methoxy derivatives by incorporating methoxy groups, which are found commonly in natural products,²⁾ into various positions on the structure of compounds A and B to form our target compounds.

This report describes the synthesis and biological activity of these target compounds and related compounds.

Results and Discussion

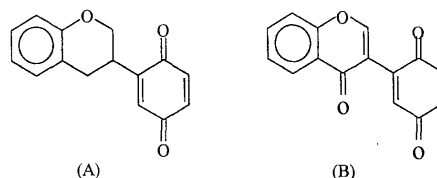
Chemistry The synthesis of 7 (or 4')-methoxyisoflavanquinone (7a or 7b) and 7 (or 4')-methoxyisoflavone quinones (9a or 9b) are illustrated schematically in Chart 1. As shown, chalcones 2a, b were first obtained from condensation of 2-hydroxy-4-substituted acetophenones in alkali with 2-benzoyloxy-4-substituted benzaldehydes 1a, b which were prepared from 2-hydroxy-4-substituted benzaldehydes.

Chalcones 2a, b were then acetylated with Ac₂O in pyridine to protect the 2'-hydroxy group. The acetylated chalcones 3a, b were subsequently treated with thallium nitrate in trimethyl orthoformate [Ti(NO₃)₃/CH(OCH₃)₃] at room temperature, according to the method published in a previous paper,¹⁾ to yield the corresponding acetals 4a, b.

The acetals 4a, b were heated on a warm bath with dil. HCl in methyl alcohol to give the corresponding isoflavones 5a, b. These products were then reduced by catalytic hydrogenation on palladium/charcoal to yield the corresponding isoflavans 6a, b with the loss of their benzyl groups.

Finally, the isoflavans 6a, b were oxidized with potassium nitrosodisulfonate (Fremy's salt) to afford the corresponding isoflavanquinones 7a, b.

On the other hand, debenzoylation of compounds 5a, b with 47% HBr yielded the corresponding 2'-hydroxyisoflavones 8a, b which were subsequently oxidized with Fremy's salt to



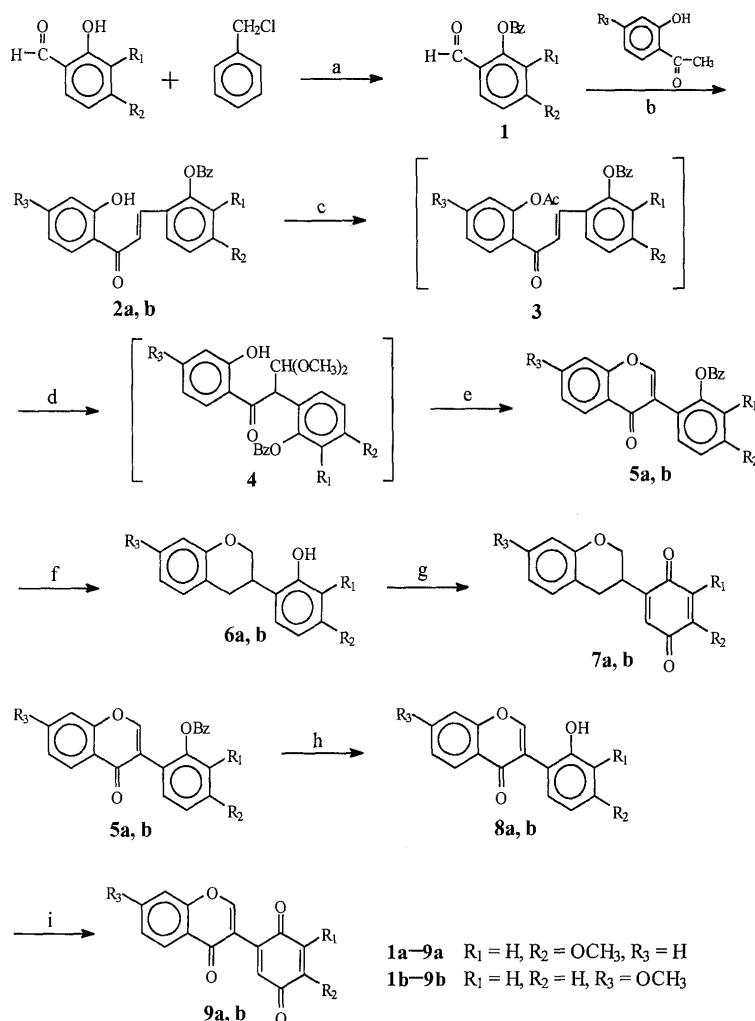
the corresponding isoflavone quinones 9a, b.

However, as indicated in Chart 2 and detailed below, the attempt to synthesize 3'-methoxyisoflavanquinone (7x) following an analogous procedure for the preparation of isoflavanquinone 7a, b, failed to furnish the target compound 7x.

First, 2-hydroxyacetophenone was condensed with 2-benzoyloxy-3-methoxybenzaldehyde (1c) to give chalcone 2c successfully. When compound 2c was acetylated with Ac₂O and subsequently treated with Ti(NO₃)₃/CH(OCH₃)₃, the molecular formula of the resulting major product 5c was determined to be C₂₃H₁₈O₄, based on its mass spectrum (*m/z* 358, M⁺) from electron impact mass (EI-MS) and on its data from elemental analysis. While its molecular formula agreed well with our expectation for compound 5x, its ¹H-NMR spectrum did not show the same result.

Due to the complexity of the ¹H-NMR spectrum of compound 5c, the complete assignment of the signals is still lacking. Despite this, compound 5c was subjected to catalytic hydrogenation to give the flavan type product 6c with saturation at the 2 and 3 positions. Further oxidation of compound 6c, with Fremy's salt, converted its B-ring to a quinone moiety forming a flavanquinone type product 7c. After comparing the ¹H-NMR spectrum of 7c with the above synthesized 4'-methoxyisoflavanquinone (7a), we noticed the presence of a set of mutually coupled signals associated with H-2, 3, 4 in the spectrum of product 7c that differed from the corresponding pattern of compound 7a. The spectrum of 7c exhibited H-3ax, H-3eq, H-4ax, H-4eq and H-2 signals at δ 1.72–1.85 (1H, m), 2.30–2.38 (1H, m), 2.75 (1H, ddd), 3.00 (1H, ddd) and 5.12 (1H, dd) respectively. This spectrum lead us to the

* To whom correspondence should be addressed. e-mail: sckuo@mail.cmc.edu.tw



reagents: (a) K_2CO_3/KI /Acetone; (b) $NaOH/EtOH/H_2O$; (c) Acetic anhydride/Pyridine;

(d) $Tl(NO_3)_3/CH(OCH_3)_3$; (e) dil. HCl/CH_3OH ; (f) $H_2/Pd(C)/CH_3COOH$;

(g) $K(SO_3)_2NO$ /Acetone/ CH_3OH ; (h) 47% HBr ; (i) $K(SO_3)_2NO$ /Acetone/ CH_3OH

Chart 1

assignment that the quinone moiety (B-ring) for **7c** was attached to the 2-position of the benzopyran and thus it is a flavanquinone, rather than the isoflavanquinone isomer.

All of the remaining spectral data of **7c** were in agreement with our structure assignment. Thus, it was apparent that the treatment of acetylated **2c** with $Tl(NO_3)_3/CH(OCH_3)_3$, followed the cyclization route to form flavone type 2'-benzoxo-3'-methoxyflavone (**5c**), instead of undergoing rearrangement, as in acetylated **2a** or **2b**, to give isoflavone type compound **5x**.

So far, the exact mechanism is still unclear. Under the same reaction conditions [$Tl(NO_3)_3/CH(OCH_3)_3$], compound **2c** did not follow the rearrangement route and instead cyclized directly to a flavone type product, whereas compound **2a, 2b** and the previously reported^{1,3,4} 2-benzoyloxy-2'-hydroxy chalcones all underwent rearrangement to form isoflavone type products. We are now working on providing the answer in the near future.

Meanwhile, in order to expand our knowledge base to include the biological activities of compounds related to our target compounds, structure modification was also conducted

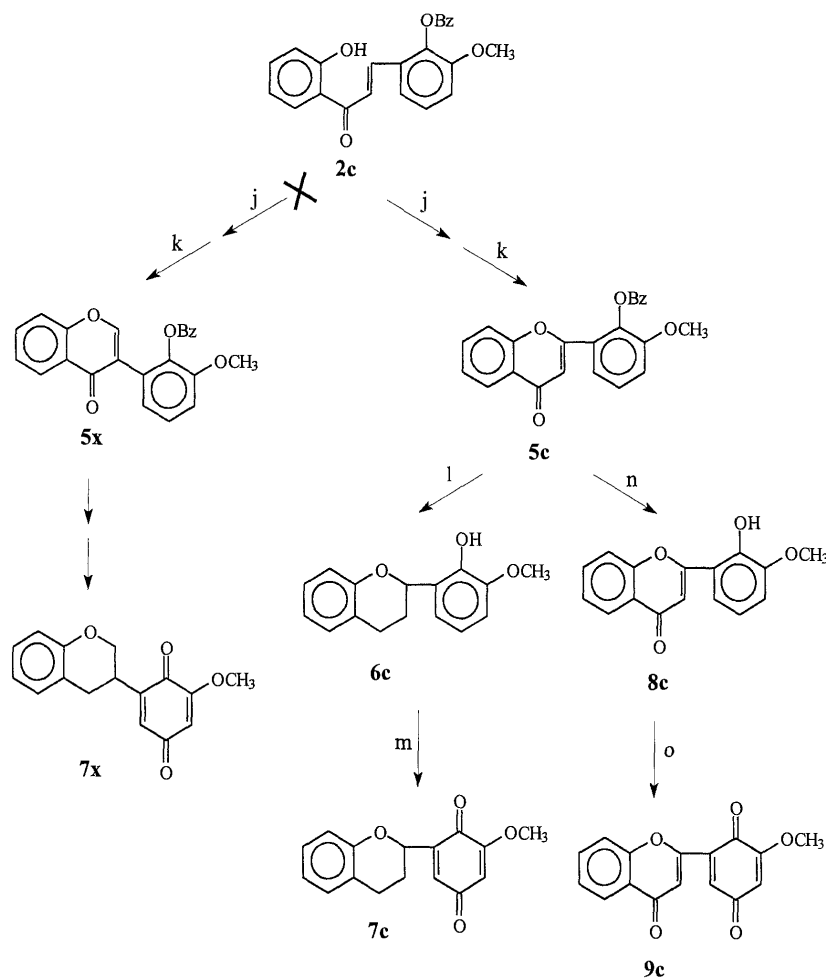
on the unexpected **5c**. The debenzoylation of compound **5c** with 47% HBr , followed by oxidation with Fremy's salt, produced 3'-methoxyflavone quinone (**9c**) which was also tested for its biological activities.

Biological Activity. Anti-platelet Activity The anti-platelet activities of all the target compounds are summarized in Table 1. Among the three chalcones **2a-c** tested, compound **2c** was the only one displaying significant activity equal to about 2 fold the inhibitory potency of aspirin against arachidonic acid (AA)-induced platelet-aggregation.

When the chalcones were first converted to flavones **5a-c** with a benzyl protection group still on the 2'-OH of their B-ring, we also tested their activity and found only the 4'-methoxy derivatives **5a** exhibited moderate activity.

Debenzoylation of the above flavones resulted in compounds **8a-c** with free 2'-OH, and elevated activities. In particular, the most potent flavone **8c** demonstrated an IC_{50} value of $3.6 \mu M$ which is about 5.5 times the inhibitory potency of aspirin against AA-induced platelet aggregation.

Furthermore, the oxidation of the B-ring of compound **8a-c** to quinones **9a-c** respectively resulted in potent ac-



Reagents : (j) $\text{Ti}(\text{NO}_3)_3/\text{CH}(\text{OCH}_3)_3$; (k) $\text{dil.HCl}/\text{CH}_3\text{OH}$; (l) $\text{H}_2/\text{Pd}(\text{C})/\text{CH}_3\text{COOH}$;

(m) $\text{K}(\text{SO}_3)_2\text{NO}/\text{Acetone}$; (n) 47% HBr ; (o) $\text{K}(\text{SO}_3)_2\text{NO}/\text{Acetone}/\text{CH}_3\text{OH}$

Chart 2

tivity for isoflavone quinone **9a, b** and flavone quinone **9c**. Especially in the flavone quinone type **9c** which displayed complete inhibition of platelet aggregation stimulated by thrombin, AA, collagen and platelet activating factor (PAF) at the concentration of $25 \mu\text{g/ml}$. Its IC_{50} value was $11.3 \mu\text{M}$ which equaled about 2 times the potency of aspirin against AA-induced aggregation.

Among the flavan and isoflavan type of compounds **6a—c** synthesized above, **6c** was the most potent one showing complete inhibition against AA-, collagen- and PAF-induced platelet aggregation at the concentration of $100 \mu\text{g/ml}$. Its IC_{50} value was $5.1 \mu\text{M}$, equal to about 4 times the potency of aspirin against AA-induced aggregation.

Conversion of flavone and isoflavones into their corresponding flavanquinone **7c** or isoflavanquinones **7a, b** further elevated their activities. Especially so in the flavanquinone type **7c** which displayed complete inhibition against platelet aggregation induced by thrombin, AA, collagen and PAF at the concentration of $100 \mu\text{g/ml}$. As a comparison, the inhibitory potency of **7c** against AA-induced platelet aggregation was about 10 fold stronger than aspirin.

From the above results, it appeared that flavonoids (**8c, 9c**) and flavanoids (**6c, 7c**) were generally superior to their corre-

sponding isoflavonoids (**8a, b, 9a, b**) and isoflavanoids (**6a, b, 7a, b**) in terms of their platelet activities.

Anti-inflammatory Activity Effect on Neutrophil Degranulation: The activities of our target compounds toward neutrophil degranulation were also examined. As summarized in Table 2, in all the compounds tested, only those with quinone type B-ring (**7a—c, 9a—c**) exhibited potent activities. Among them, 3'-methoxy flavanquinone (**7c**) notably demonstrated the highest potency ($\text{IC}_{50}=0.19 \mu\text{M}$), equivalent to about 30 times the potency of the positive control trifluoperazine ($\text{IC}_{50}=5.8 \mu\text{M}$).

As was also implicated from the data in Table 2, in general, the flavanquinone type compound (**7c**) was more potent than the isoflavanquinone type (**7a, b**), and the flavone quinone type (**9c**) was more potent than the isoflavone quinone type (**9a, b**). This seems to follow the same trend of relative efficacy as their antiplatelet activities.

Effect on Neutrophil Superoxide Formation: Table 3 shows that, with the exception of 3'-methoxyflavanquinone (**7c**) which exhibited very potent inhibitory effect ($\text{IC}_{50}=0.44 \mu\text{M}$) on formyl-Met-Leu-Phe (fMLP)-induced neutrophil superoxide formation, none of the remaining target compounds demonstrated significant effects.

Table 1. The Inhibitory Effects of Compounds on Platelet Aggregation Induced by Thrombin, AA, Collagen and PAF (*in Vitro*)

Compounds ($\mu\text{g/ml}$)		Percent aggregation			
		Thrombin	AA	Collagen	PAF
2a	Control	92.0 \pm 0.7	88.1 \pm 0.5	89.5 \pm 0.6	90.6 \pm 0.9
	100	85.3 \pm 3.3*	61.9 \pm 1.1***	48.1 \pm 8.7***	64.3 \pm 3.1***
2b	Control	92.0 \pm 0.7	88.1 \pm 0.5	89.5 \pm 0.6	90.6 \pm 0.9
	100	73.9 \pm 5.8*	46.1 \pm 7.3***	53.0 \pm 7.9***	54.2 \pm 1.8***
2c	Control	89.1 \pm 1.4	84.9 \pm 0.9	84.5 \pm 0.6	86.4 \pm 2.6
	100	74.9 \pm 3.5***	0.0 \pm 0.0***	0.0 \pm 0.0***	58.2 \pm 2.0***
	20			0.0 \pm 0.0***	
	10		0.0 \pm 0.0***	2.7 \pm 2.3***	
	5		40.0 \pm 20.0*	72.0 \pm 1.1***	
	2		78.6 \pm 2.3*	82.2 \pm 1.9	
	IC ₅₀		12.1 μM	14.9 μM	
5a	Control	90.4 \pm 1.1	90.0 \pm 0.7	90.1 \pm 1.0	89.5 \pm 0.9
	100	69.3 \pm 2.3***	0.0 \pm 0.0***	0.0 \pm 0.0***	64.2 \pm 1.1***
	50		0.0 \pm 0.0***		
	20		0.0 \pm 0.0***		
	10		80.1 \pm 2.4***		
	IC ₅₀		37.8 μM	N.D.	
5b	Control	90.4 \pm 1.1	90.0 \pm 0.7	90.1 \pm 1.0	89.5 \pm 0.9
	100	72.9 \pm 1.1**	64.9 \pm 1.7***	63.0 \pm 4.9***	60.5 \pm 7.4***
5c	Control	91.5 \pm 0.2	86.0 \pm 0.6	84.5 \pm 0.7	92.5 \pm 0.2
	100	84.5 \pm 0.3**	15.2 \pm 1.6***	26.7 \pm 1.2***	72.6 \pm 0.6***
6a	Control	90.4 \pm 1.1	90.0 \pm 0.7	90.1 \pm 1.0	89.5 \pm 0.9
	100	85.9 \pm 1.2*	0.0 \pm 0.0***	2.8 \pm 2.3***	0.0 \pm 0.0***
	50		0.0 \pm 0.0***	83.4	\pm 3.5***
	20		5.4 \pm 2.8***		
	10		84.3 \pm 2.1*		
	IC ₅₀		61.8 μM	N.D.	N.D.
6b	Control	90.4 \pm 1.1	90.0 \pm 0.7	90.1 \pm 1.0	89.5 \pm 0.9
	100	87.3 \pm 2.1	1.4 \pm 1.2***	17.4 \pm 0.9***	77.5 \pm 3.2***
	50		2.8 \pm 2.3***		
	20		56.2 \pm 3.3***		
	10		82.2 \pm 2.0*		
	IC ₅₀		96.5 μM	N.D.	
6c	Control	91.5 \pm 0.2	86.0 \pm 0.6	84.5 \pm 0.7	92.5 \pm 0.2
	100	79.7 \pm 1.2***	0.0 \pm 0.0***	0.0 \pm 0.0***	0.0 \pm 0.0***
	50		0.0 \pm 0.0***		82.8 \pm 1.1***
	0.5		0.0 \pm 0.0***		
	0.2		75.3 \pm 1.6***		
	0.1		81.0 \pm 0.6**		
	IC ₅₀		5.1 μM	N.D.	N.D.
7a	Control	90.4 \pm 1.1	90.0 \pm 0.7	90.1 \pm 1.0	89.5 \pm 0.9
	50	28.1 \pm 3.0***	0.0 \pm 0.0***	0.0 \pm 0.0***	4.2 \pm 2.0***
	20		0.0 \pm 0.0***		78.7 \pm 2.7***
	10		0.0 \pm 0.0***		
	5		0.0 \pm 0.0***		
	2		83.5 \pm 1.5***		
	IC ₅₀	N.D.	11.3 μM	N.D.	N.D.
7b	Control	90.4 \pm 1.1	90.0 \pm 0.7	90.1 \pm 1.0	89.5 \pm 0.9
	<50	28.2 \pm 2.4***	0.0 \pm 0.0***	0.0 \pm 0.0***	1.4 \pm 1.2***
	<20		0.0 \pm 0.0***		81.8 \pm 2.8*
	<10		0.0 \pm 0.0***		
	<5		0.0 \pm 0.0***		
	<2		81.8 \pm 3.9*		
	IC ₅₀	N.D.	11.2 μM	N.D.	N.D.
7c	Control	91.5 \pm 0.2	86.0 \pm 0.6	84.5 \pm 0.7	92.5 \pm 0.2
	100	0.0 \pm 0.0***	0.0 \pm 0.0***	0.0 \pm 0.0***	0.0 \pm 0.0***
	10				0.0 \pm 0.0***
	5				72.2 \pm 1.6***
	2		0.0 \pm 0.0***		83.5 \pm 1.1***
	1		21.3 \pm 1.3***		
	0.5		60.3 \pm 1.5***		
	0.2		74.4 \pm 1.1***		
	0.1		81.8 \pm 0.7***		
	IC ₅₀	N.D.	1.96 μM	N.D.	19.2 μM
8a	Control	90.4 \pm 1.1	90.0 \pm 0.7	90.1 \pm 1.0	89.5 \pm 0.9
	100	89.4 \pm 1.2	0.0 \pm 0.0***	2.8 \pm 2.3***	84.2 \pm 1.0**

Table 1. (Continued)

Compounds ($\mu\text{g/ml}$)		Percent aggregation			
		Thrombin	AA	Collagen	PAF
8a	50		0.0 \pm 0.0***		
	20		12.1 \pm 6.4***		
	10		79.2 \pm 3.1***		
	IC ₅₀		54.3 μM	N.D.	
8b	Control	90.4 \pm 1.1	90.0 \pm 0.7	90.1 \pm 1.0	89.5 \pm 0.9
	100	86.6 \pm 2.1	0.0 \pm 0.0***	6.5 \pm 3.7***	80.2 \pm 5.2
	50		0.0 \pm 0.0***		
	20		49.1 \pm 6.4***		
	10		89.0 \pm 1.1		
	IC ₅₀		81.1 μM	N.D.	
8c	Control	88.7 \pm 1.1	85.9 \pm 1.0	85.4 \pm 0.4	88.1 \pm 0.8
	100	86.7 \pm 3.1	0.0 \pm 0.0***	0.0 \pm 0.0***	79.3 \pm 5.5
	50			0.0 \pm 0.0***	
	20			6.0 \pm 5.2***	
	10			27.6 \pm 9.1***	
	5		0.0 \pm 0.0***	59.4 \pm 8.6**	
	2		10.9 \pm 9.4***	84.5 \pm 0.4	
	1		33.8 \pm 17.0**		
	0.5		80.5 \pm 0.8**		
	0.2		85.8 \pm 1.3		
	IC ₅₀		3.6 μM	28.6 μM	
9a	Control	90.4 \pm 1.1	90.0 \pm 0.7	90.1 \pm 1.0	89.5 \pm 0.9
	<50	44.3 \pm 7.0***	0.0 \pm 0.0***	0.0 \pm 0.0***	16.4 \pm 0.9***
	<20		0.0 \pm 0.0***		
	<10		77.8 \pm 1.5***		
IC ₅₀		47.4 μM			
9b	Control	90.4 \pm 1.1	90.0 \pm 0.7	90.1 \pm 1.0	89.5 \pm 0.9
	50	35.6 \pm 2.7***	0.0 \pm 0.0***	0.0 \pm 0.0***	16.2 \pm 2.3***
	20		0.0 \pm 0.0***		86.5 \pm 1.5
	10		2.8 \pm 2.3***		
	5		74.8 \pm 2.7***		
IC ₅₀	N.D.	24.8 μM	N.D.	N.D.	
9c	Control	90.4 \pm 1.1	87.2 \pm 1.1	86.7 \pm 1.7	90.5 \pm 1.8
	25	0.0 \pm 0.0***	0.0 \pm 0.0***	0.0 \pm 0.0***	0.0 \pm 0.0***
	20	13.9 \pm 7.1***	0.0 \pm 0.0***	0.0 \pm 0.0***	3.0 \pm 2.6***
	10	34.1 \pm 8.3***	0.0 \pm 0.0***	2.4 \pm 2.1***	26.1 \pm 13.8***
	5	55.8 \pm 8.0***	18.1 \pm 15.7***	15.5 \pm 8.6***	47.6 \pm 13.2**
	2	89.4 \pm 0.6	74.9 \pm 6.0	66.7 \pm 6.8**	85.9 \pm 1.9
	1		85.4 \pm 1.8	84.9 \pm 1.4	
IC ₅₀	25.2 μM	11.3 μM	12.0 μM	21.3 μM	
Aspirin IC ₅₀		N.D.	20.0 μM	N.D.	N.D.

Table 2. The Inhibitory Effect of Compounds on Neutrophil Degranulation (*in Vitro*)

Compounds (μM)		Percent release			
		β -Glucuronidase	% Inhibition	Lysozyme	% Inhibition
2a	Control	26.4 \pm 1.8		50.1 \pm 2.6	
	100	22.6 \pm 1.9	20.2 \pm 0.8	45.5 \pm 7.1	6.8 \pm 7.1
	30	21.9 \pm 2.8	23.3 \pm 4.4	48.3 \pm 6.8	0.9 \pm 6.2
2b	Control	26.4 \pm 1.8		50.1 \pm 2.6	
	100	19.5 \pm 2.8**	32.0 \pm 4.5	43.4 \pm 4.3	10.3 \pm 2.0
	30	22.7 \pm 2.6	20.2 \pm 2.5	47.6 \pm 5.9	1.9 \pm 3.8
2c	Control	23.3 \pm 2.5		43.4 \pm 3.0	
	30	22.0 \pm 0.7	2.8 \pm 9.6	44.1 \pm 7.4	0.5 \pm 10.7
	10	22.7 \pm 1.4	1.3 \pm 5.6	46.4 \pm 5.7	-5.9 \pm 6.4
5a	Control	45.8 \pm 2.0		66.7 \pm 4.1	
	30	19.9 \pm 3.4**	57.1 \pm 6.0	41.6 \pm 9.7	39.0 \pm 11.2
	10	27.7 \pm 4.3**	40.2 \pm 6.5	48.5 \pm 6.2	27.7 \pm 5.8
	3	32.7 \pm 3.7*	29.1 \pm 5.1	53.9 \pm 6.8	19.7 \pm 5.7
	IC ₅₀	21.7 μM			
5b	Control	45.8 \pm 2.0		66.7 \pm 4.1	
	100	37.5 \pm 1.5	18.2 \pm 1.4	60.2 \pm 6.6	10.2 \pm 6.0
	30	29.0 \pm 1.0**	36.7 \pm 1.6	54.7 \pm 8.9	18.8 \pm 9.5
5c	Control	19.7 \pm 0.1		42.7 \pm 0.2	
	30	16.2 \pm 1.0	17.8 \pm 5.5	38.0 \pm 1.3	10.8 \pm 3.6
	10	17.0 \pm 2.6	13.6 \pm 13.8	42.4 \pm 1.0	0.5 \pm 2.4
	3	17.4 \pm 1.4	11.6 \pm 7.9	41.3 \pm 2.4	3.3 \pm 5.4
6a	Control	45.8 \pm 2.0		66.7 \pm 4.1	
	30	10.1 \pm 1.4**	78.0 \pm 2.6	32.5 \pm 6.1*	52.0 \pm 6.5
	10	26.3 \pm 7.4*	43.8 \pm 13.3	43.7 \pm 7.2	35.0 \pm 7.8
	3	33.0 \pm 3.2*	28.2 \pm 4.2	58.4 \pm 3.9	12.1 \pm 5.7
	IC ₅₀	13.7 μM			
6b	Control	45.8 \pm 2.0		66.7 \pm 4.1	
	100	24.3 \pm 0.9	47.1 \pm 0.8	55.7 \pm 6.4	16.9 \pm 5.7
	30	32.0 \pm 2.4*	30.2 \pm 7.2	57.3 \pm 6.7	14.5 \pm 6.2
6c	Control	19.7 \pm 0.1		42.7 \pm 0.2	
	30	20.1 \pm 2.1	-1.9 \pm 10.7	46.5 \pm 2.0	-8.8 \pm 4.1
	10	15.1 \pm 2.5	23.3 \pm 12.8	43.3 \pm 2.5	-1.6 \pm 6.0
	3	16.1 \pm 1.2	18.3 \pm 6.4	38.6 \pm 3.5	9.6 \pm 8.2
7a	Control	45.8 \pm 2.0		66.7 \pm 4.1	
	30	-0.1 \pm 0.7**	100.1 \pm 1.6	22.5 \pm 2.7**	66.3 \pm 2.7
	10	21.0 \pm 3.2**	54.6 \pm 5.7	56.0 \pm 5.8	16.1 \pm 5.4
	3	28.4 \pm 5.0**	38.7 \pm 8.0	59.9 \pm 3.2	9.8 \pm 5.4
	IC ₅₀	7.4 μM			
7b	Control	45.8 \pm 2.0		66.7 \pm 4.1	
	30	-0.8 \pm 0.3**	101.8 \pm 0.7	0.8 \pm 0.4**	98.7 \pm 0.6
	3	28.4 \pm 3.9**	38.5 \pm 6.2	46.0 \pm 11.4	32.7 \pm 13.6
	1	34.9 \pm 4.2	24.4 \pm 5.7	54.7 \pm 8.6	19.0 \pm 8.3
7c	Control	18.2 \pm 1.1		36.8 \pm 3.8	
	1	-1.1 \pm 0.6**	106.7 \pm 3.6	-1.7 \pm 1.0**	105.2 \pm 3.7
	0.3	1.8 \pm 0.4**	89.4 \pm 3.1	10.8 \pm 4.2**	70.9 \pm 10.4
	0.1	9.0 \pm 0.3**	50.3 \pm 3.7	33.9 \pm 5.2	8.7 \pm 7.3
	IC ₅₀	0.19 μM			
8a	Control	45.8 \pm 2.0		66.7 \pm 4.1	
	100	28.9 \pm 1.1**	36.9 \pm 3.2	54.7 \pm 8.8	18.7 \pm 8.7
	30	30.0 \pm 2.3**	35.3 \pm 4.8	55.8 \pm 7.8	17.0 \pm 6.8
8b	Control	45.8 \pm 2.0		66.7 \pm 4.1	
	100	29.1 \pm 1.2**	36.6 \pm 1.5	57.7 \pm 5.2	13.8 \pm 3.0
	30	31.6 \pm 0.8**	31.1 \pm 1.0	59.8 \pm 5.4	10.7 \pm 3.8
8c	Control	25.6 \pm 1.0		39.9 \pm 0.5	
	30	25.6 \pm 1.0	-1.5 \pm 7.8	35.1 \pm 1.7	12.3 \pm 3.1
	10	25.1 \pm 1.2	1.9 \pm 6.8	35.9 \pm 2.0	10.2 \pm 4.1
9a	Control	45.8 \pm 2.0		66.7 \pm 4.1	
	30	0.5 \pm 0.2**	98.9 \pm 0.6	1.8 \pm 0.6**	97.0 \pm 1.1
	3	11.6 \pm 1.9**	74.7 \pm 4.3	54.6 \pm 5.2	18.3 \pm 4.6
	1	35.9 \pm 3.8	22.1 \pm 5.4	63.7 \pm 3.9	4.0 \pm 6.9
	IC ₅₀	6.3 μM			
9b	Control	45.8 \pm 2.0		66.7 \pm 4.1	
	30	0.7 \pm 0.1**	98.4 \pm 0.6	-4.8 \pm 1.0**	107.1 \pm 1.3
	3	4.0 \pm 0.3**	91.1 \pm 0.8	11.4 \pm 1.0**	82.9 \pm 1.4
	0.3	31.9 \pm 2.2**	30.8 \pm 1.5	58.6 \pm 1.9	12.5 \pm 1.3
	0.03	38.1 \pm 2.9	17.2 \pm 1.9	62.7 \pm 1.2	6.4 \pm 1.5
9c	Control	21.7 \pm 0.2		55.3 \pm 4.9	
	3	-0.1 \pm 1.5**	100.5 \pm 0.9	2.6 \pm 1.4**	95.6 \pm 2.3
	1	10.1 \pm 1.5**	53.6 \pm 7.0	14.5 \pm 2.5**	74.2 \pm 2.2
	0.3	17.0 \pm 1.2	21.9 \pm 4.8	40.2 \pm 4.7	27.5 \pm 2.0
	IC ₅₀	3.9 μM			
Trifluoperazine IC ₅₀		5.8 μM			

The neutrophil suspension was preincubated at 37°C with 0.5% DMSO or tested compound for 3 min in the presence of cytochalasin B (5 $\mu\text{g}/\text{ml}$). Forty-five minutes after the addition of FMLP (1 μM), β -glucuronidase and lysozyme in the supernatant was determined. Values are presented as mean \pm S.E., $n=3-5$, *: $p<0.05$, **: $p<0.01$.

Table 3. The Inhibitory Effect of Compounds on the Neutrophil Superoxide Formation (*in Vitro*)

Compounds (μM)		Superoxide formation	
		n mol/ 10^6 cells	% Inhibition
2a	Control	1.72 \pm 0.07	
	100	0.93 \pm 0.13**	46.2 \pm 7.5
	30	1.08 \pm 0.12**	37.4 \pm 6.0
2b	Control	1.72 \pm 0.07	
	100	1.62 \pm 0.19	-0.7 \pm 11.6
	30	1.47 \pm 0.11	8.2 \pm 9.6
2c	Control	1.84 \pm 0.09	
	30	1.30 \pm 0.10	26.7 \pm 2.7
	10	1.41 \pm 0.07	19.5 \pm 8.8
5a	Control	0.93 \pm 0.07	
	100	0.99 \pm 0.03	-0.9 \pm 10.1
	30	0.89 \pm 0.06	4.3 \pm 3.8
5b	Control	0.93 \pm 0.07	
	100	0.47 \pm 0.10**	51.1 \pm 6.4
	30	0.76 \pm 0.09*	27.7 \pm 3.3
	10	0.78 \pm 0.24	11.3 \pm 1.6
	IC ₅₀	84.3 μM	
5c	Control	1.14 \pm 0.03	
	30	0.67 \pm 0.08**	42.1 \pm 8.7
	10	0.82 \pm 0.06**	29.1 \pm 7.4
	3	0.80 \pm 0.05**	31.8 \pm 3.2
6a	Control	0.93 \pm 0.07	
	100	0.81 \pm 0.06	12.1 \pm 6.6
	30	0.75 \pm 0.08	19.0 \pm 13.0
6b	Control	0.93 \pm 0.07	
	100	0.65 \pm 0.04*	29.7 \pm 4.4
	30	0.52 \pm 0.03**	44.2 \pm 2.9
6c	Control	1.14 \pm 0.03	
	30	1.14 \pm 0.04	-1.1 \pm 7.7
	10	0.07 \pm 0.01	14.2 \pm 4.3
	3	1.00 \pm 0.09	12.1 \pm 8.3
7a	Control	0.93 \pm 0.07	
	100	3.78 \pm 0.09**	-314.8 \pm 34.5
	30	3.43 \pm 0.11**	-276.6 \pm 31.9
7b	Control	0.93 \pm 0.07	
	100	3.52 \pm 0.01**	-270.4 \pm 29.9
	30	3.35 \pm 0.08**	-251.8 \pm 22.1
7c	Control	1.58 \pm 0.12	
	0.3	0.43 \pm 0.15**	74.0 \pm 8.7
	0.1	0.79 \pm 0.07**	48.8 \pm 5.7
	0.03	1.04 \pm 0.15**	32.7 \pm 13.4
	IC ₅₀	0.44 μM	
8a	Control	0.93 \pm 0.07	
	100	1.12 \pm 0.03	-18.1 \pm 11.6
	30	0.90 \pm 0.12	3.7 \pm 8.1
8b	Control	0.90 \pm 0.07	
	100	1.11 \pm 0.17	-19.1 \pm 15.2
	30	1.32 \pm 0.15	-10.0 \pm 9.1
8c	Control	1.58 \pm 0.11	
	30	1.14 \pm 0.11	26.4 \pm 10.3
	10	1.08 \pm 0.19*	32.2 \pm 8.9
	3	1.12 \pm 0.07	28.9 \pm 1.4
8c	Control	0.93 \pm 0.07	
	100	3.45 \pm 0.12**	-277.1 \pm 27.8
	30	3.34 \pm 0.27**	-269.4 \pm 27.1
9a	Control	0.93 \pm 0.07	
	100	3.56 \pm 0.01**	-316.0 \pm 8.7
	30	1.92 \pm 0.11**	103.2 \pm 24.9
9c	Control	2.38 \pm 0.15	
	100	4.77 \pm 0.24**	-102.4 \pm 17.1
	30	5.04 \pm 0.31**	-125.9 \pm 15.6
Trifluoperazine IC ₅₀		8.0 μM	

The neutrophil suspension was preincubated at 37°C with 0.5% DMSO or tested compound for 3 min in the presence of cytochalasin B (5 $\mu\text{g}/\text{ml}$). Fifteen minutes after the addition of FMLP (0.3 μM), the absorbance was determined at 550 nm. Values are presented as mean \pm S.E., $n=3-5$, *: $p<0.05$, **: $p<0.01$.

Table 4. The Inhibitory Effect of Compounds on Mast Cell Degranulation (*in Vitro*)

Compound (μM)		Percent release			
		β -Glucuronidase	% Inhibition	Histamine	% Inhibition
2a	Control	53.5 \pm 2.9		51.5 \pm 3.0	
	100	48.4 \pm 2.0	7.3 \pm 6.2	55.6 \pm 2.4	-1.5 \pm 2.2
	30	45.5 \pm 3.5	12.4 \pm 0.2	51.1 \pm 4.0	7.0 \pm 3.4
2b	Control	53.5 \pm 2.9		51.5 \pm 3.0	
	100	49.1 \pm 5.1	7.0 \pm 6.8	52.9 \pm 5.1	3.8 \pm 4.3
	30	50.9 \pm 6.4	4.2 \pm 6.1	53.4 \pm 5.7	3.3 \pm 5.3
2c	Control	15.4 \pm 2.7		27.6 \pm 4.3	
	30	9.7 \pm 1.8*	44.8 \pm 5.1	15.7 \pm 1.7*	41.1 \pm 6.4
	10	10.0 \pm 1.8	35.3 \pm 6.2	18.7 \pm 3.8	32.0 \pm 9.9
5a	Control	34.9 \pm 1.9		64.6 \pm 2.1	
	100	32.2 \pm 2.0	7.4 \pm 2.0	57.6 \pm 1.2	10.2 \pm 4.1
	30	33.0 \pm 1.4	4.9 \pm 2.9	61.0 \pm 1.7	4.9 \pm 3.8
5b	Control	34.9 \pm 1.9		64.6 \pm 2.1	
	100	32.9 \pm 3.3	6.0 \pm 2.5	61.6 \pm 6.0	5.1 \pm 3.2
	30	32.6 \pm 2.6	6.6 \pm 0.2	60.7 \pm 5.1	6.1 \pm 1.9
5c	Control	16.8 \pm 0.1		40.5 \pm 2.5	
	30	21.3 \pm 1.0	-27.0 \pm 5.2	39.2 \pm 1.7	-1.3 \pm 0.4
	10	19.6 \pm 1.4	-16.7 \pm 7.7	37.4 \pm 1.3	3.1 \pm 5.0
6a	Control	34.9 \pm 1.9		64.6 \pm 2.1	
	100	17.4 \pm 1.6**	49.4 \pm 6.1	24.9 \pm 1.8**	61.1 \pm 3.4
	30	28.5 \pm 3.1	18.5 \pm 2.1	55.3 \pm 4.4	14.5 \pm 1.4
6b	Control	34.9 \pm 1.9		64.6 \pm 2.1	
	100	31.7 \pm 2.2	8.7 \pm 2.8	58.8 \pm 5.0	9.2 \pm 2.1
	30	30.9 \pm 3.6	11.5 \pm 3.3	58.0 \pm 4.7	10.4 \pm 1.6
6c	Control	16.8 \pm 0.1		40.5 \pm 2.5	
	10	17.2 \pm 1.2	-2.8 \pm 8.4	28.8 \pm 2.6	25.8 \pm 0.2
	3	14.1 \pm 0.4	16.5 \pm 2.8	34.4 \pm 5.8	12.1 \pm 7.2
7a	Control	34.9 \pm 1.9		64.6 \pm 2.1	
	10	8.4 \pm 2.4**	76.0 \pm 6.7	12.5 \pm 1.9**	80.5 \pm 3.4
	3	22.2 \pm 1.4**	36.4 \pm 0.8	50.3 \pm 2.1	22.2 \pm 1.1
7b	Control	34.9 \pm 1.9		64.6 \pm 2.1	
	30	4.3 \pm 0.4**	87.4 \pm 1.9	0.02 \pm 0.9**	99.8 \pm 1.4
	10	8.8 \pm 0.9**	74.6 \pm 3.2	13.6 \pm 1.8**	78.8 \pm 3.3
7c	Control	26.2 \pm 2.8		37.6 \pm 3.4	
	(1)	-4.8 \pm 3.0**	124.2 \pm 14.4	0.7 \pm 5.3**	97.2 \pm 15.8
	(0.3)	13.2 \pm 2.5	34.3 \pm 15.0	24.7 \pm 7.3	30.9 \pm 14.2
8a	Control	34.9 \pm 1.9		64.6 \pm 2.1	
	100	30.5 \pm 2.1	12.4 \pm 2.0	60.3 \pm 3.8	6.5 \pm 0.1
	30	31.8 \pm 2.4	8.7 \pm 3.5	62.6 \pm 5.8	3.4 \pm 2.8
8b	Control	34.9 \pm 1.9		64.6 \pm 2.1	
	100	30.1 \pm 2.7	13.8 \pm 1.1	52.0 \pm 3.8	19.6 \pm 1.1
	30	32.1 \pm 3.0	8.2 \pm 2.5	56.3 \pm 3.8	12.9 \pm 0.4
8c	Control	32.7 \pm 0.7		30.9 \pm 2.2	
	30	26.3 \pm 1.3	19.5 \pm 4.0	27.7 \pm 3.4	10.7 \pm 4.4
	10	27.7 \pm 0.2	15.0 \pm 2.7	29.6 \pm 3.0	3.9 \pm 7.5
9a	Control	34.9 \pm 1.9		64.6 \pm 2.1	
	100	6.0 \pm 0.8**	82.8 \pm 1.0	6.8 \pm 0.7**	89.3 \pm 1.5
	10	8.2 \pm 0.5**	72.4 \pm 4.0	14.1 \pm 4.2**	77.4 \pm 7.7
9b	Control	34.9 \pm 1.9		64.6 \pm 2.1	
	30	7.7 \pm 1.8**	78.5 \pm 4.1	10.7 \pm 1.5**	83.2 \pm 2.9
	10	26.4 \pm 1.9	24.3 \pm 2.7	53.8 \pm 2.2	16.5 \pm 4.5
9c	Control	41.4 \pm 1.2		71.2 \pm 1.6	
	10	4.5 \pm 0.5**	89.0 \pm 1.4	3.5 \pm 0.4**	94.9 \pm 0.7
	3	11.1 \pm 1.1**	73.1 \pm 2.7	17.9 \pm 1.8**	74.6 \pm 2.8
Mepacrine	Control	34.9 \pm 1.9		64.6 \pm 2.1	
	100	6.0 \pm 0.8**	82.8 \pm 1.0	6.8 \pm 0.7**	89.3 \pm 1.5
	10	8.2 \pm 0.5**	72.4 \pm 4.0	14.1 \pm 4.2**	77.4 \pm 7.7
IC ₅₀	Control	34.9 \pm 1.9		64.6 \pm 2.1	
	30	7.7 \pm 1.8**	78.5 \pm 4.1	10.7 \pm 1.5**	83.2 \pm 2.9
	10	26.4 \pm 1.9	24.3 \pm 2.7	53.8 \pm 2.2	16.5 \pm 4.5
IC ₅₀	Control	34.9 \pm 1.9		64.6 \pm 2.1	
	30	7.7 \pm 1.8**	78.5 \pm 4.1	10.7 \pm 1.5**	83.2 \pm 2.9
	10	26.4 \pm 1.9	24.3 \pm 2.7	53.8 \pm 2.2	16.5 \pm 4.5
IC ₅₀	Control	34.9 \pm 1.9		64.6 \pm 2.1	
	30	7.7 \pm 1.8**	78.5 \pm 4.1	10.7 \pm 1.5**	83.2 \pm 2.9
	10	26.4 \pm 1.9	24.3 \pm 2.7	53.8 \pm 2.2	16.5 \pm 4.5
IC ₅₀	Control	34.9 \pm 1.9		64.6 \pm 2.1	
	30	7.7 \pm 1.8**	78.5 \pm 4.1	10.7 \pm 1.5**	83.2 \pm 2.9
	10	26.4 \pm 1.9	24.3 \pm 2.7	53.8 \pm 2.2	16.5 \pm 4.5
IC ₅₀	Control	34.9 \pm 1.9		64.6 \pm 2.1	
	30	7.7 \pm 1.8**	78.5 \pm 4.1	10.7 \pm 1.5**	83.2 \pm 2.9
	10	26.4 \pm 1.9	24.3 \pm 2.7	53.8 \pm 2.2	16.5 \pm 4.5
IC ₅₀	Control	34.9 \pm 1.9		64.6 \pm 2.1	
	30	7.7 \pm 1.8**	78.5 \pm 4.1	10.7 \pm 1.5**	83.2 \pm 2.9
	10	26.4 \pm 1.9	24.3 \pm 2.7	53.8 \pm 2.2	16.5 \pm 4.5
IC ₅₀	Control	34.9 \pm 1.9		64.6 \pm 2.1	
	30	7.7 \pm 1.8**	78.5 \pm 4.1	10.7 \pm 1.5**	83.2 \pm 2.9
	10	26.4 \pm 1.9	24.3 \pm 2.7	53.8 \pm 2.2	16.5 \pm 4.5
IC ₅₀	Control	34.9 \pm 1.9		64.6 \pm 2.1	
	30	7.7 \pm 1.8**	78.5 \pm 4.1	10.7 \pm 1.5**	83.2 \pm 2.9
	10	26.4 \pm 1.9	24.3 \pm 2.7	53.8 \pm 2.2	16.5 \pm 4.5
IC ₅₀	Control	34.9 \pm 1.9		64.6 \pm 2.1	
	30	7.7 \pm 1.8**	78.5 \pm 4.1	10.7 \pm 1.5**	83.2 \pm 2.9
	10	26.4 \pm 1.9	24.3 \pm 2.7	53.8 \pm 2.2	16.5 \pm 4.5
IC ₅₀	Control	34.9 \pm 1.9		64.6 \pm 2.1	
	30	7.7 \pm 1.8**	78.5 \pm 4.1	10.7 \pm 1.5**	83.2 \pm 2.9
	10	26.4 \pm 1.9	24.3 \pm 2.7	53.8 \pm 2.2	16.5 \pm 4.5
IC ₅₀	Control	34.9 \pm 1.9		64.6 \pm 2.1	
	30	7.7 \pm 1.8**	78.5 \pm 4.1	10.7 \pm 1.5**	83.2 \pm 2.9
	10	26.4 \pm 1.9	24.3 \pm 2.7	53.8 \pm 2.2	16.5 \pm 4.5
IC ₅₀	Control	34.9 \pm 1.9		64.6 \pm 2.1	
	30	7.7 \pm 1.8**	78.5 \pm 4.1	10.7 \pm 1.5**	83.2 \pm 2.9
	10	26.4 \pm 1.9	24.3 \pm 2.7	53.8 \pm 2.2	16.5 \pm 4.5
IC ₅₀	Control	34.9 \pm 1.9		64.6 \pm 2.1	
	30	7.7 \pm 1.8**	78.5 \pm 4.1	10.7 \pm 1.5**	83.2 \pm 2.9
	10	26.4 \pm 1.9	24.3 \pm 2.7	53.8 \pm 2.2	16.5 \pm 4.5
IC ₅₀	Control	34.9 \pm 1.9		64.6 \pm 2.1	
	30	7.7 \pm 1.8**	78.5 \pm 4.1	10.7 \pm 1.5**	83.2 \pm 2.9
	10	26.4 \pm 1.9	24.3 \pm 2.7	53.8 \pm 2.2	16.5 \pm 4.5
IC ₅₀	Control	34.9 \pm 1.9		64.6 \pm 2.1	
	30	7.7 \pm 1.8**	78.5 \pm 4.1	10.7 \pm 1.5**	83.2 \pm 2.9
	10	26.4 \pm 1.9	24.3 \pm 2.7	53.8 \pm 2.2	16.5 \pm 4.5
IC ₅₀	Control	34.9 \pm 1.9		64.6 \pm 2.1	
	30	7.7 \pm 1.8**	78.5 \pm 4.1	10.7 \pm 1.5**	83.2 \pm 2.9
	10	26.4 \pm 1.9	24.3 \pm 2.7	53.8 \pm 2.2	16.5 \pm 4.5
IC ₅₀	Control	34.9 \pm 1.9		64.6 \pm 2.1	
	30	7.7 \pm 1.8**	78.5 \pm 4.1	10.7 \pm 1.5**	83.2 \pm 2.9
	10	26.4 \pm 1.9	24.3 \pm 2.7	53.8 \pm 2.2	16.5 \pm 4.5
IC ₅₀	Control	34.9 \pm 1.9		64.6 \pm 2.1	
	30	7.7 \pm 1.8**	78.5 \pm 4.1	10.7 \pm 1.5**	83.2 \pm 2.9
	10	26.4 \pm 1.9	24.3 \pm 2.7	53.8 \pm 2.2	16.5 \pm 4.5
IC ₅₀	Control	34.9 \pm 1.9		64.6 \pm 2.1	
	30	7.7 \pm 1.8**	78.5 \pm 4.1	10.7 \pm 1.5**	83.2 \pm 2.9
	10	26.4 \pm 1.9	24.3 \pm 2.7	53.8 \pm 2.2	16.5 \pm 4.5
IC ₅₀	Control	34.9 \pm 1.9		64.6 \pm 2.1	
	30	7.7 \pm 1.8**	78.5 \pm 4.1	10.7 \pm 1.5**	83.2 \pm 2.9
	10	26.4 \pm 1.9	24.3 \pm 2.7	53.8 \pm 2.2	16.5 \pm 4.5
IC ₅₀	Control	34.9 \pm 1.9		64.6 \pm 2.1	
	30	7.7 \pm 1.8**	78.5 \pm 4.1	10.7 \pm 1.5**	83.2 \pm 2.9
	10	26.4 \pm 1.9	24.3 \pm 2.7	53.8 \pm 2.2	16.5 \pm 4.5
IC ₅₀	Control	34.9 \pm 1.9		64.6 \pm 2.1	
	30	7.7 \pm 1.8**	78.5 \pm 4.1	10.7 \pm 1.5**	83.2 \pm 2.9
	10	26.4 \pm 1.9	24.3 \pm 2.7	53.8 \pm 2.2	16.5 \pm 4.5
IC ₅₀	Control	34.9 \pm 1.9		64.6 \pm 2.1	
	30	7.7 \pm 1.8**	78.5 \pm 4.1	10.7 \pm 1.5**	83.2 \pm 2.9
	10	26.4 \pm 1.9	24.3 \pm 2.7	53.8 \pm 2.2	16.5 \pm 4.5
IC ₅₀	Control	34.9 \pm 1.9		64.6 \pm 2.1	
	30	7.7 \pm 1.8**	78.5 \pm 4.1	10.7 \pm 1.5**	83.2 \pm 2.9
	10	26.4 \pm 1.9	24.3 \pm 2.7	53.8 \pm 2.2	16.5 \pm 4.5
IC ₅₀	Control	34.9 \pm 1.9		64.6 \pm 2.1	
	30	7.7 \pm 1.8**	78.5 \pm 4.1	10.7 \pm 1.5**	83.2 \pm 2.9
	10	26.4 \pm 1.9	24.3 \pm 2.7	53.8 \pm 2.2	16.5 \pm 4.5
IC ₅₀	Control	34.9 \pm 1.9		64.6 \pm 2.1	
	30	7.7 \pm 1.8**	78.5 \pm 4.1	10.7 \pm 1.5**	83.2 \pm 2.9
	10	26.4 \pm 1.9	24.3 \pm 2.7	53.8 \pm 2.2	16.5 \pm 4.5
IC ₅₀	Control	34.9 \pm 1.9		64.6 \pm 2.1	
	30	7.7 \pm 1.8**	78.5 \pm 4.1	10.7 \pm 1.5**	83.2 \pm 2.9
	10	26.4 \pm 1.9	24.3 \pm 2.7	53.8 \pm 2.2	16.5 \pm 4.5
IC ₅₀	Control	34.9 \pm 1.9		64.6 \pm 2.1	
	30	7.7 \pm 1.8**	78.5 \pm 4.1	10.7 \pm 1.5**	83.2 \pm 2.9
	10	26.4 \pm 1.9	24.3 \pm 2.7	53.8 \pm 2.2	16.5 \pm 4.5
IC ₅₀	Control	34.9 \pm 1.9		64.6 \pm 2.1	
	30	7.7 \pm 1.8**	78.5 \pm 4.1	10.7 \pm 1.5**	83.2 \pm 2.9
	10	26.4 \pm 1.9	24.3 \pm		

Table 5. Physical and Spectral Data of the Methoxyisoflavanquinones and Related Compounds

Compd No.	R ₁	R ₂	R ₃	Yield (%)	mp (°C)	MS (M ⁺) (m/z)	UV, λ _{max} (log ε)	IR ν _{C=O} cm ⁻¹	¹ H-NMR (ppm) ^{a)}	Analysis (%) Calcd. (Found) C H	
1a	H	OCH ₃		84		242	273.4 (4.42)	1675	3.85 (3H, s, -OCH ₃), 5.16 (2H, s, -OCH ₂ -), 6.52 (1H, d, J=2.2 Hz, H-3), 6.56 (1H, dd, J=8.8, 0.56 Hz, H-5), 7.38—7.45 (5H, m, H-2', 3', 4', 5', 6'), 7.85 (1H, d, J=8.6 Hz, H-6), 10.39 (1H, s, -CHO)	74.36 (74.12)	5.82 (5.81)
1b	H	H		87		212	253.6 (4.00)	1685	5.20 (2H, s, -OCH ₂ -), 7.04—7.06 (2H, m, H-3, 5), 7.35—7.46 (5H, m, H-2', 3', 4', 5', 6'), 7.53 (1H, ddd, J=8.4, 7.5, 1.7 Hz, H-4), 7.86 (1H, dd, J=8.0, 2.0 Hz, H-6), 10.56 (1H, s, -CHO)	79.23 (78.93)	5.70 (5.71)
1c	OCH ₃	H		89		242	259.6 (3.90)	1693	3.94 (3H, s, -OCH ₃), 5.18 (2H, s, -OCH ₂ -), 7.10—7.20 (2H, m, H-4, 5), 7.33—7.40 (6H, m, H-6, 2', 3', 4', 5', 6'), 10.23 (1H, s, -CHO)	74.36 (74.21)	5.82 (5.83)
2a	H	OCH ₃	H	80	166—167	360	383.0 (4.55)	1628	3.87 (3H, s, -OCH ₃), 5.15 (2H, s, -OCH ₂ -), 6.56 (1H, d, J=1.6 Hz, H-5), 6.60 (1H, s, H-3), 6.72 (1H, ddd, J=7.6, 7.1, 1.1 Hz, H-5'), 6.97 (1H, d, J=8.3 Hz, H-3'), 7.35—7.50 (7H, m, H-6, 4', 2'', 3'', 4'', 5'', 6''), 7.56 (1H, d, J=4.9 Hz, H-6'), 7.83 (1H, d, J=15.5 Hz, H-α), 8.02 (1H, d, J=15.5 Hz, H-β), 13.12 (1H, s, -OH)	76.65 (76.40)	5.59 (5.54)
2b	H	H	OCH ₃	85	116—117	360	365.0 (4.23)	1628	3.85 (3H, s, -OCH ₃), 5.18 (2H, s, -OCH ₂ -), 6.28 (1H, dd, J=8.9, 2.6 Hz, H-5'), 6.43 (1H, d, J=2.5 Hz, H-3'), 7.04 (1H, dd, J=7.3, 7.3 Hz, H-5), 7.06 (1H, d, J=8.1 Hz, H-3), 7.28 (1H, d, J=4.4 Hz, H-6), 7.35 (1H, dd, J=3.9, 2.2 Hz, H-4), 7.38—7.56 (5H, m, H-2'', 3'', 4'', 5'', 6''), 7.59 (1H, s, H-6'), 7.85 (1H, d, J=15.6 Hz, H-α), 8.04 (1H, d, J=15.6 Hz, H-β), 13.59 (1H, s, -OH)	76.65 (76.73)	5.59 (5.56)
2c	OCH ₃	H	H	85	101—103	360	358.5 (4.34)	1635	3.93 (3H, s, -OCH ₃), 5.09 (2H, s, -OCH ₂ -), 6.82 (1H, ddd, J=8.1, 7.2, 1.2 Hz, H-5'), 7.00 (1H, dd, J=8.4, 1.2 Hz, H-3'), 7.02 (1H, dd, J=7.8, 1.5 Hz, H-4), 7.12 (1H, dd, J=7.8, 7.8 Hz, H-5), 7.23 (1H, dd, J=7.8, 1.5 Hz, H-6), 6.30—7.49 (6H, m, H-4', 2'', 3'', 4'', 5'', 6''), 7.64 (1H, dd, J=8.1, 1.8 Hz, H-6'), 7.70 (1H, d, J=15.6 Hz, H-α), 8.09 (1H, d, J=15.6 Hz, H-β), 12.88 (1H, s, -OH)	76.65 (76.52)	5.59 (5.59)
5a	H	OCH ₃	H	85	127—128	358	274.0 (3.93)	1651	3.82 (3H, s, -OCH ₃), 5.08 (2H, s, -OCH ₂ -), 6.58 (1H, d, J=2.4 Hz, H-5'), 6.62 (1H, s, H-3'), 7.27—7.38 (5H, m, H-2'', 3'', 4'', 5'', 6''), 7.42 (1H, d, J=1.0 Hz, H-6'), 7.45 (1H, dd, J=2.9, 1.0 Hz, H-6), 7.48 (1H, s, H-8), 7.67 (1H, ddd, J=7.8, 7.7, 1.7 Hz, H-7), 7.99 (1H, s, H-2), 8.32 (1H, dd, J=8.0, 1.7 Hz, H-5)	77.08 (77.27)	5.06 (5.07)
5b	H	H	OCH ₃	80	163—164	358	266.8 (4.14)	1652	3.91 (3H, s, -OCH ₃), 5.10 (2H, s, -OCH ₂ -), 6.85 (1H, d, J=2.4 Hz, H-8), 7.00 (1H, dd, J=8.9, 2.4 Hz, H-6), 7.05 (2H, m, H-3', 5'), 7.27—7.39 (7H, m, H-4', 6', 2'', 3'', 4'', 5'', 6''), 7.94 (1H, s, H-2), 8.23 (1H, d, J=8.9 Hz, H-5)	77.08 (76.68)	5.06 (5.01)
5c	OCH ₃	H	H	80	140—141	358	320.0 (4.33)	1705	3.84 (3H, s, -OCH ₃), 5.09 (2H, s, -OCH ₂ -), 6.98 (1H, dd, J=8.0, 8.0 Hz, H-5'), 7.10 (1H, dd, J=8.0, 1.2 Hz, H-4'), 7.27 (1H, s, H-3), 7.29—7.40 (5H, m, H-2'', 3'', 4'', 5'', 6''), 7.46 (1H, d, J=2.1 Hz, H-6'), 7.49 (1H, ddd, J=8.5, 7.0, 1.0 Hz, H-6), 7.53 (1H, dd, J=8.7, 1.0 Hz, H-8), 7.75 (1H, ddd, J=8.7, 7.0, 1.5 Hz, H-7), 8.30 (1H, dd, J=8.5, 1.5 Hz, H-5)	77.08 (76.64)	5.06 (5.05)
6a	H	OCH ₃	H	90	104—105	256	278.2 (3.73)		3.04 (1H, ddd, J=16.4, 5.5, 1.9 Hz, H-4ax.), 3.07 (1H, dd, J=16.4, 1.2 Hz, H-4eq.), 3.54—3.60 (1H, m, H-3), 3.77 (3H, s, -OCH ₃), 4.08 (1H, dd, J=10.4, 10.4 Hz, H-2ax.), 4.35 (1H, ddd, J=10.4, 3.4, 1.9 Hz, H-2eq.), 5.15 (1H, s, -OH), 6.37 (1H, d, J=2.5 Hz, H-3'), 6.49 (1H, dd, J=8.5, 2.5 Hz, H-5'), 6.86 (1H, d, J=7.4 Hz, H-8), 6.88 (1H, ddd, J=8.2, 6.1, 1.2 Hz, H-6), 7.01—7.16 (3H, m, H-5, 7, 6')	75.02 (75.18)	6.25 (6.30)
6b	H	H	OCH ₃	90	130—131	256	276.2 (3.81)		3.07 (1H, ddd, J=16.5, 5.4, 2.0 Hz, H-4ax.), 3.09 (1H, dd, J=16.5, 1.2 Hz, H-4eq.), 3.53—3.57 (1H, m, H-3), 3.77 (3H, s, -OCH ₃), 4.07 (1H, dd, J=10.2, 10.2 Hz, H-2ax.), 4.37 (1H, ddd, J=10.2, 3.4, 2.0 Hz, H-2eq.), 5.16 (1H, s, -OH), 6.93 (1H, d, J=2.2 Hz, H-8), 6.96 (1H, dd, J=7.9, 1.2 Hz, H-6), 7.04—7.20 (4H, m, H-5, 3', 4', 5'), 7.35 (1H, dd, J=8.4, 1.7 Hz, H-6'),	75.02 (75.23)	6.25 (6.41)

Table 5. (Continued)

Compd No.	R ₁	R ₂	R ₃	Yield (%)	mp (°C)	MS (M ⁺) (m/z)	UV, λ _{max} (log ε)	IR ν _{C=O} cm ⁻¹	¹ H-NMR (ppm) ^{a)}	Analysis (%) Calcd. (Found) C H	
6c	OCH ₃	H	H	90	71—73	256	279.7 (3.75)		2.98—3.08 (2H, m, H-3ax., 4ax.), 3.15—3.27 (2H, m, H-3eq., 4eq.), 3.90 (3H, s, -OCH ₃), 5.10—5.20 (1H, m, H-2), 5.91 (1H, s, -OH), 6.79—6.86 (5H, m, H-6, 8, 4', 5', 6'), 7.09—7.17 (2H, m, H-5, 7)	75.02 (75.12)	6.25 (6.30)
7a	H	OCH ₃	H	66	172—173	270	264.8 (4.09)	1675 1644	2.80 (1H, dd, J=16.5, 6.7 Hz, H-4ax.), 3.12 (1H, dd, J=16.5, 6.9 Hz, H-4eq.), 3.46—3.54 (1H, m, H-3), 3.82 (3H, s, -OCH ₃), 4.08 (1H, dd, J=10.5, 6.6 Hz, H-2ax), 4.28 (1H, dd, J=10.5, 2.3 Hz, H-2eq), 5.97 (1H, s, H-3'), 6.48 (1H, s, H-6'), 6.81 (1H, d, J=8.6 Hz, H-8), 6.87 (1H, dd, J=7.8, 7.3 Hz, H-6), 7.06 (1H, d, J=6.8 Hz, H-5), 7.11 (1H, dd, J=7.9, 7.4 Hz, H-7)	71.10 (70.89)	5.22 (5.21)
7b	H	H	OCH ₃	65	176—178	270	236.4 (4.18)	1675 1644	2.78 (1H, dd, J=16.5, 6.6 Hz, H-4ax.), 3.09 (1H, dd, J=16.5, 6.6 Hz, H-4eq.), 3.44—3.48 (1H, m, H-3), 3.79 (3H, s, -OCH ₃), 4.05 (1H, dd, J=10.5, 6.7 Hz, H-2ax), 4.26 (1H, dd, J=10.5, 2.2 Hz, H-2eq), 5.98 (1H, s, H-6'), 6.46 (1H, dd, J=9.8, 2.0 Hz, H-4'), 6.53 (1H, d, J=9.8 Hz, H-3'), 7.03 (1H, d, J=2.4 Hz, H-8), 7.07 (1H, ddd, J=8.6, 2.2 Hz, H-6), 7.24 (1H, d, J=8.6 Hz, H-5)	71.10 (70.86)	5.22 (5.18)
7c	OCH ₃	H	H	53	150—152	270	265.6 (4.16)	1685 1651	1.72—1.85 (1H, m, H-3ax.), 2.30—2.38 (1H, m, H-3eq.), 2.75 (1H, ddd, J=16.65, 4.58, 4.5 Hz, H-4ax), 3.00 (1H, ddd, J=16.65, 10.8, 5.85 Hz, H-4eq), 3.85 (3H, s, -OCH ₃), 5.12 (1H, dd, J=9.45, 2.4 Hz, H-2), 5.94 (1H, d, J=2.4 Hz, H-4'), 6.86—6.92 (3H, m, H-6', 8, 6), 7.08 (1H, dd, J=7.2, 0.9 Hz, H-5), 7.13 (1H, ddd, J=8.4, 7.5, 0.9 Hz, H-7)	71.10 (70.95)	5.22 (5.30)
8a	H	OCH ₃	H	86	166—167	268	276.0 (4.06)	1721	3.83 (3H, s, -OCH ₃), 6.56 (1H, dd, J=8.5, 2.6 Hz, H-5'), 6.67 (1H, d, J=2.5 Hz, H-3'), 7.09 (1H, d, J=8.5 Hz, H-6'), 7.51 (1H, ddd, J=8.1, 7.5, 1.0 Hz, H-6), 7.55 (1H, dd, J=9.0, 8.1 Hz, H-8), 7.78 (1H, ddd, J=7.8, 7.8, 1.7 Hz, H-7), 8.15 (1H, s, H-2), 8.37 (1H, dd, J=8.2, 1.6 Hz, H-5), 9.08 (1H, s, -OH)	71.64 (71.31)	4.51 (4.31)
8b	H	H	OCH ₃	84	127—128	268	278.0 (4.13)	1711	3.95 (3H, s, -OCH ₃), 6.94 (1H, d, J=2.4 Hz, H-8), 6.99 (1H, dd, J=7.3, 1.3 Hz, H-6), 7.08 (1H, dd, J=9.0, 2.4 Hz, H-3'), 7.10 (1H, dd, J=8.1, 1.2 Hz, H-5'), 7.18 (1H, dd, J=7.7, 1.7 Hz, H-4'), 7.36 (1H, ddd, J=8.4, 7.8, 1.0 Hz, H-6'), 8.10 (1H, s, H-2), 8.27 (1H, d, J=9.0 Hz, H-5), 9.01 (1H, s, -OH)	71.64 (71.25)	4.51 (4.56)
8c	OCH ₃	H	H	84	207—209	268	254.6 (4.40)	1701	3.84 (3H, s, -OCH ₃), 6.92 (1H, dd, J=8.0, 8.0 Hz, H-5'), 7.06 (1H, dd, J=8.0, 1.3 Hz, H-4'), 7.27 (1H, s, H-3), 7.31 (1H, dd, J=7.5, 7.46 Hz, H-6), 7.54 (1H, d, J=8.9 Hz, H-8), 7.74—7.81 (3H, m, H-5, 7, 6'), 9.6 (1H, br, -OH)	71.64 (71.37)	4.51 (4.53)
9a	H	OCH ₃	H	50	243—244	282	298.0 (4.04)	1659 1628	3.83 (3H, s, -OCH ₃), 6.23 (1H, s, H-3'), 7.08 (1H, s, H-6'), 7.54 (1H, ddd, J=8.2, 5.6, 0.9 Hz, H-6), 7.70 (1H, dd, J=8.2, 0.9 Hz, H-8), 7.85 (1H, ddd, J=8.4, 5.6, 1.0 Hz, H-7), 8.18 (1H, dd, J=8.2, 1.0 Hz, H-5), 8.47 (1H, s, H-2)	68.09 (67.73)	3.57 (3.76)
9b	H	H	OCH ₃	45	214—216	282	298.2 (4.14)	1657 1636	3.82 (3H, s, -OCH ₃), 6.88 (1H, dd, J=10.8, 1.7 Hz, H-4'), 6.94 (1H, d, J=10.8 Hz, H-3'), 7.00 (1H, d, J=1.7 Hz, H-6'), 7.11 (1H, dd, J=8.8, 1.6 Hz, H-6), 7.20 (1H, d, J=1.6 Hz, H-8), 7.93 (1H, dd, J=8.4, 1.9 Hz, H-5), 8.42 (1H, s, H-2)	68.09 (68.12)	3.57 (3.72)
9c	OCH ₃	H	H	53	210—211	282	298.8 (4.04)	1652 1644	3.84 (3H, s, -OCH ₃), 6.18 (1H, d, J=2.5 Hz, H-4'), 6.98 (1H, d, J=2.5 Hz, H-6'), 7.34 (1H, s, H-3), 7.50 (1H, d, J=8.1 Hz, H-6), 7.65 (1H, dd, J=8.4, 1.7 Hz, H-8), 7.89 (1H, ddd, J=8.4, 7.1, 1.5 Hz, H-7), 8.29 (1H, dd, J=8.1, 1.5 Hz, H-5)	68.09 (67.98)	3.57 (3.70)

a) Compounds 7c, 9a, 9b, 9c were dissolved in DMSO-d₆ and the others in CDCl₃.

85%) as colorless needles (Table 5).

2'-Benzyloxy-7-methoxyisoflavone (**5b**): Compound **2b** (10.8 g, 30 mmol) was treated in the same manner as described for compound **5a** to afford **5b** (5.7 g, 80%) as colorless needles (Table 5).

2'-Benzyloxy-3'-methoxyflavone (**5c**): Compound **2c** (10.80 g, 30 mmol) was treated in the same manner as described for compound **5a**. The residue was eluted through a silica gel column with benzene, and recrystallized from EtOH to give compound **5c** (8.59 g, 80%) as colorless needles (Table 5).

2'-Hydroxy-4'-methoxyisoflavan (**6a**): Compound **5a** (1.1 g, 3 mmol) was suspended in AcOH (30 ml) containing 10% Pd/C (1.0 g) and shaken under an H₂ stream for 2 h at room temperature. After removing the catalyst by filtration, water (100 ml) was added to the filtrate, and the mixture was extracted with CHCl₃. The organic layer was dried over MgSO₄, and evaporated *in vacuo*. The residue was eluted through a silica gel column with benzene, and recrystallized from EtOH to give compound **6a** (0.7 g, 90%) as white prism crystals (Table 5).

2'-Hydroxy-7-methoxyisoflavan (**6b**): Compound **5b** (1.1 g, 3 mmol) was treated in the same manner as described for compound **6a** to afford **6b** (0.7 g, 90%) as white prism crystals (Table 5).

2'-Hydroxy-3'-methoxyflavan (**6c**): Compound **5c** (1.00 g, 2.8 mmol) was treated in the same manner as described for compound **6a** to afford **6c** (0.65 g, 90%) as white prism crystals (Table 5).

4'-Methoxyisoflavanquinone (**7a**): To a solution of compound **6a** (0.3 g, 1.3 mmol) in acetone/MeOH (4:1) (45 ml) was added 0.17 M KH₂PO₄ (45 ml) and potassium nitrosodisulfonate (3 g) in water (45 ml). The mixture was stirred at 25±3 °C for 4 h, poured into water (100 ml) and extracted with CHCl₃. The organic layer was dried over MgSO₄ and evaporated *in vacuo*. The residue was eluted through a silica gel column with CHCl₃ to yield compound **7a** (0.2 g, 66%) as a red-brown powder (Table 5).

7-Methoxyisoflavanquinone (**7b**): Compound **6b** (0.3 g, 1.3 mmol) was treated in the same manner as described for compound **7a** to afford **7b** (0.2 g, 65%) as a red-brown powder (Table 5).

3'-Methoxyflavanquinone (**7c**): Compound **6c** (0.31 g, 1.2 mmol) was treated in the same manner as described for compound **7a** to afford **7c** (0.17 g, 53%) as a red-brown powder (Table 5).

2'-Hydroxy-4'-methoxyisoflavone (**8a**): A suspension of compound **5a** (2.2 g, 6 mmol) in 47% HBr (80 ml) was stirred at 50±2 °C for 2 h. The reaction mixture was poured into water (100 ml) and extracted with CHCl₃. The organic layer was dried over MgSO₄ and evaporated *in vacuo*. The residue was eluted through a silica gel column with CHCl₃ to obtain compound **8a** (1.4 g, 86%) as colorless prism crystals (Table 5).

2'-Hydroxy-7-methoxyisoflavone (**8b**): Compound **5b** (2.2 g, 6 mmol) was treated in the same manner as described for compound **8a** to afford **8b** (1.4 g, 84%) as colorless prism crystals (Table 5).

2'-Hydroxy-3'-methoxyflavone (**8c**): Compound **5c** (2.00 g, 5.6 mmol) was treated in the same manner as described for compound **8a**. The residue was eluted through a silica gel column with benzene/EtOAc (9:1) to obtain compound **8c** (1.26 g, 84%) as colorless prism crystals (Table 5).

4'-Methoxyisoflavone quinone (**9a**): Compound **8a** (0.3 g, 1.25 mmol) was treated in the same manner as described for compound **7a** to afford **9a** (0.2 g, 50%) as a yellow brown powder (Table 5).

7-Methoxyisoflavone quinone (**9b**): Compound **8b** (0.3 g, 1.25 mmol) was treated in the same manner as described for compound **7a** to afford **9b** (0.2 g, 45%) as a yellow brown powder (Table 5).

3'-Methoxyflavone quinone (**9c**): Compound **8c** (0.34 g, 1.25 mmol) was treated in the same manner as described for compound **7a** to afford **9c** (0.19 g, 53%) as a yellow brown powder (Table 5).

Evaluation of Antiplatelet Activity. Material Collagen (type I, bovine achilles tendon), obtained from Sigma Chemical Co., was homogenized in 25 ml acetic acid and then stored at -70 °C. AA, EDTA (disodium salt), sodium citrate, DMSO, and PAF were purchased from Sigma Chemical Co. Thrombin (bovine) was obtained from Park Davis Co. and dissolved in 50% (v/v) glycerol to give a stock solution of 100 NIH units/ml.

Methods Platelet Suspension Preparation: Blood, collected from the marginal ear vein of rabbits was mixed with EDTA to a final concentration of 6 mM and centrifuged at 90 g for 10 min at room temperature to obtain platelet-rich plasma. The latter was further centrifuged at 500 g for 10 min and the platelets were washed with Tyrode's solution without EDTA. After centrifugation at the same conditions, the platelets were suspended in Tyrode's solution with the following compositions (mM): NaCl (136.8), KCl (2.8), NaHCO₃ (11.9), MgCl₂ (1.1), NaH₂PO₄ (0.33), CaCl₂ (1.0), and glucose (11.2). Platelet numbers were determined with a Coulter Counter (Model ZM) and adjusted to 4.5×10⁸ platelets/ml.

Platelet Aggregation: Aggregation was measured by the turbidimetric

method with a dual-channel Lumi aggregometer (Model 1020, Payton, Canada).⁵⁾ All glassware was siliconized. Test compounds were added one minute before the addition of the aggregation inducer and the platelet suspension was stirred at 900 rpm. The percentage of aggregation was calculated as previously described.⁶⁾

Evaluation of Anti-inflammatory Activity. Material Sodium pentobarbital, bovine serum albumin (BSA), ferricytochrome *c*, superoxide dismutase (SOD), fMLP, phenolphthalein-β-D-glucuronide, *Micrococcus lysodeikticus* and Triton X-100 were purchased from Sigma Chemical Co.

Methods Isolation of Neutrophils: EDTA-mixed fresh blood was obtained from the abdominal aorta of pentobarbital (60 mg/kg, ip)-anesthetized rats (Sprague-Dawley, 300–350 g). Neutrophils were separated from other blood cells by dextran sedimentation and centrifugation on Ficoll-hypaque.⁷⁾ Erythrocytes in the pellets were lysed by suspending the cells in 0.05% NaCl for 15 s, followed by washing with 1.75% NaCl containing 0.25% BSA. Cells were resuspended in Hanks' balanced salt solution containing 4 mM NaHCO₃ and 10 mM N-[2-hydroxyethyl]piperazine-N'-[2-ethanesulfonic acid] (HEPES), pH 7.4 Hank's balanced salt solution (HBSS) to a final concentration of 2×10⁶ cells/ml. The cell preparations consisted of 90–95% neutrophils (viability approximately 95% by trypan blue exclusion).

Measurement of β-Glucuronidase and Lysozyme Release: The neutrophil suspension was preincubated at 37 °C with DMSO or test compound for 3 min in the presence of cytochalasin B (5 μg/ml), and the release reaction was triggered by the addition of 1 μM fMLP. The reaction was stopped 45 min later by the addition of ice-cold Tyrode's solution and the mixture was centrifuged for 10 min at 1000 g. β-Glucuronidase activity in the supernatant was determined by spectrophotometry at 550 nm after reaction with phenolphthalein-β-glucuronide as substrate.⁸⁾ Lysozyme activity in the supernatant was measured, with *Micrococcus lysodeikticus* as substrate by spectrophotometry at 450 nm.⁹⁾ The release of β-glucuronidase and lysozyme was expressed as percentage release=[(release elicited by secretagogue-spontaneous release)/total content]×100. The total content was measured after treatment of the cell suspension with Triton X-100. Spontaneous release was less than 10%.

Measurement of Superoxide Anion Production: The production of superoxide anion (O₂⁻) was determined by SOD-inhibitable ferricytochrome *c* reduction as previously described¹⁰⁾ with modifications. Assay mixtures contained 0.2 ml cell suspension (5×10⁶ cells/ml) and 0.9 mg/ml of ferricytochrome *c* in a final volume of 0.4 ml. The reference tube also received 12.5 μg/ml of SOD. Both reference and sample tubes were incubated at 37 °C for 3 min. The reactions were then started by the addition of 0.3 μM fMLP and incubated at 37 °C for 30 min with occasional agitation. After centrifugation, the supernatant was transferred to a 96-well plate, and the absorbance at 550 nm was recorded with a microplate reader. The amount of O₂⁻ in the reaction mixture was calculated from the formula:¹¹⁾ O₂⁻ (nmol)=19.08×absorbance.

Evaluation of Antiallergic Activity. Materials Heparin (grade I-A; from porcine intestinal mucosa), compound 48/80 and *o*-phthaldialdehyde were purchased from Sigma Chemical Co.

Methods Rat Peritoneal Mast Cell Preparation: Rat peritoneal mast cells were isolated as previously described.¹²⁾ Briefly, heparinized Tyrode's solution was injected into the peritoneal cavity of exsanguinated rats (Sprague-Dawley, 250–300 g). After abdominal massage, the cells in the peritoneal fluid were harvested and separated in 38% BSA in glucose-free Tyrode's solution. The cell pellet was washed and suspended in Tyrode's solution of the following composition (mM): NaCl (137), KCl (2.7), NaHCO₃ (12), MgCl₂ (1.0), NaH₂PO₄ (0.3), CaCl₂ (1.0), glucose (5.6) and 0.1% BSA. The mast cell count was adjusted to 1–1.5×10⁶ cells/ml. Cell viability (>95%) was assessed by the trypan blue exclusion test.

Measurement of Histamine and β-Glucuronidase Release: The mast cell suspension was preincubated at 37 °C with DMSO or test compound for 3 min, and the release reaction was triggered by the addition of 10 μg/ml of compound 48/80. The reaction was stopped 15 min later by the addition of ice-cold Tyrode's solution and the mixture was centrifuged for 10 min at 1000 g. Histamine in the supernatant was determined by fluorescence spectrophotometry at 350/450 nm after condensation with *o*-phthaldialdehyde.¹³⁾ β-Glucuronidase activity in the supernatant was measured as described above. The release of histamine and β-glucuronidase was expressed as percentage release=[(release elicited by secretagogue-spontaneous release)/total content]×100. The total content was measured after treatment of cell suspensions with Triton X-100. Spontaneous release was less than 10%.

Acknowledgements This work was supported by a research grant from the National Science Council of the Republic of China (NSC86-2314-B-

039-001-M25).

References

- 1) Fwu S. Y., Chang C. Y., Huang L. J., Teng C. M., Wang J. P., Chen S. C., Kuo S. C., *Chin. Pharm. J.*, **51**, 255—169 (1999).
- 2) Lupi A., Monache F. D., Marini-Bettolo G. B., Barros Costa D. L., D'Albuquerque I. L., *Gazz. Chem. Ital.*, **10**, 9—12 (1979).
- 3) Farkas L., Gottsegen A., N6grádi M., *J. Chem. Soc., Perkin Trans. I*, **1974**, 305—312.
- 4) Lupi A., Marta M., Lintas G., Marini-Bettolo G. B., *Gazz. Chim. Ital.*, **110**, 625—628 (1980).
- 5) O'Brien J. R., *J. Clin. Pathol.*, **15**, 452—455 (1962).
- 6) Teng C. M., Chen W. Y., Ko W. C., Ouyang C., *Biochem. Biophys. Acta*, **924**, 375—382 (1987).
- 7) Wang J. P., Raung S. L., Kuo Y. H., Teng C. M., *Eur. J. Pharmacol.*, **288**, 341—348 (1995).
- 8) Barret A. P., "Lysosomes in A Laboratory Handbook," ed. by Dingle J. T., Elsevier, Amsterdam, 1972, pp. 118—120.
- 9) Absolom D. R., *Methods Enzymol.*, **132**, 95—179 (1986).
- 10) Cohen H. J., Chovaniec M. E., *J. Clin. Invest.*, **61**, 1081—1087 (1978).
- 11) Markert M., Andrews P. C., Babior B. M., *Methods Enzymol.*, **105**, 358—365 (1984).
- 12) Wang J. P., Hsu M. F., Ouyang C., Teng C. M., *Eur. J. Pharmacol.*, **161**, 143—149 (1989).
- 13) Håkanson R., R6nnberg A. L., *Anal. Biochem.*, **60**, 560—567 (1974).

Pyrinodemins B—D, Potent Cytotoxic *bis*-Pyridine Alkaloids from Marine Sponge *Amphimedon* sp.

Keiko HIRANO,^a Takaaki KUBOTA,^a Masashi TSUDA,^a Yuzuru MIKAMI,^b and Jun'ichi KOBAYASHI^{*,a}

Graduate School of Pharmaceutical Sciences, Hokkaido University,^a Sapporo 060–0812, Japan and Research Center for Pathogenic Fungi and Microbial Toxicoses, Chiba University,^b Chiba 260–8673, Japan.

Received January 5, 2000; accepted March 27, 2000

New *bis*-pyridine alkaloids, pyrinodemins B—D (1—3), have been isolated together with pyrinodemin A (4) and related 3-alkyl pyridine alkaloids 5—8 from the Okinawan marine sponge *Amphimedon* sp. and the structures were elucidated from spectroscopic data. Pyrinodemins B—D (1—3) showed potent cytotoxicity, while compounds 5—8 exhibited antimicrobial activity.

Key words sponge; *Amphimedon* sp.; *bis*-pyridine alkaloids; cytotoxicity; antimicrobial activity

A number of 3-alkyl pyridine alkaloids have been isolated from marine sponges of several genera.¹⁾ Almost of them possessed a long aliphatic chain with a various nitrogen-containing terminus,^{2–7)} and some had dimeric or polymeric structures of the 3-alkyl pyridine.^{8–11)} During our search for bioactive metabolites from Okinawan marine sponges,^{12,13)} we previously isolated cytotoxic pyridine alkaloids from sponges of the genera *Theonella*⁴⁾ and *Nyphates*.^{14–16)} More recently, potent cytotoxic *bis*-pyridine alkaloids with a unique *cis*-cyclopent[*c*]isoxazolidine moiety, pyrinodemins B—D (1—3), have been isolated together with pyrinodemin A¹⁷⁾ (4) and its related 3-alkyl pyridine alkaloids 5—8 from the Okinawan marine sponge *Amphimedon* sp. Here we describe the isolation and structure elucidation of 1—3 and 5—8, and potent cytotoxicity of 1—3 against tumor cell lines as well as antimicrobial activity of 5—8.

The sponge *Amphimedon* sp. (SS-955) was collected off Nakijin, Okinawa, and extracted with MeOH. EtOAc-soluble materials of the MeOH extract were subjected to silica gel columns (CHCl₃–MeOH and then hexane–EtOAc) followed by reversed-phase HPLC on 6-(phenyl)hexylsilyl (MeOH–H₂O or CH₃CN–H₂O) to afford pyrinodemins B (1, 0.00009%, wet weight), C (2, 0.00005%), and D (3, 0.00004%), and compounds 5 (0.0005%), 6 (0.0004%), 7 (0.0004%), and 8 (0.0003%), together with pyrinodemin A (4, 0.00011%).

High resolution (HR) FAB-MS data (m/z 562.4758 [$M+H$]⁺, Δ +2.2 mmu) of pyrinodemin B¹⁸⁾ (1) established the molecular formula, C₃₈H₅₉N₃O. ¹H- and ¹³C-NMR data indicated that 1 was an analogue of pyrinodemin A (4). The ¹³C-NMR spectrum revealed five *sp*² carbon signals [C-2 and C-2' δ_C 146.5 (2C, d); C-3 and C-3', δ_C 137.5 (2C, s); C-4 and C-4', δ_C 122.5 (2C, d); C-5 and C-5', δ_C 135.4 (2C, d); C-6 and C-6', δ_C 150.0 (2C, d)] due to two pyridine rings, *sp*³ carbon signals due to three methines (C-15, δ_C 77.2; C-16, δ_C 49.3; C-20, δ_C 72.2), one methylene (C-19', δ_C 57.3) at relatively lower field, and methylenes in a long alkyl chain (δ_C 26–34). Aromatic proton signals [H-2 and H-2', δ_H 8.42 (2H); H-4 and H-4', δ_H 7.48 (2H); H-5 and H-5', δ_H 7.19 (2H); H-6 and H-6', δ_H 8.44 (2H)] in the ¹H-NMR spectrum suggested the presence of two 3-alkyl-substituted pyridine rings. Proton and carbon chemical shifts of three methines at C-15 (δ_H 4.05; δ_C 77.2, d), C-16 (δ_H 2.83; δ_H 49.3, d), and C-20 (δ_H 3.46; δ_C 72.2, d) corresponded well to

those of 4, suggesting the presence of an isoxazolidine ring. The presence of a cyclopent[*c*]isoxazolidine moiety was deduced from the intense fragment ion peak at m/z 270 [(C₁₉H₂₈N)⁺] in the electron impact mass spectrum (EI-MS), which might be generated from 1 through Hoffmann-like elimination of the isoxazolidine ring.¹⁹⁾ Detailed analysis of the EI-MS fragmentation pattern (Fig. 1) suggested the presence of the two alkyl chains from C-7 to C-14 and from C-7' to C-19'. In the ¹H-NMR spectrum of 4, two olefin proton signals (H-16 and H-17) were observed at δ 5.34 (2H), while such olefin signals were not observed for 1. The *cis*-ring junction of the bicyclic system was deduced from the nuclear Overhauser effect spectroscopy (NOESY) correlation for H-16/H-20. NOESY correlations of H-15/H-16 and H-15/H-20 indicated that the relative stereochemistry of H-15 and H-16 was *cis*. Therefore the structure of pyrinodemin B was concluded to be 1.

Pyrinodemins C (2) and D (3) were revealed to have the molecular formulae, C₃₇H₅₇N₃O and C₃₆H₅₇N₃O, respectively, by the HR-FAB-MS data. The structures of 2 and 3 were elucidated to be analogues lacking one of CH₂ units from C-7' to C-16' in the alkyl side chain of pyrinodemin A (4) and from C-7' to C-19' in that of pyrinodemin B (1), respectively, by analyses of ¹H-NMR and EI-MS data. The position of the disubstituted olefin in 2 was assigned to C-15' on the basis of EI-MS fragment ions at m/z 190 [(C₁₄H₂₂N)⁺] and 217 [(C₁₆H₂₅N)⁺], and the *Z*-geometry of the olefin was implied by the chemical shifts of the allylic carbons (C-14' and C-17', δ_C ca. 27),²⁰⁾ which were deduced from HMQC cross-peaks.

Compound 5 was shown to have the molecular formula, C₁₉H₃₀N₂O, by HREIMS (m/z 302.2352 [M]⁺, Δ –0.6 mmu). The ¹H- and ¹³C-NMR spectra suggested that 5 was a monomer 3-alkyl pyridine alkaloid with a disubstituted double bond. In the ¹H- and ¹³C-NMR spectra, a pair of *sp*² methine signals [δ_H 6.71 (0.4H, t, H-20) and 7.43 (0.6H, t, H-20); δ_C 152.3 (0.6C, d, C-20) and 152.8 (0.4C, d, C-20)] were observed, corresponding to *E* and *Z*-type oximino groups.¹⁴⁾ The ratio of *E* and *Z*-forms was estimated to be 3 : 2 by the intensity of the imino proton signals. The EI-MS fragment ions at m/z 285 and 244 indicated the presence of an oxime terminus (Fig. 2). The position of the double bond was determined to be C-9–C-10 by ¹H–¹H correlation spectroscopy (COSY) cross-peaks for H₂-7/H₂-8 and H₂-8/H-9

* To whom correspondence should be addressed. e-mail: jkobay@pharm.hokudai.ac.jp

and EI-MS fragment ion peaks at m/z 106 and 132. The *Z*-geometry of the double bond was deduced from the ^{13}C chemical shifts for the allylic methylene carbons (C-8, δ_{C} 28.8; C-11, δ_{C} 27.1).²⁰⁾ Thus compound **5** was assigned as a 3-alkyl (C₁₄) pyridine with *E* and *Z*-forms (3 : 2) at the oxime terminus.

The molecular formula, C₁₉H₃₀N₂O, of compound **6** was established by HR-EI-MS (m/z 302.2362 [M]⁺, Δ +0.4 mmu). ¹H-NMR data revealed a 3-alkyl pyridine moiety, a disubstituted olefin, and an oxime terminus consisting of a 3:2 mixture of *E*- and *Z*-forms. The position of the olefin was inferred as C-15–C-16 by EI-MS fragment ion peaks at m/z 190 and 216 (Fig. 2). This was also supported by EI-MS fragment ions at m/z 190, 205, and 220 observed for the re-

duction product (**9**) of **6** with D₂. The carbon chemical shifts of C-14 and C-17 (δ_{C} 29.2 and 30.5, respectively) of **6** were indicative of 15*Z*-geometry.²⁰⁾ Thus compound **6** was elucidated to be a $\Delta^{15(16)}$ analogue of **5**.

Compounds **7** and **8** were revealed to possess the molecular formulae, C₁₈H₃₀N₂O and C₁₇H₂₈N₂O, respectively, by

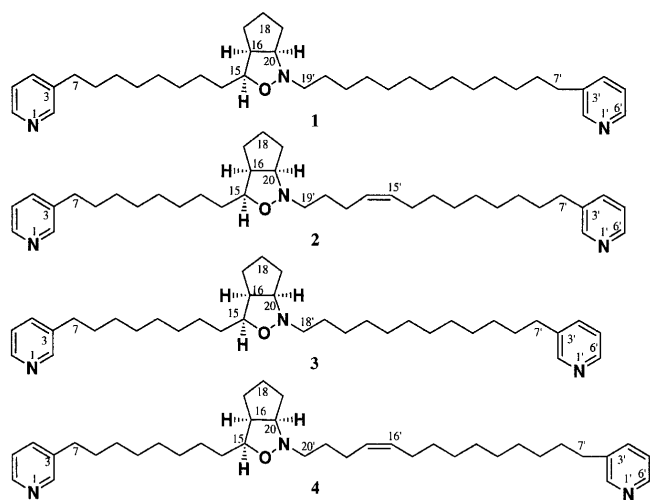


Chart 1. Structures of 1–4

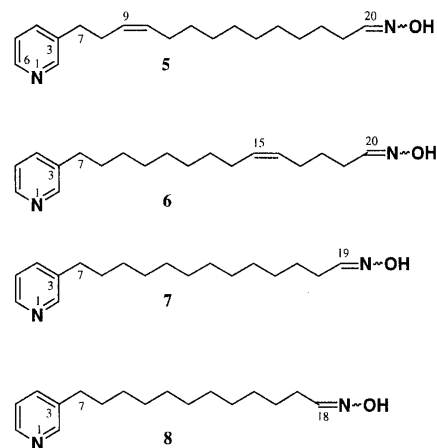


Chart 2. Structures of 5–8

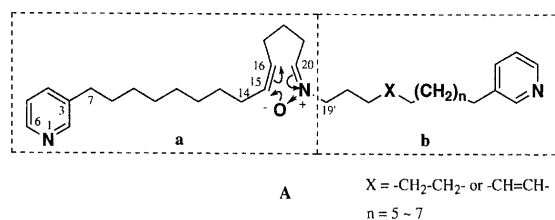


Chart 3. Structure of A

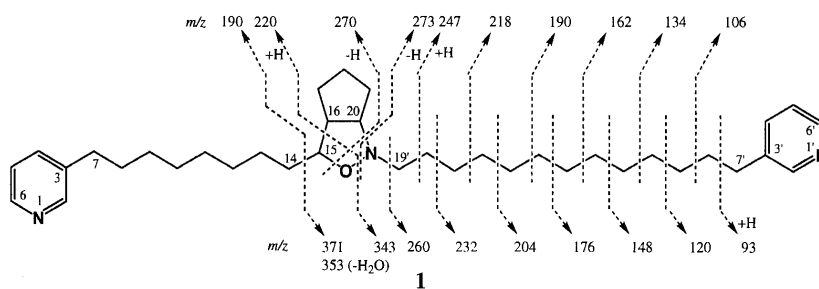


Fig. 1. Fragmentation Pattern of Pyrindemin B (**1**) in EI-MS (Parent Ion; m/z 561 [M]⁺)

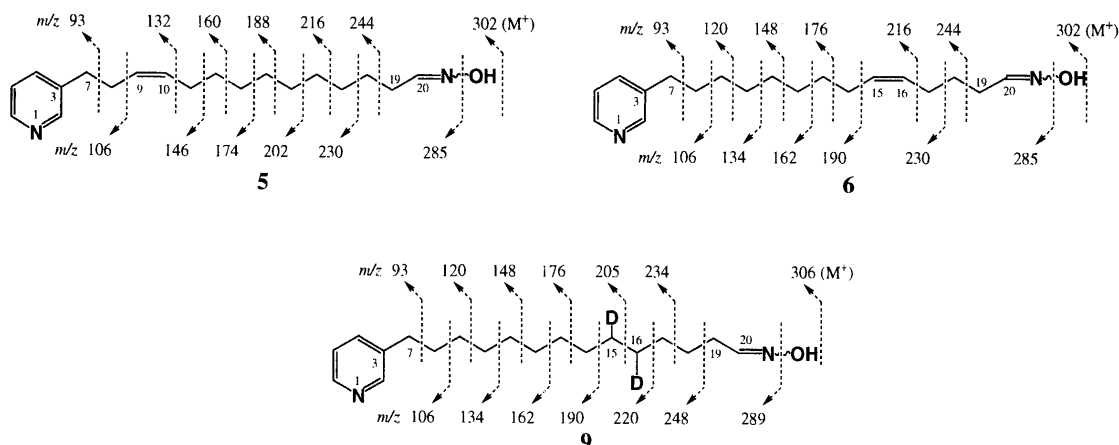


Fig. 2. Fragmentation Patterns of Compounds **5** and **6** and Reduction Product (**9**) of **6** in EI-MS

Table 1. Antimicrobial Activity of Pyrinodemin A (4) and Compounds 5–8

Test organisms	MIC ($\mu\text{g/ml}$)				
	4	5	6	7	8
<i>Candida albicans</i> ATCC 90028	>33	>33	16	16	33
<i>Cryptococcus neoformans</i> ATCC 900112	33	33	16	16	16
<i>Aspergillus niger</i> ATCC 40406	33	>33	8	4	8
<i>Paecilomyces variotii</i> YM-1	33	33	16	16	16
<i>Trichophyton mentagrophytes</i> ATCC 40769	>33	>33	>33	>33	16
<i>Staphylococcus aureus</i> 209P	>33	8	4	2	16
<i>Micrococcus luteus</i> IFM 2066	>33	16	16	8	16
<i>Bacillus subtilis</i> PCI 189	>33	33	>33	8	16
<i>Corynebacterium xerosis</i> IFM 2057	>33	33	4	4	8
<i>Escherichia coli</i> NIH JC2	>33	>33	>33	>33	>33

Mueller Hinton broth and Sabouraud dextrose broth were used for bacteria and fungi, respectively.

HR-EI-MS. ^1H -NMR data of **7** and **8** indicated that both have a 3-alkyl pyridine moiety and an oxime terminus consisting of a 3 : 2 mixture of *E*- and *Z*-forms. The ^1H -NMR spectra of compounds **7** and **8** showed that both had no internal double bond. Analyses of EI-MS fragmentation patterns of **7** and **8** implied the presence of the saturated linear C_{12} and C_{11} alkyl chains, respectively, between the pyridine ring and the oxime group. Compounds **7** and **8** were thus identified as saturated analogues of compound **5** (or **6**), respectively.

Pyrinodemins B–D (**1**–**3**) are unique *bis*-3-alkylpyridine alkaloids with a *cis*-cyclopent[*c*]isoxazolidine moiety like pyrinodemin A (**17**) (**4**). Biosynthetically, the cyclopent[*c*]isoxazolidine moiety in pyrinodemins may be generated from a linear *bis*-pyridine such as A through 1,3-dipolar cycloaddition. Furthermore, the structure of unit **a** in A corresponds to that of compound **6**, while the structure of unit **b** in A corresponds to that of **6**–**8**, or their homologues without the N–OH unit. Pyrinodemins B–D (**1**–**3**) exhibited potent cytotoxicity against murine leukemia L1210 (IC_{50} , 0.07, 0.06, and 0.08 $\mu\text{g/ml}$, respectively) and KB epidermoid carcinoma cells (IC_{50} , 0.5 $\mu\text{g/ml}$, each) *in vitro*, comparable to pyrinodemin A (**17**) (**4**), whereas compounds **5**–**8** did not show cytotoxicity (IC_{50} > 10 $\mu\text{g/ml}$). On the other hand, compounds **5**–**8** exhibited antimicrobial activity against some fungi and Gram-positive bacteria (Table 1), and pyrinodemin A (**4**) showed relatively weak antifungal activity.

Experimental

IR and UV spectra were recorded on JASCO FT/IR-5300 and JASCO Ubest-35 spectrophotometers, respectively. ^1H - and ^{13}C -NMR spectra were recorded on Bruker AMX-600 and ARX-500 spectrometers, respectively. EI-MS were obtained on a JEOL DX-303 spectrometer at 70 eV, and positive ion FAB-MS were measured on a JEOL HX-110 spectrometer using glycerol as a matrix.

Extraction and Isolation The sponge *Amphimedon* sp. (1.0 kg, wet weight) collected off Okinawa Island was extracted with MeOH (11 \times 2). The methanolic extract (71 g) was partitioned between EtOAc (400 ml \times 3) and 1 M NaCl solution. Parts (1.5 g) of the EtOAc soluble materials (5.11 g) were subjected to a silica gel column (CHCl_3 –MeOH, 100 : 0 \rightarrow 95 : 5). The fraction eluting with 98% CHCl_3 –MeOH was subjected to silica gel column chromatography (hexane–EtOAc, 1 : 2) and reversed-phase HPLC (Luna Phenyl-hexyl, 5 μm , Phenomenex[®], 4.6 \times 250 mm; eluent: MeOH– H_2O , 91 : 9; flow rate: 1 ml/min; UV detection at 264 nm) to afford pyrinodemins B (**1**, 0.00009%, wet weight, t_R 28 min), C (**2**, 0.00005%, t_R 26 min), and D (**3**, 0.00004%, t_R 24 min) together with pyrinodemin A (**4**, 0.00011%, t_R 31 min). The fraction eluting with 95% CHCl_3 –MeOH was separated on a silica gel column (hexane–EtOAc, 1 : 1) and then reversed-phase HPLC (Luna Phenyl-hexyl; eluent: CH_3CN – H_2O , 45 : 55; flow rate: 1 ml/min; UV detection at 264 nm) to yield compounds **5** (0.0005%, t_R 42 min), **6**

(0.0004%, t_R 38 min), **7** (0.0004%, t_R 35 min), and **8** (0.0003%, t_R 28 min).

Pyrinodemin B (1): UV λ_{max} (MeOH) nm (ϵ): 264 (6000). IR (neat) cm^{-1} : 1575. ^1H -NMR (CDCl_3) δ : 1.2–1.3 (24H), 1.33 (4H, m, H_{2-9} and $\text{H}_{2-9'}$), 1.40 (1H, m, H-17), 1.42 (1H, m, H-18), 1.44 (1H, m, H-14), 1.50 (2H, m, $\text{H}_{2-18'}$), 1.55 (1H, m, H-14), 1.60 (4H, m, H_{2-8} and $\text{H}_{2-8'}$), 1.64 (1H, m, H-17), 1.65 (1H, m, H-19), 1.66 (1H, m, H-18), 1.76 (1H, m, H-19), 2.59 (1H, m, H-19'), 2.60 (4H, t, $J=7.6$ Hz, H_{2-7} and $\text{H}_{2-7'}$), 2.83 (1H, m, H-16), 2.84 (1H, m, H-19'), 3.46 (1H, m, H-20), 4.05 (1H, m, H-15), 7.19 (2H, brt, $J=7.0$ Hz, H-5 and H-5'), 7.48 (2H, d, $J=7.5$ Hz, H-4 and H-4'), 8.42 (2H, brs, H-2 and H-2'), 8.44 (2H, m, H-6 and H-6'). ^{13}C -NMR (CDCl_3) δ : 26.3 (t), 26.5 (t), 27.9 (t), 28.9 (2C, t), 29.2 (2C, t), 29.4–29.8 (12C, t), 31.2 (2C, t), 33.0 (2C, t), 33.6 (t), 49.3 (d), 57.3 (t), 72.2 (d), 77.2 (d), 122.5 (2C, d), 135.4 (2C, d), 137.5 (2C, s), 146.5 (2C, d), 150.0 (2C, d). FAB-MS m/z : 562 [$\text{M}+\text{H}$]⁺. HR-FAB-MS m/z : 562.4758 (Calcd for $\text{C}_{37}\text{H}_{60}\text{N}_3\text{O}$ [$\text{M}+\text{H}$]⁺: 562.4736).

Pyrinodemin C (2): UV λ_{max} (MeOH) nm (ϵ): 263 (5800). IR (neat) cm^{-1} : 1575. ^1H -NMR (CDCl_3) δ : 1.2–1.3 (16H), 1.33 (4H, m), 1.40 (1H, m), 1.42 (1H, m), 1.44 (1H, m), 1.55 (1H, m), 1.58 (2H, m), 1.60 (4H, m), 1.64 (1H, m), 1.65 (1H, m), 1.66 (1H, m), 1.76 (1H, m), 2.03 (4H, m), 2.59 (1H, m), 2.60 (4H, t, $J=7.6$ Hz), 2.82 (1H, m), 2.84 (1H, m), 3.46 (1H, m), 4.05 (1H, m), 5.34 (2H, m), 7.19 (2H, brt, $J=7.0$ Hz), 7.48 (2H, d, $J=7.5$ Hz), 8.42 (2H, brs), 8.44 (2H, m). EI-MS m/z (rel. int. %): 93 (100), 106 (98), 120 (11), 134 (7), 148 (8), 162 (12), 176 (18), 190 (8), 217 (5), 220 (26), 230 (4), 270 (5), 271 (18), 301 (9), 315 (5), 339 (2), 351 (36), 369 (5), 541 (2), 559 ([M]⁺, 2). FAB-MS m/z : 560 [$\text{M}+\text{H}$]⁺. HR-FAB-MS m/z : 560.4558 (Calcd for $\text{C}_{37}\text{H}_{58}\text{N}_3\text{O}$ [$\text{M}+\text{H}$]⁺: 560.4579).

Pyrinodemin D (3): UV λ_{max} (MeOH) nm (ϵ): 264 (6200). IR (neat) cm^{-1} : 1575. ^1H -NMR (CDCl_3) δ : 1.2–1.3 (22H), 1.33 (4H, m), 1.40 (1H, m), 1.42 (1H, m), 1.44 (1H, m), 1.50 (2H, m), 1.55 (1H, m), 1.60 (4H, m), 1.64 (1H, m), 1.65 (1H, m), 1.66 (1H, m), 1.76 (1H, m), 2.59 (1H, m), 2.60 (4H, t, $J=7.6$ Hz), 2.83 (1H, m), 2.84 (1H, m), 3.46 (1H, m), 4.05 (1H, m), 7.19 (2H, brt, $J=7.0$ Hz), 7.48 (2H, d, $J=7.5$ Hz), 8.42 (2H, brs), 8.44 (2H, m). EI-MS m/z (rel. int. %): 93 (100), 106 (93), 120 (11), 134 (7), 148 (8), 162 (12), 176 (18), 190 (10), 204 (6), 218 (12), 220 (26), 233 (8), 259 (20), 270 (4), 301 (10), 315 (6), 329 (4), 339 (43), 357 (3), 529 (2), 547 ([M]⁺, 1). FAB-MS m/z : 548 [$\text{M}+\text{H}$]⁺. HR-FAB-MS m/z : 548.4559 (Calcd for $\text{C}_{36}\text{H}_{58}\text{N}_3\text{O}$ [$\text{M}+\text{H}$]⁺: 548.4580).

Compound 5: UV λ_{max} (MeOH) nm (ϵ): 264 (3300). IR (neat) cm^{-1} : 3200, 2925, 1575. ^1H -NMR (CDCl_3) δ : 1.2–1.3 (12H), 1.45 (2H, m, H_{2-18}), 1.92 (2H, m, H_{2-11}), 2.19 (1.2H, m, H_{2-19}), 2.36 (2.8H, m, H_{2-8} and H_{2-19}), 2.66 (2H, t, $J=7.6$ Hz, H_{2-7}), 5.37 (2H, m, H-9 and H-10), 6.71 (0.4H, t, $J=5.1$ Hz, H-20), 7.21 (1H, t, $J=5.6$ Hz, H-5), 7.43 (0.6H, t, $J=6.0$ Hz, H-20), 7.49 (1H, d, $J=5.6$ Hz, H-4), 8.47 (2H, m, H-2 and H-6). ^{13}C -NMR (CDCl_3) δ : 24.4 (0.4C, t, C-19), 27.1 (t, C-11), 28.8 (t, C-8), 28.9 (t), 29.1 (0.6C, t, C-19), 29.4–29.8 (5C, t), 33.1 (t, C-7), 123.2 (d, C-5), 127.7 (d, C-9), 131.5 (d, C-10), 136.1 (d, C-4), 137.5 (s, C-3), 147.2 (d, C-2), 149.9 (d, C-6), 152.3 (0.6C, d, C-20), 152.8 (0.4C, d, C-20). HR-EI-MS m/z : 302.2352 (Calcd for $\text{C}_{19}\text{H}_{30}\text{N}_2\text{O}$ [M]⁺: 302.2358).

Compound 6: UV λ_{max} (MeOH) nm (ϵ): 264 (3200). IR (neat) cm^{-1} : 3200, 2925, 1575. ^1H -NMR (CDCl_3) δ : 1.2–1.3 (10H), 1.45 (2H, m), 1.55 (2H, m), 2.02 (2H, m), 2.10 (2H, m), 2.19 (1.2H, m), 2.38 (0.8H, m), 2.65 (2H, t, $J=7.6$ Hz), 5.37 (1H, m), 5.40 (1H, m), 6.71 (0.4H, t, $J=5.1$ Hz), 7.21 (1H, t, $J=5.6$ Hz), 7.43 (0.6H, t, $J=6.0$ Hz), 7.49 (1H, d, $J=5.6$ Hz), 8.47 (2H, m). HR-EI-MS m/z : 302.2362 (Calcd for $\text{C}_{19}\text{H}_{30}\text{N}_2\text{O}$ [M]⁺: 302.2358).

Compound 7: UV λ_{\max} (MeOH) nm (ϵ): 264 (3100). IR (neat) cm^{-1} : 3200, 2925, 1575. $^1\text{H-NMR}$ (CDCl_3) δ : 1.2—1.3 (16H), 1.45 (2H, m), 1.55 (2H, m), 2.19 (1.2H, m), 2.38 (0.8H, m), 2.65 (2H, t, $J=7.6$ Hz), 6.71 (0.4H, t, $J=5.1$ Hz), 7.21 (1H, t, $J=5.6$ Hz), 7.43 (0.6H, t, $J=6.0$ Hz), 7.49 (1H, d, $J=5.6$ Hz), 8.47 (2H, m). EI-MS m/z (rel. int. %): 93 (100), 106 (93), 120 (28), 134 (12), 148 (18), 162 (29), 176 (33), 190 (16), 204 (22), 218 (24), 232 (78), 273 (9), 290 ($[\text{M}]^+$, 4). HR-EI-MS m/z : 290.2337 (Calcd for $\text{C}_{18}\text{H}_{30}\text{N}_2\text{O}$ $[\text{M}]^+$: 290.2358).

Compound 8: UV λ_{\max} (MeOH) nm (ϵ): 264 (3200). IR (neat) cm^{-1} : 3200, 2925, 1575. $^1\text{H-NMR}$ (CDCl_3) δ : 1.2—1.3 (14H), 1.45 (2H, m), 1.55 (2H, m), 2.19 (1.2H, m, H_2-17), 2.38 (0.8H, m), 2.65 (2H, t, $J=7.6$ Hz), 6.71 (0.4H, t, $J=5.1$ Hz), 7.21 (1H, t, $J=5.6$ Hz), 7.43 (0.6H, t, $J=6.0$ Hz), 7.49 (1H, d, $J=5.6$ Hz), 8.47 (2H, m). EI-MS m/z (rel. int. %): 93 (100), 106 (86), 120 (20), 134 (9), 148 (14), 162 (13), 176 (16), 190 (10), 204 (18), 218 (74), 259 (4), 276 ($[\text{M}]^+$, 2). HR-EI-MS m/z : 276.2185 (Calcd for $\text{C}_{17}\text{H}_{28}\text{N}_2\text{O}$ $[\text{M}]^+$: 276.2202).

Reduction of Compound 6 To a solution of compound 6 (0.1 mg) in MeOH-d_4 (70 μl) was added 5% palladium on activated carbon (10 μg), and the mixture was stirred at room temperature for 1 h under a deuterium atmosphere. After filtration of the catalyst, the filtrate was evaporated *in vacuo* to afford compound 9 (0.08 mg): HR-EI-MS m/z : 306.2630 (Calcd for $\text{C}_{19}\text{H}_{30}\text{D}_2\text{N}_2\text{O}$ $[\text{M}]^+$: 306.2638).

Acknowledgments We thank Mr. Z. Nagahama for his help with sponge collection and Dr. J. Fromont, Western Australian Museum, for identification of the sponge. This work was partly supported by a Grant-in-Aid for Scientific Research from the Ministry of Education, Science, Sports, and Culture of Japan.

References and Notes

- 1) Faulkner D. J., *Nat. Prod. Rep.*, **16**, 155—198 (1999) and previous reviews cited therein.
- 2) Quiñoa E., Crews P., *Tetrahedron Lett.*, **28**, 2467—2468 (1987).
- 3) Sakemi S., Totton L. E., Sun H. H., *J. Nat. Prod.*, **53**, 995—999 (1990).
- 4) Stierle D. B., Faulkner D. J., *J. Nat. Prod.*, **54**, 1134—1136 (1991).
- 5) Wang G.-Y.-S., Kuramoto M., Uemura D., *Tetrahedron Lett.*, **37**, 1813—1816 (1996).
- 6) Carroll A. R., Scheuer P. J., *Tetrahedron*, **46**, 6637—6644 (1990).
- 7) Matsunaga S., Shinoda K., Fusetani N., *Tetrahedron Lett.*, **34**, 5953—5954 (1993).
- 8) Schmitz F. J., Hollenbeak K. H., Campbell D. C., *J. Org. Chem.*, **43**, 3913—3922 (1978).
- 9) Fusetani N., Yasumuro K., Matsunaga S., Hirota H., *Tetrahedron Lett.*, **30**, 6891—6894 (1989).
- 10) Talpia R., Rudi A., Ilan M., Kashman Y., *Tetrahedron Lett.*, **33**, 3033—3034 (1992).
- 11) Davies-Coleman M. T., Faulkner D. J., Dubowchik G. M., Roth G. P., Polson C., Fairchild C., *J. Org. Chem.*, **58**, 5925—5930 (1993).
- 12) Tsuda M., Uemoto H., Kobayashi J., *Tetrahedron Lett.*, **40**, 5709—5712 (1999).
- 13) Tsuda M., Shimbo K., Kubota T., Mikami Y., Kobayashi J., *Tetrahedron*, **55**, 10305—10314 (1999).
- 14) Kobayashi J., Murayama T., Ohizumi Y., Sasaki T., Ohta T., Nozoe S., *Tetrahedron Lett.*, **30**, 4833—4836 (1989).
- 15) Kobayashi J., Murayama T., Kosuge S., Kanda F., Ishibashi M., Kobayashi H., Ohizumi Y., Ohta T., Nozoe S., Sasaki T., *J. Chem. Soc., Perkin Trans. 1*, **1990**, 3301—3303.
- 16) Kobayashi J., Zeng C.-M., Ishibashi M., Shigemori H., Sasaki T., Mikami Y., *J. Chem. Soc., Perkin Trans. 1*, **1992**, 1291—1294.
- 17) Tsuda M., Hirano K., Kubota T., Kobayashi J., *Tetrahedron Lett.*, **40**, 4819—4820 (1999).
- 18) The small amounts of 1—3 obtained from this sponge prevented measurement of their specific rotations.
- 19) Liguori A., Sindona G., Uccella N., *Tetrahedron*, **40**, 1901—1906 (1984).
- 20) Breitmaier E., Voelter W., "Carbon-13 NMR Spectroscopy," VCH Publishers, Weinheim, 1990, p. 192.

Studies on Adsorption Characteristics of Bile Acids and Methotrexate to a New Type of Anion-Exchange Resin, Colestimide

Yoshiteru HONDA and Masahiro NAKANO*

Department of Pharmacy, Kumamoto University Hospital, 1-1-1 Honjo, Kumamoto 860-8556, Japan.

Received January 5, 2000; accepted March 27, 2000

The adsorption characteristics of various bile acids and methotrexate to a new type of anion-exchange resin, colestimide, were studied *in vitro* and compared with those to cholestyramine. For bile acids, colestimide was shown to have a higher capacity than cholestyramine. For example, approximately 1.4-fold higher for cholic acid and 2.0-fold for deoxycholic acid in water. In the presence of physiological anions, the degree of adsorption of cholic acid to both resins was greatly reduced, whereas adsorption of deoxycholic acid was only slightly reduced. Furthermore, the bed-volume of colestimide swelled about 6.8-fold in water, hence the anion-exchange groups of this resin are expected to be able to function effectively in adsorption of bile acids in the gut. In addition, colestimide was found to have high adsorption capacity for methotrexate, not only in water but also in media containing various physiological anions, and thus it is suggested that colestimide is a potential oral antidote to reduce possible toxicity by methotrexate through interruption of enterohepatic circulation.

Key words colestimide; anion-exchange resin; methotrexate; bile acid adsorption; methotrexate adsorption; methotrexate toxicity

Anion-exchange resins, a representative of which is cholestyramine, have been studied extensively and have been proven to be most effective in reducing cholesterol levels in patients with hypercholesterolemia.^{1,2)} It is also well known that these resins have rather low *in vivo* adsorption efficacy, in spite of high bile acid binding capacity *in vitro*.³⁾ This low *in vivo* adsorption appears to be due largely to poor dispersion of the resins in the intestine because of their insolubility in water and inaccessibility of bile acids to binding sites on the resins on account of their bulky steroid nucleus, and thus large doses (8–12 g/d) of these resins are required in order to produce hypolipidemic effects. Accordingly, clinical use of the conventional anion-exchange resins is limited, particularly in Japan, because of poor patient compliance. If a more potent resin can be developed, effective lowering of serum cholesterol levels may be achieved with a smaller dose and adverse effects such as constipation, nausea and meteorism associated with the resin may be less likely to occur.

Colestimide is a new type of anion-exchange resin with an imidazolium salt on an epoxide polymer skeleton that exhibits clinical pharmacological effects similar to those of cholestyramine at approximately a quarter (one-sixth on the basis of preparation) of the dose of cholestyramine⁴⁾ and thus may be expected to be useful as a bile acid sequestrant. However, little is known about the sorption characteristics of the resin. The present communication describes the results of an *in vitro* study on the sorption characteristics of colestimide for bile acids under various conditions.

From the standpoint of development of further applications other than hypercholesterolemia, the adsorption behavior of colestimide for methotrexate (MTX), an antifolate antineoplastic agent, was also examined. MTX is an anionic drug with two carboxyl groups in the structure and its molecular weight is similar to the bile acids. Additionally, it is known that the enterohepatic circulation plays an important role in the pharmacokinetics of the drug,⁵⁾ and that cholestyramine can accelerate excretion of the drug in patients suffering from MTX toxicity associated with high-dose MTX therapy and/or renal insufficiency, through binding of

MTX in the gut and interruption of the enterohepatic circulation of the drug.^{6,7)} Similarly with colestimide, the potential for application to modulating adverse reactions of MTX is suggested.

Experimental

Materials Colestimide is a new type of anion-exchange resin, and was a generous gift from Mitsubishi Chemical Co., Tokyo, Japan. Cholestyramine resin was purchased from Sigma Chemical Co., St. Louis, Missouri. The bile acids cholate, taurocholate, glycocholate, deoxycholate, chenodeoxycholate, ursodeoxycholate and glycodeoxycholate were kindly supplied as sodium salts by Mitsubishi Tokyo Pharmaceutical Co., Tokyo. Total Bile Acids-Test Wako for bile acid measurement was purchased from Wako Pure Chemical Industries, Osaka, Japan. Methotrexate was kindly supplied through Japan Wyeth Lederle Co., Tokyo, Japan. All other chemicals used were of the highest purity commercially available.

***In Vitro* Adsorption Studies** Adsorption studies were carried out at 37°C by batch methods.⁸⁾ Accurately weighed amounts (5–10 mg) of colestimide or cholestyramine resin were placed in 50-ml screw-capped polypropylene test-tubes. Bile acid solutions of known concentrations (10 ml) were added to each of the test-tubes and the tubes were mechanically shaken for 30 min at 37°C. Since adsorption equilibrium to both resins was rapidly established within several minutes of incubation (results not shown), it was decided that a 30 min incubation time would guarantee adsorption equilibrium. After equilibration, the contents of each tube were filtered through a membrane filter (Millex-HA, 0.45 µm), appropriately diluted, and assayed for the concentration of unadsorbed (*i.e.*, free) bile acids by means of the enzymatic color-comparative method with 3α-hydroxysteroid dehydrogenase. The amount of bile acid adsorbed was calculated as the difference between the total amount of bile acid introduced into the system and the amount of unadsorbed bile acid. The maximum binding capacities of the resins were calculated according to the Langmuir adsorption equation.⁸⁾ In the methotrexate adsorption test, incubation was similar to that for bile acids, with the exception of the determination method, *i.e.*, spectrophotometric analysis at 370 nm. Water, saline, 2nd fluid of JPXIII Disintegration Test and 0.05 M bicarbonate buffer containing 0.15 M NaCl were used as the incubation media. Absorbance was determined using a Shimadzu model UV-240 double beam spectrophotometer.

Swelling Test Swelling of the resins in water was examined. One gram of each resin was placed in a 50-ml measuring cylinder and an appropriate amount of water was added. The changes of the bed-volume of the resin were measured at predetermined times.

Results and Discussion

Adsorption of Bile Acids Figure 1 presents the adsorp-

* To whom correspondence should be addressed. e-mail: nakano@kaiju.medic.kumamoto-u.ac.jp

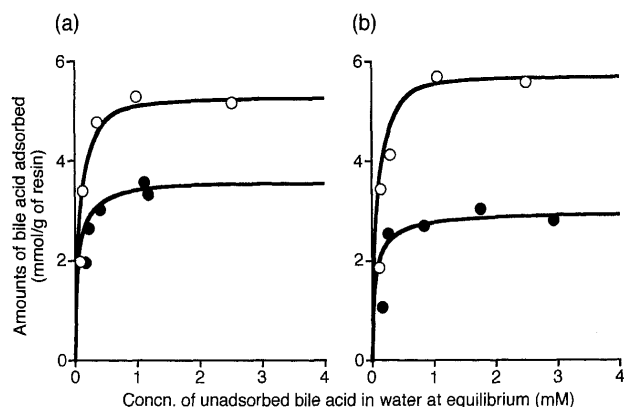


Fig. 1. Adsorption Isotherms for Binding of (a) Cholate and (b) Deoxycholate to Colestimide and Cholestyramine in Water at 37 °C

○, colestimide; ●, cholestyramine.

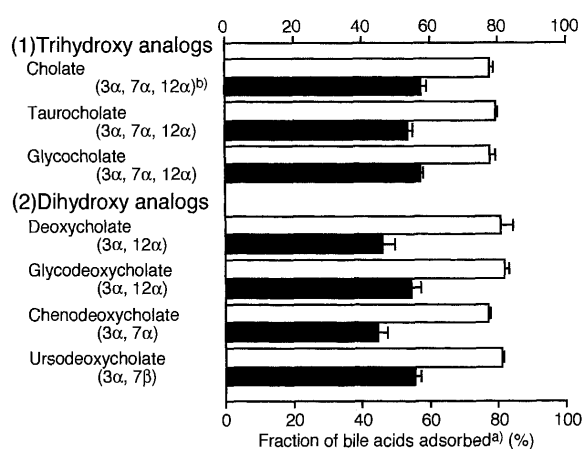


Fig. 2. Comparison of Bile Acid Adsorptive Powers of Colestimide and Cholestyramine in Water at 37 °C

a) The percent adsorbed was determined for 5 mg of either resin equilibrated with 10 ml of 3 mM of each bile acid. Each value represents the mean \pm S.E. of three determinations. b) The position and orientation of hydroxyl groups are shown in parentheses. □, colestimide; ■, cholestyramine.

tion isotherms for the binding of two representative bile acids in water at 37 °C. For both bile acids; cholate, a representative of bile acids which possess three hydroxyl groups, and deoxycholate, a dihydroxy analog, colestimide displayed greater adsorptive power than cholestyramine. The maximum binding capacities of colestimide for cholate and deoxycholate calculated according to the Langmuir equation were 5.38 and 5.86 mmol/g, and those of cholestyramine were 3.83 and 2.92 mmol/g, respectively. Thus, the adsorptive power of colestimide was shown to be approximately 1.4 times greater for cholic acid, and 2.0 times greater for deoxycholic acid than cholestyramine.

Adsorption behavior of the resins for a selected series of bile acids, under the following conditions, 10 ml of 3 mM bile salts solution; 5 mg resin, are also shown in Fig. 2. It was found that the rate of uptake of bile salts from solutions by colestimide is generally larger than that with cholestyramine, and is especially pronounced for dihydroxy analogs. With colestimide, there was no significant difference between unconjugated bile salt anions and their corresponding amino acid conjugates, *i.e.*, among the cholates or deoxycholates; cholate, taurocholate and glycocholate, deoxycholate, glycodeoxycholate, chenodeoxycholate and ursodeoxycholate.

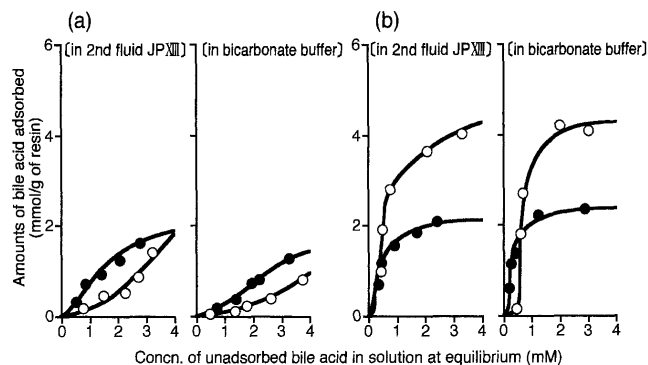


Fig. 3. Effects of Media on the Adsorption of (a) Cholate and (b) Deoxycholate to Colestimide and Cholestyramine at 37 °C

○, colestimide; ●, cholestyramine.

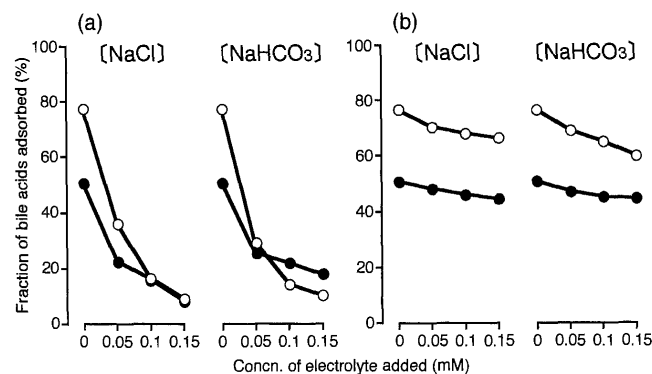


Fig. 4. Effects of Sodium Chloride and Sodium Bicarbonate on the Adsorption of (a) Cholate and (b) Deoxycholate to Colestimide and Cholestyramine in Water at 37 °C

The percent adsorbed was determined for 5 mg of either resin equilibrated with 10 ml of 3 mM of each bile acid.

Since the primary mechanism of the interaction between bile acids and anion-exchange resins is most probably electrostatic in nature (*i.e.*, between the negatively charged carboxyl groups of the bile salt anions and the positively charged anion-exchange groups on the resin),⁹ bile acid adsorption seems to be readily influenced by the various anions in the gut. Figure 3 presents the adsorption isotherms of the resins in solutions containing various electrolytes. All isotherms showed sigmoidal curves and thus no attempt was made to calculate the maximum binding capacities. Using the 2nd fluid of JPXIII and bicarbonate buffer, which are similar to physiological conditions in the gut,¹⁰ the adsorption capacity of both resins for cholate was dramatically reduced in contrast to that in water. However, the reduction in the capacity of both resins for deoxycholic acid was not as great and colestimide exhibited nearly twice as high a capacity as that of cholestyramine, similar to the case when water was used as a medium.

In view of the possible influence of other anions on the adsorptive powers of the resins for bile acids, two physiological anions were introduced separately into the adsorption system. The effects of sodium chloride and sodium bicarbonate were investigated in the adsorption of cholate and deoxycholate in water (Fig. 4). As expected from the preceding results, the binding of cholate to both resins decreased markedly with increasing concentration of electrolyte. The observed reduction can best be attributed to the existence of

a competition between the chloride or bicarbonate anion and the bile salt anion for the available binding sites on the resin particle. However, in the case of deoxycholate, the resin capacities were not reduced much by the addition of inorganic salts. These findings indicate the importance of hydrophobicity of the bile salt anions in the adsorption to anion-exchange resins, and suggests that the sequestration of bile salts by the resin in the gut is greater for dihydroxy bile acids and negligible for trihydroxy analogs. Therefore, the serum cholesterol-lowering effects of anion-exchange resins are proposed to be based on the preferential adsorption of dihydroxy bile acids, which are the main components of bile acids in the gut.

The results of these adsorption experiments indicate that colestimide exhibited superior binding activities towards bile acids compared to cholestyramine. One of the reasons for the superiority of colestimide seems to be that the ion exchange capacity per gram of colestimide is 1.6 times higher than that of cholestyramine, *i.e.*, the former is 4.9 mEq/g and the latter is 3.0 mEq/g.⁴⁾ It has been demonstrated that the forces involved in the bile salt anion-cholestyramine interaction are primarily electrostatic in nature and are reinforced by an additional nonelectrostatic interaction of the steroid nucleus of bile acids with the hydrophobic portion of the resin, and the strength of the latter force is dependent on the degree of hydrophobicity of the adsorbate molecule.⁹⁾ From our observation that addition of electrolytes to the test system led to a marked reduction in binding for trihydroxy bile acids, but little reduction for dihydroxy analogs, this secondary hydrophobic binding force appears to contribute greatly to the adsorption of dihydroxy bile acids, but not for trihydroxy analogs. Furthermore, the contribution of this nonelectrostatic force to binding of bile salt anions is proposed to be much greater with colestimide compared with cholestyramine.

The phenomenon of a larger difference in adsorption capacity between colestimide and cholestyramine with the more hydrophobic dihydroxy bile salts than with the more polar trihydroxy derivatives, may be explained to some degree by the above-mentioned secondary interaction. Because the additional 7 α -hydroxyl group causes increased polarization of the cyclopentanophenanthrene ring system and increased steric hindrance of accessibility to binding sites in the resin matrix, dihydroxy derivatives are expected to be more readily adsorbed to the resin. Especially in the case of colestimide, steric hindrance due to the hydroxyl group on the bulky steroid ring seems to be a serious limiting factor for adsorption of bile salts, since it possesses many hydroxyl groups in its polymer matrix. Accordingly, it appears that the ratio of the adsorptive capacity for deoxycholate for colestimide and cholestyramine is larger than, and the ratio for cholate is smaller than, the ratio of ion exchange capacity between the resins.

Swelling in Water Since each bile acid consists of a bulky hydrophobic steroid nucleus and an ionic group, the extent of adsorption of bile acids to resins is considered to be greatly dependent on the accessibility of the anionic sites on the bile salts to the anion-exchange sites of the resins.¹¹⁾ Previously, we reported that the introduction of a spacer arm between the polymer backbone and a functional group makes binding sites readily accessible to the functional group, and thereby leads to improvement in the *in vivo* adsorptive efficiency of the resin.¹²⁾ Thus, it appears that the swelling prop-

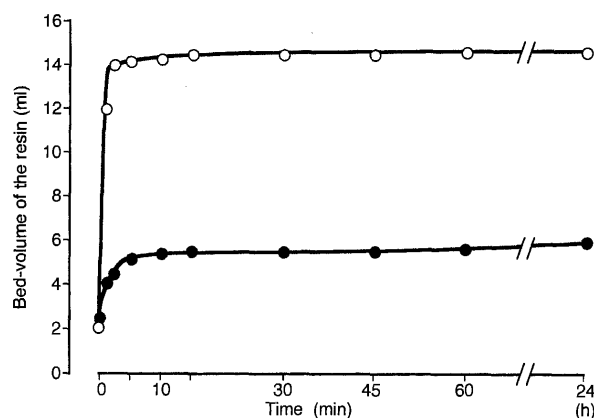


Fig. 5. Swelling Patterns of Colestimide and Cholestyramine in Water at 37°C

○, colestimide; ●, cholestyramine.

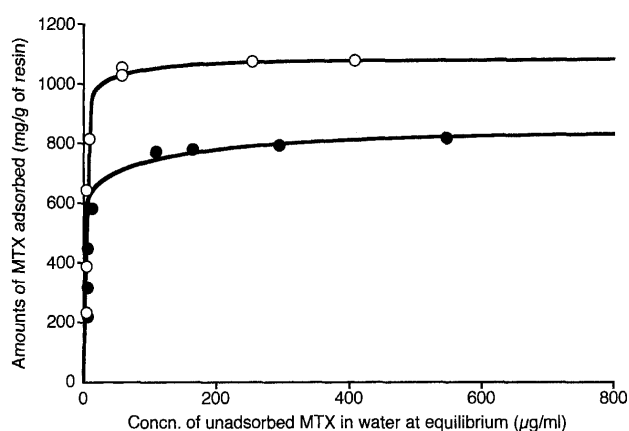


Fig. 6. Adsorption Isotherms for Binding of Methotrexate (MTX) to Colestimide and Cholestyramine in Water at 37°C

○, colestimide; ●, cholestyramine.

erty of the resin is one of the factors that influences accessibility to the binding sites.

Figure 5 presents the swelling patterns of both resins in water. Cholestyramine swelled to about 2.4 volumes within a few minutes, whereas colestimide showed much more swelling capacity, *i.e.*, the bed-volume increased about 6.8 fold. Consequently, the difference in the swelling property seems to indicate colestimide has easier accessibility to bile acids and thus more efficient adsorption of bile acids in the gut.

Adsorption of Methotrexate Because the renal clearance of MTX is markedly lower with an increase in MTX dose,¹³⁾ high-dose MTX therapy may be followed by extremely prolonged MTX elimination not only in patients with renal failure but also even in patients with normal renal function. Thus, if colestimide demonstrates a large adsorptive capacity for MTX and thereby can remove a large portion of MTX from the enterohepatic circulation, the total clearance of MTX would be greatly improved by an oral dose of colestimide.

Adsorption isotherms for the binding of MTX in water are presented for the two anion-exchange resins, colestimide and cholestyramine (Fig. 6). The curve with colestimide shows a tendency to reach a plateau at high values, *i.e.*, the amount of MTX adsorbed was over 1000 mg/g of resin. Adsorption data of the two resins fitted well to the Langmuir equation and it

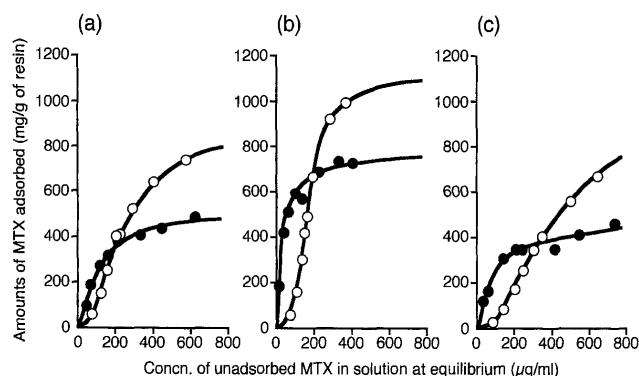


Fig. 7. Effects of Media on the Adsorption of Methotrexate (MTX) to Colestimide and Cholestyramine at 37°C

(a), in 2nd fluid JPXIII; (b), in bicarbonate buffer; (c), in saline. ○, colestimide; ●, cholestyramine.

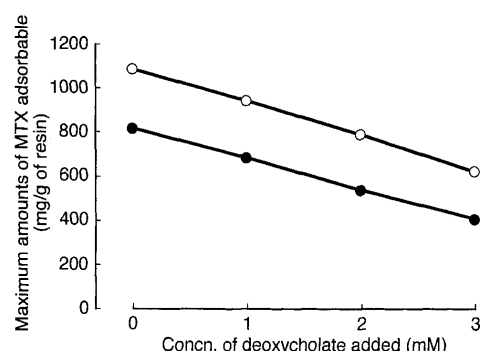


Fig. 8. Comparison of Methotrexate (MTX) Adsorptive Capacities of Colestimide and Cholestyramine in the Presence of Deoxycholate

○, colestimide; ●, cholestyramine.

was found that the maximum binding capacity of colestimide for MTX is 1087 mg/g, *i.e.*, 1.3 times as much as that of cholestyramine (820 mg/g). Not only in water but also in saline, 2nd fluid of JPXIII and the bicarbonate buffer, colestimide exhibited greater adsorptive powers as the concentration of MTX was increased. (Fig. 7). Furthermore, supposing that colestimide is used as an MTX-adsorbent in the gut, the adsorption behavior for MTX in the presence of deoxycholate is shown in Fig. 8. Although the adsorption of MTX by colestimide was smaller with increasing concentration of deoxycholate, probably through competitive binding, colestimide exhibited superior capacity compared to cholestyramine. Based on the results of these adsorption experiments

and the swelling test, it is indicated that colestimide is more suitable as an intestinal adsorbent for the early treatment of possible toxicity by MTX, and may be of clinical value in patients receiving high-dose MTX.

Conclusions

Colestimide, a new type of anion-exchange resin, had greater adsorptive capacities than cholestyramine for bile acids, by a factor of 1.4–2.0 fold in water. Although the adsorptive power of this resin for cholate, a trihydroxy bile salt anion was dramatically reduced by the addition of chloride or bicarbonate anions to the system, that for deoxycholate, a dihydroxy bile analog was almost retained. In addition, colestimide showed superior swelling properties in water, and this is expected to lead to efficient bile salt adsorption in the gut. On the other hand, since colestimide also had a higher binding capacity for MTX, a folic acid antagonist, the oral administration of colestimide may improve total body clearance of MTX by enhancing extrarenal excretion. The results obtained in this study suggest the potential of colestimide as a modulator of adverse reactions due to MTX through binding of the drug in the gut, in patients with delayed MTX elimination and/or evidence of acute renal injury. Further animal and clinical studies are indicated to assess the benefits of oral colestimide, particularly in addition to leucovorin rescue, in patients receiving high-dose MTX therapy.

References

- 1) Lipid Research Clinics Program, *JAMA*, **251**, 351–364 (1984).
- 2) Lipid Research Clinics Program, *JAMA*, **251**, 365–374 (1984).
- 3) Jansen G. R., Zanetti M. E., *J. Pharm. Sci.*, **54**, 863–867 (1965).
- 4) Toda H., Kihara K., Hashimoto M., Mizogami S., *J. Pharm. Sci.*, **77**, 531–533 (1988).
- 5) Van Den Berg H. W., Murphy R. F., Kennedy D. G., *Cancer Chemother. Pharmacol.*, **4**, 47–48 (1980).
- 6) Erttmann R., Landbeck G., *J. Cancer Res. Clin. Oncol.*, **110**, 48–50 (1985).
- 7) McAnena O. J., Ridge J. A., Daly J. M., *Cancer*, **59**, 1091–1097 (1987).
- 8) Nakano N. I., Funada S., Honda Y., Nakano M., *Chem. Pharm. Bull.*, **32**, 4096–4102 (1984).
- 9) Johns W. H., Bates T. R., *J. Pharm. Sci.*, **58**, 179–183 (1969).
- 10) Krasopoulos J. C., DE Bari V. A., Needle M. A., *Lipid*, **15**, 365–370 (1980).
- 11) Sugii A., Haratake M., Ogawa N., *Chem. Pharm. Bull.*, **37**, 1969–1938 (1989).
- 12) Honda Y., Nakano M., Haratake M., Sugii A., *J. Pharmacobio-Dyn.*, **13**, 130–135 (1990).
- 13) Lawrence J. R., Steele W. H., Stuart J. F., McNeill C. A., McVie J. G., Whiting B., *Eur. J. Clin. Pharmacol.*, **17**, 371–374 (1980).

New Antifungal 1,2,4-Triazoles with Difluoro(heteroaryl)methyl Moiety

Hiromichi ETO,* Yasushi KANEKO, and Takao SAKAMOTO^a

Central Research Labs., SS Pharmaceutical Co., Ltd., 1143 Nanpeidai, Narita, Chiba 286–8511, Japan and Graduate School of Pharmaceutical Sciences, Tohoku University,^a Aramaki-aza-Aoba, Aoba-ku, Sendai 980–8578, Japan.

Received January 12, 2000; accepted April 27, 2000

New 1,2,4-triazoles (**1**) having a difluoro(heteroaryl)methyl moiety were designed and synthesized via 1-aryl-2,2-difluoro-2-(heteroaryl)ethanones (**2**), which were prepared by two routes starting from the reaction of ethyl 2,2-difluoro(heteroaryl)acetate with phenyllithiums (Route A) and from the reaction of chlorodifluoro(heteroaryl)methane with benzaldehydes (Route B). The compounds **1** except for **1g** show antifungal activities against yeasts and filamentous fungi *in vitro*, especially (+)-**1f** have equal or superior activities compared to those of itraconazole.

Key words antifungal; 1,2,4-triazole; difluoro(heteroaryl)methyl derivatives

The treatment of systemic mycoses have been a problem in the immunocompromised patient, and partly be due to the improved recognition and diagnosis of fungal infections. Another contributory factor are the prolonged survival of patients with global defects in their host defense mechanisms including patients with neoplastic diseases, organ transplant, diabetics and AIDS.

1,2,4-Triazole antifungals inhibit the biosynthesis of the cell membrane in fungi by direct interaction with cytochrome P-450 which acts on the 14- α -demethylation of lanosterol.¹⁾ For the treatment of systemic mycoses such as candidosis and cryptococcosis in immunocompromised patients, 1,2,4-triazole antifungals such as fluconazole (FLCZ) and itraconazole (ITCZ) have been used.²⁾ However, FLCZ is not effective against aspergillosis, and ITCZ is not so efficacy *in vivo* because of its poor solubility and low bioavailability. And recently, the resistance to FLCZ in *Candida albicans* (*C. albicans*) has been reported.³⁾ Therefore more effective and safer

drugs with broader spectra have been desired and many 1,2,4-triazole antifungals containing the heterocyclic moiety were developed, such as voriconazole,⁴⁾ SCH-56592,⁵⁾ ER-30346,⁶⁾ D-0870,⁷⁾ UR-9825,⁸⁾ and TAK-187.⁹⁾

It is well known that the introduction of a fluorine atom into an organic molecule causes dramatic changes in its biological activities,¹⁰⁾ mainly due to the high electronegativity of fluorine, the strong carbon-fluorine bond, and increased solubility in lipids. Therefore, we designed the 1,2,4-triazole derivatives (**1**) with difluoro(heteroaryl)methyl moiety as shown in Chart 1. In this paper, we will describe the synthesis of **1** and their antifungal activities.

Chemistry The designed compounds **1** can be prepared from key intermediates, aryl difluoro(heteroaryl)methyl ketones (**2**), by the usual methods, which are prepared via Routes A and B. Route A consists of two reactions, namely the coupling reaction of heteroaryl halides with a copper-difluoroacetate complex, followed by the reaction of the cou-

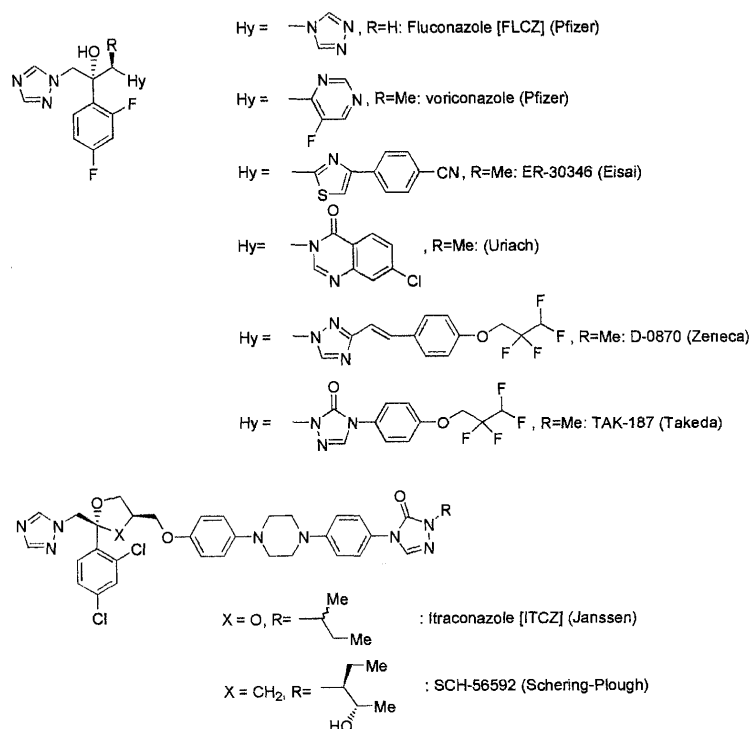


Fig. 1

* To whom correspondence should be addressed. e-mail: Hiromichi.Eto@ssp.co.jp

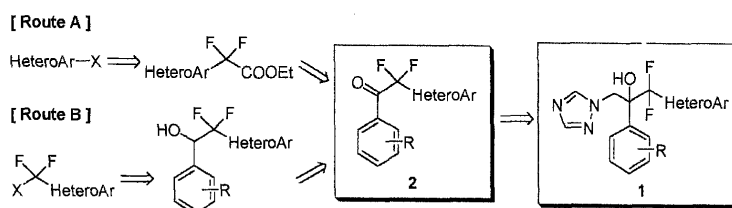


Chart 1

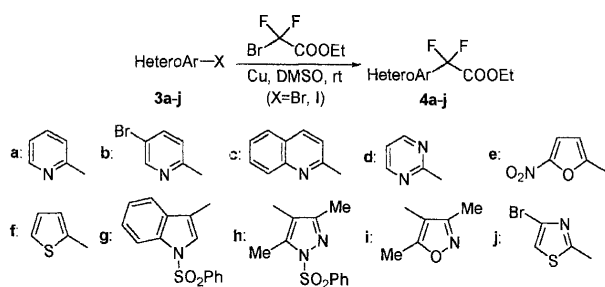


Chart 2

Table 1. Synthesis of Ethyl 2,2-Difluoro(heteroaryl)acetates (**4**) by the Reaction of Heteroaryl Halides (**3**) with Ethyl Bromodifluoroacetate in the Presence of Copper in DMSO

Run	HeteroArX (3)	X	Product (4)	Yield (%)
1	3a	Br	4a	59.5
2	3a	Br	4a	— ^{a)}
3	3b	Br	4b	62.4
4	3c	Br	4c	37.4
5	3c	I	4c	56.9 ^{b)}
6	3d	Cl	4d	—
7	3d	Br	4d	12.3 ^{c)}
8	3e	I	4e	71.7
9	3f	Br	4f	—
10	3f	Br	4f	3.8 ^{c)}
11	3f	I	4f	2.4 ^{d)}
12	3f	I	4f	74.4
13	3f	I	4f	52.4 ^{e)}
14	3g	I	4g	65.5
15	3h	I	4h	89.5
16	3i	I	4i	39.2
17	3j	I	4j	91.7

a) Reaction was carried out at 55 °C for 1 h using ethyl chlorodifluoroacetate. b) Reaction time is 5 h. c) CuI was added as an additive to the reaction. d) Reaction was carried out in DMF. e) Reaction was carried out in HMPA.

pling products, 2,2-difluoro(heteroaryl)acetates, with aryllithiums. Also Route B consists of two reactions, namely the reaction of benzaldehydes with Reformatsky reagents prepared from chlorodifluoro(heteroaryl)methanes followed by the oxidation reaction of the resulting alcohols.

The coupling reaction of the copper-difluoroacetate complex with heteroaryl halides has been reported by Kobayashi *et al.*¹¹⁾ and recently by Kumadaki *et al.*¹²⁾ Kobayashi reported the coupling reaction of aliphatic, aromatic, and heteroaromatic halides with ethyl iododifluoroacetate, and Kumadaki reported the coupling reaction of aliphatic and aromatic iodides with commercially available ethyl bromodifluoroacetate. Therefore, we carried out the coupling reaction of various heteroaryl halides with the copper-difluoroacetate complex prepared from copper powder and commercially available ethyl bromodifluoroacetate.

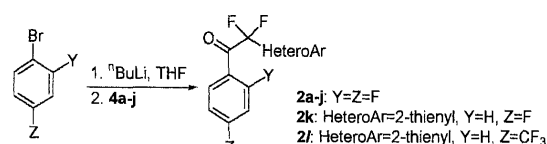


Chart 3

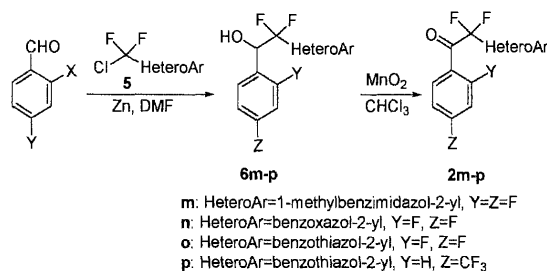


Chart 4

The results are summarized in Table 1. According to the Table 1, dimethyl sulfoxide (DMSO) (Run 12) is more preferred than *N,N*-dimethylformamide (DMF) (Run 11) and hexamethylphosphoramide (HMPA) (Run 13) as the solvent. The reactions using ethyl bromodifluoroacetate proceeded at room temperature, while the reaction using ethyl chlorodifluoroacetate did not proceed at 55 °C in DMSO (Run 2). The results in Table 1 show that most heteroaryl iodides produced products (**4**) in moderate to good yields while the bromides showed moderate yields. When the reactions did not proceed, the reaction slightly proceeded by the addition of copper(I) iodide (Run 10).

Prepared compounds (**4a—k**) were then allowed to react with 4- and 2,4-substituted phenyllithiums, which were derived from the corresponding bromides by the reaction with *n*-butyllithium in tetrahydrofuran (THF) at −78 °C, to give 1-aryl-2,2-difluoro-2-heteroarenes (**2a—l**).

In the reaction of ethyl 2-(5-bromo-2-pyridyl)-2,2-difluoroacetate (**4b**) with 2,4-difluorophenyllithium prepared from 2,4-difluorobromobenzene, the yield of 2-(5-bromo-2-pyridyl)-2,2-difluoro-1-(2,4-difluorophenyl)ethanone (**2b**) was low owing to the formation of 2,6-difluorophenyllithium by autometallation of the aryllithium.¹³⁾ Namely, 2-(5-bromo-2-pyridyl)-2,2-difluoro-1-(2,6-difluorophenyl)-1-ethanone (**2b'**) was obtained as the major product (**2b**:**2b'**=6:11) when THF was used as the solvent. However, the reaction in diethyl ether gave **2b** as the sole product in good yield without contamination of **2b'**.

Other 1-aryl-2,2-difluoro-2-heteroarenes (**2m—p**) were prepared by the oxidation of the corresponding alcohols (**6m—p**), which were synthesized from 2-(chlorodifluoromethyl)benzo-1,3-azoles (**5**)¹⁴⁾ and arylaldehydes using the

Reformatsky-type reaction.

Namely, Reformatsky-type reagents prepared from commercially available 2-(chlorodifluoromethyl)benzo-1,3-azoles (**5**) and zinc in DMF were allowed to react with 4- or 2,4-substituted benzaldehydes at 70 °C to give the 1-aryl-2,2-difluoro-2-heteroarylethanol (**6m—p**). Oxidation of the alcohols (**6m—p**) with activated manganese(IV) oxide in chloroform at room temperature for 15 h gave the corresponding ketones (**2m—p**). Other strong oxidants such as potassium permanganate, potassium dichromate, and pyridinium chlorochromate caused C–CF₂ bond cleavage of **6** to generate the corresponding benzaldehydes or benzoic acids without the formation of **2**.

Compounds **2a—p** were allowed to react with trimethylsulfoxonium iodide (TMSI) in the presence of sodium hydride in DMSO to give compounds **7a—p**. In the cases producing products (**7**) in low yields, the reaction of **2** with diazomethane is an alternative method, e.g., the yields of **7e** and **7n** were significantly improved from 9% to 81.8% and from 22.8% to 85%, respectively.

Finally, compounds **7a—p** were allowed to react with 1,2,4-triazole in the presence of potassium carbonate in DMF to give the expected compounds (**1a—p**). **1b**, **1c**, **1f** and **1o**,

which show strong antifungal activities, were optically resolved to (+)-**1** and (–)-**1** by chiral separation column chromatography.

For comparison, unfluorinated pyridylmethylene derivative (**8**)¹⁵ was prepared from 2-methylpyridine and 1-(2,4-difluorophenyl)-2-(1*H*-1,2,4-triazole-1-yl)ethanone.¹⁶

Antifungal Activities and Discussion The synthesized 1,2,4-triazole derivatives (**1a—p**) containing the difluoro(heteroaryl)methyl moiety were screened for their *in vitro* activities against *C. albicans*, *Candida krusei* (*C. krusei*), *Aspergillus fumigatus* (*A. fumigatus*), *Aspergillus flavus* (*A. flavus*), *Trichophyton mentagrophytes* (*T. mentagrophytes*), and *Trichophyton rubrum* (*T. rubrum*) in comparison with those of FLCZ and ITCZ. The minimum inhibitory concentrations (MICs) are shown in Table 2.

Many of these compounds showed excellent *in vitro* antifungal activities. Their activities were generally and exceptionally high against *C. albicans* and *T. rubrum* and were good against the others. The introduction of fluorine atoms enhanced *in vitro* antifungal activities *A. fumigatus*, *A. flavus*, *T. mentagrophytes* and *T. mentagrophyte* (**1a** and **8**).

As phenyl substituents, the 2,4-difluoro derivative (**1f**) and

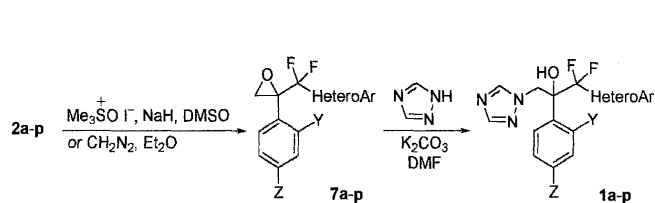


Chart 5

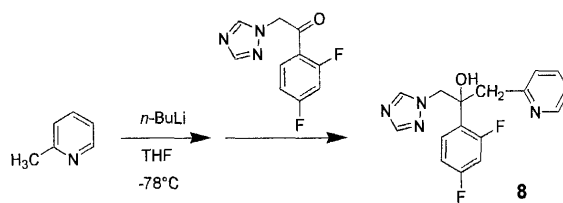


Chart 6

Table 2. *In Vitro* Antifungal Activities against Yeasts and Filamentous Fungi

	MIC (μg/ml)					
	<i>C. albicans</i> ATCC 90028	<i>C. krusei</i> ATCC 6258	<i>A. flavus</i> IFM 41935	<i>A. fumigatus</i> IFM 40808	<i>T. mentagrophytes</i> IFM 40769	<i>T. rubrum</i> IFO 6204
1a	≤0.125	1	2	1	0.25	0.25
1b	≤0.125	1	8	4	1	0.25
(–)- 1b	0.25	>8	>8	>8	>8	>8
(+)- 1b	0.031	0.25	1	0.5	0.25	0.063
1c	≤0.016	0.25	1	1	0.5	0.063
(–)- 1c	>8	>8	>8	>8	>8	>8
(+)- 1c	≤0.016	0.25	1	0.5	0.25	0.031
1d	0.5	>8	>8	>8	>8	>8
1e	0.125	4	>8	>8	4	0.25
1f	≤0.125	0.25	2	1	≤0.125	≤0.125
(–)- 1f	0.125	1	8	4	0.5	0.063
(+)- 1f	≤0.016	0.063	0.5	0.5	0.063	≤0.016
1g	>64	>64	>64	>64	>64	>64
1h	2	>8	>8	>8	>8	>8
1i	0.125	1	>8	>8	2	0.25
1j	≤0.125	0.5	2	2	0.5	≤0.125
1k	≤0.125	1	2	1	0.25	≤0.125
1l	≤0.125	2	>64	>64	64	8
1m	0.125	8	>8	>8	2	0.25
1n	0.25	1	>8	8	2	0.5
1o	≤0.016	0.25	2	2	0.25	0.063
(–)- 1o	8	>8	>8	>8	>8	>8
(+)- 1o	0.063	0.125	1	1	0.25	0.031
1p	≤0.016	0.25	4	4	2	0.25
8	0.125	1	>8	>8	4	2
FLCZ	0.5	64	>64	>64	64	64
ITCZ	0.063	0.5	0.5	0.5	0.5	0.25

4-fluoro derivative (**1k**) were superior over the 4-trifluoromethyl derivative (**1l**). As a heteroaromatic moiety, pyridine (**1a, b**), quinoline (**1c**), thiophene (**1f**), thiazole (**1j**), and the benzothiazole derivatives (**1o**) showed higher activities than pyrimidine (**1d**), furan (**1e**), pyrazole (**1h**), isoxazole (**1i**), benzimidazole (**1m**), and the benzoxazole derivatives (**1n**). On the other hand, the indole derivative (**1g**) did not show any antifungal activities.

The conformation of **1e**, **1g**, voriconazole and lanosterol were calculated by PM3.¹⁷ We used *R* configuration in PM3 calculation, because *R* configuration of **1e** is well overlapped with voriconazole, whose absolute configuration is determined. The superimposition of **1e** and voriconazole (a), and that of **1e** and lanosterol (b) are shown in Fig. 2. We presume that the compounds **1** except for **1g** interact with cytochrome P-450 with this form and show antifungal activities.

In the lowest energy conformer of **1e**, the distance of fluorine atom of difluoromethylene group and oxygen atom of hydroxy group is 2.88 Å that suggests the existence of hydrogen bond. We presume that the hydrogen bond of these atoms contributes to the stabilization of the configuration. Similar contribution of hydrogen bond were observed in compound (**6**). For example, in the ¹H-NMR spectrum of **60**, the different H–F coupling constants were observed (*J*=3 and 18 Hz) (Fig. 3).

On the other hand, a PM3 calculation of **1g**, mainly two conformations were calculated. One is an extended form, and the other is a folded form which has a 0.5 kcal/mol lower energy than extended form (Fig. 4). In the ¹H-NMR spectrum of **1g**, high magnetic field shifts of the phenyl protons were

observed at δ 6.30–6.40 and 6.65–6.75 (each 1H, m), which were due to the shielding effect of an aromatic ring. The PM3 calculation and ¹H-NMR spectra suggest that **1g** take a folded conformation, and we presume that **1g** cannot enter into the cytochrome P-450 pocket by steric hindrance and did not show any antifungal activities.

Compounds (+)-**1b**, (+)-**1c**, (+)-**1f** and (+)-**1o** showed antifungal activities, but those of (–)-form showed no significant activities. Especially, (+)-**1f** showed activities superior to FLCZ and ITCZ against *C. albicans*, *C. krusei*, *T. mentagrophytes*, and *T. rubrum*, and activities equal to itraconazole against *A. fumigatus* and *A. flavus*.

Conclusion

We designed antifungal 1,2,4-triazoles (**1**) having a heteroaryl-*gem*-difluoromethylene moiety, which were synthesized using the coupling reaction of heteroaryl halides with an ethyl difluoroacetate–copper complex or the reaction of benzaldehydes with Reformatsky type reagents prepared from chlorodifluoro(heteroaryl)methanes and zinc, as the key

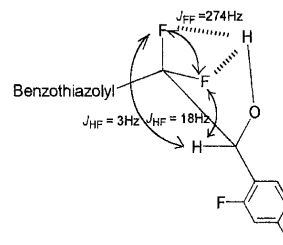


Fig. 3

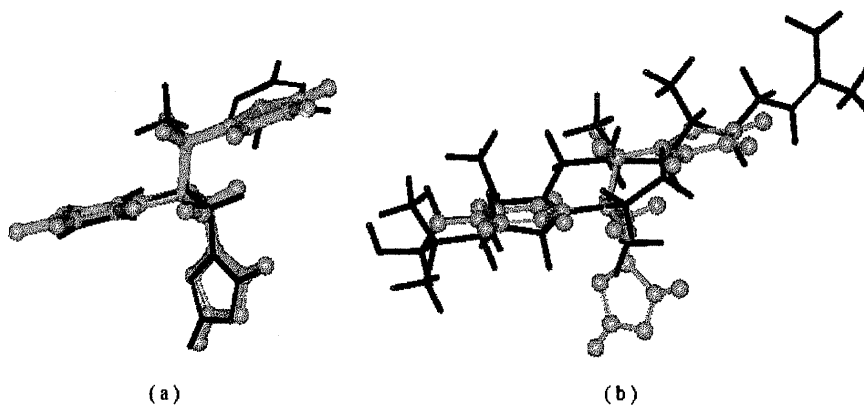


Fig. 2. Superimposition of **1e** and voriconazole (a), and that of **1e** and lanosterol (b)

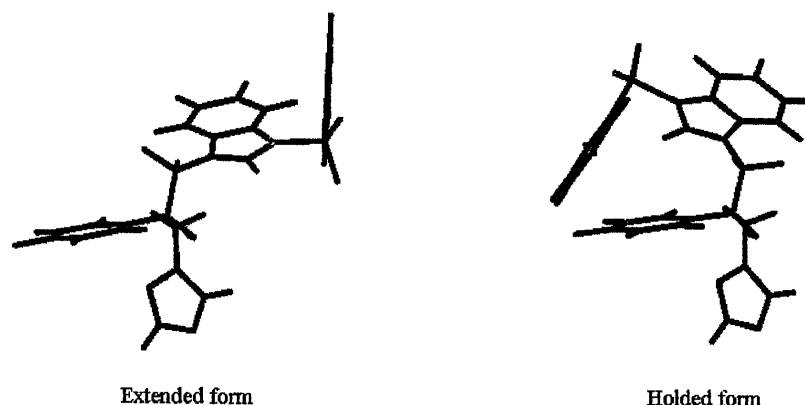


Fig. 4

reactions. The compounds **1** except for **1g** showed strong antifungal activities and especially (+)-**1f** showed activities equal or superior to ITCZ against yeasts and filamentous fungi.

Experimental

Melting points were determined on a Yanagimoto melting point apparatus without correction. IR spectra measured on a Nihon-bunko IR-810 spectrometer. ¹H-NMR spectra were recorded on a Hitachi FT-NMR R-3000 or Varian Gemini 2000 spectrometer using tetramethylsilane as a respective internal standard. ¹⁹F-NMR spectra were recorded on a JOEL JNM-EX400 FT-NMR spectrometer in CDCl₃ with trifluoroacetic acid as an external standard. The following abbreviations are used: s=singlet, d=doublet, dd=double doublet, dt=double triplet, ddd=double double doublet, t=triplet, q=quartet, m=multiplet, br=broad. MS or high-resolution mass spectra (HRMS) were obtained on a JEOL JMS-DX303 or JEOL JMS-AX500 mass spectrometer. Optical rotations were determined on a Horiba SEPA-300 polarimeter. HPLC were performed on a Hitachi L-6000 pump equipped with a Hitachi L-4000 detector. Preparative HPLC were carried out on a Yamazen 800E pump equipped with an UV-10V detector. Column chromatography was carried out on a silica gel (BW-80S Fuji-sirial). Resolution of (±)-**1** was carried out by preparative HPLC on Chiralpak AS (2 cm I.D.×25 cm) with pre-column Chiralpak AS (2 cm I.D.×5 cm) (Daicell Chemical Industries, Ltd.) and optical yields were measured by HPLC using Chiralpak AS (4.6 mm I.D.×250 mm) with pre-column Chiralpak AS (4.6 mm I.D.×50 mm) (Daicell Chemical Industries, Ltd.).

General Procedure for the Synthesis of Ethyl 2,2-Difluoro(heteroaryl)acetate (4) Ethyl bromodifluoroacetate (2 mmol) was added to a mixture of Cu powder (4 mmol) and DMSO (5 ml) at room temperature with stirring. After the mixture was stirred at the same temperature for 1 h, a heteroaryl halide (**3**) (1 mmol) was added to the solution at room temperature with stirring. The mixture was stirred at the same temperature for 15 h. After addition of aqueous NH₄Cl, the mixture was extracted with CHCl₃. The organic extract was washed with water and brine, dried over MgSO₄, and evaporated under reduced pressure. The residue was chromatographed on a silica gel column using AcOEt-*n*-hexane [1 : 9 (v/v)] to give **4**.

Ethyl 2,2-Difluoro-2-(2-pyridyl)acetate (**4a**): Colorless oil. Yield 59.5%. ¹H-NMR (CDCl₃) δ: 1.33 (3H, t, *J*=7.2 Hz), 4.38 (2H, q, *J*=7.2 Hz), 7.40–7.45 (1H, dd, *J*=5.0, 7.7 Hz), 7.74 (1H, d, *J*=8.0 Hz), 7.87 (1H, dd, *J*=7.7, 8.0 Hz), 8.66 (1H, d, *J*=5.0 Hz). MS *m/z* (%): 201 (3, M⁺), 129 (100), 128 (98). HRMS *m/z*: 201.0592 (Calcd for C₉H₉F₂N₂O₂: 201.0601). IR (neat) cm⁻¹: 1770.

Ethyl 2-(5-Bromo-2-pyridyl)-2,2-difluoroacetate (**4b**): Colorless oil. Yield 62.4%. ¹H-NMR (CDCl₃) δ: 1.33 (3H, t, *J*=7.2 Hz), 4.38 (2H, q, *J*=7.2 Hz), 7.65 (1H, d, *J*=8.2 Hz), 8.01 (1H, dd, *J*=2.2, 8.2 Hz), 8.72 (1H, d, *J*=2.2 Hz). MS *m/z* (%): 278 (18, M⁺), 206 (100). HRMS *m/z*: 278.9720 (Calcd for C₉H₈BrF₂N₂O₂: 278.9707). IR (neat) cm⁻¹: 1780.

Ethyl 2,2-Difluoro-2-(2-quinolyl)acetate (**4c**): Colorless oil. Yield 56.9%. ¹H-NMR (CDCl₃) δ: 1.36 (3H, t, *J*=7.1 Hz), 4.43 (2H, q, *J*=7.1 Hz), 7.63 (1H, dd, *J*=8.0, 7.1 Hz), 7.77 (1H, dd, *J*=7.1, 8.3 Hz), 7.81 (1H, d, *J*=7.1 Hz), 7.87 (1H, d, *J*=8.3 Hz), 8.14 (1H, d, *J*=8.5 Hz), 8.33 (1H, d, *J*=8.5 Hz). MS *m/z* (%): 251 (39, M⁺), 178 (100). HRMS *m/z*: 251.0759 (Calcd for C₁₃H₁₁F₂N₂O₂: 251.0758). IR (neat) cm⁻¹: 1790.

Ethyl 2,2-Difluoro-2-(2-pyrimidinyl)acetate (**4d**): 2 mmol of CuI was added and other procedure was same as general procedure. Colorless oil. Yield 12.3%. ¹H-NMR (CDCl₃) δ: 1.35 (3H, t, *J*=7.2 Hz), 4.42 (2H, q, *J*=7.2 Hz), 7.49 (1H, t, *J*=4.9 Hz), 8.89 (2H, d, *J*=4.9 Hz). MS *m/z* (%): 202 (7, M⁺), 129 (100). HRMS *m/z*: 202.0565 (Calcd for C₈H₈F₂N₂O₂: 202.0553). IR (neat) cm⁻¹: 1780.

Ethyl 2,2-Difluoro-2-(5-nitro-2-furanyl)acetate (**4e**): Colorless oil. Yield 71.7%. ¹H-NMR (CDCl₃) δ: 1.39 (3H, t, *J*=7.1 Hz), 4.43 (2H, q, *J*=7.1 Hz), 7.00 (1H, d, *J*=3.8 Hz), 7.35 (1H, d, *J*=3.8 Hz). MS *m/z* (%): 235 (16, M⁺), 162 (87), 86 (100). HRMS *m/z*: 235.0292 (Calcd for C₈H₈F₂N₂O₅: 235.0292). IR (neat) cm⁻¹: 1770.

Ethyl 2,2-Difluoro-2-(2-thienyl)acetate (**4f**): Colorless oil. Yield 74.4%. ¹H-NMR (CDCl₃) δ: 1.33 (3H, t, *J*=7.1 Hz), 4.37 (2H, q, *J*=7.1 Hz), 7.08 (1H, dd, *J*=3.6, 4.9 Hz), 7.40 (1H, dd, *J*=1.4, 3.6 Hz), 7.48 (1H, dd, *J*=1.4, 4.9 Hz). MS *m/z* (%): 206 (28, M⁺), 133 (100). HRMS *m/z*: 206.0235 (Calcd for C₉H₈F₂O₂S: 206.0213). IR (neat) cm⁻¹: 1760.

Ethyl 2,2-Difluoro-2-[1-(phenylsulfonyl)-3-indolyl]acetate (**4g**): Colorless oil. Yield 65.6%. ¹H-NMR (CDCl₃) δ: 1.30 (3H, t, *J*=7.2 Hz), 4.32 (2H, q, *J*=7.2 Hz), 7.32 (1H, d, *J*=7.4, 7.7 Hz), 7.39 (1H, t, *J*=7.2 Hz), 7.49 (2H, t, *J*=7.2 Hz), 7.56 (1H, d, *J*=7.4, 8.2 Hz), 7.76 (1H, d, *J*=7.7 Hz), 7.92 (2H, d,

J=7.2 Hz), 7.93 (1H, s), 7.98 (1H, d, *J*=8.2 Hz). MS *m/z* (%): 379 (49, M⁺), 306 (100), 165 (15), 141 (47). HRMS *m/z*: 379.0692 (Calcd for C₁₈H₁₅F₂N₂O₄S: 379.0690). IR (neat) cm⁻¹: 1770.

Ethyl 2-[3,5-Dimethyl-1-(phenylsulfonyl)-4-pyrazolyl]-2,2-difluoroacetate (**4h**): Colorless oil. Yield 89.5%. ¹H-NMR (CDCl₃) δ: 1.29 (3H, t, *J*=7.1 Hz), 2.30 (3H, s), 2.63 (3H, s), 4.29 (2H, q, *J*=7.1 Hz), 7.55–7.60 (2H, m), 7.65–7.75 (1H, m), 7.95–8.05 (2H, m). MS *m/z* (%): 358 (6, M⁺), 285 (100). HRMS *m/z*: Calcd for C₁₅H₁₆F₂N₂O₄S: 358.0798). IR (neat) cm⁻¹: 1760.

Ethyl 2-(3,5-Dimethyl-4-isoxazolyl)-2,2-difluoroacetate (**4i**): Colorless oil. Yield 39.2%. ¹H-NMR (CDCl₃) δ: 1.35 (3H, t, *J*=7.1 Hz), 2.33 (3H, s), 2.5 (3H, s), 4.34 (2H, q, *J*=7.1 Hz). MS *m/z* (%): 219 (17, M⁺), 146 (100). HRMS *m/z*: 219.0700 (Calcd for C₉H₁₁F₂N₂O₃: 219.0707). IR (neat) cm⁻¹: 1750.

Ethyl 2-(4-Bromo-2-thiazolyl)-2,2-difluoroacetate (**4j**): Colorless oil. Yield 91.7%. ¹H-NMR (CDCl₃) δ: 1.35 (3H, t, *J*=7.2 Hz), 4.42 (2H, q, *J*=7.2 Hz), 7.48 (1H, s). MS *m/z* (%): 285 (21, M⁺), 214 (71), 212 (68), 162 (100). HRMS *m/z*: 284.9275 (Calcd for C₇H₆BrF₂N₂O₂S: 284.9272). IR (neat) cm⁻¹: 1780.

General Procedure for the Synthesis of 1-Aryl-2,2-difluoro-2-heteroarylethanone (2) from 4 A solution of *n*-BuLi (1.37 M solution in *n*-hexane; 10 mmol) was added to a solution of 2,4-difluorobromobenzene or 4-(trifluoromethyl)bromobenzene (10.4 mmol) in THF (45 ml) with stirring at -78 °C under Ar atmosphere. The mixture was stirred at the same temperature for 0.5 h. A solution of **4** (10.4 mmol) in THF (5 ml) was added to the solution with stirring at -78 °C and stirred at the same temperature for 1 h and at room temperature for 1 h. After addition of aqueous NH₄Cl, the mixture was extracted with AcOEt. The organic extract was washed with water and brine, dried over MgSO₄, and evaporated under reduced pressure. The residue was chromatographed on a silica gel column using AcOEt-*n*-hexane [1 : 8 (v/v)] to give **2**.

2,2-Difluoro-1-(2,4-difluorophenyl)-2-(2-pyridyl)ethanone (**2a**): Colorless oil. Yield 78.4%. ¹H-NMR (CDCl₃) δ: 6.75–6.85 (1H, m), 6.90–7.00 (1H, m), 7.40–7.50 (1H, d, *J*=4.7, 7.7 Hz), 7.83 (1H, d, *J*=8.0 Hz), 7.90–7.95 (1H, m), 8.07 (1H, dd, *J*=7.7, 8.0 Hz), 8.58 (1H, d, *J*=4.7 Hz). MS *m/z* (%): 269 (3, M⁺), 141 (100), 128 (6). HRMS *m/z*: 269.0461 (Calcd for C₁₃H₇F₄N₂O: 269.0464). IR (neat) cm⁻¹: 1705.

2-(5-Bromo-2-pyridyl)-2,2-difluoro-1-(2,4-difluorophenyl)ethanone (**2b**): Colorless oil. Yield 18.6% (in THF) and 87.4% (in Et₂O). ¹H-NMR (CDCl₃) δ: 6.80–7.00 (2H, m), 7.40–7.50 (1H, m), 7.67 (1H, d, *J*=8.5 Hz), 8.02 (1H, dd, *J*=2.2, 8.5 Hz), 8.72 (1H, d, *J*=2.2 Hz). MS *m/z* (%): 346 (5, M⁺), 206 (4), 141 (100). HRMS *m/z*: 346.9569 (Calcd for C₁₃H₆BrF₄N₂O: 346.9569). IR (neat) cm⁻¹: 1720.

2-(5-Bromo-2-pyridyl)-2,2-difluoro-1-(2,6-difluorophenyl)ethanone (**2b'**): Colorless oil. Yield 32.4%. ¹H-NMR (CDCl₃) δ: 6.90–7.00 (2H, m), 7.45–7.50 (1H, m), 7.67 (1H, d, *J*=8.5 Hz), 8.02 (1H, dd, *J*=2.2, 8.5 Hz), 8.72 (1H, d, *J*=2.2 Hz). MS *m/z* (%): 346 (5, M⁺), 206 (4), 141 (100). HRMS *m/z*: 346.9557 (Calcd for C₁₃H₆BrF₄N₂O: 346.9569). IR (neat) cm⁻¹: 1720.

2,2-Difluoro-1-(2,4-difluorophenyl)-2-(2-quinolyl)ethanone (**2c**): Colorless oil. Yield 67.1%. ¹H-NMR (CDCl₃) δ: 6.85–6.95 (1H, m), 6.95–7.10 (1H, m), 7.55–7.60 (1H, m), 7.65–7.75 (1H, m), 7.80–7.90 (2H, m), 7.99 (1H, d, *J*=8.5 Hz), 8.10–8.15 (1H, m), 8.34 (1H, d, *J*=8.5 Hz). MS *m/z* (%): 319 (5, M⁺), 178 (28), 141 (100). HRMS *m/z*: 319.0620 (Calcd for C₁₇H₉F₄N₂O: 319.0610). IR (neat) cm⁻¹: 1720.

2,2-Difluoro-1-(2,4-difluorophenyl)-2-(2-pyrimidinyl)ethanone (**2d**): Colorless oil. Yield 64.1%. ¹H-NMR (CDCl₃) δ: 6.75–6.85 (1H, m), 7.00–7.05 (1H, m), 7.48 (1H, t, *J*=4.8 Hz), 8.05–8.15 (1H, m), 8.88 (2H, d, *J*=4.8 Hz). MS *m/z* (%): 270 (4, M⁺), 141 (100). HRMS *m/z*: 270.0399 (Calcd for C₁₂H₆F₄N₂O: 270.0416). IR (neat) cm⁻¹: 1720.

2,2-Difluoro-1-(2,4-difluorophenyl)-2-(5-nitro-2-furanyl)ethanone (**2e**): Colorless oil. Yield 32.0%. ¹H-NMR (CDCl₃) δ: 7.02 (1H, d, *J*=3.8 Hz), 6.90–7.00 (2H, m), 7.38 (1H, d, *J*=3.8 Hz), 7.95–8.05 (1H, m). MS *m/z* (%): 141 (100, M⁺-C₅H₂F₂N₂O₃). HRMS *m/z*: 141.0122 (Calcd for C₇H₃F₂S: 141.0151). IR (neat) cm⁻¹: 1710.

2,2-Difluoro-1-(2,4-difluorophenyl)-2-(2-thienyl)ethanone (**2f**): Colorless oil. Yield 67.2%. ¹H-NMR (CDCl₃) δ: 6.80–7.00 (2H, m), 7.07 (1H, d, *J*=3.6, 4.9 Hz), 7.37 (1H, dd, *J*=1.5, 3.6 Hz), 7.53 (1H, dd, *J*=1.5, 4.9 Hz), 7.80–7.90 (1H, m). MS *m/z* (%): 274 (4, M⁺), 141 (100), 133 (34). HRMS *m/z*: 274.0048 (Calcd for C₁₂H₆F₄O₂S: 274.0079). IR (neat) cm⁻¹: 1710.

1-(2,4-Difluorophenyl)-2,2-difluoro-2-[1-(phenylsulfonyl)-3-indolyl]ethanone (**2g**): Colorless oil. Yield 84.8%. ¹H-NMR (CDCl₃) δ: 6.9–7.0 (2H, m), 7.29 (1H, d, *J*=7.2, 7.7 Hz), 7.38 (1H, t, *J*=7.3 Hz), 7.4–7.5 (1H, m), 7.47 (2H, t, *J*=7.3 Hz), 7.50 (1H, d, *J*=7.2, 8.4 Hz), 7.74 (1H, d,

$J=7.7$ Hz), 7.88 (2H, d, $J=7.3$ Hz), 7.89 (1H, s), 7.94 (1H, d, $J=8.4$ Hz). MS m/z (%): 447 (M^+ , 14), 306 (100), 165 (9), 141 (50). HRMS m/z : 447.0553 (Calcd for $C_{22}H_{13}F_4NO_3S$ 447.0552). IR (neat) cm^{-1} : 1720.

1-(2,4-Difluorophenyl)-2-[3,5-dimethyl-1-(phenylsulfonyl)-4-pyrazolyl]-2,2-difluoroethanone (**2h**): Colorless oil. Yield: 85.1%. 1H -NMR ($CDCl_3$) δ : 2.21 (3H, s), 2.55 (3H, s), 6.85–7.0 (2H, m), 7.55–7.6 (2H, m), 7.65–7.7 (1H, m), 7.8–7.85 (1H, m), 7.95–8.0 (2H, m). MS m/z (%): 285 (100, $M^+ - C_6H_5O_2S$), 141 (48). IR (neat) cm^{-1} : 1725.

1-(2,4-Difluorophenyl)-2-(3,5-dimethyl-4-isoxazolyl)-2,2-difluoroethanone (**2i**): Colorless oil. Yield 30.7%. 1H -NMR ($CDCl_3$) δ : 2.37 (3H, s), 2.45 (3H, s), 6.9–7.05 (2H, m), 7.85–7.95 (1H, m). MS m/z (%): 288 ($M^+ + 1$, 0.2), 141 (100). HRMS m/z : 288.0644 (Calcd for $C_{13}H_{10}F_4NO_4$: 288.0648). IR (neat) cm^{-1} : 1710.

2-(4-Bromo-2-thiazolyl)-2,2-difluoro-1-(2,4-difluorophenyl)ethanone (**2j**): Colorless oil. Yield 21.6%. 1H -NMR ($CDCl_3$) δ : 6.85–6.95 (1H, m), 7.00–7.10 (1H, m), 7.50 (1H, s), 8.00–8.10 (1H, m). MS m/z (%): 353 (1, M^+), 141 (100). HRMS m/z : 352.9131 (Calcd for $C_{11}H_4BrF_4NOS$: 352.9133). IR (neat) cm^{-1} : 1720.

2,2-Difluoro-1-(4-fluorophenyl)-2-(2-thienyl)ethanone (**2k**): Colorless oil. Yield 69.3%. 1H -NMR ($CDCl_3$) δ : 7.00–7.05 (3H, m), 7.35–7.40 (1H, m), 7.50–7.60 (2H, m), 7.70–7.80 (1H, m). MS m/z (%): 256 (2, M^+), 123 (100). HRMS m/z : 256.0150 (Calcd for $C_{12}H_7F_3OS$: 256.0169). IR (neat) cm^{-1} : 1715.

2,2-Difluoro-2-(2-thienyl)-1-[4-(trifluoromethyl)phenyl]ethanone (**2l**): Colorless oil. Yield 68.1%. 1H -NMR ($CDCl_3$) δ : 7.05–7.10 (1H, m), 7.30–7.35 (1H, m), 7.55 (1H, dd, $J=1.1$, 4.9 Hz), 7.74 (2H, d, $J=8.3$ Hz), 8.18 (2H, d, $J=8.3$ Hz). MS m/z (%): 306 (6, M^+), 173 (100). HRMS m/z : 306.0173 (Calcd for $C_{13}H_7F_3OS$: 306.0137). IR (neat) cm^{-1} : 1710.

General Procedure for the Synthesis of 1-Aryl-2,2-difluoro-2-heteroarylethanone (6) A mixture of a (chlorodifluoromethyl)heteroarene (**5**) (11.4 mmol), Zn (2.6 g, 40 mmol), a benzaldehyde (20 mmol), and DMF (50 ml) was heated at 70 °C for 15 h. After addition of aqueous NH_4Cl , the precipitate was filtered and washed with AcOEt (50 ml \times 3). The filtrate was extracted with AcOEt. The combined AcOEt layer was washed with water and brine, dried over $MgSO_4$, and evaporated under reduced pressure. The residue was chromatographed on a silica gel column using AcOEt–*n*-hexane [1 : 9 (v/v)] to give **6**.

2,2-Difluoro-1-(2,4-difluorophenyl)-2-(1-methylbenzimidazol-2-yl)-ethanol (**6m**): Colorless powder. mp 195–197 °C. Yield 32.5%. 1H -NMR ($CDCl_3$) δ : 3.30 (1H, s), 3.91 (3H, s), 5.92 (1H, dd, $J_{HF}=3$, 19 Hz), 6.80–6.90 (1H, m), 6.95–7.00 (1H, m), 7.38 (1H, t, $J=7.7$ Hz), 7.44 (1H, t, $J=7.7$ Hz), 7.45 (1H, d, $J=7.7$ Hz), 7.70–7.75 (1H, m), 7.82 (1H, d, $J=7.7$ Hz). MS m/z (%): 324 (23, M^+), 182 (100). HRMS m/z : 324.0927 (Calcd for $C_{16}H_{12}F_4N_2O$: 324.0875). IR (KBr) cm^{-1} : 3100.

2-(Benzoxazol-2-yl)-2,2-difluoro-1-(2,4-difluorophenyl)ethanol (**6n**): Colorless powder. mp 146–147 °C. Yield 77.8%. 1H -NMR ($CDCl_3$) δ : 3.90 (1H, br), 5.85 (1H, dd, $J_{HF}=3$, 18 Hz), 6.80–6.90 (1H, m), 6.95–7.00 (1H, m), 7.45 (1H, dd, $J=7.4$, 7.7 Hz), 7.51 (1H, dd, $J=7.7$, 8.0 Hz), 7.60–7.70 (1H, m), 7.66 (1H, d, $J=8.0$ Hz), 7.83 (1H, d, $J=7.4$ Hz). MS m/z (%): 311 (0.3, M^+), 169 (100). HRMS m/z : 311.0567 (Calcd for $C_{15}H_9F_4NO_2$: 311.0569). IR (KBr) cm^{-1} : 3100.

2-(Benzothiazol-2-yl)-2,2-difluoro-1-(2,4-difluorophenyl)ethanol (**6o**): Colorless powder. mp 122–123 °C. Yield 57.7%. 1H -NMR ($CDCl_3$) δ : 4.37 (1H, d, $J=4.1$ Hz), 5.88 (1H, ddd, $J=4.1$, $J_{HF}=3$, 18 Hz), 6.80–6.90 (1H, m), 6.9–7.0 (1H, m), 7.56 (1H, dd, $J=7.2$, 8.0 Hz), 7.60–7.70 (1H, m), 7.62 (1H, dd, $J=7.2$, 8.0 Hz), 8.00 (1H, d, $J=8.0$ Hz), 8.16 (1H, d, $J=8.0$ Hz). ^{19}F -NMR δ : –21.4 (1F, ddd, $J=3$, 11, 274 Hz), –31.0 (1F, ddd, $J=5$, 18, 274 Hz), –33.3––33.4 (1F, m), –37.4––37.5 (1F, m). MS m/z (%): 328 (6, $M^+ + 1$), 185 (100). HRMS m/z : 328.0387 (Calcd for $C_{15}H_{10}F_4NOS$: 328.0419). IR (KBr) cm^{-1} : 3300.

2-(Benzothiazol-2-yl)-2,2-difluoro-1-(4-fluorophenyl)ethanol (**6p**): Colorless powder. mp: 142–143 °C. Yield 11.7%. 1H -NMR ($CDCl_3$) δ : 4.25 (1H, br), 5.52 (1H, dd, $J_{HF}=6$, 16 Hz), 7.50 (2H, t, $J=8.8$ Hz), 7.48 (1H, d, $J=8.8$ Hz), 7.49 (1H, d, $J=8.8$ Hz), 7.53 (1H, dd, $J=7.2$, 7.7 Hz), 7.59 (1H, dd, $J=7.2$, 8.0 Hz), 7.96 (1H, d, $J=8.0$ Hz), 8.13 (1H, d, $J=7.7$ Hz). MS m/z (%): 309 (2, M^+), 185 (100). HRMS m/z : 309.0469 (Calcd for $C_{15}H_{10}F_3NOS$: 309.0435). IR (KBr) cm^{-1} : 3140.

General Procedure for the Synthesis of 2m–p from 6 MnO_2 (2 g) was added to a solution of **6** (2.7 mmol) in $CHCl_3$ (10 ml) at room temperature with stirring for 15 h. The precipitate was filtered off, and the precipitate was washed with $CHCl_3$. The filtrate was washed with water and brine, dried over $MgSO_4$, and evaporated under reduced pressure. The residue was chromatographed on a silica gel column using AcOEt–*n*-hexane [1 : 9 (v/v)] to give **2**.

2-(1-Methylbenzimidazol-2-yl)-2,2-difluoro-1-(2,4-difluorophenyl)ethanone (**2m**): Colorless powder. mp 110–112 °C. Yield 37.4%. 1H -NMR ($CDCl_3$) δ : 4.06 (3H, s), 6.75–6.85 (1H, m), 6.95–7.05 (1H, m), 7.33 (1H, t, $J=8.2$ Hz), 7.45 (1H, t, $J=8.2$ Hz), 7.47 (1H, d, $J=8.2$ Hz), 7.8 (1H, d, $J=8.2$ Hz), 8.10–8.20 (1H, m). MS m/z (%): 322 (2, M^+), 294 (48), 141 (100). HRMS m/z : 322.0705 (Calcd for $C_{16}H_{10}F_4N_2O$: 322.0729). IR (KBr) cm^{-1} : 1710.

2-(Benzoxazol-2-yl)-2,2-difluoro-1-(2,4-difluorophenyl)ethanone (**2n**): Colorless powder. mp 71–72 °C. Yield: 43.1%. 1H -NMR ($CDCl_3$) δ : 6.80–6.90 (1H, m), 7.00–7.10 (1H, m), 7.45 (1H, dd, $J=7.7$, 8.0 Hz), 7.50 (1H, dd, $J=7.4$, 8.0 Hz), 7.68 (1H, d, $J=7.4$ Hz), 7.82 (1H, d, $J=7.7$ Hz), 8.10–8.15 (1H, m). MS m/z (%): 309 (4, M^+), 141 (100). HRMS m/z : 309.0402 (Calcd for $C_{15}H_9F_4NO_2$: 309.0412). IR (KBr) cm^{-1} : 1705.

2-(Benzothiazol-2-yl)-2,2-difluoro-1-(2,4-difluorophenyl)ethanone (**2o**): Colorless powder. mp 61–62 °C. Yield: 46.9%. 1H -NMR ($CDCl_3$) δ : 6.80–6.90 (1H, m), 6.95–7.05 (1H, m), 7.55–7.60 (1H, m), 7.55 (1H, dd, $J=7.2$, 7.7 Hz), 8.00 (1H, d, $J=7.2$ Hz), 8.08 (1H, d, $J=8.0$ Hz), 8.12 (1H, dd, $J=7.7$, 8.0 Hz). MS m/z (%): 325 (10, M^+), 141 (100). HRMS m/z : 325.0159 (Calcd for $C_{15}H_9F_4NOS$: 325.0184). IR (KBr) cm^{-1} : 1710.

2-(Benzothiazol-2-yl)-2,2-difluoro-1-(4-fluorophenyl)ethanone (**2p**): Colorless powder. mp 90–91 °C. Yield 95.4%. 1H -NMR ($CDCl_3$) δ : 7.16 (2H, dd, $J=8.6$, 8.8 Hz), 7.52 (1H, dd, $J=7.1$, 7.7 Hz), 7.57 (1H, dd, $J=7.1$; 7.4 Hz), 7.99 (1H, d, $J=7.7$ Hz), 8.09 (1H, d, $J=7.4$ Hz), 8.19 (1H, d, $J=8.6$ Hz), 8.21 (1H, d, $J=8.8$ Hz). MS m/z (%): 307 (M^+ , 6), 123 (100). HRMS m/z : 307.0296 (Calcd for $C_{15}H_8F_3NOS$: 307.0279). IR (KBr) cm^{-1} : 1705.

General Procedure for the Synthesis of 2-Aryl-2-[difluoro(heteroaryl)methyl]oxirane (7) from 2 with Trimethylsulfoxonium Iodide DMSO (10 ml) in THF (5 ml) was added to NaH (60% in oil; 64 mg, 1.6 mmol) washed twice with *n*-hexane. To the mixture, was added TMSI (349 mg, 1.6 mmol). After stirring at room temperature for 1 h, the mixture was added to **2** (1.57 mmol) in THF (5 ml) at 0 °C with stirring. The mixture was stirred at the same temperature for 1 h. After addition of aqueous $NaHCO_3$, the mixture was extracted with AcOEt. The organic extract was washed with water and brine, dried over $MgSO_4$, and evaporated under reduced pressure. The residue was chromatographed on a silica gel column using *n*-hexane–AcOEt [9 : 1 (v/v)] to give **7**.

General Procedure for the Synthesis of 7 from 2 with Diazomethane Diazomethane (0.29 M in Et_2O ; 10 ml) was added to a solution of **2e**, **n** (0.5 mmol) in Et_2O (10 ml) with stirring at 0 °C. The mixture was stirred at room temperature for 12 h, and the solvent was evaporated under reduced pressure. The residue was chromatographed on a silica gel column using AcOEt–*n*-hexane [1 : 8 (v/v)] to give **7e**, **n**.

2-[Difluoro[2-(2,4-difluorophenyl)-2-oxiranyl]methyl]pyridine (**7a**): Colorless oil. Yield 79.3%. 1H -NMR ($CDCl_3$) δ : 2.95–3.00 (1H, m), 3.45–3.50 (1H, m), 6.70–6.85 (2H, m), 7.38 (1H, dd, $J=5.0$, 8.0 Hz), 7.45–7.50 (1H, m), 7.57 (1H, d, $J=7.7$ Hz), 7.75 (1H, dd, $J=7.7$, 8.0 Hz), 8.67 (1H, d, $J=5.0$ Hz). MS m/z (%): 283 (17, M^+), 141 (10), 127 (100). HRMS m/z : 283.0647 (Calcd for $C_{14}H_9F_4NO$: 283.0620). IR (neat) cm^{-1} : 1240.

5-Bromo-2-[difluoro[2-(2,4-difluorophenyl)-2-oxiranyl]methyl]pyridine (**7b**): Colorless oil. Yield 54.9%. 1H -NMR ($CDCl_3$) δ : 2.95–3.05 (1H, m), 3.40–3.45 (1H, m), 6.85–6.95 (2H, m), 7.30–7.40 (1H, m), 7.46 (1H, d, $J=8.5$ Hz), 7.92 (1H, dd, $J=2.2$, 8.5 Hz), 8.71 (1H, d, $J=2.2$ Hz). MS m/z (%): 360 (27, M^+), 206 (24), 155 (87), 127 (100). HRMS m/z : 360.9688 (Calcd for $C_{14}H_8BrF_4NO$: 360.9725). IR (neat) cm^{-1} : 1245.

2-[Difluoro[2-(2,4-difluorophenyl)-2-oxiranyl]methyl]quinoline (**7c**): Colorless oil. Yield 89.8%. 1H -NMR ($CDCl_3$) δ : 3.00–3.05 (1H, m), 3.50–3.55 (1H, m), 6.70–6.85 (2H, m), 7.40–7.45 (1H, m), 7.59 (1H, d, $J=8.5$ Hz), 7.63 (1H, d, $J=8.2$ Hz), 7.77 (1H, dd, $J=7.7$, 8.5 Hz), 7.85 (1H, dd, $J=7.7$, 8.2 Hz), 8.17 (1H, d, $J=8.5$ Hz), 8.22 (1H, d, $J=8.5$ Hz). MS m/z (%): 333 (83, M^+), 178 (91), 127 (100). HRMS m/z : 333.0763 (Calcd for $C_{18}H_{11}F_4NO$: 333.0776). IR (neat) cm^{-1} : 1245.

2-[Difluoro[2-(2,4-difluorophenyl)-2-oxiranyl]methyl]pyrimidine (**7d**): Colorless oil. Yield 48.8%. 1H -NMR ($CDCl_3$) δ : 3.00–3.05 (1H, m), 3.55–3.65 (1H, m), 6.70–6.75 (1H, m), 6.85–6.90 (1H, m), 7.42 (1H, t, $J=4.9$ Hz), 7.55–7.50 (1H, m), 8.85 (2H, d, $J=4.9$ Hz). MS m/z (%): 284 (12, M^+), 127 (100). HRMS m/z : 284.0545 (Calcd for $C_{13}H_8F_4N_2O$: 284.0572). IR (neat) cm^{-1} : 1240.

2-[Difluoro[2-(2,4-difluorophenyl)-2-oxiranyl]methyl]-5-nitrofuran (**7e**): Colorless oil. Yield 9% (with TMSI) and 81.1% (with CH_2N_2). 1H -NMR ($CDCl_3$) δ : 3.00–3.05 (1H, m), 3.45–3.50 (1H, m), 6.78 (1H, d, $J=4.0$ Hz), 6.75–6.85 (1H, m), 6.90–6.95 (1H, m), 7.29 (1H, d, $J=4.0$ Hz), 7.40–7.50 (1H, m). MS m/z (%): 317 (1, M^+), 127 (100). HRMS m/z : 317.0288 (Calcd for $C_{13}H_7F_4NO_4$: 317.0311). IR (neat) cm^{-1} : 1250.

2-[Difluoro[2-(2,4-difluorophenyl)-2-oxiranyl]methyl]thiophene (**7f**): Colorless oil. Yield 79.9%. ¹H-NMR (CDCl₃) δ: 2.95–3.00 (1H, m), 3.20–3.25 (1H, m), 6.85–6.90 (2H, m), 7.03 (1H, dd, *J*=3.7, 5.1 Hz), 7.25 (1H, d, *J*=3.7 Hz), 7.30–7.40 (1H, m), 7.43 (1H, d, *J*=5.1 Hz). MS *m/z* (%): 288 (14, M⁺), 155 (100). HRMS *m/z*: 288.0222 (Calcd for C₁₃H₈F₄OS: 288.0223). IR (neat) cm⁻¹: 1245.

3-[Difluoro[2-(2,4-difluorophenyl)-2-oxiranyl]methyl]-1-(phenylsulfonyl)indole (**7g**): Colorless oil. Yield 54.9%. ¹H-NMR (CDCl₃) δ: 2.90–2.95 (1H, m), 3.15–3.20 (1H, m), 6.80–6.90 (2H, m), 7.26 (1H, d, *J*=6.8, 7.2 Hz), 7.30–7.40 (1H, m), 7.37 (1H, t, *J*=7.2 Hz), 7.47 (2H, t, *J*=7.2 Hz), 7.55 (1H, dd, *J*=7.2, 8.8 Hz), 7.63 (1H, d, *J*=8.8 Hz), 7.76 (1H, s), 7.89 (2H, d, *J*=7.2 Hz), 7.97 (1H, d, *J*=8.8 Hz). MS *m/z* (%): 461 (53, M⁺), 306 (100), 165 (11), 141 (39). HRMS *m/z*: 461.0738 (Calcd for C₂₃H₁₅F₄N₂O₃S: 461.0709). IR (neat) cm⁻¹: 1240.

4-[Difluoro[2-(2,4-difluorophenyl)-2-oxiranyl]methyl]-3,5-dimethyl-1-(phenylsulfonyl)pyrazole (**7h**): Colorless oil. Yield 54.3%. ¹H-NMR (CDCl₃) δ: 2.02 (3H, s), 2.30 (3H, s), 2.85–2.80 (1H, m), 3.10–3.15 (1H, m), 6.55–6.60 (1H, m), 6.65–6.75 (1H, m), 7.10–7.15 (1H, m), 7.45–7.50 (2H, m), 7.60–7.65 (1H, m), 7.85–7.90 (2H, m). MS *m/z* (%): 440 (5, M⁺), 285 (100). HRMS *m/z*: 440.0822 (Calcd for C₂₀H₁₆F₄N₂O₃S: 440.0818). IR (neat) cm⁻¹: 1240.

4-[Difluoro[2-(2,4-difluorophenyl)-2-oxiranyl]methyl]-3,5-dimethylisoxazole (**7i**): Colorless oil. Yield 59.8%. ¹H-NMR (CDCl₃) δ: 2.16 (3H, s), 2.26 (3H, s), 2.95–3.00 (1H, m), 3.25–3.30 (1H, m), 6.80–6.95 (2H, m), 7.35–7.40 (1H, m). MS *m/z* (%): 301 (16, M⁺), 155 (82), 127 (100). HRMS *m/z*: 301.0735 (Calcd for C₁₄H₁₁F₄N₂O₂: 301.0725). IR (neat) cm⁻¹: 1240.

4-Bromo-2-[difluoro[2-(2,4-difluorophenyl)-2-oxiranyl]methyl]thiazole (**7j**): Colorless oil. Yield 42.3%. ¹H-NMR (CDCl₃) δ: 3.00–3.05 (1H, m), 3.55–3.60 (1H, m), 6.80–6.90 (2H, m), 7.40–7.50 (2H, m). MS *m/z* (%): 369 (15, M⁺), 367 (15), 155 (63), 141 (20), 127 (100). IR (neat) cm⁻¹: 1260.

2-[Difluoro[2-(4-fluorophenyl)-2-oxiranyl]methyl]thiophene (**7k**): Colorless oil. Yield 78.9%. ¹H-NMR (CDCl₃) δ: 2.95–3.00 (1H, m), 3.35–3.40 (1H, m), 7.00–7.15 (3H, m), 7.15–7.20 (1H, m), 7.30–7.40 (2H, m), 7.40–7.45 (1H, m). MS *m/z* (%): 270 (35, M⁺), 137 (100). HRMS *m/z*: 270.0301 (Calcd for C₁₃H₉F₃OS: 270.0326). IR (neat) cm⁻¹: 1250.

2-[Difluoro[2-(4-trifluoromethyl)phenyl]-2-oxiranyl]methyl]thiophene (**7l**): Colorless oil. Yield 55.2%. ¹H-NMR (CDCl₃) δ: 2.90–2.95 (1H, m), 3.40–3.45 (1H, m), 6.95–7.00 (1H, m), 7.15–7.20 (1H, m), 7.35–7.40 (1H, m), 7.50–7.60 (4H, m). MS *m/z* (%): 320 (33, M⁺), 201 (80), 159 (43), 133 (100). HRMS *m/z*: 320.0273 (Calcd for C₁₄H₉F₅OS: 320.0295). IR (neat) cm⁻¹: 1250.

2-[Difluoro[2-(2,4-difluorophenyl)-2-oxiranyl]methyl]-1-methylbenzimidazole (**7m**): Colorless powder. mp 123–125 °C. Yield 62.3%. ¹H-NMR (CDCl₃) δ: 3.00–3.05 (1H, m), 3.25–3.30 (1H, m), 3.91 (3H, s), 6.80–6.90 (2H, m), 7.30–7.40 (3H, m), 7.55–7.60 (1H, m), 7.83 (1H, d, *J*=7.7 Hz). MS *m/z* (%): 336 (64, M⁺), 182 (100), 141 (51). HRMS *m/z*: 336.0894 (Calcd for C₁₇H₁₂F₄N₂O: 336.0885). IR (KBr) cm⁻¹: 1255.

2-[Difluoro[2-(2,4-difluorophenyl)-2-oxiranyl]methyl]benzoxazole (**7n**): Colorless powder. mp 91–92 °C. Yield 22.8% (with TMSI) and 85% (with CH₂N₂). ¹H-NMR (CDCl₃) δ: 3.05–3.10 (1H, m), 3.60–3.65 (1H, m), 6.75–6.80 (1H, m), 6.85–6.95 (1H, m), 7.44 (1H, dd, *J*=7.5, 7.7 Hz), 7.49 (1H, dd, *J*=7.2, 7.5 Hz), 7.50–7.60 (1H, m), 7.63 (1H, d, *J*=7.7 Hz), 7.83 (1H, d, *J*=7.2 Hz). MS *m/z* (%): 323 (43, M⁺), 189 (96), 127 (100). HRMS *m/z*: 323.0617 (Calcd for C₁₆H₉F₄N₂O₂: 323.0665). IR (KBr) cm⁻¹: 1240.

2-[Difluoro[2-(2,4-difluorophenyl)-2-oxiranyl]methyl]benzothiazole (**7o**): Colorless powder. mp 107–108 °C. Yield 22.8%. ¹H-NMR (CDCl₃) δ: 2.95–3.05 (1H, m), 3.60–3.65 (1H, m), 6.70–6.90 (2H, m), 7.46 (1H, dd, *J*=7.2, 7.7 Hz), 7.56 (1H, dd, *J*=7.2, 8.0 Hz), 7.50–7.60 (1H, m), 7.95 (1H, d, *J*=8.0 Hz), 8.16 (1H, d, *J*=7.7 Hz). MS *m/z* (%): 339 (77.5, M⁺), 184 (64), 127 (100). HRMS *m/z*: 339.0333 (Calcd for C₁₆H₉F₄NOS: 339.0341). IR (KBr) cm⁻¹: 1250.

2-[Difluoro[2-(4-fluorophenyl)-2-oxiranyl]methyl]benzothiazole (**7p**): Colorless powder. mp 57–58 °C. Yield 21.2%. ¹H-NMR (CDCl₃) δ: 2.95–3.05 (1H, m), 3.60–3.65 (1H, m), 6.98 (2H, t, *J*=8.8 Hz), 7.48 (2H, d, *J*=8.8 Hz), 7.51 (1H, dd, *J*=7.2, 8.0 Hz), 7.56 (1H, dd, *J*=7.2, 8.5 Hz), 7.92 (1H, d, *J*=8.0 Hz), 8.15 (1H, d, *J*=8.5 Hz). MS *m/z* (%): 321 (3, M⁺), 109 (100). HRMS *m/z*: 321.0422 (Calcd for C₁₆H₁₀F₃NOS: 321.0435). IR (KBr) cm⁻¹: 1240.

General Procedure for the Synthesis of 1,1-Difluoro-1-heteroaryl-3-(1,2,4-triazol-1-yl)-2-propanol (1) 1,2,4-Triazole (70 mg, 1 mmol) and K₂CO₃ (70 mg, 0.5 mmol) were added to a solution of **7** (0.93 mmol) in DMF (5 ml). The mixture was warmed at 65 °C for 5 h. After addition of aqueous NaHCO₃, the mixture was extracted with AcOEt. The organic ex-

tract was washed with water and brine, dried over MgSO₄, and evaporated under reduced pressure. The residue was chromatographed on a silica gel column using CHCl₃–MeOH [98 : 2 (v/v)] as a mobile phase to give **1**.

Resolution of (±)-1 into (+)-1 and (–)-1 Compound (±)-**1** (50 mg) was subjected to preparative HPLC (Chiralpak AS with pre-column Chiralpak AS), using *n*-hexane–2-propanol [25 : 1 (v/v)] for **1b**, **c**, **o** and [19 : 1 (v/v)] for **1f** as a mobile phase. The more mobile isomer is (+)-**1** and the less mobile isomer is (–)-**1**. Their optical yields are measured by HPLC (Chiralpak AS with pre-column Chiralpak AS) using *n*-hexane–2-propanol [9 : 1 (v/v)] as a mobile phase (flow rate: 0.5 ml/min, column temperature: 21 °C).

1,1-Difluoro-2-(2,4-difluorophenyl)-1-(2-pyridyl)-3-(1,2,4-triazol-1-yl)-2-propanol (**1a**): Colorless powder. mp 101–103 °C. Yield 63.8%. ¹H-NMR (CDCl₃) δ: 4.87 (1H, d, *J*=14.5 Hz), 5.36 (1H, d, *J*=14.5 Hz), 6.70–6.80 (2H, m), 6.86 (1H, s), 7.35–7.45 (1H, m), 7.45 (1H, dd, *J*=4.1, 7.7 Hz), 7.57 (1H, d, *J*=8.0 Hz), 7.69 (1H, s), 7.80 (1H, dd, *J*=7.7, 8.0 Hz), 8.32 (1H, s), 8.57 (1H, d, *J*=4.1 Hz). MS *m/z* (%): 353 (1, M⁺+1), 224 (47), 129 (100). HRMS *m/z*: 353.0980 (Calcd for C₁₆H₁₃F₄N₄O: 353.1025). IR (KBr) cm⁻¹: 3400. Anal. Calcd for C₁₆H₁₂F₄N₄O: C, 54.55; H, 3.43; N, 15.90. Found: C, 54.56; H, 3.57; N, 15.71.

1-(5-Bromo-2-pyridyl)-1,1-difluoro-2-(2,4-difluorophenyl)-3-(1,2,4-triazol-1-yl)-2-propanol (**1b**): Colorless powder. mp 142–143 °C. Yield 66.8%. ¹H-NMR (CDCl₃) δ: 4.73 (1H, d, *J*=14.3 Hz), 5.58 (1H, d, *J*=14.3 Hz), 5.75–5.85 (1H, m), 6.70–6.80 (2H, m), 7.15–7.25 (1H, m), 7.47 (1H, d, *J*=8.5 Hz), 7.75 (1H, s), 7.92 (1H, dd, *J*=2.2, 8.5 Hz), 8.24 (1H, s), 8.69 (1H, s). MS *m/z* (%): 433 (4, M⁺), 431 (4), 224 (48), 207 (28), 182 (100). IR (KBr) cm⁻¹: 3400. Anal. Calcd for C₁₆H₁₁BrF₄N₄O: C, 44.57; H, 2.57; N, 12.99; Br, 18.53. Found: C, 44.83; H, 2.63; N, 12.95; Br, 18.43.

(–)-**1b**: Colorless oil. e.e. 100%. [α]_D²⁴: –18.4 (c 0.1, MeOH). Retention time (min): 12.27.

(+)-**1b**: Colorless oil. e.e. 99.4%. [α]_D²⁴: 17.6 (c 0.1, MeOH). Retention time (min): 15.06.

1,1-Difluoro-2-(2,4-difluorophenyl)-1-(2-quinolyl)-3-(1,2,4-triazol-1-yl)-2-propanol (**1c**): Colorless powder. mp 136–138 °C. Yield 50.4%. ¹H-NMR (CDCl₃) δ: 4.95 (1H, d, *J*=14.4 Hz), 5.43 (1H, d, *J*=14.4 Hz), 6.60–6.80 (2H, m), 7.19 (1H, s), 7.40–7.50 (1H, m), 7.65 (1H, s), 7.60–7.70 (2H, m), 7.2 (1H, dd, *J*=8.2, 8.5 Hz), 7.88 (1H, d, *J*=8.2 Hz), 8.10 (1H, d, *J*=8.5 Hz), 8.19 (1H, s), 8.28 (1H, d, *J*=8.5 Hz). MS *m/z* (%): 403 (1, M⁺+1), 224 (22), 179 (100). HRMS *m/z*: 403.1133 (Calcd for C₂₀H₁₅F₄N₄O: 403.1182). IR (KBr) cm⁻¹: 3200. Anal. Calcd for C₂₀H₁₄F₄N₄O: C, 59.70; H, 3.51; N, 13.93. Found: C, 59.75; H, 3.55; N, 13.79.

(–)-**1c**: Colorless oil. e.e. 100%. [α]_D²⁴: –7.14 (c 0.1, MeOH). Retention time (min): 20.63.

(+)-**1c**: Colorless oil. e.e. 99.2%. [α]_D²⁴: 6.77 (c 0.1, MeOH). Retention time (min): 37.52.

1,1-Difluoro-2-(2,4-difluorophenyl)-1-(2-pyrimidinyl)-3-(1,2,4-triazol-1-yl)-2-propanol (**1d**): Colorless powder. mp 129–131 °C. Yield 14.6%. ¹H-NMR (CDCl₃) δ: 4.97 (1H, d, *J*=14.5 Hz), 5.42 (1H, d, *J*=14.5 Hz), 6.09 (1H, s), 6.70–6.80 (2H, m), 7.43 (1H, t, *J*=5.0 Hz), 7.60–7.65 (1H, m), 7.73 (1H, s), 8.15 (1H, s), 8.82 (2H, d, *J*=5.0 Hz). MS *m/z* (%): 354 (5, M⁺+1), 224 (51), 182 (100). HRMS *m/z*: 354.0991 (Calcd for C₁₅H₁₂F₄N₅O: 354.0978). IR (KBr) cm⁻¹: 3200. Anal. Calcd for C₁₅H₁₁F₄N₅O: C, 51.00; H, 3.14; N, 19.82. Found: C, 51.01; H, 3.25; N, 19.63.

1,1-Difluoro-2-(2,4-difluorophenyl)-1-(5-nitro-2-furanyl)-3-(1,2,4-triazol-1-yl)-2-propanol (**1e**): Colorless oil. Yield 49.2%. ¹H-NMR (CDCl₃) δ: 4.88 (1H, d, *J*=14.5 Hz), 5.39 (1H, d, *J*=14.5 Hz), 5.9 (1H, br), 6.73 (1H, d, *J*=3.7 Hz), 6.75–6.85 (2H, m), 7.26 (1H, d, *J*=3.7 Hz), 7.45–7.50 (1H, m), 7.84 (1H, s), 8.16 (1H, s). MS *m/z* (%): 368 (6, M⁺), 224 (100). HRMS *m/z*: 368.0601 (Calcd for C₁₈H₁₀F₄N₄O₄: 368.0639). IR (CHCl₃) cm⁻¹: 3050.

1,1-Difluoro-2-(2,4-difluorophenyl)-1-(2-thienyl)-3-(1,2,4-triazol-1-yl)-2-propanol (**1f**): Colorless powder. mp 130–132 °C. Yield 67.3%. ¹H-NMR (CDCl₃) δ: 4.72 (1H, d, *J*=14.6 Hz), 5.40 (1H, d, *J*=14.6 Hz), 5.66 (1H, s), 6.65–6.80 (2H, m), 6.96 (1H, dd, *J*=3.5, 4.9 Hz), 7.10 (1H, d, *J*=1.5, 3.5 Hz), 7.35–7.45 (1H, m), 7.40 (1H, dd, *J*=1.5, 4.9 Hz), 7.81 (1H, s), 8.10 (1H, s). MS *m/z*: 358 (2, M⁺+1), 224 (100). HRMS *m/z*: 358.0646 (Calcd for C₁₅H₁₂F₄N₃OS: 358.0637). IR (KBr) cm⁻¹: 3150. Anal. Calcd for C₁₅H₁₁F₄N₃OS: C, 50.42; H, 3.10; N, 11.76; S, 8.97. Found: C, 50.57; H, 3.12; N, 11.48; S, 8.72.

(–)-**1f**: Colorless powder. mp 99–100 °C. e.e. 100%. [α]_D²⁴: –8.21 (c 0.1, MeOH). Retention time (min): 15.33.

(+)-**1f**: Colorless powder. mp 97–98 °C. e.e. 95.2%. [α]_D²⁴: 7.99 (c 0.1, MeOH). Retention time (min): 16.99.

1,1-Difluoro-2-(2,4-difluorophenyl)-1-[1-(phenylsulfonyl)-3-indolyl]-3-(1,2,4-triazol-1-yl)-2-propanol (**1g**): Colorless powder. mp 136–138 °C.

Yield 17.0%. ¹H-NMR (CDCl₃) δ: 4.78 (1H, d, *J*=14.5 Hz), 5.47 (1H, d, *J*=14.5 Hz), 5.60 (1H, s), 6.30–6.40 (1H, m), 6.65–6.75 (1H, m), 6.95–7.05 (1H, m), 7.18 (1H, t, *J*=7.2 Hz), 7.31 (1H, dd, *J*=7.1, 7.4 Hz), 7.48 (1H, s), 7.50 (2H, t, *J*=7.2 Hz), 7.50 (1H, dd, *J*=7.1, 8.5 Hz), 7.60 (1H, d, *J*=7.4 Hz), 7.80 (1H, s), 7.84 (2H, d, *J*=7.2 Hz), 7.94 (1H, d, *J*=8.5 Hz), 8.13 (1H, s). MS *m/z* (%): 530 (2, M⁺), 306 (24), 224 (100). HRMS *m/z*: 530.1069 (Calcd for C₂₅H₁₈F₄N₄O₃S: 530.1036). IR (KBr) cm⁻¹: 3400.

1,1-Difluoro-2-(2,4-difluorophenyl)-1-[3,5-dimethyl-1-(phenylsulfonyl)-4-pyrazolyl]-3-(1,2,4-triazol-1-yl)-2-propanol (**1h**): Colorless powder. mp 175–176 °C. Yield 22.8%. ¹H-NMR (CDCl₃) δ: 1.93 (3H, br), 2.14 (3H, br), 4.78 (1H, d, *J*=14.6 Hz), 5.47 (1H, d, *J*=14.6 Hz), 5.61 (1H, br), 6.40–6.50 (1H, m), 6.65–6.75 (1H, m), 6.90–7.00 (1H, m), 7.50–7.60 (2H, m), 7.65–7.75 (1H, m), 7.78 (1H, s), 7.90–7.95 (2H, m), 8.13 (1H, s). MS *m/z* (%): 510 (0.2, M⁺+1), 285 (65), 224 (95), 145 (100). HRMS *m/z*: 510.1232 (Calcd for C₂₇H₂₀F₆N₅O₃S: 510.1223). IR (CHCl₃) cm⁻¹: 3100. Anal. Calcd for C₂₇H₁₉F₄N₅O₃S: C, 51.86; H, 3.77; N, 13.75; S, 6.30. Found: C, 51.86; H, 3.76; N, 13.75; S, 6.29.

1,1-Difluoro-2-(2,4-difluorophenyl)-1-(3,5-dimethyl-4-isoxazolyl)-3-(1,2,4-triazol-1-yl)-2-propanol (**1i**): Colorless powder. mp 188–189 °C. Yield 79.0%. ¹H-NMR (CDCl₃) δ: 1.96 (3H, s), 2.01 (3H, s), 4.82 (1H, d, *J*=14.5 Hz), 5.51 (1H, d, *J*=14.5 Hz), 5.67 (1H, s), 6.70–6.80 (2H, m), 7.20–7.25 (1H, m), 7.8 (1H, s), 8.15 (1H, s). MS *m/z* (%): 370 (0.4, M⁺), 224 (100). HRMS *m/z*: 370.1025 (Calcd for C₁₆H₁₄F₄N₄O₂: 370.1053). IR (KBr) cm⁻¹: 3150. Anal. Calcd for C₁₆H₁₄F₄N₄O₂: C, 51.90; H, 3.81; N, 15.13. Found: C, 52.03; H, 3.89; N, 15.09.

1-(4-Bromo-2-thiazolyl)-1,1-difluoro-2-(2,4-difluorophenyl)-3-(1,2,4-triazol-1-yl)-2-propanol (**1j**): Colorless powder. mp 91–93 °C. Yield 38.6%. ¹H-NMR (CDCl₃) δ: 4.92 (1H, d, *J*=14.3 Hz), 5.46 (1H, d, *J*=14.3 Hz), 5.92 (1H, s), 6.70–6.85 (2H, m), 7.44 (1H, s), 7.50–7.60 (1H, m), 7.78 (1H, s), 8.14 (1H, s). MS *m/z* (%): 437 (0.6, M⁺+1), 224 (71), 182 (100). HRMS *m/z*: 436.9675 (Calcd for C₁₄H₉BrF₄N₄O₂S: 436.9695). IR (KBr) cm⁻¹: 3400. Anal. Calcd for C₁₄H₉BrF₄N₄O₂S: C, 38.46; H, 2.07; Br, 18.28; N, 12.81; S, 7.33. Found: C, 38.50; H, 2.18; N, 13.06; Br, 18.44; S, 7.51.

1,1-Difluoro-2-(4-fluorophenyl)-1-(2-thienyl)-3-(1,2,4-triazol-1-yl)-2-propanol (**1k**): Colorless powder. mp 110–112 °C. Yield 88.3%. ¹H-NMR (CDCl₃) δ: 4.73 (1H, d, *J*=14.3 Hz), 5.45 (1H, d, *J*=14.3 Hz), 5.68 (1H, s), 6.90–7.00 (3H, m), 7.05–7.10 (1H, m), 7.20–7.25 (1H, m), 7.35–7.40 (2H, m), 7.75 (1H, s), 8.10 (1H, s). MS *m/z* (%): 340 (0.6, M⁺+1), 206 (100). HRMS *m/z*: 340.0767 (Calcd for C₁₅H₁₃F₃N₃O₂S: 340.0732). IR (KBr) cm⁻¹: 3200. Anal. Calcd for C₁₅H₁₂F₃N₃O₂S: C, 53.09; H, 3.56; N, 12.38; S, 9.45. Found: C, 53.06; H, 3.49; N, 12.19; S, 9.47.

1,1-Difluoro-1-(2-thienyl)-3-(1,2,4-triazol-1-yl)-2-[4-(trifluoromethyl)phenyl]-2-propanol (**1l**): Colorless powder. mp 117–118 °C. Yield 34.3%. ¹H-NMR (CDCl₃) δ: 4.89 (1H, d, *J*=14.5 Hz), 4.96 (1H, d, *J*=14.5 Hz), 5.6 (1H, s), 6.85–6.90 (1H, m), 6.95–7.00 (1H, m), 7.32 (1H, m), 7.52 (2H, d, *J*=8.5 Hz), 7.59 (2H, d, *J*=8.5 Hz), 7.94 (1H, s), 7.84 (1H, s). MS *m/z* (%): 390 (5, M⁺+1), 256 (100). HRMS *m/z*: 390.0681 (Calcd for C₁₆H₁₃F₃N₃O₂S: 390.0699). IR (KBr) cm⁻¹: 3200. Anal. Calcd for C₁₆H₁₂F₃N₃O₂S: C, 49.36; H, 3.11; N, 10.79; S, 8.24. Found: C, 49.41; H, 3.15; N, 10.71; S, 8.27.

1,1-Difluoro-2-(2,4-difluorophenyl)-1-(1-methylbenzimidazol-2-yl)-3-(1,2,4-triazol-1-yl)-2-propanol (**1m**): Colorless powder. mp 73–75 °C. Yield 50.4%. ¹H-NMR (CDCl₃) δ: 3.96 (3H, s), 4.95 (1H, d, *J*=14.5 Hz), 5.48 (1H, d, *J*=14.5 Hz), 6.75–6.85 (2H, m), 6.86 (1H, s), 7.35–7.40 (1H, m), 7.40–7.45 (2H, m), 7.68 (1H, s), 7.65–7.75 (1H, m), 7.80 (1H, d, *J*=8.3 Hz), 8.18 (1H, s). MS *m/z* (%): 405 (5, M⁺), 236 (85), 182 (100). HRMS *m/z*: 405.1218 (Calcd for C₁₉H₁₅F₄N₄O: 405.1213). IR (KBr) cm⁻¹: 3400. Anal. Calcd for C₁₉H₁₅F₄N₄O 2/3H₂O: C, 54.68; H, 3.94; N, 16.78. Found: C, 54.44; H, 4.08; N, 16.61.

1-(Benzoxazol-2-yl)-1,1-difluoro-2-(2,4-difluorophenyl)-3-(1,2,4-triazol-1-yl)-2-propanol (**1n**): Colorless powder. mp 147–148 °C. Yield 22.0%. ¹H-NMR (CDCl₃) δ: 4.98 (1H, d, *J*=14.5 Hz), 5.13 (1H, d, *J*=14.5 Hz), 5.88 (1H, s), 6.75–6.85 (2H, m), 7.46 (1H, dd, *J*=7.4, 7.7 Hz), 7.49 (1H, dd, *J*=7.7, 8.0 Hz), 7.55–7.65 (1H, m), 7.61 (1H, d, *J*=8.0 Hz), 7.78 (1H, s), 7.82 (1H, d, *J*=7.4 Hz), 8.15 (1H, s). MS *m/z* (%): 392 (3, M⁺), 224 (100). HRMS *m/z*: 392.0891 (Calcd for C₁₈H₁₂F₄N₄O₂: 392.0897). IR (KBr) cm⁻¹: 3400. Anal. Calcd for C₁₈H₁₂F₄N₄O₂: C, 55.11; H, 3.08; N, 14.28. Found: C, 55.29; H, 3.31; N, 14.17.

1-(Benzothiazol-2-yl)-1,1-difluoro-2-(2,4-difluorophenyl)-3-(1,2,4-triazol-1-yl)-2-propanol (**1o**): Colorless powder. mp 123–125 °C. Yield 82.9%. ¹H-NMR (CDCl₃) δ: 5.00 (1H, d, *J*=14.5 Hz), 5.51 (1H, d, *J*=14.5 Hz), 6.15 (1H, s), 6.70–6.80 (2H, m), 7.5–7.6 (1H, m), 7.51 (1H, dd, *J*=7.2, 7.7 Hz), 7.57 (1H, t, *J*=7.7 Hz), 7.73 (1H, s), 7.95 (1H, d, *J*=7.2 Hz), 8.11 (1H, d, *J*=7.7 Hz), 8.16 (1H, s). MS *m/z* (%): 408 (1, M⁺), 224 (96), 141 (100). HRMS *m/z*: 408.0678 (Calcd for C₁₈H₁₂F₄N₄O₂S: 408.0668). IR (KBr)

cm⁻¹: 3400. Anal. Calcd for C₁₈H₁₂F₄N₄O₂S: C, 52.94; H, 2.96; N, 13.72; S, 7.85. Found: C, 53.20; H, 3.09; N, 13.44; S, 8.04.

(–)-**1o**: Colorless powder. mp 56–57 °C. e.e. 100%. [α]_D²⁴: –20.3 (c 0.1, MeOH). Retention time (min): 15.56.

(+)-**1o**: Colorless powder. mp 55–56 °C. e.e. 99.7%. [α]_D²⁴: 20.1 (c 0.1, MeOH). Retention time (min): 17.39.

1-(Benzothiazol-2-yl)-1,1-difluoro-2-(4-fluorophenyl)-3-(1,2,4-triazol-1-yl)-2-propanol (**1p**): Colorless powder. mp 122–123 °C. Yield 56.4%. ¹H-NMR (CDCl₃) δ: 4.98 (1H, d, *J*=14.5 Hz), 5.13 (1H, d, *J*=14.5 Hz), 6.15 (1H, s), 6.94 (2H, t, *J*=8.2 Hz), 7.45–7.60 (4H, m), 7.89 (1H, s), 7.90 (1H, d, *J*=7.7 Hz), 8.08 (1H, d, *J*=7.8 Hz), 8.09 (1H, s). MS *m/z* (%): 390 (3, M⁺), 306 (82), 123 (100). HRMS *m/z*: 390.0782 (Calcd for C₁₈H₁₃F₃N₄O₂S: 390.0762). IR (KBr) cm⁻¹: 3450. Anal. Calcd for C₁₈H₁₃F₃N₄O₂S: C, 55.38; H, 3.36; N, 14.35; S, 8.21. Found: C, 55.43; H, 3.56; N, 14.42; S, 8.02.

Preparation of 2-(2,4-difluorophenyl)-1-(2-pyridyl)-3-(1H-1,2,4-triazol-1-yl)-2-propanol (8) A solution of *n*-BuLi (1.37 M solution in *n*-hexane; 10 mmol) was added to a solution of 2-methylpyridine (10.4 mmol) in THF (50 ml) with stirring at –78 °C under Ar atmosphere. The mixture was stirred at the same temperature for 0.5 h. A solution of 1-(2,4-difluorophenyl)-2-(1H-1,2,4-triazol-1-yl)ethanone (10 mmol) in THF (5 ml) was added to the solution with stirring at –78 °C and stirred at the same temperature for 1 h and at room temperature for 1 h. After addition of aqueous NH₄Cl, the mixture was extracted with AcOEt. The organic extract was washed with water and brine, dried over MgSO₄, and evaporated under reduced pressure. The residue was chromatographed on a silica gel column using AcOEt–*n*-hexane [1:8 (v/v)] to give 1.03 g of **8** (yield 32.5%) as a colorless oil.

¹H-NMR (CDCl₃) δ: 3.07 (1H, d, *J*=14.7 Hz), 3.55 (1H, d, *J*=14.7 Hz), 4.52 (1H, d, *J*=14.2 Hz), 4.67 (1H, d, *J*=14.2 Hz), 6.64–6.75 (2H, s), 7.01 (1H, d, *J*=7.8 Hz), 7.07 (1H, dd, *J*=4.4, 7.3 Hz), 7.35–7.45 (1H, m), 7.50 (1H, dd, *J*=7.3, 7.8 Hz), 7.81 (1H, s), 8.28 (1H, s), 8.34 (1H, d, *J*=4.4 Hz). MS *m/z* (%): 316 (0.3, M⁺), 234 (55), 141 (61), 93 (100). HRMS *m/z*: 316.1165 (Calcd for C₁₆H₁₅F₂N₄O: 316.1136). IR (KBr) cm⁻¹: 3300.

Antifungal in Vitro Activities of 1 The minimum inhibitory concentrations (MICs) of the compounds were determined by the National Committee for Clinical Laboratory Standards (NCCLS) M27-A broth microdilution method for yeasts and by the NCCLS M38-P for filamentous fungi. The compounds dissolved in DMSO (final concentration: 1%) were tested at different concentrations (from 64 to 0.016 μg/ml). *C. albicans* (ATCC 90028) and *C. krusei* (ATCC 6258) for yeast strains, and *A. flavus* (IFM 41935), *A. fumigatus* (IFM 40808), *T. mentagrophytes* (IFM 40769), and *T. rubrum* (IFO 6204) for filamentous fungi strains were used. The MICs were measured after 48 h (72 h for *Trichophyton* species) incubation at 35 °C (at 27 °C for *Trichophyton* species).

Acknowledgement We would like to thank M. Matsumoto, K. Mae-bash, and K. Ishida of SS Pharmaceutical Co., Ltd. Central Research Labs. for screening against yeasts and filamentous fungi.

References and Notes

- 1) a) Aoyama Y., Yoshida Y., Sato R., *J. Biol. Chem.*, **259**, 1661–1666 (1984), b) Hitchcock C. A., Dickinson K., Brown S. B., Evans E. G., Adams D. J., *Biochem. J.*, **266**, 475–480 (1990).
- 2) Lyman C. A., Walsh T. J., *Drugs*, **44**, 9–35 (1992).
- 3) Odds F. C., *J. Antimicrob. Agents Chemother.*, **31**, 463–471 (1993).
- 4) Fromiylng Robert A., Castaner J., *Drugs Future*, **21**, 266–271 (1996).
- 5) Fromiylng Robert A., Castaner J., *Drugs Future*, **21**, 160–166 (1995).
- 6) Naito T., Hata K., Tsuruoka A., *Drugs Future*, **21**, 20–24 (1996).
- 7) Yamada H., Tsuda T., Watanabe T., Ohashi M., Murakami K., Mochizuki H., *Antimicrob. Agents Chemother.*, **37**, 2412–2417 (1993).
- 8) Bartoli J., Yurmo E., Alguero M., Boncompte E., Vericat M. L., Conte L., Ramis J., Merlos M., Garcia-Rafanell J., Forn J., *J. Med. Chem.*, **41**, 1869–1882 (1998).
- 9) Tasaka A., Hayashi R., Kitazaki T., Tamura N., Tsutimori N., Matsusita Y., Hayashi R., Okonogi K., Itoh K., *Chem. Pharm. Bull.*, **45**, 321–326 (1997).
- 10) Filler R., Kobayashi Y., “Biomedical Aspects of Fluorine Chemistry,” Kodansha Ltd., Tokyo, Elsevier Biomedical Press, 1982.
- 11) Taguchi T., Kitagawa O., Morikawa T., Nishiwaki T., Uehara H., Endo H., Kobayashi Y., *Tetrahedron Lett.*, **27**, 6103–6106 (1986).
- 12) Sato K., Kawata R., Ama F., Omote M., Ando A., Kumadaki I., *Chem.*

- Pharm. Bull.*, **47**, 1013—1016 (1999).
- 13) a) Bridges A. J., Patt W. C., Stickney T. M., *J. Org. Chem.*, **55**, 773—775 (1990). b) Coe P. L., Waring A. J., Yawood T. D., *J. Chem. Soc., Perkin Trans. I*, **1995**, 2729—2737.
- 14) Tsukiyama T., Sato K., Japan Kokai Tokkyo Koho, JP 10-45735, Feb. 17, 1998; [*Chem. Abst.*, **128**, 140695 (1998)].
- 15) Richardson K., Brit. U. K. Patent Appl. GB 2099818, Dec. 15, 1982; [*Chem. Abst.*, **99**, 38467q (1983)].
- 16) Roger P., Andrew B., Christopher H., Subramaniyan N., Stephen R., Kenneth R., Peter T., *Bioorg. Med. Chem. Lett.*, **6**, 2031—2036 (1996).
- 17) PM3 calculation was performed using MOPAC on a Macintosh CAChe system: Stewart J. J. P., *J. Comput. Chem.*, **10**, 209—220 (1989).

An Androstane Bioside and 3'-Thiazolidinone Derivatives of Doubly-linked Cardenolide Glycosides from the Roots of *Asclepias tuberosa*

Fumiko ABE* and Tatsuo YAMAUCHI

Faculty of Pharmaceutical Sciences, Fukuoka University, 8-19-1 Nanakuma, Jonan-ku, Fukuoka 814-0180, Japan.

Received January 13, 2000; accepted March 7, 2000

Steroidal compounds in the roots of *Asclepias tuberosa* were investigated and 17 α -hydroxyandrosta-4,6,15-trien-3-one 17-*O*- α -L-arabinopyranosyl-(1 \rightarrow 6)- β -D-glucopyranoside, termed ascandroside, was isolated from the CHCl₃-soluble fraction. Among five doubly-linked cardenolide glycosides, two were identified as 3'-spiro-linked thiazolidinone (4) and *S*-oxythiazolidinone derivatives (5) of Δ^5 -calotropin. The stereochemistry at the C-3' in these two cardenolides is discussed. 3'-*O*- β -D-glucopyranosyl- Δ^5 -calotropin (3) was also isolated along with Δ^5 -calotropin and its 3'-acetate. Nine glycosides of uzarigenin, coroglaucigenin and corotoxigenin were identified.

Key words *Asclepias tuberosa*; androstane bioside; thiazolidinone-linked Δ^5 -calotropin; pleurisy root

While *Asclepias* is a genus known to contain cardenolides¹⁾ and the isolation of a large amount of glucofrugoside from the roots of *Asclepias tuberosa* L. has been described,²⁾ the roots have been called "pleurisy root" and used to treat pleurisy, bronchitis and other respiratory infections in the U.S.A. As part of a series of studies on the constituents of the Asclepiadaceae, we examined cardenolide glycosides from this plant material, in order to identify the type and the amount of cardiac glycosides present and investigate the biological effects of these substances on pleurisy. This paper deals with the isolation of an androstane glycoside and cardiac glycosides, including three unknown doubly-linked glycosides, from the roots of *A. tuberosa*.

An androstane glycoside termed ascandroside (1), showed a red spot on TLC following spraying with 10% H₂SO₄ and heating. The molecular formula of 1 was suggested to be C₃₀H₄₂O₁₁, based on high-resolution (HR)-FAB-MS. From the NMR spectra, 1 was suggested to be a bioside, based on two anomeric proton and carbon signals at δ 4.98 ($J=7$ Hz), 4.93 ($J=8$ Hz), and δ 105.3, 104.8, respectively. Upon acid hydrolysis, 1 afforded two sugars which were confirmed to be D-glucose and L-arabinose by GC of the thiazolidine derivatives,³⁾ although the isolation of the aglycone was unsuccessful. Since two 3H singlet signals were observed at δ 0.98 and

δ 1.16, as is usual for steroidal compounds, 1 was considered to be a bioside of a C-19-steroid.

The presence of a 4,6-dien-3-one system in 1 was suggested by the conjugated carbonyl carbon signal at δ 198.3 and the three olefinic proton signals at δ 5.86 (s), 6.12, 6.18 (each dd, $J=10$, 2 Hz) as well as the UV absorption at 283 nm. At a lower field, two disubstituted olefinic protons were observed at δ 6.06 (H-16, dt, $J=6$, 1 Hz) and 6.23 (H-15, ddd, $J=6$, 2, 1 Hz), which were coupled to the proton signal (H-17, δ 4.77, br s) attached to the oxygen-bearing carbon in the ¹H-¹H shift correlation spectroscopy (COSY) spectrum. Based on the small coupling constant ($J=6$ Hz) and connectivity from these olefin protons to three methine protons as δ 1.93 (H-14) \rightarrow 2.30 (H-8) \rightarrow 1.08 (H-9), the presence of a 15-en-17-ol system was suggested. The 4,6-dien-3-one and 15-en-17-ol systems in the androstane structure was further confirmed by cross peaks in the heteronuclear multiple bond connectivity (HMBC) spectrum between H-19/C-1, 5, 9, 10; H-1/C-2, 3, 10, 19; H-18/C-12, 13, 14, 17; and H-7/C-5, 8, 9, 14. The α -oriented hydroxy group at C-17 was assigned by the presence of a nuclear Overhauser effect (NOE) between H-17 and H-18. The proton signals due to H-18 and H-19 showed a response to H-8. The linkage of the sugar moiety was determined to be *via* a 17-*O*- α -L-arabi-

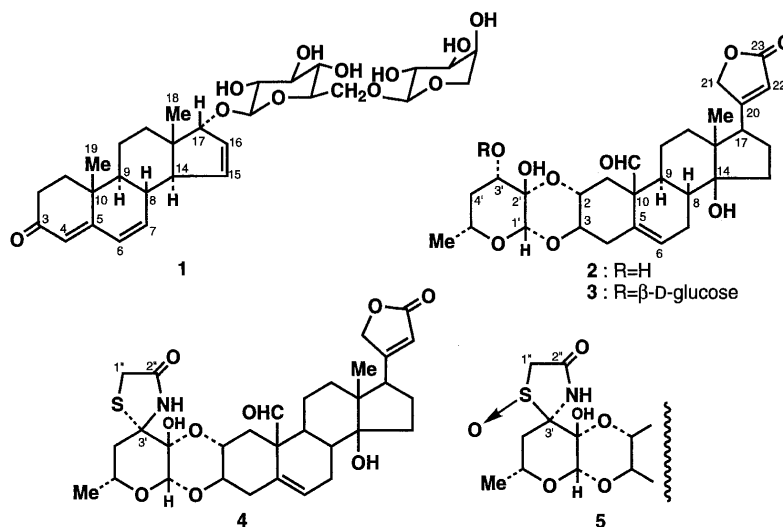


Chart 1

* To whom correspondence should be addressed. e-mail: abefumi@fukuoka-u.ac.jp

nosyl-(1→6)- β -D-glucoside, based on cross peaks between H-1_{ara}/C-6_{glc}, C-5_{ara}; H-1_{glc}/C-17; and H-17/C-1_{glc} in HMBC. The structure of **1** was, thus, established to be 17 α -hydroxy-androsta-4,6,15-trien-3-one 17-*O*- α -L-arabinopyranosyl-(1→6)- β -D-glucopyranoside.

The usual type of cardenolide glycosides, such as uzarigenin, corotoxigenin and coroglaucigenin, were isolated along with several cardenolides. They were all identified as known cardenolides and glycosides,⁴⁾ based on their NMR and FAB-MS data, and shown to be the glucoside and gentiobioside (uzarin) of uzarigenin, the glucoside and glucosyl-(1→4)-6-deoxyalloside of corotoxigenin, and the glucoside, gentiobioside, 6-deoxyalloside (frugoside), glucosyl-(1→4)-6-deoxyalloside (glucofrugoside)²⁾ and gentiobiosyl-(1→4)-6-deoxyalloside of coroglaucigenin. Of these, glucofrugoside and frugoside were the major glycosides. Of the five doubly-linked glycosides, two were identified as the already known 5,6-didehydrocalotropin (Δ^5 -calotropin, **2**) and its acetate.⁵⁾

Glycoside **3** was suggested to be a doubly-linked glycoside composed of **2** and one hexose, based on a $[M+Na]^+$ peak at m/z 715.2939 ($C_{35}H_{48}O_{14}+Na$). The signals due to **2** and glucose were identified by almost the same chemical shifts and multiplicities in the 1H - and ^{13}C -NMR spectra, except for the lower field shift of C-3'. The signals were also comparable with those of 3'-*O*-glucosylcalotropin^{1b)} over the range of shielding or deshielding affected by the Δ^5 -linkage in **3**. Since the anomeric proton of glucose (δ 5.24) showed an HMBC correlation to C-3' (δ 84.8), glucose was located at the 3'-hydroxy group. While the anomeric carbon of glucose was observed in the lower chemical shift (δ 108.0), and C-3' also showed remarkable deshielding (+10.9 ppm) with shielding of C-4' (-1.6 ppm) in comparison with those of **2**, the glucose was assigned to be one of the D-series.⁶⁾ Based on the coupling constant of the anomeric proton (d, $J=8$ Hz), the glycosidic linkage was assigned to be β . Glycoside **3** was, thus, determined to be Δ^5 -calotropin 3'-*O*- β -D-glucopyranoside.

Glycoside **4** afforded a $[M+Na]^+$ peak at m/z 624.2244, suggesting a molecular formula, $C_{31}H_{39}NO_9S$, including N and S as found in uscharin and voruscharin.^{1d)} The carbon and proton signals due to the cardenolide moiety in **4** were observed to have almost the same chemical shifts as those of **2** or **3**. In the ^{13}C -NMR spectrum, two signals at δ 32.9 and 175.1 seemed to be due to the thiazoline ring and assigned as methylene (C-1'') and carbonyl (C-2'') carbons, respectively. In the HMBC spectrum, the N-H proton at δ 10.21 showed a response to the methylene carbon at δ 32.9 and to C-3' (δ 72.7), while the methylene protons at δ 3.82 (2H, s, H-1'') showed a correlation to the carbonyl carbon at δ 175.1 and C-3'. Glycoside **4** was, therefore, appeared to link a thiazolidinone ring instead of the thiazoline ring in voruscharin.

In the HR-FAB-MS of **5**, a $[M+Na]^+$ peak at m/z 640.2202 suggested the formula, $C_{31}H_{39}NO_{10}S$, one oxygen greater than **4**. On comparing the 1H - and ^{13}C -signals with those of **4**, the cardenolide moiety in **5** seemed to have the same structure as **4**. The ^{13}C -signals of C-1'' and C-3' were deshielded as δ 55.8 and 83.5, respectively, suggesting that the extra oxygen forms an *S*-oxide. The strong absorbance at 1030 cm^{-1} in the IR spectrum also suggested the presence of an *S*-oxide. As observed in **4**, cross peaks showed a correlation between N-H/C-1'', C-2'', C-3' and H-1''/C-2'', C-3' in

Table 1. ^{13}C -NMR Spectral Data for **1**—**5** [δ ppm in Pyridine- d_5]

No.	1 ^{a)}	2	3 ^{b)}	4	5
1	33.9	35.5	35.6	35.6	35.1
2	34.3	68.9	68.8	70.1	69.5
3	198.3	72.0	72.0	71.3	71.5
4	124.1	33.7	33.6	33.4	33.2
5	163.1	140.6	140.7	140.7	140.6
6	128.2	120.9	120.9	120.9	120.9
7	140.3	29.6	29.5	29.5	29.4
8	35.0	44.9	44.9	44.9	44.7
9	51.2	38.8	38.9	38.8	38.7
10	36.2	52.3	52.4	52.3	52.3
11	20.4	23.7	23.7	23.7	23.7
12	35.5	38.8	38.8	38.9	38.7
13	52.4	50.7	50.7	50.8	50.7
14	54.8	84.4	84.3	84.4	84.3
15	135.5	39.5	39.5	39.6	39.5
16	130.0	27.9	27.9	28.0	27.9
17	91.4	50.7	50.6	50.6	50.6
18	13.2	16.1	16.1	16.1	16.0
19	16.1	206.6	206.7	206.4	206.3
20		175.2	175.3	175.3	175.2
21		73.6	73.6	73.6	73.6
22		117.9	117.8	117.9	117.9
23		174.3	174.3	174.3	174.3
1'		97.3	96.7	95.7	96.3
2'		92.7	92.7	93.0	92.6
3'		73.9	84.8	72.7	83.5
4'		39.9	38.3	46.8	35.4
5'		68.5	68.3	67.8	67.4
6'		21.5	21.3	21.3	21.2
1''				32.9	55.8
2''				175.1	171.9

a) 17-*O*-Glucosyl residue: 105.3 (C-1_{ara}), 104.8 (C-1_{glc}), 78.6 (C-3_{glc}), 77.2 (C-5_{glc}), 75.2 (C-2_{glc}), 74.3 (C-3_{ara}), 72.3 (C-2_{ara}), 71.8 (C-4_{glc}), 69.6 (C-6_{glc}), 69.1 (C-4_{ara}), 66.4 (C-5_{ara}). b) 3'-*O*-Glucosyl residue: δ 108.0 (C-1), 75.9 (C-2), 78.5 (C-3), 71.4 (C-4), 78.9 (C-5), 62.7 (C-6).

the HMBC spectrum.

In the difference (DIF)-NOE spectra of **4** and **5**, a response between H-1'/H-5' was observed for the two compounds. However, the H-1' signal showed a response in **4**, while the H-4' α in **5** required irradiation of the N-H proton (Chart 2). Therefore, the stereochemistry at C-3' was assigned as *S* in **4** and *R* in **5**. Although thiazoline or thiazolidine derivatives of doubly-linked cardenolide glycosides are known in *A. fruticosa*,^{1c,d)} **4** and **5** are the first the thiazolidinone derivatives. While all thiazoline or thiazolidine-linked glycosides, including uscharin and voruscharin, occur in the C-3'*S*-form, so far,^{1c,d)} the presence of the C-3'*R* isomer should be considered. Pregnane glycosides from the roots are described elsewhere.

Experimental

The melting points were determined on a hot-stage apparatus without correction. 1H - and ^{13}C -NMR spectra were recorded on a JNM-A500 spectrometer in pyridine- d_5 . Chemical shifts are given in δ values referred to the internal standard, tetramethylsilane (TMS), and the following abbreviations are used: s=singlet, d=doublet, t=triplet, q=quartet, m=multiplet, br=broad. HR-FAB-MS were recorded on a JEOL HX-110 spectrometer. Optical rotations were measured on a JASCO DIP 360 polarimeter. UV spectra were recorded on a Shimadzu 200S double beam spectrometer in MeOH and IR spectra were recorded on a JASCO FT/IR-230 in $CHCl_3$. GC was performed on a Shimadzu GC-17A. For silica gel column chromatography and TLC, the following solvent systems were used: $CHCl_3$ -MeOH-H₂O (bottom layer, solvent 1), EtOAc-MeOH-H₂O (top layer, solvent 2), benzene-acetone (solvent 3). For octadecyl silica (ODS) column chromatography and HPLC, MeCN-H₂O (solvent 4) was used. Spray reagent: a) 10% H₂SO₄, b)

Table 2. ^1H -NMR Spectral Data for 1–5 [δ ppm in Pyridine- d_5 , J in Hz]

No.	1 ^{a)}	2	3 ^{b)}	4	5
1	1.48 (m) 1.73 (m)	1.18 (t, 12) 2.51 (dd, 12, 5)	1.17 (t, 12) 2.55 (dd, 12, 5)	1.21 (t, 13) 2.64 (dd, 13, 5)	1.22 (t, 12) 2.36 (dd, 12, 5)
2		4.88 (m)	4.87 (m)	4.89 (m)	4.66 (m)
3		4.30 (m)	4.30 (m)	4.32 (m)	4.33 (m)
4	5.86 (s)				
6	6.12 (dd, 10, 2)	6.39 (br d, 3)	6.39 (br d, 4)	6.39 (br d, 5)	6.39 (br s)
7	6.18 (dd, 10, 2)				
8	2.30 (br t, 12)				
9	1.08 (ddd, 12, 10, 5)				
14	1.93 (ddd, 12, 2, 1)				
15	6.23 (ddd, 6, 2, 1)				
16	6.06 (dt, 6, 1)				
17	4.77 (br s)	2.81 (dd, 9, 6)	2.81 (dd, 9, 6)	2.84 (dd, 9, 6)	2.83 (dd, 9, 6)
18	1.16 (s)	0.88 (s)	0.89 (s)	0.88 (s)	0.87 (s)
19	0.98 (s)	9.88 (s)	9.88 (s)	9.83 (d, 1)	9.79 (d, 1)
21		5.04 (dd, 18, 1) 5.27 (dd, 18, 1)	5.05 (dd, 18, 2) 5.27 (dd, 18, 1)	5.05 (dd, 18, 2) 5.27 (dd, 18, 2)	5.05 (dd, 18, 2) 5.26 (dd, 18, 1)
22		6.15 (br s)	6.16 (br s)	6.17 (br s)	6.16 (br s)
1'		5.03 (s)	4.99 (s)	5.56 (s)	5.46 (s)
3'		4.13 (dd, 12, 5)	4.17 (dd, 12, 4)		
4'		2.03 (ddd, 12, 5, 2) 2.11 (br q, 12)	2.15 (br d, 12) 2.24 (br q, 12)	2.26 (dd, 13, 2) 2.56 (dd, 13, 12)	2.69 (dd, 14, 2) 2.40 (dd, 14, 11)
5'		3.74 (m)	3.68 (m)	4.49 (m)	4.29 (m)
6'		1.36 (d, 6)	1.30 (d, 6)	1.42 (d, 6)	1.37 (d, 6)
1''				3.82 (2H, s)	3.65 (d, 16) 4.60 (d, 16)

a) 17-*O*-Glycoside residue: δ 4.98 (d, $J=7$, H-1_{ara}), 4.93 (d, $J=8$, H-1_{glc}), 4.81 (dd, $J=11$, 2, H-6a_{glc}), 4.45 (dd, $J=9$, 7, H-2_{ara}), ca. 4.30 (H-6b_{glc}, H-4_{ara}, H-5a_{ara}), 4.20 (t, $J=9$, H-3_{glc}), 4.15 (dd, $J=9$, 3, H-3_{ara}), 4.14 (t, $J=9$, H-4_{glc}), 4.01 (dd, $J=9$, 8, H-2_{glc}), 4.10 (m, H-5_{glc}), 3.76 (dd, $J=13$, 3, H-5b_{ara}). b) 3'-*O*-Glucosyl residue: δ 5.24 (d, $J=8$, H-1), 4.57 (dd, $J=12$, 2, H-6a), 4.39 (dd, $J=12.5$, H-6b), 4.24 (t, $J=9$, H-3), 4.19 (t, $J=9$, H-4), 4.13 (dd, $J=8$, 9, H-2), 4.03 (m, H-5).

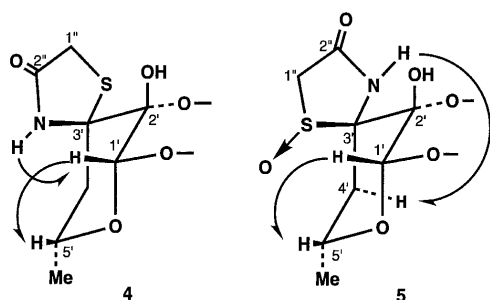


Chart 2. NOEs of 4 and 5

Kedde's reagent (1 : 1 mixture of 5% 3,5-dinitrobenzoic acid in MeOH and 2 N NaOH).

Extraction and Isolation The roots of *Asclepias tuberosa* L., collected in North Carolina in March, 1994, were purchased from Wilcox Natural Products, North Carolina. Powdered dried roots (4.5 kg) were percolated with MeOH. The concentrated MeOH extract was suspended in 50% MeOH and filtered. The filtrate was partitioned with benzene (extract 34.0 g) and then with CHCl_3 (4.5 g). The H_2O layer, after partition with CHCl_3 , was passed through an MCI-gel column (Mitsubishi Kasei Co., CHP-20P) and fractionated into five fractions (eluted with H_2O , 25%, 50%, 75%, and 100% MeOH, respectively). The CHCl_3 fraction and the 75% and 100% MeOH effluents of MCI-gel column chromatography were individually chromatographed on silica gel columns with solvents 1, 2, 3 and an ODS column or HPLC (ODS) with solvent 4, finally, to afford glycoside 1, uzarigenin (50 mg), coroglaucigenin (113 mg), calotropagenin (120 mg), coroglaucigenone-3-methyl-hemiacetal-3,19-epoxide (9 mg), uzarigenin glucoside (4.6 mg), uzarigenin gentiobioside (uzarin) (230 mg), corotoxigenin glucoside (8 mg), corotoxigenin glucosyl-(1 \rightarrow 4)-6-deoxyalloside (93 mg), coroglaucigenin glucoside (262 mg), coroglaucigenin 6-deoxyalloside (frugoside) (1 g), coroglaucigenin glucosyl-(1 \rightarrow 4)-6-deoxyalloside (glucofrugoside) (5.2 g), coroglaucigenin gentiobioside (45 mg), coroglaucigenin gentiobiosyl-(1 \rightarrow 4)-6-deoxyalloside (32 mg), Δ^5 -calotropin (2, 38 mg), Δ^5 -calotropin-3'-acetate (17 mg), glycoside 3 (14 mg), glycoside 4 (34 mg), and glycoside 5 (21 mg).

Ascandroside (1): mp 180–184 °C, $[\alpha]_D^{25} -58.7^\circ$ ($c=0.78$, MeOH), HR-FAB-MS m/z : 601.2624 (Calcd for $\text{C}_{30}\text{H}_{42}\text{O}_{11}+\text{Na}$: 601.2625), UV λ_{max} nm (log ϵ): 283 (4.04).

GC analysis: 1 (2 mg) was heated with 1 N HCl (0.5 ml) for 2 h, deacidified with IRA-410, and reacted with L-cystein methyl ester-HCl in pyridine, followed by trimethylsilylation: column Shimadzu DB-1 (0.25 mm \times 30 m), temperature column 250 °C, inj. 300 °C, detector 300 °C, carrier gas: He (30 cm/s), split ratio 1/40. t_R (min): 4.06, 6.37 (authentic specimen D-arabinose: 4.31, L-arabinose: 4.07, D-glucose: 6.37, L-glucose: 6.60).

Δ^5 -Calotropin 3'-*O*- β -D-glucopyranoside (3): mp 250–260 °C (dec.), $[\alpha]_D^{23} +38.5^\circ$ ($c=0.26$, MeOH), FAB-MS m/z : 715.2939 (Calcd for $\text{C}_{35}\text{H}_{48}\text{O}_{14}+\text{Na}$: 715.2931).

Δ^5 -Calotropin (3'*S*)-3'-thiazolidinone (4): mp 260–280 °C (dec.), $[\alpha]_D^{29} -9.6^\circ$ ($c=1.87$, MeOH), FAB-MS m/z : 624.2244 (Calcd for $\text{C}_{31}\text{H}_{39}\text{NO}_9\text{S}+\text{Na}$: 624.2243).

Δ^5 -Calotropin (3'*R*)-3'-thiazolidinone S-oxide (5): mp 240–245 °C (dec.), $[\alpha]_D^{26} +21.1^\circ$ ($c=1.07$, MeOH), FAB-MS m/z : 640.2202 (Calcd for $\text{C}_{31}\text{H}_{39}\text{NO}_{10}\text{S}+\text{Na}$: 640.2192). IR (CHCl_3) cm^{-1} : 3680, 3620, 1750, 1030.

Acknowledgments We thank Ms. Y. Iwase and Mr. H. Hanazono for obtaining NMR and MS spectra.

References

- a) Abe F., Mori Y., Yamauchi T., *Chem. Pharm. Bull.*, **39**, 2709–2711 (1991); *idem, ibid.*, **40**, 2917–2920 (1992); b) Abe F., Mori Y., Okabe H., Yamauchi T., *ibid.*, **42**, 1777–1783 (1994); c) Warashina T., Noro T., *Phytochemistry*, **37**, 217–226 (1994); d) Cheung H. T. A., Chiu F. C. K., Watson T. R., Wells R. J., *J. Chem. Soc. Perkin Trans 1*, **1983**, 2827–2835.
- Petricic J., *Arch. Pharm.*, **299**, 1007–1011 (1966).
- Hara S., Okabe H., Mihashi K., *Chem. Pharm. Bull.*, **35**, 501–505 (1987).
- Hill R. A., Kirk D. N., Makin H. L. J., Murphy G. M., "Dictionary of Steroids," Chapman & Hall, London, 1991.
- Cheung H. T. A., Nelson C. J., *J. Chem. Soc., Perkin Trans 1*, **1989**, 1563–1570.
- a) Kasai R., Suzuo M., Asakawa J., Tanaka O., *Tetrahedron. Lett.*, **1977**, 175–178; b) Tori K., Seo S., Yoshimura Y., Arita H., Tomita Y., *ibid.*, **1977**, 179–182.

Medicinal Foodstuffs. XVII.¹⁾ Fenugreek Seed. (3): Structures of New Furostanol-Type Steroid Saponins, Trigoneosides Xa, Xb, XIb, XIIa, XIIb, and XIIIa, from the Seeds of Egyptian *Trigonella foenum-graecum* L.

Toshiyuki MURAKAMI, Akinobu KISHI, Hisashi MATSUDA, and Masayuki YOSHIKAWA*

Kyoto Pharmaceutical University, Misasagi, Yamashina-ku, Kyoto 607–8414, Japan.

Received January 14, 2000; accepted March 21, 2000

Six new furostanol-type steroid saponins called trigoneosides Xa, Xb, XIb, XIIa, XIIb, and XIIIa were isolated from the seeds of Egyptian *Trigonella foenum-graecum* L. (Leguminosae) together with six known furostanol-type steroid saponins: trigoneosides Ia, Ib, and Va, glycoside D, trigonelloside C, and compound C. The structures of trigoneosides Xa, Xb, XIb, XIIa, XIIb, and XIIIa were determined on the basis of chemical and physicochemical evidence as 26-O- β -D-glucopyranosyl-(25S)-5 α -furostane-2 α ,3 β ,22 ξ ,26-tetraol 3-O- α -L-rhamnopyranosyl(1 \rightarrow 2)- β -D-glucopyranoside, 26-O- β -D-glucopyranosyl-(25R)-5 α -furostane-2 α ,3 β ,22 ξ ,26-tetraol 3-O- α -L-rhamnopyranosyl(1 \rightarrow 2)- β -D-glucopyranoside, 26-O- β -D-glucopyranosyl-(25R)-5 α -furostane-2 α ,3 β ,22 ξ ,26-tetraol 3-O- β -D-xylopyranosyl(1 \rightarrow 4)- β -D-glucopyranoside, 26-O- β -D-glucopyranosyl-(25S)-furost-4-ene-3 β ,22 ξ ,26-triol 3-O- α -L-rhamnopyranosyl(1 \rightarrow 2)- β -D-glucopyranoside, 26-O- β -D-glucopyranosyl-(25R)-furost-4-ene-3 β ,22 ξ ,26-triol 3-O- α -L-rhamnopyranosyl(1 \rightarrow 2)- β -D-glucopyranoside, and 26-O- β -D-glucopyranosyl-(25S)-furost-5-ene-3 β ,22 ξ ,26-triol 3-O- α -L-rhamnopyranosyl(1 \rightarrow 2)-[β -D-glucopyranosyl(1 \rightarrow 3)- β -D-glucopyranosyl(1 \rightarrow 4)]- β -D-glucopyranoside, respectively.

Key words *Trigonella foenum-graecum*; trigoneosides Xa—XIIIa; fenugreek; furostanol-type steroid saponin; adjuvant activity; trigonegenin A—B

Fenugreek (*Trigonella foenum-graecum* L., Leguminosae) has been widely cultivated in India, China, and Mediterranean countries. From ancient times, the seeds of this plant have been used not only as a spice or favorite food but also an antipyretic, laxative, and strengthening agent. In Chinese traditional medicine, the seeds (Japanese and Chinese name “胡蘆巴”) have been prescribed for tonic and stomachic purposes. In the course of our characterization studies on the bioactive constituents of medicinal foodstuffs,^{1,2)} we have reported the isolation of thirteen furostanol-type steroid saponins called trigoneosides Ia (7), Ib (8), IIa, IIb, IIIa, IIIb, IVa, Va (12), Vb, VI, VIIb, VIIIb, and IX from Indian fenugreek seeds and their structure elucidations.³⁾ Furthermore, we have examined the adjuvant and haemolytic activities of the saponin constituents from Indian fenugreek seeds. Among the saponin constituents, trigoneosides Ia (7), IIa, IIb, Va (12), and VI were found to show the antibody response in mice, but no haemolytic activity. Particularly, trigoneoside VI showed the potent adjuvant activity, which was stronger than quillaja saponin (QS-21).⁴⁾ As part of our continuing studies on fenugreek seeds, we have isolated six new furostanol-type steroid saponins called trigoneosides Xa (1), Xb (2), XIb (3), XIIa (4), XIIb (5), and XIIIa (6) from Egyptian fenugreek seeds. In this paper, we describe the structure elucidation of these trigoneosides (1–6) on the basis of chemical and physicochemical evidence.

The steroid saponin constituents of Egyptian fenugreek seeds were separated by the procedures shown in Chart 1. Thus, the methanolic extract from the seeds was subjected to Diaion HP-20 column chromatography to give the water-, the methanol-, and the acetone-eluted fractions. Next, the methanol-eluted fraction was separated with ordinary- and reversed-phase silica gel column chromatography and finally HPLC to afford trigoneosides Xa (1, 0.038%), Xb (2, 0.031%), XIb (3, 0.0026%), XIIa (4, 0.0071%), XIIb (5, 0.0059%), trigoneoside Ia (7, 0.0095%), trigoneoside Ib (8, 0.010%), glycoside D (9, 0.023%),

and XIIIa (6, 0.0075%) together with trigoneosides Ia³⁾ (7, 0.0095%), Ib³⁾ (8, 0.010%), and Va³⁾ (12, 0.030%), glycoside D⁵⁾ (9, 0.023%), trigonelloside C⁶⁾ (10, 0.0073%), and compound C⁷⁾ (11, 0.021%).

Trigoneoside Xa (1) was obtained as a white powder and was deduced to possess a furostanol structure based on TLC examination using the Ehrlich reagent.⁸⁾ The IR spectrum of 1 showed absorption bands at 3432, 1072, and 1044 cm^{−1} suggestive of oligoglycosidic structure. In the negative- and positive-ion FAB-MS of 1, quasimolecular ion peaks were observed at *m/z* 919 (M−H)[−] and *m/z* 943 (M+Na)⁺, respectively, and high-resolution MS analysis revealed the

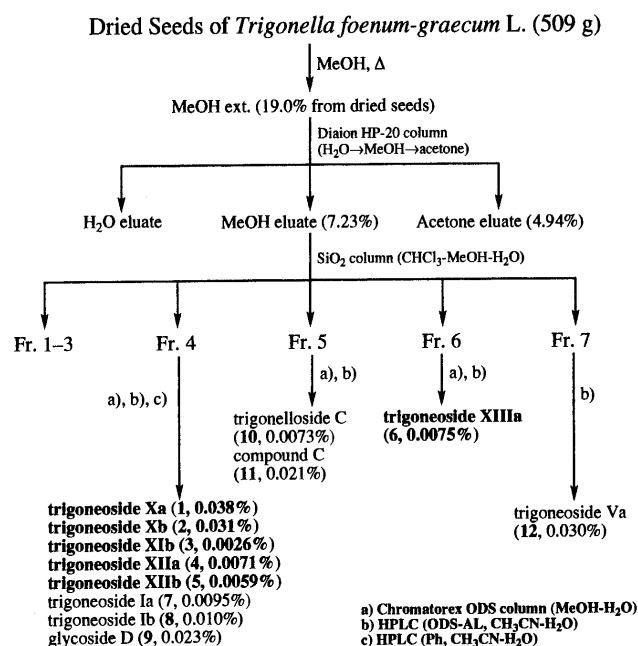


Chart 1

* To whom correspondence should be addressed. e-mail: shoyaku@mb.kyoto-phu.ac.jp

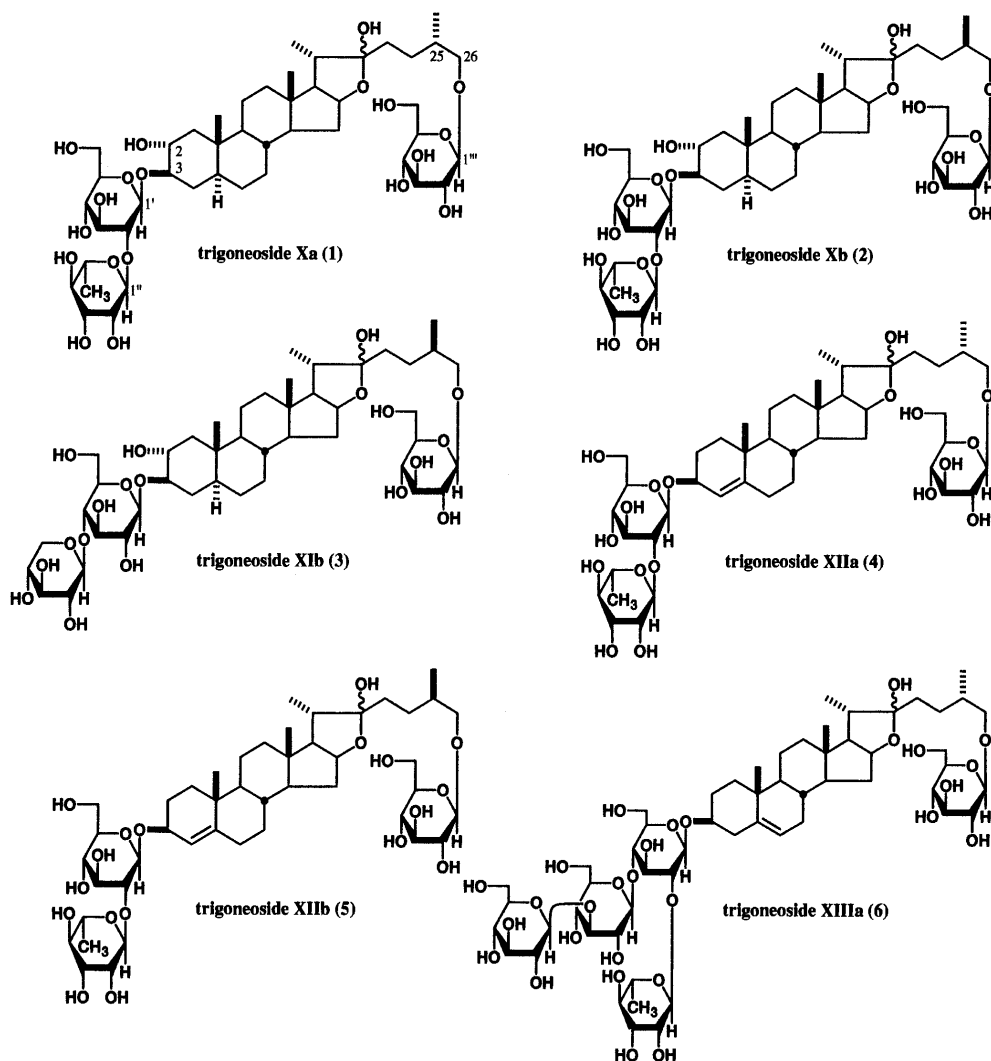


Chart 2

molecular formula of **1** to be $C_{45}H_{76}O_{19}$. Furthermore, fragment ion peaks at m/z 773 ($M-C_6H_{11}O_4$)⁻, m/z 757 ($M-C_6H_{11}O_5$)⁻, m/z 611 ($M-C_{12}H_{21}O_9$)⁻, and m/z 449 ($M-C_{18}H_{31}O_{14}$)⁻, which were derived by cleavage of the glycosidic linkage at the terminal deoxyhexose, hexose, and their diglycoside moieties, respectively, were observed in the negative-ion FAB-MS of **1**. Acid hydrolysis of **1** with 2 N hydrochloric acid (HCl)–1,4-dioxane (1:1, v/v) furnished neogitogenin (**13**)⁹ having 25*S*-configuration and gitogenin (**14**)¹⁰ having 25*R*-configuration in a 2:1 ratio. On the other hand, D-glucose and L-rhamnose, which were identified by GLC analysis of the thiazolidine derivative,¹¹ were obtained on acid hydrolysis of **1** with 5% aqueous sulfuric acid (H₂SO₄)–1,4-dioxane (1:1, v/v). Since 25*S*-steroidal aglycones were known to change to 25*R*-steroidal aglycones with acid treatment,³ the configuration at the 25-position of **1** was deduced to be *S*.

The ¹H-NMR (pyridine-*d*₅) and ¹³C-NMR (Table 1) spectra of **1**, which were assigned by various NMR analytical methods,¹² showed signals assignable to a 5α-furostane-2α,3β,22ξ,26-tetraol part [δ 0.86, 0.88 (both s, 18, 19-H₃), 1.01 (d, $J=6.2$ Hz, 27-H₃), 1.28 (d, $J=6.6$ Hz, 21-H₃), 3.47 (dd-like), 4.06 (m) (26-H₂), 3.86 (m, 3-H), 4.08 (m, 2-H), 4.90 (m, 16-H)], 3-*O*-β-D-glucopyranosyl moiety [δ 5.01 (d,

$J=7.0$ Hz, 1'-H)], 2'-*O*-α-L-rhamnopyranosyl moiety [δ 1.67 (d, $J=5.6$ Hz, 6''-H₃), 6.27 (br s, 1''-H)], and 26-*O*-β-D-glucopyranosyl moiety [δ 4.76 (d, $J=8.2$ Hz, 1'''-H)]. The 25*S*-configuration of **1** was confirmed by comparison of the 26-methylene signals for **1** with those for **7** and **8** in the ¹H-NMR spectrum.³ The carbon signals due to the sapogenol moiety in the ¹³C-NMR spectrum of **1** were superimposable on those of trigoneosides Ia (**7**) and IIa (**8**) having 5α-furostane-2α,3β,22ξ,26-tetraol 3,26-glycosidic structure.³ The 3,26-bisdesmoside structure of **1** was characterized by a heteronuclear multiple bond correlation (HMBC) experiment. Namely, long-range correlations were observed between the 1'-proton and the 3-carbon, between the 1''-proton and the 2'-carbon, and between the 1'''-proton and the 26-carbon. Consequently, the structure of trigoneoside Xa was elucidated to be 26-*O*-β-D-glucopyranosyl-(25*S*)-5α-furostane-2α,3β,22ξ,26-tetraol 3-*O*-α-L-rhamnopyranosyl-(1→2)-β-D-glucopyranoside (**1**).

Trigoneoside Xb (**2**), isolated as a white powder, was also deduced to possess a furostanol structure by the Ehrlich test. The IR spectrum of **2** was found similar to that of **1**. The negative- and positive-ion FAB-MS of **2** showed quasimolecular ion peaks at m/z 919 ($M-H$)⁻ and m/z 943 ($M+Na$)⁺, respectively, and fragment ion peaks at m/z 773

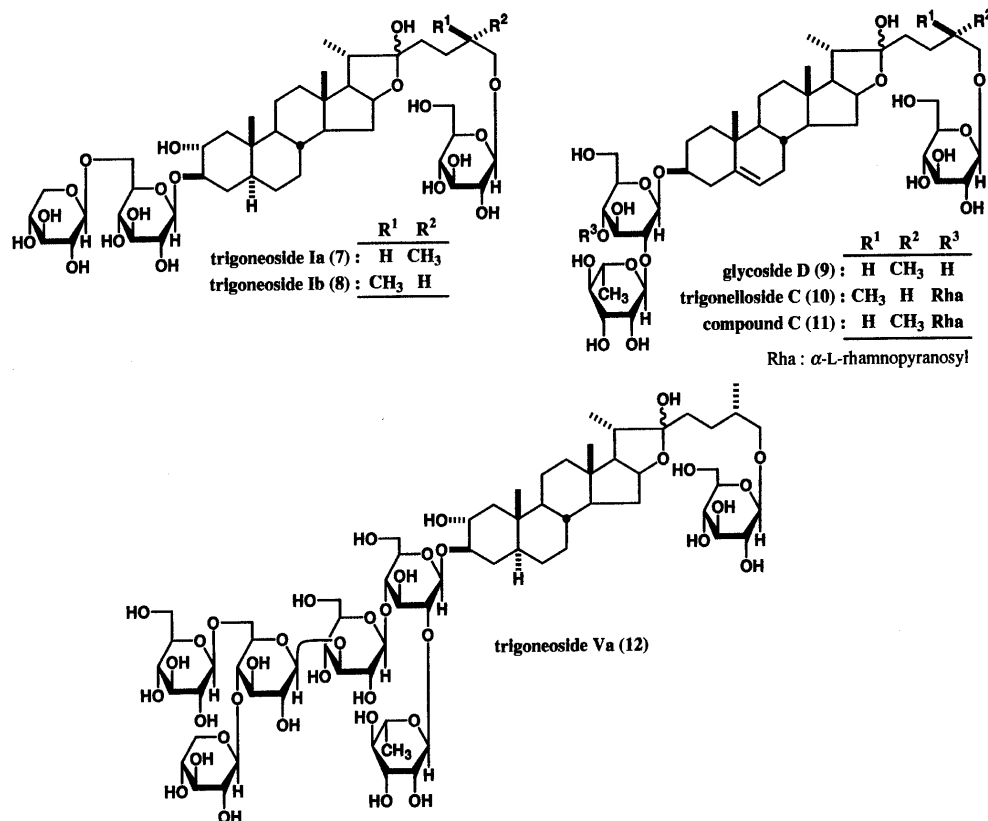


Chart 3

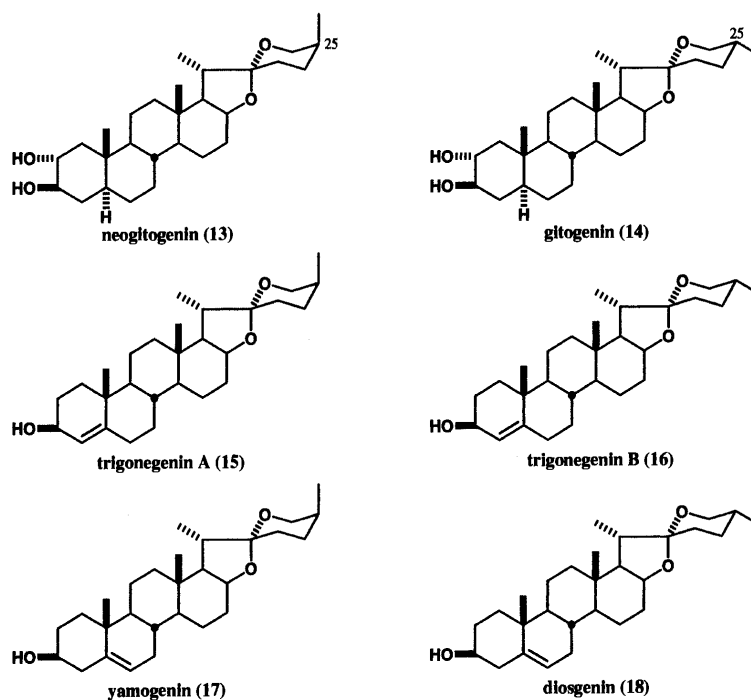


Chart 4

$(M-C_6H_{11}O_4)^-$, 757 $(M-C_6H_{11}O_5)^-$, 611 $(M-C_{12}H_{21}O_9)^-$, and 449 $(M-C_{18}H_{31}O_{14})^-$ were observed in the negative-ion FAB-MS of **2**. High-resolution MS analysis revealed the molecular formula of **2** to be $C_{45}H_{76}O_{19}$, which was the same as that of **1**. Acid hydrolysis of **2** with 2 N HCl-dioxane liberated gitogenin (**14**), while acid hydrolysis of **2** with 5% aqueous H_2SO_4 -dioxane furnished D-glucose and L-rhamnose.¹¹⁾

The 1H -NMR (pyridine- d_5) and ^{13}C -NMR (Table 1) spectra¹²⁾ of **2** were shown to be superimposable on those of **1**, except for the 26-protons [δ 3.61 (dd, $J=6.4, 9.2$ Hz), 3.96 (m)], which showed the 25*R*-configuration.³⁾ The 3,26-bisdesmoside structure of **2** was identified by a HMBC experiment, in which long-range correlations were observed between the 1''-proton and the 2'-carbon, between the 1'-proton and 3-

Table 1. ^{13}C -NMR Data for **1**—**6**, **15** and **16**

	1 ^{a)}	2 ^{a)}	3 ^{a)}	4 ^{a)}	5 ^{a)}	6 ^{a)}	15 ^{b)}	16 ^{b)}		1 ^{a)}	2 ^{a)}	3 ^{a)}	4 ^{a)}	5 ^{a)}	6 ^{a)}
C-1	45.8	45.8	45.8	35.8	35.8	37.6	35.4	35.4	C-1'	101.4	101.4	105.6	101.7	101.6	100.1
C-2	70.7	70.7	70.5	27.8	27.8	30.2	29.5	29.5	C-2'	78.1	78.1	74.7	78.2	78.3	77.3
C-3	85.6	85.6	85.2	75.5	75.5	78.4	67.9	67.9	C-3'	78.3	78.2	76.5	78.6	78.6	76.2
C-4	33.7	33.7	34.0	121.5	121.5	39.0	123.5	123.5	C-4'	71.9	72.0	80.9	72.1	72.0	81.5
C-5	44.7	44.8	44.8	147.2	147.3	140.9	147.4	147.4	C-5'	79.4	79.5	76.6	79.7	79.6	77.6
C-6	28.2	28.2	28.2	33.5	32.5	121.8	32.1	32.1	C-6'	62.6	62.6	61.8	62.9	62.9	61.7
C-7	32.3	32.3	32.3	32.6	33.5	32.4	33.2	33.2	C-1''	102.1	102.1	103.0	102.3	102.3	101.7
C-8	34.4	34.3	34.7	36.0	35.8	31.8	35.5	35.5	C-2''	72.4	72.4	75.0	72.5	72.6	72.4
C-9	54.5	54.5	54.6	54.7	54.7	50.5	54.4	54.4	C-3''	72.7	72.8	78.4	72.8	72.8	72.8
C-10	36.9	36.9	37.0	37.7	37.7	37.2	37.4	37.4	C-4''	74.1	74.1	70.8	74.1	74.1	74.2
C-11	21.5	21.5	21.5	21.1	21.1	21.2	20.9	20.8	C-5''	69.4	69.4	67.4	69.5	69.4	69.4
C-12	40.2	40.2	40.2	40.2	40.2	40.0	39.9	39.9	C-6''	18.5	18.8		18.6	18.6	18.6
C-13	41.1	41.2	41.2	41.1	41.1	40.8	40.4	40.4	C-1'''	105.0	104.9	104.9	105.1	104.9	104.5
C-14	56.3	56.4	56.4	56.2	56.2	56.7	56.0	56.0	C-2'''	75.1	75.2	75.2	75.2	75.2	73.7
C-15	32.3	32.4	32.4	32.4	32.4	32.5	31.8	31.8	C-3'''	78.5	78.5	78.6	78.5	78.6	88.3
C-16	81.1	81.1	81.2	81.1	81.1	81.2	80.8	80.8	C-4'''	71.8	71.8	71.9	71.8	71.7	69.4
C-17	63.9	64.0	64.0	63.9	63.9	63.9	62.1	62.1	C-5'''	78.2	78.2	78.4	78.3	78.4	78.4
C-18	16.7	16.7	16.7	16.7	16.7	16.5	16.3	16.4	C-6'''	62.9	62.9	63.0	62.9	62.9	61.8
C-19	13.5	13.5	13.5	18.9	18.9	19.4	18.9	19.0	C-1''''						105.8
C-20	40.7	40.7	40.7	40.8	40.7	40.7	42.1	41.6	C-2''''						75.2
C-21	16.4	16.3	16.4	16.4	16.4	16.4	14.3	14.5	C-3''''						78.3
C-22	110.6	110.6	110.7	110.7	110.7	110.7	109.7	109.2	C-4''''						71.8
C-23	37.1	37.1	37.2	37.1	37.2	37.2	25.9	31.4	C-5''''						78.6
C-24	28.4	28.4	28.4	28.3	28.4	28.3	25.8	28.8	C-6''''						62.6
C-25	34.7	34.7	34.3	34.4	34.3	34.4	27.1	30.3	C-1'''''						105.1
C-26	75.3	75.2	75.2	75.3	75.3	75.5	65.1	66.8	C-2'''''						75.2
C-27	17.4	17.4	17.5	17.5	17.5	17.4	16.1	17.1	C-3'''''						78.6
									C-4'''''						71.7
									C-5'''''						78.4
									C-6'''''						62.9

a) Pyridine- d_5 , b) CDCl_3 .

carbon, and between the 1'''-proton and the 26-carbon. Finally, by comparison of the NMR data for **2** with those for related furostanol saponins,³⁾ the structure of trigoneoside Xb was determined to be 26-*O*- β -D-glucopyranosyl-(25*R*)-5 α -furostane-2 α ,3 β ,22 ξ ,26-tetraol 3-*O*- α -L-rhamnopyranosyl-(1 \rightarrow 2)- β -D-glucopyranoside (**2**).

Trigoneoside XIb (**3**), isolated as a white powder, was positive in the Ehrlich test. Acid hydrolysis of **3** with 5% aqueous H_2SO_4 -dioxane liberated D-glucose and D-xylose,¹¹⁾ while gitogenin (**14**) was obtained by acid hydrolysis of **3** with 2*N* HCl-dioxane. The molecular formula $\text{C}_{44}\text{H}_{74}\text{O}_{19}\text{Na}$ of **3** was determined from the negative- and positive-ion FAB-MS and by high-resolution MS measurement. In the positive-ion FAB-MS of **3**, the quasimolecular ion peak was observed at m/z 929 ($\text{M}+\text{Na}$)⁺, while the negative-ion FAB-MS of **3** showed the quasimolecular ion peak at m/z 905 ($\text{M}-\text{H}$)⁻ in addition to fragment ion peaks at m/z 773 ($\text{M}-\text{C}_5\text{H}_9\text{O}_4$)⁻ and m/z 611 ($\text{M}-\text{C}_{11}\text{H}_{19}\text{O}_9$)⁻. The ^1H -NMR (pyridine- d_5) and ^{13}C -NMR (Table 1) spectra¹²⁾ of **3** indicated the presence of a (25*R*)-5 α -furostane-2 α ,3 β ,22 ξ ,26-tetraol part [δ 0.75, 0.87 (both s, 19, 18- H_3), 0.99 (d, $J=6.7$ Hz, 27- H_3), 1.31 (d, $J=7.0$ Hz, 21- H_3), 3.62, 3.93 (both m, 26- H_2), 3.84 (m, 3-H), 3.95 (m, 2-H), 4.92 (ddd-like, 16-H)], two β -D-glucopyranosyl parts [δ 5.01 (d, $J=7.6$ Hz, 1'-H), 4.79 (d, $J=7.6$ Hz, 1''-H)], and a β -D-xylopyranosyl part [δ 5.10 (d, $J=7.3$ Hz, 1'''-H)]. The carbon signals in the ^{13}C -NMR spectrum of **3** were very similar to those of **2** except for the 3-*O*-oligoglycoside structure. In the HMBC experiment of **3**, long-range correlations were observed between the following protons and carbons: 1''-H and 4'-C, 1'-H and 3-C, 1'''-H and

26-C. Those findings led us to formulate the structure of trigoneoside XIb as 26-*O*- β -D-glucopyranosyl-(25*R*)-5 α -furostane-2 α ,3 β ,22 ξ ,26-tetraol 3-*O*- β -D-xylopyranosyl-(1 \rightarrow 4)- β -D-glucopyranoside (**3**).

Trigoneosides XIIa (**4**) and XIIb (**5**), which were each isolated as a white powder, were positive in an Ehrlich test.⁷⁾ The IR spectra of **4** and **5** showed absorption bands due to hydroxyl groups. Trigoneosides XIIa (**4**) and XIIb (**5**) were found to have the same molecular formula $\text{C}_{45}\text{H}_{74}\text{O}_{18}$, which was determined from their negative- and positive-ion FAB-MS and by high-resolution MS measurement. Thus, in the positive-ion FAB-MS of **4** and **5**, the quasimolecular ion peak was observed at m/z 925 ($\text{M}+\text{Na}$)⁺, while the negative-ion FAB-MS showed the quasimolecular ion peak at m/z 901 ($\text{M}-\text{H}$)⁻ in addition to fragment ion peaks at m/z 755 ($\text{M}-\text{C}_6\text{H}_{11}\text{O}_4$)⁻, m/z 739 ($\text{M}-\text{C}_6\text{H}_{11}\text{O}_5$)⁻, m/z 593 ($\text{M}-\text{C}_{12}\text{H}_{21}\text{O}_9$)⁻, and m/z 431 ($\text{M}-\text{C}_{18}\text{H}_{31}\text{O}_{14}$)⁻. On acid hydrolysis of **4** and **5** with 5% aqueous H_2SO_4 -dioxane, D-glucose and L-rhamnose were detected in both cases. Enzymatic hydrolysis of **4** with naringinase gave a new spirostane-type aglycone termed trigonegenin A [25(*S*)-spirost-4-en-3 β -ol (**15**)], while 25*R*-stereoisomer called trigonegenin B (**16**)¹³⁾ was obtained by the enzymatic hydrolysis of **5**. The ^1H -NMR and ^{13}C -NMR (Table 1) spectra of **15** and **16** resembled those of yamogenin (**17**)^{6b,14)} and diosgenin (**18**)^{6b,14)} respectively, except for the signals due to the double bond. The 4-en-3 β -ol structures of **15**, **16**, **4**, and **5** were confirmed by various NMR experiments,¹²⁾ which included a ^1H - ^1H correlation between the 3-proton and the 4-proton in ^1H - ^1H COSY experiments on these compounds. The proton and carbon signals

due to the sugar moieties in the ^1H -NMR (pyridine- d_5) and ^{13}C -NMR (Table 1) spectra¹² of **4** and **5** were similar to those of **1** and **2**, and HMBC experiments on **4** and **5** showed long-range correlations between the following protons and carbons ($1''$ -H and $2'$ -C; $1'$ -H and 3 -C; $1'''$ -H and 26 -C). The proton signals assignable to the 26-methylene group [δ 3.48, 4.05 (both dd-like)] in the ^1H -NMR spectrum of **4** were very similar to those of **1**, while the 26-methylene signals [δ 3.63 (dd, $J=6.1$, 9.4 Hz), 3.92 (m)] of **5** were very similar to those of **2**. On the basis of the above evidence, the structures of trigoneosides XIIIa and XIIIb were formulated as 26- O - β -D-glucopyranosyl-(25*S*)-furost-4-ene-3 β ,22 ξ ,26-triol 3- O - α -L-rhamnopyranosyl(1 \rightarrow 2)- β -D-glucopyranoside (**4**) and its 25*R*-isomer (**5**).

Trigoneoside XIIIa (**6**) was found to have the molecular formula $\text{C}_{57}\text{H}_{94}\text{O}_{28}$, which was determined from the quasi-molecular ion peaks in the negative-ion [m/z 1225 ($\text{M}-\text{H}$) $^-$] and positive-ion [m/z 1249 ($\text{M}+\text{Na}$) $^+$] FAB-MS and by high-resolution MS measurement. Acid hydrolysis of **2** with 5% aqueous H_2SO_4 -dioxane liberated D-glucose and L-rhamnose, whereas yamogenin (**17**)^{6b,14} and diosgenin (**18**)^{6b,14} were obtained by acid hydrolysis of **2** with 2*N* HCl-dioxane. The ^1H -NMR (pyridine- d_5) spectrum¹² of **6** indicated the presence of the 26- O - β -D-glucopyranosyl-(25*S*)-furost-5-ene-3 β ,22 ξ ,26-triol part [δ 0.90, 1.06 (both s, 18, 19- H_3), 1.03 (d, $J=6.7$ Hz, 27- H_3), 1.31 (d, $J=6.7$ Hz, 21- H_3), 3.49, 4.06 (both dd-like, 26- H_2), 3.87 (dd-like, 3- H), 4.78 (d, $J=7.9$ Hz, $1'''$ -H), 4.93 (dd-like, 16-H), 5.30 (brs, 6-H)], three β -D-glucopyranosyl moieties [δ 4.91 (d, $J=5.8$ Hz, $1'$ -H), 5.05 (d, $J=8.0$ Hz, $1''$ -H), 5.22 (d, $J=6.7$ Hz, $1'''$ -H)], and an α -L-rhamnopyranosyl moiety [δ 1.74 (d, $J=6.1$ Hz, 6''- H_3), 6.17 (1H, brs, $1''$ -H)]. The 3,26-bisdesmoside structure of **6** was clarified by a HMBC experiment on **6**, which showed long-range correlations between the $1'''$ -proton and $3'''$ -carbon, between the $1'''$ -proton and the 4'-carbon, between the $1''$ -proton and the 2'-carbon, between the $1'$ -proton and 3-carbon, and between the $1'''$ -proton and the 26-carbon. Consequently, the structure of trigoneoside XIIIa was determined to be 26- O - β -D-glucopyranosyl-(25*S*)-furost-5-ene-3 β ,22 ξ ,26-triol 3- O - α -L-rhamnopyranosyl(1 \rightarrow 2)-[β -D-glucopyranosyl(1 \rightarrow 3)- β -D-glucopyranosyl(1 \rightarrow 4)]- β -D-glucopyranoside (**6**).

Experimental

The following instruments were used to obtain physical data: specific rotations, Horiba SEPA-300 digital polarimeter ($l=5$ cm); IR spectra, Shimadzu FTIR-8100 spectrometer; ^1H -NMR spectra, JNM-LA500 (500 MHz) spectrometer; ^{13}C -NMR spectra, JNM-LA500 (125 MHz) spectrometer with tetramethylsilane as an internal standard; MS and high-resolution MS, JEOL JMS-SX 102A mass spectrometer and JMS-GCMATE; HPLC, Shimadzu LC-10AS chromatograph.

The following experimental conditions were used for chromatography: normal-phase column chromatography; Silica gel BW-200 (Fuji Silysia Chemical, Ltd., 150–350 mesh), reversed-phase column chromatography; Chromatorex ODS DM1020T (Fuji Silysia Chemical, Ltd., 100–200 mesh); TLC, pre-coated TLC plates with Silica gel 60F₂₅₄ (Merck, 0.25 mm) (normal-phase) and Silica gel RP-18 60F₂₅₄ (Merck, 0.25 mm) (reversed-phase); HPTLC, pre-coated TLC plates with Silica gel RP-18 60WF₂₅₄ (Merck, 0.25 mm) (reversed-phase). Detection was done by spraying with 1% $\text{Ce}(\text{SO}_4)_2$ –10% aqueous H_2SO_4 , followed by heating.

Isolation of Trigoneosides Xa (1), Xb (2), XIb (3), XIIa (4), XIIb (5), and XIIIa (6) and Known Compounds (7–12) from the Seeds of *Trigonella foenum-graecum* L. The seeds of *Trigonella foenum-graecum* L. (506 g, cultivated in Egypt) were crushed and extracted three times with MeOH under reflux. Evaporation of the solvent under reduced pressure provided the MeOH extract (96.2 g, 19.0%), and the extract (90 g) was sub-

jected to Diaion HP-20 column chromatography [1 kg (Nippon Rensou Co.), $\text{H}_2\text{O} \rightarrow \text{MeOH} \rightarrow \text{acetone}$] to give the H_2O eluate, MeOH eluate (36.6 g, 7.23%) and acetone eluate (24.7 g, 4.94%). Normal-phase silica gel column chromatography [BW-200 (Fuji Silysia Ltd., 810 g), CHCl_3 – MeOH – H_2O (7:3:1, lower layer \rightarrow 65:35:10, lower layer) \rightarrow MeOH] of the MeOH eluate (27 g) gave seven fractions [fr. 1 (365.4 mg), fr. 2 (600.8 mg), fr. 3 (767.1 mg), fr. 4 (4.2 g), fr. 5 (11.1 g), fr. 6 (4.0 g), fr. 7 (5.3 g)]. Fraction 4 (4.0 g) was separated by reversed-phase silica gel column chromatography [Chromatorex DM1020T (Fuji Silysia, Ltd., 120 g), MeOH – H_2O (50:50 \rightarrow 60:40 \rightarrow 70:30, v/v) \rightarrow MeOH] and repeated HPLC [YMC-Pack ODS-AL (250 \times 20 mm i.d., YMC Co., Ltd.), CH_3CN – H_2O (25:75, v/v)] to give trigoneosides Xa (**1**, 191 mg, 0.038%), Xb (**2**, 183 mg, 0.031%), XIb (**3**, 13 mg, 0.0026%), XIIa (**4**, 38 mg, 0.0071%), and XIIb (**5**, 30 mg, 0.0059%), trigoneosides Ia (**7**, 48 mg, 0.0095%) and Ib (**8**, 51 mg, 0.010%), and glycoside D (**9**, 115 mg, 0.023%). Fraction 5 (10 g) was separated by reversed-phase silica gel column chromatography [Chromatorex DM1020T (300 g), MeOH – H_2O (50:50 \rightarrow 60:40 \rightarrow 70:30, v/v) \rightarrow MeOH] and purified by HPLC [YMC-Pack ODS-AL (250 \times 20 mm i.d.), 1) CH_3CN – H_2O (25:75, v/v); 2) CH_3CN – H_2O (30:70, v/v)] to give trigonelloside C (**10**, 37 mg, 0.0073%) and compound C (**11**, 104 mg, 0.021%). Fraction 6 (4.0 g) was separated by reversed-phase silica gel column chromatography [Chromatorex DM1020T (300 g), MeOH – H_2O (50:50 \rightarrow 60:40 \rightarrow 70:30, v/v) \rightarrow MeOH] and purified by HPLC [YMC-Pack ODS-AL (250 \times 20 mm i.d.), 1) CH_3CN – H_2O (25:75, v/v); 2) CH_3CN – H_2O (30:70, v/v)] to give trigoneoside XIIIa (**6**, 38 mg, 0.0075%). Fraction 7 (400 mg) was purified by HPLC [YMC-Pack ODS-AL (250 \times 20 mm i.d.), CH_3CN – H_2O (25:75, v/v)] to give trigoneoside Va (**12**, 152 mg, 0.030%). The known compounds (**7**–**12**) were identified by comparison of their physical data ($[\alpha]_D^{25}$, ^1H -NMR, ^{13}C -NMR) with reported values.^{3–6)}

Trigoneoside Xa (1): A white powder, $[\alpha]_D^{25} -49.2^\circ$ ($c=0.6$, MeOH). High-resolution positive-ion FAB-MS: Calcd for $\text{C}_{45}\text{H}_{76}\text{O}_{19}\text{Na}$ ($\text{M}+\text{Na}$) $^+$: 943.4879. Found: 943.4885. IR (KBr): 3432, 2932, 1072, 1044 cm^{-1} . ^1H -NMR (500 MHz, pyridine- d_5) δ : 0.86, 0.88 (3H each, both s, 18, 19- H_3), 1.01 (3H, d, $J=6.2$ Hz, 27- H_3), 1.28 (3H, d, $J=6.6$ Hz, 21- H_3), 1.67 (3H, d, $J=5.6$ Hz, 6''- H_3), 3.47 (1H, dd-like), 4.06 (1H, m) (26- H_2), 3.86 (1H, m, 3-H), 4.08 (1H, m, 2-H), 4.76 (1H, d, $J=8.2$ Hz, $1'''$ -H), 4.90 (1H, m, 16-H), 5.01 (1H, d, $J=7.0$ Hz, $1'$ -H), 6.27 (1H, brs, $1''$ -H). ^{13}C -NMR (125 MHz, pyridine- d_5) δ_C : given in Table 1. Negative-ion FAB-MS: m/z 919 ($\text{M}-\text{H}$) $^-$, 773 ($\text{M}-\text{C}_6\text{H}_{11}\text{O}_4$) $^-$, 757 ($\text{M}-\text{C}_6\text{H}_{11}\text{O}_5$) $^-$, 611 ($\text{M}-\text{C}_{12}\text{H}_{21}\text{O}_9$) $^-$, 449 ($\text{M}-\text{C}_{18}\text{H}_{31}\text{O}_{14}$) $^-$. Positive-ion FAB-MS: m/z 943 ($\text{M}+\text{Na}$) $^+$.

Trigoneoside Xb (2): A white powder, $[\alpha]_D^{25} -51.5^\circ$ ($c=0.6$, MeOH). High-resolution positive-ion FAB-MS: Calcd for $\text{C}_{45}\text{H}_{76}\text{O}_{19}\text{Na}$ ($\text{M}+\text{Na}$) $^+$: 943.4879. Found: 943.4885. IR (KBr): 3432, 2932, 1075, 1044 cm^{-1} . ^1H -NMR (500 MHz, pyridine- d_5) δ : 0.86, 0.88 (3H each, both s, 18, 19- H_3), 0.98 (3H, d, $J=6.7$ Hz, 27- H_3), 1.30 (3H, d, $J=7.0$ Hz, 21- H_3), 1.68 (3H, d, $J=6.4$ Hz, 6''- H_3), 3.61 (1H, dd, $J=6.4$, 9.2 Hz), 3.96 (1H, m) (26- H_2), 3.86 (1H, m, 3-H), 4.06 (1H, m, 2-H), 4.77 (1H, d, $J=7.6$ Hz, $1'''$ -H), 4.91 (1H, ddd-like, 16-H), 5.01 (1H, d, $J=7.6$ Hz, $1'$ -H), 6.27 (1H, d, $J=1.2$ Hz, $1''$ -H). ^{13}C -NMR (125 MHz, pyridine- d_5) δ_C : given in Table 1. Negative-ion FAB-MS: m/z 919 ($\text{M}-\text{H}$) $^-$, 773 ($\text{M}-\text{C}_6\text{H}_{11}\text{O}_4$) $^-$, 757 ($\text{M}-\text{C}_6\text{H}_{11}\text{O}_5$) $^-$, 611 ($\text{M}-\text{C}_{12}\text{H}_{21}\text{O}_9$) $^-$, 449 ($\text{M}-\text{C}_{18}\text{H}_{31}\text{O}_{14}$) $^-$. Positive-ion FAB-MS: m/z 943 ($\text{M}+\text{Na}$) $^+$.

Trigoneoside XIb (3): A white powder, $[\alpha]_D^{25} -24.7^\circ$ ($c=0.2$, MeOH). High-resolution positive-ion FAB-MS: Calcd for $\text{C}_{44}\text{H}_{74}\text{O}_{19}\text{Na}$ ($\text{M}+\text{Na}$) $^+$: 929.4722. Found: 929.4732. IR (KBr): 3432, 2926, 1076, 1044 cm^{-1} . ^1H -NMR (500 MHz, pyridine- d_5) δ : 0.75, 0.87 (3H each, both s, 19, 18- H_3), 0.99 (3H, d, $J=6.7$ Hz, 27- H_3), 1.31 (3H, d, $J=7.0$ Hz, 21- H_3), 3.62, 3.93 (1H each, both m, 26- H_2), 3.84 (1H, m, 3-H), 3.95 (1H, m, 2-H), 4.79 (1H, d, $J=7.6$ Hz, $1'''$ -H), 4.92 (1H, ddd-like, 16-H), 5.01 (1H, d, $J=7.6$ Hz, $1'$ -H), 5.10 (1H, d, $J=7.3$ Hz, $1''$ -H). ^{13}C -NMR (125 MHz, pyridine- d_5) δ_C : given in Table 1. Negative-ion FAB-MS: m/z 905 ($\text{M}-\text{H}$) $^-$, 773 ($\text{M}-\text{C}_5\text{H}_9\text{O}_4$) $^-$, 611 ($\text{M}-\text{C}_{11}\text{H}_{19}\text{O}_9$) $^-$. Positive-ion FAB-MS: m/z 929 ($\text{M}+\text{Na}$) $^+$.

Trigoneoside XIIa (4): A white powder, $[\alpha]_D^{25} -48.8^\circ$ ($c=0.6$, MeOH). High-resolution positive-ion FAB-MS: Calcd for $\text{C}_{45}\text{H}_{76}\text{O}_{18}\text{Na}$ ($\text{M}+\text{Na}$) $^+$: 925.4773. Found: 925.4776. IR (KBr): 3432, 2932, 1074, 1047 cm^{-1} . ^1H -NMR (500 MHz, pyridine- d_5) δ : 0.91, 1.07 (3H each, both s, 18, 19- H_3), 1.01 (3H, d, $J=7.2$ Hz, 27- H_3), 1.29 (3H, d, $J=6.7$ Hz, 21- H_3), 1.67 (3H, d, $J=5.8$ Hz, 6''- H_3), 3.48, 4.05 (1H each, both dd-like, 26- H_2), 4.48 (1H, dd-like, 3-H), 4.77 (1H, d, $J=7.6$ Hz, $1'''$ -H), 4.91 (1H, ddd-like, 16-H), 4.99 (1H, d, $J=7.6$ Hz, $1'$ -H), 5.81 (1H, brs, 4-H), 6.25 (1H, brs, $1''$ -H). ^{13}C -NMR (125 MHz, pyridine- d_5) δ_C : given in Table 1. Negative-ion FAB-MS: m/z 901 ($\text{M}-\text{H}$) $^-$, 755 ($\text{M}-\text{C}_6\text{H}_{11}\text{O}_4$) $^-$, 739 ($\text{M}-\text{C}_6\text{H}_{11}\text{O}_5$) $^-$, 593 ($\text{M}-\text{C}_{12}\text{H}_{21}\text{O}_9$) $^-$, 431 ($\text{M}-\text{C}_{18}\text{H}_{31}\text{O}_{14}$) $^-$. Positive-ion FAB-MS: m/z 925 ($\text{M}+\text{Na}$) $^+$.

Trigoneoside XIIb (5): A white powder, $[\alpha]_D^{22} -48.2^\circ$ ($c=0.5$, MeOH). High-resolution positive-ion FAB-MS: Calcd for $C_{45}H_{74}O_{18}Na$ ($M+Na$)⁺: 925.4773. Found: 925.4776. IR (KBr): 3432, 2932, 1071, 1048 cm^{-1} . ¹H-NMR (500 MHz, pyridine-*d*₅) δ : 0.92, 1.07 (3H each, both s, 18, 19-H₃), 0.99 (3H, d, $J=6.7$ Hz, 27-H₃), 1.32 (3H, d, $J=6.7$ Hz, 21-H₃), 1.68 (3H, d, $J=6.1$ Hz, 6''-H₃), 3.63 (1H, dd, $J=6.1$, 9.4 Hz), 3.92 (1H, m) (26-H₂), 4.49 (1H, ddd-like, 3-H), 4.78 (1H, d, $J=7.9$ Hz, 1'''-H), 4.92 (1H, ddd-like, 16-H), 4.99 (1H, d, $J=7.6$ Hz, 1'-H), 5.81 (1H, brs, 4-H), 6.23 (1H, brs, 1''-H). ¹³C-NMR (125 MHz, pyridine-*d*₅) δ_C : given in Table 1. Negative-ion FAB-MS: m/z 901 ($M-H$)⁻, 755 ($M-C_6H_{11}O_4$)⁻, 739 ($M-C_6H_{11}O_5$)⁻, 593 ($M-C_{12}H_{21}O_9$)⁻, 431 ($M-C_{18}H_{31}O_{14}$)⁻. Positive-ion FAB-MS: m/z 925 ($M+Na$)⁺.

Trigoneoside XIIIa (6): A white powder, $[\alpha]_D^{26} -31.4^\circ$ ($c=0.5$, MeOH). High-resolution positive-ion FAB-MS: Calcd for $C_{57}H_{94}O_{28}Na$ ($M+Na$)⁺: 1249.5829. Found: 1249.5817. IR (KBr): 3410, 2934, 1072, 1036 cm^{-1} . ¹H-NMR (500 MHz, pyridine-*d*₅) δ : 0.90, 1.06 (3H each, both s, 18, 19-H₃), 1.03 (3H, d, $J=6.7$ Hz, 27-H₃), 1.31 (3H, d, $J=6.7$ Hz, 21-H₃), 1.74 (3H, d, $J=6.1$ Hz, 6''-H₃), 3.49, 4.06 (1H each, both dd-like, 26-H₂), 3.87 (1H, dd-like, 3-H), 4.78 (1H, d, $J=7.9$ Hz, 1'''-H), 4.91 (1H, d, $J=5.9$ Hz, 1'-H), 4.93 (1H, dd-like, 16-H), 5.05 (1H, d, $J=8.0$ Hz, 1'''-H), 5.22 (1H, d, $J=6.7$ Hz, 1'''-H), 5.30 (1H, brs, 6-H), 6.17 (1H, brs, 1''-H). ¹³C-NMR (125 MHz, pyridine-*d*₅) δ_C : given in Table 1. Negative-ion FAB-MS: m/z 1225 ($M-H$)⁻. Positive-ion FAB-MS: m/z 1249 ($M+Na$)⁺.

Acid Hydrolysis of Trigoneosides 1–6 A solution of trigoneosides (1–6, 5 mg each) in 5% aqueous H₂SO₄–1,4-dioxane (1:1, v/v, 2 ml) was heated under reflux for 1 h. After cooling, the reaction mixture was neutralized with Amberlite IRA-400 (OH⁻ form) and the residue was removed by filtration. After removal of the solvent from the filtrate *in vacuo*, the residue was transferred to a Sep-Pak C₁₈ cartridge with H₂O and MeOH. The H₂O eluate was concentrated and the residue was treated with L-cysteine methyl ester hydrochloride (4 mg) in pyridine (0.5 ml) at 60 °C for 1 h. After reaction, the solution was treated with *N,O*-bis(trimethylsilyl)trifluoroacetamide (0.2 ml) at 60 °C for 1 h. The supernatant was then subjected to GLC analysis to identify the derivatives of D-glucose (i) from 1–6, D-xylose (ii) from 3, L-rhamnose (iii) from 1, 2, 4–6; GLC conditions: Supelco STBTM-1, 30 m×0.25 mm (i.d.) capillary column, column temperature 230 °C, He flow rate 15 ml/min, *t*_R: i (24.2 min), ii (15.4 min), iii (13.8 min).

Acid Hydrolysis of 1 Giving Neogitogenin (13) and Gitogenin (14) A solution of 1 (15 mg) in 2N HCl–dioxane (1:1, v/v, 4 ml) was heated under reflux for 1 h. After cooling, the reaction mixture was neutralized with Amberlite IRA-400 (OH⁻ form) and the insoluble portion was removed by filtration. After removal of the solvent *in vacuo* from the filtrate, the crude product (15 mg) was purified by normal-phase silica gel column chromatography [1 g, *n*-hexane–AcOEt (1:1)] to give neogitogenin (13, 4.0 mg, 54.1%) and gitogenin (14, 2.1 mg, 28.4%), which were identified by comparison of their physical data ($[\alpha]_D$, ¹H-NMR, ¹³C-NMR) with those of authentic samples.³⁾

Acid Hydrolysis of 2 Giving 14 A solution of 2 (15 mg) in 2N HCl–dioxane (1:1, v/v, 4 ml) was heated under reflux for 1 h. After cooling, the reaction mixture was neutralized with Amberlite IRA-400 (OH⁻ form) and the insoluble portion was removed by filtration. After removal of the solvent *in vacuo* from the filtrate, the crude product (15 mg) was purified by normal-phase silica gel column chromatography [1 g, *n*-hexane–AcOEt (1:1)] to give gitogenin (14, 4.4 mg, 88.7%), which was identified by comparison of the physical data ($[\alpha]_D$, ¹H-NMR, ¹³C-NMR) with those of an authentic sample.³⁾

Acid Hydrolysis of 3 Giving 14 A solution of 3 (10 mg) in 2N HCl–dioxane (1:1, v/v, 4 ml) was heated under reflux for 1 h. After cooling, the reaction mixture was neutralized with Amberlite IRA-400 (OH⁻ form) and the insoluble portion was removed by filtration. After removal of the solvent *in vacuo* from the filtrate, the crude product (10 mg) was purified by normal-phase silica gel column chromatography [1 g, *n*-hexane–AcOEt (1:1)] to give gitogenin (14, 1.9 mg, 76.0%), which was identified by comparison of the physical data ($[\alpha]_D$, ¹H-NMR, ¹³C-NMR) with those of an authentic sample.³⁾

Enzymatic Hydrolysis of Trigoneoside XIIa (4) Giving Trigonegenin A (15) A solution of 4 (10 mg) in 0.2M acetate buffer (pH 4.0, 4 ml) added with naringinase (Sigma Chemical Co., Ltd., 15 mg) was stirred at 40 °C for 10 h. After EtOH was added to the reaction mixture, the solvent was removed *in vacuo*. The crude product was purified by normal-phase silica gel column chromatography [3 g, CHCl₃–MeOH–H₂O (30:3:1, lower layer)] to give trigonegenin A (15, 2.1 mg, 46.7%), which was identified by comparison of physical data ($[\alpha]_D$, ¹H-NMR, ¹³C-NMR) with reported values.¹³⁾

Trigonegenin A (15): A white powder, $[\alpha]_D^{25} +16.2^\circ$ ($c=0.1$, CHCl₃).

High-resolution EI-MS: Calcd for $C_{27}H_{42}O_3$ (M^+): 414.3134. Found: 414.3137. IR (KBr): 3474, 1098, 1028, 803 cm^{-1} . ¹H-NMR (500 MHz, CDCl₃) δ : 0.79, 1.06 (3H each, both s, 18, 19-H₃), 0.99 (3H, d, $J=6.7$ Hz, 21-H₃), 1.08 (3H, d, $J=7.0$ Hz, 27-H₃), 3.29, 3.95 (1H each, both d, $J=11.3$ Hz, 26-H₂), 4.14 (1H, brs, 3-H), 4.39 (1H, dd-like, 16-H), 5.28 (1H, brs, 4-H). ¹³C-NMR (125 MHz, CDCl₃) δ_C : given in Table 1. EI-MS: m/z 414 (M^+).

Enzymatic Hydrolysis of 5 Giving Trigonegenin B (16) A solution of 5 (10 mg) in 0.2M acetate buffer (pH 4.0, 4 ml) added with naringinase (Sigma Chemical Co., Ltd., 15 mg) was stirred at 40 °C for 10 h. After EtOH was added to the reaction mixture, the solvent was removed *in vacuo*. The crude product was purified by normal-phase silica gel column chromatography [3 g, CHCl₃–MeOH–H₂O (30:3:1, lower layer)] to give 16 (1.9 mg, 42.2%), which was identified by comparison of physical data ($[\alpha]_D$, ¹H-NMR, ¹³C-NMR) with reported values.¹³⁾

Trigonegenin B (16): A white powder, $[\alpha]_D^{25} -17.6^\circ$ ($c=0.1$, CHCl₃). High-resolution EI-MS: Calcd for $C_{27}H_{42}O_3$ (M^+): 414.3134. Found: 414.3130. IR (KBr): 3474, 1065, 1053, 808 cm^{-1} . ¹H-NMR (500 MHz, CDCl₃) δ : 0.79, 1.06 (3H each, both s, 18, 19-H₃), 0.79 (3H, d, $J=4.3$ Hz, 27-H₃), 0.96 (3H, d, $J=6.8$ Hz, 21-H₃), 3.37 (1H, m), 3.47 (1H, dd-like) (26-H₂), 4.14 (1H, brs, 3-H), 4.37 (1H, dd-like, 16-H), 5.28 (1H, brs, 4-H). ¹³C-NMR (125 MHz, CDCl₃) δ_C : given in Table 1. EI-MS: m/z 414 (M^+).

Acid Treatment of 6 Giving Yamogenin (17) and Diosgenin (18) A solution of 6 (15 mg) in 2N HCl–dioxane (1:1, v/v, 4 ml) was heated under reflux for 1 h. After cooling, the reaction mixture was neutralized with Amberlite IRA-400 (OH⁻ form) and the insoluble portion was removed by filtration. After removal of the solvent *in vacuo* from the filtrate, the crude product (15 mg) was purified by normal-phase silica gel column chromatography [1 g, *n*-hexane–AcOEt (1:1)] to give 17 (3.0 mg, 58%) and 18 (1.4 mg, 27%), which were identified by comparison of physical data ($[\alpha]_D$, ¹H-NMR, ¹³C-NMR) with reported values.^{6b,14)}

References

- 1) Part XVI: Murakami T., Matsuda H., Inadzuki M., Hirano K., Yoshikawa M., *Chem. Pharm. Bull.*, **47**, 1717–1724 (1999).
- 2) a) Matsuda H., Li Y., Murakami T., Yamahara J., Yoshikawa M., *Eur. J. Pharmacol.*, **368**, 237–243 (1999); b) Matsuda H., Li Y., Yoshikawa M., *Life Sci.*, **65**, PL27–32 (1999); c) Matsuda H., Li Y., Murakami T., Yamahara J., Yoshikawa M., *Bioorg. Med. Chem.*, **7**, 323–327 (1999); d) Matsuda H., Li Y., Yamahara J., Yoshikawa M., *J. Pharmacol. Exp. Ther.*, **289**, 729–734 (1999); e) Matsuda H., Li Y., Yoshikawa M., *Eur. J. Pharmacol.*, **373**, 63–70 (1999); f) Matsuda H., Shimoda H., Yoshikawa M., *Bioorg. Med. Chem.*, **7**, 1445–1450 (1999); g) Matsuda H., Li Y., Yoshikawa M., *ibid.*, **7**, 1737–1741 (1999); h) Matsuda H., Shimoda H., Yamahara J., Yoshikawa M., *Biol. Pharm. Bull.*, **22**, 870–872 (1999); i) Matsuda H., Murakami T., Yashiro K., Yamahara J., Yoshikawa M., *Chem. Pharm. Bull.*, **47**, 1725–1729 (1999); j) Matsuda H., Shimoda H., Uemura T., Yoshikawa M., *Bioorg. Med. Chem. Lett.*, **9**, 2647–2652 (1999); k) Murakami T., Nakamura J., Matsuda H., Yoshikawa M., *Chem. Pharm. Bull.*, **47**, 1759–1764 (1999); l) Matsuda H., Li Y., Yoshikawa M., *Life Sci.*, **66**, PL41–46 (2000); m) Li Y., Wen S., Yamahara J., Yoshikawa M., *Eur. J. Pharmacol.*, **387**, 339–344 (2000).
- 3) a) Yoshikawa M., Murakami T., Komatsu H., Murakami N., Yamahara J., Matsuda H., *Chem. Pharm. Bull.*, **45**, 81–87 (1997); b) Yoshikawa M., Murakami T., Komatsu H., Yamahara J., Matsuda H., *Heterocycles*, **47**, 397–405 (1998).
- 4) Oda K., Matsuda H., Murakami T., Katayama S., Ohgitali T., Yoshikawa M., *Biol. Chem.*, **381** (2000), in press.
- 5) Watanabe Y., Sanada S., Ida Y., Shoji J., *Chem. Pharm. Bull.*, **31**, 3486–3495 (1983).
- 6) a) Bogacheva N. G., Kiselev V. P., Kogan L. M., *Khim. Priro. Soedin.*, **2**, 268–269 (1976) [*Chem. Abstr.*, **85**, 106634e (1976)]; b) Aquino R., Behar I., Simone F., Dagastino M., Pizzia C., *J. Nat. Prod.*, **49**, 1096–1101 (1986).
- 7) a) Kawasaki T., Komori T., Miyahara K., Nohara T., Hosokawa I., Mihashi K., *Chem. Pharm. Bull.*, **22**, 2164–2175 (1974); b) Kamel M. S., Ohtani K., Kurokawa T., Assaf M. H., El-Shanawany M. A., Ali A. A., Kasai R., Ishibashi S., Tanaka O., *ibid.*, **39**, 1229–1233 (1991).
- 8) Kiyosawa S., Hutoh M., Komori T., Nohara T., Hosokawa I., Kawasaki T., *Chem. Pharm. Bull.*, **16**, 1162–1164 (1968).
- 9) Achenbach H., Hubner H., Brandt W., Reiter S., *Phytochemistry*, **35**, 1527–1543 (1994).
- 10) a) Pataki J., Rosenkranz G., Djerassi C., *J. Am. Chem. Soc.*, **73**,

- 5375—5377 (1951); b) Jain D. C., *Phytochemistry*, **26**, 1789—1790 (1987).
- 11) Hara S., Okabe H., Mihashi K., *Chem. Pharm. Bull.*, **34**, 1843—1845 (1986).
- 12) The ^1H - and ^{13}C -NMR spectra of **1**—**6** were assigned with the aid of homo- and hetero-correlation spectroscopy (^1H — ^1H , ^1H — ^{13}C COSY), distortionless Hartmann–Hahn spectroscopy (^1H — ^1H , ^1H — ^{13}C HO-HAHA), and HMBC experiments.
- 13) a) The 1-tritium-3-acetyl derivative of **16** was reported on the synthesis from diosgenin (**18**),^{13b)} but the physical data was not cited; b) Takeda K., Minato H., Shimaoka A., Nagasaki T., *J. Chem. Soc., Perkin Trans 1*, **7**, 957—962 (1972).
- 14) Seo S., Tori K., Uomori A., Yoshimura Y., *J. Chem. Soc. Chem. Comm.*, **1981**, 895—897.

Stilbenoids Isolated from Stem Bark of *Shorea hemsleyana*

Tetsuro ITO,^a Toshiyuki TANAKA,^{*a} Yoshimi IDO,^a Ken-ichi NAKAYA,^a Munekazu INUMA,^a and Soedarsono RISWAN^b

Gifu Prefectural Institute of Health and Environmental Sciences,^a 1–1 Naka-fudogaoka, Kakamigahara 504–0838, Japan and Herbarium Bogoriense, The Indonesian Institute of Science, Research and Development Center for Biology,^b Jl Ir. Juanda 18, Bogor 16122, Indonesia. Received January 20, 2000; accepted March 7, 2000

Two new stilbene glucosides [(+)- α -viniferin 13b-O- β -glucopyranoside and resveratrol 12-C- β -glucopyranoside] and two new resveratrol oligomers, hemsleyanols A and B, were isolated from the bark of *Shorea hemsleyana* along with four known resveratrol oligomers. The structures of the isolates, including the relative configurations, were established by spectroscopic data involving long-range coupling and nuclear Overhauser effect experiments.

Key words *Shorea hemsleyana*; Dipterocarpaceae; stilbene; resveratrol oligomer; structure elucidation

Many stilbene derivatives have been isolated from various plants, and their biological effects, such as chemopreventive activity,¹⁾ anti-inflammatory activity,²⁾ inhibition of histamine release³⁾ and gastric ATPase⁴⁾ have been reported. Stilbenoids are, therefore, useful lead compounds for drug development. Plants belonging to the family Dipterocarpaceae are known to be good sources of a variety of stilbenoids.^{5,6)} In our search for bioactive compounds, phytochemical investigation of the stem bark of *Shorea hemsleyana* (Dipterocarpaceae) has been undertaken. We now report the isolation and structure elucidation of four new stilbene derivatives, (+)- α -viniferin-13b-O- β -glucopyranoside (**2**), hemsleyanols A (**3**) and B (**4**) and resveratrol-12-C- β -glucopyranoside (**5**), along with four known stilbenoids [(+)- α -viniferin (**1**), davidiol A (**6**), (–)-hopeaphenol (**7**) and (+)-isohopeaphenol (**8**)].

Compound **2** was obtained as a pale yellow amorphous solid, $[\alpha]_D^{24} +32^\circ$. The negative ion FAB-MS exhibited an $[M-H]^-$ ion peak at m/z 839 indicating its molecular weight to be 840 and an ion peak at m/z 677 $[M-H-162]^-$. The high-resolution (HR) negative FAB-MS at m/z 839.2327 showed that the molecular formula of **2** was $C_{48}H_{40}O_{14}$. The 1H - and ^{13}C -NMR spectral data (Tables 1 and 2) of **2** showed signals similar to those of **1**, except for the presence of a β -glucopyranosyl moiety [δ 5.02 (1H, d, $J=7.3$ Hz, H-1) and δ 101.9, 78.0, 77.8, 74.8, 71.5 and 62.8]. Acid hydrolysis of **2** with H_2SO_4 in MeOH gave (+)- α -viniferin. These results indicated that **2** was a β -glucopyranoside of **1**.²⁾ To confirm the location of the glucosidic linkage, the 1H - and ^{13}C -NMR signals were assigned by 1H - 1H shift correlation spectroscopy (COSY), 1H - ^{13}C long-range COSY (H–H long-range COSY), ^{13}C - 1H shift correlation spectroscopy (CH-COSY) and correlation spectroscopy involving long-range coupling (COLOC) spectra ($J=8$ Hz) (Fig. 2). In the nuclear Overhauser effect (NOE) experiment, the aromatic protons (δ 6.45 and δ 6.85) assignable to H-12b and H-14b were enhanced when the anomeric proton (δ 5.02) was irradiated. Therefore, the glucosyl moiety should be attached to C-13b of **1**. Consequently, the structure of **2** was concluded to be (+)- α -viniferin-13b-O- β -glucopyranoside.

Compound **3** (hemsleyanol A), obtained as a yellow amorphous powder, showed a positive reaction to Gibbs reagent. The compound gave an $[M-H]^-$ ion peak at m/z 469 in negative ion FAB-MS, corresponding to the molecular formula $C_{28}H_{22}O_7$, which suggested that **3** is a stilbene dimer. Methy-

lation of **3** yielded a pentamethyl ether (**3a**) which further afforded a monoacetate (**3b**), suggesting that **3** has one alcoholic hydroxyl and five phenolic groups. Thus, the remaining oxygen was attributed to an ether linkage in **3**. The 1H -NMR spectrum (Table 1) showed the presence of two sets of *ortho*-coupled aromatic protons assignable to two 4-hydroxyphenyl groups [δ 7.48 (2H, d, $J=8.3$ Hz, H-2a, 6a) and 6.94 (2H, d, $J=8.3$ Hz, H-3a, 5a); δ 6.72 (2H, d, $J=8.3$ Hz, H-2b, 6b) and 6.48 (2H, d, $J=8.3$ Hz, H-3b, 5b), two sets of *meta*-coupled aromatic protons on a 1,2,3,5-tetrasubstituted benzene ring [δ 6.24 (1H, brs, H-12a) and 6.23 (1H, brs, H-14a); δ 6.04 (1H, d, $J=2.0$ Hz, H-12b) and 5.70 (1H, d, $J=2.0$ Hz, H-14b)], an alcoholic hydroxyl group [δ 4.45 (brs)] and five phenolic hydroxyl groups [δ 8.63, 7.91 ($\times 2$), 8.01 and 8.02] in addition to two sets of mutually coupled aliphatic protons [δ 5.75 (1H, d, $J=9.8$ Hz, H-7a), 5.41 (1H, d, $J=9.8$ Hz, H-8a); δ 5.07 (1H, d, $J=5.9$ Hz, H-7b), 4.76 (1H, br d, H-8b)]. The CH-COSY spectrum gave the complete assignment of all protonated carbons as shown in Table 2. In the H–H long-range COSY spectrum, the oxymethine proton (H-7a) had a correlation with H-2a (6a) on ring A1, and H-8a had a correlation with H-14a on ring A2. In the COLOC spectrum (Fig. 3), significant correlations were observed between C-2a(6a)/H-7a, C-8a/H-14a, C-9a/H-7a, C-10b/H-8a, C-10b/H-12b and C-11b/H-8a, respectively. These results indicated that one set of benzylic methine protons (H-7a and H-8a) was assigned to the protons on a dihydrofuran ring. On the other hand, the H–H long-range COSY spectrum showed that the aliphatic hydroxyl proton at δ 4.45 was coupled with H-8b, the signal of which underwent a low-field shift in the 1H -NMR spectrum of **3b** and a hexa-acetate (**3c**), indicating the presence of a secondary alcohol substituent at C-8b. In the COLOC spectrum, long-range correlations were observed between C-11a/H-7b, C-10b/H-8b C-2b(6b)/H-7b and C-9b/OH-8b. From the above results, the planar structure of **3** could be depicted as in Fig. 3. The relative stereochemistry was substantiated by means of NOE spectrum (Fig. 4). NOEs between H-7a/H-14a, H-8a/H-2a(6a) and H-8b/H-2b(6b) in **3** indicated that both methine protons on the dihydrofuran ring (7a and 8a) and the remaining two methine protons (7b and 8b) were *trans*. NOEs were also observed between H-8a and the protons attributed to the acetyl group in **3b**. Consequently, the relative stereochemistry of **3** was confirmed as shown in Fig. 4. Previously, two resveratrol dimers having a

* To whom correspondence should be addressed.

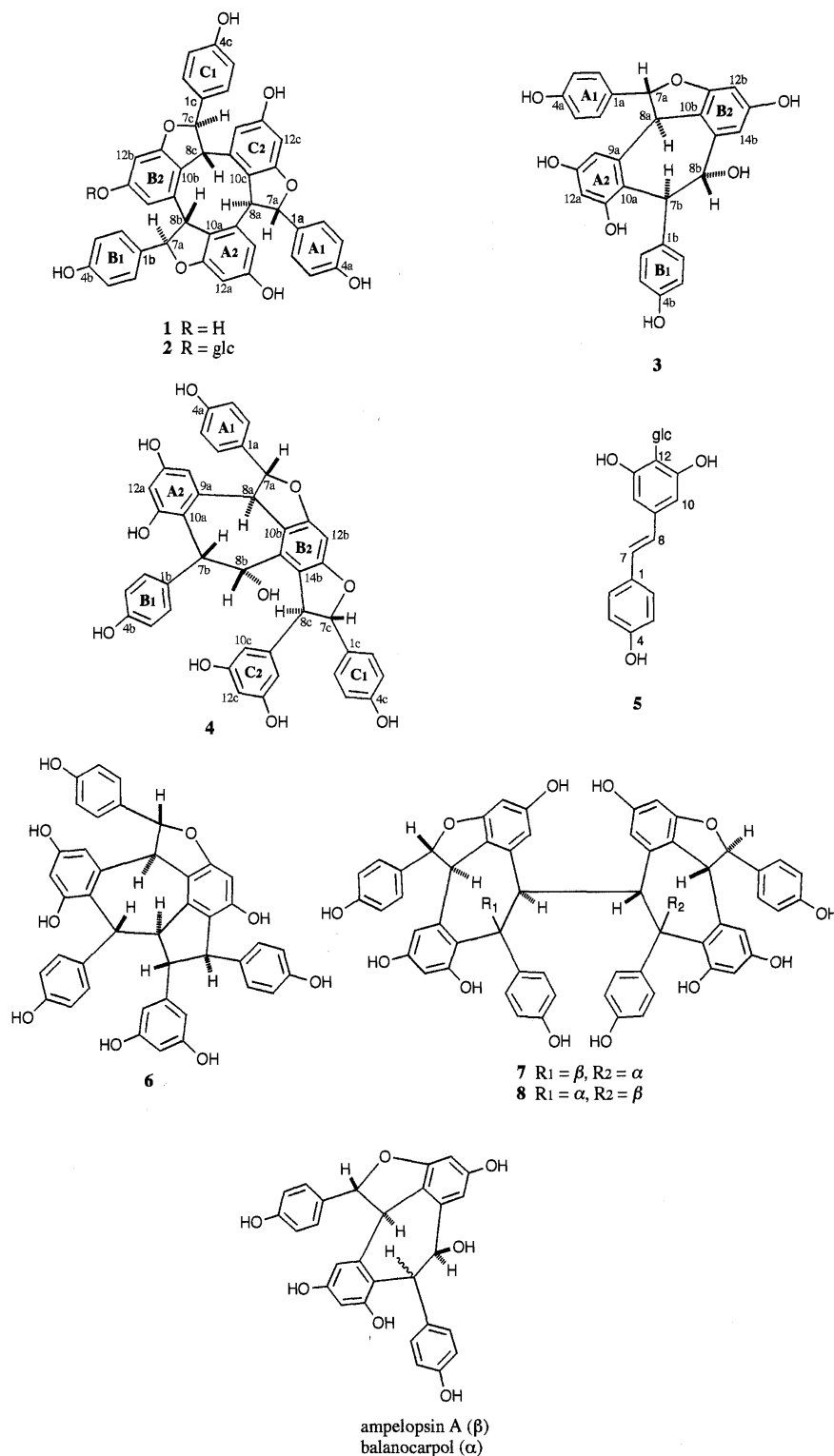


Fig. 1

same planar structure was been isolated, ampelopsin A⁷⁾ from *Ampelopsis brevipedunculata* (Vitaceae) and balanocarpol⁸⁾ from *Balanocarpus zeylanicus* (Dipterocarpaceae). Hence, **3** is one of the stereoisomers of these compounds.

Compound **4** (hemsleyanol B), a yellow amorphous powder, showed a positive reaction to Gibbs reagent. The compound gave an $[M-H]^-$ ion peak at m/z 695 in negative ion FAB-MS corresponding to the molecular formula, $C_{42}H_{32}O_{10}$, which suggested that **4** is a stilbene trimer. The 1H -NMR spectrum showed the presence of three sets of

ortho-coupled aromatic protons assignable to three 4-hydroxyphenyl groups [δ 7.08 (2H, d, $J=8.5$ Hz, H-2a, 6a) and 6.75 (2H, d, $J=8.5$ Hz, H-3a, 5a); δ 7.16 (2H, d, $J=8.8$ Hz, H-2b, 6b) and 6.59 (2H, d, $J=8.8$ Hz, H-3b, 5b); δ 7.29 (2H, d, $J=8.8$ Hz, H-2c, 6c) and 6.88 (2H, d, $J=8.8$ Hz, H-3c, 5c)], a 3,5-dihydroxyphenyl group [δ 6.10 (2H, d, $J=2.0$ Hz, H-10c, 14c) and 6.18 (1H, t, $J=2.0$ Hz, H-12c)], a set of *meta*-coupled aromatic protons on a 1,2,3,5-tetrasubstituted benzene ring [δ 6.35 (1H, d, $J=2.0$ Hz, H-12a) and 6.25 (1H, br s, H-14a)], an aromatic proton on a penta-substituted benzene ring

Table 1. ^1H -NMR Spectral Data of **1**–**5**

No.	1	2	3	4	No.	5
2a, 6a	7.04 (d, 8.8)	7.00 (d, 8.8)	7.48 (d, 8.3)	7.08 (d, 8.5)	2, 6	7.42 (d, 8.5)
3a, 5a	6.73 (d, 8.8)	6.74 (d, 8.8)	6.94 (d, 8.3)	6.75 (d, 8.5)	3, 5	6.83 (d, 8.5)
7a	6.08 (s)	6.07 (s)	5.75 (d, 9.8)	5.77 (d, 11.3)	7	6.86 (d, 16.3)
8a	3.97 (s)	3.93 (s)	5.41 (d, 9.8)	4.29 (d, 11.3)	8	7.03 (d, 16.3)
10a					10	6.55 (s)
12a	6.26 (d, 2.0)	6.25 (d, 2.0)	6.24 (br s)	6.35 (d, 2.0)		
14a	6.73 (d, 2.0)	6.71 (d, 2.0)	6.23 (br s)	6.25 (br s)	14	6.55 (s)
2b, 6b	7.22 (d, 8.8)	7.23 (d, 8.8)	6.72 (d, 8.3)	7.16 (d, 8.8)		
3b, 5b	6.78 (d, 8.8)	6.76 (d, 8.8)	6.48 (d, 8.3)	6.59 (d, 8.8)		
7b	5.96 (d, 10.0)	6.02 (d, 9.5)	5.07 (d, 5.9)	5.29 (d, 4.4)		
8b	4.71 (d, 10.0)	4.75 (d, 9.5)	4.76 (br d)	4.79 (br s)		
10b						
12b	6.24 (d, 1.8)	6.45 (d, 2.0)	6.04 (d, 2.0)	6.26 (s)		
14b	6.60 (d, 1.8)	6.85 (d, 2.0)	5.70 (d, 2.0)			
2c, 6c	7.06 (d, 8.3)	7.03 (d, 8.3)		7.29 (d, 8.8)		
3c, 5c	6.79 (d, 8.3)	6.78 (d, 8.3)		6.88 (d, 8.8)		
7c	4.91 (d, 6.3)	4.91 (d, 6.3)		5.32 (d, 5.4)		
8c	4.62 (d, 6.3)	4.64 (d, 6.3)		5.12 (d, 5.4)		
10c				6.10 (d, 2.0)		
12c	6.23 (d, 1.8)	6.25 (d, 2.0)		6.18 (t, 2.0)		
14c	6.00 (d, 1.8)	5.98 (d, 2.0)		6.10 (d, 2.0)		
OH	8.39 (br s)	8.32 (br s)	8.63 (br s, C-4a) 7.91 (br s, C-11a) 8.02 (br s, C-13a) 7.91 (br s, C-4b) 4.45 (br s, C-8b) 8.01 (br s, C-13b)	4.40 (br s, C-8b) 8.22 (br s)		
Glucose		5.02 (d, 7.3, H-1) 3.44 (m, H-2) 3.45 (m, H-3) 3.55 (m, H-4) 3.51 (m, H-5) 3.71, 3.89 (m, H-6)			Glucose	4.94 (d, 9.3, H-1) 3.68 (dd, 9.3, 9.0, H-2) 3.57 (dd, 9.0, 8.6, H-3) 3.65 (ddd, 8.6, 9.3, 1.0, H-4) 3.48 (dt, 9.3, 3.5, H-5) 3.87 (m, H-6)

Measured in acetone- d_6 (400 MHz). All protons were assigned by ^1H - ^1H , ^1H - ^1H long-range, ^{13}C - ^1H COSY and COLOC spectrum.

as a singlet [δ 6.26 (1H, s, H-12b)] and two sets of mutually coupled aliphatic protons assignable to two dihydrofuran rings [δ 5.77 (1H, d, J =11.3 Hz, H-7a), 4.29 (1H, d, J =11.3 Hz, H-8a); δ 5.32 (1H, d, J =5.4 Hz, H-7c), 5.12 (1H, d, J =5.4 Hz, H-8c)] in addition to an alcoholic hydroxyl group [δ 4.40 (br s)] as shown in Table 1. The ^1H -NMR spectrum also showed that the signals attributed to two methine protons correlated in the H–H COSY spectrum [δ 5.29 (1H, d, J =4.4 Hz, H-7b), 4.79 (1H, br s, H-8b)] and the latter proton (H-8b) also has a correlation with an alcoholic proton at δ 4.40, which indicated that the alcoholic proton was located on C-8b similar to **3**. In the H–H long-range COSY spectrum, the long-range correlations observed between methine protons and aromatic protons were as follows; H-7a/H-2a (6a), H-14a/H-8a, H-7b/H-2b(6b) and H-8c/H-10c(14c). These results indicated that **4** is the resveratrol trimer with two dihydrofuran units and a secondary alcohol. In the COLOC spectrum (Fig. 5), significant 3J long-range correlations were observed between C-2a(6a)/H-7a, C-8a/H-14a, C-9a/H-7b, C-2b(6b)/H-7b, C-9b/H-8a and C-10b/H-12b showing that the partial plane structure of **4** was the same as that of hemsleyanol A. On the other hand, long range correlations were observed between the aromatic carbons (C-13b) and the aliphatic methine protons (H-8c), indicating that resveratrol C (ring C1–C7c–C8c–ring C2) formed a dihydrobenzofuran ring with ring B2. Considering the 3J long-range correlations between an aromatic proton on ring B₂ (H-12b) and two oxy-

genated aromatic carbons (C-11b and C-13b), the plane structure of **4** was confirmed as that shown in Fig. 5, where two dihydrofuran rings were fused to ring B₂ in a linear form. For confirmation of the relative stereochemistry of **4**, NOE studies were performed (Fig. 6). In this study, **4** showed significant NOEs between H-7a/H-14a, H-8a/H-2a(6a), H-7c/H-10c(14c) and H-8c/H-2c(6c), suggesting that the orientation of both dihydrofuran rings was *trans*. Irradiation of H-2b(6b) enhanced the methine hydrogen signal (H-8a) and the alcoholic hydroxyl proton located at C-8b, which can be observed only when H-8a and the hydroxyl group are situated in the *cis* position to ring B₁. The α -configuration of H-8c was deduced from NOE data between H-8b and H-8c. On the basis of these results, the relative structure of hemsleyanol B was identified as **4**.

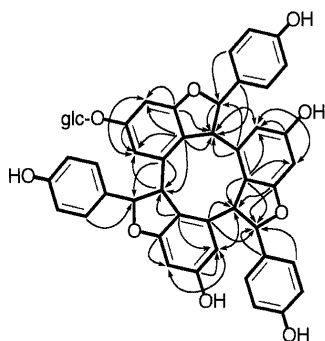
Compound **5** was positive to Gibbs reagent and had the molecular formula $\text{C}_{20}\text{H}_{22}\text{O}_8$, supported by the HR-FAB-MS (m/z 389.1229). The ^1H - and ^{13}C -NMR spectral data (Tables 1 and 2) closely resembled those of resveratrol except for the absence of an aromatic proton (H-12) and the presence of a C-glucopyranosyl moiety [δ 4.94 (1H, d, J =9.3 Hz); δ 82.2, 79.6, 77.3, 75.1, 70.7 and 61.8],⁹⁾ suggesting the location of a C-glucosyl moiety at C-12a. Therefore, **5** was identified as 12-C- β -glucopyranosylresveratrol.

Four known stilbenoids were identified as **1**,²⁾ **6**,¹⁰⁾ **7**¹¹⁾ and **8**,¹²⁾ respectively. The isolation and structural elucidation of other stilbenoids in the acetone extract are now in progress.

Table 2. ^{13}C -NMR Spectral Data of 1–5

No.	1	2	3	4	No.	5
1a	131.5	132.2	133.8	130.9	1	130.0
2a, 6a	127.4	128.0	130.4	129.9 ^{d)}	2, 6	128.9
3a, 5a	111.5	116.0	116.4	115.9	3, 5	116.5
4a	157.3 ^{a)}	158.0 ^{c)}	155.6	158.4 ^{e)}	4	158.3
7a	85.9	86.6	93.3	88.1	7	126.5
8a	45.9	47.0	51.9	50.1	8	129.4
9a	139.2	139.9	141.4	142.5	9	140.0
10a	120.4	121.0	118.4	120.7	10	107.3
11a	158.80	160.9	158.3	156.6	11	157.6
12a	96.0	96.8	102.0	101.3	12	112.0
13a	158.9	159.6	156.6	157.2	13	157.6
14a	105.7	106.4	106.6	105.1	14	107.3
1b	132.0 ^{b)}	132.4	135.2	133.0		
2b, 6b	127.7	128.5	130.5	129.8 ^{d)}		
3b, 5b	115.5 ^{f)}	116.2 ^{g)}	114.9	114.9		
4b	157.7 ^{a)}	158.4 ^{c)}	158.5	158.1		
7b	89.5	90.0	49.3	45.4		
8b	52.3	53.0	78.4	70.7		
9b	138.2	138.8	140.9	137.7		
10b	119.2	122.5	118.1	119.5		
11b	161.2	161.6	160.7	159.7		
12b	96.4	98.3	96.2	91.4		
13b	160.3	161.3	158.5	161.9		
14b	105.3	106.8	108.2	121.2		
1c	131.8 ^{b)}	132.3		134.4		
2c, 6c	128.1	128.9		128.1		
3c, 5c	115.5 ^{f)}	116.2 ^{g)}		116.1		
4c	157.8 ^{a)}	158.6 ^{c)}		155.8 ^{e)}		
7c	95.1	95.8		93.8		
8c	55.2	55.8		58.1		
9c	140.7	141.0		147.5		
10c	118.3	118.9		106.8		
11c	161.1	161.9		159.4		
12c	97.5	98.3		101.7		
13c	160.2	159.5		159.4		
14c	108.0	108.9		106.8		
Glucose		101.9 (C-1)		Glucose	77.3 (C-1)	
		74.8 (C-2)			75.1 (C-2)	
		71.5 (C-3)			79.6 (C-3)	
		77.8 (C-4)			70.7 (C-4)	
		78.0 (C-5)			82.2 (C-5)	
		62.8 (C-6)			61.8 (C-6)	

Measured in acetone- d_6 (100 MHz). a–e) Interchangeable. f–g) Overlapping. All carbons were assigned by ^{13}C - ^1H COSY and COLOC spectrum.

Fig. 2. CH Long-Range Correlations in COLOC Spectrum ($J=8$ Hz) of 2

Experimental

^1H - and ^{13}C -NMR spectra were recorded on a JNM EX-400 (JEOL) spectrometer. Chemical shifts are shown as δ -values with tetramethylsilane (TMS) as the internal reference. Peak multiplicities are quoted in Hz. Negative ion FAB-MS was measured on a JMS-DX-300 spectrometer equipped with a JMA 3500 data analysis system (JEOL). UV spectra were recorded

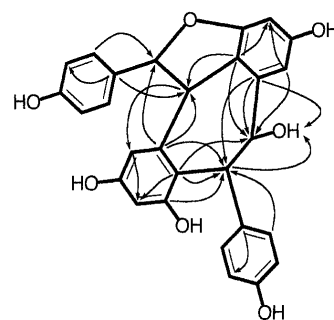
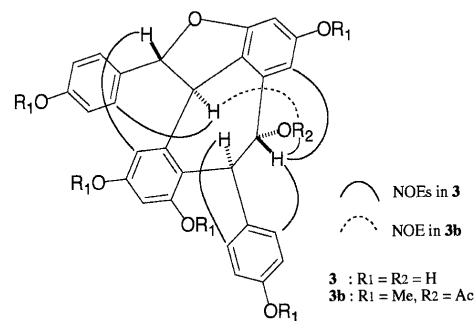
Fig. 3. COLOC Spectrum ($J=8$ Hz) of 3

Fig. 4. NOE Interactions in DIFNOE Spectrum of 3 and 3b

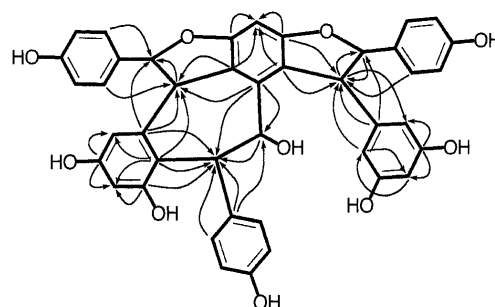
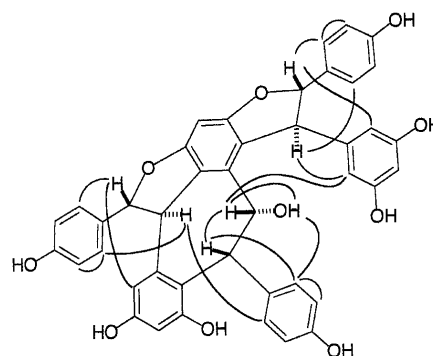
Fig. 5. COLOC Spectrum ($J=8$ Hz) of 4

Fig. 6. NOEs Observed in DIFNOE Spectrum of 4

on UV-2200 spectrometer (Shimadzu), and optical rotations on a P-1020 (JASCO) polarimeter. Silica gel 60 (70–230 mesh, Merck) and Sephadex LH-20 (Pharmacia) were used for column chromatography; Silica gel 60H (Merck) was used for vacuum liquid chromatography (VLC); Kieselgel 60 F₂₅₄ (Merck) was used for analytical and preparative TLC.

Extraction and Isolation of Compounds (1–8) The dried bark of *Shorea hemsleyana* (1 kg) collected in Indonesia in Oct., 1997 was powdered and extracted successively with acetone (31×3), MeOH (31×3) and 70% MeOH (31×3) at room temperature. A part (40 g) of the acetone extract (47 g) was chromatographed on Si-gel (800 g) and eluted with a CHCl_3 -MeOH mixture to give 34 fractions (fr. 1–34). Compound 1

(114 mg) was obtained in pure form after recrystallization (CHCl_3 -acetone) from fr. 22 [CHCl_3 -MeOH (10:1) fraction]. Fr. 23 [CHCl_3 -MeOH (10:1) fraction] was further chromatographed by vacuum liquid chromatography (VLC) using CHCl_3 -MeOH mixtures. The CHCl_3 -MeOH (10:1) fraction afforded **3** (30 mg) after purification on a Sephadex LH 20 column (MeOH). Fr. 25 [CHCl_3 -MeOH (8:1)] was chromatographed repeatedly with VLC (CHCl_3 -MeOH and benzene-EtOAc-MeOH system), Sephadex LH-20 column chromatography (MeOH), and preparative TLC (EtOAc- CHCl_3 -MeOH- H_2O =15:8:4:1) to afford **5** (5 mg) and **6** (15 mg). Compounds **2** (12 mg), **4** (12 mg), **7** (8 mg) and **8** (12 mg) were obtained from fr. 26 [CHCl_3 -MeOH (8:1)] after purification by VLC (EtOAc- CHCl_3 -MeOH- H_2O =40:20:3:1) and preparative TLC (EtOAc- CHCl_3 -MeOH- H_2O =15:8:4:1).

Compound 2 [(+)- α -Viniferin-13b-O- β -glucopyranoside] A pale yellow amorphous solid. Negative ion HR-FAB-MS: ($[\text{M}-\text{H}]^-$) m/z 839.2327 (Calcd: for $\text{C}_{48}\text{H}_{39}\text{O}_{14}$ 839.2339); Negative ion FAB-MS: m/z 839 ($[\text{M}-\text{H}]^-$), 677 ($\text{M}-\text{H}$ -glucopyranosyl moiety). UV λ_{max} (MeOH) nm: 228, 285. $[\alpha]_{\text{D}}^{24} +32^\circ$ ($c=0.1$, MeOH). The ^1H - and ^{13}C -NMR spectral data are listed in Tables 1 and 2.

Acid hydrolysis of 2 Compound **2** (2 mg) was refluxed for 6 h with 3% H_2SO_4 in MeOH. The reaction mixture was extracted with EtOAc and the resulting solid was purified with PTLC [n -hexane-EtOAc (1:1)] to afford **1** (1 mg).

Compound 3 (Hemsleyanol A) A yellow amorphous solid. Negative ion HR-FAB-MS ($[\text{M}-\text{H}]^-$) m/z 469.1277 (Calcd for $\text{C}_{28}\text{H}_{21}\text{O}_7$: 469.1287); Negative ion FAB-MS: m/z 469 ($[\text{M}-\text{H}]^-$). UV λ_{max} (MeOH) nm: 229, 285. $[\alpha]_{\text{D}}^{24} -14^\circ$ ($c=0.1$, MeOH). The ^1H - and ^{13}C -NMR spectral data are listed in Tables 1 and 2.

Methylation of 3 Compound **3** (5 mg) was allowed to react with K_2CO_3 (2 g) and MeI (0.5 g) in dry acetone under reflux for 4 h. The reaction mixture was treated in the usual manner and the crude product (5 mg) was purified by PTLC [n -hexane-EtOAc (1:1)] to afford **3a** as an amorphous colorless solid (4 mg). ^1H -NMR (400 MHz, CDCl_3) δ : 3.50, 3.58, 3.60, 3.69, 3.86 (3H each, s, OMe \times 5), 4.86 (1H, brs, H-8b), 5.20 (1H, br d, H-7b), 5.48 (1H, d, $J=10.3$ Hz, H-8a), 5.77 (1H, d, $J=10.3$ Hz, H-7a), 5.82 (1H, brs, H-14b), 6.23* (1H, brs, H-14a), 6.24* (1H, d, $J=2.0$ Hz, H-12a), 6.30* (1H, d, $J=2.0$ Hz, H-12b), 6.58 (2H, d, $J=8.8$ Hz, H-3b, 5b), 6.77 (2H, d, $J=8.8$ Hz, H-2b, 6b), 7.03 (2H, d, $J=8.8$ Hz, H-3b, 5a), 7.62 (2H, d, $J=8.8$ Hz, H-2a, 6a) (* interchangeable).

Acetylation of 3b Compound **3a** (4 mg) was dissolved in a mixture of pyridine (1 ml), acetic anhydride (1 ml). The reaction mixture was kept at room temperature for 24 h. The solution was treated in the usual manner and the resulting crude product (4 mg) was purified by PTLC [n -hexane-acetone (3:2)] to afford **3b** as an amorphous colorless solid (2 mg). ^1H -NMR (400 MHz, CDCl_3) δ : 1.97 (3H, s, OAc), 3.55, 3.56, 3.59, 3.69, 3.87 (3H each, s, OMe \times 5), 5.21 (1H, d, $J=5.9$ Hz, H-8b), 5.39 (1H, d, $J=10.2$ Hz, H-8a), 5.80 (1H, d, $J=10.2$ Hz, H-7a), 5.87 (1H, d, $J=5.9$ Hz, H-7b), 5.91 (1H, brs, H-14b), 6.25* (2H, brs, H-12b, 14a), 6.28* (1H, brs, H-12a), 6.58 (2H, d, $J=8.8$ Hz, H-3b, 5b), 6.80 (2H, d, $J=8.8$ Hz, H-2b, 6b), 7.04 (2H, d,

$J=8.8$ Hz, H-3b, 5a), 7.61 (2H, d, $J=8.8$ Hz, H-2a, 6a) (* interchangeable).

Acetylation of 3 To a solution of **3** (2 mg) in pyridine (1 ml), acetic anhydride (1 ml) was added and the mixture was kept at room temperature for 24 h. The resulting crude product (2 mg) was purified by PTLC [n -hexane-EtOAc (3:2)] to afford **3c** as an amorphous colorless solid (2 mg). ^1H -NMR (400 MHz, CDCl_3) δ : 2.00, 2.16, 2.17, 2.23, 2.24, 2.34 (3H each, s, OAc \times 6), 5.09 (1H, d, $J=5.4$ Hz, H-8b), 5.47 (1H, d, $J=9.3$ Hz, H-8a), 5.92 (1H, d, $J=5.4$ Hz, H-7b), 5.92 (1H, d, $J=9.3$ Hz, H-7a), 6.05 (1H, brs, H-14b), 6.49 (1H, d, $J=2.0$ Hz, H-12b), 6.80 (1H, d, $J=2.0$ Hz, H-12a)*, 6.84 (2H, d, $J=8.8$ Hz, H-3b, 5b), 6.85 (2H, d, $J=8.8$ Hz, H-2b, 6b), 6.89 (1H, brs, H-14a)*, 7.25 (2H, d, $J=8.8$ Hz, H-3b, 5a), 7.67 (2H, d, $J=8.8$ Hz, H-2a, 6a) (* interchangeable).

Compound 4 (Hemsleyanol B) A yellow amorphous solid. Negative ion HR-FAB-MS: ($[\text{M}-\text{H}]^-$) m/z 695.1907 (Calcd for $\text{C}_{42}\text{H}_{31}\text{O}_{10}$: 695.1916); Negative ion FAB-MS: m/z 695 ($[\text{M}-\text{H}]^-$). UV λ_{max} (MeOH) nm: 230, 284, 301. $[\alpha]_{\text{D}}^{24} -205^\circ$ ($c=0.1$, MeOH). The ^1H - and ^{13}C -NMR spectral data are shown in Tables 1 and 2.

Compound 5 (Resveratrol-12-C- β -glucopyranoside) A white amorphous powder. Negative ion HR-FAB-MS: ($[\text{M}-\text{H}]^-$) m/z 389.1229 (Calcd for $\text{C}_{20}\text{H}_{21}\text{O}_8$: 389.1236); Negative ion FAB-MS: m/z 389 ($[\text{M}-\text{H}]^-$). UV λ_{max} (MeOH) nm: 217, 309, 321. $[\alpha]_{\text{D}}^{24} +61^\circ$ ($c=0.1$, MeOH). The ^1H - and ^{13}C -NMR spectral data are listed in Tables 1 and 2.

References

- 1) Jang M., Cai L., Udeani G. O., Slowing K. V., Thomas C. F., Beecher C. W., Fong H. H. S., Farnsworth N. R., Kinghorn A. D., Mehta R. G., Moon R. C., Pezzuto J. M., *Science*, **275**, 218—220 (1997).
- 2) Kitanaka S., Ikezawa T., Yasukawa K., Yamanouchi S., Takido M., Sung H., Kim I., *Chem. Pharm. Bull.*, **38**, 432—435 (1990).
- 3) Inamori Y., Ogawa M., Tsujibo H., Baba K., Kozawa M., Nakamura H., *Chem. Pharm. Bull.*, **39**, 805—807 (1991).
- 4) Murakami S., Arai I., Muramatsu M., Otomo S., Baba K., Kido T., Kozawa M., *Biochem. Pharm.*, **44**, 33—37 (1992).
- 5) Gorham J., "The Biochemistry of the Stilbenoids," Chapman & Hall, London, 1995.
- 6) Sotheeswaran S., Pasupathy V., *Phytochemistry*, **32**, 1083—1092 (1993).
- 7) Oshima Y., Ueno U., Hikino H., *Tetrahedron*, **46**, 5121—5126 (1990).
- 8) Champika D. M. N., Sotheeswaran S., Surendrakumar S., Balasubramanian, S., Bokel M., Kraus W., *J. Chem. Soc. Perkin Trans. I*, **1985**, 1807—1809.
- 9) El-Sohly H. N., Joshi A., Li X.-C., Ros S. A., *Phytochemistry*, **52**, 141—145 (1999).
- 10) Tanaka T., Ito T., Ichise M., Iinuma M., Ohyama M., Tateishi Y., *Phytochemistry*, accepted.
- 11) Coggon P., Janes N. F., King F. E., Molyneux R. J., Morgan J. W. W., Sellars K., *J. Chem. Soc.*, **1965**, 406—508.
- 12) Ito J., Niwa M., Oshima Y., *Heterocycles*, **45**, 1809—1813 (1997).

The Constituents of the Root and Stem of *Aristolochia cucurbitifolia* Hayata and Their Biological Activity

Tian-Shung WU,* Yu-Yi CHAN, and Yann-Lii LEU

Department of Chemistry, National Cheng Kung University, Tainan, Taiwan, R.O.C.

Received January 24, 2000; accepted March 7, 2000

Four new compounds, three phenanthrene derivatives, aristolochic acid-III methyl ester (**1**), cepharanone C (**2**), and sodium 7-hydroxyl-8-methoxyaristololate (**3**), and the benzoate derivative, sodium 3,4-dimethoxybenzoate (**4**), together with 53 known compounds were isolated and characterized from the fresh root and stem of *Aristolochia cucurbitifolia*. Their structures were elucidated by spectral analyses and chemical transformations. The cytotoxicity and antiplatelet activity of the isolated compounds are also discussed.

Key words *Aristolochia cucurbitifolia*; Aristolochiaceae; aristolochic acid derivatives; antiplatelet agent; cytotoxic agent

The genus *Aristolochia* grows over wide areas from the tropics to temperate zones and consists of about 400 species.¹⁾ The fruits and roots have been used in traditional Chinese medicine as anodynes, antiphlogistics, antitussives, expectorants, and antiasthmatic agents, and also for the treatment of snakebite and lung inflammation.²⁾ Aristolochic acid derivatives, often isolated as major components from the plant of the genus *Aristolochia*, have been characterized as tumor inhibitors.^{3,4)} Our chemotaxonomic and pharmacological interests led us to investigate the constituents of the stem and root of *A. cucurbitifolia*. We report here the isolation and structural elucidation of four new compounds, **1**—**4**, and 53 known compounds. In addition, the antiplatelet activity and cytotoxicity of the compounds isolated from the root and stem of *A. cucurbitifolia* are also discussed.

Results and Discussion

Aristolochic acid-III methyl ester (**1**) was obtained as yellowish needles. The high resolution electron ionization mass spectrum (HREIMS) of **1** showed a molecular ion peak at m/z 355.0695, indicating a molecular formula of $C_{18}H_{13}NO_7$. The UV absorption of **1** at 216, 256, 278, 300, 350, and 384 nm showed it was a phenanthrene derivative.⁵⁾ The IR spectrum showed the presence of a nitro group at 1525 and 1346 cm^{-1} . In the aromatic region of the 1H -NMR spectrum, ABX-type signals at δ 7.34 (1H, dd, $J=8.8, 2.4$ Hz), 7.90 (1H, d, $J=8.8$ Hz), and 8.60 (1H, d, $J=2.4$ Hz) were attributed to H-7, H-8, and H-5, respectively. The signal of H-5 appeared at lower field at δ 8.60, due to the deshielding effect of the A ring in the aristolochic acid derivative. Two singlet signals appearing at δ 7.76 and 8.31 (each 1H) were assigned to H-2 and H-9, respectively. The methoxyl groups appeared at δ 4.02 (3H, s) and 3.87 (3H, s). In addition, δ 6.39 (2H, s) was assigned to the methylenedioxy group which was further confirmed by peaks in the IR spectrum at 1045 and 941 cm^{-1} . Based on the above results, the structure of aristolochic acid-III methyl ester is represented as **1**, which is reported for the first time to isolate from nature.

Cepharanone-C (**2**) was isolated as a yellowish powder. Its molecular formula was determined to be $C_{17}H_{11}NO_5$ by HREIMS ($[M]^+$ m/z 309.0634). The UV absorption at 236 (sh), 241, 276 (sh), 288, 357, 373 and 395 nm was consistent with a typical aristolactam derivative,⁵⁾ which was also supported by the positive reaction with Dragendorff reagent. The 1H -

NMR spectrum of **2** showed signals attributable to a methylenedioxy, a methoxyl, and a hydroxyl group at δ 6.42 (2H, s), 3.85 (3H, s) and 10.73 (1H, br s, D_2O exchange disap.), respectively. A set of *ortho* coupling aromatic protons appeared at δ 8.13 and 7.14 (each 1H, d, $J=8.8$ Hz). The lower field signal is the characteristic signal of H-5 in an aristolactam derivative. Two singlet signals at δ 7.55 (1H, s) and δ 7.18 (1H, s) could be assigned to H-2 and H-9, respectively. The relative substitution of methoxy and hydroxyl groups was deduced from the nuclear Overhauser effect spectroscopy (NOESY) experiment (Fig. 1), which showed the correlations of H-6 (δ 7.14) to H-5 and 7-OMe (δ 3.85). Thus, the structure of cepharanone-C was assigned as **2**.

Sodium 7-hydroxyl-8-methoxyaristololate (**3**) was isolated as a colorless powder. The UV absorption at 225, 265 (sh), 273, 296, 319, 352 and 371 nm, combined with the lack of a NO_2 band in the IR spectrum indicated **3** was a phenanthrene derivative.⁵⁾ In the 1H -NMR spectrum, a set of doublet signals at δ 8.27 and 7.78 (each 1H, d, $J=9.5$ Hz) were assigned to H-10 and H-9, respectively. Two *ortho*-coupling protons at δ 8.64 and 7.12 (each 1H, d, $J=9.1$ Hz) were assigned to H-5 and H-6. A singlet at δ 7.31 (1H, s) was attributed to H-2. The methoxyl and methylenedioxy groups appeared at δ 3.92 (3H, s) and 6.20 (2H, s). The positions of the methoxy and hydroxyl groups were determined by the observed NOESY correlation of 8-OMe (δ 3.92) to H-9 (δ 7.78). Based on these data, compound **3** was proposed to be 7-hydroxyl-8-methoxyaristololate. However, the carboxylic group appearing at 1558 cm^{-1} in the IR spectrum suggested compound **3** was in salt form.⁶⁾ Treatment of **3** with 5% HCl, followed by purification of the solution on a Sephadex LH-20

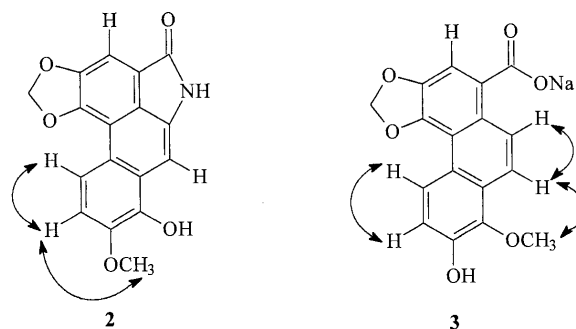


Fig. 1. The NOE Correlations of **2** and **3**

* To whom correspondence should be addressed. e-mail: tswu@mail.ncku.edu.tw

column, afforded sodium chloride which was determined by atomic absorption spectrometry. Thus, the structure of **3** was assigned as sodium 7-hydroxyl-8-methoxyaristolochate.

Sodium 3,4-dimethoxybenzoate (**4**) was isolated as a colorless powder. The UV spectrum showed absorptions at 205, 252, 286 and 291 nm, which suggested a benzenoid. In the $^1\text{H-NMR}$ spectrum, there was a set of ABX-type signals at δ 7.57 (1H, d, $J=1.9$ Hz), 7.47 (1H, dd, $J=8.0, 1.9$ Hz) and 6.75 (1H, d, $J=8.0$ Hz), and two methoxyl groups at δ 3.89 and 3.61 (each 3H, s). These data are similar to those of 3,4-dimethoxy benzoic acid.⁷ However, the IR spectrum of **4** displayed a carboxylic absorption at 1602 cm^{-1} , indicating a salt. Following acidification of **4** with 5% HCl, the solution was applied to a Sephadex LH-20 column and eluted with H_2O and then MeOH. The residue obtained from the H_2O fraction was confirmed to contain sodium ion by atomic ab-

sorption spectroscopy. The MeOH eluted fraction afforded **4a** which was identified as 3,4-dimethoxy benzoic acid. On the basis of the above data, compound **4** was assigned as sodium 3,4-dimethoxybenzoate.

Although aristolochic acid derivatives are usually isolated from the *Aristolochia* genus in free form, we had also isolated them in salt form.^{6,8–11}

The known compounds, sodium (2*R*)-3-(*p*-hydroxylphenyl) lactate (**5**)⁸ methyl pheophorbide-a (**6**),¹² aristolochic acid-I methyl ester (**7**),¹³ methyl-21-hydroxyl-(21*R*)-pheophorbide-a (**8**),¹⁴ isoscopoletin (**9**),¹⁵ aristolochic acid-II methyl ester (**10**),¹⁶ (-)hinokinin (**11**),¹⁷ aristolide-A (**12**),¹⁸ aristolide-B (**13**),¹⁸ aristolochic acid-IV methyl ester (**14**),¹⁶ aristolactam-I (**15**),¹⁶ -AII (**16**),¹⁶ -BII (**17**),¹⁹ -IIIa (**18**),⁸ 9-methoxyaristolactam-I (**19**),¹⁶ 9-methoxyaristolactam IV (**20**),²⁰ piperolactam-A (**21**),²¹ cepharadione-A (**22**),¹⁶ cepharanone-A (**23**),¹⁶ *N-trans*-cinnamoyltiramine (**24**),²² sodium aristolochate-I (**25**),⁶ -II (**26**),⁹ -III (**27**),⁶ -IVa (**28**),⁹ sodium 7-hydroxyaristolochate (**29**),⁶ aristolic acid (**30**),¹⁰ asimilobine (**31**),²³ 6-*O*-(*E*)-feruloyl-(α and β)-glucopyranoside (**32**),²⁴ adenine (**33**),²⁵ glucosyringic acid (**34**),²⁶ 4-hydroxylbenzoic acid (**35**),⁸ salidroside (**36**),²⁷ 4-hydroxylcinnamic acid (**37**),⁸ 4-hydroxyl-3-methoxycinnamic acid (**38**),⁸ vanillic acid (**39**),²⁸ isorhamnetin-3-*O*-robinobioside (**40**),¹⁶ 4,5-dioxodehydroasimilobine (**41**),¹¹ aristolochic acid-C (**42**),¹⁶ -I (**43**),¹⁶ *cis*- and *trans*-4-hydroxyl-3-methoxycinnamic acid methyl ester (**44**),⁸ allantoin (**45**),¹⁶ aristoloterpenate-III (**46**),²⁹ friedelin (**47**),³⁰ stigmat-4-ene-3,6-dione (**48**),⁹ β -sitosterol (**49**),⁹ stigmasterol (**50**),⁹ madolin-A (**51**),³¹ -B (**52**),³¹ -C (**53**),³¹ -D (**54**),³¹ -E (**55**),³¹ aristolactone (**56**)³¹ and manshurolide (**57**)³¹ were also isolated and characterized by comparison of their spectroscopic data (UV, IR, NMR and MS) with literature values.

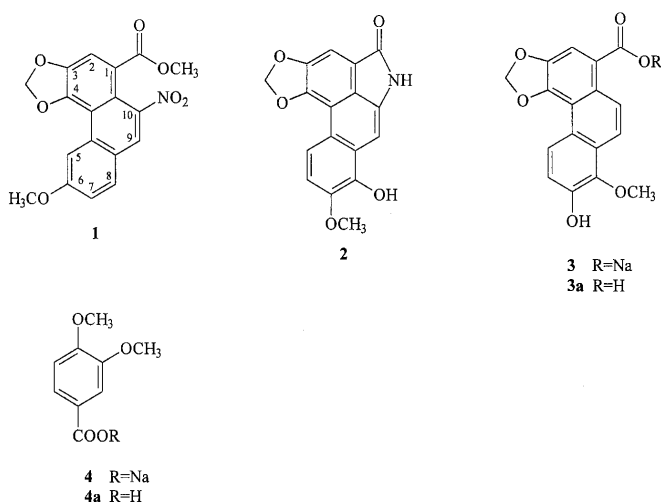


Table 1. The Effects of Compounds Isolated from the Stem and Root *Aristolochia cucurbitifolia* on the Aggregation of Washed Rabbit Platelets Induced by Collagen, Thrombin (Thr), Arachidonic Acid (AA) and Platelet Activation Factor (PAF)

Compounds	Ind. agent Compds conc. ($\mu\text{g/ml}$)	Inhibition (%)									
		Thr (0.1 $\mu\text{M/ml}$)		AA (100 μM)			Collagen (10 $\mu\text{g/ml}$)			PAF (2 ng/ml)	
		100	50	100	50	20	100	50	20	100	50
Methyl pheophorbide-a (6)		A	A	A	A	0.9 \pm 1.1	N	N	0.1 \pm 4.1	N	N
Aristolochic acid-I methyl ester (7)		N	1.7 \pm 1.7	N	N	N	N	1.6 \pm 5.1	N	N	11.3 \pm 0.8 [‡]
Aristolide-A (12)		-0.6 \pm 1.8	N	100.0 \pm 0.0 [‡]	89.6 \pm 8.6 [‡]	11.26 \pm 7.0	45.2 \pm 15.1*	15.5 \pm 6.4*	0.5 \pm 3.8	22.5 \pm 4.8 [‡]	N
Aristolactone (56)		-1.5 \pm 0.8	N	91.7 \pm 6.8 [‡]	11.2 \pm 7.3	N	13.5 \pm 4.5*	N	N	48.3 \pm 21.7*	N
Manshurolide (57)		-3.2 \pm 2.6	N	100.0 \pm 0.0 [‡]	77.3 \pm 11.5 [‡]	18.2 \pm 6.7*	21.9 \pm 5.9 [‡]	N	N	51.1 \pm 12.3 [‡]	N
Aristolactam-I (15)		1.5 \pm 1.3	N	13.1 \pm 2.8	N	N	10.3 \pm 2.4	N	N	31.4 \pm 2.9	N
Aristolactam-AII (16)		0.8 \pm 3.9	N	100.0 \pm 0.0 [‡]	100.0 \pm 0.0 [‡]	95.3 \pm 3.7 [‡]	46.8 \pm 10.2 [‡]	N	N	10.6 \pm 4.1 [†]	N
Piperolactam-A (21)		4.0 \pm 3.4	N	100.0 \pm 0.0 [‡]	100.0 \pm 0.0 [‡]	10.3 \pm 1.6 [‡]	100.0 \pm 0.0 [‡]	60.6 \pm 21.1*	22.3 \pm 2.4	38.8 \pm 13.8 [†]	N
Cepharanone-A (23)		4.0 \pm 1.7	N	4.7 \pm 1.6	N	N	8.3 \pm 1.9	N	N	25.6 \pm 1.5	N
Sodium aristolochate-I (25)		1.9 \pm 1.5	N	0.1 \pm 1.8	N	N	3.3 \pm 2.7	N	N	1.8 \pm 1.4	N
Sodium aristolochate-II (26)		-3.7 \pm 1.0	N	4.3 \pm 1.8	N	N	1.8 \pm 4.9	N	N	7.5 \pm 1.8 [†]	N
Sodium aristolochate-III (27)		-4.1 \pm 3.8	N	2.6 \pm 1.2	N	N	1.7 \pm 2.6	N	N	5.8 \pm 0.5 [†]	N
Sodium aristolochate-IVa (28)		4.6 \pm 2.3	N	10.8 \pm 2.9 [†]	N	N	21.5 \pm 8.9*	N	N	1.7 \pm 0.4	N
Aristolactam-IIIa (18)		-0.1 \pm 1.7	N	-0.5 \pm 1.8	N	N	11.6 \pm 1.0	N	N	6.0 \pm 2.4	N
Sodium (2 <i>R</i>)-3-(<i>p</i> -hydroxylphenyl) lactate (5)		2.9 \pm 1.3	N	0.8 \pm 0.2	N	N	2.4 \pm 2.0	N	N	0.7 \pm 1.0	N
Adenine (33)		3.8 \pm 2.3	N	0.0 \pm 0.4	N	N	2.6 \pm 1.9	N	N	1.7 \pm 0.3	N
Glucosyringic acid (34)		3.1 \pm 1.6	N	4.5 \pm 1.8*	N	N	2.8 \pm 2.0	N	N	2.1 \pm 0.8	N
Isohamnetin-3- <i>O</i> -robinobioside (40)		-0.4 \pm 1.4	N	18.3 \pm 1.1	N	N	3.9 \pm 1.1	N	N	0.5 \pm 2.1	N
Aristolochic acid-C (42)		-0.1 \pm 1.7	N	-0.5 \pm 1.8	N	N	11.6 \pm 1.1	N	N	6.0 \pm 2.4	N
Aristolochic acid-I (43)		4.4 \pm 1.2 [‡]	N	21.66 \pm 5.3 [†]	N	N	22.4 \pm 7.9*	N	N	10.4 \pm 1.7*	N
Allantoin (45)		4.3 \pm 3.2	N	3.2 \pm 1.4	N	N	1.4 \pm 1.9	N	N	1.2 \pm 1.1	N

Platelets were preincubated with compounds or DMSO (0.5%, control) at 37 °C for 3 min; the inducer was added. Values are means \pm S.E.M. ($n=3-4$). N=not tested. A=platelet aggregation promoted. * $p<0.05$, † $p<0.01$, ‡ $p<0.001$ were compared with the respective control.

Table 2. Cytotoxicity of Compounds Isolated from the Stem and Root *Aristolochia cucurbitifolia*

Compounds	Cell lines	ED ₅₀ conc. (μg/ml)				
		KB	P-388	A-549	HT-29	HL-60
Aristolactam-I (15)		3.3	1.0	3.2	2.6	2.4
Aristolactam-AII (16)		>50	1.3	2.7	13.2	12.9
Aristolactam-IIIa (18)		>50	8.8	>20	17.1	40
Cepharanone-A (23)		4.1	2.3	1.7	3.3	3.9
Aristolochic acid-C (42)		>50	8.8	>20	17.1	40
Aristolochic acid-I (43)		4.0	0.7	5.0	8.3×10 ⁻⁴	3.4

KB: human epidermoid carcinoma; P-388: mouse lymphocytic leukaemia; A-549: lung adenocarcinoma; HT-29: colon adenocarcinoma; HL-60: human leukaemia.

Compounds **5**, **7**, **12**, **15**, **16**, **18**, **21**, **23**, **25**—**28**, **33**, **34**, **40**, **42**, **43**, **45**, **56** and **57** were subjected to cytotoxicity testing and evaluation of their platelet aggregation effect. Among them, **12**, **16**, **21**, **56**, **57** at 100 μM showed 91—100% inhibition of rabbit platelet aggregation induced by arachidonic acid (100 μM) and **21** also produced 100% inhibition of aggregation induced by collagen (10 μg ml⁻¹) (Table 1). In addition, aristolochic acid-I (**43**) exhibited the most potent inhibition of the growth of HT-29 cells (Table 2).^{32,33}

Experimental

General Procedures Melting points (Yanagimoto apparatus) are uncorrected. Optical rotations were recorded on a Jasco DIP-370 digital polarimeter. UV spectra in MeOH solution were obtained on a Hitachi UV-3210 spectrophotometer. IR spectra in KBr discs were recorded on a Shimadzu FT-IR DR-8011 spectrophotometer. Mass and high resolution mass spectra were measured on a VG-70-250S spectrometer with a direct inlet system. ¹H-NMR and ¹³C-NMR spectra were determined on Bruker AMX-400 and Varian Unity plus 400 spectrometers. Chemical shifts are shown in δ values (ppm) with tetramethylsilane (TMS) as an internal standard.

Plant Material *Aristolochia cucurbitifolia* Hayata was collected in Yen Chao, Kaohsiung Hsien, Taiwan, in April, 1992, and verified by Prof. C.-S. Kuoh. A voucher specimen is deposited in the Herbarium of the National Cheng Kung University, Tainan, Taiwan, R.O.C.

Extraction and Isolation The stem and root (3.1 kg) were extracted with MeOH (×10) at room temperature, and concentrated to give a dark brown syrup. The MeOH extract was partitioned successively between H₂O and CHCl₃, and then *n*-BuOH. The CHCl₃ layer was filtered to obtain precipitate and filtrate. The filtrate was dried over Na₂SO₄ and then concentrated under reduced pressure to leave a brown syrup which was chromatographed directly on silica-gel and eluted with a gradient of CHCl₃ and MeOH to afford 3 fractions. Fraction 1 underwent column chromatography on silica gel and eluted with *n*-hexane-EtOAc (15:1) to obtain methyl pheophorbide-a (**6**) (24 mg), aristolochic acid-I methyl ester (**7**) (6 mg), methyl-21-hydroxyl-(21R)-pheophorbide-a (**8**) (23 mg), aristoloterpenate-III (**46**) (3 mg), isoscopoletin (**9**) (6 mg), aristolochic acid-II methyl ester (**10**) (4.5 mg), (-)hinokinin (**11**) (10 mg), aristolide-A (**12**) (6 mg), aristolide-B (**13**) (0.6 mg), aristolochic acid-IV methyl ester (**14**) (2.7 mg), aristolochic acid III methyl ester (**1**) (3 mg), madolin-A (**51**) (15 mg), -B (**52**) (5 mg), -C (**53**) (13 mg), -D (**54**) (3 mg), -E (**55**) (1 mg), aristolactone (**56**) (683 mg) and manshurolide (**57**) (23 mg), successively. Fraction 3 underwent column chromatography on silica-gel and eluted with iso-Pr₂O-Me₂CO (9:1) to give aristolactam-I (**15**) (2.1 mg), cepharanone-C (**2**) (1 mg), aristolactam-AII (**16**) (2.7 mg), piperolactam-A (**21**) (6 mg), cepharadione-A (**22**) (2 mg), 9-methoxyaristolactam-I (**19**) (2 mg), aristolactam-BII (**17**) (3 mg), cepharanone-A (**23**) (17 mg), *N*-trans-cinnamoyltyramine (**24**) (2 mg), and 9-methoxyaristolactam-IV (**20**) (1 mg). The precipitate was chromatographed on Sephadex LH-20 and eluted with a gradient of H₂O-MeOH to afford sodium aristolochate-I (**25**) (290 mg), sodium 7-hydroxyl-aristolochate (**29**) (2 mg), sodium aristolochate-II (**26**) (6 mg), sodium aristolochate-III (**27**) (6 mg), aristolic acid (**30**) (3 mg), sodium aristolochate-IVa (**28**) (24 mg), asimilobine (**31**) (5 mg), and aristololactam IIIa (**18**) (2 mg). The *n*-BuOH layer was chromatographed directly on Diaion HP-20 and eluted with a gra-

dient of MeOH and H₂O to afford 22 fractions and allantoin (**45**) (7 g). Fraction 5 underwent column chromatography on Sephadex LH-20 and eluted with a gradient of MeOH and H₂O to give sodium (2R)-3-(*p*-hydroxylphenyl) lactate (**5**) (13 mg) and adenine (**33**) (10 mg). Fraction 9 underwent column chromatography on Sephadex LH-20 and eluted with a gradient of MeOH and H₂O to give glucosyringic acid (**34**) (13 mg), 4-hydroxybenzoic acid (**35**) (4 mg), and salidroside (**36**) (11 mg). Fraction 12 underwent column chromatography on Sephadex LH-20 and eluted with a gradient of MeOH and H₂O to give sodium 3,4-dimethoxybenzoate (**4**) (13.5 mg), 4-hydroxycinnamic acid (**37**) (2 mg), and 4-hydroxyl-3-methoxy-cinnamic acid (**38**) (2 mg). Fraction 13 underwent column chromatography on Sephadex LH-20 and eluted with a gradient of MeOH and H₂O to give 6-*O*-(*E*)-feruloyl-(α and β)-glucopyranoside (**32**) (10 mg), vanillic acid (**39**) (1 mg). Fraction 16 underwent column chromatography on silica-gel and eluted with CHCl₃ and MeOH (15:1) to give isorhamnetin 3-*O*-robinobioside (**40**) (1.09 g). Fraction 19 underwent column chromatography on silica-gel and eluted with CHCl₃ and MeOH (15:1) to afford 4,5-dioxodehydroasimilobine (**41**) (3 mg), aristolochic acid-C (**42**) (20 mg), *cis*- and *trans*-4-hydroxyl-3-methoxycinnamic acid methyl ester (**44**) (6 mg), sodium 7-hydroxyl-8-methoxyaristolactate (**3**) (1 mg), and aristolochic acid-I (**43**) (280 mg), successively.

Aristolochic Acid III Methyl Ester (1): Yellowish needles. C₁₈H₁₃NO₇. mp 272—274 °C. UV λ_{max}^{MeOH} nm (log ε): 216 (4.06), 256 (4.33), 278 (sh, 3.91), 300 (3.81), 350 (3.63) and 384 (3.59). IR ν_{max}^{KBr} cm⁻¹: 1710 (C=O), 1612, 1525 (NO₂), 1346, 1228, 1045 and 941 (OCH₃O). HRMS: *Anal.* calcd for C₁₈H₁₃NO₇ (355.0692). Found: C₁₈H₁₃NO₇ (*m/z*, 355.0695). EI-MS *m/z* (rel. int.): 355 ([M]⁺, 43), 310 (20), 309 (100), 294 (67), 278 (35), 266 (16). ¹H-NMR (CDCl₃, 200 MHz) δ: 3.87 (3H, s, OCH₃), 4.02 (3H, s, OCH₃), 6.39 (2H, s, OCH₂O), 7.34 (1H, dd, *J*=8.8, 2.4 Hz, H-7), 7.76 (1H, s, H-2), 7.90 (1H, d, *J*=8.8 Hz, H-8), 8.31 (1H, s, H-9), 8.60 (1H, d, *J*=2.4 Hz, H-5).

Cepharanone-C (2): Yellowish powder. C₁₇H₁₁NO₅. UV λ_{max}^{MeOH} nm (log ε): 236 (sh, 4.45), 241 (4.49), 276 (sh, 4.35), 288 (4.49), 357 (3.85), 373 (3.83) and 395 (3.74). IR ν_{max}^{KBr} cm⁻¹: 3453 (OH), 1651 (C=O), 1560 (C=C), 1417, 1282, 1097 and 931 (OCH₂O). HRMS: *Anal.* calcd C₁₇H₁₁NO₅ (309.0637). Found (*m/z*, 309.0634). EI-MS *m/z* (rel. int.): 309 ([M]⁺, 3), 294 (17), 293 (100), 278 (68), 263 (31), 132 (36), 131 (33), 62 (33). ¹H-NMR (DMSO-*d*₆, 400 MHz) δ: 3.85 (3H, s, OCH₃), 6.42 (2H, s, OCH₂O), 7.14 (1H, d, *J*=8.8 Hz, H-6), 7.18 (1H, s, H-9), 7.55 (1H, s, H-2), 7.65 (1H, brs, NH), 8.13 (1H, d, *J*=8.8 Hz, H-5), 10.73 (1H, s, OH).

Sodium 7-Hydroxyl-8-methoxyaristolactate (3): Colorless powder. C₁₇H₁₁O₆Na. mp >300 °C. UV λ_{max}^{MeOH} nm (log ε): 225 (4.84), 265 (sh, 4.57), 273 (4.60), 296 (4.27), 319 (4.02), 352 (sh, 3.44) and 371 (3.15). IR ν_{max}^{KBr} cm⁻¹: 1558 (C=O), 1415, 1298, 1035 and 933 (OCH₂O). ¹H-NMR (CD₃OD, 400 MHz) δ: 3.92 (3H, s, OCH₃), 6.20 (2H, s, OCH₂O), 7.12 (1H, d, *J*=9.1 Hz, H-6), 7.31 (1H, s, H-2), 7.78 (1H, d, *J*=9.5 Hz, H-9), 8.27 (1H, d, *J*=9.5 Hz, H-10), 8.64 (1H, d, *J*=9.1 Hz, H-5).

Sodium 3,4-Dimethoxybenzoate (4): Colorless powder. C₉H₉O₄Na. mp >300 °C. UV λ_{max}^{MeOH} nm: 205, 252, 286 and 291. IR ν_{max}^{KBr} cm⁻¹: 1602 (C=O), 1558, 1450, 1282 and 1224. ¹H-NMR (CD₃OD, 200 MHz) δ: 3.61 (3H, s, OCH₃), 3.89 (3H, s, OCH₃), 6.75 (1H, d, *J*=8.0 Hz, H-5), 7.47 (1H, dd, *J*=8.0, 1.9 Hz, H-6), 7.57 (1H, d, *J*=1.9 Hz, H-2).

Acidification of 3 and 4: Isolated **3** (0.6 mg) and **4** (1 mg) were dissolved in 5% HCl (1 ml). The solution was eluted from a Sephadex LH-20 column with H₂O, then MeOH, to give NaCl and the acids **3a** (89%, 0.5 mg) and **4a** (85%, 0.76 mg), successively.

Antiplatelet Aggregation Assays: The antiplatelet aggregation assays were based on a method reported by Teng *et al.*³⁴

Cytotoxicity Assays: The *in vitro* KB cytotoxicity assay was carried out according to procedures described by Geran *et al.* and Ferguson *et al.*^{35,36} The assay against P-388, A-549, HT-29 and HL-60 tumor cells was based on a method reported by Lee *et al.*³⁷

Acknowledgments The authors are grateful for financial support in the form of a grant from the National Science Council of the Republic of China (NSC 84-2331-B006-074). We also thank Prof. C. M. Teng and Prof. Y. C. Wu for measuring the antiplatelet activity and carrying out the cytotoxicity testing, respectively.

References and Notes

- Hou D., "Flora of Taiwan," Vol. 2, 2nd ed., Editorial Committee of the Flora of Taiwan, 1996, p. 637.
- Jiangsu New Medicine College, "Encyclopedia of Chinese Materia Medica," Vol. 1, Shanghai Science and Technology Press, Shanghai, 1977, p. 294.

- 3) Moretti C., Rideau M., Chenieux J. C., Viel C., *Planta Med.*, **35**, 360—365 (1979).
- 4) Hinou J., Demetzos C., Harvala C., Roussakis C., *Int. J. Crude Drug Res.*, **28**, 149—151 (1990) [*Chemical Abstracts*, **114**, 160645q (1991)].
- 5) Chen Z. L., Zhu D. Y., (1987) "The Alkaloids," Vol. 31, ed. by Brossi A., Academic Press, Orlando, America, p. 29.
- 6) Leu Y. L., Chan Y. Y., Wu T. S., *Phytochemistry*, **48**, 743—745 (1998).
- 7) Pouchert C. J., Behnke J., "The Aldrich Library of ^{13}C and ^1H FTNMR Spectra," Vol. 2, Aldrich Chemical Company, 1993, 1110B.
- 8) Wu T. S., Leu Y. L., Chan Y. Y., *Chem. Pharm. Bull.*, **46**, 1624—1626 (1998).
- 9) Chiang C. Y., Leu Y. L., Chan Y. Y., Wu T. S., *J. Chin. Chem. Soc.*, **45**, 93—97 (1998).
- 10) Leu Y. L., Chan Y. Y., Hsu M. Y., Chen I. S., Wu T. S., *J. Chin. Chem. Soc.*, **45**, 539—541 (1998).
- 11) Wu T. S., Leu Y. L., Chan Y. Y., *Chem. Pharm. Bull.*, **47**, 571—573 (1999).
- 12) Ma L., Dolphin D., *Tetrahedron*, **52**, 849—860 (1996).
- 13) Wu T. S., Leu Y. L., Chan Y. Y., *Chem. Pharm. Bull.*, **46**, 1301—1302 (1998).
- 14) Nakatani Y., Ourisson G., Beck J. P., *Chem. Pharm. Bull.*, **29**, 2261—2269 (1981).
- 15) Wu T. S., Lin C. N., Yang L. K., Lin S. T., *J. Chin. Chem. Soc.*, **22**, 163—165 (1975).
- 16) Wu T. S., Ou L. F., Teng C. M., *Phytochemistry*, **36**, 1063—1068 (1994).
- 17) Jaensch M., Jakupovic J., King R. M., Robinsin H., *Phytochemistry*, **28**, 3497—3502 (1989).
- 18) Wu T. S., Chan Y. Y., Leu Y. L., *Chem. Pharm. Bull.*, **46**, 370—372 (1998).
- 19) Akasu M., Itokawa H., Fujita M., *Tetrahedron Lett.*, **1974**, 3609—3612.
- 20) Hooghton P. J., Ogutveren M., *Phytochemistry*, **30**, 253—254 (1991).
- 21) Desai S. J., Prabhu B. R., Mulchandani N. B., *Phytochemistry*, **27**, 1511—1516 (1988).
- 22) Nishioka T., Watanabe J., Kawabata J., Niki R., *Biosci. Biotechnol. Biochem.*, **61**, 1138—1141 (1997).
- 23) Chen C. L., Chang H. M., Cowling E. B., *Phytochemistry*, **15**, 547—550 (1976).
- 24) Boker M., Hever S., Wray V., Witte L., Macek T., Vanek T., Strack D., *Phytochemistry*, **30**, 3261—3265 (1991).
- 25) Ishino M., Sakaguchi T., Morimoto I., Okitsu T., *Chem. Pharm. Bull.*, **29**, 2403—2407 (1981).
- 26) Shima K., Hisada S., Inagaki I., *Phytochemistry*, **10**, 894—895 (1971).
- 27) Lalonde R. T., Wong C., Tsai A.I.-M., *J. Am. Chem. Soc.*, **98**, 3007—3012 (1976).
- 28) Pouchert C. J., Behnke J., "The Aldrich Library of ^{13}C - and ^1H -FTNMR Spectra," Vol. 2, Aldrich Chemical Company, 1993, 1115C.
- 29) Wu T. S., Chan Y. Y., Leu Y. L., Chen Z. T., *J. Nat. Prod.*, **62**, 415—418 (1999).
- 30) Teresa J. P., Bellido I. S., Gonzalez M. S., Vicente S., *Phytochemistry*, **25**, 185—190 (1986).
- 31) Wu T. S., Chan Y. Y., Leu Y. L., *J. Nat. Prod.*, **61**, 511—514 (1998).
- 32) Teng C. M., Chen W. Y., Ouyang C., *Biochim. Biophys. Acta*, **924**, 375—382 (1987).
- 33) O'Brien J. R., *J. Clin. Pathol.*, **15**, 452 (1962).
- 34) Yu S. M., Ko F. N., Su M. J., Wu T. S., Wang M. L., Huanf T. F., Teng C. M., *Arch. Pharmacol.*, **345**, 349—355 (1992).
- 35) Geran R. I., Greenberg N. H., MacDonald M. M., Schumacher A. M., Abbott B. J., *Cancer Chemother. Rep.*, **3**, 1—90 (1972).
- 36) Ferguson P. J., Fisher M. H., Stephenson J., Li D. H., Zhou B. S., Cheng Y. C., *Cancer Res.*, **48**, 5956—5964 (1988).
- 37) Lee K. H., Lin Y. M., Wu T. S., Zhang D. C., Yamagishi T., Hayashi T., Hall I. H., Chang J. J., Wu R. Y., Yang T. H., *Planta Med.*, **54**, 308—311 (1988).

Polymer-Supported Dicyanoketene Acetal as a π -Acid Catalyst: Monothioacetalization and Carbon–Carbon Bond Formation of Acetals

Nobuyuki TANAKA, Tsuyoshi MIURA, and Yukio MASAKI*

Gifu Pharmaceutical University, 5–6–1 Mitahora Higashi, Gifu 502–8585, Japan.

Received January 24, 2000; accepted March 15, 2000

Polymeric dicyanoketene acetals (DCKA) were synthesized by copolymerization of styrene and divinylbenzene or ethylene glycol dimethacrylate. These novel polymers could be used successfully as recyclable π -acid catalysts in monothioacetalization or carbon–carbon bond forming reaction of acetals.

Key words polymeric dicyanoketene acetal; π -acid; recyclable catalyst; monothioacetalization; carbon–carbon bond formation

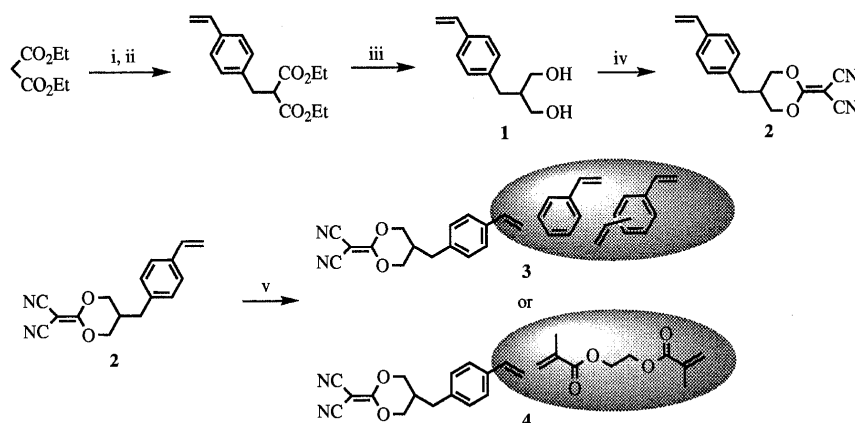
Since Merrifield's solid phase synthesis of peptides,^{1a)} polymer-supported catalysts, reagents, and substrates have attracted much attention for many years due to their inherent advantages in synthetic chemistry: simplification of reaction procedures including easy separation of products, application to automation systems leading to combinatorial chemistry, and recycling of catalysts and reagents.^{1b)}

Useful polymer-supported acid catalysts are classified into several types from the viewpoint of their elements of intrinsic acidity: 1) Lewis acids incorporated coordinately in inorganic and organic polymer matrix such as zeolites,^{2a)} clays,^{2b)} silica,^{2c)} and resins,^{2d)} 2) Lewis acidic metals introduced covalently in organic^{3a)} and mixed organic-inorganic polymer matrix,^{3b)} 3) polymeric protonic (Brønsted) acids such as proton-exchanged zeolites^{4a)} and clays,^{4b)} and protonated ion-exchange resins including hydrochloric,^{4c)} sulfonic,^{4d)} and carboxylic acid,^{4e)} and 4) organic cation species bound to a polystyrene resin.⁵⁾

In the course of our investigation on the π -acid property of tetracyanoethylene (TCNE)⁶⁾ we have found that certain capto-dative olefins, dicyanoketene acetals (DCKA), in which two geminal cyano groups are substituted with alkoxy groups, work well as a promoter in alcoholysis of epoxides,^{7a)}

tetrahydropyranylation of alcohols,^{7b)} and monothioacetalization of acetals.^{7c)} During modification of the structure of DCKA aiming at novel catalytic activities, we have designed polymer-supported dicyanoketene acetals, which are accessible by polymerization of styrene derivatives bearing dicyanoketene acetal moiety. We recently reported in preliminary communications that a polymer-supported DCKA, a new type of solid acid catalyst which does not belong to the above classification, catalyzes monothioacetalization^{8a)} and carbon–carbon bond formation^{8b)} of acetals under unhydrous conditions, and deprotects acetals and silyl ethers in aqueous media.^{8c)} We herein provide full details of monothioacetalization and carbon–carbon bond formation of acetals under mild reaction conditions using a polymer-supported DCKA.

The preparation of polymeric DCKAs (**3** and **4**) is shown in Chart 1. Condensation of diethyl malonate with an equivalent mole of 4-chloromethyl styrene in the presence of NaH gave an inseparable mixture (18:5) of monoalkylated malonate and dialkylated malonate as a by-product. This mixture was reduced with LiAlH₄ to provide a diol derivative (**1**) after chromatographic separation in 46% overall yield in two steps. Condensation of the diol (**1**) with 1.3 mole equivalent of TCNE in the presence of a catalytic amount of Et₂NH⁹⁾ in



i: 1.1 eq NaH, DMF, r.t., 1 h; ii: 0.3 eq NaI, 1.0 eq 4-chloromethyl styrene, 50 °C, 2 h; iii: 3.0 eq LiAlH₄, Et₂O, reflux, 2 h (46% for 2 steps); iv: 0.2 eq Et₂NH, 1.3 eq TCNE, THF, r.t., 2 h (67%); v: (synthesis of **3**), 0.05 eq. AIBN, 1.0 eq divinylbenzene, toluene, 100 °C, 22 h (49%); (synthesis of **4**), 0.05 eq AIBN, 1.0 eq EGDMA, toluene, 100 °C, 2 h (80%).

Chart 1

* To whom correspondence should be addressed. e-mail: masaki@gifu-pu.ac.jp

Table 1. Solvent Effect and the Reusing of **3** and **4** in the Monothioacetalization of **5**

$\text{Ph}-\text{C}(\text{OMe})_2 \xrightarrow[\text{3 h}]{\text{polymeric DCKA (3 or 4) (50mg), PhSH (1.5 eq)}} \text{Ph}-\text{C}(\text{OMe})(\text{SPh})$

5 (50 mg) **6**

Entry	Solvent	Polymeric DCKA	<i>T</i> /°C	Yield (%)		
				1st	2nd	3rd
1	CH ₃ CN	3	60	21	25	—
2	CH ₃ CN	4	60	83	88	87
3	CH ₂ Cl ₂	4	Reflux	10	—	—
4	Et ₂ O	4	Reflux	32	—	—
5	Benzene	4	60	29	—	—
6	Toluene	4	60	35	—	—
7	DMSO	4	60	42	—	—
8	DMF	4	60	61	58	60

THF produced a monomeric styrene derivative (**2**) in 67% yield, which was ascertained to have the catalytic activities in the reaction of benzaldehyde dimethyl acetal (**5**) with thiophenol (1.5 eq) in acetonitrile at 60 °C for 3 h to give the corresponding monothioacetal (**6**) in 87% yield. Copolymerization of **2** with one equivalent mole of each of styrene and divinylbenzene as cross-linking agents using a catalytic amount of AIBN as a radical initiator¹⁰ produced in 49% yield a polymer-supported DCKA (**3**) as a white powder; this was estimated to be composed of an approximate ratio 2:2:1 of **2**, styrene, and divinylbenzene from elemental analysis (2.30 mmol/g for loaded DCKA). Another DCKA (**4**) was obtained with an equivalent mole of ethylene glycol dimethacrylate (EGDMA) as a cross-linking agent according to Dhai's method¹¹ in 95% yield as a white powder, which was estimated to be composed of an approximate ratio 2:1 of **2** and EGDMA from elemental analysis (2.74 mmol/g for loaded DCKA).

The polymeric DCKAs (**3** and **4**) were evaluated as catalysts in monothioacetalization of benzaldehyde dimethyl acetal (**5**) with thiophenol. The polymer (**3** or **4**) (50 mg) was added to a solution of the dimethyl acetal (**5**) (50 mg, 0.33 mmol) and thiophenol (PhSH) (0.50 mmol) in a solvent (1.0 ml). The mixture was stirred at 60 °C and the reaction was monitored by TLC. The reaction displayed a noticeable solvent dependence as listed in Table 1. Although the polymeric DCKA (**3**) showed little catalytic activity, the other one (**4**) accelerated remarkably the monothioacetalization reaction in acetonitrile, which was the solvent of choice for providing a high yield (83%) of a monothioacetal (**6**) (entries 1 and 2). Solvents, CH₂Cl₂, Et₂O, C₆H₆, CH₃C₆H₅, and DMSO were poor to sluggish and DMF was moderate for the reaction (entries 3—8). The product could be easily isolated by filtration of the catalyst followed by the usual workup. After washing the recovered polymer successively with water and ethyl acetate followed by drying at room temperature in vacuo for 4 h, the catalysts (**3** and **4**) could be reused without loss of the activities (entries 1, 2, and 8).

Next, efficiency of the catalyst (**4**) was investigated in the monothioacetalization¹² of several aliphatic acetals including α,β -unsaturated acetals (**10**—**12**), and mixed acetals such as methoxymethyl (MOM) (**13**), tetrahydropyranyl (THP) (**14**), and tetrahydrofuranyl (THF) ethers (**15**) using PhSH as well as phenylthiotrimethylsilane (TMS-SPh) as a nucleophile,

and the results are summarized in Table 2. Typical dimethyl acetals of decyl aldehyde (**7**), 2-octanone (**8**), and cyclohexanone (**9**) smoothly underwent substitution reactions under the conditions at 60 °C within two days to give the corresponding monothioacetals (**16**), (**17**), and (**18**), respectively, although the ketone acetals (**8**, **9**) reacted more rapidly than that of the aldehyde (**7**) (entries 3, 4, 5, 7, and 9). α,β -unsaturated dimethyl acetals of *trans*-cinnamaldehyde (**10**), *trans*-2-hexenal (**11**), and 3-methyl-2-butenal (**12**) gave inseparable complex mixtures, even if the reaction was carried out at room temperature or DMF was used as a solvent (entries 10—16). Unexpectedly, no reaction was observed with dodecyl MOM ether (**13**) (entries 17 and 18). Mixed acetals, THP (**14**) and THF ethers (**15**) derived from *n*-pentanol, underwent regioselective thiolysis depending on the amount of the catalyst and the reaction time, especially when TMS-SPh was used as a nucleophile to afford selectively endo- (**20** and **22**) or exo-cyclic C—O bond cleaved products (**19** and **21**) (entry 19—23). The fact that a smaller amount of the catalyst and shorter period of reaction time led to the linear monothioacetals (**20**) selectively (entry 20) indicated that the endocyclic C—O bond of the THP ether (**14**) appears to be cleaved more rapidly than the exocyclic one, leading initially to **20** which is transformed to cyclic monothioacetal (**19**) with elimination of *n*-pentanol under the reaction conditions. Thus, the intermediate linear monothioacetal (**20**) was subjected to the reaction conditions for 20 h to produce 71% yield of the cyclic monothioacetal (**19**) (Chart 2).

Encouraged by the results of monothioacetalization, we were intrigued by the substitution reaction of aldehydes and acetals¹³ with carbon nucleophiles catalyzed by the polymeric DCKA (**4**). As a preliminary examination, catalytic activity of dicyanoketene ethylene acetal (DCKEA) (**23**) in the carbon—carbon bond forming reaction of aldehydes and ketones was investigated. Thus, benzaldehyde (**24**) when heated under reflux with TMS-CN (A) (1.5 eq) in acetonitrile in the presence of a catalytic amount of DCKEA (**23**) (0.2 eq) gave the corresponding cyanohydrin derivative (**25**) in 63% yield after acidic hydrolysis (Table 3, entry 1). Similarly, *p*-anisaldehyde (**26**), *p*-chlorobenzaldehyde (**28**) and heptanal (**30**) also reacted with TMS-CN (A) to give the corresponding cyanohydrins (**27**, **29** and **31**) in high yields under the same conditions (Table 3, entries 4—6). The methyl ketones acetophenone (**32**) and 2-octanone (**34**), however, gave low yields of the corresponding TMS ether of the cyanohydrins (**33** and **35**) in the reaction with TMS-CN (A) under the same conditions (Table 3, entries 9 and 10). Furthermore, DCKEA (**23**) was found to be a poor catalyst for the reaction of these carbonyl compounds with other silylated nucleophiles (allyltrimethylsilane (TMS-allyl) (B) and acetophenone enol TMS ether (C)) (Table 3, entries 2, 3, 7, 8, 11 and 12).

In turn, attention was focused on the reactivities of acetals with silylated nucleophiles. As shown in Table 4, *p*-anisaldehyde dimethyl acetal (**36**) (0.27 mmol) when heated under reflux for 2 h with TMS-CN (A) (1.5 eq) in acetonitrile in the presence of a catalytic amount of DCKEA (**23**) (0.2 eq) gave the corresponding cyanohydrin derivative (**37**) in 92% yield after workup (entry 1). The finding of the high catalytic activity of a monomeric DCKA (**2**) having styrene moiety to give 98% yield of **37** with 98% recovery of the catalyst (**2**) in

Table 2. Monothioacetalization of Acetals Catalyzed by 4

$\text{R}-\begin{array}{c} \text{OMe} \\ \diagup \\ \text{C} \\ \diagdown \\ \text{OMe} \end{array} \xrightarrow[\text{CH}_3\text{CN, 60 }^\circ\text{C}]{\text{polymeric DCKA (4) (50mg), Nucleophile (1.5 eq)}} \text{R}-\begin{array}{c} \text{OMe} \\ \diagup \\ \text{C} \\ \diagdown \\ \text{SPh} \end{array}$					
Entry	Substrate	Nucleophile	Time (h)	Product/Yield (%)	
1		PhSH	6		73 ^{a)}
2		PhSH	20		75
3		TMS-SPh	7		50 ^{b)}
4		TMS-SPh	20		61
5		TMS-SPh	40		86
6		PhSH	2		64
7		TMS-SPh	5		69
8		PhSH	6		29
9		TMS-SPh	7		80
					36
10		PhSH	2	Mixture	
11		TMS-SPh	20	Mixture	
12		TMS-SPh ^{c)}	27	Mixture	
13		PhSH	20	Mixture	
14		TMS-SPh ^{d)}	20	Mixture	
15		TMS-SPh ^{c)}	27	No reaction	
16		PhSH	2	Mixture	
17		PhSH	31	No reaction	
18		TMS-SPh	31	No reaction	
19		PhSH	12		73
20		TMS-SPh	19		6 ^{e)}
21		TMS-SPh	40		48 ^{f)}
					35
22		PhSH	12		86
23		TMS-SPh	40		75
					18

a) 14% of the starting material was recovered. b) 40% of the starting material was recovered. c) The reaction was carried out at room temperature. d) DMF was used as a solvent. e) 31% of the starting material was recovered. f) 21% of the starting material was recovered.

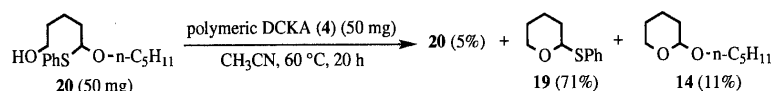


Chart 2

the same reaction prompted us to use the polymeric DCKA (4) as a catalyst in a substitution reaction of 36 with TMS-CN (A) (entry 2). Thus, a mixture of the polymeric DCKA (4) (50 mg), the dimethyl acetal (36) (50 mg, 0.27 mmol), and TMS-CN (A) (0.41 mmol) was refluxed for 2 h in acetonitrile (3 ml). Isolation by the usual workup after filtration of the catalyst (4) gave almost quantitatively the cyanohydrin derivative (37). After washing the recovered polymeric DCKA (4) successively with water and ethyl acetate followed by drying at room temperature *in vacuo* for 4 h, the catalyst (4) could be reused without loss of the activity (entry 3).

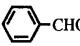
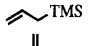
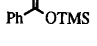
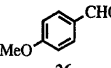
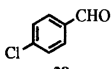

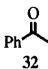

As shown in Table 5, the dimethyl acetals (36, 5 and 44) derived from aryl aldehydes, *p*-anisaldehyde, benzaldehyde and 2-furaldehyde, when treated with TMS-CN (A), TMS-allyl (B), and aryl methyl ketone enol TMS ethers (C and D) in the presence of the polymeric DCKA (4) afforded the corresponding substitution products (37–39, 40–43, 45–47)

in good yields except for allyl-substituted products (entries 1–12). The dimethyl acetals (10 and 11) derived from an α,β -unsaturated aldehyde, *trans*-cinnamaldehyde and *trans*-2-hexenal, when treated with silylated nucleophiles under the same conditions gave the corresponding substitution products (48–54) in good yields except for allyl-substituted product (49) (entries 13–19). Saturated acetals including aldehyde and ketone acetals appear less reactive than α,β -unsaturated ones under the present conditions. Thus, the reaction of decanal and 2-octanone dimethyl acetals (7 and 9) with acetophenone and 2-acetyl furan enol TMS ethers (C and D) proceeded sluggishly to give respectively low yields or no trace of the corresponding aldol methyl ethers (entries 22, 23, 25 and 26), although the reaction with TMS-CN (A) provided moderate to excellent yields of the corresponding substitution products (55 and 58) (entries 20 and 24).

As shown in Table 6, mixed acetals, THP (61) and THF

Table 3. The Reaction of Aldehydes and Ketones with Silylated Nucleophiles Catalyzed by **23**

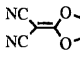
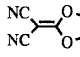
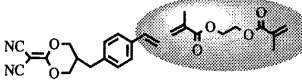
$$\begin{array}{c}
 \text{R}^1\text{C(=O)R}^2 \xrightarrow[\text{CH}_3\text{CN, reflux}]{\begin{array}{c} 0.2 \text{ eq DCKEA (23)} \\ \text{NC} \diagup \text{C} \diagdown \text{O} \\ \text{NC} \diagdown \text{C} \diagup \text{O} \end{array}} \xrightarrow[3\% \text{ HCl}]{1.5 \text{ eq TMS-Nu}} \text{R}^1\text{C(OH)(Nu)R}^2
 \end{array}$$

Entry	Substrate	TMS-Nu	Time (h)	Product	Yield (%)
1		TMS-CN (A)	3	25 Nu=CN	63
2	24		10	No reaction	
3	26		10	No reaction	
4		A	2	27 Nu=CN	Quant.
5		A	21	29 Nu=CN	90
6		A	2	31 Nu=CN	96
7	30	B	10	No reaction	
8	30	C	10	No reaction	
9		A	21	33 Nu=CN	10 ^{a)}
10		A	5	35 Nu=CN	34 ^{b)}
11	34	B	10	No reaction	
12	34	C	10	No reaction	

a) The corresponding TMS ether of the cyanohydrine was isolated as a product and 72% of the substrate (**28**) was recovered. b) The corresponding TMS ether of the cyanohydrine was isolated as a product and 27% of the substrate (**30**) was recovered.

Table 4. The Reaction of **36** with TMS-CN (A) Catalyzed by DCKAs

$$\text{36 (50mg)} \xrightarrow[\text{CH}_3\text{CN, reflux, 2h}]{\text{Catalyst, 1.5 eq TMS-CN (A)}} \text{37}$$

Entry	Catalyst	Yield (%) of 37
1	 DCKEA (23) (0.2 eq)	92
2	 Monomeric DCKA (2) (0.2 eq)	98 (Catalyst recovery; 98%)
3	 Polymeric DCKA (4) (50 mg)	1st 99 2nd quant. 3rd quant.

ethers (**63**) derived from *n*-octanol, underwent carbon-carbon bond formation reaction in the presence of the catalyst. The reactions proceeded, however, without regioselectivity to give low yields of the ring-opening products (**62** and **64**), although the other probable products, 2-cyanotetrahydropyran¹⁴⁾ and 2-cyanotetrahydrofuran¹⁵⁾ corresponding to the produced *n*-octanol (**65**) could not be isolated by the usual workup because of their low boiling points. In contrast to the thiolysis, the ring-opening product (**62**) did not undergo any change under the same reaction conditions, and was recov-

ered quantitatively.

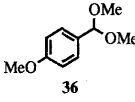
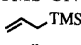
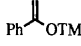
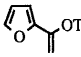
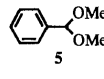
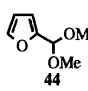
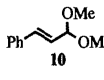
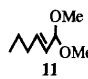
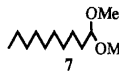
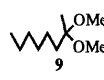
In conclusion, a novel polymer-supported DCKA (**4**) reported herein was found to be an unprecedented and recyclable polymeric π -acid and to successfully promote mild monothioacetalization and carbon-carbon bond formation of acetals.

Experimental

Melting points (Mps) were measured with a Yanagimoto micromelting point apparatus and are uncorrected. IR absorption spectra were recorded on a JASCO IRA-1 spectrometer and a Perkin Elmer Spectrum One. ¹H-NMR spectra were recorded on a JEOL JNM-GX-270 (270 MHz) and a JEOL JNM-EX-400 (400 MHz) spectrometer with SiMe₄ as an internal standard; *J* values are given in Hz. Mass spectra (MS) and high-resolution MS (HRMS) were recorded on a JEOL JMS-D300 or a JEOL JMS-SX102A spectrometer. Products were purified by silica gel chromatography or preparative TLC. Acetonitrile was distilled from CaH₂ and stored over molecular sieves.

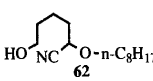
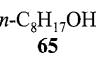
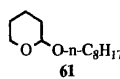
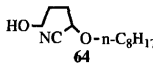
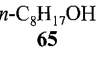
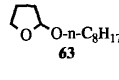
2-(4-Vinylbenzyl)-1,3-propanediol (1) A suspension of NaH (60%, 2.2 g, 55 mmol) in DMF (30 ml) was added to a solution of diethyl malonate (7.6 ml, 50 mmol) in DMF (20 ml) at 0 °C under argon atmosphere, and the mixture was stirred at room temperature for 1 h. A solution of 4-vinylbenzyl chloride (7.1 ml, 50 mmol) and NaI (1.5 g, 10 mmol) in DMF (50 ml) was added, and the mixture was stirred at 50 °C for 2 h. After cooling to room temperature, water was added, and the reaction mixture was extracted with AcOEt. The crude product thus obtained was purified by silica gel chromatography (AcOEt-hexane, 1 : 10) to give a mixture (18 : 5) of a monoalkylated product and a dialkylated one as a by-product. A solution of this mixture in ether (80 ml) was added to a suspension of LiAlH₄ in ether (20 ml), and the mixture was refluxed for 2 h. After cooling to room temperature, 2 M-HCl was added and filtered, and the reaction mixture was extracted with AcOEt. The crude product thus obtained was purified by silica gel chromatography (AcOEt-hexane, 1 : 1 to 1 : 0) to give **1** (4.4 g, 46% for 2 steps) as a colorless oil. IR (neat) cm⁻¹: 3260, 2900, 1610 (C=C), 1380, 1030, 920, 850. ¹H-NMR (CDCl₃) δ : 2.02–2.09 (3H, m+br), 2.62 (2H, d, *J*=7.8 Hz), 3.66, 3.68 (2H, each d, *J*=10.5 Hz), 3.80, 3.81 (2H, each d, *J*=10.7 Hz), 5.21 (1H, d, *J*=10.7 Hz), 5.71 (1H, d, *J*=17.6 Hz), 6.69 (1H, dd, *J*=17.6, 10.7 Hz), 7.15 (2H, d, *J*=7.8 Hz), 7.34 (2H, d, *J*=7.8 Hz).

Table 5. The Reaction of Acetals with Silylated Nucleophiles Catalyzed by **4**

$\text{R}-\begin{array}{c} \text{OMe} \\ \\ \text{OMe} \end{array} \xrightarrow[\text{CH}_3\text{CN, reflux}]{\text{polymeric DCKA (4) (50mg), 1.5 eq. TMS-Nu}} \text{R}-\begin{array}{c} \text{OMe} \\ \\ \text{Nu} \end{array}$					
Entry	Substrate	TMS-Nu	Time (h)	Product	Yield (%)
1		TMS-CN (A)	2	37 Nu=CN	99
2		 (B)	2	No reaction	
3		 (C)	6	38 Nu=CH ₂ COPh	96
4		 (D)	5	39 Nu=CH ₂ CO-2-Furyl	74
5		A	2	40 Nu=CN	95
6		B	24	41 Nu=CH ₂ CH=CH ₂	Trace
7		C	6.5	42 Nu=CH ₂ COPh	Quant.
8		D	21	43 Nu=CH ₂ CO-2-Furyl	63
9		A	3	45 Nu=CN	85
10		B	24	No reaction	
11		C	16	46 Nu=CH ₂ COPh	75
12		D	21	47 Nu=CH ₂ CO-2-Furyl	59
13		A	1.5	48 Nu=CN	94
14		B	24	49 Nu=CH ₂ CH=CH ₂	12 ^{a)}
15		C	16	50 Nu=CH ₂ COPh	98
16		D	21	51 Nu=CH ₂ CO-2-Furyl	95
17		A	1.5	52 Nu=CN	80
18		C	6	53 Nu=CH ₂ COPh	92
19		D	21	54 Nu=CH ₂ CO-2-Furyl	87
20		A	2	55 Nu=CN	96
21		B	24	56 Nu=CH ₂ CH=CH ₂	16 ^{a)}
22		C	16	57 Nu=CH ₂ COPh	38 ^{b)}
23		D	17	No reaction	
24		A	3	58 Nu=CN	63
25		C	6	59 Nu=CH ₂ COPh	44
26		D	21	60 Nu=CH ₂ CO-2-Furyl	15

a) A considerable extent of the aldehyde was obtained. b) 37% of the substrate (**7**) was recovered.

Table 6. The Reaction of Mixed Acetals with TMS-CN (A)

$\begin{array}{c} \text{Cyclohexyl-O-n-C}_8\text{H}_{17} \\ \text{61 (50 mg)} \\ \text{or} \\ \text{Cyclopentyl-O-n-C}_8\text{H}_{17} \\ \text{63 (50 mg)} \end{array} \xrightarrow[\text{CH}_3\text{CN, reflux}]{\text{Catalyst, 1.5 eq TMS-CN (A)}} \begin{array}{c} \text{HO-NC-Cyclohexyl-O-n-C}_8\text{H}_{17} \\ \text{62} \\ \text{or} \\ \text{HO-NC-Cyclopentyl-O-n-C}_8\text{H}_{17} \\ \text{64} \end{array} + \begin{array}{c} \text{61} \\ \text{or} \\ \text{63} \end{array} + \text{n-C}_8\text{H}_{17}\text{OH} \text{ (65)}$					
Entry	Substrate	Catalyst	Time (h)	Product/Yield (%)	
					
1		Polymeric DCKA (4) (50 mg)	3	11	22
2		Polymeric DCKA (4) (50 mg)	21	38	29
3		DCKEA (23) (0.2 eq)	21	24	35
					
4		Polymeric DCKA (4) (50 mg)	21	31	32
5		DCKEA (23) (0.2 eq)	21	26	43

HRMS (EI) m/z : 192.1147 (Calcd for $C_{12}H_{16}O_2$: 192.1150).

5-(4'-Vinylbenzyl)-2-dicyanomethylidene-1,3-dioxane (2) A solution of **1** (4.4 g, 23 mmol) in THF (40 ml) was added to TCNE (3.8 g, 30 mmol) in THF (20 ml) under argon atmosphere. Et_2NH (0.5 ml, 4.6 mmol) was added, and the mixture was stirred at room temperature for 4 h. The reaction mixture was extracted with AcOEt. The crude product thus obtained was purified by recrystallization (AcOEt-hexane) to give **2** (4.1 g, 67%) as a slightly yellow prism. mp 166 °C. IR ($CHCl_3$) cm^{-1} : 2235 (CN), 1570 (C=C), 1480, 1280, 1170, 905. 1H -NMR ($CDCl_3$) δ : 2.67 (1H, m), 2.75 (2H, d, $J=7.3$ Hz), 4.25, 4.28 (2H, each d, $J=10.7$ Hz), 4.56, 4.57 (2H, each d, $J=11.0$ Hz), 5.28 (1H, d, $J=11.2$ Hz), 5.76 (1H, d, $J=17.6$ Hz), 6.70 (1H, dd, $J=17.6, 10.8$ Hz), 7.11 (2H, d, $J=8.3$ Hz), 7.40 (2H, d, $J=7.8$ Hz). *Anal.* Calcd for $C_{16}H_{14}N_2O_2$: C, 72.17; H, 5.30; N, 10.52. Found: C, 72.12; H, 5.33; N, 10.62.

Polymeric DCKA (3) A solution of AIBN (3.1 mg, 0.019 mmol) in toluene (6.2 ml) was added to the mixture of **2** (100 mg, 0.376 mmol), styrene (43.1 μ l, 0.376 mmol) and divinylbenzene (55%, 96.8 μ l, 0.376 mmol), and the reaction mixture was stirred at 100 °C for 22 h. After cooling to room temperature, the reaction mixture was added to MeOH (80 ml), and filtered. The solid product thus obtained was dried *in vacuo* at 40 °C for 4 h to give **3** (80.2 mg, ca. 49%) as a white powder. This polymeric DCKA (**3**) was estimated to be composed of a 2 : 2 : 1 ratio of **2** and styrene and divinylbenzene from elemental analysis (2.30 mmol/g for loaded DCKA). IR (KBr) cm^{-1} : 3513, 3022, 2926, 2228 (CN), 1754, 1684, 1567 (C=C), 1513, 1490, 1443, 1291, 1240, 1181, 1089, 962, 909, 842, 707, 543. *Anal.* Found: C, 76.09; H, 6.19; N, 6.73.

Polymeric DCKA (4) A solution of AIBN (92.5 mg, 0.563 mmol) in toluene (185 ml) was added to the mixture of **2** (3.0 g, 11 mmol) and EGDMA (2.1 ml, 11 mmol), and the reaction mixture was stirred at 100 °C for 2 h. After cooling to room temperature, the reaction mixture was added to MeOH (1.5 l), and filtered. The solid product thus obtained was dried *in vacuo* at 40 °C for 4 h to give **4** (3.9 g, ca. 95%) as a white powder. This polymeric DCKA (**4**) was estimated to be composed of a 2 : 1 ratio of **2** and EGDMA from elemental analysis (2.74 mmol/g for loaded DCKA). IR (KBr) cm^{-1} : 3156, 2944, 2228 (CN), 1726 (C=O), 1563 (C=C), 1492, 1445, 1396, 1292, 1242, 1182, 1131, 962, 909, 712, 543. *Anal.* Found: C, 65.55; H, 5.67; N, 7.28.

General Procedure for the Reactions of Acetals with Thiophenol Catalyzed by the Polymeric DCKA (4) Benzaldehyde dimethylacetal (**5**) (50.7 mg, 0.333 mmol) and thiophenol (51.3 μ l, 0.500 mmol) were added to a suspension of polymeric DCKA (**4**) (50.0 mg) in acetonitrile (1 ml) under argon atmosphere, and the mixture was stirred at 60 °C for 3 h. After filtration of catalyst, the crude product was purified by preparative TLC (AcOEt-hexane, 1 : 10) to give methoxy(phenylthio)methyl benzene (**6**) (63.5 mg, 83%) as a slightly yellow oil. After washing the recovered polymer (**4**) successively with water and ethyl acetate followed by drying at room temperature *in vacuo* for 4 h, the catalyst (**4**) could be reused without loss of the activities (2nd. recycle; 67.6 mg, 88%, 3rd recycle; 67.1 mg, 87%).

Compounds (**6**, **17**, **18**, **19**, **21**)^{12d}, (**16**, **20**, **22**)^{7c} were identified by comparison of their spectroscopic behavior with those described in the references. The yields and reaction conditions of other products are shown in Table 2.

General Procedure for the Reactions of Aldehydes and Ketones with Silylated Nucleophiles Catalyzed by DCKEA (23) *p*-Anisaldehyde (**26**) (50.0 mg, 0.367 mmol) and TMS-CN (**A**) (73.5 μ l, 0.551 mmol) were added to a solution of DCKEA (**23**) (10.0 mg, 0.073 mmol) in acetonitrile (3 ml) under argon atmosphere, and the mixture was refluxed for 2 h. Hydrochloric acid (3%) was added to the reaction mixture which was then extracted with ether. After workup, the crude product was purified by silica gel column chromatography (AcOEt-hexane, 1 : 2) to give 2-hydroxy-2-(4-methoxyphenyl)-ethanenitrile (**27**) (59.9 mg, quant.) as a colorless oil.

Compounds (**25**, **27**, **31**, **33**)¹⁶, **29**¹⁷, **35**¹⁸ were identified by comparison of their spectroscopic behavior with those described in the references.

General Procedure for the Reactions of Acetals with Silylated Nucleophiles Catalyzed by DCKEA (23) *p*-Anisaldehyde dimethylacetal (**36**) (50.0 mg, 0.274 mmol) and TMS-CN (**A**) (54.8 μ l, 0.411 mmol) were added to a solution of DCKEA (**23**) (7.5 mg, 0.055 mmol) in acetonitrile (3 ml) under argon atmosphere, and the mixture was refluxed for 2 h. Water was added to the reaction mixture which was then extracted with ether. After workup, the crude product was purified by silica gel column chromatography (AcOEt-hexane, 1 : 2) to give 2-methoxy-2-(4-methoxyphenyl)-ethanenitrile (**37**) (44.9 mg, 92%) as a slightly yellow oil.

General Procedure for the Reactions of Acetals with Silylated Nucleophiles Catalyzed by the Polymeric DCKA (4) *p*-Anisaldehyde dimethyl-

acetal (**36**) (50.0 mg, 0.274 mmol) and TMS-CN (**A**) (54.8 μ l, 0.411 mmol) were added to a suspension of polymeric DCKA (**4**) (50.0 mg) in acetonitrile (3 ml) under argon atmosphere, and the mixture was refluxed for 2 h. After filtration of catalyst (**4**), the crude product was purified by silica gel column chromatography (AcOEt-hexane, 1 : 4) to give 2-methoxy-2-(4-methoxyphenyl)-ethanenitrile (**37**) (48.1 mg, 99%) as a slightly yellow oil. After washing the recovered polymer (**4**) successively with water and ethyl acetate followed by drying at room temperature *in vacuo* for 4 h, the catalyst (**4**) could be reused without loss of the activities (2nd recycle; 48.6 mg, quant., 3rd recycle; 48.6 mg, quant.).

Compounds (**37**, **38**, **42**, **52**, **55**)^{13e}, (**39**, **40**, **43**, **45**, **46**, **47**, **50**, **51**, **53**, **54**, **56**, **57**, **59**)^{6d}, (**48**, **49**)¹⁶, (**58**)¹⁸ were identified by comparison of their spectroscopic behavior with those described in the references. The yields and reaction conditions of other products are shown in Table 5.

1-(2-Furyl)-3-methoxy-3-methyloctane-1-one (60) Slightly yellow oil; IR ($CHCl_3$) cm^{-1} : 2950, 2870, 1665 (C=O), 1570 (C=C), 1470, 1390, 1360, 1280, 1160, 1070, 1010, 900, 880, 830. 1H -NMR ($CDCl_3$) δ : 0.87 (3H, t, $J=7.3$ Hz), 1.27 (13H, m), 1.68 (2H, m), 3.21 (3H, s), 6.54 (1H, dd, $J=3.4, 1.5$ Hz), 7.19 (1H, d, $J=3.4$ Hz), 7.59 (1H, s). HRMS (FAB) m/z : 253.1809 (Calcd for $C_{15}H_{24}O_3$: 253.1803).

1'-Cyano-5'-hydroxy-pentyl Octyl Ether (62) Colorless oil; IR ($CHCl_3$) cm^{-1} : 3340 (OH), 2900, 1460, 1330, 1100. 1H -NMR ($CDCl_3$) δ : 0.88 (3H, t, $J=6.6$ Hz), 1.27 (11H, brs), 1.61 (6H, m), 1.88 (2H, q, $J=6.8$ Hz), 3.43 (1H, dt, $J=6.4$ Hz), 3.68 (2H, t, $J=5.9$ Hz), 3.76 (1H, dt, $J=6.4$ Hz), 4.11 (1H, t, $J=6.6$ Hz). HRMS (FAB) m/z : 242.2115 (Calcd for $C_{14}H_{27}NO_2$: 242.2120).

1'-Cyano-4'-hydroxy-butyl Octyl Ether (64) Colorless oil; IR ($CHCl_3$) cm^{-1} : 3420 (OH), 2880, 1440, 1330, 1100. 1H -NMR ($CDCl_3$) δ : 0.88 (3H, t, $J=6.6$ Hz), 1.28 (10H, brs), 1.59—1.81 (5H, m), 1.97 (2H, q, $J=6.8$ Hz), 3.45 (1H, dt, $J=6.6$ Hz), 3.70 (2H, t, $J=6.1$ Hz), 3.76 (1H, dt, $J=6.6$ Hz), 4.19 (1H, t, $J=6.3$ Hz). HRMS (FAB) m/z : 228.1973 (Calcd for $C_{13}H_{25}NO_2$: 228.1963).

References and Notes

- 1) a) Merrifield B., *Science*, **232**, 341—347 (1986) and references cited therein; b) Reviews: Akelah A., Sherrington D. C., *Chem. Rev.*, **81**, 557—587 (1981); Fréchet J. M. J., *Tetrahedron*, **37**, 663—683 (1981); Shuttleworth S. J., Allin S. M., Sharma P. K., *Synthesis*, **1997**, 1217—1239.
- 2) a) Onaka M., Sugita K., Izumi Y., *Chem. Lett.*, **1986**, 1327—1328; b) Clark J. H., Martin K., Teasdale A. J., Barlow S. J., *J. Chem. Soc., Chem. Commun.*, **1995**, 2037—2040; Villemain D., Martin B., *J. Chem. Res. (S)*, **1994**, 146—147; c) Iranpoor N., Tarrian T., Movahedi Z., *Synthesis*, **1996**, 1473—1476; d) Kobayashi S., Nagayama S., *J. Org. Chem.*, **61**, 2256—2257 (1996); Tamami B., Iranpoor N., Zarchi M. A. K., *Polymer*, **34**, 2011—2013 (1993).
- 3) a) Kobayashi S., Nagayama S., *Synlett*, **1997**, 653—654; Nagahara S., Maruoka K., Yamamoto H., *Chem. Lett.*, **1992**, 1193—1196; b) Otera J., Niibo Y., Tatsumi N., Nozaki H., *J. Org. Chem.*, **53**, 275—278 (1988).
- 4) a) Kumar P., Dinesh C. U., Reddy R. S., Pandey B., *Synthesis*, **1993**, 1069—1070; Takeuchi H., Kitajima K., Yamamoto Y., Mizuno K., *J. Chem. Soc., Perkin Trans. 2*, **1993**, 199—203; b) Hoyer S., Laszlo P., *Synthesis*, **1986**, 655—657; c) Johnston R. D., Marston C. R., Krieger P. E., Goe G. L., *Synthesis*, **1988**, 393—394; d) Olah G. A., Husain A., Singh B. P., *Synthesis*, **1983**, 892—895; e) Svec F., Bares M., Zajic J., Káral J., *Chem. Ind.*, **1977**, 159.
- 5) Mukaiyama T., Iwakiri H., *Chem. Lett.*, **1985**, 1363—1366.
- 6) a) Masaki Y., Miura T., Ochiai M., *Synlett*, **1993**, 847—849; b) Masaki Y., Miura T., Ochiai M., *Chem. Lett.*, **1993**, 17—20; c) Miura T., Masaki Y., *J. Chem. Soc., Perkin Trans. 1*, **1994**, 1659—1660; d) Miura T., Masaki Y., *J. Chem. Soc., Perkin Trans. 1*, **1995**, 2155—2158.
- 7) a) Miura T., Masaki Y., *Chem. Pharm. Bull.*, **43**, 523—525 (1995); Masaki Y., Miura T., Ochiai M., *Bull. Chem. Soc. Jpn.*, **69**, 195—205 (1996); b) Miura T., Masaki Y., *Synth. Commun.*, **25**, 1981—1987 (1995); c) Miura T., Masaki Y., *Tetrahedron Lett.*, **35**, 7961—7964 (1994); *Tetrahedron*, **51**, 10477—10486 (1995).
- 8) a) Masaki Y., Tanaka N., Miura T., *Tetrahedron Lett.*, **39**, 5799—5802 (1998); b) Tanaka N., Masaki Y., *Synlett*, **1999**, 1277—1279. c) Tanaka N., Masaki Y., *Synlett*, **1999**, 1960—1962.
- 9) Middleton W. J., Engelhardt V. A., *J. Am. Chem. Soc.*, **80**, 2788—2795 (1958).
- 10) Minutolo F., Pini D., Salvadori P., *Tetrahedron Lett.*, **37**, 3375—3378

- (1996).
- 11) De B. B., Lohray B. B., Sivaram S., Dhali P. K., *Tetrahedron Asymmetry*, **6**, 2105—2108 (1995).
- 12) The most convenient method for preparation of saturated monothioacetals is the transacetalization of acetals. a) Nakatsubo F., Cocuzza A. J., Keeley D. E., Kishi Y., *J. Am. Chem. Soc.*, **99**, 4835—4836 (1977); Kieczkowski G. R., Schlessinger R. H., *J. Am. Chem. Soc.*, **100**, 1938—1940 (1978); Naruto M., Ohno K., Naruse N., *Chem. Lett.*, **1978**, 1419—1422; b) Kim S., Park J. H., Lee S., *Tetrahedron Lett.*, **30**, 6697—6700 (1989); c) Morton H. E., Guindon Y., *J. Org. Chem.*, **50**, 5379—5382 (1985); Guindon Y., Bernstein M. A., Anderson P. C., *Tetrahedron Lett.*, **28**, 2225—2228 (1987); d) Sato T., Kobayashi T., Gojo T., Yoshida E., Otera J., Nozaki H., *Chem. Lett.*, **1987**, 1661—1664; Sato T., Otera J., Nozaki H., *Tetrahedron*, **45**, 1209—1218 (1989); e) Masaki Y., Serizawa Y., Kaji K., *Chem. Lett.*, **1985**, 1933—1936.
- 13) In recent years, a variety of efficient catalysts or promoters have been developed to induce carbon-carbon bond forming reactions of aldehydes, ketones, and acetals with silylated nucleophiles. a) McCluskey A., Mayer D. M., Young D. J., *Tetrahedron Lett.*, **38**, 5217—5218 (1997); b) Ooi T., Tayama E., Takahashi M., Maruoka K., *Tetrahedron Lett.*, **38**, 7403—7406 (1997); c) Ishii A., Kotera O., Saeki T., Mikami K., *Synlett*, **1997**, 1145—1146; d) Soga T., Takenoshita H., Yamada M., Han J. S., Mukaiyama T., *Bull. Chem. Soc. Jpn.*, **64**, 1108—1117 (1991); e) Soga T., Takenoshita H., Yamada M., Mukaiyama T., *Bull. Chem. Soc. Jpn.*, **63**, 3122—3131 (1990); f) Sato T., Otera J., Nozaki H., *J. Am. Chem. Soc.*, **112**, 901—902 (1990) and references cited therein.
- 14) Nelson B. A., Hodges E. J., Simon J. I., *J. Org. Chem.*, **1956**, 798—799.
- 15) Williams N., *Ber. Dtsch. Chem. Ges.*, **60**, 2509—2514 (1927).
- 16) Torii S., Inokuchi T., Takagishi S., Horike H., Kuroda H., Uneyama K., *Bull. Chem. Soc. Jpn.*, **60**, 2173—2188 (1987).
- 17) Inagaki M., Hatanaka A., Mimura M., Hiratake J., Nishioka T., Oda J., *Bull. Chem. Soc. Jpn.*, **65**, 111—120 (1992).
- 18) Higuchi K., Onaka M., Izumi Y., *Bull. Chem. Soc. Jpn.*, **66**, 2016—2032 (1993).

Pregnane Glycosides from the Roots of *Asclepias tuberosa*¹⁾

Fumiko ABE* and Tatsuo YAMAUCHI

Faculty of Pharmaceutical Sciences, Fukuoka University, 8-19-1 Nanakuma, Jonan-ku, Fukuoka 814-0180, Japan.

Received January 25, 2000; accepted March 3, 2000

Sixteen glycosides of pregnanes, including ikemagenin, lineolon, and a new pregnane, 3 β ,8 β ,14 β ,15 β ,16 α -pentahydroxy-5 α -pregnan-20-one, termed pleurogenin, were isolated from the roots of *Asclepias tuberosa*. Among ikemagenin and lineolon glycosides, one (1) was a known glycoside, and eight (2–7, 10, 13) were glycosides with new combinations of ikemagenin or lineolon and known sugar sequences composed of D-cymarose, D-oleandrose, D-thevetose and D-glucose. The structures of four new glycosides of ikemagenin (8, 9, 11, 12) and three of pleurogenin (14–16) were determined. The new glycosides have sugar sequences ranging from tetraoside to heptaosides.

Key words pregnane glycoside; 3 β ,8 β ,14 β ,15 β ,16 α -pentahydroxy-5 α -pregnan-20-one; *Asclepias tuberosa*; Asclepiadaceae; pleurisy root; ikemagenin

During our investigations on the constituents of Asclepiadaceous plants, the isolations and structure determinations of pregnane glycosides from *Asclepias fruticosa*,²⁾ *Marsdenia tomentosa*,³⁾ *Hoya carnosa*⁴⁾ and *Tylophora tanakae*⁵⁾ were reported. In the preceding paper, we described the isolation of cardenolide glycosides including Δ^5 -calotropin 3'-O-glucoside and two Δ^5 -calotropin derivatives having a spiro-type linkage of thiazolidinone at the 3'-carbon, from the roots of *Asclepias tuberosa* L., which was used to treat pleurisy and bronchitis in North America and called "pleurisy root."¹⁾ This paper deals with the pregnane glycosides from these roots.

When the roots were percolated with MeOH, the pregnane glycosides and cardenolide glycosides were roughly partitioned in the benzene- and CHCl₃-soluble fractions, respectively, from the MeOH extract. Prior to the isolation of individual pregnane glycoside, a portion of the benzene fraction was subjected to acid hydrolysis, in order to identify the component sugars and pregnanes. The sugars were identified as D-oleandrose (Ole), D-cymarose (Cym), D-digitoxose (Dgt), D-canarose (Can), D-thevetose (Thv), and D-glucose (Glc) along with two bioses, strophanthobiose (β -D-glucosyl-D-cymarose) and glucosyl-oleandrose by direct comparisons with authentic sugars on TLC, ¹H-NMR and optical rotation data. All sugar linkages in the glycosides were assigned to be in the β -form based on the coupling constants of the anomeric protons as shown in Table 3. From the pregnane fraction in the hydrolysate, two pregnanes (**a-1**, **a-2**) were obtained, and **a-1** was identified as ikemagenin by direct comparison with an authentic sample.²⁾

Pregnane **a-2** was suggested to have the molecular formula, C₂₁H₃₄O₆, based on high resolution (HR)-FAB-MS. The NMR spectra showed the presence of an acetyl side-chain at C-17 by the signals at δ_C 32.1 (q), 213.4 (s), and δ_H 2.28 (3H, s). The methine carbon signal at δ 70.9 was assigned to C-17 by 3-bond correlation with the H-21 proton signal in the heteronuclear multiple bond connectivity (HMBC) spectrum. The proton signal of H-17 (δ 3.12, d, $J=5$ Hz) was confirmed by the ¹H-¹³C shift correlation spectroscopy (COSY) spectrum. The spin system from H-17 was observed at H-16 (δ 4.92, dd, $J=6, 5$ Hz) and then H-15 (δ 4.80, d, $J=6$ Hz) in the ¹H-¹H COSY spectrum. Corresponding tertiary carbon signals were observed at δ 81.8 and δ

81.9, respectively, suggesting the presence of hydroxy groups at C-15 and C-16, along with one at C-14. The presence of two quaternary carbons bearing oxygen was observed at δ 83.7 and 77.0, and the former signal was assigned to be C-14 by 3-bond correlations with H-17 and H-18, while the latter one was C-8, based on the coupling pattern of H-9 (br d, $J=11$ Hz). The three hydroxy groups at C-8, 14 and C-15 were assigned to have a β -orientation from the nuclear Overhauser effect (NOE) between H-9 and H-15. A 17R-configuration (17 β -acetyl) and a 16 α -OH configuration were confirmed by NOEs between H-21 and H-18, H-16, as well as the coupling constant ($J=5$ Hz) between H-16 β and H-17 α . The stereochemistry at C-5 was assigned to be 5 α -H, based on shielding of the C-19 signal to δ 13.4. The remaining hydroxy group was considered to be 3 β -OH, since a methine proton signal was observed at δ 3.86 in axial mode. Pregnane **a-2**, 3 β ,8 β ,14 β ,15 β ,16 α -pentahydroxy-5 α -pregnan-20-one, is a new compound and was called pleurogenin.

Isolation of the glycosides from the benzene extract was carried out using silica gel and octadecyl silica (ODS) column chromatography and preparative HPLC, to afford sixteen pregnane glycosides along with a small amount of free cardenolides.¹⁾ The aglycone of **1**–**12** was assigned to be ikemagenin based on the NMR data. Glycoside **1** was identical to compound **3** isolated from *Cynanchum caudatum*.⁶⁾ The sugar sequences in **2**–**7** and **10** were considered to be those represented in Chart 1 based on the difference (DIF)-NOE and/or HMBC methods. They are previously known sequences in the glycosides of pregnanes except ikemagenin, obtained from Asclepiadaceae plants,^{6,7)} and their structures were finally determined by comparison of the NMR signals from the sugar moieties.

Glycoside **8** was considered to have the molecular formula, C₆₈H₁₀₂O₂₆, based on HR-FAB-MS. The NMR spectra suggested that the sugar moiety in **8** was composed of 2 moles each of Dgt and Cym, along with one each of Can and terminal Glc. In DIF-NOE, the H-1 signals in Glc, outer Cym, outer Dgt, Can, and inner Cym showed correlations to H-4 in outer Cym, outer Dgt, Can, inner Cym, and inner Dgt, respectively. The signal of H-3 showed a response by irradiation of H-1 in inner Dgt. Furthermore, the H-4 signals of outer Cym, outer Dgt, Can, inner Cym, and inner Dgt showed cross peaks to the C-1 signals of Glc, outer Cym,

* To whom correspondence should be addressed. e-mail: abefumi@fukuoka-u.ac.jp

Table 1. NMR Spectral Data for the Aglycone Moieties of **1**–**16** and **a-2** [δ ppm in Pyridine- d_5 , J in Hz]

No.	1–12		13		14–16		a-2	
	C ^{a)}	H ^{b)}	C	H	C	H	C	H
1	38.9		39.0		38.3		38.5	
2	29.8		29.9		29.6		32.0	
3	77.6	3.85 (m)	77.7	3.86 (m)	76.6	3.86 (m)	70.7	3.86 (m)
4	39.2		39.3		34.5		38.9	
5	139.4		139.5		45.0	0.98 (m)	45.5	1.12 (m)
6	119.1	5.30 (br d, 4)	119.3	5.32 (br d, 4)	25.3		25.4	
7	35.1		34.5		34.9	2.11 (br d, 14, β)	35.0	2.13 (dt, 14,3, β)
8	74.5		74.5		77.0		77.0	
9	44.8		45.1		50.7	1.34 (br d, 11)	50.8	1.39 (br d, 11)
10	37.5		37.5		36.7		36.8	
11	24.9		29.3		18.3		18.4	
12	73.3	5.26 (dd, 12,4)	69.0	3.98 (dd, 12,4)	40.4	1.96 (br t, 12), 1.82 (br d, 12)	40.5	1.62 (td, 12,4), 2.12 (br d, 12)
13	55.8		57.9		47.5		47.5	
14	87.4		87.4		83.6		83.7	
15	34.1		35.3		81.9	4.77 (d, 5)	81.9	4.80 (d, 6)
16	21.9		22.1		81.8	4.91 (t, 5)	81.8	4.92 (dd, 6,5)
17	60.5		61.4		70.9	3.10 (d, 5)	70.9	3.12 (d, 5)
18	15.7	2.00 (s)	14.7	1.95 (s)	19.3	1.39 (s)	19.3	1.41 (s)
19	18.1	1.35 (s)	18.3	1.38 (s)	13.2	1.19 (s)	13.4	1.26 (s)
20	209.2		210.4		213.4		213.4	
21	32.1	2.27 (s)	32.0	2.42 (s)	32.1	2.27 (s)	32.1	2.28 (s)

a) 12-*O*-Cinnamoyl residue: δ 165.8 (C-1'), 119.2 (C-2'), 144.8 (C-3'), 135.0 (C-4'), 128.5 (C-5', 9'), 129.2 (C-6', 8'), 130.4 (C-7'). b) 12-*O*-Cinnamoyl residue: δ 6.78 (d, $J=16$ Hz, H-2'), 7.98 (d, $J=16$ Hz, H-3'), 7.34 (m, H-6', 7', 8'), 7.61 (br d, $J=8$ Hz, H-5', 9').

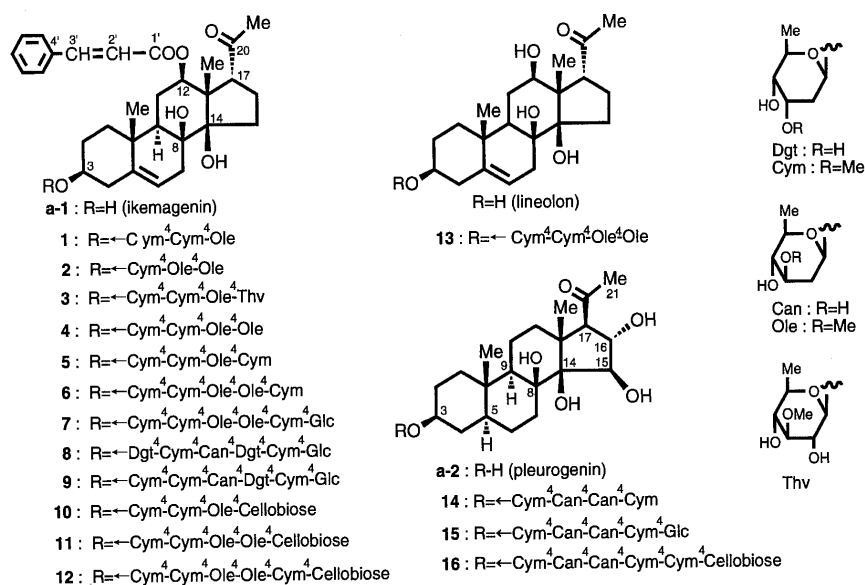


Chart 1

outer Dgt, Can, and inner Cym, respectively. Thus, **8** was determined to be ikemagenin 3-*O*- β -D-glucopyranosyl-(1 \rightarrow 4)- β -D-cymaropyranosyl-(1 \rightarrow 4)- β -D-digitoxopyranosyl-(1 \rightarrow 4)- β -D-canaropyranosyl-(1 \rightarrow 4)- β -D-cymaropyranosyl-(1 \rightarrow 4)- β -D-digitoxopyranoside.

In HR-FAB-MS, **9** was suggested to have the molecular formula, C₆₉H₁₀₄O₂₆, one CH₂ greater than **8**. Based on the NMR data, the sugar moiety of **9** was composed of 3 moles of Cym and one mole each of Dgt, Can and terminal Glc, indicating the substitution of Cym for inner Dgt in **8**. The same correlations as in **8** were observed in DIF-NOE except for the NOE between Cym (inner) and H-3. In the HMBC spectrum, cross-peaks were observed between the H-4 signals and the corresponding C-1 signals in the connecting sugars

with 3-bond relations. Consequently, **9** was identified as ikemagenin 3-*O*- β -D-glucopyranosyl-(1 \rightarrow 4)- β -D-cymaropyranosyl-(1 \rightarrow 4)- β -D-digitoxopyranosyl-(1 \rightarrow 4)- β -D-canaropyranosyl-(1 \rightarrow 4)- β -D-cymaropyranosyl-(1 \rightarrow 4)- β -D-cymaropyranoside.

The molecular formula of **11** was considered to be C₇₀H₁₀₆O₂₈, based on the HR-FAB-MS data, and the sugar moiety was composed of 2 moles each of Cym, Ole and Glc. In the same DIF-NOE and HMBC procedures as in **8** or **9**, the sugar moiety of **11** was determined to be the cellobioside of **4**, that is, β -cellobiosyl-(1 \rightarrow 4)- β -D-oleandropyranosyl-(1 \rightarrow 4)- β -D-cymaropyranosyl-(1 \rightarrow 4)- β -D-cymaropyranoside.

Glycoside **12** (C₇₇H₁₁₈O₃₁) was suggested to be a hepta-

Table 2. ^{13}C -NMR Spectral Data for the Sugar Moieties (**8**, **9**, **11**, **12**, **14**—**16**) [δ ppm in Pyridine- d_5]^{a)}

C	8	9	11	12	14	15	16
Sug-1	Dgt(1)	Cym(1)	Cym(1)	Cym(1)	Cym(1)	Cym(1)	Cym(1)
1	96.3	96.4	96.4	96.4	95.8	95.8	95.8
2	38.9	37.2	37.2 ^{b)}	37.8 ^{b)}	37.2	37.2	37.3
3	67.3 ^{b)}	77.9 ^{b)}	78.0 ^{c)}	78.0	77.9	77.9	77.5 ^{b)}
4	83.1	83.3	83.3	83.3 (Cym(2)-1)	83.6 (Can(1)-1)	83.6	83.6
5	69.4	69.4 ^{c)}	68.8	68.9 ^{c)}	68.9	68.9	68.9
6	17.9 ^{c)}	17.9 ^{d)}	18.4 ^{d)}	18.4 ^{d)}	17.6	17.5 ^{b)}	17.6 ^{c)}
Sug-2	Cym(1)	Cym(2)	Cym(2)	Cym(2)	Can(1)	Can(1)	Can(1)
1	99.6 (Dgt(1)-4)	100.4 (Cym(1)-4)	100.4 (Cym(1)-4)	100.4	101.9	101.9 (Cym(1)-4)	101.9
2	36.8	37.0	37.0 ^{b)}	37.6 ^{b)}	39.8	39.8	39.8
3	77.7	77.8 ^{b)}	77.7 ^{c)}	77.7	69.7	69.7	69.7 ^{d)}
4	83.3	83.1 ^{e)}	83.1	83.1 (Ole(1)-1)	88.1 (Can(2)-1)	88.1 (Can(2)-1)	88.1
5	69.1 ^{d)}	69.0 ^{c)}	69.0	69.0 ^{c)}	70.8	70.8	70.8
6	18.0 ^{c)}	18.0 ^{d)}	18.5 ^{e)}	18.5 ^{d)}	18.0	18.0 ^{b)}	17.9 ^{e)}
Sug-3	Can	Can	Ole(1)	Ole(1)	Can(2)	Can(2)	Can(2)
1	101.9 (Cym(1)-4)	101.9 (Cym(2)-4)	101.9 (Cym(2)-4)	101.9 (Cym(2)-4)	101.3 (Can(1)-4)	101.3 (Can(1)-4)	101.3
2	39.7	39.8	37.5 ^{b)}	37.2 ^{b)}	39.4	39.4	39.4
3	69.7	69.7	78.9	79.1 ^{e)}	69.7	69.6	69.6 ^{d)}
4	88.0	88.0 (Dgt-1)	82.6	82.7	87.6 (Cym(2)-1)	87.4 (Cym(2)-1)	87.5
5	70.9	70.9	72.0 ^{e)}	71.8 ^{d)}	71.2	71.2	71.2
6	18.3 ^{c)}	18.3 ^{d)}	18.6 ^{d)}	18.5 ^{d)}	18.4	18.1 ^{b)}	18.0 ^{c)}
Sug-4	Dgt(2)	Dgt	Ole(2)	Ole(2)	Cym(2)	Cym(2)	Cym(2)
1	99.7 (Can-4)	99.8 (Can-4)	99.9	100.1	99.7 (Can(2)-4)	99.6 (Can(2)-4)	99.7
2	38.4	38.4	37.5 ^{b)}	36.9 ^{b)}	35.5	36.3	36.7 ^{e)}
3	67.4 ^{b)}	67.2	79.7	79.0 ^{e)}	78.5	77.6	77.8 ^{b)}
4	82.5	82.5 (Cym(3)-1)	83.6 (Glc(1)-1)	82.6	73.7	82.5 (Glc-1)	82.5
5	68.5	68.8 ^{c)}	71.5 ^{e)}	71.5 ^{f)}	71.4	69.9	69.5
6	18.5 ^{c)}	18.5 ^{d)}	18.8 ^{d)}	18.6 ^{d)}	18.6	18.6 ^{b)}	18.5 ^{c)}
Sug-5	Cym(2)	Cym(3)	Glc(1)	Cym(3)		Glc	Cym(3)
1	99.8 (Dgt(2)-4)	99.7	104.2 (Ole(2)-4)	98.4		106.5 (Cym(2)-4)	100.3
2	36.4	36.4	75.2	36.8 ^{b)}		75.3	36.5 ^{e)}
3	77.8	77.7 ^{b)}	76.2	78.1		78.3	77.9 ^{b)}
4	82.8	82.8 ^{e)} (Glc-1)	81.7 (Glc(2)-1)	83.3 (Glc(1)-1)		71.8	83.0
5	69.0 ^{d)}	69.0	76.9	69.6		78.4	69.3
6	18.6 ^{c)}	18.5 ^{d)}	62.5	18.7 ^{d)}		63.0	18.6 ^{c)}
Sug-6	Glc	Glc	Glc(2)	Glc(1)			Glc(1)
1	106.4 (Cym(2)-4)	106.5 (Cym(3)-4)	104.9 (Glc(1)-4)	106.1 (Cym(3)-4)			106.1
2	75.3	75.3	74.7	74.9			74.9
3	78.3	78.3	78.2	76.5			76.5
4	71.8	71.8	71.6	81.3 (Glc(2)-1)			81.3
5	78.4	78.4	78.4	76.4			76.4
6	63.0	63.0	62.5	62.4			62.4
Sug-7				Glc(2)			Glc(2)
1				104.9			104.9
2				74.7			74.7
3				78.2			78.2
4				71.6 ^{f)}			71.5
5				78.5			78.4
6				62.4			62.4
OMe	58.6	58.6	57.2 (×2)	57.3	58.1	58.7 (×2)	58.0
	58.9	58.8	58.8 (×2)	57.4	58.7		58.8
		58.9		58.6			58.9
				58.8 (×2)			

a) Proton signals coupled via 3-bonds are shown in parentheses. b—f) Signal assignments may be interchangeable.

side. On comparing the NMR signals with those of **11**, **12** seemed to have one extra Cym. The presence of the β -cellobiosyl→Cym linkage and the array of Ole→Ole→Cym→Cym→ikemagenin in **12** were assigned by DIF-NOE and HMBC. Upon partial hydrolysis of **12** with cellulase, deglucosyl-**12** (**7**) and decellobiosyl-**12** (**6**) were observed on TLC. Therefore, the structure of **12** was determined to be ikemagenin 3-*O*- β -cellobiosyl-(1→4)- β -D-cymaropyranosyl-(1→4)- β -D-oleandropyranosyl-(1→4)- β -D-oleandropyranosyl-(1→4)- β -D-cymaropyranosyl-(1→4)- β -D-cymaropyranoside.

HR-FAB-MS of **13** suggested the molecular formula,

$\text{C}_{49}\text{H}_{80}\text{O}_{17}$, and no NMR signals due to a cinnamoyl residue were observed. The signal pattern of the aglycone moiety in **13** was similar to that of lineolon 3-*O*-glycoside.⁸⁾ The chemical shifts and multiplicities due to the sugar moiety were identical with those of **4**, and **13** was assigned to be lineolon 3-*O*- β -D-oleandropyranosyl-(1→4)- β -D-oleandropyranosyl-(1→4)- β -D-cymaropyranosyl-(1→4)- β -D-cymaropyranoside.

Since the signals due to the aglycone moieties in **14**—**16** were in good agreement with those of **a-2**, except for the deshielding of C-3 and shielding of C-2 and C-4, the sugar moieties were linked to the 3-OH of **a-2**. The molecular for-

Table 3. ¹H-NMR Spectral Data for the Sugar Moieties (**8**, **9**, **11**, **12**, **14**—**16**) [δ ppm in Pyridine-*d*₅, *J* in Hz]

H	8	9	11	12	14	15	16
H-3 α	3.86 (m) ^{a)}	3.84 (m) ^{a)}	3.84 (m) ^{a,b)}	3.84 (m) ^{a,b)}	3.86 (m)	3.86 (m)	3.86 (m) ^{a)}
Sug-1	Dgt(1)	Cym(1)	Cym(1)	Cym(1)	Cym(1)	Cym(1)	Cym(1)
1	5.46 (dd, 10, 2) ^{a)}	5.27 (dd, 10, 2) ^{a)}	5.28 (dd, 10, 2) ^{a,b)}	5.28 (dd, 10, 2) ^{a,b)}	5.29 (dd, 10, 2)	5.29 (dd, 10, 2)	5.29 (dd, 10, 2) ^{a)}
3	4.61 (brs)	4.08 (br q, 3)	4.09 (br q, 3)	4.09 (br q, 3)	4.07 (br q, 3)	4.07 (q, 3)	4.07 (br q, 3)
4	3.49 (dd, 9, 3) ^{b)}	3.51 (dd, 9, 3) ^{b)}	3.52 (dd, 9, 3) ^{c)}	3.54 (dd, 9, 3)	3.52 (dd, q, 3) ^{a)}	3.50 (dd, 9, 3)	3.52 (dd, 9, 3) ^{b)}
5	4.25 (dq, 9, 6)	4.21 (dq, 9, 6)	4.22 (dq, 9, 6)	4.23 (dq, 9, 6)	4.26 (dq, 9, 6)	4.24 (dq, 9, 6)	4.25 (dq, 9, 6)
6	1.43 (d, 6)	1.39 (d, 6)	1.40 (d, 6)	1.40 (d, 6)	1.45 (d, 6)	1.44 (d, 6)	1.45 (d, 6)
Sug-2	Cym(1)	Cym(2)	Cym(2)	Cym(2)	Can(1)	Can(1)	Can(1)
1	5.14 (dd, 10, 2) ^{b)}	5.11 (dd, 10, 2) ^{b)}	5.12 (dd, 10, 2) ^{c)}	5.13 (dd, 10, 2)	4.76 (dd, 10, 2) ^{a)}	4.76 (dd, 10, 2)	4.76 (dd, 10, 2) ^{b)}
3	4.01 (br q, 3)	4.01 (br q, 3)	4.02 (br q, 3)	4.03 (br q, 3)	3.93 (m)	3.93 (m)	3.92 (m)
4	3.38 (dd, 9, 3) ^{c)}	3.43 (dd, 9, 3) ^{c)}	3.46 (dd, 9, 3) ^{d)}	3.46 (dd, 9, 3) ^{c)}	3.27 (t, 9) ^{b)}	3.25 (t, 9)	3.26 (t, 9) ^{c)}
5	4.18 (dq, 9, 6)	4.17 (dq, 9, 6)	4.17 (dq, 9, 6)	4.18 (dq, 9, 6)	3.53 (dq, 9, 6)	3.53 (dq, 9, 6)	3.52 (dq, 9, 6)
6	1.30 (d, 6)	1.36 (d, 6)	1.39 (d, 6)	1.39 (d, 6)	1.40 (d, 6)	1.39 (d, 6)	1.39 (d, 6)
Sug-3	Can(2)	Can	Ole(1)	Ole(1)	Can(2)	Can(2)	Can(2)
1	4.72 (dd, 10, 2) ^{c)}	4.74 (dd, 10, 2) ^{c)}	4.69 (dd, 10, 2) ^{d)}	4.69 (dd, 10, 2) ^{c)}	4.82 (dd, 10, 2) ^{b)}	4.80 (dd, 10, 2)	4.79 (dd, 10, 2) ^{c)}
3	3.88 (m)	3.91 (m)	*	*	3.95 (m)	3.94 (m)	3.95 (m)
4	3.25 (t, 9) ^{d)}	3.26 (t, 9) ^{d)}	*	*	3.30 (t, 9) ^{c)}	3.25 (t, 9)	3.27 (t, 9) ^{d)}
5	3.50—3.55	3.50—3.55	*	*	3.63 (dq, 9, 6)	3.59 (dq, 9, 6)	3.60 (dq, 9, 6)
6	1.33 (d, 6)	1.34 (d, 6)	1.43 (d, 6)	1.43 (d, 6)	1.36 (d, 6)	1.31 (d, 6)	1.32 (d, 6)
Sug-4	Dgt(2)	Dgt	Ole(2)	Ole(2)	Cym(2)	Cym(2)	Cym(2)
1	5.27 (dd, 10, 2) ^{d)}	5.28 (dd, 10, 2) ^{d)}	4.89 (dd, 10, 2)	4.88 (dd, 10, 2)	5.05 (dd, 10, 2) ^{c)}	5.05 (dd, 10, 2)	5.07 (dd, 10, 2) ^{d)}
3	4.61 (brs)	4.61 (br q, 3)	*	*	3.75 (br q, 3)	4.12 (br q, 3)	4.04 (br q, 3)
4	3.42 (dd, 9, 3) ^{e)}	3.43 (dd, 9, 3) ^{e)}	3.68 (t, 9) ^{e)}	*	3.52 (dd, 9, 3)	3.64 (dd, 9, 3)	3.41 (dd, 9, 3) ^{e)}
5	4.30 (dq, 9, 6)	4.31 (dq, 9, 6)	*	*	4.16 (dq, 9, 6)	4.28 (dq, 9, 6)	4.19 (dq, 9, 6)
6	1.32 (d, 6)	1.33 (d, 6)	1.72 (d, 6)	1.43 (d, 6)	1.46 (d, 6)	1.56 (d, 6)	1.27 (d, 6)
Sug-5	Cym(2)	Cym(3)	Glc(1)	Cym(3)		Glc	Cym(3)
1	5.09 (dd, 10, 2) ^{e)}	5.10 (dd, 10, 2) ^{e)}	5.06 (d, 8) ^{e)}	5.278 (dd, 10, 2)		4.89 (d, 8)	5.04 (dd, 10, 2) ^{e)}
2	*	*	3.98 (dd, 8, 9)	*		3.96 (dd, 8, 9)	*
3	4.07 (br q, 3)	4.07 (br q, 3)	4.24 (t, 9)	4.07 (br q, 3)		4.21 (t, 9)	4.03 (br q, 3)
4	3.59 (dd, 9, 3) ^{f)}	3.60 (dd, 9, 3) ^{f)}	4.28 (t, 9) ^{f)}	3.60 (dd, 9, 3) ^{d)}		4.16 (t, 9)	3.58 (dd, 9, 3) ^{f)}
5	4.25 (dq, 9, 6)	4.25 (dq, 9, 6)	3.89 (m)	4.27 (dq, 9, 6)		3.95 (m)	4.22 (dq, 9, 6)
6	1.54 (d, 6)	1.54 (d, 6)	4.3, 4.5	1.62 (d, 6)		4.37 (dd, 12, 5)	1.59 (d, 6)
						4.56 (dd, 12, 2)	
Sug-6	Glc	Glc	Glc(2)	Glc(1)			Glc(1)
1	4.91 (d, 8) ^{f)}	4.91 (d, 8) ^{f)}	5.16 (d, 8) ^{f)}	4.87 (d, 8) ^{d)}			4.87 (d, 8) ^{f)}
2	3.98 (dd, 8, 9)	3.99 (dd, 8, 9)	4.07 (dd, 8, 9)	3.98 (dd, 8, 9)			3.98 (dd, 8, 9)
3	4.21 (t, 9)	4.22 (t, 9)	4.19 (t, 9)	4.23 (t, 9)			4.25 (t, 9)
4	4.15 (t, 9)	4.16 (t, 9)	4.16 (t, 9)	4.29 (t, 9)			4.26 (t, 9) ^{g)}
5	3.95 (m)	3.95 (m)	4.00 (m)	3.93 (m)			3.93 (m)
6	4.36 (dd, 12, 5)	4.37 (dd, 12, 4)	4.3, 4.5	4.3, 4.5			4.3, 4.5
	4.55 (dd, 12, 2)	4.56 (dd, 12, 2)					
Sug-7				Glc(2)			Glc(2)
1				5.18 (d, 8)			5.18 (d, 8) ^{g)}
2				4.09 (dd, 8, 9)			4.09 (dd, 8, 9)
3				4.19 (t, 9)			4.19 (t, 9)
4				4.17 (t, 9)			4.18 (t, 9)
5				4.00 (m)			4.00 (m)
6				4.3, 4.5			4.3, 4.5
OMe	3.51	3.52	3.49	3.50	3.46	3.52	3.50
	3.58	3.59	3.50	3.52	3.61	3.60	3.59
		3.62	3.58	3.53			3.60
			3.62	3.58			
				3.63			

* Overlapping with other signals. a—g) The signals showed response by irradiation of the corresponding a'—g'), respectively, in DIF-NOE.

mula of **14** was suggested to be C₄₇H₇₈O₁₈, based on HR-FAB-MS. The component sugars were 2 moles each of Cym and Can, and NOEs were observed between the H-1 signals of outer Cym, outer Can, inner Can/the H-4 signals of outer Can, inner Can, inner Cym, respectively. The linkages between four sugars were also confirmed by cross-peaks in the HMBC spectrum. The structure of **14** was, thus, assigned to be pleurogenin 3-*O*- β -D-cymaropyranosyl-(1 \rightarrow 4)- β -D-canaropyranosyl-(1 \rightarrow 4)- β -D-canaropyranosyl-(1 \rightarrow 4)- β -D-cymaropyranoside.

The molecular formula of **15** was considered to be

C₅₃H₈₈O₂₃, one hexose greater than **14**, and the NMR signals of **15** were observed to have almost similar chemical shifts as those of **14**, except for signals due to the extra Glc and deshielding of C-4 in the outer Cym. In the HMBC spectrum, cross-peaks were observed between H-1 of Glc/C-4 of outer Cym, and H-4 of outer Cym/C-1 of Glc, along with those in **14**. Therefore, **15** was assigned to be pleurogenin 3-*O*- β -D-glucopyranosyl-(1 \rightarrow 4)- β -D-cymaropyranosyl-(1 \rightarrow 4)- β -D-canaropyranosyl-(1 \rightarrow 4)- β -D-canaropyranosyl-(1 \rightarrow 4)- β -D-cymaropyranoside.

The molecular formula of **16** was suggested to be

$C_{66}H_{110}O_{31}$ by HR-FAB-MS. The sugar moiety was composed of 3 moles of Cym and 2 moles each of Can and Glc. Correlations in NOE were observed between the H-1 signals of outer Glc, inner Glc, outer Cym, intermediate Cym, outer Can and inner Can/the H-4 signals of inner Glc, outer Cym, intermediate Cym, outer Can, inner Can and inner Cym, respectively. A response was also observed between H-3 of **a-2/H-1** of inner Cym. The structure of **16** was, thus, determined to be pleurogenin 3-*O*- β -cellobiosyl-(1 \rightarrow 4)- β -D-cymaropyranosyl-(1 \rightarrow 4)- β -D-cymaropyranosyl-(1 \rightarrow 4)- β -D-canaropyranosyl-(1 \rightarrow 4)- β -D-canaropyranosyl-(1 \rightarrow 4)- β -D-cymaropyranoside.

Sixteen glycosides of pregnanes, including ikemagenin, lineolon and a new pregnane, pleurogenin, were isolated and their structures were elucidated. Since these glycosides foam to a lesser degree than spirostan or triterpenoid saponins, an expectorant effect can be expected when the roots are used to treat pleurisy or bronchitis.

Experimental

1H - and ^{13}C -NMR spectra were recorded on a JNM-A500 spectrometer in pyridine- d_5 . Chemical shifts are given in δ values referred to the internal standard, tetramethylsilane (TMS), and the following abbreviations are used: s=singlet, d=doublet, t=triplet, m=multiplet, brs=broad singlet, dd=doublet of doublets. HR-FAB-MS were recorded on a JEOL HX-110 spectrometer. Optical rotations were measured on a JASCO DIP 360 polarimeter. For silica gel column chromatography and TLC, the following solvent systems were applied: $CHCl_3$ -MeOH- H_2O (7:1:1.6—7:2:1.2) (bottom layer, solvent 1), EtOAc-MeOH- H_2O (8:1:1.2—6:1:1.2) (top layer, solvent 2), benzene-acetone (3:1—1:1) (solvent 3). For ODS column chromatography and HPLC, MeCN- H_2O (2:3—3:2) (solvent 4) was used. Spray reagent: 10% H_2SO_4 .

Extraction and Isolation The roots of *Asclepias tuberosa* L. collected in North Carolina in March, 1994, and purchased from Wilcox Natural Products, North Carolina (4.5 kg), were powdered and percolated with MeOH. The concentrated MeOH extract was dissolved in 50% MeOH and filtered. The filtrate was partitioned with benzene (extract 34.0 g) and then with $CHCl_3$ (extract 4.5 g). The benzene fraction was subjected to column chromatography on a silica gel column with solvent 2. A pregnane glycoside-rich aliquot obtained on initial chromatography (1.5 g) was subjected to hydrolysis. The remaining fraction was chromatographed successively on a silica gel column (solvents 1, 2, 3) and an ODS column (solvent 4) to afford 16 glycosides; **1**: 38 mg, **2**: 19 mg, **3**: 42 mg, **4**: 110 mg, **5**: 40 mg, **6**: 36 mg, **7**: 110 mg, **8**: 68 mg, **9**: 34 mg, **10**: 23 mg, **11**: 85 mg, **12**: 10 mg, **13**: 19 mg, **14**: 13 mg, **15**: 8 mg, **16**: 8 mg.

Hydrolysis of the Extract A glycoside-rich aliquot (1.5 g) from the benzene-soluble fraction was heated with 0.05 N HCl in 50% dioxane (20 ml) for 2 h at 95 °C. The mixture was deacidified with Amberlite IRA-410, diluted with H_2O and extracted with *n*-BuOH. The *n*-BuOH extract (880 mg) was chromatographed on a silica gel column with solvent 2 to give ikemagenin (**a-1**) which was further purified on a silica gel column with solvent 3 (230 mg), lineolon (10 mg), and pleurogenin (**a-2**, 8 mg). The H_2O layer, after extraction with *n*-BuOH, was chromatographed on a silica gel column with solvent 1, 2 and 3 to afford D-oleandrose: 54 mg, $[\alpha]_D^{20}$ -9.5° ($c=2.7$, H_2O , 24 h) (lit. -12.0°),⁹⁾ D-cymarose: 55 mg, $[\alpha]_D^{19}$ $+56.7^\circ$ ($c=2.8$, H_2O , 24 h) (lit. $+54.9^\circ$),⁹⁾ D-canarose: 27 mg, $[\alpha]_D^{20}$ $+22.3^\circ$ ($c=1.4$, H_2O , 24 h) (lit. $+22.8^\circ$),⁸⁾ D-digitoxose: 12 mg, $[\alpha]_D^{21}$ $+37.7^\circ$ ($c=0.6$, H_2O , 24 h) (lit. $+50.2^\circ$),⁹⁾ D-thevetose: 6 mg, $[\alpha]_D^{20}$ $+23.9^\circ$ ($c=0.3$, H_2O , 24 h) (lit. $+35.5^\circ$),⁹⁾ D-glucose: 50 mg, $[\alpha]_D^{20}$ $+50.0^\circ$ ($c=0.2$, H_2O , 24 h) (lit. $+52.5^\circ$),⁹⁾ strophanthobiose: 20 mg, $[\alpha]_D^{24}$ $+27.8^\circ$ ($c=1.0$, H_2O , 24 h) (lit. $+31.1^\circ$),⁹⁾ β -D-glucosyl-D-oleandrose: 33 mg, $[\alpha]_D^{24}$ $+12.7^\circ$ ($c=0.17$, H_2O , 24 h) (lit. $+7.0^\circ$).²⁾

Pleurogenin (**a-2**): Solid, $[\alpha]_D^{24}$ $+30.0^\circ$ ($c=0.05$, MeOH), FAB-MS (negative) m/z : 381.2277 (Calcd for $C_{21}H_{34}O_6$ -1: 381.2277).

Ikemagenin 3-*O*- β -D-oleandropyranosyl-(1 \rightarrow 4)- β -D-oleandropyranosyl-(1 \rightarrow 4)- β -D-cymaropyranoside (**2**): Solid, $[\alpha]_D^{23}$ $+7.2^\circ$ ($c=0.63$, MeOH), FAB-MS m/z : 949.4910 (Calcd for $C_{51}H_{74}O_{15}$ +Na: 949.4925). 1H -NMR δ : 5.29 (1H, dd, $J=10$, 2 Hz, H-1_{Cym}), 4.72, 4.99 (1H each, dd, $J=10$, 2 Hz, H-1_{Ole(1,2)}), 3.59, 3.53, 3.48 (3H each, s, OCH₃), 1.59, 1.48, 1.45 (3H each, d, $J=6$ Hz, H-6_{Cym,Ole}). ^{13}C -NMR δ : 100.2, 101.9 (C-1_{Ole(2,1)}), 96.3 (C-1_{Cym}), 58.7, 57.2, 56.9 (OCH₃), 18.7, 18.59, 18.56 (C-6_{Cym,Ole}).

Ikemagenin 3-*O*- β -D-thevetopyranosyl-(1 \rightarrow 4)- β -D-oleandropyranosyl-(1 \rightarrow 4)- β -D-cymaropyranosyl-(1 \rightarrow 4)- β -D-cymaropyranoside (**3**): Solid, $[\alpha]_D^{23}$ $+4.3^\circ$ ($c=2.10$, MeOH), FAB-MS m/z : 1109.5664 (Calcd for $C_{58}H_{86}O_{19}$ +Na: 1109.5661). 1H -NMR δ : 5.12, 5.28 (1H each, dd, $J=10$, 2 Hz, H-1_{Cym(2,1)}), 4.69 (1H, dd, $J=10$, 2 Hz, H-1_{Ole}), 4.95 (1H, d, $J=8$ Hz, H-1_{Thv}), 3.89, 3.62, 3.58, 3.53 (3H each, s, OCH₃), 1.70, 1.59, 1.39, 1.38 (3H each, d, $J=6$ Hz, H-6_{Cym,Ole,Thv}). ^{13}C -NMR δ : 96.3, 100.4 (C-1_{Cym(1,2)}), 101.8 (C-1_{Ole}), 104.0 (C-1_{Thv}), 60.8, 58.75, 58.84, 57.1 (OCH₃), 18.7, 18.5, 18.43, 18.40 (C-6_{Cym,Ole,Thv}).

Ikemagenin 3-*O*- β -D-oleandropyranosyl-(1 \rightarrow 4)- β -D-oleandropyranosyl-(1 \rightarrow 4)- β -D-cymaropyranosyl-(1 \rightarrow 4)- β -D-cymaropyranoside (**4**): Solid, $[\alpha]_D^{24}$ $+11.8^\circ$ ($c=0.82$, MeOH), FAB-MS m/z : 1093.5717 (Calcd for $C_{58}H_{86}O_{18}$ +Na: 1093.5712). 1H -NMR δ : 5.13, 5.28 (1H each, dd, $J=10$, 2 Hz, H-1_{Cym(2,1)}), 4.71, 4.99 (1H each, dd, $J=10$, 1 Hz, H-1_{Ole(1,2)}), 3.63, 3.59, 3.52, 3.49 (3H each, s, OCH₃), 1.60, 1.48, 1.401, 1.399 (3H each, d, $J=6$ Hz, H-6_{Cym,Ole}). ^{13}C -NMR δ : 96.4, 100.4 (C-1_{Cym(1,2)}), 100.2, 101.9 (C-1_{Ole(2,1)}), 58.8, 58.7, 57.2, 57.0 (OCH₃), 18.7, 18.6, 18.5, 18.4 (C-6_{Cym,Ole}).

Ikemagenin 3-*O*- β -D-cymaropyranosyl-(1 \rightarrow 4)- β -D-oleandropyranosyl-(1 \rightarrow 4)- β -D-cymaropyranosyl-(1 \rightarrow 4)- β -D-cymaropyranoside (**5**): Solid, $[\alpha]_D^{24}$ $+7.0^\circ$ ($c=0.63$, MeOH), FAB-MS m/z : 1093.5717 (Calcd for $C_{58}H_{86}O_{18}$ +Na: 1093.5712). 1H -NMR δ : 5.12, 5.26, 5.28 (1H each, dd, $J=10$, 2 Hz, H-1_{Cym(2,3,1)}), 4.70 (1H, dd, $J=10$, 2 Hz, H-1_{Ole}), 3.62, 3.58, 3.53, 3.47 (3H each, s, OCH₃), 1.54, 1.46, 1.393, 1.388 (3H each, d, $J=6$ Hz, H-6_{Cym,Ole}). ^{13}C -NMR δ : 96.4, 98.4, 100.4 (C-1_{Cym(1,3,2)}), 101.9 (C-1_{Ole}), 58.9, 58.8, 57.9, 57.2 (OCH₃), 18.9, 18.6, 18.5, 18.4 (C-6_{Cym,Ole}).

Ikemagenin 3-*O*- β -D-cymaropyranosyl-(1 \rightarrow 4)- β -D-oleandropyranosyl-(1 \rightarrow 4)- β -D-oleandropyranosyl-(1 \rightarrow 4)- β -D-cymaropyranosyl-(1 \rightarrow 4)- β -D-cymaropyranoside (**6**): Solid, $[\alpha]_D^{19}$ $+16.2^\circ$ ($c=1.84$, MeOH), FAB-MS m/z : 1237.6500 (Calcd for $C_{65}H_{96}O_{21}$ +Na: 1237.6498). 1H -NMR δ : 5.12, 5.26, 5.27 (1H each, dd, $J=10$, 2 Hz, H-1_{Cym(1,3,2)}), 4.69, 4.90 (1H each, dd, $J=10$, 2 Hz, H-1_{Ole(1,2)}), 3.62, 3.58, 3.55, 3.51, 3.46 (3H each, s, OCH₃), 1.53, 1.47, 1.44, 1.40, 1.39 (3H each, d, $J=6$ Hz, H-6_{Cym,Ole}). ^{13}C -NMR δ : 96.4, 98.5, 100.4 (C-1_{Cym(1,3,2)}), 100.0, 101.9 (C-1_{Ole(2,1)}), 58.83, 58.76, 57.9, 57.3 ($\times 2$) (OCH₃), 18.9, 18.7, 18.6, 18.5, 18.4 (C-6_{Cym,Ole}).

Ikemagenin 3-*O*- β -D-glucopyranosyl-(1 \rightarrow 4)- β -D-cymaropyranosyl-(1 \rightarrow 4)- β -D-oleandropyranosyl-(1 \rightarrow 4)- β -D-cymaropyranosyl-(1 \rightarrow 4)- β -D-cymaropyranoside (**7**): Solid, $[\alpha]_D^{25}$ $+11.1^\circ$ ($c=2.40$, MeOH), FAB-MS m/z : 1399.7025 (Calcd for $C_{71}H_{108}O_{26}$ +Na: 1399.7026). 1H -NMR δ : 5.12, 5.26, 5.27 (1H each, dd, $J=10$, 1 Hz, H-1_{Cym(2,3,1)}), 4.69, 4.88 (1H each, dd, $J=10$, 2 Hz, H-1_{Ole(1,2)}), 4.92 (1H, d, $J=8$ Hz, H-1_{Glc}), 3.62, 3.58, 3.534, 3.530, 3.50 (3H each, s, OCH₃), 4.56 (1H, dd, $J=12$, 2 Hz, H-6_{Glc}), 4.38 (1H, dd, $J=12$, 5 Hz, H-6_{Ole}), 1.62, 1.43 ($\times 2$), 1.40, 1.39 (3H each, d, $J=6$ Hz, H-6_{Cym,Ole}). ^{13}C -NMR δ : 96.4, 98.3, 100.4 (C-1_{Cym(1,3,2)}), 100.0, 101.9 (C-1_{Ole(2,1)}), 106.5 (C-1_{Glc}), 58.83, 58.77, 58.5, 57.4, 57.3 (OCH₃), 18.63, 18.59 ($\times 2$), 18.5, 18.4 (C-6_{Cym,Ole}).

Ikemagenin 3-*O*- β -D-glucopyranosyl-(1 \rightarrow 4)- β -D-cymaropyranosyl-(1 \rightarrow 4)- β -D-digitoxopyranosyl-(1 \rightarrow 4)- β -D-oleandropyranosyl-(1 \rightarrow 4)- β -D-cymaropyranosyl-(1 \rightarrow 4)- β -D-cymaropyranoside (**8**): Solid, $[\alpha]_D^{23}$ $+16.0^\circ$ ($c=1.29$, MeOH), FAB-MS m/z : 1357.6566 (Calcd for $C_{68}H_{102}O_{26}$ +Na: 1357.6557). NMR (see Tables 2 and 3).

Ikemagenin 3-*O*- β -D-glucopyranosyl-(1 \rightarrow 4)- β -D-cymaropyranosyl-(1 \rightarrow 4)- β -D-digitoxopyranosyl-(1 \rightarrow 4)- β -D-canaropyranosyl-(1 \rightarrow 4)- β -D-cymaropyranosyl-(1 \rightarrow 4)- β -D-cymaropyranoside (**9**): Solid, $[\alpha]_D^{24}$ $+6.4^\circ$ ($c=1.70$, MeOH), FAB-MS m/z : 1371.6713 (Calcd for $C_{69}H_{104}O_{26}$ +Na: 1371.6714). NMR (see Tables 2 and 3).

Ikemagenin 3-*O*- β -cellobiosyl-(1 \rightarrow 4)- β -D-oleandropyranosyl-(1 \rightarrow 4)- β -D-cymaropyranosyl-(1 \rightarrow 4)- β -D-cymaropyranoside (**10**): Solid, $[\alpha]_D^{19}$ $+9.4^\circ$ ($c=1.70$, MeOH), FAB-MS m/z : 1273.5985 (Calcd for $C_{63}H_{94}O_{25}$ +Na: 1273.5982). 1H -NMR δ : 5.11, 5.28 (1H each, dd, $J=10$, 2 Hz, H-1_{Cym(1,2)}), 4.68 (1H, dd, $J=10$, 2 Hz, H-1_{Ole}), 5.06, 5.16 (1H each, d, $J=8$ Hz, H-1_{Glc(1,2)}), 3.62, 3.57, 3.49 (3H each, s, OCH₃), 1.70, 1.39, 1.37 (3H each, d, $J=6$ Hz, H-6_{Cym,Ole}). ^{13}C -NMR δ : 96.4, 100.4 (C-1_{Cym(1,2)}), 101.8 (C-1_{Ole}), 104.2, 104.9 (C-1_{Glc(1,2)}), 58.9, 58.8, 57.2 (OCH₃), 18.8, 18.5, 18.4 (C-6_{Cym,Ole}).

Ikemagenin 3-*O*- β -cellobiosyl-(1 \rightarrow 4)- β -D-oleandropyranosyl-(1 \rightarrow 4)- β -D-oleandropyranosyl-(1 \rightarrow 4)- β -D-cymaropyranosyl-(1 \rightarrow 4)- β -D-cymaropyranoside (**11**): Solid, $[\alpha]_D^{24}$ $+10.1^\circ$ ($c=1.22$, MeOH), FAB-MS m/z : 1417.6780 (Calcd for $C_{70}H_{106}O_{28}$ +Na: 1417.6769). NMR (see Tables 2 and 3).

Ikemagenin 3-*O*- β -cellobiosyl-(1 \rightarrow 4)- β -D-cymaropyranosyl-(1 \rightarrow 4)- β -D-oleandropyranosyl-(1 \rightarrow 4)- β -D-oleandropyranosyl-(1 \rightarrow 4)- β -D-cymaropyranosyl-(1 \rightarrow 4)- β -D-cymaropyranoside (**12**): Solid, $[\alpha]_D^{22}$ $+15.7^\circ$ ($c=0.49$, MeOH), FAB-MS m/z : 1561.7535 (Calcd for $C_{77}H_{118}O_{31}$ +Na: 1561.7554). NMR (see Tables 2 and 3). A mixture of **12** (5 mg) and cellulase II (Sigma, 15 mg) in 20% EtOH was stirred for 6 h at 37 °C and extracted with *n*-

BuOH. On TLC (solvent 1 and 2), 2 spots at the same *R_f* values as **7** and **6** were observed.

Lineolon 3-*O*- β -D-oleandropyranosyl-(1 \rightarrow 4)- β -D-oleandropyranosyl-(1 \rightarrow 4)- β -D-cymaropyranosyl-(1 \rightarrow 4)- β -D-cymaropyranoside (**13**): Solid, $[\alpha]_D^{22} + 2.2^\circ$ ($c=0.95$, MeOH), FAB-MS *m/z*: 963.5295 (Calcd for $C_{49}H_{80}O_{17} + Na$: 963.5293). 1H -NMR δ : 5.12, 5.28 (1H each, dd, $J=10$, 2 Hz, H-1_{Cym(2,1)}), 4.71, 4.99 (1H each, dd, $J=10$, 2 Hz, H-1_{Ole(1,2)}), 3.62, 3.58, 3.52, 3.49 (3H each, s, OCH₃), 1.59, 1.48, 1.39, 1.38 (3H each, d, $J=6$ Hz, H-6_{Cym,Ole}). ^{13}C -NMR δ : 96.4, 100.4 (C-1_{Cym(1,2)}), 100.2, 101.9 (C-1_{Ole(2,1)}), 58.8, 58.7, 57.2, 57.0 (OCH₃), 18.7, 18.6, 18.5, 18.4 (C-6_{Cym,Ole}).

Pleurogenin 3-*O*- β -D-cymaropyranosyl-(1 \rightarrow 4)- β -D-canaropyranosyl-(1 \rightarrow 4)- β -D-canaropyranosyl-(1 \rightarrow 4)- β -D-cymaropyranoside (**14**): Solid, $[\alpha]_D^{22} - 5.4^\circ$ ($c=0.73$, MeOH), FAB-MS *m/z*: 953.5088 (Calcd for $C_{47}H_{78}O_{18} + Na$: 953.5086). NMR (see Tables 2 and 3).

Pleurogenin 3-*O*- β -D-glucopyranosyl-(1 \rightarrow 4)- β -D-cymaropyranosyl-(1 \rightarrow 4)- β -D-canaropyranosyl-(1 \rightarrow 4)- β -D-canaropyranosyl-(1 \rightarrow 4)- β -D-cymaropyranoside (**15**): Solid, $[\alpha]_D^{25} - 2.3^\circ$ ($c=0.39$, MeOH), FAB-MS *m/z*: 1115.5613 (Calcd for $C_{53}H_{88}O_{23} + Na$: 1115.5614). NMR (see Tables 2 and 3).

Pleurogenin 3-*O*- β -D-cellobiosyl-(1 \rightarrow 4)- β -D-cymaropyranosyl-(1 \rightarrow 4)- β -D-cymaropyranosyl-(1 \rightarrow 4)- β -D-canaropyranosyl-(1 \rightarrow 4)- β -D-canaropyranosyl-(1 \rightarrow 4)- β -D-cymaropyranoside (**16**): Solid, $[\alpha]_D^{25} + 2.7^\circ$ ($c=0.40$, MeOH), FAB-MS *m/z*: 1421.6929 (Calcd for $C_{66}H_{110}O_{31} + Na$: 1421.6929). NMR (see Tables 2 and 3).

Acknowledgments We thank Ms Y. Iwase for the NMR spectra and Mr. H. Hanazono for operating the MS.

References

- 1) Abe F., Yamauchi T., *Chem. Pharm. Bull.*, submitted.
- 2) Abe F., Mori Y., Okabe H., Yamauchi T., *Chem. Pharm. Bull.*, **42**, 1777—1783 (1994).
- 3) a) Abe F., Okabe H., Yamauchi T., Honda K., Hayashi N., *Chem. Pharm. Bull.*, **47**, 869—875 (1999); b) Abe F., Yamauchi T., Honda K., Hayashi N., *ibid.*, **48**, 154—156 (2000).
- 4) Abe F., Fujishima H., Iwase Y., Yamauchi T., Kinjo K., Yaga S., *Chem. Pharm. Bull.*, **47**, 1128—1133 (1999).
- 5) Abe F., Hirokawa M., Yamauchi T., Honda K., Hayashi N., Nishida R., *Chem. Pharm. Bull.*, **47**, 1384—1387 (1999).
- 6) Warashina T., Noro T., *Chem. Pharm. Bull.*, **43**, 977—982 (1995).
- 7) a) Mitsuhashi H., Hayashi K., *Shoyakugaku Zasshi*, **39**, 1—27 (1985); b) Yoshikawa K., Okada N., Kann Y., Arihara S., *Chem. Pharm. Bull.*, **44**, 1790—1796 (1996); *idem*, *ibid.*, **44**, 2243—2248 (1996); c) Warashina T., Noro T., *Phytochemistry*, **44**, 917—923 (1997).
- 8) Warashina T., Noro T., *Chem. Pharm. Bull.*, **48**, 99—107 (2000).
- 9) Zechmeister L. (ed.), "Progress in The Chemistry of Organic Natural Products," Vol. 14, Springer-Verlag, Vienna, 1957.

Michael-type Reaction of Ethyl Bromodifluoroacetate with α,β -Unsaturated Carbonyl Compounds in the Presence of Copper Powder

Kazuyuki SATO, Misato TAMURA, Kei TAMOTO, Masaaki OMOTE, Akira ANDO, and
Itsumaro KUMADAKI*

Faculty of Pharmaceutical Sciences, Setsunan University, 45-1 Nagaotoge-cho, Hirakata, Osaka 573-0101, Japan.

Received January 28, 2000; accepted March 13, 2000

We have reported that the reaction of ethyl bromodifluoroacetate (**1**) with alkenyl iodides in the presence of copper powder gives ethyl alkenyldifluoroacetates. As an extension of this reaction, reaction of **1** with Michael acceptors in the presence of copper powder was examined and found to give 1,4-addition products selectively, unless the acceptor has a group stabilizing a radical intermediate, such as a phenyl group.

Key words bromodifluoroacetate; copper; α,β -unsaturated carbonyl compound; Michael acceptor; 1,4-addition; δ -oxodifluoroacetate

Organofluorine compounds are now drawing much attention in biomedical fields, since many of them are used as medicines.¹⁾ Among them, difluoromethylene (CF_2) analogs of bioactive compounds have been synthesized to modify their biological activities,²⁾ and various methods have been developed for the introduction of a CF_2 group.³⁾ In conjunction with this field, we have reported the cross-coupling reaction of ethyl bromodifluoroacetate (**1**) with alkenyl or aryl iodides in the presence of copper powder, providing a convenient route to aryl- or alkenyldifluoroacetates.⁴⁾ As an extension of this reaction, now we would like to report the 1,4-addition reaction of **1** with various Michael acceptors in the presence of copper powder.

Taguchi and his colleagues reported the atom-transfer reaction of methyl difluoriodoacetate with olefins in the presence of Cu powder. They postulated that the reactive intermediate might be a difluoroacetate radical.^{5,6)} Although their reaction proceeded with olefins, it did not proceed with α,β -unsaturated carbonyl compounds. We have suggested, however, that the reactive intermediate is anionic in our reaction.⁴⁾ Therefore, we expected that the anionic intermediate would react with Michael acceptors to afford α,α -difluorocarboxylates with electron-withdrawing substituents at δ -position. So, 2-cyclohexen-1-one (**2**) was treated with **1** in the presence of Cu powder in DMSO at 55 °C. As we expected, ethyl 2,2-difluoro-2-(3-oxocyclohexyl)acetate, a Michael adduct (**3**), was obtained in the isolation yield of 45% (Chart 1). In this reaction, we could obtain neither an atom-transfer product nor a 1,2-adduct. This result strongly suggests that the reactive intermediate in this reaction is anionic.

To improve the yield of this reaction, we examined the solvent effect. In DMSO, **3** was obtained in the isolation yield of 45%, while the yield was estimated to be 63% by ¹H-NMR. The results obtained using other solvents are shown in Table 1.

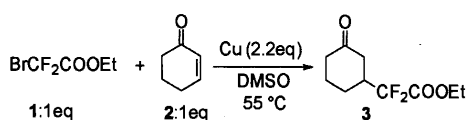


Chart 1

Next, we examined the effect of temperature using DMSO as the solvent. The results are shown in Table 2. The reaction proceeded even at room temperature, but it was very slow and gave only a poor yield of **3**. The best result was obtained at 55 °C, as in the previous reactions with alkenyl iodides.⁴⁾

These results suggested that the best condition for this reaction is to use DMSO as a solvent and to carry it out at 55 °C. Using this condition, we examined the reaction with various Michael acceptors. The results are shown in Table 3.

At first, the effects of electron withdrawing groups of Michael acceptors were investigated (entries 1 to 4). An α,β -unsaturated ketone (**4**) gave the best result, while an ester (**6**) was much less reactive. A nitrile (**8**) and a sulfone (**10**) were comparable to **4** and much better than **6** as a Michael acceptor of this reaction. Thus, the relative activating power of various groups is as follows: ketone > nitrile ~ sulfone >> ester. Taguchi and his colleagues reported that 2,2-difluoroketene silyl acetal, generated from methyl difluoriodoacetate, reacted with α,β -unsaturated carbonyl compounds to give

Table 1. Investigation of Solvent Effect

Solv.	Time ^{a)} (h)	Yield ^{b)} (%)
DMSO	3	63
HMPA	24	7 ^{c)}
DMF	56	56
CH ₃ CN	1 week	ND ^{d)}
THF	1 week	ND ^{d)}

a) Until the peak of **1** was no longer detected by GLC. b) ¹H-NMR yield (Internal standard is 1,4-dioxane). c) HMPA was eliminated by column chromatography. d) No products were detected by GLC.

Table 2. Temperature Effect

Temp. (°C)	Time ^{a)} (h)	Yield ^{b)} (%)
120	3	52
80	3	61
55	3	63
40	9	62
25	4 days	16

a) Until the peak of **1** was no longer detected by GLC. b) Estimated by ¹H-NMR: Internal standard is 1,4-dioxane.

Table 3. Reaction of **1** with Various Michael Acceptors

Entry	R' 	Time ^{a)} (h)	R'' 	Yield ^{b)} (%)
1		5		54
2		3		16
3		7		40
4		5		42
5		3		45
6		3		49
7		8		8 ^{c,d)}

a) Until the peak of **1** was no longer detected by GLC. b) Isolation yield. c) Two equivalents of **1** were used.

d) and were obtained as by-products.

Michael type 1,4-addition products.⁷⁾ However, the regioselectivity of this reaction is not high. Thus, some 1,2-addition products were obtained in many cases. Further, this reaction does not proceed with α,β -unsaturated esters or phenyl vinyl sulfone (**8**). Our reaction proceeded not only with benzyl acrylate (**6**) but with **8** to afford the 1,4-addition products (entries 2 and 3). As mentioned above, cyclic enone (**2**) gave the Michael type adduct (**3**). From entry 6, an alkyl group on the β -position did not disturb the reaction, while an aryl group on the β -carbon afforded a poor yield of the Michael adduct (**15**) with larger amounts of **16** and **17**. Hydrogenation of the latter two products gave the same product, ethyl-3-benzyl-2,2-difluoro-4-oxopentanoate (**18**), and seemed to be produced by copper-induced radical addition of bromodifluoroacetate (**1**) followed by elimination of hydrogen bromide. Namely, because of high stability of benzylic radical, a primary radical from **1** attacked the β -carbon from the phenyl group of **14**. In other cases, the radical must have reacted with copper to give the copper reagent ($\text{BrCuCF}_2\text{CO}_2\text{C}_2\text{H}_5$) postulated in the previous paper.⁴⁾

In conclusion, **1** reacted with α,β -unsaturated carbonyl compounds and other Michael acceptors in the presence of copper powder to give 1,4-addition products in the absence of substituents that stabilize a radical intermediate. These results are quite different from the reaction of copper complex from difluoroiodoacetate reported by Taguchi's group. This suggests that the intermediate of our reaction is the one shown above and it behaves as an anionic species with Michael acceptors. Although this reaction is affected by an aryl substituent at β -position, the 1,4-addition proceeds with various Michael acceptors in moderate yields.

Experimentals

General Procedures ¹H-NMR were recorded on JEOL-FX90Q and JNM-GX400 spectrometers. Tetramethylsilane was used as an internal standard. ¹⁹F-NMR were recorded on Hitachi FT-NMR R-1500, JEOL-FX90Q and GE-Omega 600 spectrometer. Benzotrifluoride was used as an internal

standard. Mass spectra were obtained by JEOL JMS-DX-300. IR spectra were recorded on a Hitachi 270-30 infrared spectrophotometer. Gas-liquid chromatography (GLC) was carried out on a Hitachi 263-50 gas chromatograph (column, 5% SE-30 3 mm \times 2 m, carrier, N₂ at 30 ml/min). Peak areas were calculated on a Shimadzu C-R5A Chromatopac.

Ethyl 2,2-Difluoro-2-(3-oxocyclohexyl)acetate (3) In an atmosphere of Ar, ethyl bromodifluoroacetate (**1**, 0.25 ml, 2.0 mmol) and 2-cyclohexen-1-one (**2**, 0.19 ml, 2.0 mmol) were added to a suspension of activated Cu powder (280 mg, 4.4 mmol) in DMSO (10 ml), and the mixture was stirred at 55 °C for 3 h. Thereafter, **1** was not detected by GLC. The mixture was poured into a mixture of ice and saturated NH₄Cl, and extracted with Et₂O. The Et₂O layer was washed with saturated NH₄Cl and saturated NaCl, and dried over MgSO₄. After evaporation of the solvent, the residue was purified by column chromatography (SiO₂, AcOEt:hexane=1:4) to give **3** (198 mg, 45%). **3**: A colorless oil; MS *m/z*: 220 (*M*⁺); HRMS Calcd for C₁₀H₁₄F₂O₃: 220.091 (*M*⁺). Found: 220.090; IR (neat) cm⁻¹: 2968, 2880, 1766, 1722, 1316, 1266, 1200, 1118, 1082, 1054; ¹H-NMR (CDCl₃) δ : 4.35 (q, 2H, *J*=7.0 Hz), 1.90–2.70 (m, 7H), 1.66 (m, 2H), 1.37 (t, 3H, *J*=7.0 Hz); ¹⁹F-NMR (CDCl₃) ppm: -50.4 (dd, 1F, *J*=256.4, 14.7 Hz), -51.0 (dd, 1F, *J*=256.4, 14.7 Hz).

Ethyl 2,2-Difluoro-5-oxohexanoate (5) In an atmosphere of Ar, **1** (0.25 ml, 2.0 mmol) and methyl vinyl ketone (**4**, 0.17 ml, 2.0 mmol) were added to a suspension of activated Cu powder (280 mg, 4.4 mmol) in DMSO (10 ml), and the mixture was stirred at 55 °C for 6 h. The mixture was worked up as in the case of **3**. After evaporation of the solvent, the residue was purified by column chromatography (SiO₂, AcOEt:hexane=1:4) to give **5** (208 mg, 54%). **5**: A colorless oil; MS *m/z*: 194 (*M*⁺); HRMS Calcd for C₈H₁₂F₂O₃: 194.075 (*M*⁺). Found: 194.076; IR (neat) cm⁻¹: 2992, 2952, 1768, 1726, 1440, 1362, 1196, 1040; ¹H-NMR (CDCl₃) δ : 4.32 (q, 2H, *J*=7.0 Hz), 2.69 (t, 2H, *J*=7.9 Hz), 2.31–2.43 (m, 2H), 2.19 (s, 3H), 1.36 (t, 3H, *J*=7.0 Hz); ¹⁹F-NMR (CDCl₃) ppm: -40.9 (t, 2F, *J*=16.1 Hz).

Ethyl Benzyl 2,2-Difluoropentandioate (7) In an atmosphere of Ar, **1** (0.25 ml, 2.0 mmol) and benzyl acrylate (**6**, 324 mg, 2.0 mmol) were added to a suspension of activated Cu powder (280 mg, 4.4 mmol) in DMSO (10 ml), and the mixture was stirred at 55 °C for 3 h. The mixture was worked up as in the case of **3**. The extract was purified by column chromatography (SiO₂, AcOEt:hexane=1:4) to give **7** (90 mg, 16%). **7**: A colorless oil; MS *m/z*: 286 (*M*⁺); HRMS Calcd for C₁₄H₁₆F₂O₄: 286.101 (*M*⁺). Found: 286.102; IR (neat) cm⁻¹: 3072, 3044, 2988, 1768, 1744, 1310, 1284, 1186, 1098; ¹H-NMR (CDCl₃) δ : 7.35 (m, 5H), 5.13 (s, 2H), 4.30 (q, 2H, *J*=7.0 Hz), 2.60 (m, 2H), 2.37–2.52 (m, 2H), 1.33 (t, 3H, *J*=7.0 Hz); ¹⁹F-NMR (CDCl₃) ppm: -44.0 (t, 2F, *J*=17.1 Hz).

Ethyl 2,2-Difluoro-4-(benzenesulfonyl)butanoate (9) In an atmosphere of Ar, **1** (0.25 ml, 2.0 mmol) was added to a suspension of activated Cu powder (280 mg, 4.4 mmol) and phenyl vinyl sulfone (**8**, 336 mg, 2.0 mmol) in DMSO (10 ml), and the mixture was stirred at 55 °C for 6 h. The mixture was worked up as in the case of **3**. The extract was purified by column chromatography (SiO₂, AcOEt:hexane=1:4) to give **9** (236 mg, 40%). **9**: A colorless oil; MS *m/z*: 219 (*M*⁺-COOEt); HRMS Calcd for C₉H₉F₂O₂S: 219.029 (*M*⁺-COOEt). Found: 219.029; IR (neat) cm⁻¹: 2992, 2770, 1476, 1312, 1192, 1152, 1090; ¹H-NMR (CDCl₃) δ : 7.93 (m, 2H), 7.71 (tt, 1H, *J*=7.6, 1.5 Hz), 7.61 (m, 2H), 4.32 (q, 2H, *J*=7.0 Hz), 3.30 (m, 2H), 2.53 (m, 2H), 1.35 (t, 3H, *J*=7.0 Hz); ¹⁹F-NMR (CDCl₃) ppm: -43.1 (t, 2F, *J*=15.9 Hz).

Ethyl 4-Cyano-2,2-difluorobutanoate (11) In an atmosphere of Ar, **1** (0.25 ml, 2.0 mmol) and acrylonitrile (**10**, 0.13 ml, 2.0 mmol) were added to a suspension of activated Cu powder (280 mg, 4.4 mmol) in DMSO (10 ml), and the mixture was stirred at 55 °C for 5 h. The mixture was worked up as in the case of **3**. The extract was purified by column chromatography (SiO₂, AcOEt:hexane=1:4) to give **11** (150 mg, 42%). **11**: A colorless oil; MS *m/z*: 178 (*M*⁺+1); HRMS Calcd for C₇H₁₀F₂NO₂: 178.067 (*M*⁺+1). Found: 178.067; IR (neat) cm⁻¹: 2992, 2256, 1770, 1446, 1378, 1320, 1222, 1198, 1098; ¹H-NMR (CDCl₃) δ : 4.37 (q, 2H, *J*=7.0 Hz), 2.63 (m, 2H), 2.48 (m, 2H), 1.38 (t, 3H, *J*=7.0 Hz); ¹⁹F-NMR (CDCl₃) ppm: -44.6 (dd, 2F, *J*=15.9, 14.7 Hz).

Ethyl 2,2-Difluoro-3-methyl-5-oxoheptanoate (13) In an atmosphere of Ar, **1** (0.25 ml, 2.0 mmol) and 4-hexen-3-one (**12**, 0.23 ml, 2.0 mmol) were added to a suspension of activated Cu powder (280 mg, 4.4 mmol) in DMSO (10 ml), and the mixture was stirred at 55 °C for 3 h. The mixture was worked up as in the case of **3**. The extract was purified by column chromatography (SiO₂, Et₂O:hexane=1:9) to give **13** (216 mg, 49%). **13**: A pale yellow oil; MS *m/z*: 222 (*M*⁺); HRMS Calcd for C₁₀H₁₆F₂O₃: 222.106 (*M*⁺). Found: 222.105; IR (neat) cm⁻¹: 2988, 2948, 1770, 1724, 1312, 1278, 1142, 1112, 1062; ¹H-NMR (CDCl₃) δ : 4.32 (q, 2H, *J*=7.0 Hz), 2.90 (m,

1H), 2.77 (dd, 1H, $J=17.7$, 4.0 Hz), 2.48 (dq, 1H, $J=17.7$, 7.3 Hz), 2.41 (dq, 1H, $J=17.7$, 7.3 Hz), 2.38 (dd, 1H, $J=17.7$, 9.2 Hz), 1.36 (t, 3H, $J=7.0$ Hz), 1.07 (t, 3H, $J=7.3$ Hz), 1.01 (d, 3H, $J=7.0$ Hz); ^{19}F -NMR (CDCl_3) ppm: -44.0 (dd, 1F, $J=252.0$, 13.2 Hz), -49.3 (dd, 1F, $J=252.0$, 14.7 Hz).

Ethyl 2,2-Difluoro-5-oxo-3-phenyl-hexanoate (15), Ethyl (Z)- and (E)-3-Acetyl-2,2-difluoro-4-phenyl-3-butenolate (16 and 17) In an atmosphere of Ar, **1** (0.25 ml, 2.0 mmol) was added to a suspension of activated Cu powder (280 mg, 4.4 mmol) and benzalacetone (**14**, 290 mg, 2.0 mmol) in DMSO (10 ml), and the mixture was stirred at 55 °C for 6 h. After this time, **1** (0.25 ml, 2.0 mmol) was added to the mixture, since **14** was detected by GLC, and the mixture was stirred for further 2 h. At this time, **14** was not detected by GLC. The mixture was worked up as in the case of **3**. The extract was purified by column chromatography (SiO_2 , $\text{AcOEt}:\text{hexane}=1:4$) to give **15** (41 mg, 8%), **16** (86 mg, 16%) and **17** (54 mg, 10%). **15**: A colorless oil; MS m/z : 270 (M^+); HRMS Calcd for $\text{C}_{14}\text{H}_{16}\text{F}_2\text{O}_3$: 270.106 (M^+). Found: 270.106; IR (neat) cm^{-1} : 3044, 2992, 1772, 1726, 1268, 1110; ^1H -NMR (CDCl_3) δ : 7.29 (m, 5H), 4.12 (q, 2H, $J=7.0$ Hz), 4.05 (dddd, 1H, $J=22.0$, 12.2, 9.2, 4.3 Hz), 3.16 (dd, 1H, $J=17.7$, 4.3 Hz), 3.03 (dd, 1H, $J=17.7$, 9.2 Hz), 2.10 (s, 3H), 1.13 (t, 3H, $J=7.0$ Hz); ^{19}F -NMR (CDCl_3) ppm: -42.9 (dd, 1F, $J=251.5$, 12.2 Hz), -51.0 (dd, 1F, $J=251.5$, 22.0 Hz). **16**: A colorless oil; MS m/z : 268 (M^+); HRMS Calcd for $\text{C}_{14}\text{H}_{14}\text{F}_2\text{O}_3$: 268.091 (M^+). Found: 268.091; ^1H -NMR (CDCl_3) δ : 7.92 (s, 1H), 7.49 (m, 2H), 7.41 (m, 3H), 4.27 (q, 2H, $J=7.0$ Hz), 2.49 (s, 3H), 1.30 (t, 3H, $J=7.0$ Hz); ^{19}F -NMR (CDCl_3) ppm: -35.8 (s, 2F). **17**: A colorless oil; MS m/z : 268 (M^+); HRMS Calcd for $\text{C}_{14}\text{H}_{14}\text{F}_2\text{O}_3$: 268.091 (M^+). Found: 268.091; ^1H -NMR (CDCl_3) δ : 7.51 (t, 1H, $J=1.83$ Hz), 7.41 (m, 3H), 7.30 (m, 2H), 4.39 (q, 2H, $J=7.0$ Hz), 2.08 (s, 3H), 1.37 (t, 3H, $J=7.0$ Hz); ^{19}F -NMR (CDCl_3) ppm: -42.0 (s, 2F).

Ethyl 3-Acetyl-2,2-difluoro-4-phenylbutanoate (18) A solution of **16** (54 mg, 0.2 mmol) in THF (5 ml) was shaken overnight in the presence of 10% Pd-C (80 mg) in an atmosphere of H_2 at room temperature. After filtration of the catalyst, the solvent was evaporated under vacuum, and the residue was purified by column chromatography (SiO_2 , $\text{Et}_2\text{O}:\text{hexane}=1:4$) to give **18** in a quantitative yield. **18**: A colorless oil; MS m/z : 270 (M^+); HRMS Calcd for $\text{C}_{14}\text{H}_{16}\text{F}_2\text{O}_3$: 270.107 (M^+). Found: 270.107; ^1H -NMR (CDCl_3) δ : 7.16–7.33 (m, 5H), 4.30 (q, 2H, $J=7.0$ Hz), 3.66 (ddt, 1H, $J=14.7$, 12.2, 7.3 Hz), 3.08 (d, 2H, $J=7.3$ Hz), 2.00 (s, 3H), 1.35 (t, 3H, $J=7.0$ Hz); ^{19}F -NMR (CDCl_3) ppm: -44.20 (dd, 2F, $J=361.4$, 12.2 Hz), -44.59 (dd, 2F, $J=361.4$, 14.7 Hz). A similar reaction of **17** gave the same product in a quantitative yield.

References

- 1) "Fussokagakunyumon," ed. by Nihon Gakujutu Shinkokai, Nikkan-kogyoshimbunsha, Osaka, 311–340 (1997).
- 2) Nakano T., Makino M., Morizawa Y., Matsumura Y., *Angew. Chem. Int. Ed. Engl.*, **35**, 1019–1021 (1996); Hertel L. W., Korin J. S., Misner J. W., Tustin J. M., *J. Org. Chem.*, **53**, 2406–2409 (1988).
- 3) Tozer M. J., Herpin T. F., *Tetrahedron*, **52**, 8619–8683 (1996).
- 4) Sato K., Kawata R., Ama F., Omote M., Ando A., Kumadaki I., *Chem. Pharm. Bull.*, **47**, 1013–1016 (1999).
- 5) Kitagawa O., Miura A., Kobayashi Y., Taguchi T., *Chem. Lett.*, **1990**, 1011–1014.
- 6) Kitagawa O., Taguchi T., Kobayashi Y., *Chem. Lett.*, **1989**, 389–392.
- 7) Kitagawa O., Hashimoto A., Kobayashi Y., Taguchi T., *Chem. Lett.*, **1990**, 1307–1310.

Triterpenes from the Spores of *Ganoderma lucidum* and Their Cytotoxicity against Meth-A and LLC Tumor Cells

Byung-Sun MIN, Jiang-Jing GAO, Norio NAKAMURA, and Masao HATTORI*

Institute of Natural Medicine, Toyama Medical and Pharmaceutical University, 2630 Sugitani, Toyama 930-0194, Japan.

Received January 28, 2000; accepted March 16, 2000

Six new highly oxygenated lanostane-type triterpenes, called ganoderic acid γ (1), ganoderic acid δ (2), ganoderic acid ϵ (3), ganoderic acid ζ (4), ganoderic acid η (5) and ganoderic acid θ (6), were isolated from the spores of *Ganoderma lucidum*, together with known ganolucidic acid D (7) and ganoderic acid C2 (8). Their structures of the new triterpenes were determined as (23*S*)-7 β ,15 α ,23-trihydroxy-3,11-dioxolanosta-8,24(*E*)-diene-26-oic acid (1), (23*S*)-7 α ,15 α ,23-trihydroxy-3,11-dioxolanosta-8,24(*E*)-diene-26-oic acid (2), (23*S*)-3 β ,7 β ,23-trihydroxy-11,15-dioxolanosta-8,24(*E*)-diene-26-oic acid (3), (23*S*)-3 β ,23-dihydroxy-7,11,15-trioxolanosta-8,24(*E*)-diene-26-oic acid (4), (23*S*)-3 β ,7 β ,12 β ,23-tetrahydroxy-11,15-dioxolanosta-8,24(*E*)-diene-26-oic acid (5) and (23*S*)-3 β ,12 β ,23-trihydroxy-7,11,15-trioxolanosta-8,24(*E*)-diene-26-oic acid (6), respectively, by chemical and spectroscopic means, which included the determination of a chiral center in the side chain by a modification of Mosher's method. The cytotoxicity of the compounds isolated from the *Ganoderma* spores was carried out *in vitro* against Meth-A and LLC tumor cell lines.

Key words ganoderic acids γ — θ ; lanostane-type triterpene; *Ganoderma lucidum*; spore; cytotoxicity

The fruiting body of *Ganoderma* (*G.*) *lucidum* (Reishi in Japanese) is a well known Chinese crude drug which has been used clinically in East Asia and gives much attention as a home remedy. Over one hundred highly oxygenated and pharmacologically active lanostane-type triterpenoids have been isolated from the fruiting bodies and the mycelium of *G. lucidum*.^{1–24} Some of them have been shown to have cytotoxicity against hepatoma cells *in vitro* (ganoderic acids U, V, W, X and Y),²⁵ anti-histamine releasing activity in rat mast cells (ganoderic acids C and D),²⁶ inhibitory activity against angiotensin converting enzyme (ganoderic acid F),²⁷ hepatoprotective activity (ganoderic acid A),²⁸ and an inhibitory effect on farnesyl protein transferase (ganoderic acid A and methyl ganoderate A).²⁹ Earlier and more recently, we reported the isolation of new triterpenoids, ganoderic acids α and β , and lucidumols A and B, with several known compounds from the spores and fruiting bodies of this mushroom.^{30,31} Of the compounds isolated, ganoderiol F and ganodermanontriol were found to have anti-human immunodeficiency virus (anti-HIV-1) activity, and ganoderic acid β , lucidumol B, and ganolucidic acid A showed an inhibitory effect on HIV-1 protease.

As part of our continuing research to find pharmacologically active constituents from *G. lucidum*, we have isolated six new lanostane-type triterpenes, called ganoderic acids γ (1), δ (2), ϵ (3), ζ (4), η (5) and θ (6), from a chloroform-soluble fraction of the spores of *G. lucidum* and examined their cytotoxicity against Meth-A (sarcoma) and LLC (Lewis lung carcinoma) mouse tumor cell lines. In this paper, we describe the characterization of these new lanostane-type triterpenes (1–6), as well as cytotoxic activity of triterpenes isolated from the spores of this mushroom.

Results and Discussion

Silica gel column chromatography (CC) and prep. HPLC with an ODS-80T_s column of a CHCl₃-soluble fraction of the MeOH extract of spores of *G. lucidum* resulted in the isolation of eight triterpenes (1–8). The structures of known compounds were identified as ganolucidic acid D (7)¹⁰ and

ganoderic acid C2 (8),¹³ which had previously been isolated from the same mushroom, by comparison with the reported data.

Ganoderic acid γ (1) was obtained as colorless needles (MeOH–H₂O), mp 243–245 °C, with a positively optical rotation ($[\alpha]_D^{25} +156^\circ$). The ultraviolet (UV) absorbance at 252 nm (log ϵ 3.82) and infrared (IR) band at 1660 cm^{–1} suggested the presence of a conjugated carbonyl group. The high-resolution electron impact mass (HR-EIMS) spectrum revealed the molecular formula of 1 to be C₃₀H₄₄O₇.

The ¹H-NMR spectrum showed signals for seven methyls including a doublet at δ 0.96 ($J=6.3$ Hz) and an allylic methyl at δ 1.88 ($J=1.5$ Hz), three oxymethylenes at δ 4.53 (dt, $J=9.2, 5.1$ Hz), 4.59 (dd, $J=9.8, 6.6$ Hz) and 4.70 (dd, $J=9.2, 6.3$ Hz), and an olefinic methine at δ 6.61 (dd, $J=9.2, 1.5$ Hz) (Table 1). The ¹³C-NMR, in combination with distortionless enhancement by polarization transfer (DEPT) and ¹H-detected multiple quantum coherence (HMQC) experiments, showed signals for seven methyls, six methylenes, seven methines (including three oxymethylenes at δ 65.9, 68.2 and 71.6, and an *sp*² methine at δ 143.2), seven quaternary carbons (including three *sp*² carbons at δ 128.4, 139.6 and 160.4), and three carbonyls at δ 170.2, 200.3 and 218.6 (Table 2). On the basis of spectroscopic evidence by ¹H–¹H-correlation spectroscopy (COSY) and HMQC experiments, all protons and carbons were assigned as shown in Tables 1 and 2, respectively. These ¹H- and ¹³C-NMR spectral data indicated a highly oxygenated lanostane-type triterpene close to the structure of ganoderic acid A (9),¹ isolated from the same mushroom, except for those of C-22 to C-27. The higher-field shifts of C-22, C-23, C-26 and C-27 by 6.8, 142.5, 6.3 and 4.3 ppm, respectively, and the lower-field shifts of C-24 and C-25 by 96.4 and 93.8 ppm, respectively, compared with those of 9 suggested that an allylic alcohol group may be located at C-23–25 in the side chain. The presence of the allylic alcohol group in the side chain of 1 supported by prominent fragment ions at m/z 401 [e]⁺, 359 [a]⁺ and 157 [b]⁺ corresponding to a loss of the side chain molecule in the EIMS spectrum (Fig. 1). The fragmentation

* To whom correspondence should be addressed. e-mail: saibo421@ms.toyama-mpu.ac.jp

Table 1. ^1H -NMR Spectral Data of Compounds **1**–**7** (400 MHz, in $\text{CDCl}_3 + \text{CD}_3\text{OD}$)

^1H	1	2	3	4
1-H (α)	1.53 dt (13.5, 7.0)	1.70 td (13.9, 4.6)	0.98 m	1.22 m
1-H (β)	2.81 ddd (13.5, 8.3, 5.9)	2.94 ddd (13.9, 8.2, 5.9)	2.78 dt (9.9, 3.5)	2.82 m
2-H (α)	2.45 dd (15.5, 7.0)	2.45 m	1.68 m	1.71 m
2-H (β)	2.53 ddd (15.5, 9.2, 5.9)	2.62 ddd (15.5, 9.6, 5.9)		
3-H (α)			3.16 dd (11.2, 5.0)	3.23 dd (10.8, 6.3)
5-H	1.72 m	2.09 dd (12.8, 2.4)	0.91 m	1.59 m
6-H (α)	2.03 m	1.74 m	2.19 m	2.62 d (15.5)
6-H (β)	1.71 m		1.55 m	2.56 dd (15.5, 3.0)
7-H (α)	4.59 dd (9.8, 6.6)		4.84 t (9.4)	
7-H (β)		4.56 br d (3.4)		
12-H (α)	2.79 d (15.7)	2.77 d (17.9)	2.90 d (16.7)	2.90 d (16.0)
12-H (β)	2.49 d (15.7)	2.40 d (17.9)	2.66 d (16.7)	2.69 d (16.0)
15-H (β)	4.70 dd (9.2, 6.3)	4.53 br t (5.1)		
16-H (α)	1.77 m	1.90 m	2.83 m	2.84 m
16-H (β)			2.07 dd (19.3, 9.7)	2.80 m
17-H	1.87 m	1.92 m	2.18 m	2.22 m
18-H ₃	0.94 s	0.82 s	0.95 s	0.81 s
19-H ₃	1.26 s	1.02 s	1.22 s	1.27 s
20-H	1.26 m	1.31 m	1.60 m	1.68 m
21-H ₃	0.96 d (6.3)	0.91 d (6.5)	1.07 d (6.1)	1.04 d (6.2)
22-H	1.45 m	1.48 m	1.55 m	1.50 m
22-H	1.62 m	1.58 br t (11.1)		
23-H	4.53 td (9.2, 5.1)	4.51 m	4.56 m	4.53 dd (13.2, 9.2)
24-H	6.61 dd (9.2, 1.5)	6.53 br d (8.7)	6.59 dd (9.2, 1.5)	6.57 br d (9.2)
27-H ₃	1.88 d (1.5)	1.87 br s	1.88 d (1.5)	1.87 br s
28-H ₃	1.13 s	1.16 s	1.03 s	1.02 s
29-H ₃	1.11 s	1.08 s	0.84 s	0.88 s
30-H ₃	1.26 s	1.28 s	1.38 s	1.54 s

^1H	5	6	7
1-H (α)	0.92 m	1.10 m	1.55 m
1-H (β)	2.57 dt (13.3, 3.9)	2.72 m	2.97 ddd (13.8, 8.3, 5.6)
2-H (α)	1.65 m	1.73 m	2.56 m
2-H (β)			
3-H (α)	3.19 dd (8.9, 7.3)	3.22 dd (8.9, 7.2)	
5-H	0.89 m	1.55 dd (14.5, 2.2)	
6-H (α)	2.25 m	2.72 m	
6-H (β)	1.64 m	2.57 dd (14.5, 2.2)	
7-H (α)	4.76 t (8.7)		
7-H (β)			
12-H (α)	4.40 s	4.51 s	2.73 d (17.2)
12-H (β)			2.41 d (17.2)
15-H (β)			4.31 dd (8.4, 5.6)
16-H (α)	2.68 dd (19.6, 8.7)	2.75 dd (18.0, 9.8)	2.44 ddd (16.6, 8.5, 6.8)
16-H (β)	2.21 dd (19.6, 9.8)	2.63 m	1.69
17-H	2.50 dd (8.7, 4.0)	1.99 dd (18.0, 8.2)	1.72 m
18-H ₃	0.75 s	0.62 s	0.85 s
19-H ₃	1.29 s	1.37 s	1.01 s
20-H	2.00 m	1.78 m	1.26 s
21-H ₃	1.16 d (6.8)	1.15 d (6.5)	0.92 d (6.3)
22-H	1.66 m	1.46 m	1.85 m
22-H		1.62 m	
23-H	4.56 ddd (12.6, 8.9, 5.1)	4.54 ddd (13.8, 8.9, 4.8)	4.51 m
24-H	6.57 br d (8.9)	6.52 br d (8.9)	6.54 d (8.9)
27-H ₃	1.88 br s	1.87 br s	1.88 br s
28-H ₃	1.02 s	1.05 s	1.08 s
29-H ₃	0.86 s	0.89 s	1.13 s
30-H ₃	1.43 s	1.68 s	1.18 s

 δ Values in ppm and coupling constants (in parentheses) in Hz.

ions m/z 498 $[\text{M}-\text{H}_2\text{O}]^+$, 480 $[\text{M}-2\text{H}_2\text{O}]^+$ and 462 $[\text{M}-3\text{H}_2\text{O}]^+$, due to the successive losses of 18 mass units, indicated the presence of three hydroxyl groups.

The connectivities of **1** were established by interpretation

of the significant heteronuclear multiple bond correlation (HMBC) spectrum. Correlations among the signals H-5 and C-3/C-7/C-9; H₃-28/H₃-29 and C-3; H₂-6 and C-8; H₃-19 and C-9; and H₂-12 and C-11, confirmed that the positions of ke-

tone and hydroxyl, and α,β -unsaturated carbonyl groups were at C-3 and C-7, and C-8, C-9 and C-11, respectively (Fig. 2). Long-range correlations between H-15/C-17 and H₃-30/C-15 indicated the presence of another hydroxyl group at C-15. On the other hand, the connectivity of an allylic alcohol group in the side chain moiety at C-23, C-24 and C-25 as shown in formula 1 was revealed by the ¹H-¹H correlations between H₂-22 and H-23; H-23 and H-24; and H-24 and H₃-

Table 2. ¹³C-NMR Spectral Data of Compounds 1–7 (100 MHz, in CDCl₃+CD₃OD)

C	1	2	3	4	5	6	7
1	35.2	34.9	35.7	33.6	34.4	33.2	34.9
2	33.9	34.3	28.0	26.9	27.1	26.7	34.0
3	218.6	219.5	78.7	77.2	78.0	76.8	219.6
4	46.4	46.6	39.7	39.0	38.4	40.0	46.8
5	48.3	45.3	50.0	50.8	49.0	51.2	51.3
6	28.1	27.7	27.6	36.2	26.5	36.4	18.4
7	68.2	66.6	67.7	199.9	66.2	199.5	29.3
8	160.4	160.9	158.4	148.6	156.6	146.2	165.1
9	139.6	139.7	143.9	151.8	142.0	151.0	137.9
10	37.6	37.9	39.4	40.4	38.1	38.8	36.8
11	200.3	200.1	200.1	200.1	199.5	201.4	199.1
12	51.5	52.0	51.2	49.6	78.2	77.6	51.6
13	46.3	47.0	46.4	44.2	51.7	49.5	46.4
14	53.7	53.4	60.3	57.0	60.1	57.5	53.3
15	71.6	71.7	218.5	209.0	217.4	207.6	72.0
16	35.6	37.5	42.0	45.6	36.8	36.7	38.1
17	48.5	49.7	47.2	42.7	46.2	45.5	49.0
18	16.6	17.3	17.6	15.9	11.9	10.6	16.7
19	18.9	17.5	18.8	17.6	18.6	17.6	18.6
20	33.1	33.5	34.0	33.1	28.5	29.4	33.1
21	19.0	19.2	20.0	19.3	22.0	21.3	18.8
22	42.9	43.3	43.7	40.4	41.3	41.8	42.9
23	65.9	66.4	66.8	65.9	67.0	66.5	66.0
24	143.2	142.4	144.2	142.8	142.7	142.2	142.4
25	128.4	130.2	129.6	128.8	129.3	129.0	129.5
26	170.2	172.0	171.2	170.8	170.8	175.0	171.5
27	12.3	13.1	13.1	12.6	12.8	12.6	12.7
28	27.0	27.5	28.6	27.5	27.9	27.4	27.5
29	20.1	20.5	16.1	15.3	15.2	15.2	20.2
30	19.0	21.0	24.9	21.6	22.9	20.1	18.7

27. This was further supported by long-range correlations between H-20 and C-23; H₂-22 and C-24; H-23 and C-25; and H-24 and C-26/C-27 in the HMBC spectrum.

Two equatorial hydroxyl groups at C-7 (β -orientation) and C-15 (α -orientation) were deduced from the multiplicities of H-7 (δ_{H} 4.59, dd, $J=9.8$ and 6.6 Hz) and H-15 (δ_{H} 4.70, dd, $J=9.2$ and 6.3 Hz), which was supported by nuclear Overhauser effect (NOE) correlations observed from H-7 to H-5 and H₃-30, and H-15 to H₃-18 in the nuclear Overhauser effect spectroscopy (NOESY) spectrum (Fig. 2). The configuration of the double bond at C-24 and C-25 was confirmed to be an *E* form by ¹H-NMR chemical shift of H-24 (δ_{H} 6.61), which resembles those of tiglic acid³²⁾ and ganoderic acids U–Z.³³⁾ Determination of the absolute configuration at C-23 was examined by a modification of Mosher's method.³⁴⁾ Under the standard reaction conditions with (*R*)-(+)- and (*S*)-(–)-MTPA for 20 h, 1 gave 15,23-di-(*R*)-(+)-MTPA ester and 7,15,23-tri-(*S*)-(–)-MTPA ester, respectively. However, 1 gave 15,23-di-(*R*)-(+)-MTPA ester (1a) and 15,23-di-(*S*)-(–)-MTPA ester (1b), respectively, when stirred for 6 h. In the ¹H-NMR spectrum of (*S*)-(–)-MTPA ester (1b), proton signals assigned for H-20, H₃-21 and H₂-22 were observed at a higher-field than those in the (*R*)-(+)-MTPA ester (1a), while signals due to H-24 and H₃-27 in the former ester were shifted to a lower-field than those in the latter ester (Fig. 3). Therefore, the absolute configuration at C-23 was concluded to be 23*S*. Consequently, the structure of 1 was determined as (23*S*)-7 β ,15 α ,23-trihydroxy-3,11-dioxolanosta-8,24(*E*)-diene-26-oic acid.

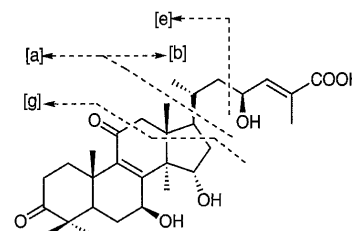


Fig. 1. Proposed Mass Fragmentation Pattern of 1

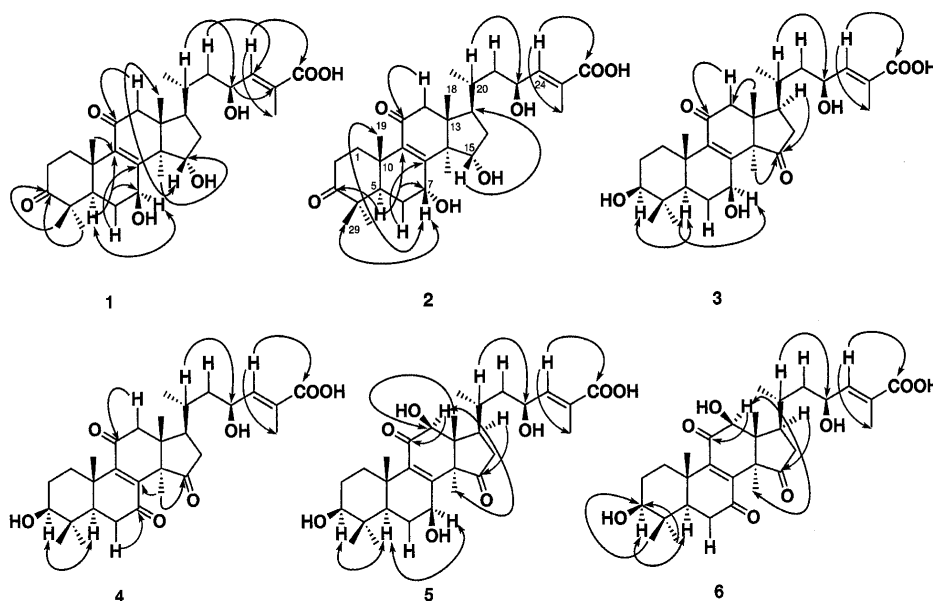


Fig. 2. Long-range and NOE Correlations Observed in the HMBC and NOESY Spectra of 1–6 (HMBC →, NOE ↔)

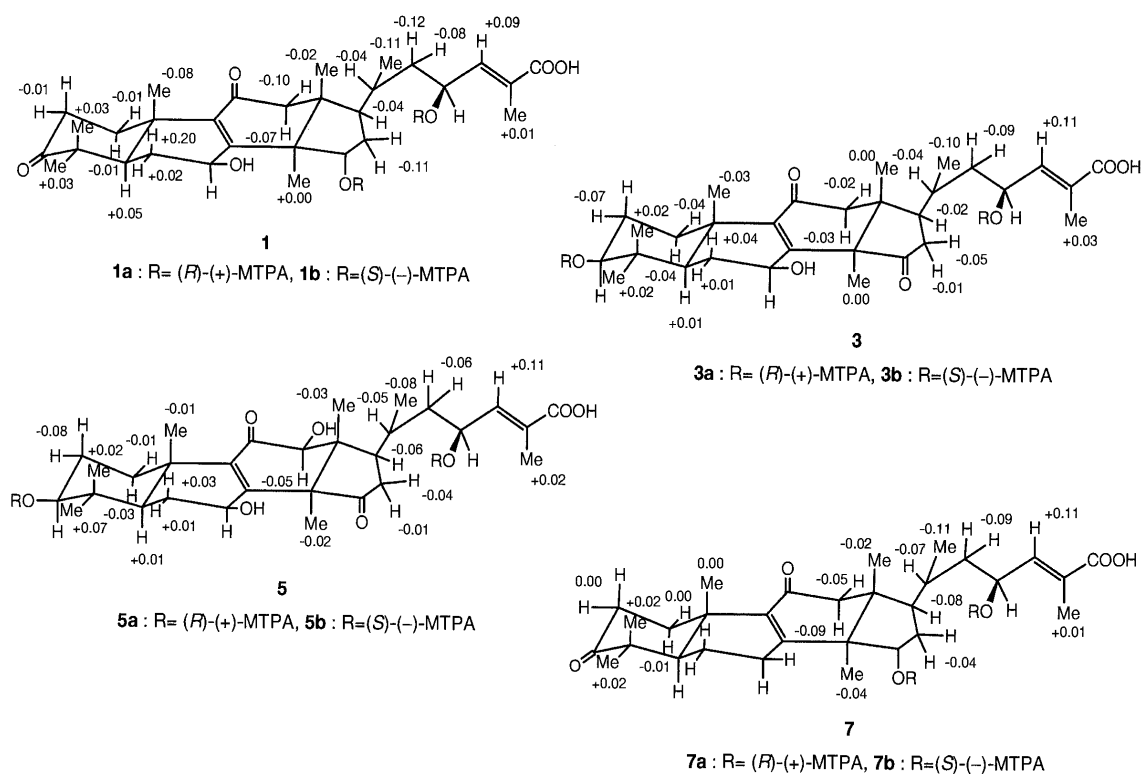


Fig. 3. Chemical Shift Difference for the (*S*)-(-)-MTPA Esters (**1b**, **3b**, **5b** and **7b**) and (*R*)-(+)-MTPA Esters (**1a**, **3a**, **5a** and **7a**) in ppm at 400 MHz

Ganoderic acid **δ** (**2**) was isolated as white amorphous powder, $[\alpha]_D^{25} +160^\circ$, and possessed the same molecular formula as that of **1**, HR-EIMS. Its UV and IR spectra exhibited absorptions at 252 nm ($\log \epsilon$ 3.70) and 1657 cm^{-1} , ascribable to a conjugated ketone. The ^1H - and ^{13}C -NMR spectra of **2** were quite similar to those of **1**. Careful examination of the spectral data, however, revealed several significant differences. The most noticeable change were higher-field shifts of H-7 (δ_{H} 4.56, brd, $J=3.4\text{ Hz}$) and H-15 (δ_{H} 4.53, brt, $J=5.1\text{ Hz}$) by 0.3 and 1.3 ppm, respectively, and a higher-field shift of C-7 by 1.6 ppm, compared with the corresponding signals of **1** in the ^1H - and ^{13}C -NMR spectra (Tables 1 and 2). In the HMBC spectrum of **2**, long-range correlations were also similar to those of **1** (Fig. 2). A detailed comparison of spectral data of **1** and **2** with ganoderic acid A (**9**) and B8 (**10**)¹³ showed that **2** was a stereoisomer of **1** with regard to a hydroxyl group at C-7. This was further supported by a NOESY experiment, which showed NOE correlations between H-7 and H₃-19/H₃-29, and H-15 to H₃-18 (Fig. 2). The configurations of C-23 and C-24 were assigned as 23*S* and 24*E* on the basis of the proton and carbon signals of the side chain moiety (C-20—27), which were very similar to those of **1**. Consequently, the structure of **2** was determined to be (23*S*)-7 α ,15 α ,23-trihydroxy-3,11-dioxolanosta-8,24(*E*)-diene-26-oic acid.

Ganoderic acid ϵ (**3**) was also obtained as colorless needles (MeOH–H₂O) of mp 249—251 °C. The molecular formula was determined as C₃₀H₄₄O₇ by HR-FABMS.

Inspection of spectral data of **3** revealed the presence of the same functional groups as in **1**, including three oxymethylenes at δ 3.16 (dd, $J=11.2, 5.0\text{ Hz}$), δ 4.84 (t, $J=9.4\text{ Hz}$) and δ 4.56 (m), and an sp^2 methine at δ 144.2 and three carbonyls (δ 171.2, 200.1 and 218.5). In the ^{13}C -NMR spectrum, most of the signals in **3** were superimposable over

those of **1**, except signals C-2, C-3, C-4, C-14, C-15 and C-16; the signals of C-2, C-3 and C-4 were shifted to a higher-field by 5.9, 139.9 and 6.7 ppm, respectively, while those of C-14, C-15 and C-16 shifted to a lower-field by 6.6, 146.9 and 6.4 ppm, respectively, compared with those of **1**, indicating a hydroxyl group at C-3 and a carbonyl group at C-15. This was further supported by HMBC correlations observed between signals of H₃-28 (δ_{H} 1.03)/H₃-29 (δ_{H} 0.84) and C-3 (δ_{C} 78.7), as well as signals between H₃-30 (δ_{H} 1.38) and C-15 (δ_{C} 218.5) (Fig. 2). Furthermore, the proton and carbon signals in **3** were also superimposable on those of ganoderic acid B (**11**),¹ except for the signals due to the side chain moiety (C-20—27), where the former possesses an allylic alcohol group at C-23—25 and the latter possesses an isolated carbonyl group.

The β orientation of hydroxyl groups at C-3 and C-7 was deduced from the multiplicities of H-3 (δ_{H} 3.16, dd, $J=11.2, 5.0\text{ Hz}$) and H-7 (δ_{H} 4.84, t, $J=9.4\text{ Hz}$). This was further confirmed by NOE correlations observed between H-3 and H-5 and between H-5 and H-7 in the NOESY spectrum (Fig. 2). For determination of absolute configuration at C-23, **3** was treated with (*R*)-(+)- and (*S*)-(-)-MTPA chloride to give 3,23-di-(*R*)-(+)-MTPA ester (**3a**) and 3,23-di-(*S*)-(-)-MTPA ester (**3b**), respectively. The chemical shift difference of **3a** and **3b** were observed in the same direction as **1a** and **1b** in the ^1H -NMR spectrum (Fig. 3). Consequently, the absolute configuration at C-23 in **3** was assigned as 23*S*. The structure of **3** was established as (23*S*)-3 β ,7 β ,23-trihydroxy-11,15-dioxolanosta-8,24(*E*)-diene-26-oic acid.

Ganoderic acid ζ (**4**) was isolated as colorless needles (MeOH–H₂O), mp 143—145 °C. Its IR spectrum exhibited absorption bands due to a five-membered carbonyl (1747 cm^{-1}) and α,β -unsaturated carbonyl (1698 cm^{-1}) groups, and the UV spectrum showed an absorption at

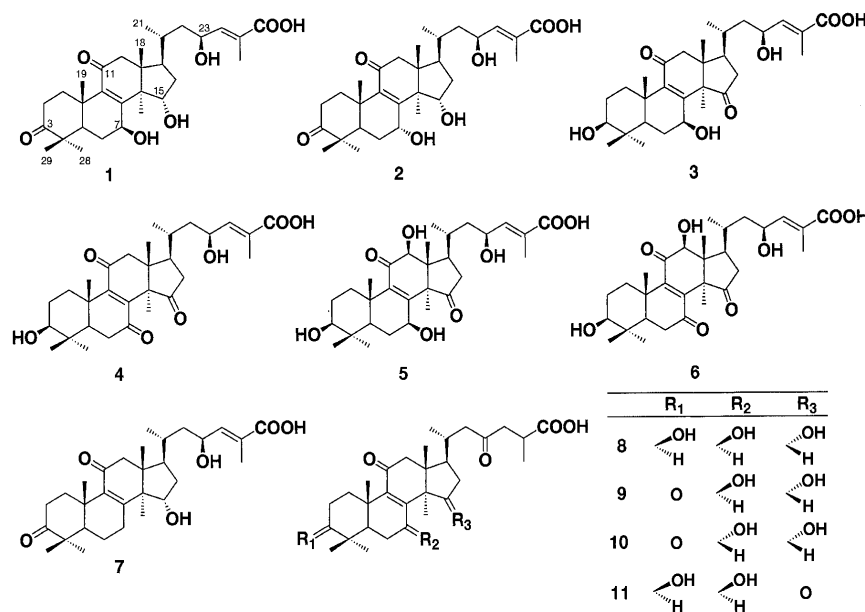


Chart 1. Structures of Compounds Isolated from the Spores of *Ganoderma lucidum*

257 nm ($\log \epsilon$, 3.81) due to an α,β -unsaturated carbonyl group. In the positive-mode FABMS of **4**, quasimolecular ion peaks were observed at m/z 515 $[M+H]^+$ and 537 $[M+Na]^+$, and the molecular formula, $C_{30}H_{42}O_7$, was determined by HR-FABMS.

The ¹H- and ¹³C-NMR spectra of **4** were similar to those of **3**. However, an oxymethylene signal (δ_H 4.84/ δ_C 67.7) observed in the spectrum of **3** was absent in that of **4**. Instead, a new signal at δ_C 199.9 was observed, indicating that **4** has a carbonyl group at C-7. The connectivity of the carbonyl group was confirmed by HMBC correlations observed between H₂-6 (δ_H 2.56 and δ_H 2.62) and C-7 (δ_C 199.9) (Fig. 2). The carbon signals at δ_C 146.8 and 151.8 assigned as C-8 and C-9 correlated with H₃-30 and H₃-19 methyl protons, respectively, in the HMBC spectrum. The carbon signal of C-8 was more shielded than that of C-9. The configuration of a hydroxyl group at C-3 was assigned as β on the basis of multiplicity (δ_H 3.22, dd, $J=10.8, 6.3$ Hz). The configurations of C-23 and C-24 were assigned as 23*S* and 24*E* on the basis of NMR data, which were similar to those of **3**. Ganoderic acid ζ (**4**) was accordingly determined as (23*S*)-3 β ,23-dihydroxy-7,11,15-trioxolanosta-8,24(*E*)-diene-26-oic acid.

Ganoderic acid η (**5**) was isolated as yellow needles (MeOH-H₂O), mp 212–214 °C, with a positive optical rotation ($[\alpha]_D^{25} +128^\circ$, EtOH). The molecular formula, $C_{30}H_{44}O_8$, of **5** was determined by positive-mode FABMS.

The ¹H- and ¹³C-NMR spectra of **5** exhibited signals due to four oxymethylenes (δ_H 3.19/ δ_C 78.0, δ_H 4.40/ δ_C 78.2, δ_H 4.56/ δ_C 67.0 and δ_H 4.76/ δ_C 66.2) and an olefinic methine (δ_H 6.57/ δ_C 142.7). The ¹H-NMR spectral feature of **5** closely resembled that of **3** except for a singlet signal at δ 4.40 due to the oxymethylene proton, instead of a pair of doublets arising from 12-methylene protons of **3** and appreciable higher-field and lower-field shifts of H₃-18 and H₃-19 signals, respectively, indicating that **5** may be a 12-hydroxy derivative of **3**. This was supported by the ¹³C-NMR spectrum analyzed by means of the HMQC spectrum. The signals of C-12 and C-13 were shifted to the lower-field by 27.0 and 5.3 ppm, respectively, and the signal due to C-18 was shifted

to the higher-field by 5.7 ppm, compared with the corresponding signals in **3**. This was confirmed by the HMBC correlations observed between signals of H₃-18 and C-12, and those of H-12 and C-11 (Fig. 2).

The β -configuration of a hydroxyl group at C-12 was inferred from NOE correlations observed between H-12 (δ 4.40) and H₃-30 (δ 1.43) in the NOESY spectrum. The absolute stereochemistry at C-23 was determined by a modification of Mosher's method. The signals due to H-20, H₃-21 and H₂-22 in 3,23-di-(*S*)-(-)-MTPA ester (**5b**) were observed at higher fields, compared to those of 3,23-di-(*R*)-(+)-MTPA ester (**5a**), while the signals due to H-24 and H₃-27 in **5b** were observed at lower-fields (Fig. 3). Thus, the absolute configuration at C-23 was assigned to be *S*. The structure of **5** was determined as (23*S*)-3 β ,7 β ,12 β ,23-tetrahydroxy-11,15-dioxolanosta-8,24(*E*)-diene-26-oic acid.

Ganoderic acid θ (**6**) was obtained as yellow needles (MeOH-H₂O), mp 131–132 °C, with a positive optical rotation ($[\alpha]_D^{25} +71.3^\circ$). In the positive-mode FABMS of **6**, quasimolecular ion peaks were observed at m/z 531 $[M+H]^+$ and 553 $[M+Na]^+$, and the molecular formula, $C_{30}H_{42}O_8$, was determined by HR-MS measurement.

The ¹H-NMR spectrum of **6** was quite similar to that of **5**, except for absence of an oxymethylene signal at δ 4.76 (t, $J=8.7$ Hz) and lower-field shifts of H-5, H $_{\alpha}$ -6 and H $_{\beta}$ -6 by 0.66, 0.93 and 0.47 ppm, respectively (Table 1); this suggested the presence of a 7-oxo group in **6**, instead of a 7-hydroxyl group in **5**. It was supported by ¹³C-NMR spectrum evidence that signals due to C-6 and C-7 (δ 9.9 and 133.3, respectively) shifted to the lower-field, reflecting the structural change in ring B. Furthermore, the HMBC spectrum showed correlation peaks between H-5 and C-7/C-9; H₂-6 and C-8; and H₃-19 and C-9, which led to the conclusion that the structure of **6** was (23*S*)-3 β ,12 β ,23-trihydroxy-7,11,15-trioxolanosta-8,24(*E*)-diene-26-oic acid.

Ganolucidic acid D (**7**) was isolated from the fruiting body of *G. lucidum* by Nishitoba *et al.*,²¹⁾ who determined the absolute configuration at C-23 as 23*S*, by converting **7** to a mono-*p*-dimethylaminobenzoate derivative and measuring its

Table 3. Cytotoxicity of Compounds Isolated from the Spores of *Ganoderma lucidum* on Tumor Cell Growth

Compound	ED ₅₀ (μg/ml)	
	Meth-A	LLC
Ganoderic acid γ (1)	15.6	>20
Ganoderic acid δ (2)	>20	>20
Ganoderic acid ε (3)	12.2	>20
Ganoderic acid ζ (4)	>20	>20
Ganoderic acid η (5)	>20	>20
Ganoderic acid θ (6)	5.7	15.2
Ganolucidic acid D	>20	>20
Ganoderic acid C2	>20	>20
Lucidumol A	4.2	2.3
Lucidumol B	8.5	16.6
Ganodermanondiol	3.4	12.5
Ganoderiol F	4.4	6.0
Ganodermanontriol	5.4	9.6
Ganoderic acid A	>20	>20
Ganoderic acid B	>20	>20
Ganoderic acid C1	>20	17.0
Ganolucidic acid A	>20	15.5
Lucideric acid α	>20	17.8
Ganoderic acid C6	>20	>20
Ganoderic acid G	6.8	>20
Adriamycin ^{a)}	0.01	0.15

a) Positive control.

CD and UV spectra.³⁵⁾ Herein, **7** was converted to 15,23-di-(*R*)-(+)-MTPA ester (**7a**) and 15,23-di-(*S*)-(–)-MTPA ester (**7b**) using a modification of Mosher's method. The chemical shift difference between **7a** and **7b** was found to be the same as those observed in the respective derivatives of **1**, **3** and **5** in the ¹H-NMR spectra (Fig. 3). Consequently, the absolute configuration at C-23 of **7** was confirmed to be 23*S*.

The compounds isolated from the spores of *G. lucidum* were tested for their cytotoxicity against Meth-A and LLC tumor cell lines. The results (ED₅₀ values) are summarized in Table 3. The ganoderic alcohols lucidumols A and B, ganodermanondiol, ganoderiol F, and ganodermanontriol showed cytotoxic effects on both tumor cells. Of these, lucidumol A exhibited the most potent cytotoxicity (ED₅₀ value, 2.3 μg/ml) against LLC tumor cells and ganodermanondiol (ED₅₀, 3.4 μg/ml) against Meth-A cells. However, ganoderic acids, including ganoderic acids γ–θ isolated in the present experiment were inactive to both tumor cells.

Experimental

Melting points were measured on a Yanagimoto micro hot-stage melting point apparatus and are not corrected. Optical rotations were measured with a DIP-360 automatic polarimeter (JASCO). UV spectra were measured with a UV-2200 UV-VIS recording spectrophotometer (Shimadzu), and IR spectra were measured with a FT/IR-230 infrared spectrometer (JASCO). ¹H- and ¹³C-NMR spectra were measured with a JNA-LAA 400 WB-FT (¹H, 400 MHz; ¹³C, 100 MHz; JEOL) spectrophotometer, the chemical shifts being represented as ppm with tetramethylsilane as an internal standard. HR-FABMS and FABMS were measured with a JMX-AX 300L spectrometer (JEOL) using glycerol as a matrix. HR-EIMS and EIMS were measured with a JMX-AX 505 HAD mass spectrophotometer (JEOL). Prep. HPLC was carried out on a Gilson HPLC system; pump: model 305 and 306, detector: 119 UV/VIS detector. Column chromatography was carried out on silica gel (Kieselgel 60, 70–230 mesh, Merck). Thin layer chromatography (TLC) was carried out on pre-coated Silica gel 60 F₂₅₄ plates (0.25 mm, Merck) and RP-18 F₂₅₄S (0.25 mm, Merck), and spots were detected under a UV light and by spraying 10% H₂SO₄ followed by heating.

Plant Materials The spore of *G. lucidum* was provided by Linzhi Gen-

eral Institute Co., Ltd. (Tokyo). The voucher specimen is deposited in the authors' laboratory.

Chemicals Lucidumols A and B, ganodermanondiol, ganoderiol F, ganodermanontriol, ganoderic acids A, B, C1, C6 and G, ganolucidic acid A, and lucideric acid α were obtained from the spores of *G. lucidum* by a method described previously.³¹⁾

Cells Meth-A cells (mouse sarcoma) and LLC (mouse lung carcinoma) were purchased from RIKEN Cell Line Bank (Tsukuba, Japan). The cells were maintained as monolayer cultures in RPMI 1640 medium supplemented with 10% fetal bovine serum, sodium bicarbonate, penicillin G and streptomycin.

Isolation Procedure The spores of *G. lucidum* KARST (250 g) were extracted with MeOH (1.5 l × 3) by refluxing for 3 h to give 35.7 g of a solid extract. The MeOH extract (30 g) was suspended in 90% MeOH (300 ml) and extracted with hexane (150 ml × 2). The resulting MeOH solution was concentrated *in vacuo* and suspended in H₂O (300 ml). The suspension was extracted with CHCl₃ (150 ml × 2) to give a CHCl₃-soluble fraction (23.2 g). The fraction (20 g) was chromatographed on a column of silica gel. Elution was started with hexane–acetone (3:2, 1:1 and 2:3) and then CHCl₃–MeOH (4:1) yielded 6 fractions (fr. A–F; 1.3, 5.5, 10.1, 1.9, 0.7 and 0.4 g, respectively). Column chromatography of fr. D on silica gel (CHCl₃–MeOH, 19:1) was separated into five subfractions (subfr. D1–D5; 0.12, 0.26, 0.24, 0.30 and 0.63 g, respectively). Purification of subfr. D4 by the prep. HPLC, a linear gradient of CH₃CN (25%→65%) in 3% AcOH, afforded **1** (11.4 mg, *R*_f 81.0 min), **2** (1.0 mg, *R*_f 82.8 min), **3** (18.6 mg, *R*_f 72.6 min), **4** (1.5 mg, *R*_f 74.4 min), **5** (12.5 mg, *R*_f 70.4 min), **6** (2.4 mg, *R*_f 67.0 min), **7** (5.0 mg, *R*_f 91.0 min) and **8** (12.0 mg, *R*_f 78.6 min).

(23*S*)-7β,15α,23-Trihydroxy-3,11-dioxolanosta-8,24(*E*)-diene-26-oic Acid (1, Ganoderic Acid γ) Colorless needles (MeOH–H₂O), mp 243–245 °C. [α]_D²⁰ +155.3° (*c*=0.1, EtOH). IR *v*_{max} cm^{−1}: 3373 (OH), 1706, 1675, 1660 (C=O). UV *λ*_{max} nm (log *ε*): 208 (4.05), 252 (3.82). EIMS *m/z* (rel. int.): 516 [M]⁺ (3), 498 [M–H₂O]⁺ (15), 480 [M–2H₂O]⁺ (27), 462 [M–3H₂O]⁺ (15), 401 [e]⁺ (8), 370 [M–C₆H₂O₄]⁺ (27), 359 [a]⁺ (7), 306 [g+H]⁺ (10), 252 [M–C₆H₂O₄]⁺ (40), 157 [b]⁺ (22), 69 (100). HR-EIMS *m/z*: 516.3092 (M⁺, Calcd for C₃₀H₄₄O₇; 516.3088). ¹H- and ¹³C-NMR data: see Tables 1 and 2. In the HMBC spectrum, the following correlations were observed: C-1/H-2,19; C-2/H-1; C-3/H-1,2,5,28,29; C-4/H-2,5,6,28,29; C-5/H-6; C-6/H-5,7; C-7/H-5,6; C-8/H-6,30; C-9/H-5,19; C-10/H-5,6,19; C-11/H-12; C-12/H-18; C-13/H-12,15,16,20; C-14/H-12,16,18; C-15/H-30; C-16/H-20; C-17/H-15,18,21,22; C-18/H-12,30; C-19/H-1,5,6; C-20/H-21,22; C-21/H-20,22; C-23/H-20,27; C-24/H-22,23,27; C-25/H-23,27; C-26/H-24,27; C-27/H-24; C-28/H-5,29; C-29/H-5,28; C-30/H-12.

(*R*)-(+)-MTPA Ester of 1 (1a) (*R*)-(+)-MTPA chloride (15 mg, 59 μmol) in pyridine (0.2 ml) was added to a solution of **1** (2.0 mg, 3.9 μmol) in CCl₄ (0.2 ml). After stirring at room temperature for 6 h, the mixture was poured into water (10 ml), and extracted with CHCl₃ (10 ml × 2). The CHCl₃ extract was concentrated *in vacuo* and purified by preparative thin layer chromatography (TLC) [hexane–acetone (1:1)] to give a 15,23-di-(*R*)-(+)-MTPA ester (**1a**, 1.5 mg) as a colorless oil. ¹H-NMR (CDCl₃): δ 1.37 (1H, m, H_α-1), 2.89 (1H, ddd, *J*=13.7, 7.8, 5.2 Hz, H_β-1), 2.45 (2H, m, H-2), 1.41 (1H, m, H-5), 1.39, 1.63 (each 1H, m, H-6), 3.63 (1H, t, *J*=7.9 Hz, H-7), 2.71 (1H, d, *J*=16.9 Hz, H_α-12), 2.51 (1H, d, *J*=16.9 Hz, H_β-12), 5.89 (1H, dd, *J*=9.7, 5.8 Hz, H-15), 1.82 (1H, m, H-16), 1.85 (1H, m, H-17), 0.92 (3H, s, H-18), 1.17 (3H, s, H-19), 1.37 (1H, m, H-20), 0.96 (3H, d, *J*=6.3 Hz, H-21), 1.80, 1.62 (each 1H, m, H-22), 5.79 (1H, ddd, *J*=18.7, 9.7, 5.1 Hz, H-23), 6.51 (1H, dd, *J*=9.7, 1.5 Hz, H-24), 2.01 (3H, d, *J*=1.5 Hz, H-27), 1.04 (3H, s, H-28), 1.03 (3H, s, H-29), 1.22 (3H, s, H-30), 3.52, 3.62 (each 3H, s, MTPA–OCH₃).

(*S*)-(–)-MTPA Ester of 1 (1b) (*S*)-(–)-MTPA chloride (15 mg) in pyridine (0.2 ml) was added to a mixture of **1** (2 mg) in CCl₄ (0.2 ml). Workup as described above gave a 15,23-di-(*S*)-(–)-MTPA ester (**1b**, 1.0 mg) as a colorless oil. ¹H-NMR (CDCl₃): δ 1.36 (1H, m, H_α-1), 2.88 (1H, ddd, *J*=13.7, 7.8, 5.2 Hz, H_β-1), 2.44 (2H, m, H-2), 1.46 (1H, m, H-5), 1.41, 1.83 (each 1H, m, H-6), 3.82 (1H, t, *J*=8.4 Hz, H-7), 2.61 (1H, d, *J*=17.2 Hz, H_α-12), 2.44 (1H, d, *J*=17.2 Hz, H_β-12), 5.93 (1H, dd, *J*=10.1, 5.8 Hz, H-15), 1.71 (1H, m, H-16), 1.80 (1H, m, H-17), 0.90 (3H, s, H-18), 1.09 (3H, s, H-19), 1.33 (1H, m, H-20), 0.85 (3H, d, *J*=6.3 Hz, H-21), 1.68, 1.54 (each 1H, m, H-22), 5.77 (1H, ddd, *J*=17.8, 9.4, 5.9 Hz, H-23), 6.62 (1H, dd, *J*=9.4, 1.5 Hz, H-24), 2.02 (3H, d, *J*=1.5 Hz, H-27), 1.07 (3H, s, H-28), 1.06 (3H, s, H-29), 1.22 (3H, s, H-30), 3.46, 3.54 (each 3H, s, MTPA–OCH₃).

(23*S*)-7α,15α,23-Trihydroxy-3,11-dioxolanosta-8,24(*E*)-diene-26-oic Acid (2, Ganoderic Acid δ) White amorphous powder, [α]_D²⁰ +160.0° (*c*=0.074, EtOH). IR *v*_{max} cm^{−1}: 3419 (OH), 1763, 1657 (C=O). UV *λ*_{max} nm (log *ε*): 207 (3.95), 252 (3.70). EIMS *m/z* (rel. int.): 516 [M]⁺ (4), 498

$[M-H_2O]^+$ (21), 480 $[M-2H_2O]^+$ (29), 370 $[M-C_6H_2O_4]^+$ (29), 306 $[M-C_{12}H_{20}O_3]^+$ (12), 252 $[M-C_6H_2O_4]^+$ (46), 106 (100). HR-EIMS m/z : 516.3056 (M^+ , Calcd for $C_{30}H_{44}O_7$: 516.3088). 1H - and ^{13}C -NMR data: see Tables 1 and 2. In the HMBC spectrum, the following correlations were observed: C-1/H-2,19; C-2/H-1; C-3/H-1,2,5,28,29; C-4/H-5,6,28,29; C-5/H-6,19,28,29; C-6/H-5,7; C-7/H-5,6; C-8/H-6,30; C-9/H-1,5,19; C-10/H-2,5,6,19; C-11/H-12; C-12/H-18; C-13/H-12,18,30; C-4/H-7,12,16,18; C-15/H-30; C-16/H-20; C-17/H-15,18,21; C-18/H-12,30; C-19/H-1,5,6; C-20/H-21,22; C-21/H-20,22; C-22/H-21,23; C-23/H-20,27; C-24/H-22,27; C-25/H-23,27; C-26/H-24,27; C-27/H-24; C-28/H-5,29; C-29/H-6,28; C-30/H-12.

(23S)-3 β ,7 β ,23-Trihydroxy-11,15-dioxolanosta-8,24(E)-diene-26-oic Acid (3, Ganoderic Acid ϵ) Colorless needles (MeOH-H₂O), mp 249—251 °C. $[\alpha]_D^{25} +153.3^\circ$ ($c=0.1$, EtOH). IR ν_{max} cm^{-1} : 3553, 3335 (OH), 1714, 1695, 1658 (C=O). UV λ_{max} nm (log ϵ): 212 (4.13), 253 (4.03). Positive-mode FABMS m/z : 517 $[M+H]^+$, 539 $[M+Na]^+$. HR positive-mode FABMS m/z : 517.3142 ($[M+H]^+$, Calcd for $C_{30}H_{45}O_7$: 517.3165). 1H - and ^{13}C -NMR data: see Tables 1 and 2. In the HMBC spectrum, the following correlations were observed: C-1/H-19; C-2/H-1; C-3/H-1,28,29; C-4/H-5,6,28,29; C-5/H-6,19,28,29; C-6/H-5,7; C-7/H-5,6; C-8/H-6,7,30; C-9/H-5,7,12,19; C-10/H-1,5,6,19; C-11/H-12; C-12/H-18; C-13/H-12,16,17,18,30; C-14/H-12,18,30; C-15/H-17,30; C-16/H-18,30; C-17/H-16,18,21; C-18/H-12,17; C-19/H-1,5; C-20/H-16,17,21,23; C-21/H-17,20,22; C-22/H-20,21,23; C-23/H-20,27; C-24/H-27; C-25/H-23,24,27; C-26/H-24,27; C-27/H-24; C-28/H-3,29; C-29/H-3,5,28.

(R)-(+)-MTPA Ester of 3 (3a) (R)-(+)-MTPA chloride (15 mg, 59 μ mol) in pyridine (0.2 ml) was added to a solution of **3** (2.0 mg, 3.9 μ mol) in CCl₄ (0.2 ml). After stirring at room temperature for 6 h, workup as mentioned above gave a 3,23-di-(R)-(+)-MTPA ester (**3a**, 1.8 mg) as a colorless oil. 1H -NMR (CDCl₃): δ 1.11 (1H, m, H _{α} -1), 2.91 (1H, dt, $J=14.0$, 3.6 Hz, H _{β} -1), 1.82 (2H, m, H-2), 4.71 (1H, dd, $J=11.6$, 5.1 Hz, H-3), 0.98 (1H, m, H-5), 2.16 (1H, m, H _{α} -6), 1.61 (1H, m, H _{β} -6), 4.79 (1H, t, $J=9.0$ Hz, H-7), 2.76 (1H, d, $J=16.8$ Hz, H _{α} -12), 2.68 (1H, d, $J=16.8$ Hz, H _{β} -12), 2.75, 2.05 (each 1H, m, H-16), 1.94 (1H, m, H-17), 0.86 (3H, s, H-18), 1.24 (3H, s, H-19), 1.50 (1H, m, H-20), 1.06 (3H, d, $J=6.5$ Hz, H-21), 1.70 (2H, m, H-22), 5.78 (1H, m, H-23), 6.49 (1H, dd, $J=9.2$, 1.2 Hz, H-24), 2.00 (3H, d, $J=1.2$ Hz, H-27), 0.93 (3H, s, H-28), 0.85 (3H, s, H-29), 1.26 (3H, s, H-30), 3.49, 3.56 (each 3H, s, MTPA-OCH₃).

(S)-(-)-MTPA Ester of 3 (3b) (S)-(-)-MTPA chloride (15 mg) in pyridine (0.2 ml) was added to a solution of **3** (2 mg) in CCl₄ (0.2 ml). Workup as mentioned above gave a 3,23-di-(S)-(-)-MTPA ester (**3b**, 1.0 mg) as a colorless oil. 1H -NMR (CDCl₃): δ 1.07 (1H, m, H _{α} -1), 2.87 (1H, dt, $J=13.7$, 3.7 Hz, H _{β} -1), 1.75 (2H, m, H-2), 4.69 (1H, dd, $J=11.8$, 4.4 Hz, H-3), 0.99 (1H, m, H-5), 2.17 (1H, ddd, $J=12.7$, 7.9, 1.1 Hz, H _{α} -6), 1.65 (1H, m, H _{β} -6), 4.79 (1H, t, $J=8.9$ Hz, H-7), 2.73 (1H, d, $J=16.6$ Hz, H _{α} -12), 2.67 (1H, d, $J=16.6$ Hz, H _{β} -12), 2.70, 2.04 (each 1H, m, H-16), 1.92 (1H, m, H-17), 0.86 (3H, s, H-18), 1.21 (3H, s, H-19), 1.46 (1H, m, H-20), 0.96 (3H, d, $J=6.8$ Hz, H-21), 1.61 (2H, m, H-22), 5.79 (1H, m, H-23), 6.60 (1H, dd, $J=9.7$, 1.2 Hz, H-24), 2.03 (3H, d, $J=1.2$ Hz, H-27), 0.95 (3H, s, H-28), 0.87 (3H, s, H-29), 1.26 (3H, s, H-30), 3.52, 3.54 (each 3H, s, MTPA-OCH₃).

(23S)-3 β ,23-Dihydroxy-7,11,15-trioxolanosta-8,24(E)-diene-26-oic Acid (4, Ganoderic Acid ζ) Colorless needles (MeOH-H₂O), mp 143—145 °C. $[\alpha]_D^{25} +213.3^\circ$ ($c=0.015$, EtOH). IR ν_{max} cm^{-1} : 3421 (OH), 1747, 1698, 1681, 1654 (C=O). UV λ_{max} nm (log ϵ): 210 (4.13), 257 (3.81). Positive-mode FABMS m/z : 515 $[M+H]^+$, 537 $[M+Na]^+$. HR positive-mode FABMS m/z : 515.3044 ($[M+H]^+$, Calcd for $C_{30}H_{43}O_8$: 515.3009). 1H - and ^{13}C -NMR data: see Tables 1 and 2. In the HMBC spectrum, the following correlations were observed: C-1/H-19; C-3/H-28,29; C-4/H-19,28,29; C-5/H-6,19,28,29; C-7/H-6; C-8/H-30; C-9/H-19; C-10/H-19; C-11/H-12; C-12/H-18; C-13/H-18,30; C-14/H-12,18,30; C-15/H-30; C-16/H-18,20; C-17/H-12,16,18; C-18/H-12,16,30; C-19/H-1,5; C-20/H-21; C-22/H-21; C-23/H-20; C-24/H-22,27; C-25/H-27; C-26/H-24,27; C-27/H-24; C-28/H-29; C-29/H-29.

(23S)-3 β ,7 β ,12 β ,23-Tetrahydroxy-11,15-dioxolanosta-8,24(E)-diene-26-oic Acid (5, Ganoderic Acid η) Yellow needles (MeOH-H₂O), mp 212—214 °C. $[\alpha]_D^{25} +128.0^\circ$ ($c=0.1$, EtOH). IR ν_{max} cm^{-1} : 3405 (OH), 1725, 1697, 1673 (C=O). UV λ_{max} nm (log ϵ): 209 (4.10), 257 (3.80). Positive-mode FABMS m/z : 533 $[M+H]^+$, 555 $[M+Na]^+$. HR positive-mode FABMS m/z : 555.2791 ($[M+Na]^+$, Calcd for $C_{30}H_{44}O_8Na$: 555.2812). 1H - and ^{13}C -NMR data: see Tables 1 and 2. In the HMBC spectrum, the following correlations were observed: C-1/H-2,19; C-2/H-1; C-3/H-1,2,28,29; C-4/H-2,3,6,28,29; C-5/H-6,19,28,29; C-6/H-7; C-7/H-5,6; C-8/H-6,7,30; C-9/H-5,7,19; C-10/H-1,19,28,29; C-11/H-12; C-12/H-18; C-13/H-12,16,17,

18,30; C-14/H-7,12,18,30; C-15/H-17; C-16/H-17,20; C-17/H-16,18,21; C-18/H-17; C-19/H-1,5; C-20/H-16,17,23; C-21/H-17; C-22/H-21; C-23/H-20; C-24/H-22,27; C-25/H-23,27; C-26/H-24; C-27/H-24; C-28/H-3,29; C-29/H-3,6,28.

(R)-(+)-MTPA Ester of 5 (5a) (R)-(+)-MTPA chloride (15 mg, 59 μ mol) in pyridine (0.2 ml) was added to a solution of **5** (2.0 mg, 3.8 μ mol) in CCl₄ (0.2 ml). The mixture was stirred at room temperature for 6 h and worked up as described above to give a 3,23-di-(R)-(+)-MTPA ester (**5a**, 1.2 mg) as a colorless oil. 1H -NMR (CDCl₃): δ 1.01 (1H, m, H _{α} -1), 2.68 (1H, dt, $J=13.8$, 3.7 Hz, H _{β} -1), 1.83 (2H, m, H-2), 4.70 (1H, dd, $J=11.0$, 5.2 Hz, H-3), 0.95 (1H, m, H-5), 2.20 (1H, m, H _{α} -6), 1.67 (1H, m, H _{β} -6), 4.77 (1H, t, $J=10.9$ Hz, H-7), 4.33 (1H, s, H-12), 2.62, 2.13 (each 1H, m, H-16), 2.51 (1H, m, H-17), 0.72 (3H, s, H-18), 1.25 (3H, s, H-19), 2.04 (1H, m, H-20), 1.19 (3H, d, $J=6.8$ Hz, H-21), 1.85 (2H, m, H-22), 5.79 (1H, m, H-23), 6.48 (1H, dd, $J=9.2$, 1.5 Hz, H-24), 2.01 (3H, d, $J=1.5$ Hz, H-27), 0.87 (3H, s, H-28), 0.86 (3H, s, H-29), 1.32 (3H, s, H-30), 3.52, 3.55 (each 3H, s, MTPA-OCH₃).

(S)-(-)-MTPA ester of 5 (5b) (S)-(-)-MTPA chloride (15 mg) and pyridine (0.2 ml) were added to a solution of **5** (2 mg) in CCl₄ (0.2 ml). Workup as mentioned above gave a 3,23-di-(S)-(-)-MTPA ester (**5b**, 0.8 mg) as a colorless oil. 1H -NMR (CDCl₃): δ 1.00 (1H, m, H _{α} -1), 2.65 (1H, dt, $J=14.0$, 2.9 Hz, H _{β} -1), 1.71 (2H, m, H-2), 4.67 (1H, dd, $J=9.4$, 4.4 Hz, H-3), 0.96 (1H, m, H-5), 2.23 (1H, m, H _{α} -6), 1.68 (1H, m, H _{β} -6), 4.77 (1H, dd, $J=8.3$, 4.1 Hz, H-7), 4.28 (1H, s, H-12), 2.58, 2.12 (each 1H, m, H-16), 2.45 (1H, m, H-17), 0.69 (3H, s, H-18), 1.24 (3H, s, H-19), 1.99 (1H, m, H-20), 1.11 (3H, d, $J=6.8$ Hz, H-21), 1.79 (2H, m, H-22), 5.81 (1H, m, H-23), 6.59 (1H, dd, $J=8.6$, 1.5 Hz, H-24), 2.03 (3H, d, $J=1.5$ Hz, H-27), 0.94 (3H, s, H-28), 0.88 (3H, s, H-29), 1.30 (3H, s, H-30), 3.51, 3.53 (each 3H, s, MTPA-OCH₃).

(23S)-3 β ,12 β ,23-Trihydroxy-7,11,15-trioxolanosta-8,24(E)-diene-26-oic Acid (6, Ganoderic Acid θ) Yellow needles (MeOH-H₂O), mp 131—133 °C. $[\alpha]_D^{25} +71.3^\circ$ ($c=0.1$, EtOH). IR ν_{max} cm^{-1} : 3404 (OH), 1747, 1685, 1653 (C=O). UV λ_{max} nm (log ϵ): 212 (4.08), 251 (3.75). Positive-mode FABMS m/z : 531 $[M+H]^+$, 553 $[M+Na]^+$. HR positive-mode FABMS m/z : 531.2933 ($[M+Na]^+$, Calcd for $C_{30}H_{43}O_8$: 531.2958). 1H - and ^{13}C -NMR data: see Tables 1 and 2. In the HMBC spectrum, the following correlations were observed: C-1/H-19; C-3/H-1,28,29; C-4/H-6,19; C-5/H-6,19,28,29; C-6/H-5; C-7/H-6; C-8/H-6,30; C-9/H-5,19; C-10/H-1,19; C-11/H-12; C-12/H-18; C-13/H-12,16; C-14/H-12,18,30; C-15/H-16,17,30; C-16/H-16,18,21; C-19/H-5; C-20/H-21,22; C-21/H-23; C-22/H-21; C-23/H-20,27; C-24/H-22,27; C-25/H-23,27; C-26/H-24,27; C-27/H-24; C-28/H-3,29; C-29/H-3,28.

(R)-(+)-MTPA Ester of 7 (7a) (R)-(+)-MTPA chloride (10 mg, 40 μ mol) in pyridine (0.1 ml) was added to a solution of **7** (1.0 mg, 2 μ mol) in CCl₄ (0.1 ml). After stirring at room temperature for 20 h, workup as mentioned above gave a 15,23-di-(R)-(+)-MTPA ester (**7a**, 0.7 mg) as a colorless oil. 1H -NMR (CDCl₃): δ 1.46 (1H, m, H _{α} -1), 2.96 (1H, ddd, $J=15.1$, 9.0, 6.0 Hz, H _{β} -1), 2.45 (2H, m, H-2), 2.68 (1H, d, $J=17.2$ Hz, H _{α} -12), 2.43 (1H, d, $J=17.2$ Hz, H _{β} -12), 5.20 (1H, dd, $J=9.7$, 5.5 Hz, H-15), 1.81 (2H, m, H-16), 1.91 (1H, m, H-17), 0.87 (3H, s, H-18), 1.05 (3H, s, H-19), 1.36 (1H, m, H-20), 0.95 (3H, d, $J=6.3$ Hz, H-21), 1.62, 1.75 (each 1H, m, H-22), 5.77 (1H, m, H-23), 6.50 (1H, dd, $J=9.4$, 1.5 Hz, H-24), 2.01 (3H, d, $J=1.5$ Hz, H-27), 1.06 (3H, s, H-28), 1.05 (3H, s, H-29), 1.13 (3H, s, H-30), 3.51, 3.63 (each 3H, s, MTPA-OCH₃).

(S)-(-)-MTPA Ester of 7 (7b) (S)-(-)-MTPA chloride (10 mg) in pyridine (0.1 ml) were added to a solution of **7** (1 mg) in CCl₄ (0.1 ml). After workup as usual, a 15,23-di-(S)-(-)-MTPA ester (**7b**, 0.6 mg) was obtained as a colorless oil. 1H -NMR (CDCl₃): δ 1.46 (1H, m, H _{α} -1), 2.95 (1H, ddd, $J=18.0$, 7.7, 5.7 Hz, H _{β} -1), 2.45 (2H, m, H-2), 2.59 (1H, d, $J=17.3$ Hz, H _{α} -12), 2.38 (1H, d, $J=17.3$ Hz, H _{β} -12), 5.21 (1H, dd, $J=9.4$, 5.6 Hz, H-15), 1.77 (2H, m, H-16), 1.83 (1H, m, H-17), 0.85 (3H, s, H-18), 1.05 (3H, s, H-19), 1.29 (1H, m, H-20), 0.84 (3H, d, $J=5.8$ Hz, H-21), 1.53, 1.66 (each 1H, m, H-22), 5.77 (1H, m, H-23), 6.61 (1H, dd, $J=8.0$, 1.5 Hz, H-24), 2.02 (3H, d, $J=1.5$ Hz, H-27), 1.08 (3H, s, H-28), 1.07 (3H, s, H-29), 1.09 (3H, s, H-30), 3.45, 3.54 (each 3H, s, MTPA-OCH₃).

Cytotoxicity Assay The *in vitro* Meth-A tumor cell assay was carried out according to the procedure by Geran *et al.*³⁶⁾ and LLC cells, by a sulforhodamin B (SRB) method³⁷⁾ as described previously.³⁸⁾

Acknowledgment Part of this study was financially supported by Linzin General Institute Co., Ltd. (Tokyo).

References and Notes

- 1) Kubota T., Asaka Y., Miura I., Mori H., *Helv. Chim. Acta*, **65**, 611—

- 619 (1982).
- 2) Nishitoba T., Sato H., Kasai T., Kawagishi H., Sakamura S., *Agric. Biol. Chem.*, **48**, 2905—2907 (1984).
- 3) Kikuchi T., Matsuda S., Kadota S., Murai Y., Ogita Z., *Chem. Pharm. Bull.*, **33**, 2624—2627 (1985).
- 4) Kikuchi T., Matsuda S., Murai Y., Ogita Z., *Chem. Pharm. Bull.*, **33**, 2628—2631 (1985).
- 5) Hirofani M., Furuya T., Shiro M., *Phytochemistry*, **24**, 2055—2061 (1985).
- 6) Komoda Y., Nakamura H., Ishihara S., Uchida M., Kohda H., Yamasaki K., *Chem. Pharm. Bull.*, **33**, 4829—4835 (1985).
- 7) Hirofani M., Asaka I., Ino C., Furuya T., Shiro M., *Phytochemistry*, **26**, 2797—2803 (1987).
- 8) Arisawa M., Fujita A., Saga M., Fukumura H., Hayashi T., Shimizu M., Morita N., *J. Nat. Prod.*, **49**, 621—625 (1986).
- 9) Hirofani M., Ino C., Furuya T., Shiro M., *Chem. Pharm. Bull.*, **34**, 2282—2285 (1986).
- 10) Nishitoba T., Sato H., Sakamura S., *Agric. Biol. Chem.*, **50**, 809—811 (1986).
- 11) Sato H., Nishitoba T., Shirasu S., Oda K., Sakamura S., *Agric. Biol. Chem.*, **50**, 2887—2890 (1986).
- 12) Fujita A., Arisawa M., Saga M., Hayashi T., Morita N., *J. Nat. Prod.*, **49**, 1122—1125 (1986).
- 13) Kikuchi T., Kanomi S., Kadota S., Murai Y., Tsubono K., Ogita Z., *Chem. Pharm. Bull.*, **34**, 3695—3712 (1986).
- 14) Kikuchi T., Kanomi S., Murai Y., Kadota S., Tsubono K., Ogita Z., *Chem. Pharm. Bull.*, **34**, 4018—4029 (1986).
- 15) Nishitoba T., Sato H., Sakamura S., *Phytochemistry*, **26**, 1777—1784 (1987).
- 16) Nishitoba T., Sato H., Oda K., Sakamura S., *Agric. Biol. Chem.*, **52**, 211—216 (1988).
- 17) Shiao M. S., Lin L. J., Yeh S. F., *Phytochemistry*, **27**, 873—875 (1988).
- 18) Shiao M. S., Lin L. J., Yeh S. F., Chou C. S., *J. Nat. Prod.*, **50**, 886—890 (1987).
- 19) Shiao M. S., Lin L. J., Yeh S. F., *Phytochemistry*, **27**, 2911—2914 (1988).
- 20) Lin L. J., Shiao M. S., Yeh S. F., *Phytochemistry*, **27**, 2269—2271 (1988).
- 21) Nishitoba T., Sato H., Sakamura S., *Agric. Biol. Chem.*, **49**, 3637—3638 (1985).
- 22) Lin L. J., Shiao M. S., Yeh S. F., *J. Nat. Prod.*, **51**, 918—924 (1988).
- 23) Chen R. Y., Yu D. Q., *Yaoxue Xuebao*, **26**, 267—273 (1991).
- 24) Hirofani M., Ino C., Furuya T., *Phytochemistry*, **33**, 379—382 (1993).
- 25) Toth J. O., Luu B., Ourisson G., *Tetrahedron Letters*, **24**, 1081—1084 (1983).
- 26) Kohda H., Tokumoto W., Sakamoto K., Fujii M., Hirai Y., Yamasaki K., Komoda Y., Nakamura H., Ishihara S., Uchida M., *Chem. Pharm. Bull.*, **33**, 1367—1374 (1985).
- 27) Morigiwa A., Kitabatake K., Fujimoto Y., Ikekawa N., *Chem. Pharm. Bull.*, **34**, 3025—3028 (1986).
- 28) Kim D. H., Shim S. B., Kim N. J., Jang I. S., *Biol. Pharm. Bull.*, **22**, 162—164 (1999).
- 29) Lee S., Park S., Oh J. W., Yang C., *Planta Medica*, **64**, 303—308 (1998).
- 30) El-Mekkawy S., Meselhy M. R., Nakamura N., Tezuka Y., Hattori M., Kakiuchi N., Shimotohno K., Kawahata T., Otake T., *Phytochemistry*, **49**, 1651—1657 (1998).
- 31) Min B. S., Nakamura N., Miyashiro H., Bae K. H., Hattori M., *Chem. Pharm. Bull.*, **46**, 1607—1612 (1998).
- 32) Fraser R. R., *Can. J. Chem.*, **38**, 549—553 (1960).
- 33) Toth J. O., Luu B., Beck J. P., Ourisson G., *J. Chem. Research (M)*, 2722 (1983).
- 34) Ohtani I., Kusumi T., Kashman H., Kakisawa H., *J. Am. Chem. Soc.*, **113**, 4092—4096 (1991).
- 35) Nishitoba T., Oda K., Sato H., Sakamura S., *Agric. Biol. Chem.*, **52**, 367—372 (1988).
- 36) Geran R. I., Greenberg N. H., McDonald M. H., Schumacher A. M., Abbott B. J., *Cancer Chemother. Rep.*, **3**, 1—103 (1972).
- 37) Skehan P., Storeng R., Scudiero D., Monks A., McMahon J., Vistica D., Warren J. T., Bokesch H., Kenney S., Boyd M. R., *J. Natl. Cancer Inst.*, **82**, 1107—1112 (1990).
- 38) Min B. S., Ahn B. Z., Bae K. H., *Arch. Pharm. Res.*, **19**, 543—550 (1996).

In Vivo Evaluation of Carborane Gadolinium–DTPA Complex as an MR Imaging Boron Carrier

Hiroyuki NAKAMURA,^a Hiroshi FUKUDA,^{*,b} Frank GIRALD,^c Tooru KOBAYASHI,^d Jun'ichi HIRATSUKA,^e Takashi AKAIZAWA,^b Hisao NEMOTO,^a Jianping CAI,^a Katsuya YOSHIDA,^c and Yoshinori YAMAMOTO^{*,a}

Department of Chemistry, Graduate School of Science, Tohoku University,^a Sendai, Department of Nuclear Medicine and Radiology, Institute of Development, Aging and Cancer (IDAC), Tohoku University,^b Sendai, Division of Advanced Technology for Medical Imaging, Institute of Radiological Sciences,^c Chiba, Research Reactor Institute, Kyoto University,^d Osaka, and Department of Radiology, Kawasaki Medical School,^e Kurashiki, Japan.

Received January 31, 2000; accepted March 9, 2000

The evaluation of the Gd-carborane complex 2 as an MR imaging and boron carrier agent was carried out *in vivo* using tumor-bearing Donryu rats, MRI, ICP-AES, and α -autoradiography. The MR imaging revealed that the carborane Gd–DTPA 2 was metabolized slower in the body than Gd–DTPA 1. The results of the ICP-AES method indicated that compound 2 was incorporated into normal tissues and metabolized quickly, whereas it was not accumulated into tumor or brain tissue. The α -autoradiography showed that a high level of boron was obtained in the internal organs and in the necrosis of tumor tissue.

Key words neutron capture therapy; MR imaging; DTPA; carborane; gadolinium

Since neutron capture therapy (NCT)^{1–5)} for brain tumor and malignant melanoma was clinically achieved by Hatanaka and his colleagues^{6,7)} and Mishima *et al.*,⁸⁾ much attention has been paid to the synthesis of boron carriers which would selectively accumulate in a tumor. It has been difficult to estimate the boron content of the tumor, however, using available technologies. In order to improve and optimize efficient NCT treatment, it is necessary to follow the distribution of a carrier in the body in real time. For this purpose, positron emission tomography (PET) using fluorine-18-labeled fluoroboronophenylalanine (¹⁸F-BPA) has recently been evaluated in humans.^{9–14)}

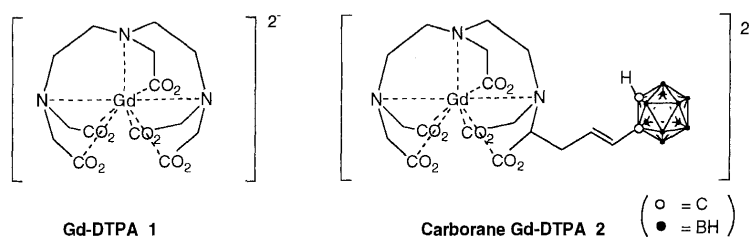
Magnetic resonance imaging (MRI) can also be used to follow the kinetics of the boron compounds.^{15–20)} It is indeed a noninvasive tool, and contrast can be modified by the injection of extrinsic contrast agents. Although boron-11 MRI has been studied for this purpose,^{15–18)} the actual nucleus for neutron capture reaction is boron-10, and therefore the administration of extra amounts of boron-11 compound (which does not undergo the nucleic reaction) is needed for MR imaging. A gadolinium–DTPA complex 1, which is commercially available under the trade name of “Magnevist” and is used as an MR imaging contrast medium, is paramagnetic; therefore, its effect on the contrast of the images can best be seen on T₁-weighted images with short repetition times. The effect is caused by the gadolinium ion in the center, which induces an enhancement of T₁ relaxation. It has been observed that the blood-brain barrier of a brain tumor is disrupted, and that the complex 1 can pass through this disrupted barrier and enter into the tumor tissue.^{21–25)} Furthermore, gadolinium-

ium-157 has a higher thermal neutron capture cross section (255000 b) in comparison with that of boron-10 (3838 b). It occurred to us that a combination of gadolinium-157 and boron-10 might prove effective not only as an MR imaging but also as a neutron capture therapy.²⁶⁾ We have recently succeeded in the synthesis of the gadolinium–DTPA complex 2 which contains a carborane unit attached *via* a palladium catalyzed C–C bond formation reaction.^{27,28)} Herein we report *in vivo* evaluation of the complex 2 in tumor-bearing rats using MRI, ICP, and α -autoradiographic methods.

Results

MR Imaging of Rat Tumor with Gd–Carborane Complex 2 Figure 1a shows the sagittal T₁-weighted MR image of a rat with a tumor implanted on its back before injection of any compounds, and Figs. 1b–d show the images at 4 min 23 s (b), 11 min 32 s (c), and 50 min 54 s (d) after injection of compound 2. The signal intensity of kidney, liver, bladder, heart, and tumor on the images is calculated by Philips software and the intensity of the images versus time is plotted in Figs. 2a and 2b. The signal intensity is plotted as the ordinate and the time after injection is plotted on the horizontal axis. Although the dynamic change of the intensity in each tissue can be seen from these images, comparison of the intensity among the tissues is not possible since the signal intensity strongly depends on the distance between the tissue and the surface coil.

A contrast enhancement was observed in the center of the tissue, which is indicated by the circle in Figs. 1c and 1d. The signal intensity of tumor tissues also increased rapidly



* To whom correspondence should be addressed. e-mail: yoshi@yamamoto1.chem.tohoku.ac.jp

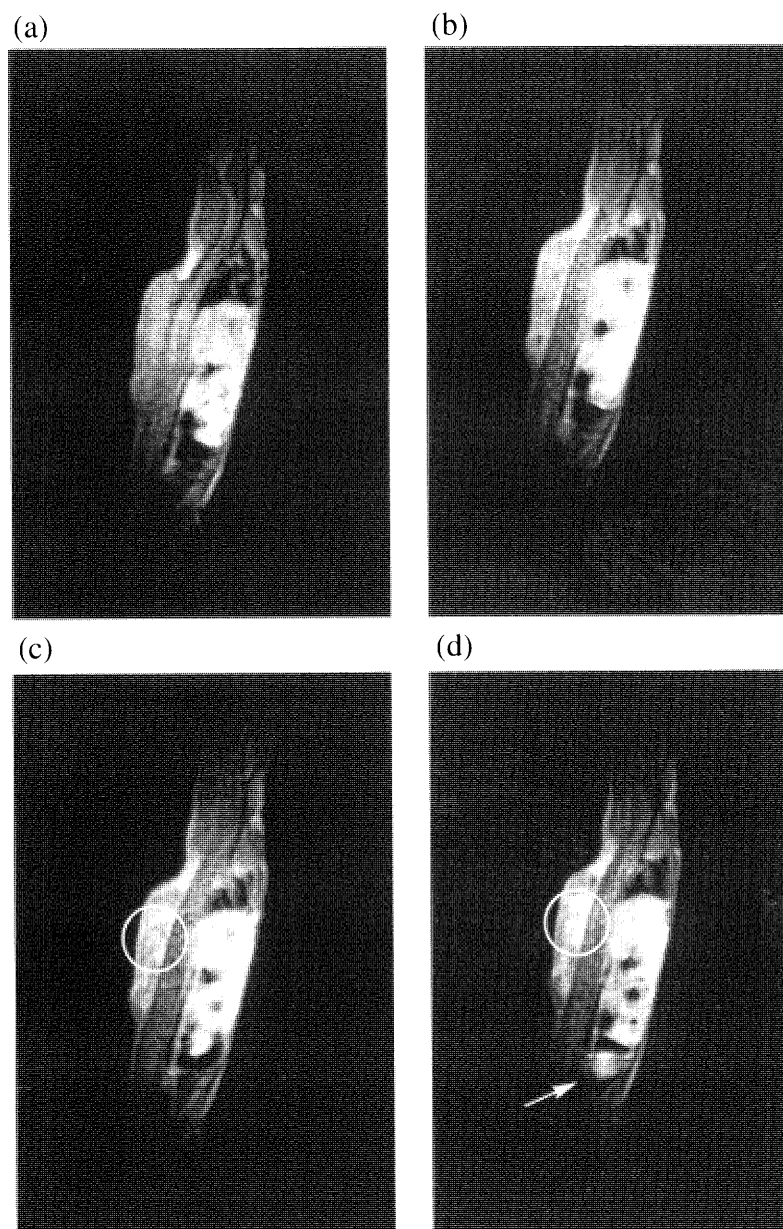


Fig. 1. Sagittal T_1 -Weighted MR Imaging of a Rat Bearing AH109A Tumor on the Back: (a) before Injection of Compound **2**, (b) at 4 min 23 s, (c) at 11 min 32 s, (d) at 50 min 54 s, after Injection of Compound **2**

Circles indicate the necrotic inner part of tumor tissues in which compound **2** is distributed. Arrow indicates the bladder containing compound **2** in the urea.

after injection of compound **2** and then decreased slowly (Fig. 2b). The signal intensity of kidney rapidly increased after injection of the compound and remained constant throughout the experimental period, whereas that of liver, heart, and tumor rapidly increased after injection and then slowly decreased (Fig. 2). Further, the contrast enhancement was also observed in the bladder at 50 min after injection, which is indicated by the arrow in Fig. 1d. The signal intensity of the bladder increased at 45 min after injection (Fig. 2a). On the other hand, the signal intensity of all tissues increased rapidly after injection of normal Gd-DTPA **1** and decreased rapidly after 10 min (Fig. 3). The signal intensity of bladder also increased rapidly after injection.

Gadolinium Concentrations in Various Tissues of Rats with Gd-Carborane Complex **2** Using ICP-AES Method

The distribution of gadolinium in the body of rats is shown in Fig. 4. The concentration of gadolinium (ppm) in 100 mg of

tissue is plotted as the ordinate and the time after injection is plotted on the horizontal axis. The gadolinium concentration in blood was 9.1 ppm at 5 min after injection and then decreased very rapidly. The concentrations in kidney and liver increased after injection, reached a maximum value at 20 min and then decreased. However, the concentration of gadolinium in tumor and brain was very low.

Boron Distribution in the Body of Tumor-Bearing Rats Visualized by α -Autoradiography The α -autoradiography of the rats bearing tumor is shown in Fig. 5. The boron was mainly distributed in the blood pool and the concentration was relatively high in heart, lung, and kidney at 15 min after injection (Fig. 5a). However, the concentration of boron in the blood decreased whereas it was still high in the intestines and kidney at 60 min after injection (Fig. 5b). Although the boron concentration in the tumor was relatively low at 15 min, higher accumulation of boron was visualized in the

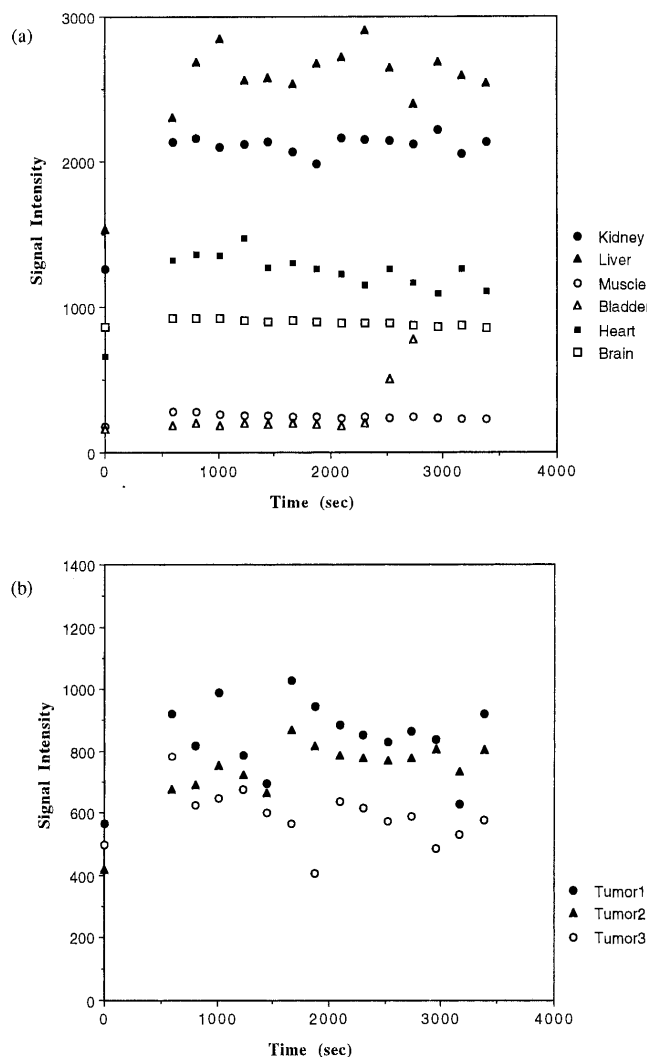


Fig. 2. Dynamic Curves of Signal Intensities for Various Parts of a Rat after Injection of Compound 2: (a) Normal Tissues, (b) Different Parts of the Tumor

Tumors 1 and 2 show different inner parts of the tumor and Tumor 3 shows the outer part of the tumor. The values for the signal intensity are relative and not comparable to those in Fig. 3.

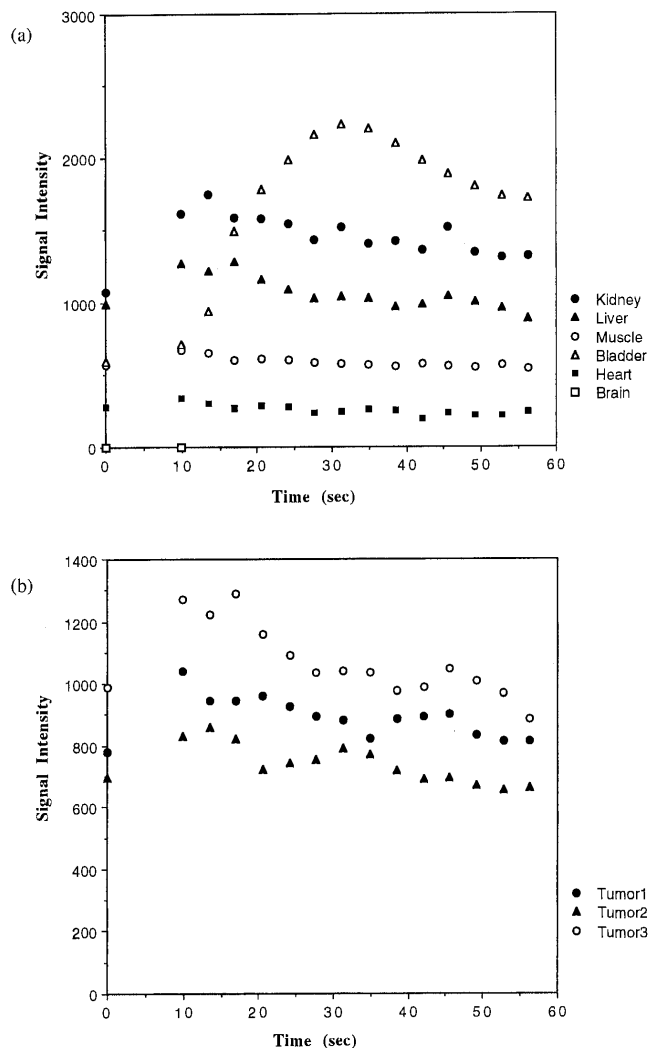


Fig. 3. Dynamic Curves of Signal Intensities for Various Parts of a Rat after Injection of Gd-DTPA 1: (a) Normal Tissues, (b) Different Parts of the Tumor

Tumors 1 and 2 show different inner parts of the tumor and Tumor 3 shows the outer part of the tumor. The values for the signal intensity are relative and not comparable to those in Fig. 2.

center of the tumor tissue and in the intestines at 60 min.

Discussion

It is important to learn whether gadolinium complex is stable in the body or if gadolinium is dissociated from the boronated DTPA scaffold. We tried to determine the boron concentrations in various tissues of rats. However, it was difficult to measure them by ICP-AES since unidentified strong signals and the boron signals overlapped each other, which made it difficult to observe precise and correct boron concentration. Nevertheless, even under these difficult conditions, we determined the boron concentrations in the brain tissue as 17 ppm at 20 min and 12 ppm at 60 min. The gadolinium concentration, however, was too low to be detected. There are two possible explanations for this strange observation. First, gadolinium was dissociated from the boronated DTPA scaffold in the body and only boron was incorporated in the tissue. Second, the values of boron concentration were wrong and perhaps no boron was present in the tissue. The experiment using α -autoradiography clearly indicates that the second possibility is correct and that boron is not accumulated

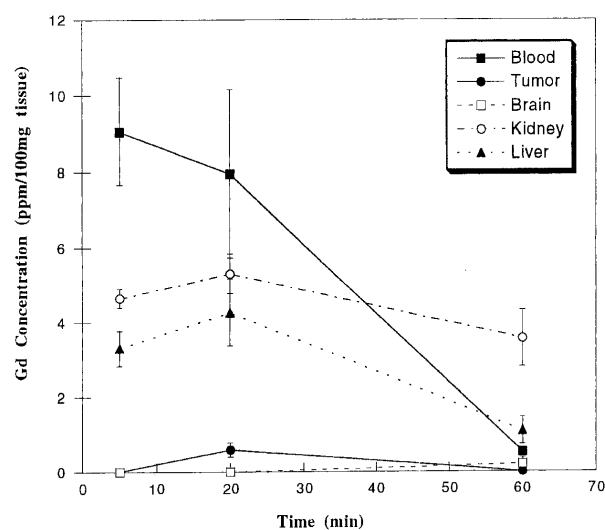


Fig. 4. The Distribution of Gadolinium Incorporated into Various Tissues of Rats after Injection of Compound 2

The concentration of gadolinium was determined by ICP-AES. Each point represents the mean \pm S.E. of triplicate experiments.

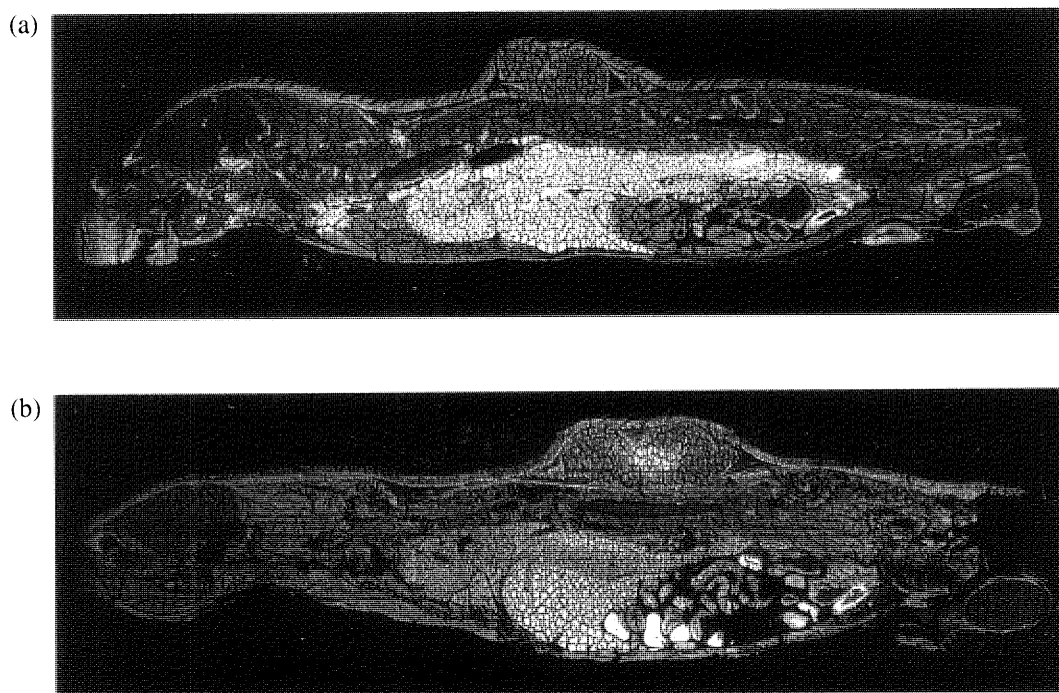


Fig. 5. α -Autoradiography of a Rat Bearing AH109A Tumor on the Back, (a) at 15 min, (b) at 60 min, after Injection of Compound 2

in the brain portion (see Fig. 5). The data of the boron concentration obtained from the ICP-AES experiment are therefore not reliable, and only the gadolinium concentration determined by this experiment is discussed in this paper.

The visible contrast enhancement effected by compound 2 was obtained from the MR imaging experiment. Compound 2 is distributed in the necrotic inner part of tumor tissue (Figs. 1c–d and 2b). The same tendency is observed in Fig. 5, although low uptake into the tumor tissue is observed in Fig. 4. These different observations reflect which part of the tissue is measured. Actually, the outer part (not the necrotic part) of tumor tissue was removed and used for the ICP-AES experiment; thus, low gadolinium concentration is obtained in tumor tissue in Fig. 4. The outside of the necrotic part of tumor is not visualized by the α -autoradiography in Fig. 5, which supports the results obtained from the ICP-AES experiment. The tumor/blood ratio of the compound is very low (0.075 at 20 min after injection in Fig. 4) and the higher ratio is required for boron carriers (for example, the tumor/blood ratio of BSH, which is clinically utilized for brain tumor, is *ca.* 1).⁷⁾ Compound 2 is also incorporated into kidney and liver and excreted gradually (Figs. 2 and 4), whereas Gd-DTPA 1 is excreted rapidly from the body (Fig. 3). The lipophilic functional group, carborane, attached to the molecule is believed to make the gadolinium–DTPA complex remain longer in the tissues. The intestines are visualized at 60 min in Fig. 5, which indicates that compound 2 is also metabolized via the liver and excreted in the bile.

Conclusion

Carborane containing Gd–DTPA 2 has been synthesized as a dual labeled probe for MR imaging and neutron capture therapy. It is clear from the MRI experiment that compound 2 is effective for contrast enhancement and remains in the body for a long period of time in comparison with ordinary Gd–DTPA 1. Although no selective accumulation in the

tumor tissue was observed in these experiments, the present findings provide the promising result that the distribution of the boron carrier in the body can be followed in real time using MRI. We are now at the second stage to synthesize the compounds that can be accumulated into tumor as well as visualized by MRI for reliable estimation in the body.

Experimental

MR Imaging of Rat Tumor with Gd–Carborane Complex 2 The experiments were performed with four male tumor-bearing Donryu rats. Their age ranged from 4 to 6 weeks and their weights from 130 to 150 g. The tumors (AH109A—ascitic hepatoma) were implanted previously on the back, and allowed to grow for 2 weeks. This tumor line was established in the Institute of Development, Aging and Cancer, Tohoku University, and serially transplanted into these rats in ascitic form. Before each examination, the animals were anaesthetized with an intraperitoneal injection of 10 ml/kg of a 4% chloral hydrate solution. The MRI system of Gyroscan S 15 (Philips) with an 8 cm surface coil was used for this experiment. The scan parameters are as follows: spin echo sequence with TR time of 500 ms, TE time of 20 ms, 15 dynamic scan with a scan duration of 214 s, slice thickness of 3–5 mm.

Compound 2 (55 mg) was dissolved in NaHCO₃ aqueous solution (2: 0.05 M, NaHCO₃: 0.13 M). The solution (0.3 ml) was injected intravenously through a catheter previously implemented in the jugular vein, at a dose of 0.1 mmol/kg body weight, and sagittal T₁-weighted images were acquired following the protocol. A standard surface coil 8 cm in diameter was used for the images. To follow the excretion of compound 2, sagittal multisection T₁-weighted images were obtained. A dynamic study was performed with 15 dynamic scans. The first scan was recorded manually, and then 14 scans were carried out during 53 min 45 s (214 s/each scan) after the injection of the compound. For the sake of comparison, normal Gd–DTPA 1 (Magnevist) was given to two rats at the same dose.

Gadolinium Concentrations in Various Tissues of Rats with Gd–Carborane Complex 2 Using ICP-AES Method The distribution of the compound *in vivo* was examined using ICP-AES. This method is very useful to obtain the concentration of elements in tissues. The rats bearing tumor used in this experiment were the same as those used in MRI experiments. Compound 2 (227 mg) was dissolved in 10 ml of NaHCO₃ aqueous solution (finally, 2: 0.03 M, NaHCO₃: 0.07 M). The pH value of this solution was 7.7. The solution (0.5 ml) was injected intravenously through the lateral tail vein at a dose of 0.1 mmol/kg body weight. Rats weighing 130–150 g (total number of rats was 9) were used for this experiment. To determine the con-

centrations of gadolinium in the tissues, the rats were killed and blood, kidney, tumor, brain, and liver were removed at 5, 20, and 60 min after injection of the compound and dissolved in $\text{H}_2\text{O}_2\text{-HClO}_4$ (2/1) solution at 70 °C for 3 h. The solution was filtered with a membrane filter (Millipore 0.22 $\mu\text{m}\phi$) and then the gadolinium concentration in the solution obtained was determined by ICP-AES.

Boron Distribution in the Body of Tumor-Bearing Rats Visualized by α -Autoradiography The experiments were performed with two tumor-bearing Donryu rats. The tumors (AH109A—ascitic hepatoma) were implanted previously on the back, and allowed to grow for 2 weeks. Compound **2** (0.1 mmol/kg body weight) was injected intravenously through the lateral tail vein. The rats were killed at 15 and 60 min after injection and frozen in a dry-ice acetone bath (−80 °C). The frozen rats were coated with 4% of CMC (carboxymethyl cellulose) to make a block and frozen again at −80 °C. Blocks were sliced in 40 μm thicknesses, and the slices obtained were dried at −80 °C for two weeks and then placed in contact with the etching films (Baryotrack). The films were irradiated with a thermal neutron of the Kyoto University Reactor (a power of 5 MW, Cd ratio of 5000) with a total fluence of $1.6\text{--}1.9 \times 10^{13}$ n/cm² and etched with KOH (30%) at 70 °C for 3 h.

Acknowledgment Part of this work was supported by a Grant-in-Aid for Scientific Research (No. 09470196) from the Ministry of Education, Science, Culture and Sports, Japan.

References

- 1) Locher G. L., *Am. J. Roentgenol.*, **36**, 1 (1936).
- 2) Yamamoto Y., *Pure. Appl. Chem.*, **63**, 423—426 (1991).
- 3) Hawthorne M. F., *Angew. Chem., Int. Ed. Engl.*, **32**, 950—984 (1993).
- 4) Barth R. F., Soloway A. H., Fairchild R. G., *Cancer Res.*, **50**, 1061—1070 (1990).
- 5) Soloway A. H., Tjarks W., Barnum B. A., Rong F.-G., Barth R. F., Codogni I. M., Wilson J. G., *Chem. Rev.*, **98**, 1515—1562 (1998).
- 6) Soloway A. H., Hatanaka H., Davis M. A., *J. Med. Chem.*, **10**, 714—717 (1967).
- 7) Hatanaka H., Nakagawa Y., *Int. J. Radiation Oncology Biol. Phys.*, **28**, 1061—1066 (1994), and references cited therein.
- 8) Mishima Y., Ichihashi M., Hatta S., Honda C., Yamamura K., Nakagawa T., *Pigm. Cell*, **2**, 226—234 (1989).
- 9) Ishiwata K., Ido T., Kawamura M., Kubota K., Ichihashi M., Mishima Y., *Nucl. Med. Biol.*, **18**, 745—751 (1991).
- 10) Ishiwata K., Ido T., Honda C., Kawamura M., Ichihashi M., Mishima Y., *Nucl. Med. Biol.*, **19**, 311—318 (1992).
- 11) Ishiwata K., Shiono M., Kubota K., Yoshino K., Hatazawa J., Ido T., Honda C., Ichihashi M., Mishima Y., *Melanoma Res.*, **2**, 171—174 (1992).
- 12) Reddy N. K., Kabalka G. W., Longford C. P. D., Roberts J., Gotsick T., *J. Lab. Comp. Radiopharm.*, **37**, 599—600 (1995).
- 13) Kabalka G. W., Smith G. T., Reid W. S., Longford C. P. D., Roberts J., Reddy N. K., Buonocore E., Hubner K. F., *J. Nucl. Med.*, **38**, 1762—1767 (1997).
- 14) Imahori Y., Ueda S., Ohmori Y., Kusuki T., One K., Fujii R., Ido T., *J. Nucl. Med.*, **39**, 325—333 (1998).
- 15) Kabalka G. W., Davis M., Bendel P., *Magn. Reson. Med.*, **8**, 231—237 (1988).
- 16) Kabalka G. W., Tang C., Bendel P., *Neuro-Oncol.*, **33**, 153—161 (1997).
- 17) Bendel P., Zilberstein J., Salomon Y., *Magn. Reson. Med.*, **32**, 170—174 (1994).
- 18) Bradshaw K. M., Schweizer M. P., Glover G. H., Hadley J. R., Tippetts R., Tang P.-P., Davis W. L., Heilbrun M. P., Johnson S., Ghanem T., *Magn. Reson. Med.*, **34**, 48—56 (1995).
- 19) Huang L. R., Straubinger R. M., Kahl S. B., Koo M. S., Alletto J. J., Mazurchuk R., Chau R. I., Thamer S. L., Fiel R. J., *J. Magn. Res. Imaging*, **3**, 351—356 (1993).
- 20) Weinmann H. J., Brasch R. C., Press W. R., Wesbey G. E., *ARJ*, **142**, 619—624 (1984).
- 21) Runge V. M., Clanton J. A., Price A. C., Wehr C. J., Herzer W. A., Partain C. L., James A. E., Jr., *J. Magn. Res. Imaging*, **3**, 43—56 (1985).
- 22) Runge V. M., Clanton J. A., Price A. C., Herzer W. A., Allen J. H., Partain C. L., James A. E., Jr., *Am. J. Neuroradiology*, **6**, 139—147 (1985).
- 23) Stack J. P., Antoun N. M., Jenkins J. P. R., Metcalfe R., Isherwood I., *Neuroradiology*, **30**, 145—154 (1988).
- 24) Makita S., Nishimura T., Naito H., Yamada N., Yamamoto K., Takamiya M., Yamada Y., Sakashita Y., Minamikawa J., *Neuroradiology*, **29**, 422—429 (1987).
- 25) Runge V. M., Jacobson S., Wood M. L., Kaufman D., Adelman L. S., *Radiology*, **166**, 835—838 (1988).
- 26) Shih J. L., Brugger R. M., *Med. Phys.*, **19**, 733—744 (1992).
- 27) Nemoto H., Cai J., Yamamoto Y., *Tetrahedron Lett.*, **37**, 539—542 (1996).
- 28) Nemoto H., Cai J., Nakamura H., Fujiwara M., Yamamoto Y., *J. Organomet. Chem.*, **581**, 170—175 (1999).

Medicinal Foodstuffs. XVIII.¹⁾ Phytoestrogens from the Aerial Part of *Petroselinum crispum* MILL. (PARSLEY) and Structures of 6''-Acetylapiin and a New Monoterpene Glycoside, Petroside

Masayuki YOSHIKAWA,^{*,a} Toshiaki UEMURA,^a Hiroshi SHIMODA,^a Akinobu KISHI,^a Yuzo KAWAHARA,^b and Hisashi MATSUDA^a

Kyoto Pharmaceutical University,^a Misasagi, Yamashina-ku, Kyoto 607–8414, Japan and Research and Development Division, Morishita Jintan Co., Ltd.,^b 1–1–30 Tamatsukuri, Chuo-ku, Osaka 540–8566, Japan.

Received January 31, 2000; accepted March 28, 2000

In the course of our screening for natural estrogenic compounds from Occidental medicinal herbs, the extracts of several herbs were found to show proliferative activity in MCF-7 (an estrogen-sensitive breast cancer cell line). Among these active herbs, the methanolic extract from the aerial parts of *Petroselinum crispum* (parsley) showed potent estrogenic activity, which was equal to that of isoflavone glycosides from soybean. Through bioassay-guided separation, we isolated several flavone glycosides and a new flavone glycoside, 6''-acetylapiin, with estrogenic activity together with a new monoterpene glucoside, petroside. The structures of 6''-acetylapiin and petroside were characterized by the chemical and physicochemical evidence. Estrogenic activities of these flavone glycosides were found to be enhanced by removal of their glycoside moieties. The EC₅₀ values (concentration needed to enhance the MCF-7 proliferation 50% compared to non-estrogen treated cell) of their aglycones are as follows, apigenin (1.0 μ M), diosmetin (2.9 μ M), and kaempferol (0.56 μ M). The estrogenic activities of these flavones are nearly equal to those of the isoflavones, daidzein (0.61 μ M) and genistein (0.60 μ M). The methanolic extract of parsley, apiin, and apigenin restored the uterus weight in ovariectomized mice when orally administered for consecutive 7 days.

Key words phytoestrogen; *Petroselinum crispum*; 6''-acetylapiin; petroside; flavone glycoside; breast cancer cell line

Insufficiency of internal estrogen (estrone, estradiol) secretion is known to cause several physical disorders shown in postmenopausal women, such as osteoporosis, blood cholesterol elevation, and symptoms of menopause (hot flashes and depression). Synthetic estrogen (ethynyl estradiol, 17 β -estradiol) replacement therapy was reported to have a curative effect on these conditions. Recently, the estrogenic activity of isoflavones, lignans, and coumarins, which are widely distributed in vegetables, fruits, and medicinal plants, has been investigated; these compounds are generically called phytoestrogens.²⁾ Isoflavones, representative phytoestrogens, were shown to prevention of bone loss³⁾ and arteriosclerosis,⁴⁾ and to have cardioprotective⁵⁾ and anticarcinogenic⁶⁾ activities.

In a search for new phytoestrogens effective in preventing postmenopausal diseases, the estrogenic activities of many Occidental medicinal herbs were examined using the proliferation activity of MCF-7 (an estrogen sensitive cell line).⁷⁾ The methanolic extract from several of these herbs was found to possess estrogenic activity in the range of 1 to 10 μ g/ml (Table 1). Particularly, the extracts of the aerial part of *Petroselinum crispum* MILL. (parsley, cultivated in U.S.A. and Japan) showed reproducible estrogenic activity comparable to that of the isoflavone glucoside fraction⁸⁾ from soybean. Through bioassay-guided separation, we isolated two benzoxoles, myristicin (**3**)⁹⁾ and apiole (**4**)⁹⁾ two furocoumarins, cnidilin (**5**)¹⁰⁾ and isoimperatorin (**6**)¹⁰⁾ and four flavone glycosides, apigetrin (**7**)¹¹⁾ apiin (**8**)¹²⁾ diosmetin 7-*O*- β -D-glucopyranoside (**9**)¹³⁾ and kaempferol 3-*O*- β -D-glucopyranoside (**10**)¹⁴⁾ together with a new glycoside, 6''-acetylapiin (**1**), from American dried parsley. A new monoterpene glucoside called petroside (**2**) was isolated from Japanese fresh parsley together with **8** and icariside F₂ (**11**). This paper deals with the isolation of phytoestrogens from American

and Japanese parsley and the structure elucidation of the two new glycosides, **1** and **2**.

Estrogenic Activities of Medicinal Herbs We tested the estrogenic activities of various medicinal herbs originating in European and South Asian countries. Table 1 shows the MCF-7 proliferative activities of the methanolic extract (at 1.0 and 10 μ g/ml) from twelve Occidental herbs. The extracts of agrimony, raspberry, dill, vervain, and parsley exhibited estrogenic activities at 1.0 μ g/ml. Among them, the extract from parsley showed reproducible and potent estrogenic activity equal to that of the isoflavone glycoside fraction of soybean.⁸⁾

Bioassay-Guided Separation of the Constituents from Parsley The methanolic extract from American dried parsley was separated into ethyl acetate- and water-soluble fractions which showed estrogenic activity (Table 2). An ethyl acetate-soluble extract was separated into five fractions by silica gel column chromatography. Fractions 1, 2, 4, and 5 with the activity were further subjected to SiO₂ and reversed phase column chromatography, and finally HPLC. Two benzoxoles, myristicin (**3**, 0.0051%) and apiole (**4**, 0.0016%), were isolated from fraction 1, and two furocoumarins, cnidilin (**5**, 0.0010%) and isoimperatorin (**6**, 0.0021%), were obtained from fraction 2. Known flavone glycosides, apigetrin (**7**, 0.0037%), apiin (**8**, 0.0063%), diosmetin 7-*O*- β -D-glucopyranoside (**9**, 0.0013%), and kaempferol 3-*O*- β -D-glucopyranoside (**10**, 0.0024%) and a new flavone glycoside, 6''-acetylapiin (**1**, 0.0075%) was isolated from fraction 4 and 5. From the water-soluble extract, **8** (1.5%) was also isolated using similar separation procedures. Furthermore, we isolated a new monoterpene glucoside, petroside (**2**, 0.0004%), from the methanolic extract of Japanese fresh parsley, which also showed potent estrogenic activity, together with **8**

* To whom correspondence should be addressed. e-mail: shoyaku@mb.kyoto-phu.ac.jp

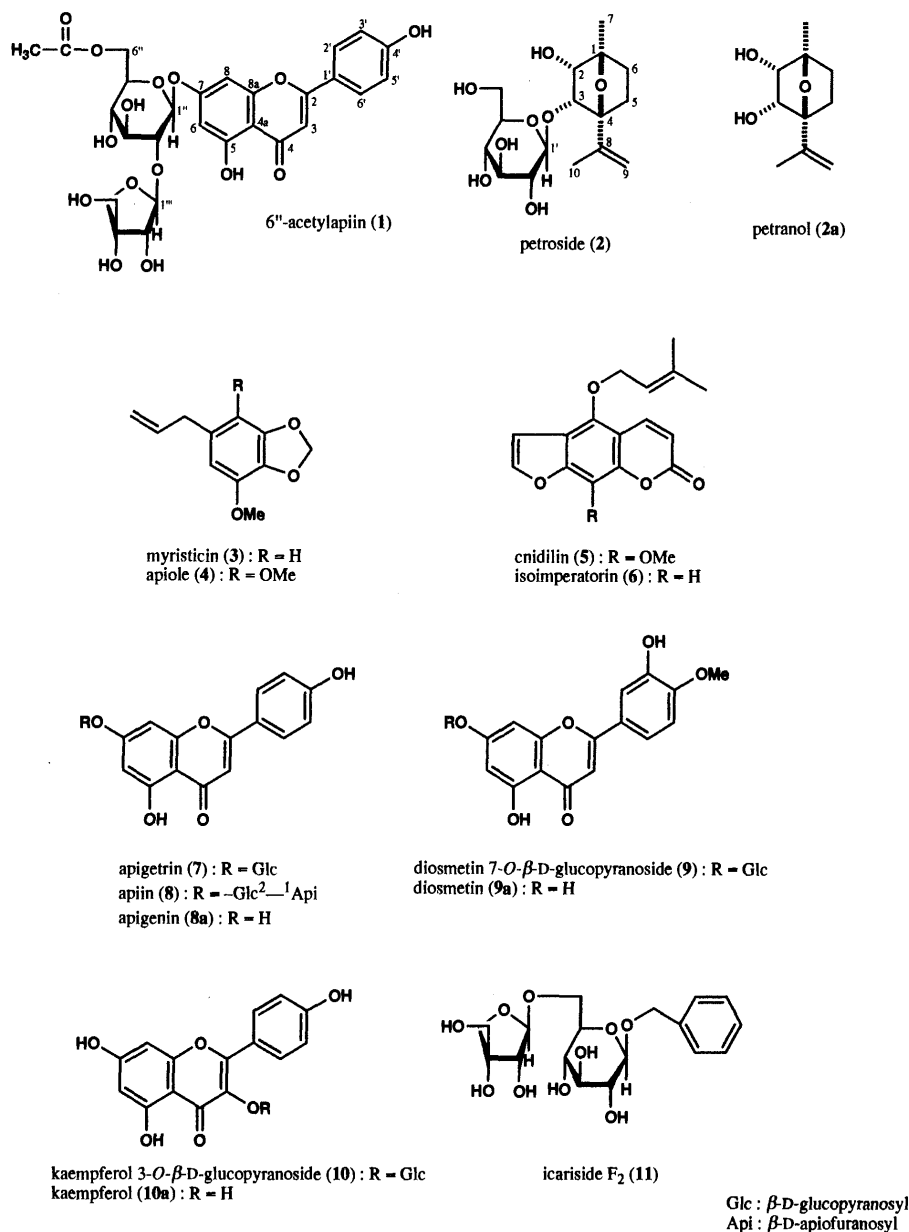


Chart 1. Chemical Constituents Isolated from Parsley

(0.0011%) and icaride F₂ (11, 0.0019%).

Estrogenic Activities of the Constituents from Parsley

Table 3 shows estrogenic activities of constituents from parsley and their derivatives. Benzooxoles (3, 4) and kaempferol 3-O-β-D-glucopyranoside (10) had no activity, and flavone glycosides such as 6''-acetylapiin (1), apiin (8), and diosmetin 7-O-β-D-glucoside (9) showed weak activity at 10 μM but it was not significant. Only apigetrin (7) revealed a potent activity (EC₅₀: 2.2 μM). Apigenin (8a), diosmetin (9a), and kaempferol (10a), the aglycones of 7, 8, 9, and 10, showed significant activities at 1.0 and 10 μM. The ED₅₀ of 8a and 10a were 1.0 and 0.56 μM, respectively, which were nearly equal to those of the isoflavones, daidzein⁸⁾ (0.61 μM) and genistein⁸⁾ (0.69 μM).

Increase by the Methanolic Extracts, Apiin (8), and Apigenin (8a) on Uterus Weight in Ovariectomized Mice

Fig. 1 shows the restoration effects of the methanolic extracts, apiin (8), and apigenin (8a) on uterus weight gain in ovariectomized mice. The mean uterus weight of ovariectomized mice was decreased to 18.6 and 24.2% of sham operated

groups. Consecutive treatment (7 days) of the methanolic extract tended to increase the uterus weight up to 17.5 and 27.0% at a dose of 1000 and 2000 mg/kg, respectively. Apiin (8), a principal flavone glycoside, and apigenin (8a), an aglycone of 8, also restored uterus weight up to 17.4 to 22.4%, and 15.0 to 17.5%, respectively, at a dose of 250 and 500 mg/kg. Although those effects were not significant but weak, all samples showed the activity was dose-dependent.

Structures of 6''-Acetylapiin (1) and Petroside (2) 6''-Acetylapiin (1) was obtained as a white powder and its IR spectrum showed absorption bands at 1735, 1661, and 1607 cm⁻¹ ascribable to carbonyl, chelated carbonyl, and aromatic ring functions, and strong absorption bands at 3415 and 1078 cm⁻¹ suggestive of its oligoglycosidic structure. The UV spectrum of 1 showed absorption maxima (log ε) at 334 (4.1) and 269 (4.0) nm, which suggested the flavone structure. The negative- and positive-ion FAB-MS of 1 showed quasimolecular ions at *m/z* 605 (M-H)⁻ and *m/z* 607 (M+H)⁺, respectively, and high-resolution MS analysis revealed the molecular formula of 1 to be C₃₄H₃₀O₁₅. Fur-

Table 1. Proliferative Activities of Methanolic Extracts from Occidental Herbs on MCF-7

Source	Conc. ($\mu\text{g/ml}$)	Proliferation (% of control)
Rosemary, leaf (<i>Rosmarinus officinalis</i>)	1	103.0 \pm 3.2
	10	122.5 \pm 5.3*
Agrimony, aerial part (<i>Agrimonia eupatoria</i>)	1	117.0 \pm 2.5**
	10	158.3 \pm 2.8**
Raspberry, leaf (<i>Rubus idaeus</i>)	1	163.3 \pm 3.2**
	10	177.7 \pm 4.2**
Lemon verbena, leaf (<i>Aloysia triphylla</i>)	1	102.1 \pm 3.5
	10	125.5 \pm 3.3**
Pennyroyal, leaf (<i>Mentha pulegium</i>)	1	99.1 \pm 2.9
	10	130.4 \pm 6.0**
Dill, seed (<i>Anethum graveolens</i>)	1	128.4 \pm 4.1**
	10	146.8 \pm 2.3**
Fennel, fruit (<i>Foeniculum vulgare</i>)	1	108.3 \pm 3.6
	10	126.5 \pm 2.5**
Alfalfa, aerial part (<i>Medicago sativa</i>)	1	110.7 \pm 5.0
	10	139.4 \pm 3.0**
Vervain, leaf (<i>Verbena officinalis</i>)	1	147.1 \pm 5.0**
	10	152.1 \pm 5.0**
Borage, aerial part (<i>Borago officinalis</i>)	1	109.0 \pm 4.6
	10	141.9 \pm 1.5**
Mugwort, aerial part (<i>Artemisa vulgaris</i>)	1	113.0 \pm 4.3
	10	133.0 \pm 7.3**
American Parsley, aerial part (<i>Petroselinum crispum</i>)	1	134.7 \pm 5.1**
	10	156.0 \pm 5.4**
Soybean isoflavone glycoside fraction	1	130.1 \pm 4.9**
	10	157.1 \pm 14.8**

Each value represents mean with the S.E. of 6 experiments. Asterisks denote significant differences from the control *: $p < 0.05$, **: $p < 0.01$, respectively.

Table 2. Proliferative Activities of Extracts and Fractions of Parsley

Sample	Conc. ($\mu\text{g/ml}$)	Proliferation (% of control)
American Parsley		
MeOH extract	1	134.7 \pm 5.1**
	10	156.0 \pm 5.4**
AcOEt-soluble extract	2.5	114.8 \pm 4.5
	5	118.3 \pm 7.3
	10	146.2 \pm 10.2**
H ₂ O-soluble extract	2.5	116.5 \pm 10.2
	5	119.2 \pm 6.4
	10	133.5 \pm 6.6**
Fr. 1	2.5	119.2 \pm 2.8**
	5	125.6 \pm 4.3**
	10	146.1 \pm 4.1**
Fr. 2	2.5	117.8 \pm 3.7*
	5	124.3 \pm 5.4**
	10	145.3 \pm 5.8**
Fr. 3	2.5	115.1 \pm 3.2
	5	121.9 \pm 2.1*
	10	117.0 \pm 8.5
Fr. 4	2.5	120.7 \pm 2.5**
	5	120.8 \pm 3.2**
	10	129.0 \pm 2.6**
Fr. 5	2.5	159.8 \pm 4.9**
	5	159.4 \pm 3.1**
	10	176.0 \pm 4.0**
Japanese Parsley		
MeOH extract	1	145.5 \pm 4.5**
	10	158.7 \pm 2.4**

Each value represents mean with the S.E. of 6 experiments. Asterisks denote significant differences from the control *: $p < 0.05$, **: $p < 0.01$, respectively.

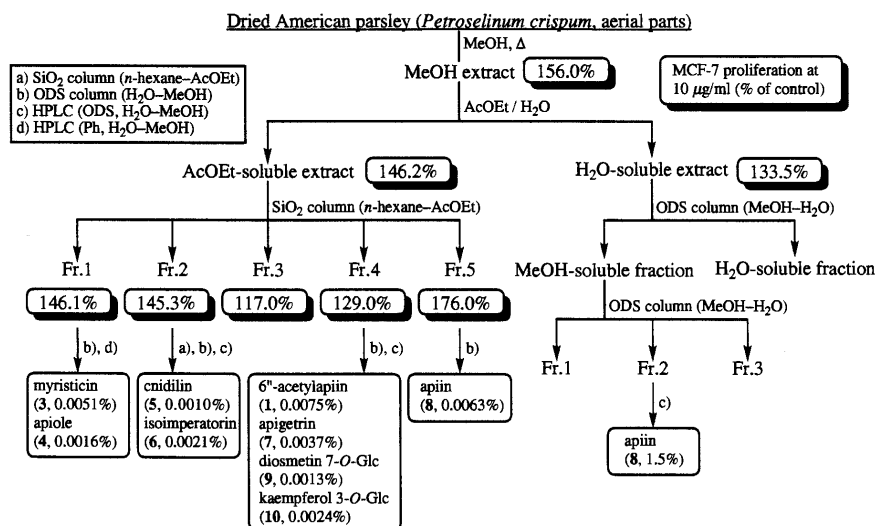


Chart 2

thermore, fragment ion peaks at m/z 473 ($\text{M}-\text{C}_5\text{H}_9\text{O}_4$)⁻ and 269 ($\text{M}-\text{C}_{13}\text{H}_{21}\text{O}_{10}$)⁻, which were derived by cleavage of the glycoside linkage at the 2''- and 7-positions, were observed in the negative-ion FAB-MS of **1**. The proton and carbon signals in the ¹H-NMR (DMSO-*d*₆) and ¹³C-NMR (Table 4) spectra¹⁶ of **1**, were similar to those of apiin (**8**), except for the signals due to an acetyl moiety [δ 2.01 (s)] in **1**. Comparison of the ¹H- and ¹³C-NMR data for **1** with those for **8** revealed an acylation shift around the 6''-position of **1**. In the HMBC experiment on **1**, HMBC correlations were observed between the 1''-proton and the 7-carbon, between the 1'''-pro-

ton and the 2''-carbon, and between the 6''-protons and the acetyl carbonyl carbon. Finally, deacetylation of **1** with sodium methoxide furnished **8** and consequently, the structure of 6''-acetylapiin was determined to be apigenin 7-*O*- β -D-apiofuranosyl(1 \rightarrow 2)-6''-*O*-acetyl- β -D-glucopyranoside (**9**).

Petroside (**2**) was isolated as a white powder. The IR spectrum of **2** showed absorption bands assignable to hydroxyl and *exo*-methylene functions at 3410, 1649, 1452, and 1078 cm⁻¹. The electron impact (EI) MS of **2** showed a molecular ion peak at m/z 346 (M^+) in addition to a fragment ion peak at m/z 183 (100). The molecular formula C₁₆H₂₆O₈ of **2**

was confirmed from the molecular ion peak and by high-resolution MS measurement. Enzymatic hydrolysis of **2** with β -glucosidase liberated a new monoterpene aglycone petranol (**2a**), while acid hydrolysis of **2** with 5% aqueous sulfuric

Table 3. Estrogenic Activities of Constituents Isolated from Parsley

Source	Conc. (μ M)	Proliferation (% of control)	EC ₅₀ (μ M)
6''-Acetylapiin (1)	0.1	103.3 \pm 6.0	—
	1	116.7 \pm 6.5	
	10	119.2 \pm 3.0	
Myristicin (3)	0.1	94.4 \pm 5.8	—
	1	102.4 \pm 5.4	
	10	92.7 \pm 5.4	
Apiole (4)	0.1	89.9 \pm 3.6	—
	1	83.3 \pm 5.0	
	10	92.9 \pm 4.5	
Apigetrin (7)	0.1	102.6 \pm 5.5	2.2
	1	98.7 \pm 11.5	
	10	206.4 \pm 7.0**	
Apiin (8)	0.1	96.8 \pm 8.8	—
	1	106.5 \pm 6.4	
	10	115.1 \pm 17.7	
Apigenin (8a)	0.1	109.3 \pm 3.5	1.0
	1	148.0 \pm 3.6**	
	10	200.1 \pm 6.2**	
Diosmethin 7- <i>O</i> - β -D-glucopyranoside (9)	0.1	100.8 \pm 10.3	—
	1	102.3 \pm 12.4	
	10	112.7 \pm 12.8	
Diosmethin (9a)	0.1	91.4 \pm 5.8	—
	1	127.9 \pm 5.4**	
	10	133.9 \pm 2.3**	
Kaempferol 3- <i>O</i> - β -D-glucopyranoside (10)	0.1	95.9 \pm 3.8	—
	1	89.1 \pm 6.4	
	10	100.7 \pm 3.3	
Kaempferol (10a)	0.1	130.2 \pm 1.8**	0.56
	1	182.3 \pm 4.0**	
	10	199.6 \pm 4.9**	
Daidzein	0.1	135.0 \pm 4.3**	0.61
	1	170.9 \pm 3.7**	
	10	170.1 \pm 7.4**	
Genistein	0.1	141.7 \pm 9.4**	0.60
	1	171.5 \pm 5.8**	
	10	197.2 \pm 12.4**	

Each value represents mean with the S.E. of 6 experiments. Asterisks denote significant differences from the control **: $p < 0.01$.

acid-1,4-dioxane furnished D-glucose, which was identified by GLC analysis of the thiazolidine derivative.¹⁵⁾ The ¹H-NMR (CD₃OD) and ¹³C-NMR (Table 4) spectra of **2a**, which were assigned on the basis of various NMR experiments,¹⁶⁾ indicated the presence of two tertiary methyls [δ 1.36, 1.79 (both s, 7, 10-H₃)], two methylenes [δ 1.28 (m), 2.12 (ddd-like) (5-H₂), 1.45 (m), 2.26 (ddd-like) (6-H₂)], two methines bearing hydroxyl group [δ 3.52 (d-like, 3-H), 3.72 (d, $J=10.6$ Hz, 2-H)], and *exo*-methylene [δ 4.82, 4.86 (both brs, 9-H₂)] together with three quaternary carbons (1, 4, 8-C). The plane structure of **2a** was constructed on the basis of ¹H-¹H correlation spectroscopy (H-H COSY) and the heteronuclear multiple bond correlation (HMBC) experiment on **2a** shown in Fig. 2. Thus, the H-H COSY experiment on **2a** indicated the presence of two partial structures shown by thick lines (C-2—C-3 and C-5—C-6). In the HMBC experiment, long-range correlations were observed between the following protons and carbons of **2a** (7-H₃ and 1, 2, 6-C; 10-H₃ and 4, 8, 9-C), so that the connectivities of the quaternary carbons in **2a** were identified. The above-mentioned evidence led us to confirm that the plane structure of **2a** was 1,4-epoxy-*p*-menth-8-en-2,3-diol.

The ¹H-NMR (CD₃OD) and ¹³C-NMR (Table 4) spectra¹⁶⁾ of **2** showed signals assignable to a petrol moiety [δ 1.35, 1.82 (both s, 7, 10-H₃), 1.35, 2.13 (both m, 6-H₂), 1.51 (dt-like), 2.32 (m) (5-H₂), 3.62 (m, 2-H), 4.04 (d, $J=8.6$ Hz, 3-H), 4.83, 5.14 (both brs, 9-H₂)] and a β -D-glucopyranosyl moiety [δ 4.42 (d, $J=7.6$ Hz, 1'-H)]. In the HMBC experiment on **2**, long-range correlations were observed between 1'-H and 3-C. The stereostructure of **2** was characterized by a phase-sensitive NOESY experiment on **2**, which showed NOE correlations between the 2-proton and the 3-proton, between the 2-proton and the 7-protons, between the 2-proton and the 6 β -proton, between the 3-proton and the 1'-proton, between the 6 β -proton and the 7-protons, and between the 7-protons and the 10-protons. Finally, the absolute stereostructure of **2** was identified using the glycosylation shift rule,¹⁷⁾ which is achieved by comparison of the 3-carbon signal in the ¹³C-NMR spectrum for **2a** with that for **2**. Thus, the shift value [$\Delta\delta = \delta$ glucoside (**2**) - δ alcohol (**2a**)] is 6.5 ppm, which indicates the absolute configuration of the 3-position to be *R*. On the basis of the above evidence, the structure of

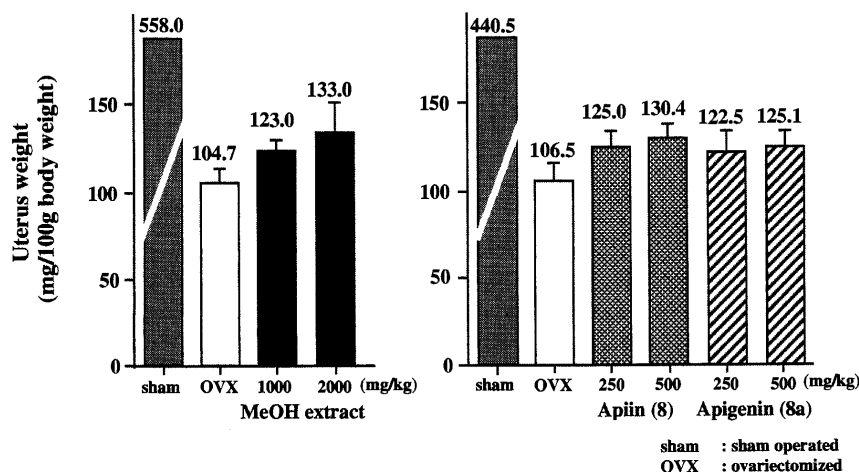


Fig. 1. Effects of Methanolic Extract of Parsley, Apiin (**8**), and Apigenin (**8a**) on Uterus Weight Decrease in Ovariectomized Mice

Mice aged 5 weeks were ovariectomized and kept for 7 d. Samples suspended in 5% Acaica solution were given to mice for the next 7 d. On the last day, mice were sacrificed and the uterus was removed. Each column represents mean with the S.E. of 5 to 7 mice.

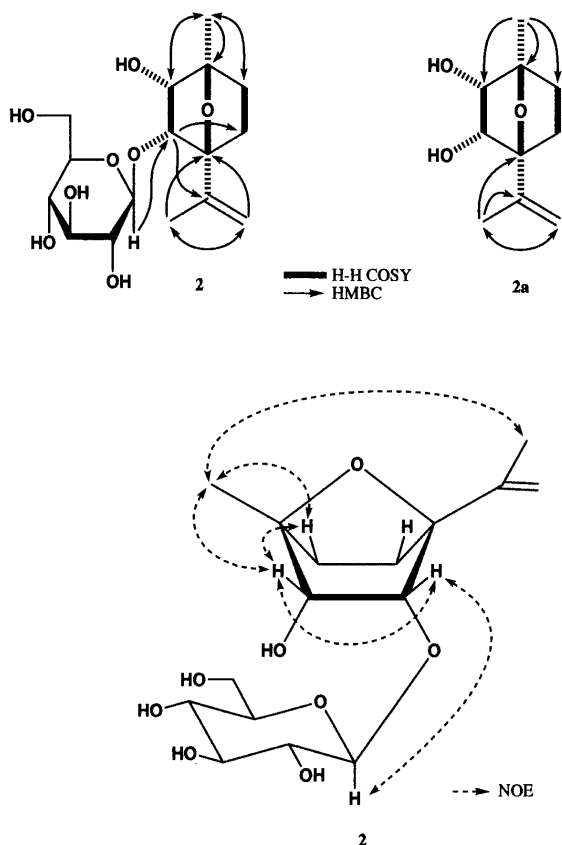


Fig. 2

Table 4. ^{13}C -NMR Data for 6''-Acetylapiin (1), Apiin (8), Petroside (2), Petranol (2a) (68 MHz, CD_3OD , $\text{DMSO}-d_6$)

	1 ^b	8 ^b		2 ^a	2a ^a
C-1			C-1	86.7	86.9
C-2	164.3	164.3	C-2	74.8	74.6
C-3	103.1	103.1	C-3	79.7	73.2
C-4	181.9	181.9	C-4	90.5	91.8
C-4a	161.3	161.4	C-5	30.3	30.3
C-5	99.3	99.4	C-6	30.0	29.3
C-6	162.4	162.7	C-7	20.3	20.4
C-7	94.8	94.8	C-8	145.9	146.7
C-8	156.8	156.9	C-9	111.5	110.6
C-8a	105.4	105.4	C-10	19.4	19.2
C-1'	121.0	121.0	Glc-1'	104.2	
C-2'	128.5	128.5	-2'	75.4	
C-3'	115.9	115.9	-3'	78.3	
C-4'	161.1	161.1	-4'	71.5	
C-5'	115.9	116.0	-5'	78.2	
C-6'	128.5	128.5	-6'	62.8	
Glc-1''	98.0	98.2			
-2''	75.7	75.9			
-3''	76.1	76.1			
-4''	70.0	69.8			
-5''	76.1	77.0			
-6''	63.3	60.6			
Api-1'''	108.7	108.7			
-2'''	76.4	76.7			
-3'''	79.2	79.1			
-4'''	73.9	73.9			
-5'''	64.1	64.2			
Ac-1	170.6				
-2	20.4				

a) In CD_3OD , b) in $\text{DMSO}-d_6$.

petroside (2) was determined as shown.

Experimental

The following instruments were used to obtain physical data: specific rotations, Horiba SEPA-300 digital polarimeter ($l=5\text{ cm}$); UV spectra, Shimadzu UV-1200 spectrometer; IR spectra, Shimadzu FTIR-8100 spectrometer; ^1H -NMR spectra, JEOL EX-270 (270 MHz) and JNM-LA500 (500 MHz) spectrometer; ^{13}C -NMR spectra, JEOL EX-270 (68 MHz) and JNM-LA500 (125 MHz) spectrometers with tetramethylsilane as an internal standard; MS and high-resolution MS, JEOL JMS-SX 102A mass spectrometer and JMS-GCMATE; HPLC, Shimadzu LC-10AS chromatograph.

The following experimental conditions were used for chromatography: normal-phase column chromatography; silica gel BW-200 (Fuji Silysia Chemical, Ltd., 150–350 mesh), reversed-phase column chromatography; Chromatorex ODS DM1020T (Fuji Silysia Chemical, Ltd., 100–200 mesh); TLC, pre-coated TLC plates with silica gel 60F₂₅₄ (Merck, 0.25 mm) (normal-phase) and silica gel RP-18 60F₂₅₄ (Merck, 0.25 mm) (reversed-phase); HPTLC, pre-coated TLC plates with silica gel RP-18 60WF_{254S} (Merck, 0.25 mm) (reversed-phase). Detection was done by spraying with 1% $\text{Ce}(\text{SO}_4)_2$ –10% aqueous H_2SO_4 , followed by heating.

Preparation of Herbal Extract Dried herbs were purchased from Tochimoto Tenkaido Co., Ltd. (Osaka, Japan). Each herb was extracted with 5 volumes of MeOH 3 times at 80 °C for 3 h, and the extract was evaporated under reduced pressure at under 40 °C to give the MeOH extract.

Cell Culture MCF-7 cells¹⁸⁾ were kindly provided by the Institute of Development, Aging and Cancer, Tohoku University. Cells were maintained in Dulbecco's modified Eagle medium (D-MEM, Gibco BRL, Life Technologies) supplemented with 10% fetal calf serum (FCS, Biowhittaker) and an antibiotic [penicillin (100 unit/ml) and streptomycin (100 $\mu\text{g}/\text{ml}$) mixture (Gibco BRL, Life Technologies)], and subcultured every 3 or 4 d.

Estrogenic Activity of Herb Estrogenic activity was investigated with MCF-7 according to the previous report.¹⁹⁾ MCF-7 collected by trypsinization was washed (80 \times g, 3 min, 4 °C) 3 times with phenol red-free D-MEM. Cells (2000 cells/100 μl) were suspended in phenol red-free D-MEM containing 5% estrogen free FCS (charcoal and dextran treated FCS),²⁰⁾ and were seeded in a 96-well culture plate. After 24 h culture, the medium was changed with 90 μl fresh medium and 10 μl sample solution, and the cells were continuously cultured for 4 days. Proliferation of cells was assessed by MTT assay.²¹⁾ Each samples were dissolved in dimethyl sulfoxide (DMSO) and diluted with medium. The final concentration of DMSO was adjusted to 0.1 or 0.01% in each experiment.

Measurement of Uterus Weight Increase in Ovariectomized Mice Mice aged 5 weeks (Kiwa Laboratory Animals, Wakayama, Japan) were ovariectomized and were kept for 7 d. The methanolic extracts, apigenin, and apiin were suspended with 5% Acacia in water, and given to ovariectomized mice for 7 consecutive days. On the last day, mice were sacrificed by cervical vertebra dislocation and the uterus was removed. The uterus was weighed immediately and its ratio to total body weight was calculated.

Statistical Analysis Dunnett's multiple range test²²⁾ was used to evaluate any significant difference from the control group.

Extraction and Isolation. i) **American Parsley** The dried aerial parts of *Petroselinum crispum* MILL. cultivated in U.S.A. (900 g, purchased from Tochimoto Tenkaido Co., Ltd., Osaka) were powdered and extracted three times with MeOH under reflux. Evaporation of the solvent under reduced pressure provided the MeOH extract (320.9 g, 36%), and the MeOH extract (300 g) was partitioned in an AcOEt–H₂O (1:1, v/v) mixture. Removal of the solvent from the AcOEt-soluble and H₂O-soluble fractions under reduced pressure yielded the AcOEt-soluble extract (77.8 g, 8.6%) and the H₂O-soluble extract (202.2 g, 24%). The AcOEt-soluble extract (72.8 g) was separated by normal-phase silica gel column chromatography [BW-200 (Fuji Silysia Ltd., 810 g), *n*-hexane–AcOEt (4:1→2:1, v/v)→CHCl₃–MeOH (30:1→15:1→5:1, v/v)→MeOH] to afford seven fractions [fr. 1 (8.1 g), fr. 2 (6.9 g), fr. 3 (25.7 g), fr. 4 (7.7 g), fr. 5 (6.8 g)]. Fraction 1 (6.8 g) was separated by reversed-phase silica gel column chromatography [Chromatorex DM1020T (Fuji Silysia Ltd., 120 g), MeOH–H₂O (70:30→95:5, v/v)→CHCl₃–MeOH–H₂O (6:4:1, v/v)→MeOH] and HPLC [YMC-Pack Ph (250 \times 20 mm i.d., YMC Co., Ltd.), MeOH–H₂O (60:40, v/v)] to give myristicin (3, 46 mg, 0.0051%) and apiole (4, 15 mg, 0.0016%). Fraction 2 (6.0 g) was separated by normal-phase [200 g, *n*-hexane–AcOEt (9:1→5:1→3:1→2:1, v/v)→MeOH], reversed-phase silica gel column chromatography [50 g, MeOH–H₂O (70:30→80:20→95:5, v/v)→CHCl₃–MeOH–H₂O (6:4:1, v/v)→MeOH], and HPLC [YMC-Pack ODS-A (250 \times 20 mm i.d., YMC Co., Ltd.), MeOH–H₂O (75:25, v/v)] to give cnicidil (5, 8.9 mg, 0.0010%) and isoimperatorin (6, 19 mg, 0.0021%). Fraction

4 (7.0 g) was separated by reversed-phase silica gel column chromatography [200 g, MeOH-H₂O (50:50→70:30→90:10→95:5, v/v)→CHCl₃-MeOH-H₂O (6:4:1, v/v)→MeOH] to give fr. 4-1 (1.3 g), 4-2 (783 mg), 4-3 (158 mg), 4-4 (535 mg, fatty acid mixture), 4-5 (592 mg), 4-6 (2.9 g, daucosterin), 4-7 (569 mg). Fraction 4-1 (450 mg) was purified by HPLC [MeOH-H₂O (45:55, v/v)] to give apigetrin (7, 33 mg, 0.0037%), diosmetin 7-*O*-β-D-glucopyranoside (9, 12 mg, 0.0013%), and kaempferol 3-*O*-β-D-glucopyranoside (10, 21 mg, 0.0024%). Fraction 4-2 (175 mg) was purified by HPLC [MeOH-H₂O (60:40, v/v)] to give 6''-acetylapiin (1, 68 mg, 0.0075%). Fraction 5 (5.7 g) was separated by reversed-phase silica gel column chromatography [180 g, MeOH-H₂O (50:50→60:40→70:30→90:10, v/v)→CHCl₃-MeOH-H₂O (6:4:1, v/v)→MeOH] to give apiin (8, 56 mg, 0.0063%). The H₂O-soluble fraction (23.3 g) was separated by reversed-phase silica gel column chromatography [700 g, MeOH-H₂O (30:70→50:50→70:30)→MeOH→CHCl₃-MeOH-H₂O (6:4:1, v/v)→MeOH] to give 8 (1.3 g, 1.5%). The known compounds (3–10) were identified by comparison of their physical data ([α]_D, ¹H-NMR, ¹³C-NMR) with reported values.^{9–14)}

6''-Acetylapiin (1): A white powder, [α]_D²⁵ −151.6° (c=0.4, MeOH). High-resolution positive-ion FAB-MS: Calcd for C₃₄H₃₁O₁₅ (M+H)⁺: 607.1658. Found: 607.1671. UV [λ_{max}^{MeOH} nm (log ε)]: 334 (4.1), 269 (4.0). IR (KBr): 3415, 2926, 1735, 1661, 1607, 1078 cm^{−1}. ¹H-NMR (270 MHz, DMSO-*d*₆) δ: 2.01 (3H, s, Ac-2), 5.19 (1H, d, *J*=7.6 Hz, 1''-H), 5.36 (1H, brs, 1'''-H), 6.43 (1H, d-like, 6-H), 6.77 (1H, d-like, 8-H), 6.84 (1H, s, 3-H), 6.94 (2H, d, *J*=8.9 Hz, 3', 5'-H), 7.94 (2H, d, *J*=8.9 Hz, 2', 6'-H). ¹³C-NMR (DMSO-*d*₆, 68 MHz) δ_C: given in Table 4. Negative-ion FAB-MS: (*m*-H)[−], 473 (M-C₅H₉O₄)[−], 269 (M-C₁₃H₂₁O₁₀)[−]. Positive-ion FAB-MS: *m/z* 607 (M+H)⁺.

ii) **Japanese Parsley** The fresh aerial parts of Japanese parsley (2.2 kg) cultivated in Chiba Prefecture, Japan were cut and extracted three times with MeOH under reflux. Evaporation of the solvent under reduced pressure provided the MeOH extract (120 g, 5.5%), and 100 g of this extract was partitioned in an AcOEt-H₂O (1:1, v/v) mixture. Removal of the solvent from the AcOEt-soluble and H₂O-soluble fractions under reduced pressure yielded the AcOEt-soluble extract (14.5 g, 0.8%) and H₂O-soluble extract (85.5 g, 4.7%). The H₂O-soluble extract (85.5 g) was separated by reversed-phase silica gel column chromatography [Chromatorex DM1020T (Fuji Silysia Ltd., 120 g), H₂O→MeOH→CHCl₃-MeOH-H₂O (5:5:1, v/v)→MeOH→acetone→MeOH] to afford seven fractions [fr. 1 (11.1 g), fr. 2 (184 mg), fr. 3 (99 mg), fr. 4 (70 mg), fr. 5 (67 mg), fr. 6 (63 mg), fr. 7 (49 mg)]. Fraction 1 (10 g) was separated by normal-phase silica gel column chromatography [BW-200 (Fuji Silysia Ltd., 500 g), CHCl₃-MeOH-H₂O (15:3:1, lower layer→6:4:1, v/v)] to give fr. 1-1 (790 mg), 1-2 (406 mg), 1-3 (496 mg), 1-4 (269 mg), 1-5 (3.2 g), 1-6 (1.8 g), and 1-7 (1.2 g). Fraction 1-2 (400 mg) was separated by reversed-phase silica gel column chromatography [10 g, H₂O→MeOH] and purified by HPLC [YMC-Pack ODS-AL (250×20 mm i.d.), MeOH-H₂O (50:50, v/v)] to give petroside (2, 10 mg, 0.0006%). Fraction 1-4 (260 mg) was separated by reversed-phase silica gel column chromatography [10 g, H₂O→MeOH] and purified by HPLC [MeOH-H₂O (35:65, v/v)] to give icarisside F₂ (11, 24 mg, 0.0015%). Fraction 1-6 (1.8 g) was separated by reversed-phase silica gel column chromatography [90 g, H₂O→MeOH] and purified by HPLC [MeOH-H₂O (45:55, v/v)] to give apiin (8, 318 mg, 0.0193%). The known compounds (8, 11) were identified by comparison of their physical data ([α]_D, ¹H-NMR, ¹³C-NMR) with reported values.^{12,23)}

Petroside (2): A white powder, [α]_D²⁵ −13.8° (c=0.3, MeOH). High-resolution EI-MS: Calcd for C₁₆H₂₆O₈ (M⁺): 346.1627. Found: 346.1631. IR (KBr): 3410, 2928, 1649, 1452, 1078 cm^{−1}. ¹H-NMR (270 MHz, CD₃OD) δ: 1.35, 1.82 (3H each, both s, 7, 10-H₃), 1.35, 2.13 (1H each, both m, 6-H₂), 1.51 (1H, dt-like), 2.32 (1H, m) (5-H₂), 3.62 (1H, m, 2-H), 4.04 (1H, d, *J*=8.6 Hz, 3-H), 4.42 (1H, d, *J*=7.6 Hz, 1'-H), 4.83, 5.14 (1H each, both brs, 9-H₂). ¹³C-NMR (68 MHz, CD₃OD) δ_C: given in Table 4. EI-MS: *m/z* 346 (M⁺, 3.8), 183 (100.0).

Deacetylation of 6''-Acetylapiin (1) A solution of 1 (1 mg) in 0.1% NaOMe-MeOH (1.0 ml) was stirred at room temperature for 15 min. The reaction solution was neutralized with Dowex HCR W2 (H⁺ form) and the insoluble portion was removed by filtration. After removal of the solvent *in vacuo* from the filtrate, the crude product was purified by normal-phase silica gel column chromatography [1 g, *n*-hexane-AcOEt (1:1)] to give apiin (8, 1 mg), which was identified by comparison of physical data ([α]_D, ¹H-NMR) and TLC with an authentic sample.

Enzymatic Hydrolysis of Petroside (2) Given Petranol (2a) A solution of 2 (6 mg) in 0.2 M acetate buffer (pH 4.4, 1.0 ml) was treated with β-glucosidase (Oriental Yeast Co., Japan, 6.0 mg) and the reaction mixture was

stirred at 38 °C for 12 h. The reaction mixture was then poured into H₂O and the whole was extracted with AcOEt. The AcOEt extract was washed with sat. aq. NaHCO₃ and brine, then dried over MgSO₄ and filtered. After removal of the solvent under reduced pressure, the residue (3 mg) was purified by silica gel column chromatography [5.0 g, *n*-hexane-AcOEt (1:1)] to give 2a (2 mg).

Petranol (2a): A white powder, [α]_D²⁷ +18.7° (c=0.1, MeOH). High-resolution EI-MS: Calcd for C₁₀H₁₆O₃ (M⁺): 184.1099. Found: 184.1101. IR (KBr) 3436, 2361, 1385, 1117 cm^{−1}. ¹H-NMR (270 MHz, CD₃OD) δ: 1.28 (1H, m), 2.12 (1H, ddd-like) (5-H₂), 1.36, 1.79 (3H each, both s, 7, 10-H₃), 1.45 (1H, m), 2.26 (1H, ddd-like) (6-H₂), 3.52 (1H, d-like, 3-H), 3.72 (1H, d, *J*=10.6 Hz, 2-H), 4.82, 4.86 (1H each, both brs, 9-H₂). ¹³C-NMR (CD₃OD, 68 MHz) δ_C: given in Table 4.

Acid Hydrolysis of Petroside (2) A solution of petroside (2, 2 mg) in 5% aqueous H₂SO₄-1,4-dioxane (1:1, v/v, 2 ml) was heated under reflux for 1 h. After cooling, the reaction mixture was neutralized with Amberlite IRA-400 (OH[−] form) and the residue was removed by filtration. After removal of the solvent from the filtrate *in vacuo*, the residue was passed through a Sep-Pak C₁₈ cartridge with H₂O and MeOH. The H₂O eluate was concentrated and the residue was treated with L-cysteine methyl ester hydrochloride (4 mg) in pyridine (0.5 ml) at 60 °C for 1 h. After reaction, the solution was treated with *N,O*-bis(trimethylsilyl)trifluoroacetamide (0.2 ml) at 60 °C for 1 h. The supernatant was then subjected to GLC analysis to identify the derivatives of D-glucose from 2; GLC conditions: Supelco STBTM-1, 30 m×0.25 mm (i.d.) capillary column, column temperature 230 °C, He flow rate 15 ml/min, *t*_R: 24.2 min.

References and Notes

- 1) Part XVII: Murakami T., Kishi A., Matsuda H., Yoshikawa M., *Chem. Pharm. Bull.* submitted (No. 100015).
- 2) a) Hutchins A. M., Lampe J. W., Martini M. C., Campbell D. R., Slavin J. L., *J. Am. Diet. Assoc.*, **95**, 769–774 (1995); b) Milligan S. R., Kalita J. C., Heyerick A., Rong H., De Cooman L., De Keukeleire D., *J. Clin. Endocrinol. Metab.*, **84**, 2249–2252 (1999).
- 3) Fanti P., Monier-Faugere M. C., Geng Z., Schmidt J., Morris P. E., Cohen D., Malluche H. H., *Osteoporos Int.*, **8**, 274–281 (1998).
- 4) Meng Q. H., Lewis P., Wahala K., Adlercreutz H., Tikkanen M. J., *Biochim. Biophys. Acta*, **1438**, 369–376 (1999).
- 5) Deodato B., Altavilla D., Squadrito G., Campo G. M., Arlotta M., Minutoli L., Saitta A., Cucinotta D., Calapai G., Caputi A. P., Miano M., Squadrito F., *Br. J. Pharmacol.*, **128**, 1683–1690 (1999).
- 6) Lamartiniere C. A., Moore J. B., Brown N. M., Thompson R., Hardin M. J., Barnes S., *Carcinogenesis*, **16**, 2833–2840 (1995).
- 7) Wakeling A. E., Newbould E., Peters S. W., *J. Mol. Endocrinol.*, **2**, 225–234 (1989).
- 8) Kitagawa I., Yoshikawa M., Yoshioka I., *Chem. Pharm. Bull.*, **24**, 121–129 (1976).
- 9) Yakushiji K., Tohshima T., Suzuki R., Murata H., Lu S. T., Furukawa H., *Chem. Pharm. Bull.*, **31**, 2879–2883 (1983).
- 10) Kuo-Hsiung L., Soine T. O., *J. Pharm. Sci.*, **58**, 681–683, (1969).
- 11) Redaelli C., Formentini L., Santaniello E., *Phytochemistry*, **19**, 985–986 (1980).
- 12) Markham K. R., Ternai B., Stanley R., Geiger H., Mabry T. L., *Tetrahedron*, **34**, 1389–1397 (1978).
- 13) Matsuzaki K., Wang Y. Q., Takahashi K., Okuyama T., *Shoyakugaku Zasshi*, **44**, 251–253 (1990).
- 14) Okuyama T., Hosoyama K., Hiraga Y., Kurono G., Takemoto T., *Chem. Pharm. Bull.*, **26**, 3071–3074 (1978).
- 15) Hara S., Okabe H., Mihashi K., *Chem. Pharm. Bull.*, **34**, 1843–1845 (1986).
- 16) The ¹H- and ¹³C-NMR spectra of 9 and 10 were assigned with the aid of homo- and hetero-nuclear correlation spectroscopy (¹H-¹H, ¹H-¹³C COSY), and HMBC experiments.
- 17) Inoshiri S., Saiki M., Kohda H., Otsuka H., Yamasaki K., *Phytochemistry*, **27**, 2869–2871 (1988).
- 18) Soule H. D., Vazquez A., Long A., Albert S., Brennan M., *J. Natl. Cancer Inst.*, **51**, 1409–1416 (1973).
- 19) Kawamura I., Mizota T., Lacey E., Tanaka Y., Manda T., Shimomura K., Kohsaka M., *Jpn. J. Pharmacol.*, **63**, 27–34 (1993).
- 20) Devleeschouwer N., Body J. J., Legros N., Muquardt C., Donnay I., Wouters P., Leclercq G., *Anticancer Res.*, **12**, 789–794 (1992).
- 21) Mossman T., *J. Immunol. Methods*, **65**, 55–63 (1983).
- 22) a) Dunnett C. W., *J. Am. Stat. Assoc.*, **75**, 789–795 (1980); b) *Idem*, *ibid.*, **75**, 796–800 (1980).
- 23) Miyase T., Ueno A., Takizawa N., Kobayashi H., Oguchi H., *Chem. Pharm. Bull.*, **36**, 2475–2484 (1988).

Bioactive Saponins and Glycosides. XVI.¹⁾ Nortriterpene Oligoglycosides with Gastroprotective Activity from the Fresh Leaves of *Euptelea polyandra* SIEB. et ZUCC. (1): Structures of Eupteleasaponins I, II, III, IV, V, and V Acetate

Masayuki YOSHIKAWA,* Toshiyuki MURAKAMI, Hideo OOMINAMI, and Hisashi MATSUDA

Kyoto Pharmaceutical University, Misasagi, Yamashina-ku, Kyoto, 607–8414, Japan.

Received February 14, 2000; accepted March 25, 2000

The saponin fraction from the fresh leaves of *Euptelea polyandra* SIEB. et ZUCC. was found to exhibit potent gastroprotective activity. Fourteen new nortriterpene saponins called eupteleasaponins were isolated from the saponin fraction with gastroprotective activity. The structures of eupteleasaponins I, II, III, IV, V, and V acetate were determined on the basis of chemical and physicochemical evidence as 3-*O*- α -L-rhamnopyranosyl(1 \rightarrow 2)- β -D-glucopyranosyl(1 \rightarrow 3)- β -D-xylopyranosylakebonoic acid 28-*O*- β -D-glucopyranosyl ester, 3-*O*- α -L-rhamnopyranosyl(1 \rightarrow 2)-[α -L-rhamnopyranosyl(1 \rightarrow 4)]- β -D-glucopyranosyl(1 \rightarrow 3)- β -D-xylopyranosylakebonoic acid 28-*O*- β -D-glucopyranosyl ester, 3-*O*- α -L-rhamnopyranosyl(1 \rightarrow 2)-[α -L-arabinopyranosyl(1 \rightarrow 4)]- β -D-glucopyranosyl(1 \rightarrow 3)- β -D-xylopyranosylakebonoic acid 28-*O*- β -D-glucopyranosyl ester, 3-*O*- α -L-rhamnopyranosyl(1 \rightarrow 2)-[α -L-rhamnopyranosyl(1 \rightarrow 4)]- β -D-glucopyranosyl(1 \rightarrow 3)- β -D-xylopyranosylakebonoic acid 28-*O*- β -D-glucopyranosyl ester, 3-*O*- α -L-rhamnopyranosyl(1 \rightarrow 2)-[α -L-arabinopyranosyl(1 \rightarrow 4)]- β -D-glucopyranosyl(1 \rightarrow 3)- β -D-xylopyranosylakebonoic acid, 3-*O*- α -L-rhamnopyranosyl(1 \rightarrow 2)- β -D-glucopyranosyl(1 \rightarrow 3)- β -D-xylopyranosyleupteleogenin, and 3-*O*- α -L-rhamnopyranosyl(1 \rightarrow 2)-6"-*O*-acetyl- β -D-glucopyranosyl(1 \rightarrow 3)- β -D-xylopyranosyleupteleogenin.

Key words *Euptelea polyandra*; eupteleasaponin; gastroprotective activity; akebonoic acid; eupteleogenin; Eupteleaceae

Euptelea (*E.*) *polyandra* SIEB. et ZUCC., which is endemic to Japan, is a medium height tree of 7 to 8 m belonging to the small family Eupteleaceae. An aqueous methanolic extract from the fresh leaves of this plant was earlier reported to show anti-microbial activity.²⁾ From the extract, two triterpene glycosides were isolated and the structure of the common aglycone, eupteleogenin, was reported,²⁾ but detailed chemical elucidation of the glycoside constituents was left undetermined.

In the course of our studies on bioactive saponins of natural medicines and medicinal foodstuffs,^{1,3)} we found that the saponin fraction from the fresh leaves of *E. polyandra* exhibited potent gastroprotective activity. From this fraction, we isolated fourteen new nortriterpene oligoglycosides, eupteleasaponins I (1), II (2), III (3), IV (4), V (5), V acetate (6), VI, VI acetate, VII, VIII acetate, IX, X, XI, and XII. This paper deals with the isolation of eupteleasaponins and the structure elucidation of eupteleasaponins I (1), II (2), III (3), IV (4), V (5), and V acetate (6).

The saponin constituents of the fresh leaves of *E. polyandra*, which were collected in the Kitayama area of Kyoto prefecture, were separated by the procedure shown in Chart 1. The methanolic extract obtained from the leaves was partitioned into an ethyl acetate and water mixture to give an ethyl acetate extract and an aqueous phase. The aqueous phase was subjected to reversed-phase silica gel column chromatography to remove the sugar components and to give the methanol eluate fraction (saponin fraction). As apparent from Fig. 1, oral administration of the saponin fraction was found to cause potent gastroprotective activity against hydrochloric acid (HCl) and ethanol-induced lesions in rats. The saponin fraction significantly reduced the mucosal lesions in a dose-dependent manner and its activity was much stronger than that of the reference medicine omeprazole. The saponin fraction was subjected to normal- and reversed-phase silica-gel column chromatography and finally HPLC to

give eupteleasaponins I (1, 0.0021%), II (2, 0.0015%), III (3, 0.0015%), IV (4, 0.0008%), V (5, 0.0058%), V acetate (6, 0.0143%), VI (0.0045%), VI acetate (0.0032%), VII (0.0038%), VIII acetate (0.0023%), IX (0.0018%), X (0.0013%), XI (0.0014%), and XII (0.0018%).

Structures of Eupteleasaponin I, II, III, IV, V, and V acetate Eupteleasaponin I (1) was isolated as colorless fine crystals from CHCl₃–MeOH of mp 201–203 °C with positive optical rotation ($[\alpha]_D^{28} +17.7^\circ$). The IR spectrum of 1 showed absorption bands at 3432, 1744, 1680, and 1075 cm⁻¹ due to hydroxyl, carbonyl, and *exo*-methylene groups. In the negative- and positive-ion FAB-MS of 1, quasimolecular ion peaks were observed at *m/z* 1041 (M–H)⁻ and *m/z* 1065 (M+Na)⁺ and the molecular formula C₅₂H₈₂O₂₁ was determined by high-resolution MS measurement. Acid hydrolysis of 1 with 5% aqueous sulfuric acid–1,4-dioxane (1:1, v/v) furnished D-xylose, D-glucose, and L-rhamnose, which were identified by GLC analysis of the thiazolidine derivatives.⁴⁾ Furthermore, fragment ion peaks were observed at *m/z* 895 (M–C₆H₁₁O₄)⁻ and 879 (M–C₆H₁₁O₅)⁻, which were derived by cleavage of the glycoside linkage at the rhamnose and glucose, respectively, in

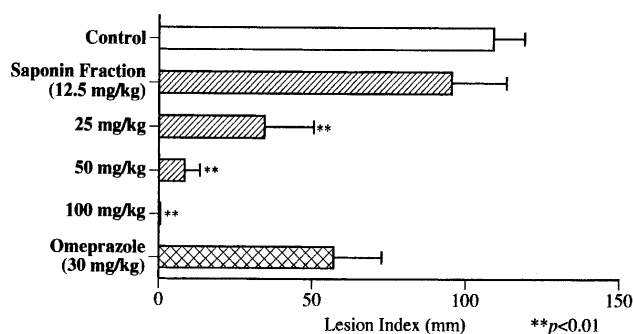


Fig. 1. Gastromucosal Protective Activity of the Saponin Fraction from the Leaves of *Euptelea polyandra*

* To whom correspondence should be addressed. e-mail: shoyaku@mb.kyoto-phu.ac.jp

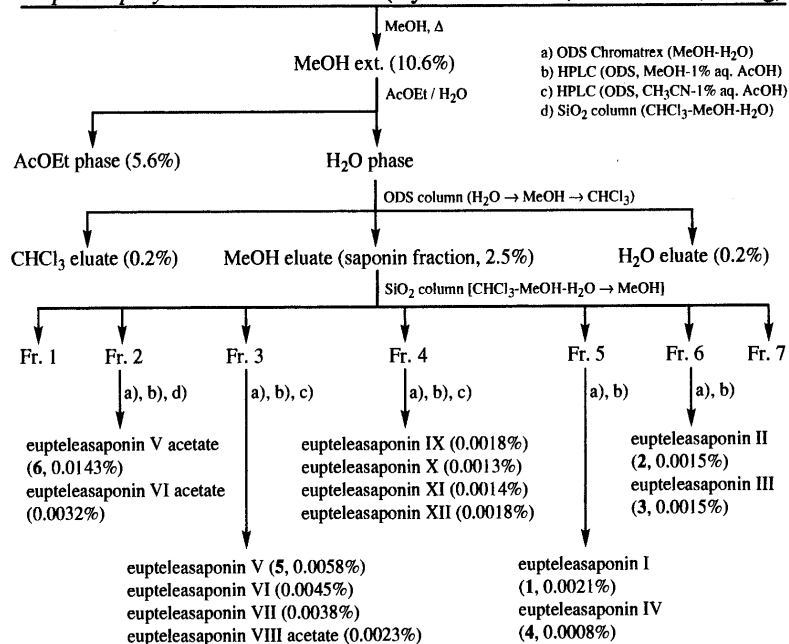
Euptelea polyandra SIEB. et ZUCC. (Kyoto Prefecture, fresh leaves, 2.6 kg)

Chart 1

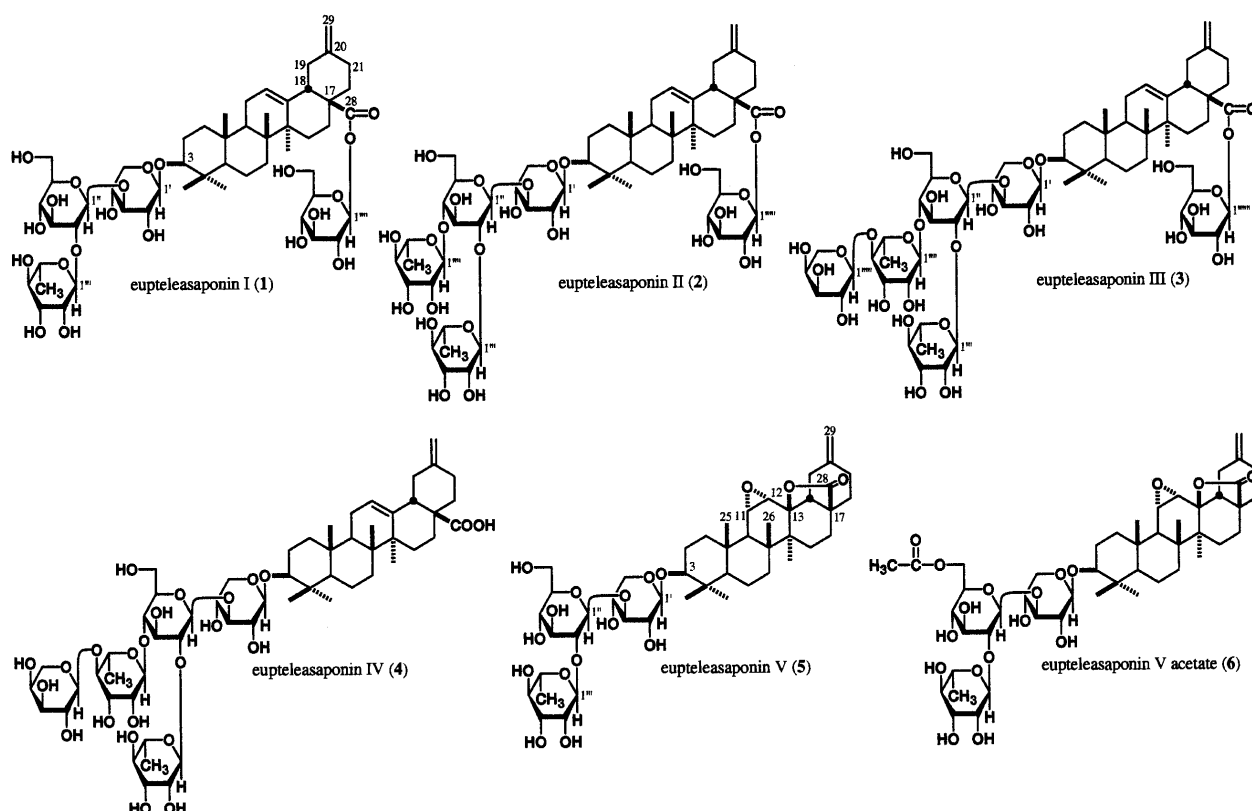


Chart 2

the negative-ion FAB-MS of **1**. The ¹H-NMR (pyridine-*d*₅) and ¹³C-NMR (Table 1) spectra of **1**, which were assigned by various NMR analytical methods,⁵⁾ indicated the presence of a β -D-xylopyranosyl moiety [δ 4.87 (d, $J=5.2$ Hz, 1'-H)], two β -D-glucopyranosyl moieties [δ 5.06 (d, $J=7.6$ Hz, 1''-H), 6.23 (d, $J=7.0$ Hz, 1'''-H)], an α -L-rhamnopyranosyl moiety [δ 1.61 (d, $J=5.8$ Hz, 6'''-H₃), 6.05 (brs, 1'''-H)], and a nortriterpene sapogenol moiety [δ 3.10 (dd-like, 18-H),

3.30 (dd, $J=3.5, 11.3$ Hz, 3-H), 4.68, 4.74 (both s, 29-H₂), 5.43 (brs, 12-H)]. The carbon signals due to the aglycone structure in the ¹³C-NMR data were very similar to those of known akebonoic acid glycosides.⁶⁾ The HMBC experiment on **1** showed long-range correlations between the protons and the carbons depicted in Fig. 2, which confirmed the sapogenol of **1** to be akebonoic acid having the 29-*exo*-methylene group (29-H₂ and 19, 21-C; 18-H and 17, 19-C) and the

oligoglycoside structure (1'-H and 3-C; 1''-H and 3'-C; 1'''-H and 2''-C; 1''''-H and 28-C). Consequently, eupteleasaponin I was determined to be 3-*O*- α -L-rhamnopyranosyl(1 \rightarrow 2)- β -D-glucopyranosyl(1 \rightarrow 3)- β -D-xylopyranosylakebonoic acid 28-*O*- β -D-glucopyranosyl ester (1).

Eupteleasaponin II (2) was isolated as colorless fine crystals from CHCl_3 -MeOH of mp 191–193 °C. The IR spectrum of 2 showed absorption bands at 3410, 1736, 1655, and 1078 cm^{-1} assignable to hydroxyl, carbonyl, and *exo*-methylene groups. In the negative- and positive-ion FAB-MS of 2, quasimolecular ion peaks were observed at m/z 1187 ($\text{M}-\text{H}$)⁻ and m/z 1211 ($\text{M}+\text{Na}$)⁺ and the molecular formula $\text{C}_{58}\text{H}_{92}\text{O}_{25}$ was determined by high-resolution MS measurement. Furthermore, fragment ion peaks were observed at m/z 1041 ($\text{M}-\text{C}_6\text{H}_{11}\text{O}_4$)⁻ and 1025 ($\text{M}-\text{C}_6\text{H}_{11}\text{O}_5$)⁻ in the nega-

tive-ion FAB-MS of 2. Acid hydrolysis of 2 with 5% aqueous sulfuric acid–1,4-dioxane (1 : 1, v/v) furnished D-xylose, D-glucose, and L-rhamnose.⁴⁾ The ¹H-NMR (pyridine-*d*₅) and ¹³C-NMR (Table 1) spectra⁵⁾ of 2 showed signals assignable to a β -D-xylopyranosyl moiety [δ 4.85 (d-like, 1'-H)], two β -D-glucopyranosyl moieties [δ 5.01, 6.24 (both d, $J=7.9$ Hz, 1''-H, 1'''-H)], and two α -L-rhamnopyranosyl moieties [δ 1.62, 1.68 (both d, $J=6.1$ Hz, 6'''-H₃, 6''''-H₃), 5.77, 6.05 (both br s, 1''''-H, 1'''-H)], together with the akebonoic acid moiety. The oligoglycoside structure of 2 was characterized by an HMBC experiment on 2. That is, long-range correlations observed between the following protons and carbons: 1'-H and 3-C; 1''-H and 3'-C; 1'''-H and 2''-C; 1''''-H and 4''-C; 1''''-H and 28-C. The carbon signals in the ¹³C-NMR spectrum of 2 were very similar to those of 1, except for the signals due to 4''-*O*- α -L-rhamnopyranosyl moiety of 2. Consequently, eupteleasaponin II was determined to be 3-*O*- α -L-rhamnopyranosyl(1 \rightarrow 2)-[α -L-rhamnopyranosyl(1 \rightarrow 4)]- β -D-glucopyranosyl(1 \rightarrow 3)- β -D-xylopyranosylakebonoic acid 28-*O*- β -D-glucopyranosyl ester (2).

Eupteleasaponin III (3), isolated as colorless fine crystals from CHCl_3 -MeOH of mp 232–235 °C, liberated D-xylose, D-glucose, L-rhamnose, and L-arabinose on acid hydrolysis,⁴⁾ and its IR spectrum showed absorption bands due to hydroxyl, carbonyl, and *exo*-methylene functions. Here again, the molecular formula $\text{C}_{63}\text{H}_{100}\text{O}_{29}$ of 3 was identified from its

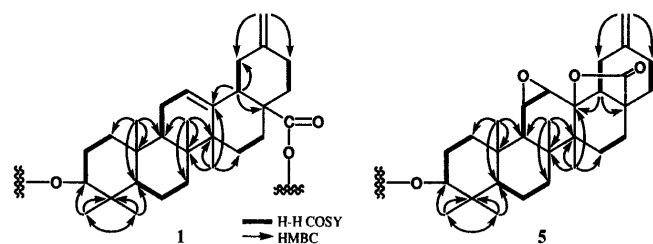


Fig. 2. H-H COSY and HMBC Correlations of Eupteleasaponins I (1) and V (5)

Table 1. ¹³C-NMR Data for Eupteleasaponins I (1), II (2), III (3), IV (4), V (5), and V Acetate (6)

	1	2	3	4	5	6		1	2	3	4	5	6
C-1	39.1	39.1	39.1	39.1	38.8	38.7	C-1'	104.7	104.7	104.7	104.8	104.7	104.8
C-2	26.6	26.6	26.6	26.6	26.2	26.2	C-2'	74.8	74.9	74.9	75.0	74.9	74.9
C-3	88.2	88.3	88.3	88.3	88.0	88.1	C-3'	81.8	81.8	81.6	81.9	82.0	82.3
C-4	39.6	39.6	39.7	39.6	39.7	39.6	C-4'	68.1	68.1	68.1	68.2	68.1	68.2
C-5	56.1	56.1	56.1	56.1	55.3	55.3	C-5'	64.8	64.7	64.7	64.8	64.8	64.5
C-6	18.6	18.5	18.6	18.6	17.8	17.8	C-1''	104.6	104.4	104.4	104.5	104.7	104.7
C-7	33.2	33.2	33.2	33.2	31.4	31.4	C-2''	74.9	75.1	75.2	75.3	75.0	74.7
C-8	40.0	40.0	40.0	39.9	41.7	41.7	C-3''	78.2	76.4	76.3	76.3	78.3	78.0
C-9	48.1	48.1	48.1	48.1	51.2	51.2	C-4''	71.3	78.4	77.5	77.5	71.6	71.5
C-10	37.1	37.1	37.1	37.1	36.5	36.5	C-5''	79.2	77.3	77.3	77.3	78.6	75.3
C-11	23.6	23.6	23.6	23.8	52.9	52.8	C-6''	62.4	61.4	61.3	61.3	62.8	64.9
C-12	123.8	123.8	123.8	123.1	57.2	57.1	C-1'''	101.9	102.0	102.0	102.0	102.0	102.0
C-13	143.4	143.4	143.4	144.2	87.0	87.0	C-2'''	72.3	72.3	72.4	72.4	72.4	72.4
C-14	42.1	42.2	42.2	42.2	41.0	41.0	C-3'''	72.6	72.6	72.6	72.6	72.6	72.6
C-15	28.2	28.2	28.2	28.4	27.0	27.1	C-4'''	73.9	73.9	73.9	74.0	74.0	73.9
C-16	23.7	23.8	23.8	23.9	32.3	32.3	C-5'''	70.1	70.1	70.2	70.2	70.1	70.0
C-17	47.3	47.4	47.4	47.1	44.1	44.1	C-6'''	18.6	18.5	18.4	18.4	18.6	18.6
C-18	47.7	47.7	47.7	48.0	54.8	54.8	C-1''''	95.8	102.7	102.4	102.5		
C-19	41.7	41.7	41.7	42.0	34.7	34.7	C-2''''	74.0	72.6	72.6	72.1		
C-20	148.5	148.5	148.5	149.2	147.1	147.0	C-3''''	78.5	72.8	72.9	73.0		
C-21	30.2	30.2	30.2	30.4	30.2	30.2	C-4''''	71.5	74.0	83.0	83.1		
C-22	37.6	37.7	37.7	38.4	22.0	22.0	C-5''''	78.8	70.4	70.1	70.1		
C-23	28.2	28.2	28.2	28.2	27.8	27.8	C-6''''	62.6	18.6	18.6	18.6		
C-24	17.0	17.0	17.0	17.0	16.5	16.4	C-1'''''		95.9	107.2	107.2		
C-25	15.7	15.7	15.7	15.6	17.4	17.4	C-2'''''		74.1	73.2	73.2		
C-26	17.5	17.5	17.5	17.4	20.3	20.3	C-3'''''		78.8	74.5	74.6		
C-27	26.1	26.1	26.1	26.2	18.9	18.9	C-4'''''		71.3	69.4	69.4		
C-28	175.7	175.5	175.8	179.4	178.2	178.1	C-5'''''		79.2	67.0	67.0		
C-29	107.2	107.2	107.2	107.0	109.8	109.8	C-6'''''		62.4				
Ac-1						170.8	C-1'''''			95.9			
Ac-2						20.7	C-2'''''			74.1			
							C-3'''''			78.8			
							C-4'''''			71.3			
							C-5'''''			79.2			
							C-6'''''			62.4			

negative- and positive-ion FAB-MS [quasimolecular ion peaks: m/z 1319 ($M-H$)⁻, m/z 1321 ($M+H$)⁺, m/z 1343 ($M+Na$)⁺] by high-resolution MS measurement. The ¹H-NMR (pyridine-*d*₅) and ¹³C-NMR (Table 1) spectra⁵⁾ of **3** showed the presence of a β -D-xylopyranosyl moiety [δ 4.85 (d, $J=5.4$ Hz, 1'-H)], two β -D-glucopyranosyl moieties [δ 4.99 (d, $J=7.9$ Hz, 1''-H), 6.24 (d, $J=8.0$ Hz, 1'''-H)], two α -L-rhamnopyranosyl moieties [δ 1.63, 1.64 (both d, $J=5.8$ Hz, 6'''-H₃, 6'''-H₃), 5.78, 6.03 (both br s, 1'''-H, 1'''-H)], and an α -L-arabinopyranosyl moiety [δ 5.20 (d, $J=7.4$ Hz, 1''''-H)], together with the akebonoic acid moiety [δ 3.11 (dd, $J=4.9$, 13.1 Hz, 18-H), 3.31 (dd, $J=3.9$, 11.6 Hz, 3-H), 4.70, 4.75 (both s, 29-H₂), 5.44 (br s, 12-H)]. The glycosidic structure of **3** was characterized by the HMBC experiment, in which long-range correlations were observed between the following protons and carbons: 1'-H and 3-C; 1''-H and 3'-C; 1'''-H and 2''-C; 1''''-H and 4''-C; 1''-H and 4'''-C; 1''''-H and 28-C. The carbon signals in the ¹³C-NMR data of **3** closely resembled those of **2**, except for the signals due to the 4'''-O- α -L-arabinopyranosyl moiety of **3**. On the basis of the evidence, the structure of eupteleasaponin III was characterized as 3-O- α -L-rhamnopyranosyl(1 \rightarrow 2)-[α -L-arabinopyranosyl(1 \rightarrow 4)]- α -L-rhamnopyranosyl(1 \rightarrow 4)]- β -D-glucopyranosyl(1 \rightarrow 3)- β -D-xylopyranosylakebonoic acid 28-O- β -D-glucopyranosyl ester (**3**).

Eupteleasaponin IV (**4**) was also obtained as colorless fine crystals from CHCl₃-MeOH of mp 177–179 °C, liberated D-xylose, D-glucose, L-rhamnose, and L-arabinose on acid hydrolysis.⁴⁾ The IR spectrum of **4** showed absorption bands at 1736 and 1655 cm⁻¹ ascribable to carboxyl and *exo*-methylene groups and strong absorption bands at 3432 and 1075 cm⁻¹ suggestive of its oligoglycosidic structure. In the negative- and positive-ion FAB-MS of **4**, quasimolecular ion peaks were observed at m/z 1157 ($M-H$)⁻, m/z 1159 ($M+H$)⁺, and m/z 1181 ($M+Na$)⁺ and the molecular formula C₅₇H₉₀O₂₄ was determined by high-resolution MS measurement. Furthermore, fragment ion peaks were observed at m/z 1025 ($M-C_5H_9O_4$)⁻, m/z 1011 ($M-C_6H_{11}O_4$)⁻, and m/z 879 ($M-C_{11}H_{20}O_8$)⁻, which were derived by cleavage of the glycoside linkage at the arabinose and/or rhamnose, in the negative-ion FAB-MS of **4**. The ¹H-NMR (pyridine-*d*₅) and ¹³C-NMR (Table 1) spectra⁵⁾ of **4** showed signals due to the akebonoic acid moiety [δ 3.22 (dd-like, 18-H), 3.32 (dd, $J=4.0$, 11.6 Hz, 3-H), 4.75, 4.80 (both s, 29-H₂), 5.48 (br s, 12-H)], a β -D-xylopyranosyl moiety [δ 4.86 (d, $J=5.8$ Hz, 1'-H)], a β -D-glucopyranosyl moiety [δ 5.00 (d, $J=7.6$ Hz, 1''-H)], two α -L-rhamnopyranosyl moieties [δ 1.64 (d, $J=6.1$ Hz, 6'''-H₃), 1.65 (d, $J=6.2$ Hz, 6'''-H₃), 5.80 (br s, 1'''-H), 6.06 (br s, 1'''-H)], and an α -L-arabinopyranosyl moiety [δ 5.21 (d, $J=7.1$ Hz, 1''''-H)]. Alkaline hydrolysis of **3** with 5% aqueous sodium hydroxide liberated eupteleasaponin IV (**4**). Consequently, eupteleasaponin IV was determined to be 3-O- α -L-rhamnopyranosyl(1 \rightarrow 2)-[α -L-arabinopyranosyl(1 \rightarrow 4)]- α -L-rhamnopyranosyl(1 \rightarrow 4)]- β -D-glucopyranosyl(1 \rightarrow 3)- β -D-xylopyranosylakebonoic acid (**4**).

Eupteleasaponin V (**5**) was isolated as colorless fine crystals from CHCl₃-MeOH of mp 175–177 °C. The IR spectrum of **5** showed absorption bands ascribable to hydroxyl, γ -lactone, and *exo*-methylene functions at 3432, 1781, 1655, and 1075 cm⁻¹. The molecular formula C₄₆H₇₀O₁₇ was also determined from the negative- and positive-ion FAB-

MS [m/z 893 ($M-H$)⁻, m/z 917 ($M+Na$)⁺, m/z 939 ($M+2Na-H$)⁺] and by high-resolution MS measurement. Upon acid hydrolysis with 5% aqueous sulfuric acid–1,4-dioxane (1 : 1, v/v), **5** gave D-xylose, D-glucose, and L-rhamnose.⁴⁾ The ¹H-NMR (pyridine-*d*₅) and ¹³C-NMR (Table 1) spectra⁵⁾ of **5** showed signals assignable to a β -D-xylopyranosyl moiety [δ 4.87 (d, $J=4.7$ Hz, 1'-H)], a β -D-glucopyranosyl moiety [δ 5.08 (d, $J=7.9$ Hz, 1''-H)], and an α -L-rhamnopyranosyl moiety [δ 1.64 (d, $J=6.1$ Hz, 6'''-H₃), 6.09 (br s, 1'''-H)], together with a nortriterpene sapogenol moiety [δ 2.35 (dd, $J=3.1$, 13.4 Hz, 18-H), 3.05 (br s, 11-H), 3.15 (d, $J=3.9$ Hz, 12-H), 3.30 (dd, $J=4.0$, 11.9 Hz, 3-H), 4.70, 4.73 (both s, 29-H₂)]. The carbon signals due to the glycosidic structures in the ¹³C-NMR data of **5** were superimposable on those of **1**, whereas the signals of the sapogenol moiety were very similar to those of known eupteleogenin.^{2,7)} The 11,12-epoxy-13,28-lactone structure in the eupteleogenin moiety was elucidated on the basis of H–H COSY and HMBC experiments as shown in Fig. 2. Furthermore, the stereostructure of the eupteleogenin moiety in **5** was clarified by a phase-sensitive ROESY experiment, which showed NOE correlations between the following proton pairs (11 β -H and 25-CH₃; 12 β -H and 11 β , 18 β -H, 26-CH₃). Consequently, the structure of eupteleasaponin V was determined to be 3-O- α -L-rhamnopyranosyl(1 \rightarrow 2)- β -D-glucopyranosyl(1 \rightarrow 3)- β -D-xylopyranosyleupteleogenin (**5**).

Eupteleasaponin V acetate (**6**) was also obtained as colorless fine crystals from CHCl₃-MeOH of mp 180–182 °C and its IR spectrum showed absorption bands due to hydroxyl, ester, γ -lactone, and *exo*-methylene functions. In the negative- and positive-ion FAB-MS of **6**, quasimolecular ion peaks were observed at m/z 937 ($M+H$)⁺, m/z 959 ($M+Na$)⁺, and m/z 935 ($M-H$)⁻ and the molecular formula C₄₈H₇₂O₁₈ was determined by high-resolution MS measurement. Furthermore, fragment ion peaks were observed at m/z 893 ($M-C_2H_3O$)⁻, m/z 789 ($M-C_6H_{11}O_4$)⁻, and m/z 747 ($M-C_8H_{13}O_5$)⁻, which were derived by cleavage of the acetyl and/or glycoside linkage at the rhamnose moiety, were observed in the negative-ion FAB-MS of **6**. Upon acid hydrolysis with 5% aqueous sulfuric acid–1,4-dioxane (1 : 1, v/v), **6** gave D-xylose, D-glucose, and L-rhamnose,⁴⁾ while alkaline treatment of **6** with 0.1% NaOMe–MeOH furnished eupteleasaponin V (**5**). The ¹H-NMR (pyridine-*d*₅) and ¹³C-NMR (Table 2) spectra⁵⁾ of **6** showed signals assignable to an acetyl moiety [δ 2.07 (3H, s, Ac-2)], together with the eupteleasaponin V part [δ 2.35 (dd-like, 18-H), 3.06 (br s, 11-H), 3.15 (d, $J=3.6$ Hz, 12-H), 3.30 (dd, $J=4.0$, 11.2 Hz, 3-H), 4.70, 4.73 (both s, 29-H₂), 4.85 (d, $J=6.9$ Hz, 1'-H), 5.01 (d, $J=7.9$ Hz, 1''-H), 6.06 (br s, 1'''-H)]. The HMBC experiment of **6** showed long-range correlations between the 6''-protons of 3'-O-glucopyranosyl moiety and the acetyl carbonyl carbon. Furthermore, comparison of the ¹³C-NMR data for **6** with those for **5** revealed an acetylation shift around the 6''-position of the glucose moiety in **6**. Consequently, the structure of eupteleasaponin V acetate was elucidated as 3-O- α -L-rhamnopyranosyl(1 \rightarrow 2)-6''-O-acetyl- β -D-glucopyranosyl(1 \rightarrow 3)- β -D-xylopyranosyleupteleogenin (**6**).

Experimental

The following instruments were used to obtain physical data: specific rotations, Horiba SEPA-300 digital polarimeter ($l=5$ cm); IR spectra, Shimadzu FTIR-8100 spectrometer; ¹H-NMR spectra, JNM-LA500 (500 MHz)

spectrometer; ^{13}C -NMR spectra, JNM-LA500 (125 MHz) spectrometers with tetramethylsilane as an internal standard; MS and high-resolution MS, JEOL JMS-SX 102A mass spectrometer; HPLC, Shimadzu LC-10AS chromatograph.

The following experimental conditions were used for chromatography: normal-phase column chromatography; Silica gel BW-200 (Fuji Silysia Chemical, Ltd., 150–350 mesh), reversed-phase column chromatography; Chromatorex ODS DM1020T (Fuji Silysia Chemical, Ltd., 100–200 mesh); TLC, pre-coated TLC plates with Silica gel 60F₂₅₄ (Merck, 0.25 mm) (normal-phase) and Silica gel RP-18 60F₂₅₄ (Merck, 0.25 mm) (reversed-phase); HPTLC, pre-coated TLC plates with Silica gel RP-18 60WF₂₅₄ (Merck, 0.25 mm) (reversed-phase). Detection was done by spraying with 1% $\text{Ce}(\text{SO}_4)_2$ –10% aqueous H_2SO_4 , followed by heating.

Isolation of Eupteleasaponins I (1), II (2), III (3), IV (4), V (5), V Acetate (6), VI, VI Acetate, VII, VIII, IX, X, XI, and XIII from the Fresh Leaves of *E. polyandra* The fresh leaves of *E. polyandra* SIEB. et ZUCC. (2.6 kg, collected in the Kitayama area of Kyoto Prefecture) were cut and extracted three times with MeOH under reflux. Evaporation of the solvent under reduced pressure provided the MeOH extract (275 g, 10.6%), and a part of it (250 g) was partitioned in an AcOEt – H_2O (1 : 1, v/v) mixture. Removal of the solvent from the AcOEt -soluble and H_2O -soluble fractions under reduced pressure yielded AcOEt extract (145 g, 5.6%) and H_2O phase. The H_2O phase was subjected to reversed-phase silica gel column chromatography [Chromatorex DM1020T (Fuji Silysia, Ltd., 2 kg), H_2O → MeOH → CHCl_3] to give the H_2O eluate, MeOH eluate (60.1 g, 2.3%), and CHCl_3 eluate (6.1 g, 0.2%). Normal-phase silica gel column chromatography [BW-200 (Fuji Silysia, Ltd., 1.5 kg), CHCl_3 – MeOH – H_2O (7 : 3 : 1, lower layer→6 : 4 : 1, v/v)→ MeOH] of the MeOH eluate (55 g) gave seven fractions [fr. 1 (2.1 g), fr. 2 (4.9 g), fr. 3 (10.4 g), fr. 4 (9.0 g), fr. 5 (7.8 g), fr. 6 (14.5 g), fr. 7 (6.0 g)]. Fraction 2 (4.7 g) was separated by reversed-phase silica gel column chromatography [120 g, MeOH – H_2O (70 : 30→80 : 20, v/v)→ MeOH], HPLC [YMC-Pack ODS-A (250×20 mm i.d., YMC Co., Ltd.), MeOH –1% aq. AcOH (80 : 20, v/v)], and normal-phase silica gel column chromatography [30 g, CHCl_3 – MeOH – H_2O (7 : 3 : 1, lower layer→6 : 4 : 1, v/v)→ MeOH] to give eupteleasaponins V acetate (6, 372 mg, 0.0143%) and VI acetate (82 mg, 0.0032%). Fraction 3 (10.1 g) was separated by normal-phase silica gel column chromatography [300 g, CHCl_3 – MeOH – H_2O (10 : 3 : 1, lower layer→7 : 3 : 1, lower layer)→ MeOH] to give fr. 3-1 (36 mg), 3-2 (115 mg), 3-3 (2.2 g), 3-4 (2.0 g), 3-5 (3.5 g), 3-6 (1.1 g), and 3-7 (266 mg). Fraction 3-2 (115 mg) was purified by reversed-phase silica gel column chromatography [3 g, MeOH – H_2O (60 : 40, v/v)] and HPLC [MeOH –1% aq. AcOH (70 : 30, v/v)] to give eupteleasaponin VIII acetate (60 mg, 0.0023%). Fraction 3-3 (2.16 g) was purified by HPLC [MeOH –1% aq. AcOH (70 : 30, v/v)] to give eupteleasaponin IX (100 mg, 0.0038%). Fraction 3-5 (3.5 g) was purified by reversed-phase silica gel column chromatography [10 g, MeOH – H_2O (70 : 30, v/v)→ MeOH] and HPLC [MeOH –1% aq. AcOH (80 : 20, v/v)] to give eupteleasaponins V (5, 151 mg, 0.0058%) and VI (116 mg, 0.0045%). Fraction 4 (8.0 g) was separated by reversed-phase silica gel column chromatography [3 g, MeOH – H_2O (70 : 30→80 : 20→85 : 15→90 : 10, v/v)→ MeOH] and HPLC [1] MeOH –1% aq. AcOH (75 : 25, v/v); 2) MeOH –1% aq. AcOH (80 : 20, v/v); 3) CH_3CN –1% aq. AcOH (40 : 60, v/v)] to give eupteleasaponins IX (46 mg, 0.0018%), X (33 mg, 0.0013%), XI (37 mg, 0.0014%), and XII (46 mg, 0.0018%). Fraction 5 (7.0 g) was separated by reversed-phase silica gel column chromatography [200 g, MeOH – H_2O (65 : 35→75 : 25→80 : 20, v/v)→ MeOH] and HPLC [MeOH –1% aq. AcOH (85 : 15, v/v)] to give eupteleasaponins I (1, 55 mg, 0.0021%) and IV (4, 20 mg, 0.0008%). Fraction 6 (500 mg) was purified by HPLC [MeOH – H_2O (75 : 25, v/v)] to give eupteleasaponins II (2, 38 mg, 0.0015%) and III (3, 39 mg, 0.0015%).

Eupteleasaponin I (1): Colorless fine crystals from CHCl_3 – MeOH , mp 201–203 °C, $[\alpha]_D^{28} + 17.7^\circ$ ($c=0.1$, MeOH). High-resolution positive-ion FAB-MS: Calcd for $\text{C}_{52}\text{H}_{82}\text{O}_{21}\text{Na}$ ($\text{M}+\text{Na}$)⁺: 1065.5246. Found: 1065.5258. IR (KBr): 3432, 1744, 1680, 1075 cm^{-1} . ^1H -NMR (500 MHz, pyridine- d_5) δ : 0.86, 1.06, 1.10, 1.20, 1.24 (3H each, all s, 25, 26, 24, 23, 27- H_3), 1.61 (3H, d, $J=5.8$ Hz, 6"- H_3), 3.10 (1H, dd-like, 18-H), 3.30 (1H, dd, $J=3.5$, 11.3 Hz, 3-H), 4.68, 4.74 (1H each, both s, 29- H_2), 4.87 (1H, d, $J=5.2$ Hz, 1'-H), 5.06 (1H, d, $J=7.6$ Hz, 1"-H), 5.43 (1H, brs, 12-H), 6.05 (1H, brs, 1"-H), 6.23 (1H, d, $J=7.0$ Hz, 1"-H). ^{13}C -NMR (125 MHz, pyridine- d_5) δ_C : given in Table 1. Negative-ion FAB-MS: m/z 1041 ($\text{M}-\text{H}$)[−], 895 ($\text{M}-\text{C}_6\text{H}_{11}\text{O}_4$)[−], 879 ($\text{M}-\text{C}_6\text{H}_{11}\text{O}_3$)[−]. Positive-ion FAB-MS: m/z 1065 ($\text{M}+\text{Na}$)⁺.

Eupteleasaponin II (2): Colorless fine crystals from CHCl_3 – MeOH , mp 191–193 °C, $[\alpha]_D^{28} + 14.3^\circ$ ($c=0.1$, MeOH). High-resolution positive-ion FAB-MS: Calcd for $\text{C}_{58}\text{H}_{92}\text{O}_{25}\text{Na}$ ($\text{M}+\text{Na}$)⁺: 1211.5825. Found: 1211.5812.

IR (KBr): 3410, 1736, 1655, 1078 cm^{-1} . ^1H -NMR (500 MHz, pyridine- d_5) δ : 0.87, 1.07, 1.11, 1.21, 1.24 (3H each, all s, 25, 26, 24, 23, 27- H_3), 1.62 (3H, d, $J=6.1$ Hz, 6"- H_3), 1.68 (3H, d, $J=6.1$ Hz, 6"- H_3), 3.11 (1H, dd, $J=4.5$, 12.8 Hz, 18-H), 3.31 (1H, dd, $J=3.9$, 11.9 Hz, 3-H), 4.68, 4.75 (1H each, both s, 29- H_2), 4.85 (1H, d-like, 1'-H), 5.01 (1H, d, $J=7.9$ Hz, 1"-H), 5.44 (1H, brs, 12-H), 5.77 (1H, brs, 1"-H), 6.05 (1H, brs, 1"-H), 6.24 (1H, d, $J=7.9$ Hz, 1"-H). ^{13}C -NMR (125 MHz, pyridine- d_5) δ_C : given in Table 1. Negative-ion FAB-MS: m/z 1187 ($\text{M}-\text{H}$)[−], 1041 ($\text{M}-\text{C}_6\text{H}_{11}\text{O}_4$)[−], 1025 ($\text{M}-\text{C}_6\text{H}_{11}\text{O}_3$)[−]. Positive-ion FAB-MS: m/z 1211 ($\text{M}+\text{Na}$)⁺.

Eupteleasaponin III (3): Colorless fine crystals from CHCl_3 – MeOH , mp 232–235 °C, $[\alpha]_D^{28} + 11.1^\circ$ ($c=0.1$, MeOH). High-resolution positive-ion FAB-MS: Calcd for $\text{C}_{63}\text{H}_{100}\text{O}_{29}\text{Na}$ ($\text{M}+\text{Na}$)⁺: 1343.6248. Found: 1343.6250. IR (KBr): 3432, 1744, 1655, 1075 cm^{-1} . ^1H -NMR (500 MHz, pyridine- d_5) δ : 0.87, 1.07, 1.11, 1.21, 1.24 (3H each, all s, 25, 26, 24, 23, 27- H_3), 1.63 (3H, d, $J=5.8$ Hz, 6"- H_3), 1.64 (3H, d, $J=5.8$ Hz, 6"- H_3), 3.11 (1H, dd, $J=4.9$, 13.1 Hz, 18-H), 3.31 (1H, dd, $J=3.9$, 11.6 Hz, 3-H), 4.70, 4.75 (1H each, both s, 29- H_2), 4.85 (1H, d, $J=5.4$ Hz, 1'-H), 4.99 (1H, d, $J=7.9$ Hz, 1"-H), 5.20 (1H, d, $J=7.4$ Hz, 1"-H), 5.44 (1H, brs, 12-H), 5.78 (1H, brs, 1"-H), 6.03 (1H, brs, 1"-H), 6.24 (1H, d, $J=8.0$ Hz, 1"-H). ^{13}C -NMR (125 MHz, pyridine- d_5) δ_C : given in Table 1. Negative-ion FAB-MS: m/z 1319 ($\text{M}-\text{H}$)[−], 1157 ($\text{M}-\text{C}_6\text{H}_{11}\text{O}_3$)[−]. Positive-ion FAB-MS: m/z 1321 ($\text{M}+\text{H}$)⁺, 1343 ($\text{M}+\text{Na}$)⁺.

Eupteleasaponin IV (4): Colorless fine crystals from CHCl_3 – MeOH , mp 177–179 °C, $[\alpha]_D^{28} + 14.6^\circ$ ($c=0.1$, MeOH). High-resolution positive-ion FAB-MS: Calcd for $\text{C}_{57}\text{H}_{90}\text{O}_{24}\text{Na}$ ($\text{M}+\text{Na}$)⁺: 1181.5720. Found: 1181.5702. IR (KBr): 3432, 1736, 1655, 1075 cm^{-1} . ^1H -NMR (500 MHz, pyridine- d_5) δ : 0.85, 0.98, 1.12, 1.23, 1.28 (3H each, all s, 25, 26, 24, 23, 27- H_3), 1.64 (3H, d, $J=6.1$ Hz, 6"- H_3), 1.65 (3H, d, $J=6.2$ Hz, 6"- H_3), 3.22 (1H, dd-like, 18-H), 3.32 (1H, dd, $J=4.0$, 11.6 Hz, 3-H), 4.75, 4.80 (1H each, both s, 29- H_2), 4.86 (1H, d, $J=5.8$ Hz, 1'-H), 5.00 (1H, d, $J=7.6$ Hz, 1"-H), 5.21 (1H, d, $J=7.1$ Hz, 1"-H), 5.48 (1H, brs, 12-H), 5.80 (1H, brs, 1"-H), 6.06 (1H, brs, 1"-H). ^{13}C -NMR (125 MHz, pyridine- d_5) δ_C : given in Table 1. Negative-ion FAB-MS: m/z 1157 ($\text{M}-\text{H}$)[−], 1025 ($\text{M}-\text{C}_6\text{H}_9\text{O}_4$)[−], 1011 ($\text{M}-\text{C}_6\text{H}_9\text{O}_4$)[−], 879 ($\text{M}-\text{C}_{11}\text{H}_{20}\text{O}_8$)[−]. Positive-ion FAB-MS: m/z 1159 ($\text{M}+\text{H}$)⁺, 1181 ($\text{M}+\text{Na}$)⁺.

Eupteleasaponin V (5): Colorless fine crystals from CHCl_3 – MeOH , mp 175–177 °C, $[\alpha]_D^{27} + 15.5^\circ$ ($c=0.1$, MeOH). High-resolution positive-ion FAB-MS: Calcd for $\text{C}_{46}\text{H}_{70}\text{O}_{17}\text{Na}$ ($\text{M}+\text{Na}$)⁺: 917.4511. Found: 917.4502. IR (KBr): 3432, 1781, 1655, 1075 cm^{-1} . ^1H -NMR (500 MHz, pyridine- d_5) δ : 0.92, 1.19, 1.20 (3H each, all s, 25, 27, 23- H_3), 1.10 (6H, s, 24, 26- H_3), 1.64 (3H, d, $J=6.1$ Hz, 6"- H_3), 2.35 (1H, dd, $J=3.1$, 13.4 Hz, 18-H), 3.05 (1H, brs, 11-H), 3.15 (1H, d, $J=3.9$ Hz, 12-H), 3.30 (1H, dd, $J=4.0$, 11.9 Hz, 3-H), 4.70, 4.73 (1H each, both s, 29- H_2), 4.87 (1H, d, $J=4.7$ Hz, 1'-H), 5.08 (1H, d, $J=7.9$ Hz, 1"-H), 6.09 (1H, brs, 1"-H). ^{13}C -NMR (125 MHz, pyridine- d_5) δ_C : given in Table 1. Negative-ion FAB-MS: m/z 893 ($\text{M}-\text{H}$)[−]. Positive-ion FAB-MS: m/z 917 ($\text{M}+\text{Na}$)⁺, 939 ($\text{M}+2\text{Na}-\text{H}$)⁺.

Eupteleasaponin V Acetate (6): Colorless fine crystals from CHCl_3 – MeOH , mp 180–182 °C, $[\alpha]_D^{26} + 41.5^\circ$ ($c=0.1$, MeOH). High-resolution positive-ion FAB-MS: Calcd for $\text{C}_{48}\text{H}_{72}\text{O}_{18}\text{Na}$ ($\text{M}+\text{Na}$)⁺: 959.4616. Found: 959.4632. IR (KBr): 3432, 1775, 1744, 1649, 1074 cm^{-1} . ^1H -NMR (500 MHz, pyridine- d_5) δ : 0.93 (3H, s, 25- H_3), 1.09, 1.20 (6H each, both s, 24, 26, 23, 27- H_3), 1.62 (3H, d, $J=6.3$ Hz, 6"- H_3), 2.07 (3H, s, Ac-2), 2.35 (1H, dd-like, 18-H), 3.06 (1H, brs, 11-H), 3.15 (1H, d, $J=3.6$ Hz, 12-H), 3.30 (1H, dd, $J=4.0$, 11.2 Hz, 3-H), 4.70, 4.73 (1H each, both s, 29- H_2), 4.85 (1H, d, $J=6.9$ Hz, 1'-H), 5.01 (1H, d, $J=7.9$ Hz, 1"-H), 6.06 (1H, brs, 1"-H). ^{13}C -NMR (125 MHz, pyridine- d_5) δ_C : given in Table 1. Negative-ion FAB-MS: m/z 935 ($\text{M}-\text{H}$)[−], 893 ($\text{M}-\text{C}_2\text{H}_3\text{O}$)[−], 789 ($\text{M}-\text{C}_6\text{H}_{11}\text{O}_4$)[−], 747 ($\text{M}-\text{C}_6\text{H}_{13}\text{O}_3$)[−]. Positive-ion FAB-MS: m/z 937 ($\text{M}+\text{H}$)⁺, 959 ($\text{M}+\text{Na}$)⁺.

Acid Hydrolysis of Eupteleasaponins I (1), II (2), III (3), IV (4), V (5), and V Acetate (6) A solution of eupteleasaponins (1–6, 5 mg each) in 5% aq. H_2SO_4 –1,4-dioxane (1 : 1, v/v, 2 ml) was heated under reflux for 1 h. After cooling, the reaction mixture was neutralized with Amberlite IRA-400 (OH^- form) and residue was removed by filtration. After removal of the solvent from the filtrate *in vacuo*, the residue was transferred to a Sep-Pak C₁₈ cartridge with H_2O and MeOH . The H_2O eluate was concentrated and the residue was treated with L-cysteine methyl ester hydrochloride (4 mg) in pyridine (0.5 ml) at 60 °C for 1 h. After reaction, the solution was treated with *N,O*-bis(trimethylsilyl)trifluoroacetamide (0.2 ml) at 60 °C for 1 h. The supernatant was then subjected to GLC analysis to identify the derivatives of D-xylose (i), D-glucose (ii), L-rhamnose (iii), and L-arabinose (iv): i, ii, and iii from 1–6, iv from 3, 4; GLC conditions: Supelco STBTM-1, 30 m×0.25 mm (i.d.) capillary column, column temperature 230 °C, He flow rate 15 ml/min, t_R : i (19.3 min), ii (24.2 min), iii (15.4 min), iv (15.0 min).

Alkaline Hydrolysis of Eupteleasaponin III (3) with 5% Aqueous

NaOH Giving Eupteleasaponin IV (4) A solution of **3** (20 mg) in 5% aqueous NaOH (2 ml) was stirred under reflux for 2 h. The reaction mixture was neutralized with Dowex HCR W2 (H^+ form) and the resin was removed by filtration. Evaporation of the solvent from filtrate *in vacuo* yielded a product which was separated by reversed-phase silica gel column chromatography [0.5 g, $H_2O \rightarrow MeOH-H_2O$ (90:10, v/v)] to give eupteleasaponin IV (**4**, 17 mg). **4** was identified on the basis of TLC, $[\alpha]_D$, and 1H - and ^{13}C -NMR spectra comparisons with an authentic sample.

Alkaline Hydrolysis of Eupteleasaponin V Acetate (6) with 0.1% NaOMe–MeOH Giving Eupteleasaponin V (5) A solution of **6** (10 mg) in 0.1% NaOMe–MeOH (1 ml) was stirred at room temperature (27°C) for 1 h. The reaction mixture was neutralized with Dowex HCR W2 (H^+ form) and the resin was removed by filtration. Evaporation of the solvent from filtrate *in vacuo* yielded a product, which was separated by normal-phase silica gel column chromatography [0.3 g, $CHCl_3$ –MeOH– H_2O (65:35:10, lower layer, v/v)] to give eupteleasaponin V (**5**, 8 mg). **5** was identified on the basis of TLC, $[\alpha]_D$, and 1H - and ^{13}C -NMR spectra comparisons with an authentic sample.

Gastroprotective Activity Acute gastric lesions were induced by intra-gastric application of ethanol. Briefly, 99.5% ethanol (1.5 ml) was orally administered to 24–26 h fasted rats (about 250 g) by means of a metal orogastric tube. One hour later, the animals were sacrificed by cervical dislocation under ether anesthesia, and the stomach was dissected out and inflated by injection of 10 ml of 1.5% formalin to fix the inner and outer layers of the gastric walls. Subsequently, the stomach was incised along the greater curvature and the lengths of the necrotizing lesions were examined at 10× magnification by 2 or 3 observers unaware of the treatment. Samples were taken orally 1 h prior to the application of ethanol. Omeprazole was used as a reference drug in this experiment.

Statistics Values were expressed as means \pm S.E.M. Statistical significance was assessed by one-way analysis of variance following Dunnett's test

for parametric data.⁸⁾

Acknowledgments The authors are grateful to Dr. Johji Yamahara of Research Institute for Production and Development for his kind help in collecting of the plant materials.

References and Notes

- 1) Part XV: Murakami T., Nakamura J., Matsuda H., Yoshikawa M., *Chem. Pharm. Bull.*, **47**, 1759–1764 (1999).
- 2) a) Goto M., Imai S., Murata T., Noguchi T., Fujioka S., *Yakugaku Zasshi*, **90**, 736–743 (1970); b) Murata T., Imai S., Imanishi M., Goto M., *ibid.*, **90**, 744–751 (1970); c) Goto M., Imai S., Noguchi T., Fujioka S., Murata T., *Shoyakugaku Zasshi*, **24**, 18–20 (1970).
- 3) Murakami T., Kishi A., Matsuda H., Yoshikawa M., *Chem. Pharm. Bull.*, **48** (2000), in press.
- 4) Hara S., Okabe H., Mihashi K., *Chem. Pharm. Bull.*, **34**, 1843–1845 (1986).
- 5) The 1H - and ^{13}C -NMR spectra were assigned on the basis of homo- and hetero-correlation spectroscopy (1H – 1H , 1H – ^{13}C COSY), homo- and hetero-nuclear Hartmann–Hahn spectroscopy (1H – 1H , 1H – ^{13}C HOHAHA), heteronuclear multiple bond connectivity (HMBC), and rotating Overhauser effect spectroscopy (ROESY) experiments.
- 6) Yoshikawa M., Murakami T., Kadoya M., Yamahara J., Matsuda H., *Chem. Pharm. Bull.*, **46**, 1758–1763 (1998).
- 7) a) Kitagawa I., Kitazawa K., Aoyama K., Asanuma M., Yosioka I., *Tetrahedron*, **28**, 923–931 (1972); b) Yoshikawa M., Wang H. K., Tosirisuk V., Kitagawa I., *Chem. Pharm. Bull.*, **30**, 3057–3060 (1982).
- 8) a) Dunnett C. W., *J. Am. Statist. Assoc.*, **75**, 789–795 (1980); b) *Idem*, *ibid.*, **75**, 796–800 (1980).

Chalcone and Stilbene Synthases Expressed in Eucaryotes Exhibit Reduced Cross-Reactivity *in Vitro*

Dae-Yeon SUH,^a Junichi KAGAMI,^a Kazuki FUKUMA,^a Naoko IWANAMI,^a Yasuyo YAMAZAKI,^a Hiroya YURIMOTO,^b Yasuyoshi SAKAI,^b Nobuo KATO,^b Masaaki SHIBUYA,^c Yutaka EBIZUKA,^c and Ushio SANKAWA^{*,a,d}

Faculty of Pharmaceutical Sciences, Toyama Medical and Pharmaceutical University,^a Toyama 930-0194, Division of Applied Life Sciences, Graduate School of Agriculture, Kyoto University,^b Kyoto 606-8502, Graduate School of Pharmaceutical Sciences, The University of Tokyo,^c Tokyo 113-0033, and International Traditional Medicine Research Center, Toyama International Health Complex,^d Toyama 939-8224, Japan.

Received February 18, 2000; accepted March 24, 2000

Chalcone synthase (CHS) and stilbene synthase (STS) catalyze different cyclization reactions of the common tetraketide to give different products, naringenin chalcone and resveratrol, respectively. We have previously observed *in vitro* cross-reaction of CHS and STS overexpressed in *Escherichia coli*, resveratrol production by CHS and chalcone production by STS. When expressed in eucaryotic cells, or in *E. coli* as thioredoxin-fusion proteins, CHS and STS exhibited reduced cross-reaction. STS refolded from inclusion bodies also showed reduced cross-reaction. While addition of bovine serum albumin and pH in the reaction were without noticeable effect, addition of glycerol decreased the cross-reaction of CHS likely due to its stabilizing effect on enzyme conformation. These results were interpreted to provide supporting evidence to our earlier proposition (Yamaguchi T. *et al.*, *FEBS Lett.*, 460, 457–461 (1999)) that the *in vitro* cross-reaction of CHS and STS is due to intrinsic capability of these enzymes to catalyze different types of cyclization, which, in turn, is endowed by conformational flexibility of their active sites.

Key words Chalcone synthase; stilbene synthase; cross-reaction; heterologous expression

Flavonoids protect plants from UV irradiation and are responsible for the color in flowers.¹⁾ The first committed reaction of flavonoid biosynthesis is catalyzed by chalcone synthase (CHS, E.C. 2.3.1.74).²⁾ In contrast, stilbene synthase (STS, E.C. 2.3.1.95), found in a limited number of plants, synthesizes the backbone of the stilbene phytoalexins which have antifungal properties and contribute to the plant defense against pathogens.^{3,4)} Belonging to the CHS superfamily,⁵⁾ CHS and STS share common starting materials with identical stoichiometry (a starter CoA ester from the phenylpropanoid pathway such as *p*-coumaroyl-CoA and three molecules of malonyl-CoA) and use the same decarboxylative condensation mechanism up to the common tetraketide intermediate (Fig. 1). However, they catalyze different ring closure reactions involving different atoms to give rise to differ-

ent products, chalcones and stilbenes, respectively. CHS and STS are homodimers of 43 kDa subunits and the amino acid homology between these two enzymes is more than 65%.

It has been thought that the difference in products of CHS and STS is strictly controlled in nature. However, this distinction was not absolute under certain *in vitro* conditions, as we have previously reported *in vitro* cross-reaction of CHS and STS overexpressed in *Escherichia coli*.⁶⁾ Purified *Pueraria lobata* CHS overexpressed in *E. coli* produced resveratrol, the natural product of STS, up to 4% of its chalcone production, whereas purified *Arachis hypogaea* STS overexpressed in *E. coli* produced naringenin chalcone up to 2% of its resveratrol production. This cross-reaction probably does not occur in nature, but it was taken to reflect close semblance of the active sites of the two enzymes. It has been pro-

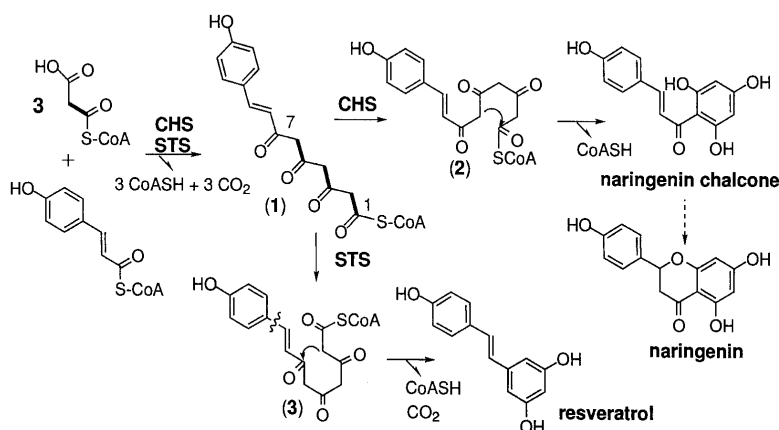


Fig. 1. Reactions Catalyzed by Chalcone Synthase (CHS) and Stilbene Synthase (STS)

Both enzymes catalyze decarboxylative Claisen-type condensations between *p*-coumaroyl-CoA starter unit and three malonyl-CoA extender units leading to the enzyme-bound tetraketide intermediate (1). CHS catalyzes a cyclization reaction (acylation) involving C-1 and C-6 (6→1), producing naringenin chalcone, whereas STS catalyzes a cyclization involving C-2 and C-7 (2→7) accompanied by loss of carboxylate, producing resveratrol. Naringenin chalcone was chemically transformed to naringenin under the reaction conditions used.⁶⁾

* To whom correspondence should be addressed. e-mail: sankawa@toyama-pref-ihc.or.jp

posed that the cyclization reactions in CHS and STS are under pure topological control. Different spatial folding of the linear tetraketide ((2) and (3) in Fig. 1) governed by different surface geometry of the enzyme active sites would lead to different cyclization products.^{7,8)} Then, the observed *in vitro* cross-reaction of CHS and STS might be due to the intrinsic conformational flexibility of the enzyme active sites, which was exposed under non-optimal folding conditions during bacterial overexpression and/or under certain enzyme reaction conditions. Hence, to study the effects of expression hosts and reaction conditions on the cross-reaction, CHS and STS were expressed in eucaryotes, yeasts and insect cells, and also in *E. coli* as thioredoxin-fusion proteins, all of which are expected to provide better environments for adequate folding. In addition, active enzymes were refolded from inclusion bodies produced during overexpression in *E. coli*. The cross-reaction activities of these various enzyme preparations were compared under varying reaction conditions.

Experimental

Heterologous Expression of *P. lobata* CHS and *A. hypogaea* STS in *Candida boidinii* The full-length CHS and STS inserts⁶⁾ were introduced into the *NotI* site of a yeast expression vector pNotel⁹⁾ by blunt-end ligation, yielding pNotel-CHS and pNotel-STS, respectively. Direction of the inserted cDNA was confirmed by restriction enzyme mapping of the plasmids. Transformation of methylotrophic yeast, *C. boidinii* TK62¹⁰⁾ was performed by the modified lithium acetate method as described.¹¹⁾ Colonies of transformants were subcultured at 30 °C for 30 h in 3 ml of YNB medium (0.67% yeast nitrogen base, 2% glucose). The cells were then transferred for induction to 50 ml of YME medium (0.67% yeast nitrogen base, 0.5% yeast extract, 1.5% methanol) and allowed to grow aerobically at 28 °C for 40 h. The cells were harvested by centrifugation at 2000×g for 10 min and disrupted by french-press with a CRYO-PRESS CP-100W (Microtech Nichion, Japan). The cell lysates were suspended in 20 ml of 0.1 M potassium phosphate (pH 7.5) containing 2 mM DTT and cell-free extracts were obtained after centrifugation at 10000×g for 10 min. Colonies that allowed higher expression of CHS and STS were selected by SDS-PAGE analysis of the cell-free extracts. Insertion of the CHS and STS genes into the yeast DNA was further confirmed by PCR using appropriate primers designed from the sequences of 5'- and 3'-ends of the CHS and STS cDNAs. Total yeast DNA purified following a standard method¹²⁾ was used as template.

Heterologous Expression of CHS and STS in *Spodoptera frugiperda* Sf9 Cells The full-length *P. lobata* CHS and *A. hypogaea* STS cDNA were blunt-ligated into the *SmaI* site of the baculovirus expression vector pAcYM1¹³⁾ produced from *Autographa californica* nuclear polyhedrosis virus (AcNPV), yielding pAc-CHS and pAc-STS, respectively. Transfection of *Spodoptera frugiperda* (Sf9) cells with the derived recombinant baculovirus and insect cell culture were performed using the kit (BaculoGold, PharMingen) according to the manufacturer's protocol. The cells were harvested 72 h after infection by centrifugation at 2500×g for 5 min. The precipitated cells were ruptured with a CRYO-PRESS and suspended in a proper volume (4×10⁶ cells/ml) of 0.1 M potassium phosphate (pH 7.5) containing 2 mM DTT. The resulting cell-free extracts (1 mg/ml) were analyzed by SDS-PAGE for enzyme expression and used as enzyme source without further purification.

Expression in *E. coli*, Isolation of Inclusion Bodies and Refolding of Enzymes Construction of expression plasmids pET3d-CHS and pET3d-STS coding *P. lobata* CHS and *A. hypogaea* STS, respectively, their expression in *E. coli* BL21(DE3)pLysE, and purification were previously described.⁶⁾

Inclusion bodies were isolated from the induced *E. coli* cells according to the literature¹⁴⁾ with some modifications. The recombinant *E. coli* cells harboring pET3d-CHS or pET3d-STS were grown at 37 °C for 4 h after induction by 0.4 mM IPTG. Following a freeze/thaw cycle, the cells suspended in 1/25 culture volume of cold 40 mM potassium phosphate buffer (*I*=0.1, pH 7.4), 2 mM EDTA (KPE buffer) were subjected to bursts (3×5 s) of sonication to complete lysis. After centrifugation at 6000×g for 10 min, the inclusion body pellet was sequentially washed with 1/10 culture volume of 0.1% Triton X-100 in KPE buffer and twice with 2 M urea in KPE buffer. The in-

clusion bodies were dissolved in denaturation buffer (8 M urea, 0.1 M β -mercaptoethanol in KPE buffer) to a concentration of 3 mg/ml. Refolding was performed by dialysis at 4 °C against KPE buffer containing 5 mM cysteine with two changes of the buffer for >24 h. The volume and protein concentration of the dialysate were 1 ml and 3.5 to 5 μ g/ml, respectively. The refolded enzymes were finally dialyzed against 0.1 M potassium phosphate (pH 7.4), 2 mM DTT prior to enzyme activity measurements. Protein concentration was determined by Bradford's dye method (BioRad)¹⁵⁾ using Trx-CHS as standard.

Expression in *E. coli* and Purification of Thioredoxin-Fusion Proteins Expression of CHS and STS as thioredoxin-HisTag-fusion proteins (Trx-CHS and Trx-STS) and purification by nickel chelation chromatography will be described elsewhere.

Enzyme Assay and Quantification of Cross-reaction Both CHS and STS reactions were carried out in the presence of 0.1 mM *p*-coumaroyl-CoA and 16.8 μ M [2-¹⁴C]malonyl-CoA (2.2 GBq/mmol, NEN) as substrates and analyzed by radio-TLC and an imaging plate analyzer (BAS2000, Fuji) as described previously.⁶⁾ The specific enzyme activity was expressed in pmol of the product produced/s/mg (pkat/mg).

To study cross-reaction of the enzymes expressed in yeasts and in insect cells, the enzyme reaction was carried out in a total volume of 1 ml containing 100 μ g (yeasts) or 800 μ g (insect cells) of proteins, 0.1 mM *p*-coumaroyl-CoA and 16.8 μ M [2-¹⁴C]malonyl-CoA (37 kBq) in 0.1 M potassium phosphate (pH 7.5) containing 2 mM DTT. After incubation at 37 °C for 15 to 30 min, the reaction was stopped by addition of 50% acetic acid (0.5 ml). The reaction products were then extracted with ethyl acetate (2×1 ml) and the solvent was removed using a spin-vac. The residue was dissolved in 0.5 ml of the HPLC mobile phase (methanol:H₂O:acetic acid=50:50:1, v/v) and authentic naringenin (2 μ g) and resveratrol (1.5 μ g) were added as internal standards. HPLC was performed using a ODS-80TM column (TOSOH, 5 μ m, 4.6×150 mm) at a flow rate of 1 ml/min; compounds were detected by their absorbance at 254 nm. Radioactivity of each 0.5 ml fraction was measured with a β -scintillation counter and the fractions containing the products were pooled. For carrier dilution analysis, recrystallization of the radioactive products with carrier compounds was performed four times in two different solvent systems (methanol and hexane/ethyl acetate) and specific radioactivity was measured after each recrystallization step.

Results and Discussion

Heterologous Expression in Yeasts and Insect Cells

Using a homologous recombination-based integrative transformation system, *P. lobata* CHS and *A. hypogaea* STS were functionally expressed in the methylotrophic yeast, *C. boidinii*. The constructed plasmids, pNotel-CHS and pNotel-STS, were linearized by *Bam*HI, and used for the transformation of *C. boidinii* TK62 (*ura3*). As the inserts were placed under the *C. boidinii* alcohol oxidase (*AOD1*) promoter, the CHS and STS proteins were produced at a high level when methanol was used as the carbon source. About 80% of the Ura⁺ transformants selected (>100) showed the distinctive CHS or STS band on SDS-PAGE, and a single transformant with apparently higher expression was chosen for further study (Fig. 2A). Being non-glycoproteins, CHS and STS expressed in eucaryotes were indistinguishable on SDS-PAGE from the enzymes expressed in *E. coli*. The other 20% of the Ura⁺ transformant colonies seemed not to contain the insert DNA, likely due to gene conversion or double crossing over within the *URA3* locus,¹⁰⁾ and this was confirmed by PCR. Total DNA from yeasts with or without enzyme (CHS or STS) activity was obtained and PCR-amplified using 5'- and 3'-flanking CHS or STS primer.⁶⁾ Only those DNA templates obtained from yeast colonies that exhibited enzyme activity showed the single DNA band corresponding to the full-length insert sequence (data not shown). It has been established that synonymous codons for any single amino acid are not randomly used and that this non-random usage is taxon specific.¹⁶⁾ However, no appreciable change in expression

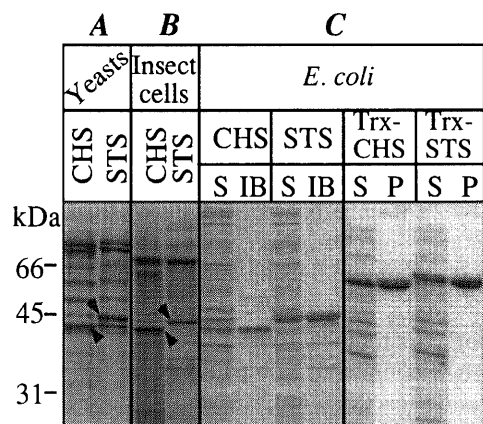


Fig. 2. SDS-PAGE of Various CHS (C) and STS (S) Preparations

A, B: Total cell-free extracts of transformed yeasts (A) and insect cells (B). C: Soluble fractions (S), isolated inclusion bodies (IB) of CHS and STS overexpressed in *E. coli*, and thioredoxin-HisTag-fusion enzymes (Trx-CHS and Trx-STS) purified by Ni^{2+} -chelation chromatography (P). SDS-PAGE was performed on 12% acrylamide minislab gels and the proteins were stained with Coomassie blue R250 (Bio-Rad). The protein bands corresponding to CHS and STS are indicated by arrowheads.

level was observed when codons for a few N-end amino acids of CHS and STS (plant enzymes) were substituted with those preferred by yeast.

CHS and STS were also functionally expressed in *S. frugiperda* Sf9 cells using a baculovirus-based expression system. Both enzymes were overexpressed so as to give major bands on SDS-PAGE when total cell extracts were analyzed (Fig. 2B). Integration of the CHS and STS insert into the viral DNA was also confirmed by nested-PCR using primers derived from internal sequences of the enzymes and viral DNA as template.

Purification of Inclusion Bodies and Refolding of CHS and STS *E. coli* cells were disrupted with a combination of lysozyme (coded for by the pLysE plasmid), a freeze/thaw cycle and sonication. Inclusion bodies, sedimented with low speed centrifugation, were washed with detergent and urea for further purification (Fig. 2C). The inclusion bodies were solubilized in 8 M urea in the presence of β -mercaptoethanol as reducing agent, and refolding was performed by slowly removing the denaturing agent by dialysis. The yield of refolding depends on a number of variables including pH, temperature, protein concentration and additives.¹⁴ Therefore, refolding experiments were performed under varying conditions in order to find better refolding conditions. The yield of active enzyme was higher at pH 7.4 ($I=0.1$) than at pH 9.0 ($I=0.1$); at 4 °C than at 23 °C, and at a protein concentration of 3.5 $\mu\text{g/ml}$ than at 7 $\mu\text{g/ml}$. The addition of free CoA at 0.5 mM in the dialysis buffer had little effect on the yield (data not shown). Cystein at 5 mM was used as redox agent and other redox agents were not tested. The recently solved 3-D structure of alfalfa CHS revealed no disulfide bond even though each CHS subunit contains seven cystein residues.⁸ Specific activities of the refolded enzymes under the chosen conditions ($I=0.1$, pH 7.4, 4 °C, 3.5 $\mu\text{g/ml}$, 5 mM Cys) were: refolded CHS, 2.7 ± 1.8 pkat/mg for naringenin production, and refolded STS, 14 ± 2.8 pkat/mg for resveratrol production. These values were substantially lower (6 to 19%) than those of Trx-fusion enzymes (see below). As a result, reliable cross-reaction data could not be obtained with refolded CHS due to the lower activity.

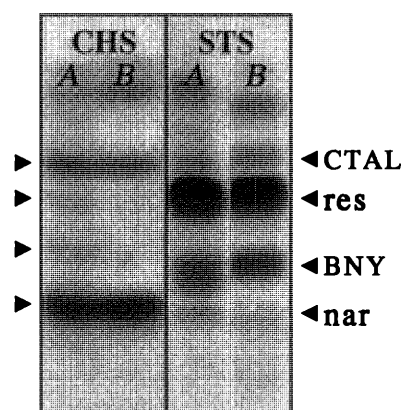


Fig. 3. Radio Thin-Layer Chromatogram of Enzyme Assays Using Trx-CHS and Trx-STS

Enzyme reaction was carried out in 0.1 M potassium phosphate buffer (pH 7.5) in the presence (A) or absence (B) of 2 mM DTT. Cross-reaction products (resveratrol by CHS and naringenin by STS) are visible along with derailment products, bisnoryangonin (BNY) and *p*-coumaroyltriacetic acid lactone (CTAL).⁶

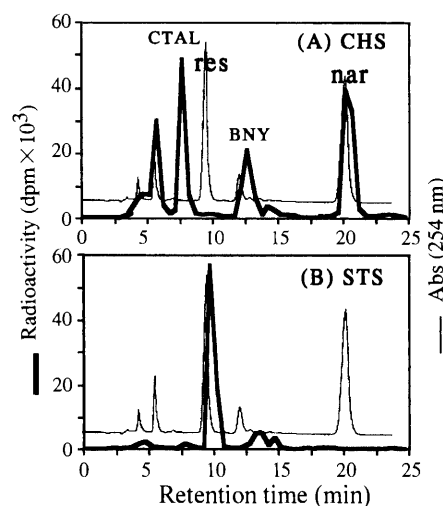


Fig. 4. HPLC Analysis of Reaction Products Produced by *P. lobata* Chalcone Synthase (A) and *A. hypogaea* Stilbene Synthase (B) Overexpressed in *S. frugiperda* Sf9 Cells

Authentic resveratrol and naringenin were added to the reaction products to aid detection by UV (thin line). Radioactivity (thick line) of each fraction (0.5 ml) was measured and fractions corresponding to the cross-reaction products (resveratrol for CHS and naringenin for STS) as well as the natural products were pooled and used for carrier dilution analysis.

Expression and Purification of Thioredoxin-Fusion Proteins Trx-CHS and Trx-STS were overexpressed and purified to apparent homogeneity by a single step of Ni^{2+} -chelation chromatography (Fig. 2C). When expressed as thioredoxin-fusion proteins (60 kDa), more enzymes were recovered in soluble fractions allowing higher yields of purified enzymes (8 mg/100 ml culture). The specific activities of purified Trx-CHS and Trx-STS were 49 ± 1.8 pkat/mg (for naringenin production) and 75 ± 16 pkat/mg (for resveratrol production), respectively.

Cross-Reaction Cross-reaction was analyzed both by radio-TLC (Fig. 3) and HPLC (Fig. 4) followed by carrier dilution assay. In radio-TLC analysis, cross-reaction was calculated from the amounts of radioactive products quantitated with an imaging plate analyzer using standards of known specific radioactivity. In carrier dilution assay, four successive rounds of recrystallization of radioactive product in the

Table 1. Cross-Reaction Obtained from Carrier-Dilution Assays

Enzyme	Yeasts	Expression hosts Insect cells	<i>E. coli</i> ^{a)}
CHS	1.2%	1.4%	2.7—4.2%
STS	0.48%	0.36%	1.4—2.3%

a) Values from ref. 6. Enzyme reaction was carried out in 0.1 M potassium phosphate, pH 7.5, containing 2 mM DTT as described in Experimental.

Table 2. Cross-Reaction under Various Reaction Conditions Calculated from Radio-TLC

Enzyme	Reaction conditions	
	0.1 M potassium phosphate, pH 7.5, 2 mM DTT	0.1 M potassium phosphate, pH 7.2, 10% glycerol, 1 mM DTT
CHS expressed in <i>E. coli</i> ^{a)}	8.0±3.3 ^{d)}	
CHS expressed in yeasts	3.4±0.34 ^{d)}	
Trx-CHS ^{b)}	6.0±2.4	4.3±0.94
STS expressed in <i>E. coli</i> ^{a)}	4.1±0.64 ^{d,e)}	
STS expressed in yeasts	1.2±0.13 ^{d)}	
Refolded STS ^{c)}	2.6±0.49 ^{e)}	
Trx-STS ^{b)}	2.7±1.6 ^{e)}	2.0±0.25

Data are expressed as mean±S.D. (n=3—6). a) Purified enzymes overexpressed in *E. coli* BL21.⁶⁾ b) Purified thioredoxin-HisTag-fusion enzymes overexpressed in *E. coli* AD494. c) Refolded enzyme from inclusion bodies isolated from *E. coli* BL21. d, e) Significantly different at $p<0.01$, ^{d)} $p<0.05$, ^{e)} (Student's *t*-test).

presence of a non-labeled carrier compound yielded crystals of constant specific radioactivity. For example, for CHS expressed in yeasts, the specific radioactivity of naringenin produced was 1.2×10^5 dpm/mmol (methanol), 1.1×10^5 (methanol), 1.1×10^5 (methanol) and 1.0×10^5 (ethyl acetate/hexane), whereas that of resveratrol produced was 1.5×10^3 dpm/mmol (methanol), 1.3×10^3 (methanol), 1.3×10^3 (methanol) and 1.4×10^3 (ethyl acetate/hexane), yielding 1.2% of cross-reaction.

Cross-reactions of CHS and STS obtained using different expression systems were compared under otherwise identical reaction conditions. Both CHS and STS expressed in eucaryotic cells showed reduced cross-reaction as compared to the enzymes overexpressed in *E. coli* when analyzed by carrier dilution assay (Table 1) and radio-TLC (Table 2). The higher values obtained from radio-TLC were attributed to band tailing and high backgrounds. Similarly, the Trx-fusion enzymes and *in vitro* refolded STS also showed lower values of cross-reaction than those of purified *E. coli* overexpressed in intact enzymes (Table 2). We also studied cross-reaction by the Trx-fusion enzymes under varying reaction conditions, and the cross-reaction of CHS was found to be reaction condition-dependent. While protein concentration controlled by BSA and pH were without noticeable effect, addition of gly-

cerol showed a tendency to decrease the cross-reaction, likely due to its stabilizing effect on enzyme conformation. These results were interpreted to provide supporting evidence to our earlier proposition⁶⁾: that *in vitro* cross-reaction of CHS and STS are due to the intrinsic capability of these enzymes to catalyze different types of cyclization, which, in turn, is endowed by conformational flexibility of their active sites. The higher cross-reaction observed with the enzymes overexpressed in *E. coli* could thus be attributed to greater manifestation of this otherwise cryptic capability under a non-optimal folding environment during bacterial overexpression. This notion is completely compatible with the proposal that the cyclization reactions in CHS and STS are modulated by active site geometry.^{7,8)} Overexpression in *E. coli* often leads to misfolding especially for membrane-associated eucaryotic proteins, as bacteria lack intracellular membrane environments that may be necessary for efficient and accurate folding.¹⁷⁾ Both CHS and STS are shown to be weakly membrane-associated in the plant cells.^{4,18,19)}

Acknowledgements The authors are grateful to the Ministry of Education, Science, Sports and Culture of Japan for Grants-in Aid for Scientific Research (B) (No. 09044212) and (C) (No. 10680564). D.-Y. Suh is a recipient of a fellowship (TBRF-98-10) from the Tokyo Biochemistry Research Foundation.

References

- 1) Harborne J. B. (ed), "The Flavonoids, Advances in Research," Chapman & Hall, London, 1994.
- 2) Kreuzaler F., Hahlbrock K., *FEBS Lett.*, **28**, 69—72 (1972).
- 3) Gorham J., "The Biochemistry of the Stilbenoids," Chapman & Hall, London, 1995.
- 4) Rupprich N., Kindl H., *Hoppe-Seyler's Z. Physiol. Chem.*, **359**, 165—172 (1978).
- 5) Schröder J., *Trends. Plant Sci.*, **2**, 373—378 (1997).
- 6) Yamaguchi T., Kurosaki F., Suh D.-Y., Sankawa U., Nishioka M., Akiyama T., Shibuya M., Ebizuka Y., *FEBS Lett.*, **460**, 457—461 (1999).
- 7) Schöppner A., Kindl H., *J. Biol. Chem.*, **259**, 6806—6811 (1984).
- 8) Ferrer J.-L., Jez J. M., Bowman M. E., Dixon R. A., Noel J. P., *Nat. Str. Biol.*, **6**, 775—784 (1999).
- 9) Sakai Y., Akiyama M., Kondoh H., Shibano Y., Kato N., *Biochim. Biophys. Acta*, **1308**, 81—87 (1996).
- 10) Sakai Y., Kazarimoto T., Tani Y., *J. Bacteriol.*, **173**, 7458—7463 (1991).
- 11) Sakai Y., Goh T. K., Tani Y., *J. Bacteriol.*, **175**, 3556—3562 (1993).
- 12) Moreno S., Klar A., Nurse P., *Methods Enzymol.*, **194**, 795—823 (1991).
- 13) Matsuura Y., Possee R. D., Overton H. A., Bishop D. H. L., *J. Gen. Virol.*, **68**, 1233—1250 (1987).
- 14) Marston A. O., *Biochem. J.*, **240**, 1—12 (1986).
- 15) Bradford M. M., *Anal. Biochem.*, **72**, 248—254 (1976).
- 16) Sharp P. M., Li W.-H., *Nucleic Acids Res.*, **15**, 1281—1295 (1987).
- 17) Moreno S., Klar A., Nurse P., *Methods Enzymol.*, **194**, 795—823 (1991).
- 18) Hrazdina G., Zobel A. M., Hoch H. C., *Proc. Natl. Acad. Sci. U.S.A.*, **84**, 8966—8970 (1987).
- 19) Kreuzaler F., Hahlbrock K., *Arch. Biochem. Biophys.*, **169**, 84—90 (1975).

Prolyl Endopeptidase Inhibitory Activity of Fourteen Kampo Formulas and Inhibitory Constituents of Tokaku-joki-to (桃核承氣湯)

Wenzhe FAN, Yasuhiro TEZUKA, and Shigetoshi KADOTA*

Institute of Natural Medicine, Toyama Medical and Pharmaceutical University, 2630-Sugitani, Toyama 930-0194, Japan.

Received February 21, 2000; accepted March 24, 2000

Prolyl endopeptidase (PEP, EC 3.4.21.26) is an enzyme playing a role in the metabolism of proline-containing neuropeptides which have been suggested to be involved in learning and memory processes. In screening for PEP inhibitors from fourteen traditional Kampo formulas, we found that Tokaku-joki-to (桃核承氣湯) shows a significant inhibitory activity. Examination of the constituents of the Kampo formula resulted in the isolation of two new compounds, *cis*-3,5,4'-trihydroxystilbene 4'-*O*- β -D-(6-*O*-galloyl)glucopyranoside (10) and 4-(4-hydroxyphenyl)-2-butanone 4'-*O*- β -D-(6-*O*-galloyl-2-*O*-cinnamoyl)glucopyranoside (16), along with twenty-five known compounds, cinnamic acid (1), protocatechuic acid (2), gallic acid (3), torachrysone 8-*O*- β -D-glucoside (4), emodin (5), emodin 8-*O*- β -D-glucoside (6), 3,5,4'-trihydroxystilbene 4'-*O*- β -D-glucopyranoside (7), 3,5,4'-trihydroxystilbene 4'-*O*- β -D-(2-*O*-galloyl)glucopyranoside (8), 3,5,4'-trihydroxystilbene 4'-*O*- β -D-(6-*O*-galloyl)glucopyranoside (9), 4-(4-hydroxyphenyl)-2-butanone 4'-*O*- β -D-glucopyranoside (11), isolindleyin (12), lindleyin (13), 4-(4-hydroxyphenyl)-2-butanone 4'-*O*- β -D-(2,6-di-*O*-galloyl)glucopyranoside (14), 4-(4-hydroxyphenyl)-2-butanone 4'-*O*- β -D-(2-*O*-galloyl-6-*O*-cinnamoyl)glucopyranoside (15), 1-*O*-galloylglucose (17), 1,2,6-tri-*O*-galloylglucose (18), gallic acid 4-*O*- β -D-(6-*O*-galloyl)glucopyranoside (19), liquiritigenin (20), liquiritigenin 4'-*O*- β -D-glucoside (21), liquiritigenin 7,4'-diglucoside (22), liquiritigenin 4'-*O*- β -D-apiofuranosyl-(1 \rightarrow 2)- β -D-glucopyranoside (23), licuroside (24), (–)-epicatechin (25), (–)-epicatechin 3-*O*-gallate (26) and (+)-catechin (27). Among these compounds, twelve (7–10, 14–16, 18, 19, 24–26) showed noncompetitive inhibition with an IC₅₀ of 22.9, 3.0, 14.9, 2.8, 10.5, 0.69, 8.2, 0.44, 9.39, 26.5, 28.1 and 0.052 μ M, respectively.

Key words prolyl endopeptidase inhibitor; Tokaku-joki-to (桃核承氣湯); Kampo formula; *cis*-3,5,4'-trihydroxystilbene 4'-*O*- β -D-(6-*O*-galloyl)glucopyranoside; 4-(4-hydroxyphenyl)-2-butanone 4'-*O*- β -D-(6-*O*-galloyl-2-*O*-cinnamoyl)glucopyranoside

Prolyl endopeptidase (PEP, EC 3.4.21.26) is a serine protease and specifically cleaves the peptide bonds at the carboxyl side of proline residues.¹⁾ This enzyme was first discovered in the human uterus as an oxytocin-degrading enzyme²⁾ and was thereafter found to widely distribute in various tissues, particularly in human brain.³⁾ In the central nervous system, PEP is suspected to hydrolyze proline-containing neuropeptides, which are suggested to participate in learning and memory processes, *e.g.*, vasopressin, substance P and thyrotropin-releasing hormone (TRH).⁴⁾ Moreover, this enzyme was proposed to be essential for the morphogenetic process of imaginal discs and to participate in DNA synthesis in insect cell proliferation.⁵⁾

Abnormal PEP level is considered to be related to neuropathological disorders, such as post-traumatic stress disorder, major depression, mania, schizophrenia and senile dementia of the Alzheimer's type.⁶⁾ In addition, PEP-like immunoreactivity has been detected in the hippocampus of senescence-accelerated mouse,⁷⁾ and PEP activity is reported to be significantly high in Alzheimer's patients.⁸⁾ Specific inhibitors of PEP are thus expected to have anti-amnesic effects, and many inhibitors have been synthesized⁹⁾ or identified from natural resources¹⁰⁾ as candidates for such neuropathological disorders. Studies on the inhibitors have suggested that they could improve memory by blocking the metabolism of endogenous neuropeptides and have possible potential as anti-amnesic drugs for preventing and/or curing amnesia.¹¹⁾

In our search for bioactive constituents in natural medicines, we made a screening for PEP inhibitory activity of crude drugs contained in Kampo formulas having a kidney-tonifying effect¹²⁾ and reported the inhibitory constituents of

Sheng-di-hong-jing-tian (聖地紅景天, underground part of *Rhodiola sacra*).¹³⁾ The combination of the crude drugs, *i.e.*, Kampo formula, is generally used in clinics. In our continuing study we examined the PEP inhibitory activity of fourteen Kampo formulas, and we describe here the activity of these fourteen formulas and the constituents of Tokaku-joki-to (桃核承氣湯) which showed the strongest activity.

PEP Inhibitory Activity of Fourteen Kampo Formulas

In the theory of traditional Chinese medicine, Kampo, amnesia or dementia is believed to be derived from breathing stagnation and blood stasis (the term of Kampo, ki-tai-ketsu-o, 氣滯血瘀) or insufficiency of the liver and kidney (kan-jin-fusoku, 肝腎不足). Thus, a blood-quickenening and stasis-transforming formula (kakketsu-ka-o-zai, 活血化癥劑) or a kidney tonifying formula (hojin-zai, 補腎劑) is clinically used. We selected fourteen Kampo formulas from among "kakketsu-ka-o-zai" and "hojin-zai" and examined their PEP inhibitory activity. As can be seen in Table 1, only Tokaku-joki-to, a kind of "kakketsu-ka-o-zai", showed strong activity.

Constituents of Tokaku-joki-to Powder of Tokaku-joki-to was suspended on distilled water and separated into CHCl₃-, EtOAc-, BuOH- and H₂O-soluble fractions. The EtOAc-soluble (IC₅₀, 1.75 μ g/ml) and BuOH-soluble (IC₅₀, 7.39 μ g/ml) fractions showed strong inhibitory activity (Chart 1). Chemical examination was made of these fractions and two new compounds, 10 and 16, were isolated together with twenty-five known ones. The known compounds were identified by analyses of the spectroscopic data and comparison of their data with those in the literatures to be: cinnamic acid (1), protocatechuic acid (2), gallic acid (3), torachrysone 8-*O*- β -D-glucoside (4),¹⁴⁾ emodin (5),¹⁵⁾ emodin 8-*O*- β -D-glu-

* To whom correspondence should be addressed. e-mail: Kadota@ms.toyama-mpu.ac.jp

Table 1. Constituents of Kampo Formulas Used in This Study and Their PEP Inhibitory Activity at 100 μ g/ml

Formula	Constituent ^{a)}	Inhibition (%) ^{b)}
Kakkon-to (葛根湯)	Puerariae Radix (4), Cinnamomi Cortex (2), Ephedrae Herba (3), Paeoniae Radix (2), Glycyrrhizae Radix (2), Zingiberis Rhizoma (2), Zizyphi Fructus (3).	15.6 \pm 2.7
Zokumei-to (統命湯)	Ginseng Radix (3), Cinnamomi Cortex (3), Ephedrae Herba (3), Gypsum Fibrosum (6), Glycyrrhizae Radix (2), Zingiberis Rhizoma (2), Chungxiong Rhizoma (2), Angelicae Radix (3), Armeniacae Semen (4).	-11.1 \pm 3.4
Ninjin-to (人參湯)	Ginseng Radix (3), Atractylodis Rhizoma (3), Glycyrrhizae Radix (3), Zingiberis Rhizoma (3).	-9.8 \pm 3.3
Unsei-in (溫清飲)	Angelicae Radix (3), Paeoniae Radix (3), Rehmanniae Radix (3), Coptidis Rhizoma (1.5), Scutellariae Radix (3), Gardeniae Fructus (2), Chungxiong Rhizoma (3).	-15.6 \pm 4.5
Shimotsu-to (四物湯)	Angelicae Radix (3), Paeoniae Radix (2), Chungxiong Rhizoma (2), Rehmanniae Radix (3).	-10.7 \pm 2.3
Tokaku-joki-to (桃核承氣湯)	Rhei Rhizoma (3), Cinnamomi Cortex (4), Persicae Semen (5), Sulfas Natrii (2), Glycyrrhizae Radix (1.5).	99.6 \pm 0.2
Hochu-ekki-to (補中益氣湯)	Ginseng Radix (3), Bupleuri Radix (2), Atractylodis Rhizoma (4), Glycyrrhizae Radix (1.5), Astragali Radix (4), Citri Leiocarpae Exocarpium (2), Zingiberis Rhizoma (1.5), Zizyphi Fructus (2).	-1.9 \pm 0.5
Hachimi-gan-ryo (八味丸料)	Poria (3), Cinnamomi Cortex (1), Rehmanniae Radix (3), Corni Fructus (3), Dioscoreae Rhizoma (3), Moutan Cortex (3), Aconiti Tuber (1.5), Alismatis Rhizoma (3).	2.6 \pm 0.8
Toki-shakuyaku-san (当歸芍藥散)	Angelicae Radix (3), Paeoniae Radix (4), Chungxiong Rhizoma (3), Poria (4), Alismatis Rhizoma (4), Atractylodis Rhizoma (4).	0.8 \pm 2.0
Kami-shoyo-san (加味逍遙散)	Bupleuri Radix (3), Angelicae Radix (3), Atractylodis Rhizoma (3), Moutan Cortex (1.5), Paeoniae Radix (3), Menthae Herba (1), Glycyrrhizae Radix (1.5), Zingiberis Rhizoma (1), Poria (3), Gardeniae Fructus (2).	3.9 \pm 1.6
San-o-shashin-to (三黃瀉心湯)	Rhei Rhizoma (2), Coptidis Rhizoma (1), Scutellariae Radix (1).	30.9 \pm 10
Oren-gedoku-to (黃連解毒湯)	Phellodendri Cortex (1.5), Coptidis Rhizoma (2), Scutellariae Radix (3), Gardeniae Fructus (2).	26.4 \pm 9.4
Yokukan-san-ka-chinpi-to (抑肝散加陳皮湯)	Uncariae Ramulus et Uncus (3), Glycyrrhizae Radix (1.5), Atractylodis Rhizoma (4), Bupleuri Radix (2), Angelicae Radix (3), Chungxiong Rhizoma (3), Pinelliae Rhizoma (5), Poria (4), Citri Leiocarpae Exocarpium (3).	19.3 \pm 6.2
Choto-san (釣藤散)	Uncariae Ramulus et Uncus (3), Ginseng Radix (2), Glycyrrhizae Radix (1), Zingiberis Rhizoma (1.5), Poria (3), Pinelliae Rhizoma (3), Ophiopogonis Radix (3), Ledebouriellae Radix (2), Citri Leiocarpae Exocarpium (3), Gypsum Fibrosum (5), Chrysanthemi Flos (2).	16.7 \pm 9.1

a) Ratio of the crude drugs in parentheses. b) Mean \pm S.D. (n=3).

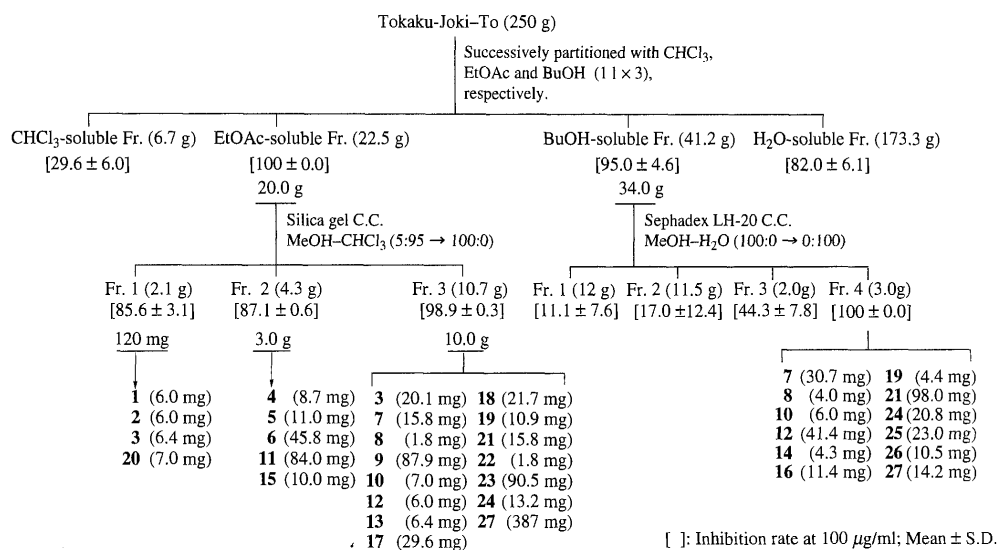


Chart 1

copyranoside (6),¹⁶⁾ *trans*-3,5,4'-trihydroxystilbene 4'-*O*- β -D-glucopyranoside (7),¹⁷⁾ *trans*-3,5,4'-trihydroxystilbene 4'-*O*- β -D-(2-*O*-galloyl)glucopyranoside (8),¹⁸⁾ *trans*-3,5,4'-trihydroxystilbene 4'-*O*- β -D-(6-*O*-galloyl)glucopyranoside (9),¹⁸⁾ 4-(4-hydroxyphenyl)-2-butanone 4'-*O*- β -D-glucopyranoside (11),¹⁹⁾ isolindleyin (12),²⁰⁾ lindleyin (13),¹⁹⁾ 4-(4-hydroxyphenyl)-2-butanone 4'-*O*- β -D-(2,6-di-*O*-galloyl)glucopyranoside (14),²⁰⁾ 4-(4'-hydroxyphenyl)-2-butanone 4'-*O*- β -D-(2-

O-galloyl-6-*O*-cinnamoyl)glucopyranoside (15),²⁰⁾ 1-*O*-galloylglucose (17),¹⁹⁾ 1,2,6-tri-*O*-galloylglucose (18),¹⁹⁾ gallic acid 4-*O*- β -D-(6-*O*-galloyl)glucopyranoside (19),¹⁸⁾ liquiritigenin (20),²¹⁾ liquiritigenin 4'-*O*- β -D-glucopyranoside (21),²¹⁾ liquiritigenin 7,4'-diglucoside (22),²¹⁾ liquiritigenin 4'-*O*- β -D-apiofuranosyl-(1 \rightarrow 2)- β -D-glucopyranoside (23),²²⁾ licuroside (24),²²⁾ (-)-epicatechin (25), (-)-epicatechin 3-*O*-gal-late (26) and (+)-catechin (27) (Chart 2).

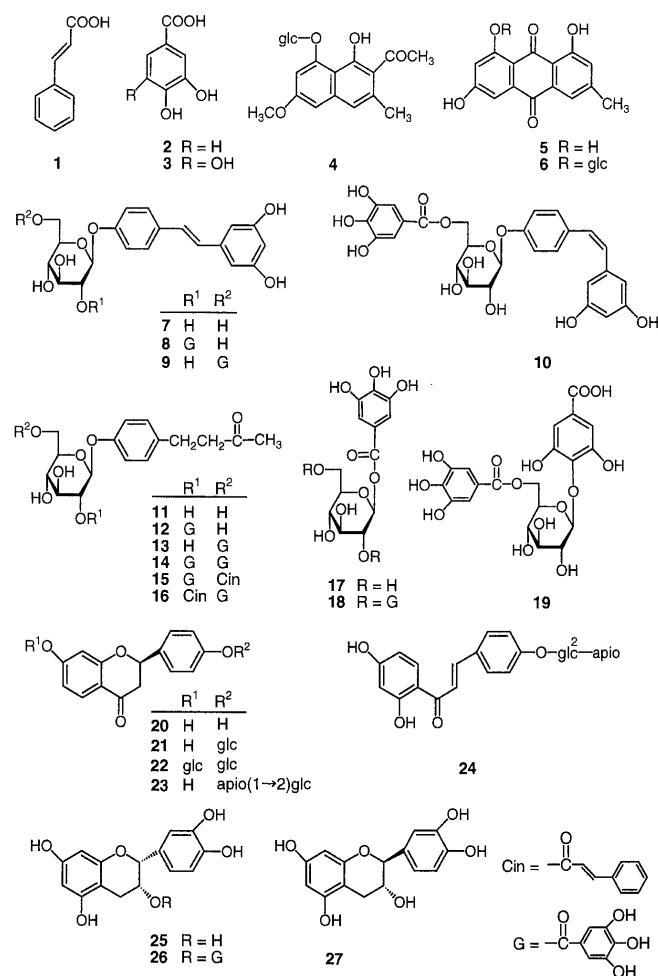
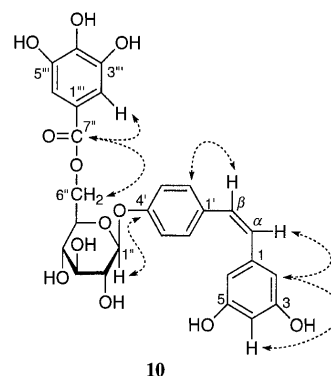


Chart 2

Compound **10** was isolated as a pale brown powder having $[\alpha]_D^{25}$ of -124° ($c=0.027$, MeOH). The negative ion FAB-MS of **10** showed a quasimolecular ion at m/z 541 ($M-H$)⁻, and high-resolution FAB-MS (HR-FAB-MS) analysis of the quasimolecular ion revealed the molecular formula of **10** to be $C_{27}H_{26}O_{12}$. The 1H - and ^{13}C -NMR spectra of **10** were similar to those of stilbenes **7**–**9**, especially of **9** (Table 2), and indicated the presence of a stilbene, a glucose and a galloyl moiety. The coupling constant ($J=12$ Hz) of the olefinic protons ($H-\alpha$, $H-\beta$) of **10** was smaller than that ($J=16.5$ Hz) of other compounds, indicating **10** to have *cis*-olefin.²³ The glucose moiety was concluded to be a β anomer from the coupling constant ($J=7.8$ Hz) of the anomeric proton. In the field gradient-pulsed (FG-pulsed) heteronuclear multiple bond correlation (HMBC) spectrum (Fig. 1), long-range correlations were observed between the anomeric proton (δ 4.88) and C-4' of the stilbene moiety (δ 102.4) and between the ester carbonyl carbon of the gallic acid moiety (δ 168.2)

Fig. 1. Long-Range Correlations Observed in the FG-Pulsed HMBC spectrum of **10**Table 2. 1H - and ^{13}C -NMR Data for Stilbene Derivatives **7**–**10** in CD_3OD

		7		8		9		10	
		δ_H	δ_C	δ_H	δ_C	δ_H	δ_C	δ_H	δ_C
Stilbene moiety									
1			141.0		140.9		141.1		140.8
2,6	6.45 d (2.0)		106.0	6.44 d (2.0)	105.9	6.50 d (2.0)	106.1	6.18 d (2.0)	108.2
3,5			159.6		159.6		159.6		159.6
4	6.17 t (2.0)		103.0	6.16 t (2.0)	103.0	6.17 t (2.0)	102.9	6.10 t (2.0)	102.4
α	7.01 d (16.5)		128.9	6.96 d (16.5)	128.7	6.92 d (16.5)	128.6	6.41 d (12.0)	130.5
β	6.85 d (16.5)		128.6	6.85 d (16.5)	128.6	6.80 d (16.5)	128.6	6.35 d (12.0)	130.4
1'			133.2		133.6		133.2		132.8
2',6'	7.44 d (8.0)		128.6	7.39 d (8.0)	128.7	7.29 d (8.0)	128.8	7.11 d (8.0)	131.3
3',5'	7.07 d (8.0)		117.9	7.09 d (8.0)	117.9	7.01 d (8.0)	117.9	6.89 d (8.0)	117.7
4'			158.6		158.5		158.4		157.9
Glucose moiety									
1''	4.92 d (7.8)		102.2	5.16 d (7.8)	103.0	4.87 d (7.8)	102.3	4.88 d (7.8)	102.1
2''			74.9	5.17 dd (8.0, 7.8)	78.4		74.9		74.8
3''	3.50–3.60 m (4H)		78.1 ^{a)}	3.50–3.60 m (2H)	75.3	3.35–3.12 m (3H)	78.0	3.44–3.52 m (3H)	77.9
4''			71.3		71.6		71.9		71.6
5''			78.0 ^{a)}	3.76 ddd (8.0, 5.0, 2.0)	76.2	3.78 ddd (8.0, 5.0, 2.0)	75.7	3.73 ddd (8.0, 5.0, 2.0)	75.6
6''	3.72 dd (12.0, 5.0)		62.5	3.77 dd (12.0, 5.0)	62.5	4.44 dd (12.0, 5.0)	64.9	4.42 dd (12.0, 5.0)	64.7
	3.91 dd (12.0, 2.0)			3.95 dd (12.0, 2.0)		4.60 dd (12.0, 2.0)		4.55 dd (12.0, 2.0)	
Galloyl moiety									
1'''					121.4		121.5		121.4
2'''				7.13 s	110.3	7.15 s	110.4	7.09 s	110.3
3'''					146.4		146.6		146.5
4'''					140.9		140.0		139.9
7'''					167.7		168.2		168.2

a) May be interchanged.

Table 3. ^1H - and ^{13}C -NMR Data for Phenylbutanones **11**–**16** in CD_3OD

	11		12		13	
	δ_{H}	δ_{C}	δ_{H}	δ_{C}	δ_{H}	δ_{C}
Phenylbutanone moiety						
1	2.09 s	30.7	2.08 s	30.7	2.09 s	30.0
2		211.9		211.9		211.5
3	2.76 m	30.7	2.74 m	30.7	2.68 m	29.9
4		46.7		46.7		45.8
1'		137.1		137.6		136.3
2',6'	7.10 d (8.5)	131.0	7.05 d (8.5)	131.1	6.97 d (8.5)	130.3
3',5'	7.00 d (8.5)	118.6	6.88 d (8.5)	118.9	6.93 d (8.5)	118.1
4'		158.1		158.2		157.2
Glucose moiety						
1''	4.85 d (7.8)	103.1	5.10 d (8.0)	102.2	4.80 d (7.8)	102.4
2''		75.6	5.12 d (9.0, 8.0)	79.2		75.6
3''	3.35–3.60 m (4H)	78.7	3.50–3.60 m (3H)	76.9	3.37–3.50 m (4H)	78.1
4''		72.1		72.4		72.1
5''		78.6		77.0		75.4
6''	3.70 dd (12.0, 4.0) 3.88 dd (12.0, 2.2)	63.2	3.75 dd (12.0, 7.6) 3.94 dd (12.0, 2.2)	63.6	4.41 dd (12.0, 8.0) 4.57 dd (12.0, 2.2)	65.0
Galloyl moiety						
1'''				122.2		121.5
2''',6'''			7.08 s	111.1	7.10 s	110.4
3''',5'''				147.3		146.6
4'''				140.7		139.9
7'''				168.4		168.2
Cinnamoyl moiety						
1''''						
2''',6'''						
3''',5'''						
4''''						
7''''						
8''''						
9''''						

	14		15		16	
	δ_{H}	δ_{C}	δ_{H}	δ_{C}	δ_{H}	δ_{C}
Phenylbutanone moiety						
1	2.09 s	29.9	2.04 s	29.9	2.03 s	30.6
2		210.6		210.9		211.9
3	2.69 m	30.0	2.61 m	29.9	2.58 m	30.6
4		45.8		45.7		46.6
1'		138.6		136.8		137.6
2',6'	6.94 d (8.5)	130.2	6.96 d (8.5)	130.2	6.97 d (8.5)	130.1
3',5'	6.82 d (8.5)	118.0	7.49 d (8.5)	118.2	6.85 d (8.5)	119.0
4'		157.0		157.1		157.9
Glucose moiety						
1''	5.07 d (8.0)	101.2	5.13 d (8.0)	101.2	5.10 d (8.0)	102.0
2''	5.16 dd (9.0, 8.0)	77.0	5.18 dd (9.0, 8.0)	76.2	5.17 d (9.0, 8.0)	77.0
3''	3.50–3.60 m (3H)	76.3	3.50–3.60 m (3H)	75.7	3.50–3.60 m (3H)	76.4
4''		72.2		72.2		72.9
5''		75.3		75.2		76.0
6''	4.47 dd (12.0, 7.6) 4.65 dd (12.0, 2.2)	64.6	4.43 dd (12.0, 7.5) 4.58 dd (12.0, 2.2)	64.6	4.45 dd (12.0, 7.0) 4.60 dd (12.0, 2.2)	65.5
Galloyl moiety						
1'''		121.4, 121.6		121.4		122.2
2''',6'''	7.05 s; 7.13 s	110.4, 110.3	7.08 s	110.3	7.09 s	111.2
3''',5'''		146.7, 146.5		146.8		147.2
4'''		140.1, 139.3		139.4		140.7
7'''		168.8, 168.6		168.9		168.4
Cinnamoyl moiety						
1''''				136.8		136.5
2''',6'''			6.98 m	130.2	7.42 m	130.9
3''',5'''			6.82 m	131.3	7.63 m	131.0
4''''			6.95 m	118.2	7.40 m	118.9
7''''			6.36 d (16.0)	146.5	6.58 (16.0)	147.3
8''''			7.65 d (16.0)	146.5	7.73 (16.0)	147.3
9''''				167.6		167.8

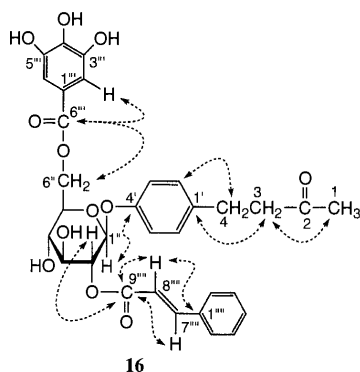


Fig. 2. Long-Range Correlations Observed in the FG-Pulsed HMBC Spectrum of **16**

and 6''-H₂ of the β -glucose moiety (δ 4.55, 4.22), indicating the locations of the β -glucose and gallic acid moieties to be at C-4' and at C-6'', respectively. The negative sign of the optical rotation indicated that the β -glucose moiety should have D configuration. Thus, compound **10** was determined to be *cis*-3,5,4'-trihydroxystilbene 4'-O- β -D-(6-O-galloyl)glucopyranoside.

Compound **16** was obtained as a pale brown amorphous solid with $[\alpha]_D^{25}$ of -94.9° ($c=0.015$, MeOH). The negative ion FAB-MS and HR-FAB-MS of **16** indicated the molecular formula C₃₂H₃₂O₁₂ (Mw 608). The ¹H- and ¹³C-NMR spectra of **16** were similar to those of phenylbutanones **11**–**15**, especially of **15** (Table 3), and indicated the presence of a 4-(4-hydroxyphenyl)-2-butanone, a glucose, a cinnamoyl and a galloyl moiety. The ¹H-NMR spectrum of **16** was almost the same as that of **15** but was characterized by high-field shift of the signals for the cinnamoyl moiety [**16**: δ 6.98 (2H, m), 6.82 (3H, m); **15**: δ 7.42 (2H, m), 7.63 (3H, m)]. Thus, **16** was considered to be a regioisomer of **15** on the locations of the cinnamoyl and galloyl moieties. The locations of these moieties, and also the structure of **16**, were determined by the FG-pulsed HMBC spectrum (Fig. 2). The ester carbonyl carbon at δ 167.8 showed long-range correlations with the olefinic protons of the cinnamoyl moiety (δ 6.58, 7.73) and 2''-H of the glucose moiety (δ 5.17), while the ester carbonyl carbon at δ 168.4 had correlations with the protons of the galloyl moiety (δ 7.09) and 6''-H of the glucose moiety (δ 4.45, 4.60). Thus, the locations of the cinnamoyl and galloyl moieties were determined to be C-2'' and C-6'', respectively. These and a negative sign of the optical rotation led to the conclusion that compound **16** is 4-(4'-hydroxyphenyl)-2-butanone 4'-O- β -D-(2-O-cinnamoyl-6-O-galloyl)glucopyranoside.

Among the isolated compounds, nineteen (**2**–**9**, **11**–**15**, **17**–**19**, **25**–**27**) have been reported as constituents of Rhei Rhizoma,^{14–20} four (**1**, **25**–**27**) of Cinnamomi Cortex^{21,24} and five (**20**–**24**) of Glycyrrhizae Radix.^{21,22} The stilbenes **7**–**9** and the phenylbutanones **11**–**15** both were isolated only from Rhei Rhizoma. Thus, the new stilbene **10** and the new phenylbutanone **16** also would be derived from Rhei Rhizoma, although it is uncertain whether they are contained in the original plant or produced during the preparation of the Kampo formula.

PEP Inhibitory Activity PEP inhibitory activities of the twenty-seven compounds were examined against *Flavobacterium* PEP and are listed in Table 4, together with those of

Table 4. PEP Inhibitory Activity of Isolated Compounds

Compound	Concentration (μ M)	Inhibition (%) ^{a)}	IC ₅₀ (μ M)	K _i (μ M) ^{b)}
1	100	14.6 \pm 6.8		
2			27.8 ^{c)}	26.6 \pm 0.6 ^{c)}
3	100	33.0 \pm 5.2		
4	100	19.9 \pm 6.5		
5	100	20.6 \pm 4.3		
6	100	19.1 \pm 3.6		
7	100	81.9 \pm 3.4	22.9	30.9 \pm 18.5
	10	32.1 \pm 7.0		
	1	11.4 \pm 1.1		
8	100	99.7 \pm 0.1	3.0	8.82 \pm 7.80
	10	75.5 \pm 4.9		
	1	26.4 \pm 6.4		
9	100	93.3 \pm 1.5	14.9	17.3 \pm 10.3
	10	40.9 \pm 2.4		
	1	19.3 \pm 1.5		
10	100	99.9 \pm 0.1	2.8	6.73 \pm 4.49
	10	86.7 \pm 3.4		
	1	20.2 \pm 1.5		
11	100	2.1 \pm 1.4		
12	100	44.1 \pm 7.7		
13	100	24.2 \pm 4.5		
14	100	98.4 \pm 0.3	10.5	11.3 \pm 4.44
	10	48.9 \pm 8.5		
	1	19.0 \pm 12.7		
15	100	100.0 \pm 0.0	0.69	1.17 \pm 0.013
	10	75.2 \pm 9.0		
	1	54.3 \pm 8.7		
16	100	98.4 \pm 2.2	8.2	8.45 \pm 3.44
	10	53.8 \pm 3.6		
	1	32.7 \pm 3.9		
17	100	14.3 \pm 3.7		
18	100	99.5 \pm 0.0	0.44	0.149 \pm 0.011
	10	98.9 \pm 0.3		
	1	62.8 \pm 21.2		
19	100	84.6 \pm 8.9	9.39	8.16 \pm 1.30
	10	49.3 \pm 23.6		
	1	18.8 \pm 8.5		
20	100	9.4 \pm 0.8		
21	100	11.0 \pm 1.8		
22	100	13.4 \pm 5.8		
23	100	12.2 \pm 8.4		
24	100	71.1 \pm 3.9	26.5	14.1 \pm 4.83
	10	34.5 \pm 9.2		
	1	11.3 \pm 6.9		
25	100	66.3 \pm 8.0	28.1	14.3 \pm 2.74
	10	35.3 \pm 7.5		
	1	11.4 \pm 3.6		
26	1	96.6 \pm 1.5	0.052	0.103 \pm 0.066
	0.1	59.2 \pm 2.2		
	0.01	24.5 \pm 3.5		
27	100	35.0 \pm 2.9		
Z-Pro-prolinol			641 ^{c)}	283 \pm 5 ^{c)}
Z-Pro-prolinal			2.55 nM ^{c)}	0.421 \pm 0.173 nM ^{c)}

a) The values are the means \pm S.D. of triplicate experiments. b) K_i values were obtained from Dixon Plot. c) Data from ref. 13.

positive controls, Z-Pro-prolinol and Z-Pro-prolinal. Thirteen of these compounds (**2**, **7**–**10**, **14**–**16**, **18**, **19**, **24**–**26**) showed the inhibitory activity concentration-dependently with an IC₅₀ of 27.8, 22.9, 3.0, 14.9, 2.8, 10.5, 0.69, 8.2, 0.44, 9.39, 26.5, 28.1 and 0.052 μ M, respectively. The inhibition mode of twelve compounds, other than **2** of a competitive inhibitor,¹³⁾ was determined to be non-competitive by analysis of the Lineweaver–Burk plot. The inhibitory activity of **26** (IC₅₀, 0.052 μ M) was almost the same as poststatin

(IC₅₀, 0.055 μ M),²⁵⁾ a peptidic and the strongest inhibitor obtained from a natural source.

Stilbenes **8**–**10** (IC₅₀, 3.0–14.9 μ M) with a galloyl group showed stronger inhibitory activity than stilbene **7** (IC₅₀, 22.9 μ M) without a galloyl group. Thus, the galloyl moiety in **8**–**10** should be required for the potent inhibitory activity. Similar tendency was observed also in phenylbutanones **11**–**16**, galloylglucoses **17**–**19** and epicatechins **25** and **26**, and the inhibitory activity increased with the number of galloyl moieties; the order of inhibitory activity was **11**<**12**, **13**<**14**–**16**; **17**<**19**<**18**; **25**<**26**.

Moreover, compounds **8**, **12** and **15**, having a galloyl group at C-2 of glucose, showed much more potent activity than the corresponding compounds (**9**, **13**, **16**) having a galloyl group at C-6 of glucose. Though a galloyl group locates at C-6 of glucose, the inhibitory activity of *cis*-stilbene **10** (IC₅₀, 2.8 μ M) was stronger than the corresponding *trans*-stilbene **9** (IC₅₀, 14.9 μ M) and almost the same as stilbene **8** (IC₅₀, 3.0 μ M) with a galloyl group at C-2 of glucose. Thus, the spatial disposition between the galloyl group and the oxygen-function (phenolic hydroxyl in **8**–**10**, **18** and **26**; ketone carbonyl group in **12**–**16**; and carboxylic acid group in **19**) may be important for the PEP inhibition.

As mentioned above, the eleven known compounds showing the PEP inhibitory activity have been reported to be constituents of Rhei Rhizoma (**2**, **7**–**9**, **14**, **15**, **18**, **19**, **25**, **26**), Cinnamomi Cortex (**25**, **26**) and Glycyrrhizae Radix (**24**).^{14–22,24)} In addition, two new compounds (**10**, **16**) are believed to be derived from Rhei Rhizoma. Rhei Rhizoma is also contained in San-o-shashin-to (三黃瀉心湯), and Cinnamomi Cortex and/or Glycyrrhizae Radix is present in Kakkon-to (葛根湯), Zokumei-to (續命湯), Ninjin-to (人參湯), Hochu-ekki-to (補中益氣湯), Hachimi-gan-ryo (八味丸料), Kami-shoyo-san (加味逍遙散), Yokukan-san-ka-chinpi-to (抑肝散加陳皮湯) and Choto-san (釣藤散). However, these Kampo formulas showed weak or no inhibitory activity at 100 μ g/ml (Table 1). Thus, the combination of the crude drugs could affect the PEP inhibitory activity through a qualitative and/or quantitative change of constituents. This is under investigation and will be reported elsewhere.

Experimental

Optical rotations were measured with a JASCO DIP-4 digital polarimeter and UV spectra were obtained with a Shimadzu UV 160A spectrometer. FAB-MS and HR-FAB-MS were measured with JEOL JMS-700T and NMR spectra were recorded on a JEOL JNM-GX400 spectrometer with tetramethylsilane (TMS) as internal standard. PEP inhibitory activity was measured with a Perkin-Elmer HTS7000 bioassay reader. Column chromatography was performed over silica gel (Fuji Silysia BW-820MH) or Sephadex LH-20 (Pharmacia), and TLC was conducted on precoated Merck Kieselgel 60F₂₅₄ or RP-18F₂₅₄ plates.

PEP Inhibitory Activity PEP (*Flavobacterium meningosepticum* origin) was purchased from Seikagaku Corporation (Tokyo, Japan), and Z-Gly-Pro-pNA from Bachem Fine Chemical Co. (Switzerland). Two positive controls, Z-Pro-prolinol and Z-Pro-prolinol, were synthesized by the method in the literature.²⁶⁾ Kampo formulas used in this study (Table 1) were supplied by Kotaro Kampo Pharmaceutical Co., Ltd. (Osaka, Japan). PEP inhibitory activities and inhibitor constants (*K_i*) were measured by the method of Yoshimoto *et al.*,²⁷⁾ as described in the previous papers.^{12,13)}

Process of Isolating Constituents of Tokaku-joki-to Tokaku-joki-to used in this study was prepared by Kotaro Kampo Pharmaceutical Co., Ltd. It consists of Rhei Rhizoma (*Rheum palmatum* LINNE, Sichuan Province in China), Cinnamomi Cortex (*Cinnamomum cassia* BLUME, Guangdong Province in China), Persicae Semen (*Prunus persica* BATSCH, Shanxi Province in China) and Glycyrrhizae Radix (*Glycyrrhiza uralensis* FISHER,

Hebei Province in China). Powder of Tokaku-joki-to (250 g) was suspended on distilled water and the suspension was extracted successively with CHCl₃, EtOAc and BuOH (each 1 l, $\times 3$) (Chart 1). Each extract was evaporated to dryness *in vacuo* to give a CHCl₃-soluble (6.7 g), an EtOAc-soluble (22.5 g) and a BuOH-soluble (41.2 g) fraction, respectively, while the remaining water layer was freeze-dried to give an H₂O-soluble (173.3 g) fraction.

EtOAc-soluble fraction (20.0 g) was subjected to silica gel (1.0 kg) column chromatography with a MeOH–CHCl₃ solvent system (5:95→100:0) and eluates were separated into three fractions by their behavior on TLC. Fraction 1 (120 mg) was separated by normal-phase preparative TLC with MeOH–CHCl₃ (1:6) to give cinnamic acid (**1**, 6.0 mg), protocatechuic acid (**2**, 6.0 mg), gallic acid (**3**, 6.4 mg) and liquiritigenin (**20**, 7.0 mg). Fraction 2 (3.0 g) was chromatographed over silica gel (400 g) with MeOH–CHCl₃ (1:9) to give torachrysone 8-*O*- β -D-glucoside (**4**, 8.7 mg), emodin (**5**, 11.0 mg), emodin 8-*O*- β -D-glucoside (**6**, 45.8 mg), 4-(4-hydroxyphenyl)-2-butanone 4'-*O*- β -D-glucopyranoside (**11**, 84.0 mg) and 4-(4'-hydroxyphenyl)-2-butanone 4'-*O*- β -D-(2-*O*-galloyl-6-*O*-cinnamoyl)glucopyranoside (**15**, 10.0 mg). Fraction 3 (10 g) was separated by a combination of column chromatography with Sephadex LH-20 (800 g) (H₂O–MeOH, 100:0→0:100) and reversed-phase preparative TLC (H₂O–MeOH, 1:1) to furnish **3** (20.1 mg), *trans*-3,5,4'-trihydroxystilbene 4'-*O*- β -D-glucopyranoside (**7**, 15.8 mg), *trans*-3,5,4'-trihydroxystilbene 4'-*O*- β -D-(2-*O*-galloyl)glucopyranoside (**8**, 1.8 mg), *trans*-3,5,4'-trihydroxystilbene 4'-*O*- β -D-(6-*O*-galloyl)glucopyranoside (**9**, 87.9 mg), **10** (7.0 mg), isolindleyin (**12**, 6.0 mg), lindleyin (**13**, 6.4 mg), 1-*O*-galloylglucose (**17**, 29.6 mg), 1,2,6-tri-*O*-galloylglucose (**18**, 21.7 mg), gallic acid 4-*O*- β -D-(6-*O*-galloyl)glucopyranoside (**19**, 10.9 mg), liquiritigenin 4'-*O*- β -D-glucopyranoside (**21**, 15.8 mg), liquiritigenin 7,4'-diglucoside (**22**, 1.8 mg), liquiritigenin 4'-*O*- β -D-apiofuranosyl-(1→2)- β -D-glucopyranoside (**23**, 90.5 mg), licuroside (**24**, 13.2 mg) and (+)-catechin (**27**, 387 mg).

BuOH-soluble fraction (34.0 g) was chromatographed over Sephadex LH-20 (1.5 kg) with a MeOH–H₂O solvent system (0:100→100:0) to afford four fractions. Fraction 4 was further subjected to Sephadex LH-20 (200 g) column chromatography with a H₂O–MeOH solvent system (100:0→0:100) and the eluates were separated by reversed-phase preparative TLC (H₂O–MeOH, 1:1) to furnish **7** (30.7 mg), **8** (4.0 mg), **10** (6.0 mg), **12** (41.4 mg), 4-(4-hydroxyphenyl)-2-butanone 4'-*O*- β -D-(2,6-di-*O*-galloyl)glucopyranoside (**14**, 4.3 mg), 4-(4-hydroxyphenyl)-2-butanone 4'-*O*- β -D-(6-*O*-galloyl-2-*O*-cinnamoyl)glucopyranoside (**16**, 11.4 mg), **19** (4.4 mg), **21** (98 mg), **24** (20.8 mg), (–)-epicatechin (**25**, 23.0 mg), (–)-epicatechin 3-*O*-gallate (**26**, 10.5 mg) and **27** (14.2 mg).

cis-3,5,4'-Trihydroxystilbene 4'-*O*- β -D-(6-*O*-Galloyl)glucopyranoside (**10**): Pale brown powder, $[\alpha]_D^{25}$ –124° (*c*=0.027, MeOH). UV λ_{max} (MeOH) nm (log ϵ): 210 (4.78), 275 (4.38). Negative ion HR-FAB-MS *m/z*: 541.1325 [Calcd for C₂₇H₂₅O₁₂ (M–H)[–] 541.1346]. ¹H- and ¹³C-NMR: Table 2.

4-(4-Hydroxyphenyl)-2-butanone 4'-*O*- β -D-(6-*O*-Galloyl-2-*O*-cinnamoyl)glucopyranoside (**16**): Pale brown amorphous solid, $[\alpha]_D^{25}$ –94.9° (*c*=0.015, MeOH). UV λ_{max} (MeOH) nm (log ϵ): 218 (4.34), 275 (3.90). Negative ion HR-FAB-MS *m/z*: 607.1812 [Calcd for C₃₂H₃₁O₁₂ (M–H)[–] 607.1816]. ¹H- and ¹³C-NMR: Table 3.

Acknowledgements We thank Kotaro Kampo Pharmaceutical Co., Ltd. for their generosity in supplying the Kampo formulas. One of the authors (W. Fan) is grateful to the Rotary Club for his Yoneyama Scholarship.

References and Notes

- Wilk S., *Life Sci.*, **33**, 2149–2157 (1983); Yoshimoto T., *Nippon Nogekigaku Kaishi*, **58**, 1147–1154 (1984); *idem*, *Yakugaku Zasshi*, **111**, 345–358 (1991); Aoyagi T., Muraoka Y., *Tanpakushitsu Kakusan Koso*, **38**, 1971–1986 (1993).
- Walter R., Shlank H., Glass J. D., Schwartz I. L., Kerenyi T. D., *Science*, **173**, 827–829 (1971).
- Yoshimoto T., Ogita K., Walter R., Koida M., Tsuru D., *Biochim. Biophys. Acta*, **569**, 184–192 (1979); Kalwant S., Porter A. G., *Biochem. J.*, **276**, 237–244 (1991).
- Burbach J. P. H., Kovács G. L., De Wied D., Van Nispen J. W., Greven H. M., *Science*, **221**, 1310–1312 (1983); De Wied D., Gaffori O., Van Ree J. M., De Jong W., *Nature* (London), **308**, 276–278 (1984).
- Ohtsuki S., Homma K., Kurata S., Komano H., Natori S., *J. Biochem.*, **115**, 449–453 (1994); Ohtsuki S., Homma K., Kurata S., Natori S., *ibid.*, **121**, 1176–1181 (1997); Ishino T., Ohtsuki S., Homma K., Natori S., *ibid.*, **123**, 540–545 (1998).
- Maes M., Lin A. H., Bonaccorso S., Goossens F., Van Gastel A.,

- Delmeire L., Scharpe S., *J. Affect. Disord.*, **53**, 27—34 (1999); Maes M., Goossens F., Scharpe S., Calabrese J., Desnyder R., Meltzer H. Y., *Psych. Res.*, **58**, 217—225 (1995); Ichai C., Chevallier N., Delaere P., Dournaud P., Epelbaum J., Hauw J.-J., Vincent J.-P., Checler F., *J. Neurochem.*, **62**, 645—655 (1994).
- 7) Fukunari A., Kato A., Sakai Y., Yoshimoto T., Ishiura S., Suzuki K., Nakajima T., *Neurosci. Lett.*, **176**, 201—204 (1994).
- 8) Aoyagi T., Wada T., Nagai M., Kojima F., Harada S., Takeuchi T., Takahashi H., Hirokawa K., Tsumita T., *Experientia*, **46**, 94—97 (1990).
- 9) Vendeville S., Buisine E., Williard X., Schrevel J., Grellier P., Santana J., Sergheraert C., *Chem. Pharm. Bull.*, **47**, 194—198 (1999); Tsutsumi S., Okonogi T., Shibahara S., Ohuchi S., Hatsushiba E., Patchett A., Christensen B. G., *J. Med. Chem.*, **37**, 3492—3502 (1994); Tanaka Y., Niwa S., Nishioka H., Yamanaka T., Torizuka M., Yoshinaga K., Kobayashi N., Ikeda Y., Arai H., *ibid.*, **37**, 2071—2078 (1994); Angelucci L., Calvisi P., Catini R., Cosentino U., Cozzolino R., De Witt P., Ghirardi O., Giannesi F., Ciuliani A., Guaraldi D., Misiti D., Ramacci M. T., Scolastico C., Tinti M. O., *ibid.*, **36**, 1511—1519 (1993); see also references cited therein.
- 10) Hwang J. S., Song K. S., Kim W. G., Lee T. H., Koshino H., Yoo I. D., *J. Antibiot.*, **50**, 773—777 (1997); Kimura K., Kanou F., Takahashi H., Esumi Y., Uramoto M., Yoshihama M., *ibid.*, **50**, 373—378 (1997); Christner C., Zerlin M., Grafe U., Heinze S., Kullertz G., Fischer G., *ibid.*, **50**, 384—389 (1997); Kimura K., Kanou F., Koshino H., Uramoto M., Yoshihama M., *ibid.*, **50**, 291—296 (1997); Nagai M., Ogawa K., Muraoka Y., Naganawa H., Aoyagi T., Takeuchi T., *ibid.*, **44**, 956—961 (1991); see also references cited therein.
- 11) The following are recent reports: Shishido Y., Tanaka T., Tanabe S., Furushiro M., Hashimoto S., Yokokura T., Shibata S., Tanabe S., *Pharmaceut. Res.*, **16**, 463—465 (1999); Umemura K., Kondo K., Ikeda Y., Nishimoto M., Hiraga Y., Yoshida Y., Nakashima M., *J. Clin. Pharmacol.*, **39**, 462—470 (1999); Katsube N., Sunaga K., Aishita H., Chung D. M., Ishitana R., *J. Pharmacol. Exp. Ther.*, **288**, 6—13 (1999); Shinoda M., Miyazaki A., Toide K., *Behav. Brain Res.*, **99**, 17—25 (1999); Toide K., Shinoda M., Miyazaki A., *Rev. Neurosci.*, **9**, 17—29 (1998); see also references cited therein.
- 12) Tezuka Y., Fan W., Kasimu R., Kadota S., *Phytomedicine*, **6**, 197—203 (1999).
- 13) Fan W., Tezuka Y., Komatsu K., Namba T., Kadota S., *Biol. Pharm. Bull.*, **22**, 157—161 (1999).
- 14) Tsuboi M., Minami M., Nonaka G., Nishioka I., *Chem. Pharm. Bull.*, **25**, 2708—2712 (1977).
- 15) Cohen P. A., Towers G. H. N., *J. Nat. Prod.*, **58**, 520—526 (1995).
- 16) Coskun M., Satake T., Hori K., Saiki Y., Tanker M., *Phytochemistry*, **29**, 2018—2020 (1990).
- 17) Nonaka G., Minami M., Nishioka I., *Chem. Pharm. Bull.*, **25**, 2300—2305 (1977).
- 18) Nonaka G., Nishioka I., *Chem. Pharm. Bull.*, **31**, 1652—1658 (1983).
- 19) Nonaka G., Nishioka I., Nagasawa T., Oura H., *Chem. Pharm. Bull.*, **29**, 2862—2870 (1981).
- 20) Kashiwada Y., Nonaka G., Nishioka I., *Chem. Pharm. Bull.*, **34**, 3237—3243 (1986).
- 21) Yahara S., Nishioka I., *Phytochemistry*, **23**, 2108—2109 (1984).
- 22) Kinjo J., Furusawa J., Baba J., Takeshita T., Yamasaki M., Nohara T., *Chem. Pharm. Bull.*, **35**, 4846—4850 (1987).
- 23) Kashiwada Y., Nonaka G., Nishioka I., *Chem. Pharm. Bull.*, **32**, 3501—3517 (1984).
- 24) Otsuka H., Fujioka S., Komiya T., Mizuta E., Takamoto M., *Yakugaku Zasshi*, **102**, 162—172 (1982).
- 25) Aoyagi T., Nagai M., Ogawa K., Kojima F., Okada M., Ikeda T., Hamada M., Takeuchi T., *J. Antibiot.*, **44**, 949—955 (1991).
- 26) Bakker A. V., Jung S., Spencer R. W., Vinick F. J., Faraci W. S., *Biochem. J.*, **271**, 559—562 (1990).
- 27) Yoshimoto T., Walter R., Tsuru D., *J. Biol. Chem.*, **255**, 4786—4792 (1980).

Steroidal Oligoglycosides from *Solanum nigrum*¹⁾

Tsuyoshi IKEDA, Hidetsugu TSUMAGARI, and Toshihiro NOHARA*

Faculty of Pharmaceutical Sciences, Kumamoto University, 5-1 Oe-honmachi, Kumamoto 862-0973, Japan.

Received February 21, 2000; accepted April 27, 2000

Two new steroidal saponins, named nigrumnins I and II, together with two known saponins were obtained from the whole plant of *Solanum nigrum* L. On the basis of spectroscopic analysis (¹H-NMR, ¹³C-NMR, ¹H-¹H COSY, TOCSY, HMQC, HMBC and FAB-MS), nigrumnin I was established as (25*R*)-5α-spirostan-3β-ol 3-*O*-β-D-xylopyranosyl-(1→3)-[α-L-arabinopyranosyl-(1→2)]-β-D-glucopyranosyl-(1→4)-[α-L-rhamnopyranosyl-(1→2)]-β-D-galactopyranoside (1), and nigrumnin II was elucidated as (25*R*)-3β,17α-dihydroxy-5α-spirostan-12-one 3-*O*-β-D-xylopyranosyl-(1→3)-[α-L-arabinopyranosyl-(1→2)]-β-D-glucopyranosyl-(1→4)-[α-L-rhamnopyranosyl-(1→2)]-β-D-galactopyranoside (2).

Key words *Solanum nigrum*; Solanaceae; steroidal saponin; tigogenin; (25*R*)-3β,17α-dihydroxy-5α-spirostan-12-one; nigrumnin

Our search for bioactive compounds among solanaceous plants has resulted in the isolation of cytotoxic²⁾ and anti-herpes³⁾ steroidal saponins. In order to obtain new cytotoxic and anti-herpes steroidal saponins, and to study the relationship between the structure and bioactivity, we investigated steroidal saponins from the whole plant of *Solanum nigrum* L.

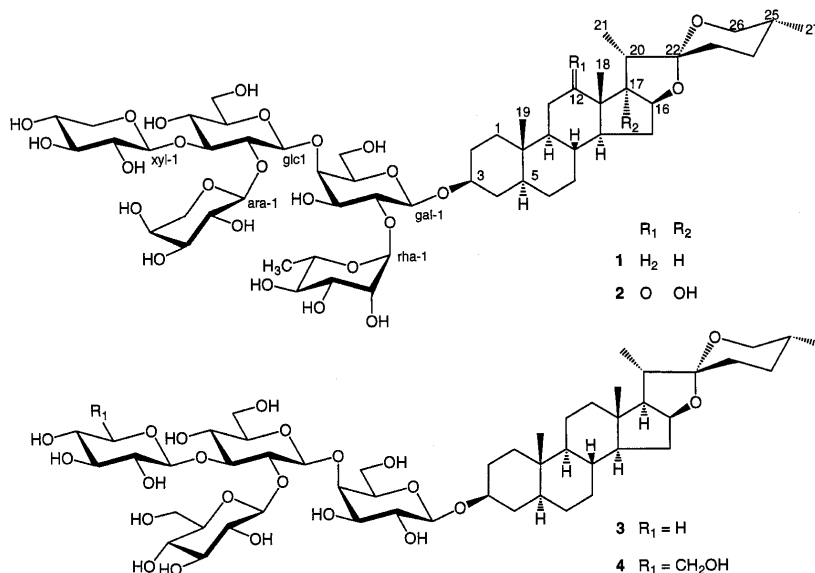
The whole plant of *S. nigrum* L. has been used traditionally as a remedy for various cancers in the Shanghai region of China⁴⁾ and in the Sendai area of Miyagi Prefecture in Japan. Previously, we analyzed the constituents of the immature fruits of this plant and found steroidal glycosides, proto-desgalactotigogenin, desgalactotigogenin, tigogenin 3-*O*-β-D-glucopyranosyl-(1→2)-[β-D-glucopyranosyl-(1→3)]-β-D-glucopyranosyl-(1→4)-β-D-galactopyranoside, together with steroidal alkaloids, solamargine and solasonine.⁵⁾ Furthermore, four new steroidal alkaloids, which were enzymatically derived from the original constituents, were obtained from the berries of this plant.⁶⁾ This paper deals with the isolation and structural elucidation of two new spirostanol steroidal saponins, together with two known saponins from the whole plant of *S. nigrum*.

The methanolic extract of the whole plant of *S. nigrum*

was partitioned between *n*-hexane and 80% MeOH. The 80% MeOH fraction was subjected to Diaion HP-20, silica gel, Chromatorex ODS column chromatography to give new steroidal oligoglycosides, named nigrumnins I (1) and II (2), together with the known saponins, compounds 3 and 4.

Compounds 3 and 4 were known steroidal saponins and identified as desgalactotigogenin,⁷⁾ and tigogenin 3-*O*-β-D-glucopyranosyl-(1→2)-[β-D-glucopyranosyl-(1→3)]-β-D-glucopyranosyl-(1→4)-β-D-galactopyranoside,⁵⁾ based on their NMR spectral data and by comparison of their physical properties with those reported in the literatures.

Nigrumnin I (1) was isolated as an amorphous powder, [α]_D -56.2° (pyridine). It showed a quasi-molecular ion peak of [M+Na]⁺ at *m/z* 1173, and fragment ion peaks due to [M+Na-pentose]⁺ at *m/z* 1041 and [M+H-pentose-methylpentose]⁺ at *m/z* 873 in the positive FAB-MS. The high-resolution (HR) FAB-MS gave an [M+Na]⁺ ion at *m/z* 1173.5669, which corresponds to the composition C₅₅H₉₀O₂₅Na. The ¹H-NMR spectrum in pyridine-*d*₅ displayed signals for four steroidal methyl groups at δ 0.82, and 0.86 (each 3H, s), 0.70 (3H, d, *J*=6.1 Hz), and 1.14 (3H, d, *J*=6.7 Hz), one secondary methyl group of a methylpentose at δ 1.71 (3H, d, *J*=6.1 Hz), and five anomeric protons at δ



* To whom correspondence should be addressed. e-mail: none@gpo.kumamoto-u.ac.jp

Table 1. ^1H - and ^{13}C -NMR Data for the Sugar Moiety of **1** and **2** in Pyridine- d_5

	1 δ_{H}	$J(\text{Hz})$	1 δ_{C}	2 δ_{C}
Gal-1	4.85 1H d	7.4	100.1	100.1
2	4.38 1H dd	7.4, 9.1	77.4	77.3
3	4.13 1H *		76.2	76.2
4	4.49 1H *		81.5	81.5
5	3.95 1H *		75.1	75.1
6	4.74 1H *		60.4	60.3
6'	4.18 1H *			
Glc-1	4.95 1H d	7.9	105.4	105.4
2	4.22 1H dd	7.9, 8.5	81.5	81.4
3	4.05 1H dd	8.5, 9.2	87.9	87.9
4	3.79 1H *		70.4	70.3
5	3.81 1H *		77.7	77.6
6	4.51 1H *		62.9	62.9
6'	4.00 1H *			
Ara-1	5.33 1H d	7.3	105.8	105.8
2	4.40 1H dd	7.3, 9.1	73.3	73.2
3	4.01 1H dd	9.1, 3.7	74.7	74.7
4	4.16 1H br dd	3.7, 2.2	69.7	69.7
5	4.64 1H dd	11.1, 2.2	67.3	67.3
5'	3.60 1H br d	11.1		
Xy-1	5.20 1H d	7.9	105.0	104.9
2	3.96 1H dd	7.9, 9.2	75.1	75.1
3	4.07 1H dd	9.2, 9.2	78.7	78.7
4	4.11 1H ddd	9.2, 11.0, 5.5	70.7	70.7
5	4.19 1H dd	11.1, 5.5	67.3	67.3
5'	3.64 1H dd	11.0, 11.1		
Rha-1	6.27 1H br s		101.7	101.6
2	4.77 1H m		72.4	72.4
3	4.53 1H dd	9.2, 3.1	72.7	72.7
4	4.29 1H dd	9.2, 9.8	74.0	74.0
5	4.90 1H dq	9.8, 6.1	69.6	69.6
6	1.71 3H d	6.1	18.5	18.4

* Overlapped.

4.85 (1H, d, $J=7.4$ Hz), 4.95 (1H, d, $J=7.9$ Hz), 5.20 (1H, d, $J=7.9$ Hz), 5.33 (1H, d, $J=7.3$ Hz) and 6.27 (1H, br s). Acid hydrolysis of **1** with 1 M HCl in dioxane- H_2O (1 : 1) afforded D-glucose, D-galactose, L-rhamnose, D-xylose, and L-arabinose in a ratio of 1 : 1 : 1 : 1 : 1 as carbohydrate components by GLC analysis following the conversion to the thiazolidine derivatives,⁸⁾ while the aglycone was identified as tigogenin by TLC on comparison with an authentic sample.⁹⁾ To determine the glycosidic linkage, ^1H - ^1H shift correlation spectroscopy (COSY), totally correlated spectroscopy (TOCSY), heteronuclear multiple quantum coherence (HMQC) and heteronuclear multiple bond correlation (HMBC) experiments were carried out for assignment of the respective proton and carbon signals (Table 1). The rhamnosyl H-1 at δ 6.27 and the galactosyl C-2 at δ 77.4, the arabinosyl H-1 at δ 5.33 and the glucosyl C-2 at δ 81.5, the xylosyl H-1 at δ 5.20 and the glucosyl C-3 at δ 87.9, and the glucosyl H-1 at δ 4.95 and the galactosyl C-4 at δ 81.5 were correlated by the HMBC spectrum, so that the sugar moiety of **1** was disclosed to be β -D-xylopyranosyl-(1 \rightarrow 3)-[α -L-arabinopyranosyl-(1 \rightarrow 2)]- β -D-glucopyranosyl-(1 \rightarrow 4)-[α -L-rhamnopyranosyl-(1 \rightarrow 2)]- β -D-galactopyranoside. Furthermore, the galactosyl H-1 at δ 4.85 and the C-3 of aglycone carbon at δ 77.0 were also correlated.

Thus, the structure of nigrumnin I was determined to be tigogenin 3-O- β -D-xylopyranosyl-(1 \rightarrow 3)-[α -L-arabinopyranosyl-(1 \rightarrow 2)]- β -D-glucopyranosyl-(1 \rightarrow 4)-[α -L-rhamnopyra-

Table 2. ^1H - and ^{13}C -NMR Data for the Aglycone Moiety of **1** and **2** in Pyridine- d_5

	1 δ_{C}	2 δ_{C}	2 δ_{H}	$J(\text{Hz})$
C-1	37.2	36.6	0.74 1H m	
			1.37 1H *	
2	30.0	29.7	1.72 1H *	
			1.98 1H m	
3	77.0	76.7	3.88 1H m	
4	34.4	34.2	1.63 1H *	
			1.91 1H m	
5	44.7	44.2	0.86 1H *	
6	29.0	28.5	1.15 1H m	
			0.87 1H *	
7	32.4	31.5	1.60 1H *	
			0.82 1H *	
8	35.3	34.6	1.76 1H m	
9	54.4	54.7	0.99 1H m	
10	35.9	36.3		
11	21.3	38.8	2.37 1H dd	14.0, 14.0
			2.24 1H *	
12	40.2	215.8		
13	40.8	59.3		
14	56.5	52.4	2.45 1H m	
15	32.1	32.4	1.61 1H *	
			2.25 1H *	
16	81.1	86.9	4.40 1H *	
17	63.0	89.8		
18	16.6	16.6	0.99 3H s	
19	12.4	11.8	0.87 3H s	
20	42.0	45.1	2.22 1H q	6.7
21	15.0	8.8	1.33 3H d	6.7
22	109.2	109.7		
23	31.8	30.2	1.27 1H *	
			1.59 1H *	
24	29.3	28.8	1.55 1H *	
			1.55 1H *	
25	30.6	30.3	1.57 1H *	
26	66.9	66.8	3.49 1H dd	10.4, 10.4
			3.59 1H dd	10.4, 3.3
27	17.3	17.3	0.68 3H d	6.1

* Overlapped.

nosyl-(1 \rightarrow 2)]- β -D-galactopyranoside (**1**).

Nigrumnin II (**2**) was isolated as an amorphous powder, $[\alpha]_{\text{D}} - 34.2^\circ$ (MeOH). It showed a *quasi*-molecular ion peak due to $[\text{M}+\text{Na}]^+$ at m/z 1203 and a fragment ion peak due to $[\text{M}+\text{H}-\text{pentose}-\text{methylpentose}]^+$ in the positive FAB-MS. The HR-FAB-MS gave an $[\text{M}+\text{Na}]^+$ ion at m/z 1203.5460, which corresponds to the composition $\text{C}_{55}\text{H}_{88}\text{O}_{27}\text{Na}$. Acid hydrolysis of **2** gave D-glucose, D-galactose, L-rhamnose, D-xylose, and L-arabinose in a ratio of 1 : 1 : 1 : 1 : 1, while the genuine aglycone decomposed under the acidic conditions. The results of the acid hydrolysis and the ^1H - and ^{13}C -NMR spectral data provided the identity of the saccharide sequences between **1** and **2**. In the aglycone moiety, when the ^1H - and ^{13}C -NMR spectral data of **2** were compared with that of **1** (tigogenin), the A, B, and F ring signals were identical. On the other hand, the presence of a carbonyl group and a quaternary carbon signal was recognized in the ^{13}C -NMR spectrum (δ 215.8 and δ 89.8) of **2**. The complete assignment of the ^1H - and ^{13}C -NMR signals of the aglycone part of **2** was carried out by the concerted use of the ^1H - ^1H COSY, HMQC and HMBC spectra as shown in Table 2. HMBC correlations were observed between the carbonyl carbon signal

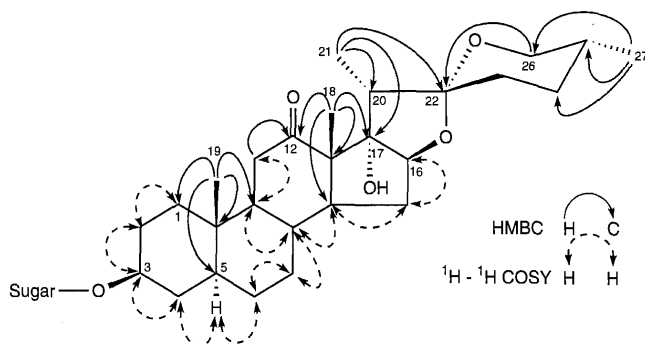


Fig. 1. HMBC and ^1H - ^1H COSY Correlations of the Aglycone Moiety of **2**

at δ 215.8 and the proton signals at δ 0.99 (H_3 -18) and δ 2.37 (H -11 β), and the quaternary carbon signal at δ 89.8 and the proton signals at δ 0.99 (H_3 -18) and δ 1.33 (H_3 -21) (Fig. 1). Thus, the locations of the carbonyl and hydroxyl groups were assigned to C-12 and C-17, respectively. A nuclear Overhauser exchanged spectroscopy (NOESY) between H -20 [δ 2.22 (1H, q, $J=6.7$ Hz)] and H_3 -18 (δ 0.99) indicated the α -orientation of the C-17 hydroxyl group.

Thus, the structure of nigrumnin II was determined to be (25*R*)-3 β ,17 α -dihydroxy-5 α -spirostan-12-one (=17 α -hydroxyhecogenin) 3-*O*- β -D-xylopyranosyl-(1 \rightarrow 3)-[α -L-arabinopyranosyl-(1 \rightarrow 2)]- β -D-glucopyranosyl-(1 \rightarrow 4)-[α -L-rhamnopyranosyl-(1 \rightarrow 2)]- β -D-galactopyranoside (**2**).

The cytotoxicity against human cancer cell lines and anti-herpes simplex virus type 1 (HSV-1) activity of these oligoglycosides is now in progress.

Experimental

Optical rotations were measured on a JASCO DIP-360 automatic digital polarimeter. The NMR spectra were recorded at 500 MHz for ^1H and 125 MHz for ^{13}C on a JEOL α -500 spectrometer and chemical shifts were given on a δ (ppm) scale with tetramethylsilane as the internal standard. Standard pulse sequences were employed for the distortionless enhancement by polarization transfer (DEPT), HMQC, and HMBC experiments. NOESY spectra were measured with mixing time of 600 ms. The FAB-MS were measured with a JEOL DX-300 and/or SX102A spectrometer. The HR-FAB-MS were measured with a JEOL DX-303 HF spectrometer and taken in a glycerol, triethylene glycol and *m*-nitrobenzyl alcohol matrix. GLC was performed on a HP5890A gas chromatograph with a flame ionization detector. TLC was performed on precoated Kieselgel 60 F_{254} plates (Merck). Column chromatography was carried out on Kieselgel 60 (70–230 mesh, 230–400 mesh), Diaion HP-20 (Mitsubishi Chemical, Ind.), Sephadex LH-20 (Pharmacia), and Chromatorex ODS-DU 3050MT (Fuji Silysia).

Extraction and Isolation The whole plant of *Solanum nigrum* L. (2.2 kg), collected at Jyonanmachi, Kumamoto Prefecture, Japan, on 28 August 1998, were cut into pieces and extracted with MeOH at room temperature. The extract was concentrated (79.5 g) and partitioned between hexane and 80% MeOH. The 80% MeOH fraction was subjected to Diaion HP-20 column chromatography using $\text{H}_2\text{O} \rightarrow \text{MeOH}$ to give fractions 1 to 5. A part (2.1 g) of fraction 4 (80% MeOH eluate; 12.1 g) was further purified by silica gel column chromatography ($\text{CHCl}_3 : \text{MeOH} : \text{H}_2\text{O} = 8 : 2 : 0.2 \rightarrow 7 : 3 :$

0.5) to give nigrumnin I (**1**) (31.9 mg) and **4** (7.6 mg). Fraction 5 (MeOH eluate; 2.5 g) was further purified by Chromatorex ODS (70% MeOH \rightarrow MeOH) and silica gel column chromatography ($\text{CHCl}_3 : \text{MeOH} : \text{H}_2\text{O} = 8 : 2 : 0.2 \rightarrow 7 : 3 : 0.5$) to yield nigrumnin II (**2**) (14.0 mg) and **3** (420 mg).

Nigrumnin I (1): An amorphous powder, $[\alpha]_D^{25} -56.2^\circ$ ($c=0.29$, pyridine). Positive FAB-MS (m/z) 1173 $[\text{M}+\text{Na}]^+$, 1041 $[\text{M}+\text{Na}-\text{pentose}]^+$, 873 $[\text{M}+\text{H}-\text{pentose}-\text{methylpentose}]^+$. HR FAB-MS (m/z) 1173.5690 $[\text{M}+\text{Na}]^+$ (Calcd for $\text{C}_{55}\text{H}_{90}\text{O}_{25}\text{Na}$; 1173.5670). ^1H -NMR (pyridine- d_5) δ : 0.70 (3H, d, $J=6.1$ Hz, H_3 -27), 0.82 (3H, s, H_3 -18), 0.86 (3H, s, H_3 -19), 1.08 (3H, d, $J=6.7$ Hz, H_3 -21), 3.50 (1H, t, $J=10.4$ Hz, H -26 α), 3.58 (1H, overlapped, H -26 β); Table 1. ^{13}C -NMR (pyridine- d_5) δ : Tables 1 and 2.

Nigrumnin II (2): An amorphous powder, $[\alpha]_D^{25} -34.2^\circ$ ($c=0.23$, MeOH). Positive FAB-MS (m/z) 1203 $[\text{M}+\text{Na}]^+$, 903 $[\text{M}+\text{H}-\text{pentose}-\text{methylpentose}]^+$. HR FAB-MS (m/z) 1203.5460 $[\text{M}+\text{Na}]^+$ (Calcd for $\text{C}_{55}\text{H}_{88}\text{O}_{27}\text{Na}$; 1203.5417). ^1H -NMR (pyridine- d_5) δ : 1.71 (3H, d, $J=6.1$ Hz, rha-6), 4.88 (1H, d, $J=7.4$ Hz, gal-1), 4.96 (1H, d, $J=7.7$ Hz, glc-1), 5.19 (1H, d, $J=7.8$ Hz, xyl-1), 5.34 (1H, d, $J=7.4$ Hz, ara-1), 6.29 (1H, brs, rha-1); Table 2. ^{13}C -NMR (pyridine- d_5) δ : Tables 1 and 2.

Acid Hydrolysis of 1 and 2 Compound **1** (1 mg) was hydrolyzed with 1 M HCl in dioxane- H_2O (1:1) for 4 h at 80 $^\circ\text{C}$. The reaction mixture was neutralized with 2 mol/l NaOH in H_2O and extracted with CHCl_3 . The organic layer was identified as a tigogenin by TLC [R_f value: 0.50 (hexane-aceton=1:1)] comparing with an authentic sample. The aqueous layer was concentrated to dryness *in vacuo* to give a residue which was dissolved in dry pyridine, to which was added L-cysteine methyl ester hydrochloride.⁸⁾ The reaction mixture was heated for 2 h at 60 $^\circ\text{C}$ and concentrated to dryness by blowing N_2 gas. To the residue was added trimethylsilylimidazole, followed by heating for 1 h at 60 $^\circ\text{C}$. The residue was extracted with hexane and H_2O , and the organic layer was analyzed by GLC; column: OV-17 (0.32 mm \times 30 m), detector: FID, column temp.: 230 $^\circ\text{C}$, detector temp.: 270 $^\circ\text{C}$, injector temp.: 270 $^\circ\text{C}$, carrier gas: He (2.6 kg/cm 2). One peak was observed at t_R (min): 6.84 min (D-Glc), 7.34 min (D-Gal), 4.76 min (L-Rha), 3.91 min (D-Xyl), and 4.05 min (L-Ara) in a ratio of 1:1:1:1:1. The standard monosaccharides were subjected to the same reaction and GLC analysis under the same conditions. Following this procedure, **2** (1 mg) was subjected to acid hydrolysis to yield D-Glc, D-Gal, L-Rha, D-Xyl, and L-Ara in a ratio of 1:1:1:1:1. In this procedure, an aglycone decomposed under acidic conditions.

Acknowledgments We are grateful to Mr. K. Takeda and Mr. T. Iriguchi of the Analytical Center of Kumamoto University for NMR and MS measurements.

References and Notes

- 1) Part 49 in a series of studies on solanaceous plants.
- 2) Nakamura T., Komori C., Lee Y., Hashimoto F., Yahara S., Nohara T., Ejima A., *Biol. Pharm. Bull.*, **19**, 564–566 (1996).
- 3) Ikeda T., Ando J., Miyazono A., Zhu X.-H., Tsumagari H., Nohara T., Yokomizo K., Uyeda M., *Biol. Pharm. Bull.*, **23**, 363–364 (2000).
- 4) Jiangsu New Medical College (ed.), "Chinese Drug Dictionary," Vol. 1, Shanghai Science and Technology Publishing Co., 1978, pp. 630–631.
- 5) Saijo R., Murakami K., Nohara T., Tomimatsu T., Sato A., Matsuoka K., *Yakugaku Zasshi*, **102**, 300–305 (1982).
- 6) Yoshida K., Yahara S., Saijo R., Murakami K., Tomimatsu T., Nohara T., *Chem. Pharm. Bull.*, **35**, 1645–1648 (1987).
- 7) Mahato S. B., Ganguly A. N., Sahu N. P., *Phytochemistry*, **21**, 959–978 (1982).
- 8) Hara S., Okabe H., Mihashi K., *Chem. Pharm. Bull.*, **35**, 501–507 (1987).
- 9) Agrawal P. K., Jain D. C., Gupta R. K., Thakur R. S., *Phytochemistry*, **24**, 2479–2496 (1985).

Application of Liquid Chromatography-Atmospheric Pressure Chemical Ionization Mass Spectrometry to the Differentiation of Stereoisomeric Diterpenoid Alkaloids

Koji WADA,* Takao MORI, and Norio KAWAHARA

Hokkaido College of Pharmacy, 7-1 Katsuraoka-cho, Otaru 047-0264, Japan.

Received March 10, 2000; accepted April 27, 2000

High-performance liquid chromatography-atmospheric pressure chemical ionization mass spectrometry (HPLC-APCI-MS) was successfully applied to seven stereoisomeric diterpenoid alkaloids at position 1 or 12. Comparison of the breakdown curves, observed by changing the potential difference between the first electrode and the second electrode of the APCI ion source, revealed stereochemical dependence of different fragmentations. The APCI spectra of alkaloids were predominantly the $[M+H]^+$ ion and the major fragment ion, corresponding to the $[M+H-H_2O]^+$ ion or the $[M+H-CH_3COOH]^+$ ion, and comparison of the APCI spectra showed that the abundance of fragment ions was significantly higher for C-1 β -form alkaloids than for C-1 α -form alkaloids, and for C-12 β -form alkaloids than for C-12 α -form alkaloids. The characteristic fragment ions were formed due to the loss of an acetic acid or a water molecule at position 12. The fragmentation mechanisms depending on the stereochemistry of the precursor ion could be discerned by recording the spectra in a deuterated solvent system of 0.05 M ammonium acetate in D_2O -acetonitrile-tetrahydrofuran. Loss of CH_3COOD or D_2O from the precursor ion gave the fragment ion. This result indicated that the proton of protonation was included in the leaving acetic acid and water molecule, respectively. The peak intensity ratio for $R=[M+H]^+/[M+H-H_2O]^+ + [M+H-CH_3COOH]^+$ manifested the stereochemical differentiation of alkaloids at position 1 or 12.

Key words atmospheric pressure chemical ionization; diterpenoid alkaloid; 12-*epi*-lucidusculine 12,15-diacetyl-1-*epi*-luciculine; lucidusculine; mass spectrometry

The structural elucidation of organic compounds of natural and synthetic origin has been one of the major analytical applications of mass spectrometry (MS). In general, mass spectra provide useful information on the stereochemistry of the compound under investigation, and the stereochemical information arises from sterically controlled ionic fragmentations.¹⁾ The fragmentation pattern manifested in a conventional mass spectrum is a direct reflection of the internal energy distribution of precursor ions. Consequently, stereochemical differentiation, which generally depends on one particular fragmentation pathway among various dissociation channels, is very sensitive to the experimental conditions of ionization. Several analytical methods have been developed in order to control the amount of internal energy deposited on the precursor ion of interest with regard to the fragment ion yield.^{2–4)} A number of reports on the stereochemistry of indoloquinolizine alkaloids,⁵⁾ quinolizine alkaloids⁶⁾ and eburnane-type alkaloids,⁷⁾ and indoloquinolizine⁸⁾ and indole⁹⁾ alkaloids by electrospray ionization have appeared in recent years.

Various *Aconitum* (Ranunculaceae) plants produce norditerpenoid and diterpenoid alkaloids.¹⁰⁾ Structure studies of diterpenoid alkaloids involving mass spectrometry have been carried out essentially by electron impact (EI) ionization and conventional analysis.^{11–17)} EI spectra of *Aconitum* alkaloids showed a molecular ion together with many fragment ions. In general, atmospheric pressure chemical ionization (APCI) has a wider range of applications for elucidation of structures of organic compounds and generates protonated molecules ($[M+H]^+$) with remarkable ease and efficiency. We applied an APCI-MS method to the analysis of *Aconitum* alkaloids,^{18–20)} and the APCI mass spectra of *Aconitum* alkaloids showed predominantly the $[M+H]^+$ ion together with major

fragment ions. We previously reported that high-performance liquid chromatography (HPLC)-APCI-MS was useful for the structural elucidation of six stereoisomeric norditerpenoid neoline-type alkaloids at position 6,²¹⁾ corresponding to neoline, 14-acetylneoline, chasmanine, subcusine, subcumine and 6-*epi*-chasmanine; and for the structural elucidation of ten stereoisomeric norditerpenoid neoline-type alkaloids, corresponding to neoline, 14-acetylneoline, 8-acetyl-14-benzoylneoline, 1-*epi*-neoline, 14-acetyl-1-*epi*-neoline and 8-acetyl-14-benzoyl-1-*epi*-neoline; and delcosine-type alkaloids, corresponding to delcosine, 14-acetyldelcosine, 1-*epi*-delcosine and 14-acetyl-1-*epi*-delcosine, at position 1.²²⁾ Comparison of APCI spectra of these alkaloids showed that the abundance of fragment ions was significantly higher for C-6 β -form alkaloids, corresponding to subcusine, subcumine and 6-*epi*-chasmanine, than for C-6 α -form alkaloids, corresponding to neoline, 14-acetylneoline and chasmanine, and for C-1 β -form alkaloids, corresponding to 1-*epi*-neoline, 14-acetyl-1-*epi*-neoline, 8-acetyl-14-benzoyl-1-*epi*-neoline, 1-*epi*-delcosine and 14-acetyl-1-*epi*-delcosine, than for C-1 α -form alkaloids, corresponding to neoline, 14-acetylneoline, 8-acetyl-14-benzoylneoline, delcosine and 14-acetyldelcosine.

In the present paper, we report the results of an HPLC-APCI-MS study of diterpenoid alkaloids, 12,15-diacetyluciculine (1),²³⁾ 12,15-diacetyl-1-*epi*-luciculine (2), 1,12,15-triacetyluciculine (3),²³⁾ 1,12,15-triacetyl-1-*epi*-luciculine (4), lucidusculine (5),²³⁾ 12-*epi*-lucidusculine (6),²⁴⁾ and 1,12,15-triacetyl-12-*epi*-luciculine (7), for resolving structural problems related to the differentiation of stereoisomers. These alkaloids differ in the stereochemistry at position 1 or 12, alkaloids 2, 4, 6 and 7 being characterized by a β -form and alkaloids 1, 3 and 5 by an α -form.

* To whom correspondence should be addressed. e-mail: kowada@hokuyakudai.ac.jp

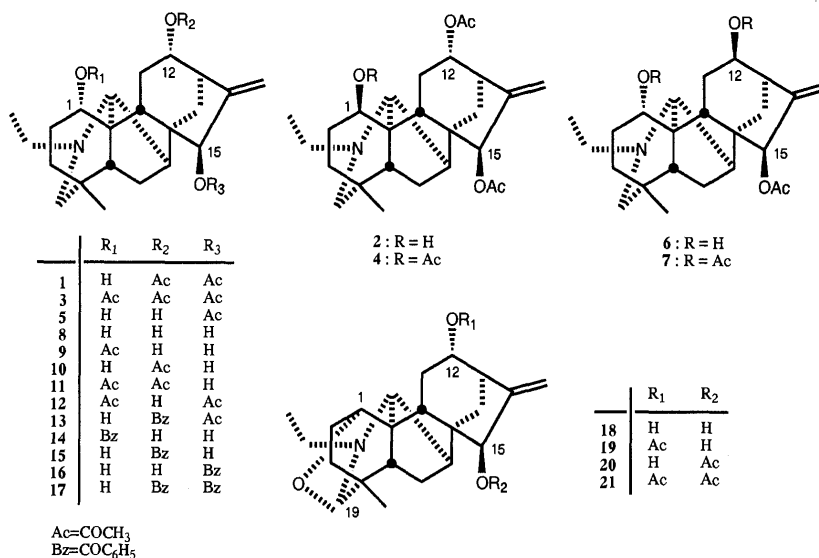


Chart 1

Results and Discussion

We applied an HPLC-APCI-MS method to the investigation of stereochemical differentiation of diterpenoid alkaloids **1**—**4**, which contain a C-1 α - or β -form, and alkaloids **5**—**7**, which contain a C-12 α - or β -form. At first, the APCI mass spectra obtained by HPLC-APCI-MS of alkaloids **1**—**4** were examined (Fig. 1). When APCI mass spectra of alkaloids **1**—**4** were recorded at the drift voltage of 140 V between the first electrode and the second electrode of the APCI ion source, the $[M+H]^+$ ion and a characteristic product ion were obtained (Table 1). The spectra of **1** and **2** showed a very intense ion peak at m/z 444, corresponding to the $[M+H]^+$ ion, and fragment ions at m/z 426 and 384, which were formed due to the loss of a water and an acetic acid molecule, respectively. Drift collision-induced dissociation (drift-CID) analysis^{25,26} of **1** and **2** (Fig. 2) clearly showed that the abundance of fragment ions increased. Comparison of the two spectra showed a remarkable increase in the relative abundance of the ion peaks at m/z 426 and 384 in the case of **2**. The spectra of **3** and **4** revealed a strong $[M+H]^+$ ion at m/z 486 and a fragment ion at m/z 426, which was formed due to the loss of an acetic acid molecule (Table 1). Drift-CID analysis of **3** and **4** showed that the abundance of the fragment ion increased. Comparison of these spectra indicated that the abundance of the m/z 426 ion for **4** was greater than that for **3**. These results indicated that the relative abundance of the characteristic fragment ions for C-1 β -form alkaloids, which contain **2** and **4**, was greater than that for C-1 α -form alkaloids, which contain **1** and **3**.

APCI mass spectra of alkaloids **1**—**4** showed characteristic fragment ions, which were formed due to the loss of a water and an acetic acid molecule. Therefore, evidence of fragmentation mechanisms depending on the precursor ion was provided by the study of fragmentation behaviors of luciculine (**8**), 1-acetylliciculine (**9**), 12-acetylliciculine (**10**), 1,12-diacetylliciculine (**11**), 1,15-diacetylliciculine (**12**), 12-benzoylluciculine (**13**), 1-benzoylluciculine (**14**), 12-benzoylluciculine (**15**), 15-benzoylluciculine (**16**), 12,15-dibenzoylluciculine (**17**), dehydroluciculine (**18**), 12-acetyldehydroluciculine (**19**), dehydroluciculine (**20**) and 12-

acetyldehydroluciculine (**21**) (Table 1). The spectra of **10**, **11**, **19** and **21**, which contain an acetyl group at C-12, showed a fragment ion peak corresponding to the $[M+H-CH_3COOH]^+$ ion. Similarly, the spectra of **15** and **17**, which contain a benzoyl group at C-12, showed a fragment ion peak corresponding to the $[M+H-C_6H_5COOH]^+$ ion. The spectra of **13**, which contains a benzoyl group at C-12, showed a major fragment ion peak at m/z 384 corresponding to the $[M+H-C_6H_5COOH]^+$ ion. The spectra of **8**, **9**, **12**, **14**, **16**, **18** and **20**, which contain an OH group at C-12, showed a fragment ion peak corresponding to the $[M+H-H_2O]^+$ ion. These results indicated that the characteristic fragment ions were formed due to the loss of a water, an acetic acid or a benzoic acid molecule at position 12.

In order to compare the stabilities of the $[M+H]^+$ ions of **1** and **2** towards the fragmentation processes, we proceeded to the study of energy dependence of the ion abundances. This experiment was carried out in a simple manner: the drift voltage was increased by 15 V every three scans in the range 0—240 V, and the ion peak intensity values were calculated by averaging the signals measured in each set of three scans.²¹⁾

The results for the ions at m/z 426 and 384 are shown in Fig. 3. The ion appearing at m/z 384 was of very similar abundance for the two isomers. In contrast, the conditions for the formation of the ion at m/z 426 appear to be closely related to the stereochemistry of the compounds under investigation and were sensitive to energy variation. The curve of the ion at m/z 426 was completely different. In the case of **2**, the loss of a water molecule remained the major fragmentation pathway over the whole energy range. The situation is completely reversed for **1**, in favor of the m/z 384 fragment ion, whose abundance reaches a maximum around 140 V. For comparison, energy dependence of the fragmentation pathway in relation to the stereochemistry of the protonated molecules was examined (Fig. 4). The formation of the ion at m/z 426 clearly required a greater amount of energy in the case of **1** than in the case of **2**. The two curves obtained were separated from 40—50 V, evidently corresponding to the stability difference between the $[M+H]^+$ ions of **1** and **2** towards this

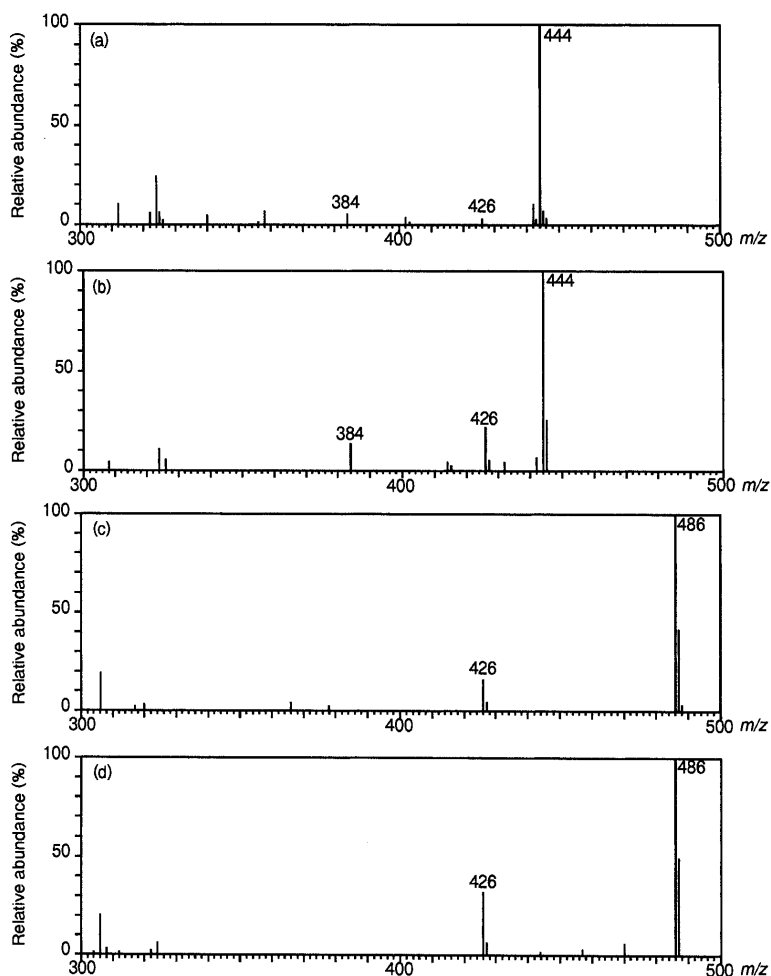


Fig. 1. APCI Mass Spectra of Alkaloids

(a) 12,15-Diacetylluciculine (**1**), (b) 12,15-diacetyl-1-*epi*-luciculine (**2**), (c) 1,12,15-triacetylluciculine (**3**), (d) 1,12,15-triacetyl-1-*epi*-luciculine (**4**). The drift voltage between the first and the second electrodes was 140 V.

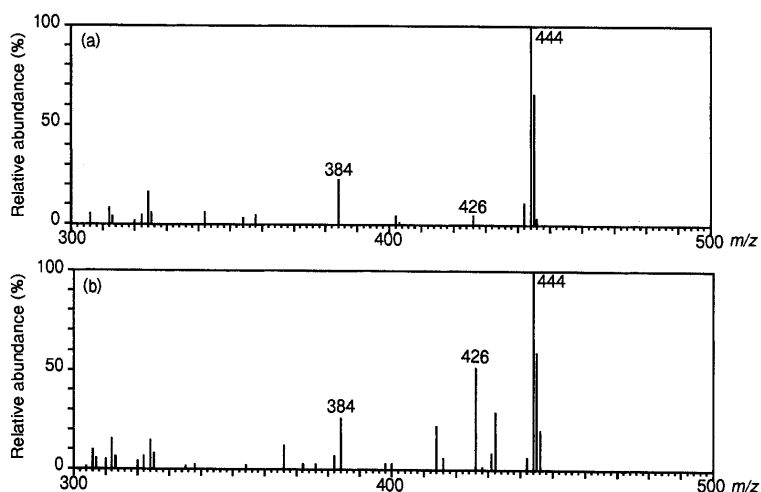


Fig. 2. APCI Mass Spectra of Alkaloids 12,15-Diacetylluciculine (**1**; a) and 12,15-Diacetyl-1-*epi*-luciculine (**2**; b)

The drift voltage between the first and the second electrodes was 160 V.

fragmentation pathway. Also, the formation of the ion at m/z 384 appeared in the decreasing parts of curves that were identical for the two compounds. The two curves obtained were separated from about 40 V, evidently corresponding to the stability difference between the $[M+H]^+$ ions **1** and **2** towards this fragmentation pathway. These results indicated

that the formation of the fragment ions at m/z 426 and 384 clearly required a greater amount of energy in the case of **1**, which contains a C-1 α -form, than in the case of **2**, which contains a C-1 β -form.

The fragmentation mechanisms depending on the stereochemistry of the precursor ion could be discerned by record-

Table 1. m/z and Relative Abundances (%) of the Mass Spectral Fragments of Diterpenoid Alkaloids

	$[M+H]^+$	$[M+H-H_2O]^+$	$[M+H-RCOOH]^+$	$[M-d_n+D]^+$	$[M-d_n+D-D_2O]^+$	$[M-d_n+D-CH_3COOD]^+$
1	444 (100%)	426 (3%)	384 (6%)	446 (100%)	426 (6%)	385 (1%)
2	444 (100%)	426 (22%)	384 (12%)	446 (100%)	426 (14%)	385 (4%)
3	486 (100%)	—	426 (15%)	487 (100%)	—	426 (32%)
4	486 (100%)	—	426 (32%)	—	—	—
5	402 (100%)	384 (10%)	342 (7%)	405 (100%)	385 (2%)	344 (4%)
6	402 (100%)	384 (12%)	342 (24%)	405 (100%)	385 (8%)	344 (13%)
7	486 (100%)	—	426 (28%)	—	—	—
8	360 (100%)	342 (3%)	—	364 (100%)	344 (6%)	—
9	402 (100%)	384 (4%)	342 (29%)	—	—	—
10	402 (100%)	—	342 (27%)	—	—	—
11	444 (68%)	—	384 (14%)	—	—	—
12	444 (100%)	426 (3%)	384 (45%)	—	—	—
13	506 (100%)	488 (9%)	446 (10%), 384 (68%)	—	—	—
14	464 (100%)	446 (3%)	342 (53%)	—	—	—
15	464 (100%)	—	342 (23%)	—	—	—
16	464 (100%)	446 (8%)	342 (9%)	—	—	—
17	568 (100%)	—	446 (20%)	—	—	—
18	358 (100%)	340 (39%)	—	—	—	—
19	400 (100%)	—	340 (11%)	—	—	—
20	400 (100%)	382 (1%)	340 (18%)	—	—	—
21	442 (100%)	—	382 (2%)	—	—	—

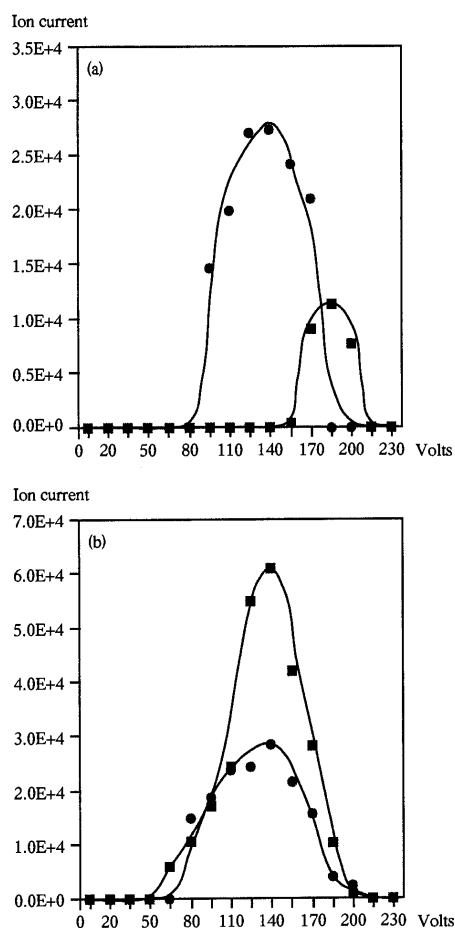


Fig. 3. Ion Currents of the Fragment Ions at m/z 426 (■) and m/z 384 (●) Arising from Alkaloids 12,15-Diacetyluciculine (1; a) and 12,15-Diacetyl-1-*epi*-luciculine (2; b) as a Function of the Drift Voltage between the First and the Second Electrodes of the APCI Ion Source

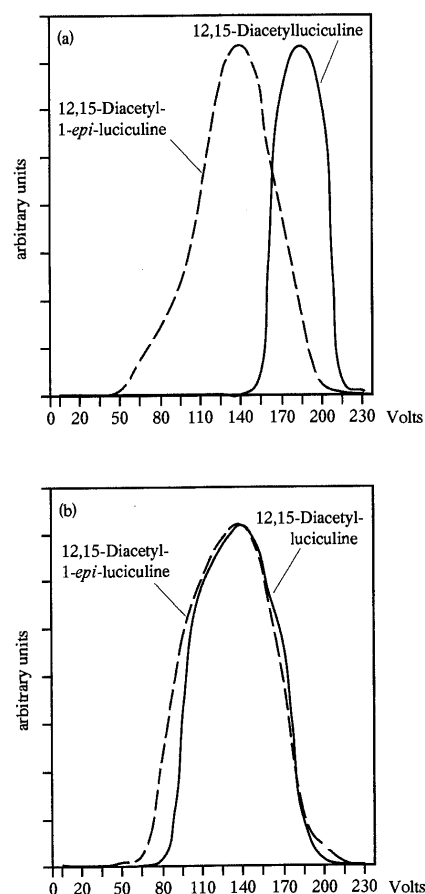


Fig. 4. Ion Currents of the Fragment Ions at m/z 426 (a) and m/z 384 (b) Arising from Alkaloids 12,15-Diacetyluciculine (1, Solid Line) and 12,15-Diacetyl-1-*epi*-luciculine (2, Dashed Line) as a Function of the Drift Voltage between the First and the Second Electrodes of the APCI Ion Source

For a better comparison, the tops of the curves were equalized in the figure.

ing the spectra of alkaloids 1 and 2 in a deuterated solvent system of 0.05 M ammonium acetate in D_2O -acetonitrile-tetrahydrofuran. These spectra showed a major ion peak at

m/z 446 corresponding to the $[M-d+D]^+$ ions formed by deuterium exchange of hydroxyl hydrogen and addition of D^+ on the molecules (Fig. 5). Loss of D_2O and CH_3COOD

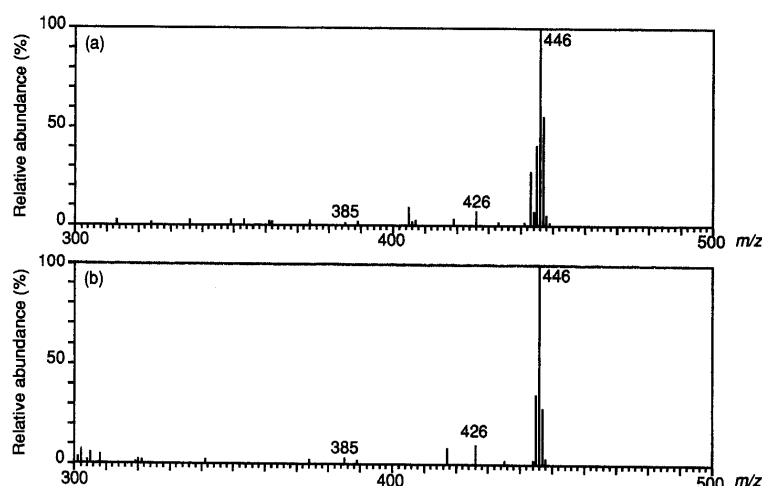


Fig. 5. APCI Mass Spectra of Alkaloids Recorded by Solvent System of 0.05 M Ammonium Acetate in D_2O -Acetonitrile-Tetrahydrofuran (a) 12,15-Diacetyluciculine (1), (b) 12,15-diacetyl-1-*epi*-luciculine (2). The drift voltage between the first and the second electrodes was 140 V.

from this precursor ion gave the fragment ions at m/z 426 and 385, respectively (Table 1). This result indicated that the proton of protonation was included in the leaving water molecule and acetic acid molecule, irrespective of the stereochemistry at position 1. As we have reported,²¹⁾ the site of protonation in the norditerpenoid alkaloids was at a nitrogen atom, and proton chelation occurred between the amino group and the C-1 hydroxyl group. Similarly, the site of protonation in the diterpenoid alkaloids was at a nitrogen atom, and proton chelation occurred between the amino group and the C-1 hydroxyl group (Chart 2a). The fragment ion at m/z 384 was formed so that the proton of protonation could be transferred to the C-12 acetyl group and fragmented as an acetic acid molecule.

The stabilization of the $[M+H]^+$ ion of **1** relative to the stereoisomer **2** towards the loss of a water molecule is thought to be due to an intramolecular H-bonded system (Chart 2a). Therefore, in the case of **2**, it was presumed that proton chelation cannot occur (Chart 2b), and proton transfer occurred more easily in alkaloid **2** than in **1**, and that the formation of the ion at m/z 384 was easier in the case of **2** than in the case of **1**. Also, the formation of the ion at m/z 426 was due to the elimination of a water molecule at position 1. In the case of **2**, it was presumed that proton chelation cannot occur, and the axial positions of the corresponding substituents (C-1 β hydroxyl group and the hydrogen at C-3, C-5 and C-9) suggested a 1,3-diaxial interaction effect of the fragmentation (Chart 2b). In fact, the abundance of the fragment ion m/z 426 increased more in the case of **2** than in the case of **1**.

We considered the peak intensity ratio for alkaloids **1**–**4** to be $R = [M+H]^+ / [M+H-H_2O]^+ + [M+H-CH_3COOH]^+$. The R values of alkaloids **1** and **3**, which contain a C-1 α -hydroxyl group, were 6.7–11.1, respectively, whereas those of alkaloids **2** and **4**, which contain a C-1 β -hydroxyl group, were 2.9–3.1, respectively. These results indicated that the R value showed stereochemical differentiation of alkaloids at position 1.

Next, the APCI mass spectra of alkaloids **5** and **6** exhibited at m/z 402 a highly intense ion peak corresponding to the $[M+H]^+$ ion (Fig. 6). The spectra of **5** and **6** showed fragment ions at m/z 384 and 342, and the fragment ions were

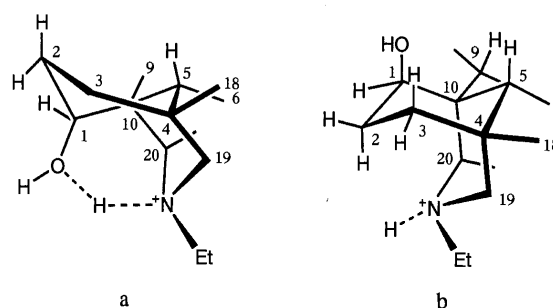


Chart 2

formed from the $[M+H]^+$ ion due to the loss of a water and an acetic acid molecule, respectively (Table 1). The drift-CID spectra of **5** and **6** indicated that the abundance of fragment ions at m/z 384 and 342 increased, and the abundance of the ion at m/z 342 was greater for **6**, which contains a C-1 β -form, than for its epimer **5**, which contains a C-1 α -form (Fig. 7).

In order to compare the stabilities of the $[M+H]^+$ ion of **5** and **6** towards the fragmentation processes, we proceeded to the study of energy dependence of the ion abundances. The results for the ions at m/z 342 and 384 are shown in Fig. 8. The ion appearing at m/z 384 was of very similar abundance for the two isomers. In contrast, the conditions for the formation of the ion at m/z 342 appear to be closely related to the stereochemistry of the compounds under investigation and were sensitive to energy variation. The curves of the ions at m/z 342 and 384 were completely different. In the case of **6**, the loss of an acetic acid molecule remained the major fragmentation pathway over the whole energy range. The situation is completely reversed for **5**, in favor of the m/z 384 fragment ion, whose abundance reaches a maximum at around 140 V. The top of the m/z 342 ion curves corresponding to **6** seemed to be located at voltage values lower than **5**.

For comparison, energy dependence of the fragmentation pathway in relation to the stereochemistry of the protonated molecules was examined (Fig. 9). In the m/z 384 ion curves, even though the increasing part of the curve was shifted to higher energies at about 70 V in the case of **5**, it was noteworthy that the m/z 384 ion current became strong in the case

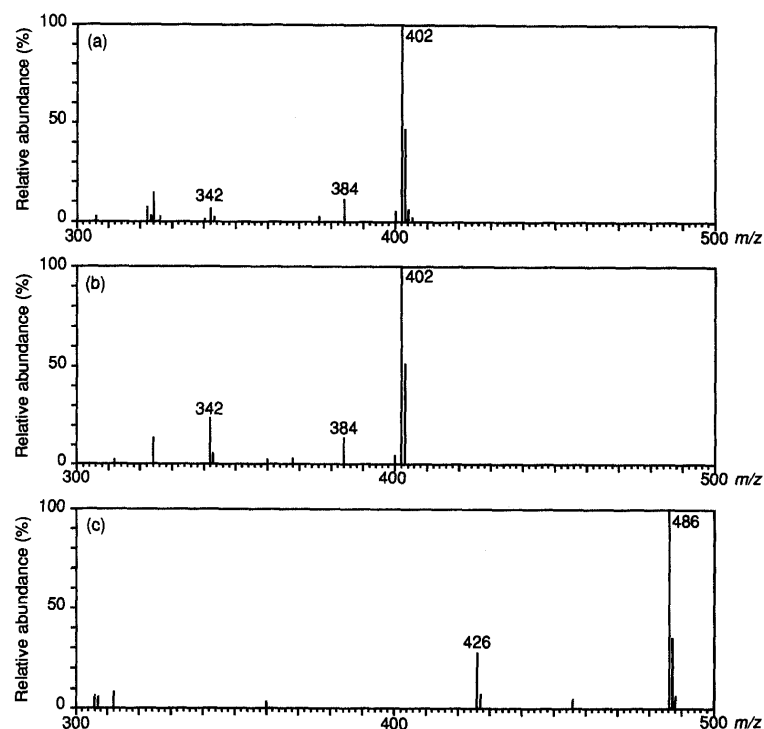


Fig. 6. APCI Mass Spectra of Alkaloids

(a) Lucidusculine (5), (b) 12-*epi*-lucidusculine (6), (c) 1,12,15-triacetyl-12-*epi*-lucidusculine (7). The drift voltage between the first and the second electrodes was 140 V.

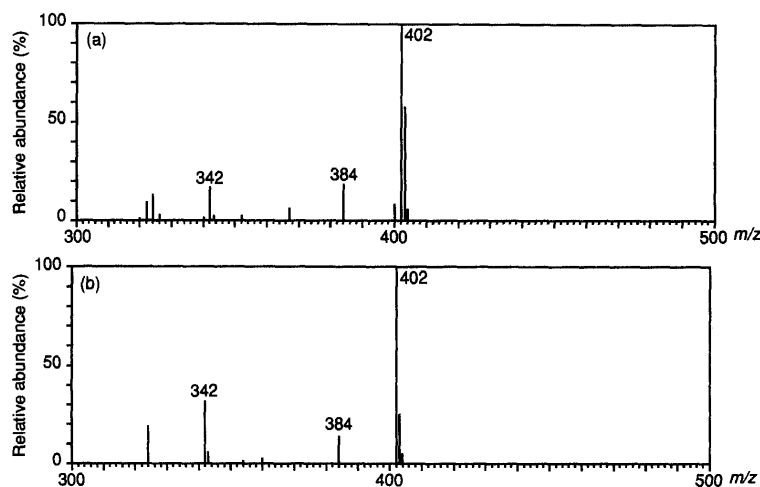


Fig. 7. APCI Mass Spectra of Alkaloids Lucidusculine (5; a) and 12-*Epi*-lucidusculine (6; b)

The drift voltage between the first and the second electrodes was 160 V.

of 6. In contrast, the formation of the ion at m/z 342 clearly required a greater amount of energy in the case of 5 than in the case of 6. The two curves obtained were separated by 65–70 V, evidently corresponding to the stability difference between the $[M+H]^+$ ions 5 and 6 towards this fragmentation pathway. These results indicated that the formation of the fragment ions at m/z 342 and 384 clearly required a greater amount of energy in the case of 5, which contains a C-12 α -form, than the case of 6, which contains a C-12 β -form.

The spectrum of alkaloid 7 revealed a strong $[M+H]^+$ ion at m/z 486. A fragment ion was observed at m/z 426. This ion could be explained by the loss of an acetic acid molecule from the $[M+H]^+$ ion. Drift-CID analysis of 7 showed that the abundance of the fragment ion increased. Comparison of

7 and 3 spectra indicated that the abundance of the m/z 426 ion for 7 was greater than that for 3.

In the spectra of 3 and 5–7, the abundance of the fragment ion was greater for C-12 β -form alkaloids, which correspond to 6 and 7, than for its epimer C-12 α -form alkaloids, which correspond to 3 and 5. Comparison of spectra of 5 and 6 showed a remarkable increase in the relative abundance of the fragment ion peaks at m/z 342 and 384 in the case of 6. Similarly, the m/z 426 ion abundance was higher for 7 than for 3. These results suggested that in the case of alkaloids 6 and 7, it was caused by the steric interactions of the substituents (C-9 hydrogen, C-12 β -hydroxyl, C-15 β -acetyl group) (Chart 3).

The fragmentation mechanisms depending on the stereochemistry of the precursor ion could be discerned by record-

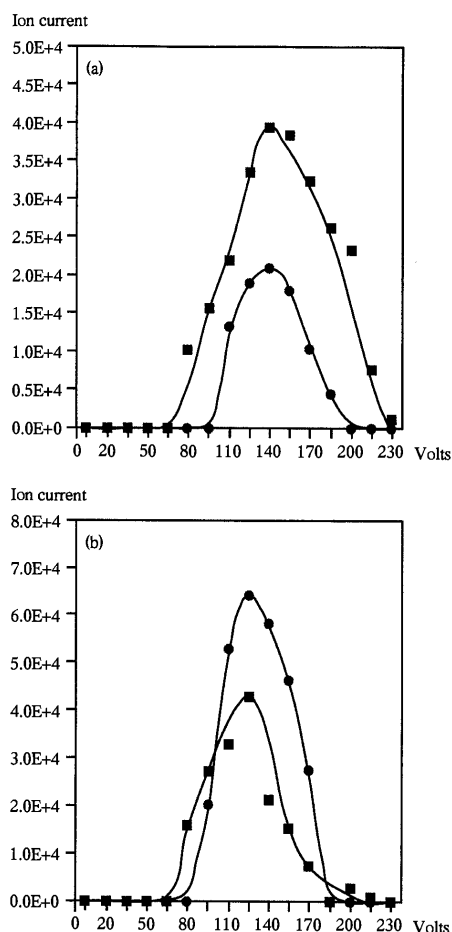


Fig. 8. Ion Currents of the Fragment Ions at m/z 384 (■) and m/z 342 (●) Arising from Alkaloids Lucidusculture (5; a) and 12-Epi-lucidusculture (6; b) as a Function of the Drift Voltage between the First and the Second Electrodes of the APCI Ion Source

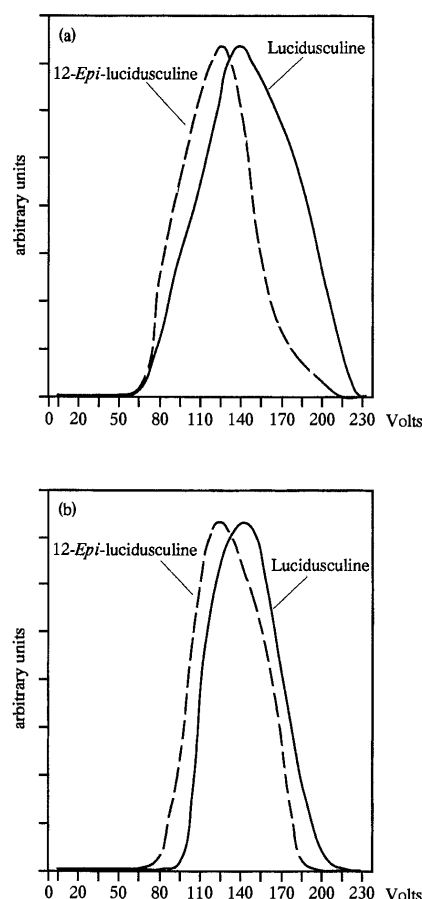


Fig. 9. Ion Currents of the Fragment Ions at m/z 384 (a) and m/z 342 (b) Arising from Alkaloids Lucidusculture (5, Solid Line) and 12-Epi-lucidusculture (6, Dashed Line) as a Function of the Drift Voltage between the First and the Second Electrodes of the APCI Ion Source

For a better comparison, the tops of the curves were equalized in the figure.

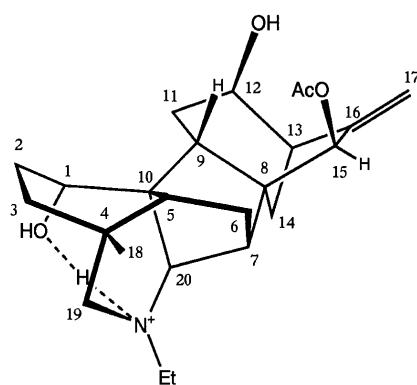


Chart 3

ing the spectra of alkaloids 5 and 6 in a deuterated solvent system of 0.05 M ammonium acetate in D_2O -acetonitrile-tetrahydrofuran. These spectra showed a major ion peak at m/z 405 corresponding to the $[M-d_2+D]^+$ ions formed by deuterium exchange of hydroxyl hydrogen and addition of D^+ on the molecules (Fig. 10). Loss of CH_3COOD and D_2O from this precursor ion gave the fragment ions at m/z 344 and 385, respectively. This result indicated that the proton of protonation was included in the leaving water or acetic acid molecule, irrespective of the stereochemistry at position 12.

We considered the peak intensity ratio for alkaloids 3 and

5–7 to be $R = [M+H]^+ / [M+H-H_2O]^+ + [M+H-CH_3COOH]^+$. The R values of alkaloids 3 and 5, which contain a C-12 α -form, were 5.9–6.7, whereas those of alkaloids 6 and 7, which contain a C-12 β -form, were 2.8–3.6. These results indicated that the R value showed stereochemical differentiation of alkaloids at position 12.

In conclusion, the APCI spectra of diterpenoid alkaloids were remarkably simple and very similar with respect to characteristic fragments. APCI-MS was successfully applied to seven stereoisomeric diterpenoid alkaloids at position 1 or 12. APCI-MS was useful for the structural elucidation of seven stereoisomeric diterpenoid alkaloids. Comparison of the APCI spectra of these alkaloids showed that the abundance of fragment ions was significantly higher for C-1 β -form alkaloids than for C-1 α -form alkaloids, and for C-12 β -form alkaloids than for C-12 α -form alkaloids. The peak intensity ratio for $R = [M+H]^+ / [M+H-H_2O]^+ + [M+H-CH_3COOH]^+$ manifested the stereochemical differentiation of alkaloids at position 1 or 12. We are considering a future APCI-MS study of diterpenoid alkaloids 8–21 to resolve the structural problems related to the differentiation of stereoisomers. APCI-MS experiments can be useful for detecting subtle structural characteristics of organic molecules, including stereochemical differentiation.

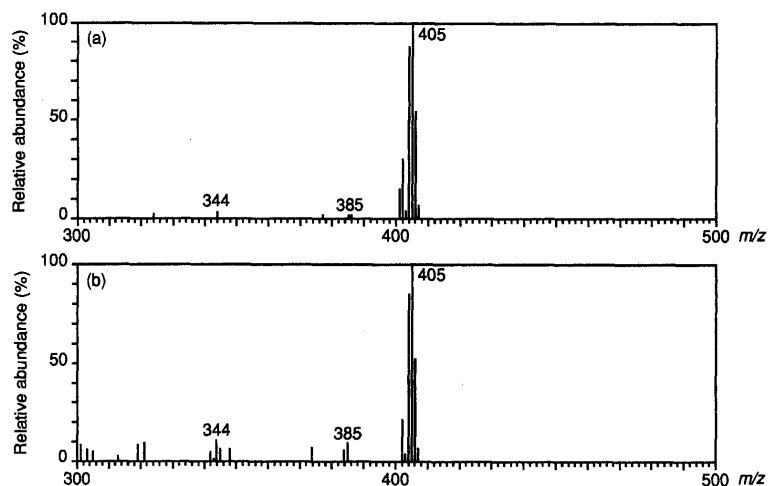


Fig. 10. APCI Mass Spectra of Alkaloids Recorded by Solvent System of 0.05 M Ammonium Acetate in D_2O -Acetonitrile-Tetrahydrofuran (a) Lucidusculine (5), (b) 12-*epi*-lucidusculine (6). The drift voltage between the first and the second electrodes was 140 V.

Experimental

All melting points were measured on a Yanagimoto micromelting point apparatus without correction. IR spectra were recorded using a Model FT/IR 7000 spectrometer (Jasco, Tokyo, Japan). 1H -NMR spectra were measured with a Model GX-270 spectrometer (JEOL, Tokyo, Japan) using trimethylsilyl or tetramethylsilane (TMS) as an internal standard. MS was performed with a Model M-2000 mass spectrometer (Hitachi, Tokyo, Japan).

Materials 12,15-Diacetyluciculine (1), lucidusculine (5), luciculine (8), 1-acetyluciculine (9), dehydrolucidusculine (20) and 12-acetyldehydrolucidusculine (21) were purified from *Aconitum yessoense* var. *macrotysoense* roots and identified as described previously.²³⁾ 1,12,15-Triacetyluciculine (3),²³⁾ 12-acetyluciculine (10),²⁷⁾ dehydrolucidusculine (18)²³⁾ and 12-acetyldehydrolucidusculine (19)²⁷⁾ were prepared as described previously. 12,15-Diacetyl-1-*epi*-luciculine (2), 1,12,15-triacetyl-1-*epi*-luciculine (4), 12-*epi*-lucidusculine (6),²⁴⁾ 1,12,15-triacetyl-12-*epi*-luciculine (7), 1,12-diacetyluciculine (11), 1,15-diacetyluciculine (12),²⁸⁾ 12-benzoyllucidusculine (13), 1-benzoylluciculine (14), 12-benzoylluciculine (15), 15-benzoylluciculine (16) and 12,15-dibenzoylluciculine (17) were synthesized from 12,15-diacetyluciculine (2), dehydrolucidusculine (20), 1-acetyluciculine (9), 1,12,15-triacetyluciculine (3), lucidusculine (5) and luciculine (8), respectively. Ammonium acetate of reagent grade was purchased from Kanto Chemicals (Tokyo, Japan), and acetonitrile and tetrahydrofuran of HPLC grade were purchased from Wako Pure Chemical Industries (Osaka, Japan).

Preparation of 12,15-Diacetyl-1-*epi*-luciculine (2) 1) Oxidation of 12,15-Diacetyluciculine: A solution of 12,15-diacetyluciculine (1: 30.6 mg) in dichloromethane (9 ml) was mixed with pyridinium dichromate (PDC; 78 mg). The mixture was stirred at 0 °C for 4 h 50 min. The reaction mixture was passed through a short column of florisil and then purified by column chromatography on silica gel (5–1% hexane-ether saturated with 28% ammonia) to give 12,15-diacetyl-1-dehydrolucidusculine (19.2 mg, 63%) and the starting material (15.8 mg). Amorphous. IR (KBr) cm^{-1} : 1742, 1696, 1232, 1164, 907. 1H -NMR ($CDCl_3$) δ : 0.80 (3H, s, 18- CH_3), 1.08 (3H, t, $J=7.0$ Hz, $N-CH_2CH_3$), 2.02, 2.11 (each 3H, s, $OCOCH_3$), 4.63 (1H, dd, $J=7.0, 9.7$ Hz, 12 β -H), 4.98, 5.29 (each 1H, s, 17- H_2), 5.49 (1H, s, 15 α -H). HR-EI-MS m/z : 441.2491 (Calcd for $C_{26}H_{33}NO_5$: 441.2514). EI-MS m/z : 441 (M^+), 398 ($M^+ - COCH_3$, base peak), 382 ($M^+ - OCOCH_3$).

2) Reduction of 12,15-Diacetyl-1-dehydrolucidusculine: 12,15-Diacetyl-1-dehydrolucidusculine (23.0 mg), dissolved in MeOH-absolute EtOH (1:1, 4 ml), was treated with $NaBH_4$ (5 mg). The resulting solution was stirred at room temperature for 50 min. Water was added, and the mixture was extracted with $CHCl_3$. The combined extracts were washed with 5% aqueous $NaHCO_3$ and brine, dried over anhydrous $MgSO_4$, and evaporated in vacuum to give a residue, which was separated by column chromatography on silica gel (10% hexane-ether saturated with 28% ammonia) to give 12,15-diacetyl-1-*epi*-luciculine (2; 5.6 mg, 24%) and 12,15-diacetyluciculine²³⁾ (1; 13.5 mg, 58%).

2: Amorphous. IR (KBr) cm^{-1} : 3450, 1738, 1647, 1236, 1027, 900. 1H -NMR ($CDCl_3$) δ : 0.74 (3H, s, 18- CH_3), 1.03 (3H, t, $J=7.0$ Hz, $N-CH_2CH_3$), 2.04, 2.12 (each 3H, s, $OCOCH_3$), 4.10 (1H, brs, 1 α -H), 4.68 (1H, dd, $J=7.3, 10.2$ Hz, 12 β -H), 4.97, 5.28 (each 1H, s, 17- H_2), 5.50 (1H, s, 15 α -

H). HR-EI-MS m/z : 443.2678 (Calcd for $C_{26}H_{37}NO_5$: 443.2671); EI-MS m/z : 443 (M^+ , base peak), 425 ($M^+ - H_2O$), 400 ($M^+ - COCH_3$), 384 ($M^+ - OCOCH_3$).

Preparation of 1,12,15-Triacetyl-1-*epi*-luciculine (4) Acetic anhydride (0.7 ml) was added to a solution of 12,15-diacetyl-1-*epi*-luciculine (2; 10.3 mg) in pyridine (0.7 ml), and the mixture was then kept at 70 °C for 3 h. The usual work-up and purification by column chromatography on silica gel (15% hexane-ether saturated with 28% ammonia) afforded 1,12,15-triacetyl-1-*epi*-luciculine (4; 7.3 mg, 65%). Amorphous. IR (KBr) cm^{-1} : 1738, 1649, 1243, 1162, 901. 1H -NMR ($CDCl_3$) δ : 0.75 (3H, s, 18- CH_3), 1.02 (3H, t, $J=7.0$ Hz, $N-CH_2CH_3$), 2.03, 2.07, 2.16 (each 3H, s, $OCOCH_3$), 4.63 (1H, dd, $J=7.0, 10.0$ Hz, 12 β -H), 4.99, 5.30 (each 1H, s, 17- H_2), 5.14 (1H, brs, 1 α -H), 5.50 (1H, s, 15 α -H). HR-EI-MS m/z : 485.2770 (Calcd for $C_{28}H_{39}NO_6$: 485.2777). EI-MS m/z : 485 (M^+ , base peak), 442 ($M^+ - COCH_3$), 426 ($M^+ - OCOCH_3$).

Preparation of 12-*Epi*-lucidusculine (6) 1) Oxidation of Dehydrolucidusculine: A solution of dehydrolucidusculine (15: 197 mg) in dichloromethane (56 ml) was mixed with PDC (743.2 mg). The mixture was stirred at room temperature for 3 h. The reaction mixture was passed through a short column of florisil and then purified by column chromatography on silica gel (20% hexane-ether saturated with 28% ammonia) to give 12-dehydro-dehydrolucidusculine (41.6 mg, 21%) and the starting material (69.7 mg). mp 132–135 °C. IR (KBr) cm^{-1} : 1742, 1723, 1680, 1234, 1178, 898. 1H -NMR ($CDCl_3$) δ : 0.84 (3H, s, 18- CH_3), 1.03 (3H, t, $J=7.0$ Hz, $N-CH_2CH_3$), 2.15 (3H, s, $OCOCH_3$), 3.71 (1H, s, 19-H), 3.99 (1H, d, $J=5.3$ Hz, 1-H), 4.96, 5.28 (each 1H, s, 17- H_2), 5.64 (1H, s, 15 α -H). HR-EI-MS m/z : 397.2240 (Calcd for $C_{24}H_{31}NO_4$: 397.2251). EI-MS m/z : 397 (M^+ , base peak), 354 ($M^+ - COCH_3$), 341 ($M^+ - C_3H_5O$).

2) Reduction of 12-Dehydro-dehydrolucidusculine: $NaBH_4$ (15 mg) was added to the stirred solution of 12-dehydro-dehydrolucidusculine (70.6 mg) in MeOH-absolute EtOH (1:1, 12 ml) at room temperature. After 1 h 30 min, water was added. Work-up of the reaction mixture in the usual manner resulted in a residue, which was separated by column chromatography on silica gel ($CHCl_3$ saturated with 28% ammonia) to give 12-*epi*-lucidusculine (6; 37.1 mg, 52%). mp 204 °C (dec.). IR (KBr) cm^{-1} : 3374, 1742, 1661, 1234, 1127, 899. 1H -NMR ($CDCl_3$) δ : 0.79 (3H, s, 18- CH_3), 1.13 (3H, t, $J=7.0$ Hz, $N-CH_2CH_3$), 2.13 (3H, s, $OCOCH_3$), 3.90 (1H, dd, $J=6.3, 8.3$ Hz, 1 β -H), 4.18 (1H, brs, 12 α -H), 5.17, 5.23 (each 1H, s, 17- H_2), 5.59 (1H, s, 15 α -H). HR-EI-MS m/z : 401.2542 (Calcd for $C_{24}H_{35}NO_4$: 401.2564). EI-MS m/z : 401 (M^+ , base peak), 384 ($M^+ - OH$), 358 ($M^+ - COCH_3$), 342 ($M^+ - OCOCH_3$).

Preparation of 1,12,15-Triacetyl-12-*epi*-luciculine (7) Acetic anhydride (0.6 ml) and pyridine (0.6 ml) were added to 12-*epi*-lucidusculine (6; 13 mg), and the mixture was kept at 70 °C for 2 h. The usual work-up afforded 1,12,15-triacetyl-12-*epi*-luciculine (7; 15.0 mg, 96%). mp 153 °C (dec.). IR (KBr) cm^{-1} : 1734, 1247, 1170, 911. 1H -NMR ($CDCl_3$) δ : 0.73 (3H, s, 18- CH_3), 1.05 (3H, t, $J=7.0$ Hz, $N-CH_2CH_3$), 1.92, 2.05, 2.11 (each 3H, s, $OCOCH_3$), 4.89, 5.04 (each 1H, s, 17- H_2), 5.01 (1H, ddd, $J=8.7, 6.1, 1.4$ Hz, 12 α -H), 5.09 (1H, dd, $J=6.5, 10.7$ Hz, 1 β -H), 5.59 (1H, s, 15 α -H). HR-EI-MS m/z : 485.2780 (Calcd for $C_{28}H_{39}NO_6$: 485.2777). EI-MS m/z :

485 (M^+), 442 ($M^+ - \text{COCH}_3$), 426 ($M^+ - \text{OCOCH}_3$, base peak).

Preparation of 1,12-Diacetyluciculine (11) A mixture of 1-acetyluciculine (**9**; 16 mg), pyridine (1 ml) and acetic anhydride (1 ml) was kept at 0 °C for 1 h 20 min. The usual work-up and purification by column chromatography on silica gel (50% hexane–ether saturated with 28% ammonia) afforded 1,12,15-triacetyluciculine²³ (**3**; 1.6 mg, 12%) and 1,12-diacetyluciculine (**11**; 6.1 mg, 34%).

11: Amorphous. IR (KBr) cm^{-1} : 3375, 1730, 1640, 1245, 900. $^1\text{H-NMR}$ (CDCl_3) δ : 0.74 (3H, s, 18- CH_3), 1.07 (3H, t, $J=7.3$ Hz, $N\text{-CH}_2\text{CH}_3$), 2.01, 2.04 (each 3H, s, OCOCH_3), 4.16 (1H, s, 15 α -H), 4.40 (1H, dd, $J=6.3$, 10.0 Hz, 12 β -H), 5.04 (1H, dd, $J=6.8$, 10.7 Hz, 1 β -H), 5.21, 5.33 (each 1H, s, 17- H_2). HR-EI-MS m/z : 443.2697 (Calcd for $\text{C}_{26}\text{H}_{37}\text{NO}_5$: 443.2671). EI-MS m/z : 443 (M^+), 384 ($M^+ - \text{OCOCH}_3$, base peak).

Preparation of 1,15-Diacetyluciculine (12) A mixture of 1,12,15-triacetyluciculine (**3**; 145.3 mg) and K_2CO_3 -aqueous MeOH (16 ml, pH 9.0) was refluxed for 16 h. The usual work-up and purification by column chromatography on silica gel (CHCl_3 saturated with 28% ammonia) afforded 1,15-diacetyluciculine²⁶ (**12**; 28.1 mg, 21%) and 1-acetyluciculine²³ (**9**; 48.1 mg, 40%).

12: Amorphous. IR (KBr) cm^{-1} : 3400, 1720, 1640, 1230, 910. $^1\text{H-NMR}$ (CDCl_3) δ : 0.74 (3H, s, 18- CH_3), 1.11 (3H, t, $J=7.3$ Hz, $N\text{-CH}_2\text{CH}_3$), 2.08, 2.10 (each 3H, s, OCOCH_3), 3.55 (1H, dd, $J=6.3$, 9.5 Hz, 12 β -H), 4.93, 5.11 (each 1H, s, 17- H_2), 5.05 (1H, dd, $J=6.9$, 10.5 Hz, 1 β -H), 5.49 (1H, s, 15 α -H). HR-EI-MS m/z : 443.2691 (Calcd for $\text{C}_{26}\text{H}_{37}\text{NO}_5$: 443.2671). EI-MS m/z : 443 (M^+), 384 ($M^+ - \text{OCOCH}_3$, base peak).

Preparation of 12-Benzoyllucidusculine (13) A mixture of lucidusculine (**5**; 50.4 mg), pyridine (1 ml) and benzoyl chloride (0.059 ml) was kept at 0 °C for 1 h. The usual work-up and purification by column chromatography on silica gel (2% hexane–ether saturated with 28% ammonia) afforded 12-benzoyllucidusculine (**13**; 60.6 mg, 95%). mp 122–123 °C. IR (KBr) cm^{-1} : 3456, 1740, 1717, 1560, 1278, 1236, 907. $^1\text{H-NMR}$ (CDCl_3) δ : 0.78 (3H, s, 18- CH_3), 1.08 (3H, t, $J=7.0$ Hz, $N\text{-CH}_2\text{CH}_3$), 2.13 (3H, s, OCOCH_3), 3.95 (1H, dd, $J=6.1$, 7.5 Hz, 1 β -H), 4.85 (1H, t, $J=8.3$ Hz, 12 β -H), 5.04, 5.36 (each 1H, s, 17- H_2), 5.55 (1H, s, 15 α -H), 7.43 (2H, t, $J=7.5$ Hz, COC_6H_5), 7.55 (1H, t, $J=7.5$ Hz, COC_6H_5), 8.54 (2H, dd, $J=1.4$, 8.5 Hz, COC_6H_5). HR-EI-MS m/z : 505.2834 (Calcd for $\text{C}_{31}\text{H}_{39}\text{NO}_5$: 505.2827). EI-MS m/z : 505 (M^+ , base peak), 488 ($M^+ - \text{OH}$), 462 ($M^+ - \text{COCH}_3$), 446 ($M^+ - \text{OCOCH}_3$), 384 ($M^+ - \text{OCOC}_6\text{H}_5$).

Preparation of 1-Benzoylluciculine (14), 12-Benzoylluciculine (15) and 12,15-Dibenzoylluciculine (21) 1) A mixture of luciculine (**8**; 200 mg), pyridine (4 ml) and benzoyl chloride (0.45 ml) was kept at room temperature for 3 h 10 min. The usual work-up and purification by column chromatography on silica gel (50% hexane–ether saturated with 28% ammonia) afforded 12-benzoylluciculine (**15**; 73.8 mg, 29%), 1,12-dibenzoylluciculine (60.2 mg, 19%), 12,15-dibenzoylluciculine (**17**; 80.1 mg, 25%) and 1,12,15-tribenzoylluciculine (99.2 mg, 27%).

15: Amorphous. IR (KBr) cm^{-1} : 3410, 1715, 1603, 1584, 1278, 903. $^1\text{H-NMR}$ (CDCl_3) δ : 0.73 (3H, s, 18- CH_3), 1.03 (3H, t, $J=7.0$ Hz, $N\text{-CH}_2\text{CH}_3$), 3.90 (1H, dd, $J=5.8$, 7.5 Hz, 1 β -H), 4.17 (1H, d, $J=7.8$ Hz, 15 α -H), 4.70 (1H, t, $J=8.5$ Hz, 12 β -H), 5.21, 5.37 (each 1H, s, 17- H_2), 7.37 (2H, t, $J=7.8$ Hz, COC_6H_5), 7.49 (1H, t, $J=7.5$ Hz, COC_6H_5), 8.00 (2H, dd, $J=1.4$, 8.3 Hz, COC_6H_5). HR-EI-MS m/z : 463.2707 (Calcd for $\text{C}_{29}\text{H}_{37}\text{NO}_4$: 463.2720). EI-MS m/z : 463 (M^+), 446 ($M^+ - \text{OH}$), 342 ($M^+ - \text{OCOC}_6\text{H}_5$, base peak), 105 ($[\text{COC}_6\text{H}_5]^+$).

1,12-Dibenzoylluciculine: Amorphous. IR (KBr) cm^{-1} : 3420, 1710, 1603, 1584, 1276, 905. $^1\text{H-NMR}$ (CDCl_3) δ : 0.79 (3H, s, 18- CH_3), 1.17 (3H, t, $J=7.0$ Hz, $N\text{-CH}_2\text{CH}_3$), 4.22 (1H, d, $J=7.8$ Hz, 15 α -H), 4.52 (1H, dd, $J=6.5$, 10.5 Hz, 12 β -H), 5.26, 5.43 (each 1H, s, 17- H_2), 5.37 (1H, dd, $J=7.0$, 10.5 Hz, 1 β -H), 7.18 (2H, t, $J=7.5$ Hz, COC_6H_5), 7.38 (2H, t, $J=8.5$ Hz, COC_6H_5), 7.46 (3H, t, $J=8.7$ Hz, COC_6H_5), 7.59 (1H, t, $J=7.3$ Hz, COC_6H_5), 8.08 (2H, d, $J=8.5$ Hz, COC_6H_5). HR-EI-MS m/z : 567.2976 (Calcd for $\text{C}_{36}\text{H}_{41}\text{NO}_5$: 567.2982). EI-MS m/z : 567 (M^+), 446 ($M^+ - \text{OCOC}_6\text{H}_5$, base peak), 105 ($[\text{COC}_6\text{H}_5]^+$).

17: mp 128–130 °C. IR (KBr) cm^{-1} : 3372, 1717, 1624, 1578, 1272, 903. $^1\text{H-NMR}$ (CDCl_3) δ : 0.61 (3H, s, 18- CH_3), 1.02 (3H, t, $J=7.0$ Hz, $N\text{-CH}_2\text{CH}_3$), 3.96 (1H, dd, $J=6.1$, 8.0 Hz, 1 β -H), 4.86 (1H, t, $J=8.5$ Hz, 12 β -H), 5.05, 5.32 (each 1H, s, 17- H_2), 5.76 (1H, s, 15 α -H), 7.34–7.55, 7.98–8.04 (10H, m, COC_6H_5). HR-EI-MS m/z : 567.2974 (Calcd for $\text{C}_{36}\text{H}_{41}\text{NO}_5$: 567.2982). EI-MS m/z : 567 (M^+), 462 ($M^+ - \text{COC}_6\text{H}_5$), 444 (base peak), 105 ($[\text{COC}_6\text{H}_5]^+$).

1,12,15-Tribenzoylluciculine: Amorphous. IR (KBr) cm^{-1} : 1717, 1603, 1584, 1270, 895. $^1\text{H-NMR}$ (CDCl_3) δ : 0.67 (3H, s, 18- CH_3), 1.17 (3H, t, $J=7.0$ Hz, $N\text{-CH}_2\text{CH}_3$), 4.67 (1H, dd, $J=6.3$, 9.2 Hz, 12 β -H), 5.11, 5.40 (each 1H, s, 17- H_2), 5.45 (1H, dd, $J=7.3$, 10.5 Hz, 1 β -H), 5.81 (1H, s, 15 α -

H), 7.16–8.12 (15H, m, COC_6H_5). HR-EI-MS m/z : 671.3259 (Calcd for $\text{C}_{43}\text{H}_{45}\text{NO}_6$: 671.3245). EI-MS m/z : 671 (M^+), 566 ($M^+ - \text{COC}_6\text{H}_5$), 550 ($M^+ - \text{OCOC}_6\text{H}_5$), 105 ($[\text{COC}_6\text{H}_5]^+$, base peak).

2) Hydrolysis of 1,12-Dibenzoylluciculine: A mixture of 1,12-dibenzoylluciculine (60.2 mg) and 28% ammonia–MeOH– CHCl_3 (4–5.2–2 ml) was stirred at 70 °C for 10 d. The reaction mixture was evaporated, and then purification by column chromatography on silica gel (33% hexane–ether saturated with 28% ammonia) afforded 1-benzoylluciculine (**14**; 17.3 mg, 35%) and the starting material (24.5 mg). Amorphous. IR (KBr) cm^{-1} : 3452, 1700, 1584, 1276, 907. $^1\text{H-NMR}$ (CDCl_3) δ : 0.78 (3H, s, 18- CH_3), 1.15 (3H, t, $J=7.0$ Hz, $N\text{-CH}_2\text{CH}_3$), 3.36 (1H, m, 12 β -H), 4.18 (1H, d, $J=7.8$ Hz, 15 α -H), 5.14 (2H, s, 17- H_2), 5.34 (1H, dd, $J=7.0$, 10.4 Hz, 1 β -H), 7.45 (2H, t, $J=7.5$ Hz, COC_6H_5), 7.53 (1H, t, $J=7.5$ Hz, COC_6H_5), 8.05 (2H, dd, $J=1.4$, 8.3 Hz, COC_6H_5). HR-EI-MS m/z : 463.2722 (Calcd for $\text{C}_{29}\text{H}_{37}\text{NO}_4$: 463.2720). EI-MS m/z : 463 (M^+), 342 ($M^+ - \text{OCOC}_6\text{H}_5$, base peak), 105 ($[\text{COC}_6\text{H}_5]^+$).

Preparation of 15-Benzoylluciculine (16) A mixture of 12,15-dibenzoylluciculine (**17**; 80.1 mg) and 28% ammonia–MeOH– CHCl_3 (4–5.2–2 ml) was stirred at 70 °C for 4 d. The reaction mixture was evaporated, and then purification by column chromatography on silica gel (10% MeOH–ether saturated with 28% ammonia) afforded 15-benzoylluciculine (**16**; 25.9 mg, 40%) and the starting material (35.3 mg). mp 126–129 °C. IR (KBr) cm^{-1} : 3384, 1719, 1603, 1584, 1272, 895. $^1\text{H-NMR}$ (CDCl_3) δ : 0.65 (3H, s, 18- CH_3), 1.07 (3H, t, $J=7.0$ Hz, $N\text{-CH}_2\text{CH}_3$), 3.72 (1H, t, $J=7.8$ Hz, 12 β -H), 3.99 (1H, dd, $J=6.1$, 8.3 Hz, 1 β -H), 4.99, 5.13 (each 1H, s, 17- H_2), 5.77 (1H, s, 15 α -H), 7.48 (2H, t, $J=7.3$ Hz, COC_6H_5), 7.60 (1H, t, $J=7.3$ Hz, COC_6H_5), 8.06 (2H, dd, $J=1.4$, 8.3 Hz, COC_6H_5). HR-EI-MS m/z : 463.2720 (Calcd for $\text{C}_{29}\text{H}_{37}\text{NO}_4$: 463.2720). EI-MS m/z : 463 (M^+), 358 ($M^+ - \text{COC}_6\text{H}_5$, base peak), 105 ($[\text{COC}_6\text{H}_5]^+$).

HPLC-APCI-MS Conditions²¹ A model M-2000 mass spectrometer (Hitachi, Tokyo, Japan) through an APCI interface was used as the HPLC-APCI-MS system. The HPLC system consisted of a Model L-6200 chromatographic pump (Hitachi, Tokyo, Japan) and a Rheodyne (Cotati, CA, U.S.A.) Model 7125 injector with a 20- μl loop. Direct injection analysis was performed without HPLC columns. The eluent was transferred at the flow rate of 0.8 ml/min directly to the APCI interface. The solvent consisted of 0.05 M ammonium acetate–acetonitrile–tetrahydrofuran (60:25:15, v/v). The mass spectrometer interface consisted of nebulizing and vaporizing units. The temperature of the nebulizer was set to 280 °C to give optimum abundance of the target ions. The desolvation temperature was set to 400 °C. Vaporized sample and solvent molecules were passed into the ion source of the APCI-MS system. The solvent molecules were ionized by corona discharge, and then the sample molecules and ionized solvent molecules underwent ion-molecule reactions.

Deuterium Exchange Studies²¹ Sample solution dissolved in deuterated methanol. The solvent consisted of 0.05 M ammonium acetate in D_2O –acetonitrile–tetrahydrofuran (60:25:15, v/v). The conditions were the same as those stated above.

References

- 1) Splitter J. S., Turecek F. (eds.), "Application of Mass Spectrometry of Organic Stereochemistry," VCH, New York, 1994, pp. 83–671.
- 2) Fetterolf D. D., Yost R. A., *Int. J. Mass Spectrom. Ion Phys.*, **44**, 37–50 (1982).
- 3) McLuckey S. A., Cooks R. G., "Tandem Mass Spectrometry," ed. by McLafferty F. W., Wiley-Intersciences, New York, 1983, pp. 303–320.
- 4) Hayes R. N., Gross M. L., *Methods Enzymol.*, **193**, 237–263 (1990).
- 5) Beckett A. H., Dwuuma-Badu D., Haddock R. E., *Tetrahedron*, **25**, 5961–5969 (1969).
- 6) Fujisawa H., *Chem. Pharm. Bull.*, **36**, 4136–4143 (1988).
- 7) Czira G., Tamás J., Kalaus G., *Org. Mass Spectrom.*, **19**, 555–562 (1984).
- 8) Laprévotte O., Ducrot P., Thal C., Serani L., Das B. C., *J. Mass Spectrom.*, **31**, 1149–1155 (1996).
- 9) Laprévotte O., Serani L., Das B. C., *J. Mass Spectrom.*, **32**, 339–340 (1997).
- 10) Amiya T., Bando H., "The Alkaloids," Vol. 34, ed. by Brossi A., Academic Press, San Diego, 1988, pp. 95–179.
- 11) Edwards O. E., "The Alkaloids," Vol. 1, ed. by Saxton J. E., The Chemical Society, London, 1971, pp. 343–381.
- 12) Pelletier S. W., Page S. W., "The Alkaloids," Vol. 3, ed. by Saxton J. E., The Chemical Society, London, 1973, pp. 232–257.
- 13) Pelletier S. W., Page S. W., "The Alkaloids," Vol. 8, ed. by Grudon M. F., The Chemical Society, London, 1978, pp. 219–245.

- 14) Pelletier S. W., Page S. W., "The Alkaloids," Vol. 10, ed. by Grudon M. F., The Chemical Society, London, 1981, pp. 211—226.
- 15) Yunusov M. S., *Natural Product Reports*, **8**, 499—526 (1991).
- 16) Yunusov M. S., *Natural Product Reports*, **10**, 471—486 (1993).
- 17) Yunusov M. S., Rashkes Ya. V., Yunusov S. Yu., *Khim. Prir. Soedin.*, **8**, 85—87 (1972).
- 18) Wada K., Bando H., Kawahara N., *J. Chromatogr.*, **644**, 43—48 (1993).
- 19) Wada K., Bando H., Kawahara N., Mori T., Murayama M., *Biol. Mass Spectrom.*, **23**, 97—102 (1994).
- 20) Wada K., Bando H., Kawahara N., *Natural Medicines*, **51**, 37—39 (1997).
- 21) Wada K., Mori T., Kawahara N., *J. Mass Spectrom.*, **35**, 432—439 (2000).
- 22) Wada K., Mori T., Kawahara N., *Chem. Pharm. Bull.*, **48**, 660—668 (2000).
- 23) Bando H., Wada K., Amiya T., *Heterocycles*, **26**, 2623—2637 (1987).
- 24) Takayama H., Wu F. E., Eda H., Aimi N., Sakai S., *Chem. Pharm. Bull.*, **39**, 1644—1646 (1991).
- 25) Kambara H., Kanomata I., *Anal. Chem.*, **49**, 270—275 (1977).
- 26) Sakairi M., Kambara H., *Anal. Chem.*, **60**, 774—780 (1988).
- 27) Wada K., Ishizuki S., Mori T., Bando H., Murayama M., Kawahara N., *Biol. Pharm. Bull.*, **20**, 978—982 (1997).
- 28) Takayama H., Tokita A., Miyuki I., Sakai S., Kurosaki F., Okamoto T., *Yakugaku Zasshi*, **102**, 245—257 (1982).

Three New Phenylethanoid Glycosides from *Caryopteris incana* and Their Antioxidative Activity

Jianjun GAO, Kiharu IGARASHI,* and Manabu NUKINA

Faculty of Agriculture, Yamagata University, Tsuruoka-shi, Yamagata 997–8555, Japan.

Received December 13, 1999; accepted April 10, 2000

Three new phenylethanoid glycosides, incanoside C, incanoside D and incanoside E were isolated together with one known glycoside, β -D-fructofuranosyl- α -D-(6-O-[*E*]-sinapoyl) glucopyranoside from the whole plant of *Caryopteris incana* (THUNB.) MIQ. On the basis of chemical and spectral analyses, the structures of the new compounds were elucidated to be 1-O-(3,4-dihydroxyphenyl)ethyl-O- β -D-glucopyranosyl(1→2)- α -L-rhamnopyranosyl(1→3)-4-O-feruloyl- β -D-glucopyranoside (incanoside C), 1-O-(3-hydroxy-4-methoxyphenyl)ethyl-O- β -D-glucopyranosyl(1→2)- α -L-rhamnopyranosyl(1→3)-4-O-feruloyl- β -D-glucopyranoside (incanoside D) and 1-O-(3-methoxy-4-hydroxyphenyl)ethyl-O- β -D-glucopyranosyl(1→2)- α -L-rhamnopyranosyl(1→3)-4-O-feruloyl- β -D-glucopyranoside (incanoside E). The three new phenylethanoid glycosides exhibited radical scavenging activities against DPPH radical and inhibitory activities against the oxidation of linoleic acid.

Key words *Caryopteris incana* (THUNB.) MIQ.; Verbenaceae; phenylethanoid glycoside; incanoside; antioxidative activity

Recent developments in biomedical science have shown that free radicals are involved in many diseases. They attack the unsaturated fatty acids in the biomembrane resulting in membrane lipid peroxidation, which is strongly connected to aging, carcinogenesis and atherosclerosis.^{1–3} Free radicals also attack DNA and cause mutation leading to cancer.⁴ In addition, lipid peroxidation is an important deterioration reaction in the processing and storage of foods. Therefore, it is important to look for new effective radical scavengers.

In a continuation of our antioxidant discovery program, we isolated potent radical-scavenging phlinoside A (**1**) and four other phenylpropanoid glycosides from *C. incana* (THUNB.) MIQ.⁵ Further fractionation of radical scavengers has led to the isolation of four other active glycosides. These were identified as three new phenylethanoid glycosides, incanoside C (**2**), incanoside D (**3**) and incanoside E (**4**), and

one known compound, β -D-fructofuranosyl- α -D-(6-O-[*E*]-sinapoyl)glucopyranoside (**5**). Herein we report their isolation, structural elucidation and antioxidative activities.

Compound **5** was identified as β -D-fructofuranosyl- α -D-(6-O-[*E*]-sinapoyl)glucopyranoside on the basis of comparison of its spectral data with those of β -D-fructofuranosyl- α -D-(6-O-[*E*]-feruloyl)glucopyranoside.⁶

Incanoside C (**2**) was isolated as an amorphous powder. Its molecular formula, C₃₆H₄₈O₂₀, was determined from its high-resolution FAB mass spectra (m/z 801.2892 [M+H]⁺, Calcd for 801.2820). Its spectral data, including UV, IR, FAB-MS, and NMR, indicated that it was related to phlinoside A (**1**). The ¹H- and ¹³C-NMR spectra of **2** showed that the signals were in good agreement with those of **1**, except for differences in the acyl ester moiety, *i.e.* the existence of an additional methoxyl group [δ_H 3.88 (3H, s); δ_C 56.7 (OMe)]. Key

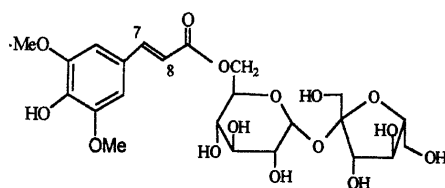
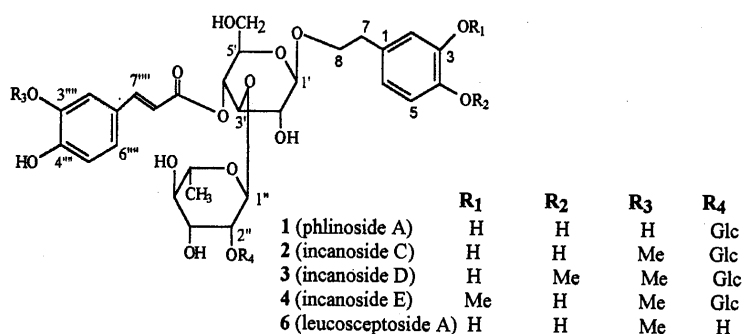


Fig. 1. Structures of Phenylethanoid Glycosides from *Caryopteris incana*

* To whom correspondence should be addressed. e-mail: igarashi@tds1.tr.yamagata-u.ac.jp

Table 1. ^1H - and ^{13}C -NMR Spectral Data of Compounds **2**–**4** (400 MHz and 100 MHz, Respectively, CD_3OD)

C	2		3		4	
	δ_{H}	δ_{C}	δ_{H}	δ_{C}	δ_{H}	δ_{C}
Aglycone						
1		131.6		132.9		131.6
2	6.73 (br s)	117.2	6.73 (d, 1.9)	112.9	6.85 (d, 1.9)	113.8
3		144.7		147.6		145.9
4		146.1		147.7		148.8
5	6.70 (d, 8.3)	116.5	6.82 (d, 8.3)	117.3	6.69 (br s)	116.1
6	6.57 (d, 8.3)	121.5	6.69 (dd, 8.3, 1.9)	121.2	6.69 (br s)	122.4
7	2.78 m	36.7	2.80 m	36.5	2.78 m	36.8
8	3.71 m, 4.04 m	72.4	3.72 m, 4.06 m	72.1	3.73 m, 4.08 m	72.2
OMe			3.81 (s)	56.4	3.84 (s)	56.4
Inner glucose						
1'	4.37 (d, 7.8)	104.3	4.37 (d, 7.8)	104.2	4.37 (d, 7.8)	104.2
2'	3.39 (dd, 9.3, 7.8)	76.2	3.39 (dd, 9.3, 7.8)	76.1	3.39 (dd, 9.3, 7.8)	76.1
3'	3.78 (t, 9.3)	82.9	3.77 (t, 9.3)	82.8	3.77 (t, 9.3)	82.8
4'	4.92 (t, 9.3)	70.5	4.91 (t, 9.3)	70.4	4.91 (t, 9.3)	70.4
5'	3.54 m	76.0	3.54 m	76.0	3.54 m	76.0
6'	3.52 ^a , 3.66 ^a	62.4	3.52 ^a , 3.65 ^a	62.3	3.53 ^a , 3.66 ^a	62.4
Rhamnose						
1''	5.58 brs	102.4	5.58 brs	102.2	5.58 brs	102.2
2''	3.98 (dd, 3.4, 1.5)	83.0	3.97 (dd, 3.4, 1.5)	83.0	3.97 (dd, 3.4, 1.5)	83.0
3''	3.67 (dd, 9.6, 3.4)	71.9	3.66 (dd, 9.6, 3.4)	71.8	3.66 (dd, 9.6, 3.4)	71.8
4''	3.30 ^a	74.2	3.29 ^a	74.1	3.29 ^a	74.1
5''	3.56 m	70.5	3.56 m	70.4	3.56 m	70.4
6''	1.08 (d, 6.4)	18.5	1.07 (d, 6.4)	18.4	1.08 (d, 6.4)	18.4
Outer glucose						
1'''	4.41 (d, 7.3)	107	4.39 (d, 7.3)	106.9	4.41 (d, 7.3)	106.9
2'''	3.28 ^a	75.5	3.28 ^a	75.4	3.28 ^a	75.4
3'''	3.34 ^a	78.0	3.34 ^a	77.9	3.34 ^a	77.9
4'''	3.30 ^a	71.5	3.30 ^a	71.4	3.30 ^a	71.4
5'''	3.30 ^a	78.2	3.30 ^a	78.1	3.30 ^a	78.1
6'''	3.90 (d, 11.7, 1.5) 3.64 ^a	63.0	3.90 (d, 11.7, 1.5) 3.63 ^a	62.8	3.90 (d, 11.7, 1.5) 3.64 ^a	62.8
Ester moiety						
1'''		127.8		127.6		127.6
2'''	7.19 (d, 2.0)	112.0	7.19 (d, 2.0)	111.8	7.19 (d, 2.0)	111.8
3'''		149.2		149.4		149.4
4'''		150.9		150.8		150.8
5'''	6.81 (d, 8.3)	116.7	6.81 (d, 8.3)	116.5	6.81 (d, 8.3)	116.5
6'''	7.08 (d, 8.3, 2.0)	124.5	7.08 (d, 8.3, 2.0)	124.3	7.08 (d, 8.3, 2.0)	124.3
7'''	7.66 (d, 16.0)	148.0	7.66 (d, 16.0)	147.9	7.66 (d, 16.0)	147.9
8'''	6.38 (d, 16.0)	115.2	6.38 (d, 16.0)	115.0	6.38 (d, 16.0)	115
CO		168.4		168.2		168.2
OMe	3.88 (s)	56.7	3.88 (s)	56.5	3.88 (s)	56.5

a) Overlapped with other signals.

correlation via long-range coupling (COLOC) correlation (Fig. 2) observed between this methoxyl group and C-3''' (δ 146.8) of the ester group, indicated that the additional methoxyl was attached to C-3''' of the ester group. Acid hydrolysis of compound **2** afforded two glucoses, one rhamnose (identified by GC) and ferulic acid (identified by HPLC). The absolute configurations of the two glucoses and rhamnose were identified as D and L, respectively, by the Oshima method.⁷⁾ Thus, the structure of **2** was established as 1-*O*-(3,4-dihydroxyphenyl)ethyl-*O*- β -D-glucopyranosyl(1 \rightarrow 2)- α -L-rhamnopyranosyl(1 \rightarrow 3)-4-*O*-feruloyl- β -D-glucopyranoside. In good agreement with this, mild hydrolysis of **2** furnished leucosceptoside A (**6**) identified by co-TLC with the authentic sample.⁸⁾

The ^1H - and ^{13}C -NMR spectra of compound **3** were similar to those of **2** but differed from the signals arising from their aglycone moieties due to the presence of one additional

methoxyl group in **3**. The nuclear overhauser effect (NOE) spectrum showed that the irradiation of this methoxyl group (δ 3.81) caused enhancement of the H-5 signal (δ 6.82) of the phenylethoxy group, indicating that this additional methoxyl group is attached to C-4. Its heteronuclear multiple bond correlation (HMBC) spectrum also supports this fact (Fig. 2). The FAB-MS spectra of **2** and **3** exhibited molecular ion peaks at m/z 801 and 815 $[\text{M}+\text{H}]^+$, respectively, confirming these structural differences. The absolute configurations of the two glucoses and rhamnose were also identified as D and L, respectively, by the Oshima method.⁷⁾ Thus, the structure of incanoside D (**3**) was determined to be 1-*O*-(3-hydroxy-4-methoxyphenyl)ethyl-*O*- β -D-glucopyranosyl(1 \rightarrow 2)- α -L-rhamnopyranosyl(1 \rightarrow 3)-4-*O*-feruloyl- β -D-glucopyranoside.

The FAB-MS spectrum of compound **4** showed the same molecular ion and main fragments (m/z 815 $[\text{M}+\text{H}]^+$, 653

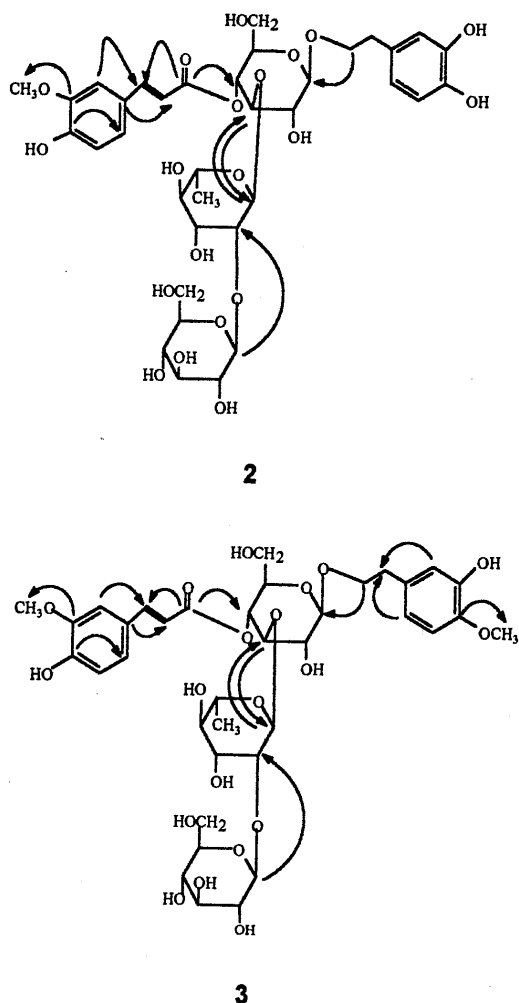


Fig. 2. COLOC or HMBC Correlation ($^{13}\text{C} \rightarrow ^1\text{H}$) of Incanoside C (2) and D (3) (COLOC for 2 and HMBC for 3)

$[\text{M}-\text{glc}+\text{H}]^+$, 507 $[\text{M}-\text{glc}-\text{rha}+\text{H}]^+$, 339 $[\text{M}-\text{glc}-\text{rha}-\text{aglycone}+\text{H}]^+$, 177 $[\text{feruloyl}]^+$ as those of 3. The UV, IR, ^1H - and ^{13}C -NMR spectra for 3 and 4 were also just about the same except for the signals given from phenylethoxy groups with the methoxyl group at a different position. In the NOE spectrum, the methoxy signal in phenylethoxy group at δ 3.84 exhibited a NOE with H-2 signal at δ 6.85, indicating that the aglycone of 4 is (3-methoxy-4-hydroxy phenyl)-ethoxy group. Thus, the structure of compound 4 was 1-*O*-(3-methoxy-4-hydroxyphenyl)ethyl-*O*- β -D-glucopyranosyl-(1 \rightarrow 2)- α -L-rhamnopyranosyl(1 \rightarrow 3)-4-*O*-feruloyl- β -D-glucopyranoside.

1,1-Diphenyl-2-picrylhydrazyl (DPPH) Radical Scavenging and Antioxidative Activity Phenylethanoid glycosides are water soluble natural products widely distributed in the plant kingdom, most of which are isolated from traditional medicinal plants. Significant biological activities, such as enzyme inhibition, and immunomodulatory, antiviral and cytotoxic effects have been reported.^{9,10} Recently some phenylethanoid glycosides have been reported to be good antioxidants and free radical scavengers in some *vitro* antioxidative assay models, and the number of phenolic hydroxyl groups in the structures of the phenylethanoids is related to their scavenging activities.^{11,12}

Figure 3 shows the DPPH radical scavenging activity of

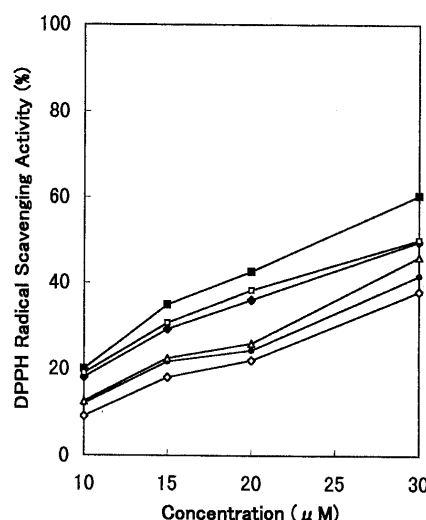


Fig. 3. DPPH Radical Scavenging Activity of Compounds 2–5, *dl*- α -Tocopherol and Ascorbic Acid

Each value is the average of duplicate determinations. Incanoside C (2) —■—, incanoside D (3) —◆—, incanoside E (4) —□—, compound 5 —◇—, *dl*- α -tocopherol —●—, ascorbic acid —△—.

compounds 2–5. Compounds 2–4 have potent DPPH radical scavenging activities, more than *dl*- α -tocopherol and ascorbic acid, which are known as natural antioxidants. Thus, compounds 2–4 may also be good radical scavengers.

It is generally thought that the inhibition of lipid peroxidation by antioxidants may be due to their free radical scavenging activities. Superoxide indirectly initiates lipid peroxidation because superoxide anion acts as a precursor of singlet oxygen and hydroxyl radical.¹³ Hydroxyl radical eliminates hydrogen atoms from the membrane lipid which results in lipid peroxidation. The inhibition of the above phenylethanoid glycosides against the oxidation of linoleic acid was therefore tested using the β -carotene bleaching method.¹⁴ The inhibitory percentages of phlinoside A (1), incanoside C (2), incanoside D (3) and *dl*- α -tocopherol were 39%, 33%, 22%, and 73%. Thus, the inhibitory activity of these compounds may also be related to the number of their phenolic hydroxyl groups.

Experimental

General The experimental procedures and plant material were the same as reported in ref. 5.

Isolation Fraction 6 (1.8 g) reported in ref. 5 had DPPH radical scavenging activity and was further purified by a second polyamide column (60 g, 2.5 \times 30 cm), eluted with H_2O -MeOH [1:0 (800 ml); 7:3 (800 ml); 1:1 (500 ml)] and followed by Sephadex LH-20 column chromatography (MeOH- H_2O 1:1) to give compound 5 (20 mg) and a mixture containing 3 and 4. The mixture was further purified by a semi-preparative HPLC on a C_{18} (Develosil-HG-5, 10 \times 200 mm, MeOH- H_2O 4:6, 1.5 ml/min) to give pure 3 (15 mg) and 4 (6 mg). Fraction 9 (2.2 g) mostly containing 2 had potent DPPH radical scavenging activity and was purified by polyamide column (60 g, 2.5 \times 30 cm) chromatography eluted with increasing amounts of MeOH in H_2O , and further purified by Sephadex LH-20 column chromatography (MeOH) to give compound 2 (250 mg).

Incanoside C (2) Off-white amorphous powder. ^1H - and ^{13}C -NMR spectral data are shown in Table 1. IR: ν_{max} (KBr) cm^{-1} : 3390 (br, OH), 1691 (O=C=O), 1625, 1596, 1513, 1368, 1278, 1158. UV: λ_{max} (MeOH) nm (ϵ): 219 (24660), 289 (15000), 329 (20510). FAB-MS: m/z 801 $[\text{M}+\text{H}]^+$, 639 $[\text{M}-\text{glc}+\text{H}]^+$, 493 $[\text{M}-\text{glc}-\text{rha}+\text{H}]^+$, 339 $[\text{M}-\text{glc}-\text{rha}-\text{aglycone}+\text{H}]^+$. High-resolution FAB-MS m/z 801.2892 (Calcd for $\text{C}_{36}\text{H}_{49}\text{O}_{20}$: 801.2820).

Incanoside D (3) Off-white amorphous powder. ^1H - and ^{13}C -NMR

spectral data are shown in Table 1. IR: ν_{\max} (KBr) cm^{-1} : 3389 (br, OH), 1691 (O=C=O), 1620, 1695, 1515, 1370, 1278, 1155. UV: λ_{\max} (MeOH) nm (ϵ): 219 (15000), 288 (8280), 328 (11470). FAB-MS: m/z 815 $[\text{M}+\text{H}]^+$, 653 $[\text{M}-\text{glc}+\text{H}]^+$, 507 $[\text{M}-\text{glc}-\text{rha}+\text{H}]^+$, 339 $[\text{M}-\text{glc}-\text{rha}-\text{aglycone}+\text{H}]^+$, 177 $[\text{feruloyl}]^+$. High-resolution FAB-MS m/z 815.3003 (Calcd for $\text{C}_{37}\text{H}_{51}\text{O}_{20}$: 815.2977).

Incanoside E (4) Off-white amorphous powder. ^1H - and ^{13}C -NMR spectral data are shown in Table 1. IR: ν_{\max} (KBr) cm^{-1} : 3388 (br, OH), 1691 (O=C=O), 1620, 1690, 1514, 1370, 1275, 1155. UV: λ_{\max} (MeOH) nm (ϵ): 218 (15200), 289 (8300), 327 (11450). FAB-MS: m/z 815 $[\text{M}+\text{H}]^+$, 653 $[\text{M}-\text{glc}+\text{H}]^+$, 507 $[\text{M}-\text{glc}-\text{rha}+\text{H}]^+$, 339 $[\text{M}-\text{glc}-\text{rha}-\text{aglycone}+\text{H}]^+$, 177 $[\text{feruloyl}]^+$. High-resolution FAB-MS m/z 815.3002 (Calcd for $\text{C}_{37}\text{H}_{51}\text{O}_{20}$: 815.2977).

β -D-Fructofuranosyl- α -D-(6-O-[E]-sinapoyl)glucopyranoside (5) Off-white amorphous powder, ^1H -NMR (400 MHz, CD_3OD) δ : 3.20–4.20 (m), 3.87 (6H, s, OCH_3), 4.27 (1H, dd, $J=11.9$, 5.3 Hz, H-6 of glucose), 4.50 (1H, dd, $J=11.9$, 1.9 Hz, H-6 of glucose), 5.42 (1H, d, $J=3.4$ Hz, H-1 of glucose); sinapoyl 6.47 (1H, d, $J=16.0$ Hz, H-8), 6.93 (2H, s, H-2, H-6), 7.63 (1H, d, $J=16.0$ Hz, H-7). ^{13}C -NMR (100 MHz, CD_3OD) δ : glucose 93.2 (C-1), 73.2 (C-2), 74.6 (C-3), 71.8 (C-4), 72.0 (C-5), 65.1 (C-6); fructose 105.2 (C-2), 79.2 (C-3), 76.0 (C-3), 83.8 (C-4), 64.2 (C-5 or C-6), 64.3 (C-1 or C-6); sinapoyl 126.6 (C-1), 106.9 (C-2 and C-6), 149.4 (C-3, C-5), 139.6 (C-4), 147.2 (C-7), 115.7 (C-8), 169.1 (C-9).

Mild Acid Hydrolysis¹⁵ Mild acid hydrolysis of compound **2** (0.5% in MeOH) was carried out on four TLC plates by adding 5 μl of a solution of **2** and 5 μl of 3 N HCl to the start as a spot. Each plate was heated to 100 °C for 5, 10, 15 and 30 min and then developed with $\text{CHCl}_3:\text{CH}_3\text{OH}:\text{H}_2\text{O}$ (7:3:0.5). The products of hydrolysis were identified after spraying with H_2SO_4 (5%) reagent and comparing with authentic samples of Leucosceptoside A.

Acid Hydrolysis A solution of compounds **2** and **3** (ca. 4 mg each) in 4% H_2SO_4 (5 ml) was heated at 90 °C for 3 h. After cooling and filtering, the residue was dissolved in 30 ml H_2O and then extracted with EtOAc (3 \times 30 ml). The EtOAc layer was concentrated to dryness, the residue was analyzed by HPLC and the retention time was compared with those of authentic materials. Conditions: Column: ODS-HG-5, 150 mm \times 4.6 mm. Flow rate: 1.0 ml/min. Eluent: linear gradient of MeOH (0–100%) in 5% MeOH containing 1% AcOH. t_{R} : ferulic acid 18.6 min. The aqueous layer was neutralized with BaCO_3 and filtered. The filtrate was passed through an Amberlite IR-45 (OH^-) column, followed by an Amberlite IR-120 (H^+) column. The final eluate was concentrated and the residue was dissolved in distilled water containing inositol as an internal standard. The mixture was evaporated to dryness. The residue was trimethylsilylated and detected by GC. The GC conditions were as follows: column: 3% Silicone OV-1/Gaschrom Q (60–80 mesh), 1.5 m \times 2 mm; column temperature: 80–300 °C at a rate of 4 °C/min; carrier gas N_2 ; t_{R} (min): 18.58, 20.40 (trimethylsilyl(TMSi) derivatives of rhamnose); 26.15 and 29.01 (TMSi derivatives of glucose).

Determination of the Configuration of Sugars in Compounds **2 and **3**** A solution of compound **2** or **3** (8 mg each) in 4% H_2SO_4 (5 ml) was hydrolyzed using the same method as above. The sugar residue was dissolved in 1 ml H_2O , L-(–)- α -methylbenzylamine (8 mg) and $\text{Na}(\text{BH}_3\text{CN})$ (5 mg) in EtOH (1 ml) was added. The mixture was allowed to stand overnight, followed by the addition of AcOH (0.2 ml) and then was evaporated to dryness. The reaction mixture was acetylated with 1:1 Ac_2O –pyridine (1 ml) and was heated in a sealed tube for 1 h at 100 °C. Water (1 ml) was added and the mixture was evaporated to dryness so that it gave an oily residue. The residue was dissolved in 1 ml water, and extracted with chloroform. HPLC of the extract showed that glucose and rhamnose in **2** and **3** were D and L configurations, respectively, according to the method of Oshima *et al.*⁷⁾

Scavenging Effect against DPPH Radical Using TLC¹⁶⁾ A 6×10^{-5} M DPPH solution was sprayed on a developed TLC plate. The active compounds against DPPH radical showed light yellow spots on a plate of purple

DPPH background.

Scavenging Effect against DPPH Radical Using the Colorimetry Method¹⁷⁾ A MeOH solution (0.2 ml) of test compounds at various concentrations was added to a 2.8 ml MeOH solution containing DPPH (1.5×10^{-4} M). The reaction mixture was shaken vigorously and then kept at room temperature for 30 min. The absorbance of the remaining DPPH was measured in 1 cm cubettes using a Shimadzu UV-1200 spectrophotometer at 520 nm, and the radical-scavenging activity of each compound was expressed by the ratio of decrease in the absorbance of DPPH (%), relative to the absorbance (100%) of DPPH solution in the absence of sample.

Measurement of Antioxidative Activity by β -Carotene Bleaching Method¹⁵⁾ A β -carotene solution was prepared at a concentration of 3.7 mm in acetone. The concentration of linoleic acid solution was 4.3 mm in a pH 7 McIlvaine buffer containing Tween 80 at a concentration of 0.8 mg/ml. Lipoxigenase (Oriental Co., from soybean, 126500 units/mg) was used after diluting with H_2O to a concentration of 0.2 mg/ml. A 50 μl aliquot of lipoxigenase solution was added to a mixture containing 2.4 ml of the McIlvaine buffer (pH=7), 0.5 ml of a linoleic acid solution, 0.2 ml of the β -carotene solution and 50 μl of a 3 mm phenylethanoid solution. After 1 min, the bleaching rate of β -carotene was measured at 460 nm. The inhibitory ratio (I.R.) of each compound toward carotene bleaching is expressed as follows: I.R. (%) = $100\times[(a-b)/a]$, where a is the decrease in absorbance at 460 nm due to β -carotene decomposition in control, b is the decrease in absorbance at 460 nm of the β -carotene solution with added samples.

Acknowledgements This work was supported by a JSPS (Japan Society for the promotion of Science) Postdoctoral Fellowship for Foreign Researchers in Japan (to Dr. Gao) and by a Grant-in Aid for Scientific Research from the Ministry of Education, Science, Sports and Culture of Japan for Foreign Researchers in Japan (to Prof. Igarashi and Dr. Gao).

References

- 1) Floyd R. A., *FASEB J.*, **4**, 2587–2597 (1990).
- 2) Yagi K., *Chem. Phys. Lipids*, **45**, 337–341 (1987).
- 3) Halliwell B., Gutteridge J. M. C., Gross E. E., *J. Lab. Clin. Med.*, **119**, 598–620 (1992).
- 4) Ames B. N., Gold L. S., Willett W. C., *Proc. Natl. Acad. Sci. U.S.A.*, **92**, 5258–5265 (1995).
- 5) Gao J., Igarashi, K., Nukina M., *Biosci. Biotechnol. Biochem.*, **63**, 983–988 (1999).
- 6) Mimaki Y., Sashida Y., *Phytochemistry*, **30**, 937–939 (1991).
- 7) Oshima R., Yamauchi Y., Kumanotani J., *Carbohydrate Res.*, **107**, 169–176 (1982).
- 8) Jia Z. J., Gao J. J., Liu Z. M., *Indian J. Chem.*, **33B**, 460–464, (1994).
- 9) Nicoletti M., Serafini M., Tomassini L., *Annali Di Botanica*, **XLV**, 197–216 (1987).
- 10) Jimenez C., Rigueria R., *Natural Product Reports*, **1994**, 591–606.
- 11) Xiong Q., Kadota S., Tani T., Namba T., *Biol. Pharm. Bull.*, **19**, 1580–1585 (1996).
- 12) Wang P., Kang J., Zheng R., Yang Z., Lu J., Gao J., Jia Z., *Biochem. Pharmacol.*, **51**, 687–691 (1996).
- 13) Shahidi F., Wanasundara P. K., *Crit. Rev. Food Sci. Nutr.*, **32**, 67–103 (1992).
- 14) Igarashi K., Yoshida T., Suzuki E., *Nippon Shokuhin Kogyo Gakkaishi*, **40**, 138–143 (1993).
- 15) Seidel V., Bailieul F., Libot F., Tiliequin F., *Phytochemistry*, **44**, 691–693 (1997).
- 16) Blois M. S., *Nature (London)*, **181**, 1199–1200 (1958).
- 17) Yoshida T., Mori K., Hatano T., Okumura T., Uehara I., Komagoe K., Fujita Y., Okuda T., *Chem. Pharm. Bull.*, **37**, 1919–1921 (1989).

A Novel Agarofuran Sesquiterpene, Celahin D from *Celastrus hindsii* BENTH.

Hui-Chi HUANG,^{a,b} Chien-Chang SHEN,^b Chieh-Fu CHEN,^b Yang-Chang WU,^{*,a} and Yao-Haur KUO^{*,b,c}

Graduate Institute of Natural Products, Kaohsiung Medical College,^a Kaohsiung 807, Taiwan, R.O.C., National Research Institute of Chinese Medicine,^b No. 155-1, Li-Nong St., Sec. 2, Shih-Pai, Taipei 112, Taiwan, R.O.C., and Department of Applied Chemistry, Chinese Culture University,^c Taipei 113, Taiwan, R.O.C.

Received December 13, 1999; accepted March 7, 2000

A novel agarofuran sesquiterpene polyol ester, 1 β ,2 β ,6 α ,15 β -tetracetoxo-8 β ,9 α -dibenzoyloxy- β -dihydroagarofuran (celahin D) (**1**), two known analogues of 1,1 β -acetoxo-8 β ,9 α -dibenzoyloxy-4 α ,6 α -dihydroxy-2 β -(α -methylbutanoyloxy)- β -dihydroagarofuran (**2**) and 1 β -acetoxo-8 β ,9 α -dibenzoyloxy-6 α -hydroxy-2 β -(α -methylbutanoyloxy)- β -dihydroagarofuran (**3**), and a known cytotoxic sesquiterpene pyridine alkaloid, emarginatine E (**4**) were isolated from the stems of *Celastrus hindsii* BENTH. Three known triterpenes, loranthol (**5**), lupenone (**6**) and friedelinol (**7**) were also obtained from the titled plant. Structural elucidation of compound **1** was established by 2D NMR spectra.

Key words *Celastrus hindsii* BENTH; cytotoxicity; 1 β ,2 β ,6 α ,15 β -tetracetoxo-8 β ,9 α -dibenzoyloxy- β -dihydroagarofuran; celahin D; emarginatine E

In the search for potential antitumor agents from the plant family Celastraceae, we have isolated several cytotoxic sesquiterpene pyridine alkaloids.^{1–4} Recently, we reported on the isolation and structural elucidation of several new sesquiterpene polyol esters with β -dihydroagarofuran skeletons⁵ and novel triterpenes⁶ from *Celastrus hindsii* Benth. Further investigation of *C. hindsii* has led to the isolation of a new agarofuran sesquiterpene polyol ester, 1 β ,2 β ,6 α ,15 β -tetracetoxo-8 β ,9 α -dibenzoyloxy- β -dihydroagarofuran (celahin D) (**1**), two known agarofuran sesquiterpenes, 1 β -acetoxo-8 β ,9 α -dibenzoyloxy-4 α ,6 α -dihydroxy-2 β -(α -methylbutanoyloxy)- β -dihydroagarofuran (**2**) and 1 β -acetoxo-8 β ,9 α -dibenzoyloxy-6 α -hydroxy-2 β -(α -methylbutanoyloxy)- β -dihydroagarofuran (**3**), a known agarofuran sesquiterpene with pyridine alkaloid, emarginatine E (**4**), and three known triterpenes, loranthol (**5**), lupenone (**6**) and epifriedelinol (**7**). The structure of compound **1** was established by 2D NMR spectra, including ¹H–¹H COSY, ¹H–¹³C heteronuclear multiple quantum coherence (HMQC), ¹H–¹³C heteronuclear multiple bonds coherence (HMBC), and 2D nOe (nuclear Overhauser effect) studies. Among these isolates, except for emarginatine E, no cytotoxic effect was found after the cytotoxicity test.

Celahin-D (**1**), amorphous powder, mp 107–108 °C, had the empirical formula C₃₇H₄₂O₁₃ determined by high resolution MS: *m/z* 694.2561. The nature of the structure was deduced from ¹³C- and ¹H-NMR spectra, together with the IR spectrum with bands at 1740 (ester CO), 1650 and 1450 (aromatic) cm⁻¹. The NMR spectra confirmed the presence of four acetate esters [¹H-NMR: δ 1.45, 2.03, 2.05, 2.10 (each 3H, s); ¹³C-NMR: δ 20.3, 21.2, 21.3 and 25.9 (each –OCOME), δ 169.3, 169.7, 169.9 and 170.7 (each –OCO–)] and two benzoate esters [¹H-NMR: δ 7.41 (2H, m), 7.46 (2H, m), 7.55 (1H, m), 7.57 (1H, m), 8.02 (2H, m) and 8.16 (2H, m); ¹³C-NMR: δ 128.4–133.6 (Ph \times 2), 164.3 and 165.5 (–OCO–)]. One AB quartet at δ 4.52, 5.12 (2H, ABq, *J*=12.9 Hz) was assigned to a methylene attached to the primary ester group. The signals at δ 5.52, 5.59, 5.70, 5.75, and 6.53 were assigned to five protons attached to the carbon

atoms bearing secondary ester groups. The ¹³C-NMR spectrum suggested that **1** possesses a sesquiterpene skeleton including three methyls, two methylenes, seven methines, and three quaternary carbons. From the ¹H–¹H COSY spectrum of **1**, the correlated signals at 5.75 (1H, s), 5.52 (1H, d, *J*=2.8 Hz), 2.49 (1H, d, *J*=2.8 Hz) were assigned as H-9, H-8 and H-7, respectively. The signals at 5.70 (1H, d, *J*=4.0 Hz), 5.59 (1H, m), 1.76, 2.52 (2H, m), 2.40 (1H, m), and 1.15 (3H, d, *J*=7.8 Hz) were assigned as H-1, H-2, H-3_{ax}, H-3_{eq}, H-4, and H-14, respectively. These data suggested that **1** is a β -dihydroagarofuran sesquiterpene substituted with two benzoyl and four acetyl esters.

¹H–¹³C long-range correlation (HMBC) spectrum was a useful tool to confirm the location of the benzoyl and acetyl ester groups. Thus, the carbonyl signals at δ 164.3 and 165.5 were correlated with the proton signals at δ 8.16 (benzoyl-H) and 5.75 (H-9), and δ 8.02 (benzoyl-H) and 5.52 (H-8), respectively, revealing that the two benzoates were located at C-9 and C-8, respectively. Also, four acetyl esters were positioned at C-1, C-2, C-6, and C-15, respectively, because the carbonyl signals at δ 169.3, 169.7, 169.9 and 170.7 were correlated with the proton signals H-1, H-2, H-6, and H-15, respectively. As usually found in this class of skeleton, H-6 and H-1 have axial stereochemistry.^{7–9} From the NOESY spectrum of **1** (Fig. 2), the correlation between H-6 and H-15a and H-14, and between H-9 and H-15a indicated the presence of equatorial stereochemistry of H-9. From this data,

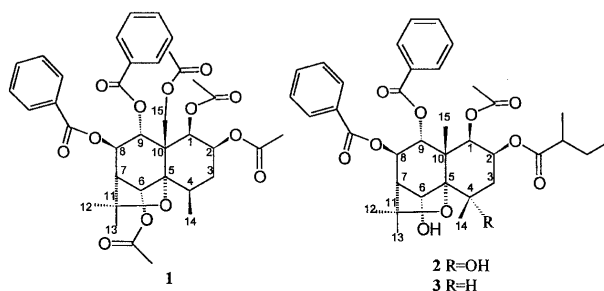


Fig. 1

* To whom correspondence should be addressed. e-mail:

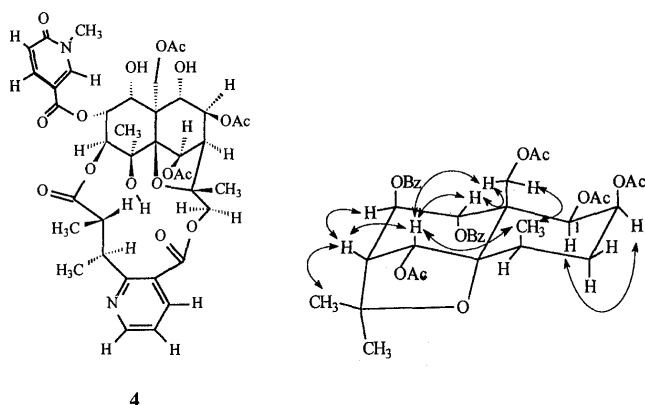


Fig. 2. Partial nOe Correlation of **1**

compound **1** was identified as 1 β ,2 β ,6 α ,15 β -tetracetoxo-8 β ,9 α -dibenzoyloxy- β -dihydroagarofuran, and given the trivial name, celahin-D.

Furthermore, the isolated sesquiterpene polyol esters and triterpenoids, **1**–**7**, were assayed for cytotoxicity in four cancer cell lines: nasopharynx carcinoma (KB), colon carcinoma (COLO-205), hepatoma (Hepa-3B), and cervical carcinoma (Hela). Emarginatine-E (**4**) exhibited cytotoxicity against KB (ED₅₀=1.7 μ g/ml) and COLO-205 (ED₅₀=4.1 μ g/ml) cancer cells. In contrast, the ED₅₀ values for compounds **1**–**3** and **5**–**6** all exceeded 10 μ g/ml.

Experimental

General Experimental Procedures ¹H- and ¹³C-spectra were run on a Bruker AM-300 spectrometer. Samples for IR spectral measurements were prepared as KBr disk. The spectra of heteronuclear correlation, HMQC was established by the coupling of 8 Hz. HREIMS was performed on a JEOL SX-102 instrument. HPLC was employed by using the semipreparative 5C₁₈ column. Si gel (Merck 70–230 mesh, ASTM) was used for column chromatography, and precoated Si gel (Merck 60 F-254) for TLC. Melting points were determined on a Fisher–Johns apparatus and are uncorrected.

Plant Material The stems of *C. hindsii* were collected in September 1992 in Taichung Hsien, Taiwan. A voucher specimen is deposited at the National Research Institute of Chinese Medicine, Taipei, Taiwan, R.O.C.

Extraction and Isolation The dried stems of *C. hindsii* Benth. (5.2 kg) were extracted exhaustively with EtOH. Extract (200 g) was chromatographed on silical gel (2.5 kg) eluting with *n*-hexane–EtOAc to give 10 frs. Fr. 3 was chromatographed on silica gel eluting with CHCl₃:MeOH (30:1→4:1) to give 8 frs. Fr. 3-5 was chromatographed on silica gel eluting with CH₂Cl₂:acetone (10:1→4:1). Fr. 3-5-4 was further separated by HPLC (MeOH:H₂O=1:1→0.9) to yield 1 β ,2 β ,6 α ,15 β -tetracetoxo-8 β ,9 α -dibenzoyloxy- β -dihydroagarofuran (**1**) (4.5 mg), 1 β -acetoxo-8 β ,9 α -dibenzoyloxy-4 α ,6 α -dihydroxy-2 β -(α -methylbutanoyloxy)- β -dihydroagarofuran (**2**)⁸ (7.5 mg), 1 β -acetoxo-8 β ,9 α -dibenzoyloxy-6 α -hydroxy-2 β -(α -methylbu-

tanoyloxy)- β -dihydroagarofuran (**3**)⁹ (1.5 mg), and emarginatine-E (**4**)¹ (2.2 mg). Fr. 3-4 was chromatographed on silica gel eluting with CHCl₃:acetone (10:1→4:1) to yield loranthol (**5**)¹⁰ (2.4 mg), lupenone (**6**)¹¹ (3.4 mg) and friedelinol (**7**)^{12,13} (3.1 mg).

Celahin-D (1**):** Amorphous powder, [α]_D –21° (*c*=0.3, CHCl₃); IR ν_{\max} cm^{–1}: 1740 (ester CO), 1650 and 1450 (aromatic); HREIMS *m/z*: 694.2561 [M]⁺ (Calcd for C₃₇H₄₂O₁₃: 694.2625); ¹H-NMR: 5.70 (1H, d, *J*=4.0 Hz, H-1), 5.59 (1H, m, H-2), 1.76, 2.52 (2H, m, H-3), 2.40 (1H, m, H-4), 6.53 (1H, s, H-6), 2.49 (1H, d, *J*=2.8 Hz, H-7), 5.52 (1H, d, *J*=2.8 Hz, H-8), 5.75 (1H, s, H-9), 1.64 (3H, s, H-12), 1.47 (3H, s, H-13), 1.15 (3H, d, *J*=7.8 Hz, H-14), 4.52, 5.12 (2H, ABq, *J*=12.9 Hz, H-15), 1.45 (3H, s, OAc-1), 2.10 (3H, s, OAc-2), 2.05 (3H, s, OAc-6), 2.03 (3H, s, OAc-15), 8-OBz: 7.41 (2H, m), 7.55 (1H, m), 8.02 (2H, m), 9-OBz: 7.46 (2H, m), 7.57 (1H, m), 8.16 (2H, m); ¹³C-NMR: 73.6 (C-1), 71.7 (C-2), 30.1 (C-3), 32.8 (C-4), 89.8 (C-5), 69.1 (C-6), 53.5 (C-7), 77.6 (C-8), 74.9 (C-9), 52.7 (C-10), 81.5 (C-11), 25.9 (C-12), 30.3 (C-13), 16.7 (C-14), 65.9 (C-15), 25.9, 169.3 (OAc-1), 21.3, 169.7 (OAc-2), 21.2, 169.9 (OAc-6), 20.3, 170.7 (OAc-15), 128.4–133.6 (128.4, 128.7, 129.9, 130.2, 133.3 and 133.6, Ph×2), 165.5 (–OCO-8) and 164.3 (–OCO-9).

Cytotoxicity Assay The *in vitro* cytotoxicity assay was performed as previously described.¹⁴

Acknowledgments The authors thank the National Science Council (NSC 85-2113-M-077-002) and National Research Institute of Chinese Medicine for the financial support to Y. H. Kuo.

References

- 1) Kuo Y. H., Chen C. H., Kuo L. M. Y., Wu T. S., Lee K. H., *Phytochemistry*, **35**, 803–807 (1994).
- 2) Kuo Y. H., Ou J. C., Lee K. H., Chen C. F., *J. Nat. Prod.*, **58**, 1103–1108 (1995).
- 3) Kuo Y. H., King M. L., Chen C. F., Chen H. Y., Chen C. H., Chen K., Lee K. H., *J. Nat. Prod.*, **57**, 263–269 (1994).
- 4) Kuo Y. H., Chen C. F., Kuo Y. L. M., King M. L., Chen C. F., Lee K. H., *J. Nat. Prod.*, **58**, 1735–1738 (1995).
- 5) Kuo Y. H., Chou C. J., Kuo Y. L. M., Hu Y. Y., Chen Y. C., Chen C. F., *Phytochemistry*, **41**, 549–551 (1996).
- 6) Kuo Y. H., Kuo Y. L. M., *Phytochemistry*, **44**, 1275–1281 (1997).
- 7) Wakabayashi N., Wu W. J., Waters R. M., Redfern R. E., Mills G. D., Demilo A. B., Lusby W. R., Andrzejewski D., *J. Nat. Prod.*, **51**, 537–542 (1988).
- 8) Tu Y. Q., *Phytochemistry*, **31**, 2155–2157 (1992).
- 9) Tu Y. Q., Chen Y., *Phytochemistry*, **30**, 4169–4171 (1991).
- 10) Rahman A. U., Khan M. A., Khan N. H., *Phytochemistry*, **28**, 3004–3006 (1973).
- 11) Wenkert E., Baddeley G. V., Burfitt I. R., Moreno L. N., *Org. Mag. Res.*, **11**, 337–343 (1978).
- 12) Betancor C., Freire R., Gonzalez A. G., Salazar J. A., Pascard C., Prange T., *Phytochemistry*, **19**, 1989–1993 (1980).
- 13) Kuo Y. H., Li S. Y., Shen C. C., Yang L. M., Huang H. C., Liao W. B., Chang C. I., Kuo Y. H., Chen C. F., *Chinese Pharmaceut. J.*, **49**, 207–216 (1997).
- 14) Kuo Y. H., Huang H. C., Kuo Y. L. M., Chen C. F., *J. Org. Chem.*, **64**, 7023–7027 (1999).

Macrophyllosaponin E: A Novel Compound from the Roots of *Astragalus oleifolius*

Erdal BEDİR,^{a,b} Ihsan CALIS,^a and Ikhlas A. KHAN^{*,b,c}

Hacettepe University, Faculty of Pharmacy, Department of Pharmacognosy,^a TR-06100 Ankara, Turkey, National Center for Natural Products Research, Research Institute of Pharmaceutical Sciences,^b and Department of Pharmacognosy, School of Pharmacy,^c The University of Mississippi, University, MS 38677, U.S.A.

Received December 17, 1999; accepted March 17, 2000

Macrophyllosaponin E, a novel cycloartane-type triterpene, has been isolated from the roots of *Astragalus oleifolius*. The structure elucidation of the compound was achieved by a combination of one- and two-dimensional NMR techniques [¹H–¹H-correlation spectroscopy (COSY), ¹H–¹³C-heteronuclear multiple quantum correlation spectroscopy (HMQC), and ¹H–¹³C-heteronuclear multiple-bond correlation spectroscopy (HMBC)] and high resolution electrospray ionization Fourier transformation mass spectrometry (HR-ESI-FT-MS).

Key words *Astragalus oleifolius*; cycloartane-type triterpene; macrophyllosaponin E, Leguminosae

Astragalus L., the largest genus in the family Leguminosae, is represented by 380 species in the flora of Turkey.¹⁾ The roots of *Astragalus* species represent a very old and well-known drug in traditional medicine for its usage as an antiperspirant, diuretic and tonic drug. It has also been used in the treatment of diabetes mellitus, nephritis, leukemia and uterine cancer.²⁾ In the district of Anatolia, located in South Eastern Turkey, an aqueous extract of the roots of *Astragalus* is traditionally used against leukemia and for its wound-healing properties. Known biologically active constituents of *Astragalus* roots represent two major classes of compounds, polysaccharides and saponins.²⁾ *Astragalus* polysaccharides are already known to have anticancer and immune enhancing properties in both *in vitro* and *in vivo* experiments.^{3–5)} Chemical studies on *Astragalus* saponins have reported the presence of cycloartane-type triterpenoid glycosides which were found to exert biological activities (e.g. anti-inflammatory, analgesic, diuretic, hypotensive and sedative effects).⁶⁾

Our earlier investigations performed on *Astragalus* species resulted in the isolation of a series of cycloartane-type triterpenic saponins,^{7–13)} as well as the compounds which were evaluated in lymphocyte stimulation tests showed immunomodulatory activity. The activity is relatively potent and thereby deserves further attention.⁸⁾

We previously reported the isolation and the structure determination of macrophyllosaponins A–D from *Astragalus oleifolius*.⁷⁾ In our continuing search, we have isolated a novel cycloartane-type triterpene glycoside, named as macrophyllosaponin E (**1**). This paper deals with the isolation and the structural elucidation of **1**.

The high resolution electrospray ionization Fourier transformation mass spectrometry (HR-ESI-FT-MS) spectra of **1** exhibited ion peak for [M+Na]⁺ at *m/z* 839.4721, which is compatible with the molecular formulae C₄₂H₇₂O₁₅.

Taking into account the results of our comprehensive ¹H- and ¹³C-NMR studies and previous knowledge derived from metabolites isolated from the genus *Astragalus*,^{7–13)} the main features of a cycloartane-type triterpene were evident: characteristic signals due to cyclopropane-methylene protons as an AX system (δ 0.44, 0.79, J_{AX} =4.5 Hz, H₂-19), six tertiary methyl groups (δ 0.89, 1.05, 1.07, 1.09, 1.2, 1.27; respectively, H₃-29, H₃-18, H₃-30, H₃-28, H₃-27, H₃-26) and a sec-

ondary methyl group (0.95 d, J =6.3; H₃-21). Additionally, the resonances for two anomeric protons were observed at δ 4.54 (d, J =7.8 Hz) and 4.36 (d, J =7.8 Hz), indicative of the presence of two β -linked sugar units. Thus, **1** was considered to be a cycloartane-type triterpene diglycoside. This observation was supported by the ¹³C-NMR spectral data of **1** (Table 1). The ¹H- and ¹³C-NMR data (Table 1) supported the assignment of the sugar moieties in **1** as two β -D-glucopyranose.¹⁴⁾ The remaining carbon and proton resonances were consistent with C₃₀H₅₂O₅ for the aglycon moiety. This implied five saturated ring systems because there were no olefinic protons.

Among the sugar signals, the remaining signals showed correlations with the resonances at highfield, indicating the presence of four protons geminal to oxygenated carbons of the sapogenol moiety (δ 3.47, dd, J =5.8, 11.6 Hz, H-24; δ 3.54, dd, J =3.6, 2.7 Hz, H-1; δ 3.57 ddd, 10.5, 8.3, 5.0 Hz, H-7; δ 3.73, dd, J =4.3, 12.0 Hz, H-3). The resonances for the oxygenated carbons also indicated the presence of four oxymethine carbons (δ 70.2, d, C-7; δ 73.1, d, C-1; δ 77.0, d, C-24; δ 84.1, d, C-3) and an oxygenated quaternary carbon (δ 80.5, s, C-25).

To complete the assignment of the chemical shifts of the triterpene skeleton and its substitution pattern had to be determined for which task the ¹H–¹H-correlation spectroscopy (COSY) spectrum proved to be most useful. Detailed examination of this spectrum indicated the presence of seven spin systems (Chart 2). In order to establish the interfragment relationship, a heteronuclear multiple-bond correlation experiment (HMBC) was performed (Chart 2). Thus, the anomeric proton at δ 4.36 (d, J =7.8 Hz) showed a long range correlation with the carbon resonance at δ 84.10 (d, C-3) while the anomeric proton at δ 4.54 (d, J =7.8 Hz) exhibited a long range correlation with the carbon resonance at δ 80.50 (s, C-25), indicating the bidesmosidic structure of **1**.

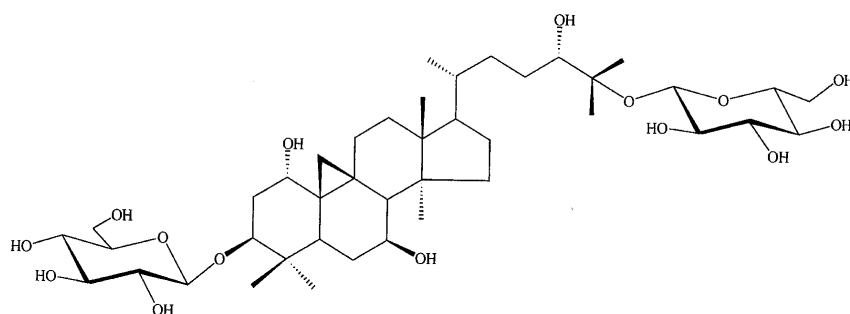
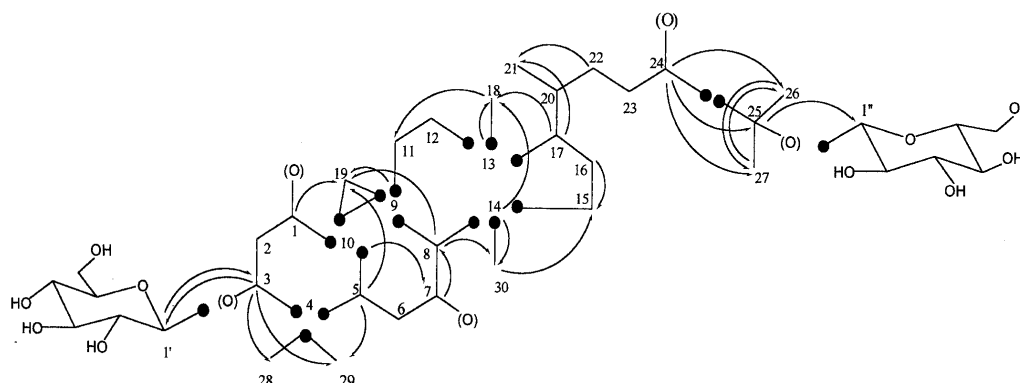
¹³C-NMR data for C-24 is comparable to those reported for analogous compounds having a 24(*S*) configuration.^{15,16)} It has to be mentioned that the ¹³C-NMR data can be regarded as characteristic parameters in the determination of absolute configurations of C-24. In the case of 24(*R*) configuration δ_{C-24} gives resonance at 80.0–80.5 ppm,^{17,18)} while for the 24(*S*) configuration δ_{C-24} gives resonance at 77.0–77.2

* To whom correspondence should be addressed. e-mail: rikhan@olemiss.edu

Table 1. ^1H - and ^{13}C -Assignments of **1**, (in CD_3OD ; at 500 and 125 MHz, Respectively)

C/H	δ (ppm), J (in Hz)	δ (ppm)	C/H	δ (ppm), J (in Hz)	δ (ppm)
1	3.54 dd (2.7, 3.6)	73.1 d	23	1.45 m	28.0 t
2	2.17 m, 1.86 ddd (11.8, 2.7, 1.6)	36.4 t	24	3.47 dd (5.8, 11.6)	77.0 d
3	3.73 dd (12.0, 4.3)	84.1 d	25	—	80.5 s
4	—	40.7 s	26	1.27 s	22.0 q
5	2.16 t (12.0, 4.8)	39.3 d	27	1.23 s	21.6 q
6	1.05 m, 1.75 m	31.0 t	28	1.09 s	24.8 q
7	3.57 ddd (10.5, 8.3, 5.0)	70.2 d	29	0.89 s	13.5 q
8	1.56 m	55.1 d	30	1.07 s	18.2 q
9	—	21.0 s			
10	—	30.4 s	1'	4.36 d (7.8)	105.7 d
11	2.27 m, 1.36 m	26.0 t	2'	3.22 ^{a)}	74.3 d
12	1.70 m	33.0 t	3'	3.37 ^{a)}	77.2 ^{b)} d
13	—	45.9 s	4'	3.30 ^{a)}	70.8 d
14	—	48.9 s	5'	3.28 ^{a)}	76.8 ^{c)} d
15	1.58 m	37.5 t	6'	3.84 dd (10.3, 2.0)	61.8 t
16	1.36 m, 1.96 m	28.6 t		3.65 ^{a)}	
17	1.58 m	52.2 d	1''	4.54 d (7.8)	97.0 d
18	1.05 s	17.4 q	2''	3.20 ^{a)}	74.7 d
19	0.44 d (4.5), 0.79 d (4.5)	28.4 t	3''	3.37 ^{a)}	77.3 ^{b)} d
20	1.45 m	36.2 d	4''	3.30 ^{a,b)}	70.6 d
21	0.95 d (6.3)	17.9 q	5''	3.28 ^{a)}	77.0 ^{c)} d
22	1.56 m, 1.35 m	33.7 t	6''	3.91 dd (10.1, 2.0)	62.1 t
				3.65 ^{a)}	

Assignments confirmed by COSY, HMQC and HMBC experiments. a) Signal pattern was unclear due to overlapping. b, c) Assignments may be interchangeable.

Chart 1. Structure of **1**Chart 2. Partial Structures Deduced from 2D-NMR Measurements (HMQC, COSY) and Key HMBC of **1**

ppm.^{15,16)} Additionally, the relative configurations of the oxygenated carbon atoms were determined from the magnitude of the vicinal proton–proton coupling constants to be: C-1 (α -OH; δ 3.54 dd, $J=2.7, 3.6$ Hz, $H_{\text{eq}}-1$), C-3 (β -OH; δ 3.73 dd, $J=12.0, 4.3$ Hz, $H_{\text{ax}}-3$), C-7 (β -OH; δ 3.57 ddd, $J=10.5, 8.3, 5.0$ Hz, $H_{\text{ax}}-7$), and C-24 (δ 3.47 dd, $J=11.6, 5.8$ Hz, H -24).

Consequently, the structure of **1** was established as 3,25-di- O - β -D-glucopyranosyl-1 α ,3 β ,7 β ,24(S),25-pentahydroxy-

cycloartane.

Experimental

General The 1D- and 2D-NMR spectra were obtained on a Bruker® Avance DRX 500 FT spectrometer operating at 500 and 125 MHz, respectively. The chemical shift values are reported as parts per million (ppm) units relative to tetramethylsilane (TMS) for ^1H - and ^{13}C -; and the coupling constants are in Hz (in parentheses). For the ^{13}C -NMR spectra, multiplicities were determined by a distortionless enhancement by polarization transfer (DEPT) experiment. HR-ESI-FT-MS were obtained using a Bruker BioApex

FT-MS in ESI mode.

Chromatographic Conditions TLC: precoated Si 250F plates (Baker); developing system: CHCl_3 -MeOH- H_2O (70:30:3); visualization: 30% H_2SO_4 . Column chromatography: silica gel 230–400 mesh (Merck).

Plant Material *Astragalus oleifolius* DC. was collected from Ahlatlibel, Ankara, Central Anatolia, Turkey in May 1994. Voucher specimens (94-004) have been deposited at the Herbarium of the Department of Pharmacognosy, Faculty of Pharmacy, Hacettepe University, Ankara, Turkey.

Extraction and Isolation Air-dried and powdered roots of *A. oleifolius* (250 g) were kept in EtOH- H_2O (4:1; 2l) overnight, then refluxed for 2 h and filtered. The filtrate was concentrated to dryness *in vacuo* (65.0 g, yield 26%). An aliquot of the extract (30.0 g) was partitioned in H_2O and subjected to vacuum liquid chromatography (VLC) using reversed phase material (Sepalyte 40 μm ; 250 g), employing H_2O , H_2O -MeOH (90:10→10:90) and MeOH as the eluents. Fractions rich in saponins were combined (7.0 g). This fraction further subjected to column chromatography (silica gel, 150 g) eluted with CH_2Cl_2 -MeOH (85:15) and CH_2Cl_2 -MeOH- H_2O mixtures (80:20:1; 80:20:2; 70:30:3) to give six main fractions (frs. A–F). Fr. E (166 mg) was subjected to VLC using reversed phase material as stationary phase (Sepalyte 40 μm ; 15 g). Elution with increasing amount of MeOH in H_2O (40:60→70:30) yielded compound **1** (11.5 mg).

Compound **1** 3,25-di-*O*- β -D-glucopyranosyl-1 α ,3 β ,7 β ,24(*S*),25-pentahydroxy-cycloartane: ^1H - and ^{13}C -NMR: see Table 1. HR-ESI-FT-MS: $[\text{M}+\text{Na}]^+$ at m/z 839.4721.

Acknowledgments We are grateful to Dr. Chuck Dunbar for conducting the HR-ESI-MS analysis. We also thank Mr. Frank Wiggers for his assistance in obtaining the 2D-NMR spectra of **1**. This work was supported in part by the United States Dept. of Agricultural, ARS Specific Cooperative Agreement No. 58-6408-7-012.

References

- 1) Davis P. H., "Flora of Turkey and East Aegean Islands," Vol. 4, University Press, Edinburgh, 1970, pp. 49–254.
- 2) Tang W., Eisenbrand G., "Chinese Drugs of Plant Origin," Springer-Verlag, Berlin, 1992.
- 3) Smee D. F., Verbiscar A. J., *Antiviral Chem. Chemother.*, **6**, 385–390 (1995).
- 4) Yang H., Zhao G., *Zhongguo Zhongliu Linchang*, **25**, 669–672 (1998).
- 5) Liu X., Wang M., Wu H., Zhao X., Li H., *Tianran Chanwu Yanjiu Yu Kaifa*, **6**, 23–31 (1994).
- 6) Isaev M. I., Gorovits M. B., Abubakirov N. K., *Khim. Prir. Soedin.*, **1998**, 156–175.
- 7) Calis I., Zor M., Saracoglu I., Isimer A., Rüegger H., *J. Nat. Prod.*, **59**, 1019–1023 (1996).
- 8) Bedir E., Calis I., Zerbe O., Sticher O., *J. Nat. Prod.*, **61**, 503–505 (1998).
- 9) Bedir E., Calis I., Aquino R., Piacente S., Pizza C., *J. Nat. Prod.*, **61**, 1469–1472 (1998).
- 10) Bedir E., Calis I., Aquino R., Piacente S., Pizza C., *J. Nat. Prod.*, **62**, 563–568 (1999).
- 11) Bedir E., Calis I., Aquino R., Piacente S., Pizza C., *Phytochemistry*, **51**, 1017–1020 (1999).
- 12) Calis I., Yusufoglu H., Zerbe O., Sticher O., *Phytochemistry*, **50**, 843–847 (1999).
- 13) Yuruker A., Tasdemir D., Wright A. D., Sticher O., Luo Y. D., Pezzuto J. M., *Planta Med.*, **63**, 183–186 (1997).
- 14) Agrawal P. K., Jain D. C., Gupta R. K., Thakur R. S., *Phytochemistry*, **24**, 2479–2496 (1985).
- 15) Fadeev Y. M., Isaev M. I., Akimov Y. A., Kintya P. K., Gorovits M. B., Abubakirov N. K., *Khim. Prir. Soedin.*, **1987**, 817–824.
- 16) Hirotani M., Zhou Y., Rui H., Furuya T., *Phytochemistry*, **37**, 1403–1407 (1994).
- 17) Isaev M. I., Gorovits M. B., Abdullaev N. D., Abubakirov N. K., *Khim. Prir. Soedin.*, **1982**, 458–464.
- 18) Isaev M. I., Gorovits M. B., Abdullaev N. D., Abubakirov N. K., *Khim. Prir. Soedin.*, **1984**, 732–735.

Isolation of Lignan Glucosides and Neolignan Sulfate from the Leaves of *Glochidion zeylanicum* (Gaertn) A. Juss

Hideaki OTSUKA,^{*,a} Eiji HIRATA,^b Takakazu SHINZATO,^c and Yoshio TAKEDA^d

Institute of Pharmaceutical Sciences, Hiroshima University Faculty of Medicine,^a 1-2-3 Kasumi, Minami-ku, Hiroshima 734-8551, Japan, Faculty of Agriculture, University of the Ryukyus,^b 1 Senbaru, Nishihara-cho, Nakagami-gun, Okinawa 903-0129, Japan, University Forest, Faculty of Agriculture, University of the Ryukyus,^c 685 Yona, Kunigami-son, Kunigami-gun, Okinawa 905-1427, Japan, and Faculty of Integrated Arts and Sciences, The University of Tokushima,^d 1-1 Minamijosanjima-cho, Tokushima 770-8502, Japan. Received January 19, 2000; accepted March 7, 2000

Six lignan and neolignan derivatives (1–6) were isolated from the *n*-BuOH-soluble fraction of a MeOH extract of the leaves of *Glochidion zeylanicum*. On the basis of spectral data, their structures were elucidated to be (+)-isolarisiresinol 3a-*O*- β -D-glucopyranoside (1), dihydrodehydrodiconiferyl alcohol 4-, 9- and 9'-*O*- β -D-glucopyranosides (2–4, respectively), (+)-isolarisiresinol 2a-*O*- β -D-glucopyranoside (5), and dihydrodehydrodiconiferyl alcohol 9-*O*-sulfate (6), and 5 and 6 were new compounds.

Key words *Glochidion zeylanicum*; Euphorbiaceae; lignan; (+)-isolarisiresinol 2a-*O*- β -D-glucopyranoside; neolignan; dihydrodehydrodiconiferyl alcohol 9-*O*-sulfate

In our continuing studies on plants collected in the Okinawa islands, we investigated the constituents of *Glochidion zeylanicum* (Euphorbiaceae).¹⁾ Plants belonging to the Euphorbiaceae family are of taxonomic interest, since it contains various morphologically different plants. From the *n*-BuOH-soluble fraction of a MeOH extract of the leaves, several butenolide glucosides have been isolated,²⁾ and further investigation of the same fraction afforded six lignan derivatives (1–6). Following spectroscopic analyses, compounds 1–4 were found to be the known, (+)-isolarisiresinol 3a-*O*- β -D-glucopyranoside,³⁾ and dihydrodehydrodiconiferyl alcohol 4-, 9- and 9'-*O*- β -D-glucopyranosides,⁴⁾ respectively, and the structures of the two new compounds (5 and 6) were elucidated by spectroscopic methods. This paper deals with their structural elucidation.

Compound 5, $[\alpha]_D^{25} +26.5^\circ$, was isolated as an amorphous powder and the elemental composition was determined to be C₂₆H₃₄O₁₁ by negative-ion high-resolution (HR)-FAB-MS. The ¹H- and ¹³C-NMR spectra indicated the presence of two aromatic rings, both of which have two electronegative substituents, three methylenes, two of which have an oxygen

atom, three methines, and a β -glucopyranose unit. These spectral data of 5 were similar to those of (+)-isolarisiresinol 3a-*O*- β -D-glucopyranoside (1), except for significant upfield shifts of C-2 and C-3a, and downfield shifts of C-2a and C-3 in the ¹³C-NMR spectrum (Table 1). Thus, the structure of 5 was proposed to be isolarisiresinol 2a-*O*- β -D-glucopyranoside. This was confirmed by heteronuclear multiple bond correlation (HMBC) spectroscopy, in which the anomeric proton (δ_H 4.29) crossed the carbon signal at δ_C 73.9, and by the results of difference NOE experiments, in which significant enhancement was observed on the proton (δ_H 3.68) of C-2, on irradiation of H-1' (δ_H 4.29). The absolute configuration of the chiral centers was expected to be the same as that of 1 from the results of circular dichroism (CD) spectral analyses.³⁾ Therefore, the structure of 5 was elucidated to be as shown in Fig. 1. Glycosides of aryltetrahydronaphthalene-type lignans are widely distributed in many plant species and the site of glycosylation is limited to the hydroxyl group at the 3a-position. Although an extensive survey of the literature was carried out, 2a-*O*-glucopyranoside is rare in the plant kingdom.

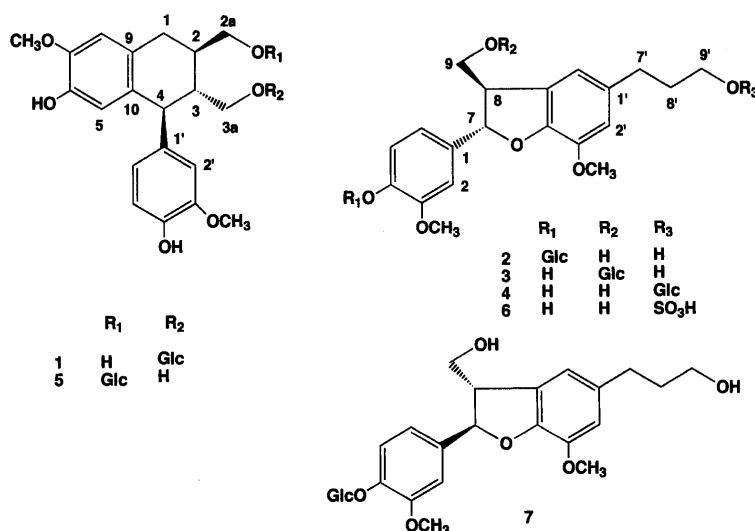


Fig. 1. Structures of Compounds 1–7

* To whom correspondence should be addressed. e-mail: hide@pharm.hiroshima-u.ac.jp

Table 1. ^{13}C -NMR Data for (+)-Isolarisiresinol 3a- (1) and 2a- (5) *O*- β -D-Glucopyranosides (CD_3OD , 100 MHz)

Carbon No.	1	5
1	33.9	33.9
2	39.6	37.5
2a	65.3	73.9
3	46.0	48.3
3a	69.6	61.8
4	47.9	48.0
5	117.4	117.5
6	145.2	145.4
7	147.2	147.3
8	112.5	112.6
9	129.2	129.2
10	134.4	134.3
1'	138.7	138.7
2'	114.4	114.1
3'	149.0	149.1
4'	145.9	146.0
5'	116.1	116.1
6'	123.2	123.3
1''	105.2	104.7
2''	75.2	75.3
3''	78.2	78.2
4'	71.7	71.8
5''	77.9	78.1
6''	62.8	62.9
OMe	56.5 \times 2	56.5 \times 2

Compound **6**, $[\alpha]_{\text{D}} +5.1^\circ$, was also isolated as an amorphous powder and the elemental composition was determined to be $\text{C}_{20}\text{H}_{24}\text{O}_9\text{S}$ by HR-FAB-MS. The ^1H - and ^{13}C -NMR spectra indicated that **6** was a derivative of a dihydrobenzofuran-type neolignan, judging from the characteristic signals at δ_{H} 5.50 (d, $J=6$ Hz) on δ_{C} 89.1 and δ_{H} 3.84 (m) on δ_{C} 55.5 (see ^{13}C -NMR data of **2** and **4** in Table 1). Although in the ^{13}C -NMR spectrum no signals assignable to those of a sugar moiety were observed, the mobility of **6** on TLC was much lower than that of **4**. From the results of HR-FAB-MS, compound **6** was expected to be the sulfuric acid ester of dihydrodehydrodiconiferyl alcohol. The position of the sulfuric acid group was determined to be the hydroxyl group at the 9'-position by comparison of the ^{13}C -NMR data for **2** and **4** with those for **6** (Table 2). From the CD spectral data for 7*S*,8*R*- and 7*R*,8*S*-dihydrodehydrodiconiferyl alcohol 4-*O*- β -D-glucopyranosides [2: $\Delta\epsilon +5.49$ (290 nm) and 7: -9.70 (283 nm), respectively],^{4a)} compound **6** was isolated in a significantly racemised state, in which the 7*S*,8*R* isomer was slightly predominant [$\Delta\epsilon +0.41$ (290 nm)].

Experimental

The following instruments were used to record physical data. Optical rotations: Union Giken PM-101 polarimeter; UV spectra: Shimadzu UV-160A spectrophotometer; NMR spectra: JEOL α -400 spectrometer at 400 MHz for ^1H and 100 MHz for ^{13}C spectra with TMS as an internal standard; CD spectra: JASCO J-702 spectropolarimeter; HR-FAB-MS: JEOL SX-102 mass spectrometer in a negative-ion mode with PEG-400 as a matrix.

Plant Material The leaves of *Glochidion zeylanicum* were collected in Okinawa, Japan, in August 1990, and a voucher specimen was deposited in the Herbarium of the Institute of Pharmaceutical Sciences, Hiroshima University Faculty of Medicine (90-GZ-Okinawa-0822).

Extraction and Isolation Air-dried leaves of *G. zeylanicum* (4.72 kg) were extracted with MeOH three times. Parts of the extraction and isolation procedures were described in a previous paper.²⁾ The 40% MeOH eluate (28.7 g) obtained on Diaion HP-20 column chromatography was suc-

Table 2. ^{13}C -NMR Data for Dihydrodehydrodiconiferyl Alcohol 4- (2) and 9'- (4) *O*- β -D-Glucopyranosides, and 9'-*O*-Sulfate (6) (CD_3OD , 100 MHz)

Carbon No.	2	4	6
1	138.4	134.9	135.0
2	111.3	110.6	110.7
3	147.7	149.1	149.2
4	151.0	147.9	147.8
5	118.2	116.2	116.2
6	119.4	119.8	119.8
7	88.5	89.0	89.1
8	55.7	55.5	55.5
9	65.1	65.1	65.0
1'	129.7	129.9	136.5
2'	114.3	114.3	114.9
3'	145.3	145.2	145.3
4'	147.7	147.5	147.5
5'	137.1	136.9	129.9
6'	118.0	118.1	118.2
7'	32.9	33.0	32.7
8'	35.8	33.0	32.8
9'	62.3	70.1	68.2
1''	102.9	105.2	
2''	75.0	75.2	
3''	78.2	78.2	
4'	71.4	71.7	
5''	77.9	77.9	
6''	62.6	62.8	
OMe	56.8	56.5	56.5
	56.9	56.9	56.9

sively separated by silica gel (CHCl_3 -MeOH), reversed-phase gravity octadecyl silica gel (MeOH - H_2O), droplet counter-current (CHCl_3 - MeOH - H_2O -*n*-PrOH, 9:12:8:2), and Sephadex LH-20 (MeOH) chromatography to give 6.5 mg of **6**. The following amounts of compounds **1**—**5** were similarly obtained by a combination of the aforementioned chromatographic techniques from the 60% MeOH eluate (25.9 g) obtained by Diaion HP-20 column chromatography: **1** (36 mg), **2** (39 mg), **3** (43 mg), **4** (25 mg), and **5** (13 mg).

(+)-Isolarisiresinol 2a-*O*- β -D-Glucopyranoside (5) Amorphous powder. $[\alpha]_{\text{D}}^{22} +26.5^\circ$ ($c=0.83$, MeOH). UV λ_{max} (MeOH) nm (log ϵ): 211 (4.37), 224 sh (4.15), 284 (3.80); ^1H -NMR (CD_3OD) δ : 1.80 (1H, tt, $J=3$ and 10 Hz, H-3), 2.18 (1H, m, H-2), 2.84 (2H, m, H_2 -1), 3.21 (1H, dd, $J=8$ and 9 Hz, H-2''), 3.39 (1H, dd, $J=3$ and 12 Hz, H-3aa), 3.66 (1H, dd, $J=6$ and 12 Hz, H-6'a), 3.68 (1H, dd, $J=5$ and 10 Hz, H-2aa), 3.73 (1H, dd, $J=3$ and 12 Hz, H-3ab), 3.77 (3H, s, -OMe on C-7), 3.80 (3H, s, -OMe on C-3'), 3.86 (1H, br d, $J=10$ Hz, H-4), 3.87 (1H, dd, $J=2$ and 12 Hz, H-6'b), 4.00 (1H, dd, $J=4$ and 10 Hz, H-2ab), 4.29 (1H, d, $J=8$ Hz, H-1''), 6.19 (1H, s, H-5), 6.61 (1H, dd, $J=2$ and 8 Hz, H-6'), 6.65 (1H, s, H-8), 6.68 (1H, d, $J=2$ Hz, H-2'), 6.74 (1H, d, $J=8$ Hz, H-5'); ^{13}C -NMR (CD_3OD): Table 1; CD $\Delta\epsilon$ (nm): +10.8 (214), +6.80 (238), +3.71 (275), -5.50 (291) ($c=7.99 \times 10^{-5}$ M, MeOH); HR-FAB-MS (negative-ion mode) m/z : 521.2025 $[\text{M}-\text{H}]^-$ (Calcd for $\text{C}_{26}\text{H}_{33}\text{O}_{11}$: 521.2023).

Dihydrodehydrodiconiferyl Alcohol 9'-*O*-Sulfate (6) Amorphous powder. $[\alpha]_{\text{D}}^{22} +5.1^\circ$ ($c=0.43$, MeOH). UV λ_{max} (MeOH) nm (log ϵ): 212 (4.40), 228sh (4.16), 282 (3.75); UV λ_{max} (H_2O) nm (log ϵ): 212 (4.48), 221 (4.19), 281 (3.71); ^1H -NMR (CD_3OD) δ : 1.94 (2H, m, H_2 -8'), 2.68 (2H, t, $J=7$ Hz, H_2 -7'), 3.47 (1H, dd, $J=6$ and 11 Hz, H-9a), 3.76 (1H, dd, $J=7$ and 11 Hz, H-9b), 3.83 (3H, s, -OMe), 3.84 (1H, m, H-8), 3.87 (3H, s, -OMe), 4.01 (2H, t, $J=6$ Hz, H_2 -9'), 5.50 (1H, d, $J=6$ Hz, H-7), 6.68 (2H, s, H-2' and 6'), 6.77 (1H, d, $J=8$ Hz, H-5), 6.83 (1H, dd, $J=2$ and 8 Hz, H-6), 6.95 (1H, d, $J=2$ Hz, H-2); ^{13}C -NMR (CD_3OD): Table 1; CD $\Delta\epsilon$ (nm): +2.60 (211), -0.27 (223), +0.69 (240), +0.41 (290) ($c=7.90 \times 10^{-5}$ M, MeOH); HR-FAB-MS (negative-ion mode) m/z : 439.1046 $[\text{M}-\text{H}]^-$ (Calcd for $\text{C}_{20}\text{H}_{23}\text{O}_9\text{S}$: 439.1063); TLC: R_f : 0.19 (Merck silica gel plate, 0.25 mm thickness, CHCl_3 -MeOH- H_2O , 15:6:1) (cf. R_f of **4**: 0.37).

Acknowledgements The authors are grateful for access to the superconducting NMR instrument in the Analytical Center of Molecular Medicine of

Hiroshima University Faculty of Medicine. Thanks are also due to the Okinawa Foundation for in the form of financial support of an Okinawa Research Promotion Award (H.O.).

References

- 1) Hatusima S., "Flora of the Ryukyus," Okinawa Society of Biological Education and Research, Naha, Okinawa, 1975, pp. 371—372.
- 2) Otsuka H., Hirata E., Takushi A., Shinzato T., Takeda Y., Bando M., Kido M., *Chem. Pharm. Bull.*, **48**, 547—551 (2000).
- 3) Achenbach H., Lowel M., Waibel R., Gupta M., Solis P., *Planta Med.*, **58**, 270—272 (1992).
- 4) a) Matsuda N., Sato H., Yaoita Y., Kikuchi M., *Chem. Pharm. Bull.*, **44**, 1122—1123 (1996); b) Abe F., Yamauchi T., *ibid.*, **34**, 4340—4345 (1986); c) Takeda Y., Mima C., Masuda T., Hirata E., Takushi A., Otsuka H., *Phytochemistry*, **49**, 2137—2139 (1998).

A New Cytotoxic Polyhydroxysterol from Soft Coral *Sarcophyton trocheliophorum*

Hui DONG,^{*,a,b} Yu-Lin GOU,^a R. Manjunatha KINI,^a Hong-Xi XU,^b Shao-Xing CHEN,^c
Serena Lay Ming TEO,^a and Paul Pui-Hay BUT^b

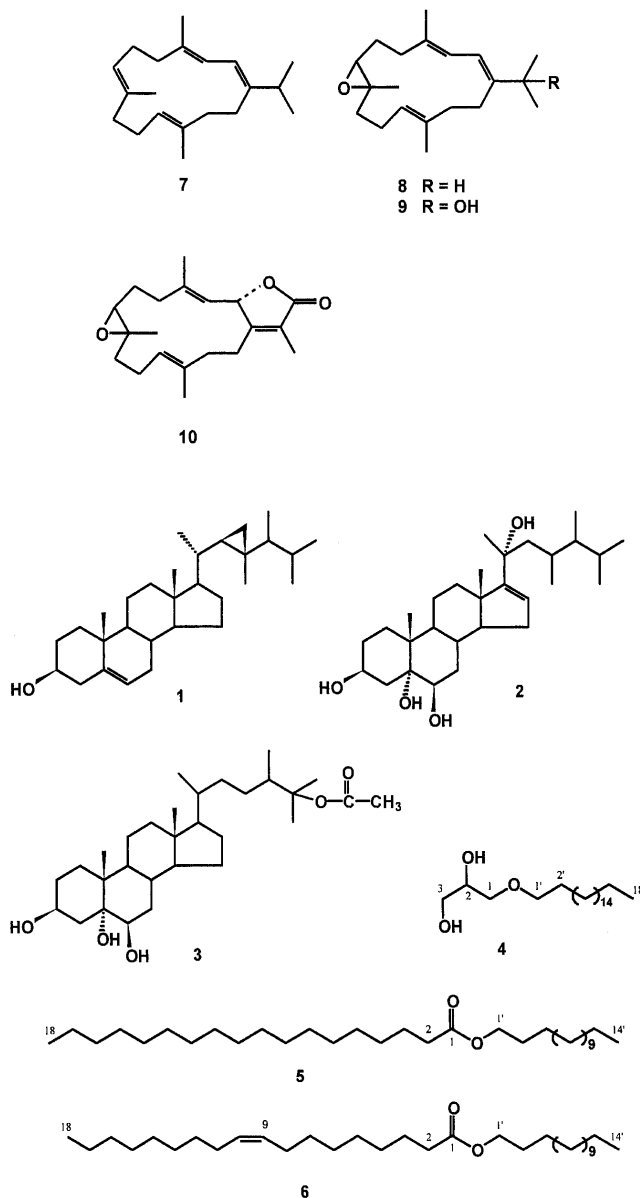
Bioscience Center, Department of Biological Science, Faculty of Science, National University of Singapore,^a 10 Kent Ridge Crescent, Singapore 119260, Singapore, Chinese Medicinal Material Research Center, The Chinese University of Hong Kong,^b Shatin, Hong Kong, and Department of Scientific Service, Institute of Science and Forensic Medicine,^c 11 Outram Road, Singapore 169078, Singapore. Received January 24, 2000; accepted March 17, 2000

A new cytotoxic polyhydroxysterol, 23,24-dimethylcholest-16(17)-E-en-3 β ,5 α ,6 β ,20(S)-tetraol (2), together with nine known compounds was isolated from the soft coral *Sarcophyton trocheliophorum*. Their structures were determined by spectroscopic methods. Compound 2 showed potent growth inhibitory activity against human HL60 leukemia, M14 skin melanoma, and MCF7 breast carcinoma cells with EC₅₀ values of 2.8, 4.3, and 4.9 μ g/ml, respectively, and exhibited minimal toxicity to normal human peripheral blood lymphocytes.

Key words Soft coral; *Sarcophyton trocheliophorum*; polyhydroxysterol

A variety of constituents, such as sterols, terpenoids, and alicyclic compounds have been isolated from soft coral species of the *Sarcophyton* genus.¹⁾ Some of these compounds have been shown to have cytotoxic,²⁾ cancer chemopreventative,^{3,4)} and anti-inflammatory potential.⁵⁾ The hexane soluble extract of the soft coral *Sarcophyton trocheliophorum* Von Marenzeller showed growth inhibitory activity against human tumor cells. In this paper, we report the isolation and structure determination of a new cytotoxic polyhydroxysterol, 23,24-dimethylcholest-16(17)-E-ene-3 β ,5 α ,6 β ,20(S)-tetraol (2), together with nine known compounds, gorosten-5(E)-3 β -ol (1), 24-methylcholestane-3 β ,5 α ,6 β ,25-tetraol 25-monoacetate (3), 2,3-dihydroxypropyl octadecyl ether (4), tetradecyl octadecanoate (5), tetradecyl-9-Z-octadecenoate (6), isoneocembrene A (7), 7,8-epoxy-1(E),3(E),11(E)-cembratriene (8), 7,8-epoxy-1(E),3(E),11(E)-cembratrien-15-ol (9), and sarcophine (10) from the hexane soluble fraction of the soft coral *Sarcophyton trocheliophorum* (Alcyoniidae) and their cytotoxic activity on human tumor cells.

Compound 2 was obtained as colorless amorphous powder. The molecular formula was determined as C₂₉H₅₀O₄ by HREIMS (M⁺ 462.3716, Calc. 462.3709). The ¹³C NMR and DEPT spectra showed twenty nine signals including characteristic signals of eight methylene carbons, eight methine carbons, five quaternary carbons, one olefinic carbon, and seven methyl carbons. In the ¹H NMR spectrum of compound 2, four methyl groups appeared as four doublets (*J*=6.6, 7.9, 7.2, and 7.2 Hz) at δ 0.75, 0.77, 0.86, and 0.88 and three methyl groups appeared as three singlets at δ 0.98, 1.20, and 1.36, respectively. These data indicated the presence of the partial structure of the side chain of 23,24-dimethyl cholesterol derivatives. It was further confirmed in the mass spectrum by the fragmentation pattern with peaks at *m/z* 349 [M-C₈H₁₇], 331 [M-C₈H₁₇-H₂O], 313 [M-C₈H₁₇-2H₂O], and 295 [M-C₈H₁₇-3H₂O], which corresponded to the cleavage of the side chain of 23,24-dimethyl cholesterol derivatives. Furthermore, the ¹H-¹H COSY and HMBC spectra of this compound also gave good information for supporting the assignment of the side chain. There were long-range correlations between C-24 (δ 45.89) with Me-26 (δ 0.77),



* To whom correspondence should be addressed. e-mail: dongh@cuhk.edu.hk

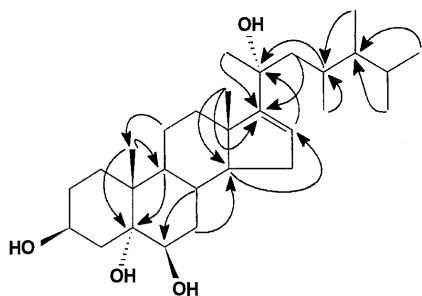


Fig. 1. Selected HMBC Correlations in Compound 2

Me-27 (δ 0.75), Me-28 (δ 0.86), and Me-29 (δ 0.88), C-23 (δ 29.59) with Me-28 and Me-29, and C-22 (δ 49.09) with Me-21 (δ 1.36) and Me-29 in the HMBC spectrum. The ^1H NMR spectrum also showed an olefinic proton at δ 5.47 which appeared as a broad singlet and two secondary carbinol methines at δ 3.55 (1H, br) and 4.08 (1H, br m). The broad methine multiplet at δ 4.08 had the normal complexity for the 3α -carbinol proton of an A/B *trans*-steroid. This unusually downshifted signal is typical of 3β -hydroxysterols bearing a 5α -hydroxyl group.^{6,7} Two double doublets at δ 2.05 ($J=11.2$ and 12.5 Hz) and δ 1.76 ($J=12.5$ and 3.9 Hz), mutually coupled and coupled with the 3α -proton at δ 4.08, were assigned, respectively, to the 4-H_{ax} and 4-H_{eq} protons next to the C-5 substituted position.⁸ The downshift of the C-19 methyl group signal at δ 1.20 was indicative of the β -orientation of the C-6 hydroxyl group.⁹ These data suggested the $3\beta,5\alpha,6\beta$ -trihydroxyl substitutions of compound 2. This partial structure was further confirmed by observation of the long-range correlations between C-3 (δ 67.63) with $\text{H}_{\text{ax}}\text{-4}$ (δ 2.05) and H-1 (δ 1.40) and C-5 (δ 76.78) with Me-19 (δ 1.23) and H-6 (δ 3.55) in the HMBC spectrum. Likewise, the HMBC spectrum permitted the location of another hydroxylated quaternary carbon (δ 75.97) at C-20 and a double bond (δ 123.69 and 160.90) at C-16(17) due to the unambiguous correlations between C-20 (δ 75.97) with H-16 (δ 5.47), Me-21 (δ 1.36), and $\text{H}_2\text{-22}$ (δ 1.47 and 1.58) and C-17 (δ 160.90) with Me-18 (δ 0.98), Me-21 (δ 1.36), and $\text{H}_2\text{-15}$ (δ 1.89 and 2.02) (Fig. 1). The relative stereochemistry of compound 2 was elucidated on the basis of NOESY correlations. The NOESY spectrum showed cross-peaks of H-4 β /Me-19 and H-8/Me-19 which confirmed a *trans*-junction between rings A and B and the $3\beta,5\alpha,6\beta$ -oriented substitutions.¹⁰ NOESY correlations for H-16/Me-21, H-15 β /Me-21, Me-18/Me-21, and H-12 β /Me-21 suggested that the relative stereochemistry at C-20 was *S* configuration. From the above data, the structure of compound 2 was concluded to be 23,24-dimethylcholest-16(17)-*E*-ene- $3\beta,5\alpha,6\beta,20(S)$ -tetraol. The ^1H - and ^{13}C -NMR data of compound 2 were assigned by analysis of DEPT, ^1H , ^1H COSY, ^1H , ^{13}C COSY, HMQC, and HMBC spectral data.

The other nine compounds, gorosten-5(*E*)- 3β -ol (1),¹¹ 24-methylcholestane- $3\beta,5\alpha,6\beta,25$ -tetraol 25-monoacetate (3),^{12,13} 2,3-dihydroxypropyl octadecyl ether (4),¹⁴ tetradecyl octadecanoate (5),¹⁵ tetradecyl-9-*Z*-octadecenoate (6),¹⁵ isoneocembrene A (7),¹⁶ 7,8-epoxy-1(*E*),3(*E*),11(*E*)-cembratriene (8),¹⁷ 7,8-epoxy-1(*E*),3(*E*),11(*E*)-cembratrien-15-ol (9),¹⁸ and sarcophine (10)¹⁸ were identified by comparing their MS, ^1H -, and ^{13}C -NMR spectral data with those reported in the literature. The assignment of ^{13}C -NMR data of

Table 1. ^{13}C -NMR Spectral Data of Compounds 2 and 3^{a)} (125 MHz, CDCl_3)

C	2	3 ^{b)}	C	2	3
1	32.21, t ^{c)}	32.41, t	16	123.69, d	24.16, t
2	30.82, t	30.88, t	17	160.90, s	55.95, d
3	67.63, d	67.66, d	18	18.39, q	12.19, q
4	40.72, t	40.78, t	19	16.76, q	16.89, q
5	76.78, s	76.12, s	20	75.97, s	36.24, d
6	75.93, d	76.09, d	21	29.65, q	18.97, q
7	34.28, t	34.57, t	22	49.09, t	34.69, t
8	28.89, d	30.25, d	23	29.59, d	27.79, t
9	45.99, d	45.89, d	24	45.89, d	41.98, d
10	38.54, s	38.34, d	25	30.94, d	85.96, s
11	21.19, t	21.20, t	26	20.91, q	14.52, q
12	36.26, t	39.96, t	27	15.78, q	23.36, q
13	47.76, s	42.78, s	28	11.59, q	22.94, q
14	57.33, d	55.99, d	29	21.49, q	
15	30.85, t	28.14, t	OAc		170.49, s

a) δ in ppm. b) Data assigned by analysis of ^1H , ^1H COSY, HMQC, and HMBC spectral data. c) Multiplicities determined by DEPT sequences.

Table 2. Cytotoxicity of Compounds 1–10 ($n=3$ –6)

Compound	Cell line EC ₅₀ ($\mu\text{g/ml}$)		
	HL60	M14	MCF7
1	54.1	20.3	30.2
2	2.8	4.3	4.9
3	19.6	13.2	34.5
4	46.9	20.1	29.8
5	76.8	17.2	30.2
6	53.1	10.4	26.3
7	37.2	74.6	72.8
8	34.2	>100	>100
9	63.8	>100	56.4
10	61.8	>100	>100

compound 3 was different from the data reported in the literature¹² and is listed in Table 1.

Constituents such as polyhydroxysterols and cembranoid diterpenes from soft corals are well known for their cytotoxic and cancer chemopreventative activities.^{2–4} In this study, we examined the growth inhibitory activity of compounds 1–10 against human HL60 leukemia, M14 skin melanoma, and MCF7 breast carcinoma cells. As shown in Table 2, compound 2 showed the most potent growth inhibitory activity against human HL60, M14, and MCF7 cells with EC₅₀ values of 2.8, 4.3, and 4.9 $\mu\text{g/ml}$, respectively, and in a dose-dependent manner. Compound 3 also exhibited strong growth inhibitory activity against these tested tumor cells. Compound 1, however, showed less activity than either compound 2 or 3. Of these sterols, compound 1 has only one hydroxyl group at C-3 position. Compounds 2 and 3 are polyhydroxysterols with the same $3\beta,5\alpha,6\beta$ -oriented partial structure, but compound 2 has one more free hydroxyl group at C-20 position, whereas compound 3 has one acetyl group at C-25 position.

Triggered by our finding of the antitumor activity of compound 2, we next investigated the effect of this compound on normal human peripheral blood lymphocytes (PBLs). Our data showed that compound 2 had minimal toxicity to normal human PBLs. Indicating its selective targeting of human tumor cell lines.

Data obtained from this study indicated that compound **2** showed potent inhibitory activity on human tumor cells and minimal toxicity to the normal human peripheral blood lymphocytes. Further investigations on this compound as a chemotherapeutic agent are in progress.

Experimental

General The optical rotation was obtained on a Perkin-Elmer 241 polarimeter. EIMS were obtained on a MACROMASS 7035E mass spectrometer at 70 eV. All spectra (^1H , ^{13}C , COSY, HMQC, NOESY, and HMBC) were recorded on a Bruker AMX 500 spectrometer (500 MHz for ^1H and 125 MHz for ^{13}C), and the chemical shifts are reported in ppm using TMS as an internal standard. TLC was performed on 0.25-mm Si gel (60 F₂₅₄, Merck) plates. Spots were visualized by spraying 10% H_2SO_4 aqueous and heating for 5 min.

Animal Materials The soft coral *Sarcophyton trocheliophorum* was collected in April 1998 from Pulau Hantu, an island south of Singapore, at a depth of 10 m. The voucher specimen (SC980401) is deposited in the Herbarium of Bioscience Center, Department of Biological Science, Faculty of Science, National University of Singapore, Singapore.

Extraction and Isolation The fresh material (2.5 kg, wet wt.) was sliced and percolated with acetone- H_2O (7:3) three times (8×3 l) at room temperature. The acetone was evaporated *in vacuo*. The aqueous portion was partitioned by hexane (4 l, 32 g) and EtOAc (2 l, 4 g). The hexane extract (32 g) was subjected to column chromatography over Si gel 60 and eluted by CH_2Cl_2 , CH_2Cl_2 -MeOH (8:2), CH_2Cl_2 -MeOH (1:1), and CH_2Cl_2 -MeOH- H_2O (1:1:0.1) solvent systems to afford four fractions, fractions A—D. Fraction A (5.6 g) was purified again by column chromatography over Si gel and eluted under gradient conditions with increasing amounts of EtOAc in hexane to afford **1** (30 mg), **5** (200 mg), **6** (150 mg), and **7** (20 mg). Fraction B (0.5 g) was further purified by repeated Si gel chromatography under the above conditions and/or preparative TLC to give **8** (12 mg), **9** (40 mg), and **10** (8 mg). Fraction D (1.2 g) was subjected to column chromatography over LiChroprep RP-18 (60–43 μm) and elution with ethanol- H_2O (6:4) to give **2** (6 mg), **3** (12 mg), and **4** (70 mg).

23,24-Dimethylcholest-16(17)-*E*-ene-3 β ,5 α ,6 β ,20(*S*)-tetraol (**2**): Colorless amorphous powder. A spot sprayed with 5% H_2SO_4 and heated for 5 min showed a light blue color. $[\alpha]_D^{20} = -14.1^\circ$ (*c* 0.16, EtOH); IR (KBr) ν_{max} 3422 (OH), 2938, 1376, 1083 cm^{-1} . UV λ_{max} (log ϵ): 225 (0.26) nm. HREIMS 462.3716 (calcd for $\text{C}_{29}\text{H}_{50}\text{O}_4$, 462.3709); EIMS *m/z* 426 (M^+ , 1.2), 349 (64), 331 (24), 313 (18), 295 (30), 280 (20), 271 (14), 269 (26), 229 (12), 133 (30), 95 (48), 43 (100); ^1H NMR (500 MHz, CDCl_3) δ 0.75 (3H, d, *J*=6.6 Hz, Me-27), 0.77 (3H, d, *J*=7.9 Hz, Me-26), 0.86 (3H, d, *J*=7.2 Hz, Me-29), 0.88 (3H, d, *J*=7.2 Hz, Me-28), 0.98 (3H, s, Me-18), 1.06 (1H, m, H-24), 1.20 (3H, s, Me-19), 1.31 (1H, m, H-23), 1.33 (1H, m, H-9), 1.36 (3H, s, Me-21), 1.61 (1H, m, H-12), 1.71 (1H, ddd, *J*=3.9, 11.8, 15.4 Hz, H-12), 1.76 (1H, dd, *J*=3.9, 12.5 Hz, H_{eq} -4), 1.96 (1H, m, H-8), 2.05 (1H, dd, *J*=11.2, 12.5 Hz, H_{ax} -4), 3.55 (1H, br s, H-6), 4.08 (1H, br m, H-3), 5.47 (1H, br s, H-16); ^{13}C NMR (125 MHz, CDCl_3) see Table 1.

Cytotoxicity Assays¹⁹ Human promyelocytic leukemia cell line HL60, human skin melanoma cell line M14, and human breast carcinoma cell line MCF7 were obtained from ATCC (Rockville, MD) and maintained in culture in RPMI 1640 supplemented with 10% fetal bovine serum (FBS; HyClone, Logan, UT) in an atmosphere of 5% CO_2 at 37 °C. Normal human PBLs were obtained from blood donated by healthy volunteers by ficoll hypaque density centrifugation. For HL60 cells and normal PBLs, 1×10^5 cells/well in a 96-well plate were exposed to different concentrations of compounds **1**—**10** for 24 h. M14 cells and MCF7 cells were plated in 96-

well plates (2×10^4) for 24 h before the addition of compounds **1**—**10** with different concentrations. Medium was then aspirated and replaced with fresh RPMI 1640+10% FBS containing compounds **1**—**10** for 24 h. Equal concentration of DMSO was used in the control wells. Viability was determined by the MTT assay for HL60 cells and for PBLs, or by the crystal violet assay for M14 and MCF7 cells. For MTT assay, 10 μl of 5 mg/ml of MTT was added to each well and incubated for 4 h at 37 °C. Elution of the precipitate was performed with 200 μl of DMSO+10 μl of Tris-glycine buffer (0.1 M Tris, 0.1 M Glycine, pH 10.5, with 1 N NaOH). Cell viability was calculated from absorption values obtained at 570 nm using an automated enzyme-linked immunosorbent assay (ELISA) reader. For crystal violet assays, medium was aspirated and replaced for 10 min with 50 μl of 0.75% crystal violet in 50% ethanol, 0.25% NaCl, and 1.75% formaldehyde solution. Cells were then washed with water, air-dried, and the dye eluted with PBS+1% sodium dodecyl sulfate (SDS) solution. Cell viability was assessed by dye absorbance measured at 595 nm on an automated ELISA reader.

Acknowledgments The authors acknowledge the technical assistance of Mr. Mohamed Ali-syed and Mr. Wen-Cai Ye. This work was supported by the grants RP950389 and RP960319 from the National University of Singapore.

References and Notes

- 1) Anjaneyulu A. S. R., Rao G. V., *J. Ind. Chem. Soc.*, **74**, 272—278 (1997).
- 2) Duh T. Y., Hou R. S., *J. Nat. Prod.*, **59**, 595—598 (1996).
- 3) Fujiki H., Suganuma M., Suguri H., Yoshizawa S., Takagi K., Kobayashi M., *J. Cancer Res. & Clin. Oncology*, **115**, 25—28 (1989).
- 4) Narisawa T., Takahashi M., Niwa M., Fukaura Y., Fujiki H., *Cancer Res.*, **49**, 3287—3289 (1989).
- 5) Norton R. S., Kazlauskas R., *Experientia*, **36**, 276—278 (1980).
- 6) Bridgeman J. E., Cherry P. C., Clegg A. S., Evans J. M., Jones E. R. H., Kasal A., Kumar V., Meakins G. D., Morisawa Y., Richards E. E., Woodgate P. D., *J. Chem. Soc. (C)*, 250—257 (1970).
- 7) Su J. Y., Yu X. Q., Zeng L. M., *J. Nat. Prod.*, **52**, 934—940 (1989).
- 8) Piccialli V., Sica D., *J. Nat. Prod.*, **50**, 915—920 (1987).
- 9) Demarco P. V., Farkas E., Doddrell D., Mylari B. L., Wenkert E., *J. Am. Chem. Soc.*, **90**, 5480—5486 (1968).
- 10) Barabas A., Botar A. A., Gocan A., Popovici N., Hodosan F., *Tetrahedron*, **34**, 2191—2194 (1978).
- 11) Hale R. L., LeClerc J., Tursch B., Djerassi C., Gross R. A., Jr., Weinheimer A. J., Gupta K., Scheuer P. J., *J. Am. Chem. Soc.*, **92**, 2179—2180 (1970).
- 12) Raju B. L., Subbaraju G. V., Reddy M. C., Rao D. V., Rao C. B., Raju V. S., *J. Nat. Prod.*, **55**, 904—911 (1992).
- 13) Kobayashi M., Kanda F., Rao C. V. L., Kumar S. M. D., Trimurtulu G., Rao C. B., *Chem. Pharm. Bull.*, **38**, 1724—1726 (1990).
- 14) Wang G. Y. S., Liu Q., Zeng L. M., *Acta Scientiarum Naturalium Universitatis Sunyatseni*, **34**, 110—113 (1995).
- 15) Dembitsky V. M., Rezanka T., *Phytochemistry*, **42**, 1075—1080 (1996).
- 16) Suleimanove A. M., Kalinovakii A. I., Raldugin A. I., Shevtsov S. A., Bagryanskaya I. Y., Gatilov Y. V., Kuznetsova T. A., Elyakov G. B., *Khim. Priir. Soedin*, 535—640 (1988).
- 17) Coll J. C., Hawes G. B., Liyanage N., Oberhansli W., Wells R. J., *Aust. J. Chem.*, **30**, 1305—1309 (1977).
- 18) Duh C. Y., Hou R. S., *J. Nat. Prod.*, **59**, 595—598 (1996).
- 19) Clement M. V., Hirpara J. L., Chawhury S. H., Pervaiz S., *Blood*, **92**, 996—1002 (1998).

Conduritol F Glucosides and Terpenoid Glucosides from *Cynanchum liukiuense* and Distribution of Conduritol F Glucosides in Several Asclepiadaceous Plants

Fumiko ABE,*^a Tatsuo YAMAUCHI,^a Keiichi HONDA,^b and Nanao HAYASHI^b

^aFaculty of Pharmaceutical Sciences, Fukuoka University,^a 8-19-1 Nanakuma, Jonan-ku, Fukuoka 814-0180, Japan,

^bFaculty of Integrated Arts and Sciences, Hiroshima University,^b 1-7-1 Kagamiyama, Higashihiroshima 739-8521, Japan.

Received February 3, 2000; accepted March 9, 2000

Conduritol F 3-*O*- and 4-*O*-glucosides were obtained from *Cynanchum liukiuense*, along with conduritol F which was identified in all Asclepiadaceous plants examined, *Tylophora tanakae*, *Asclepias curassavica* and *A. fruticosa*, as well as in *Marsdenia tomentosa*. The pattern of the glucosidic linkage to conduritol F differed between individual species, 2-*O*-glucoside from *T. tanakae* and *M. tomentosa*, 3-*O*-glucoside from *A. curassavica*, but none from *A. fruticosa*. Along with conduritol F glucosides, an 11-glucosyloxy-megastigmane and a monoterpenoid glucoside were isolated from *C. liukiuense*.

Key words *Cynanchum liukiuense*; conduritol F glucoside; 11-glucosyloxy-megastigmane; *Tylophora tanakae*; *Asclepias curassavica*; *Asclepias fruticosa*

During studies on the constituents of Apocynaceae and Asclepiadaceous plants, we have described that the pyrrolizidine alkaloids in *Parsonia laevigata* ALSTON¹⁾ and phenanthroindolizidine alkaloids in *Tylophora tanakae* MAXIM.²⁾ act as an oviposition-activating substance for Danaid butterflies, *Idea leuconoe* and *Ideopsis similis*, respectively. Since *Parantica sita* lays eggs on the leaves of *Marsdenia tomentosa* MORREN et DECAISNE and cyclitols such as conduritol A, conduritol F and their glucosides in this plant are involved in host-recognition,³⁾ we have investigated polar compounds, including cyclitols, in other Asclepiadaceous plants. This paper deals with the isolation of conduritol F and its glucosides, along with a megastigmane glucoside and a monoterpenoid glucoside from *Cynanchum liukiuense* WARB., which is known as a host-plant for *Salatura genutia* CRAMER, one of the Danaid butterflies in the Ryukyu district. We also describe the comparison of conduritol F and its glucosides from *T. tanakae*, *A. curassavica* L. and *A. fruticosa* L.

The leaves of *C. liukiuense*, collected in the Yaeyama Islands, were homogenized with MeOH, and the MeOH extract was partitioned with CHCl₃ and then *n*-BuOH. The water layer was fractionated on a charcoal column and eluted with H₂O, 5–50% EtOH, and MeOH. Each fraction was then pu-

rified on a silica gel column and subjected to HPLC to afford five substances (1–5). Substance 1, obtained from the H₂O effluent, was identified as conduritol F (L-leuchanthemitol).³⁾

Substance 2 was obtained from the 10–20% EtOH effluent, and has the molecular formula, C₁₂H₂₀O₉, based on high resolution (HR)-FAB-MS. In addition to the signals due to a β -glucopyranosyl moiety (δ_C 105.4 and δ_H 4.81, $J=8$ Hz), signals due to conduritol F were observed in the ¹H- and ¹³C-NMR spectra, suggesting 2 to be a conduritol F glucoside (Table 1). Upon acid hydrolysis of 2, the glucose was confirmed to be in the D-form by GC analysis of the thiazolidine derivative.⁴⁾ Based on the deshielding of C-3 (+8.9 ppm) and the shielding of C-2 (–1.4 ppm) and C-4 (–0.5 ppm), in comparison with the signals for 1, 2 was determined to be 3-*O*- β -D-glucopyranosyl-conduritol F.

Substance 3 was accompanied by 2 and isolated finally by HPLC. HR-FAB-MS of 3 suggested that it has the same molecular formula as 2, C₁₂H₂₀O₉. The NMR spectra showed a similar pattern to 2, except for the deshielding of C-4 (+9.1 ppm) and the shielding of C-3 (–1.4 ppm) and C-5 (–1.4 ppm) in the ¹³C-NMR spectrum. Therefore, the linkage of glucose was assigned to be at C-4–OH. In the same way as for 2, glucose was confirmed to be in the D-form, and 3 was determined to be 4-*O*- β -D-glucopyranosyl-conduritol F.

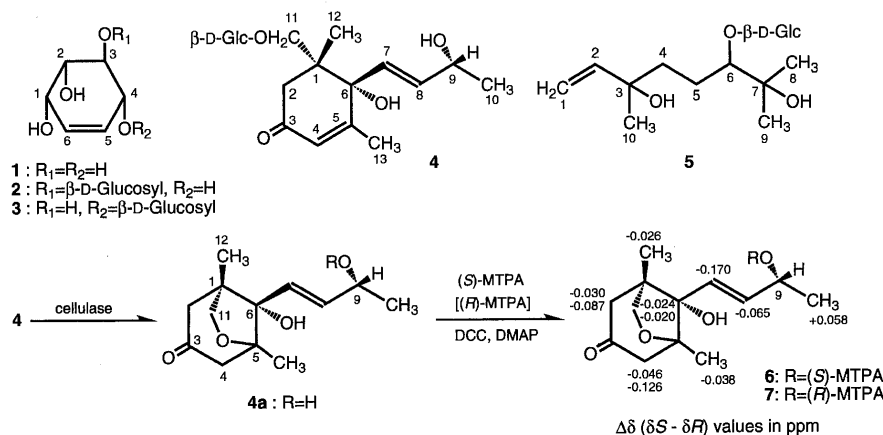


Chart 1

* To whom correspondence should be addressed. e-mail: abefumi@fukuoka-u.ac.jp

Table 1. ^{13}C - and ^1H -NMR Spectral Data for **1**–**5** and **4a** (J =Hz in Parentheses)

No.	1^{a)}		2^{a)}		3^{a)}		4^{b)}		4a^{b)}		5^{b)}	
	C	H	C	H	C	H	C	H	C	H	C	H
1	69.4	4.28 (t, 4)	69.3	4.33 (t, 5)	69.0	4.28 (d, 4)	46.2		49.5		112.0	5.01 (dd, 11,2) 5.19 (dd, 17,2)
2	73.5	3.59 (dd, 11,4)	72.1	3.71 (dd, 10,4)	73.3	3.63 (dd, 11,4)	45.6	2.35 (d, 17, β) 2.64 (d, 17, α)	53.3	2.67 (dd, 18,3) 2.34 (dd, 18,3)	146.6	5.91 (dd, 17,11)
3	75.2	3.64 (dd, 11,7)	84.1	3.91 (dd, 10,8)	73.8	3.88 (dd, 11,7)	200.9		211.2		73.9	
4	75.1	4.08 (dt, 7, 2)	74.6	4.31 (dt, 8,2)	84.2	4.29 (d, 7)	127.8	5.90 (br s)	53.9	2.75 (d, 18) 2.47 (dd, 18,3)	39.5	1.54 (m) 2.03 (m)
5	135.1	5.80 (dd, 10,2)	134.8	5.79 (dd, 10,2)	133.7	5.92 (br d, 10)	167.1		87.4		27.1	1.55 (m) 1.65(m)
6	129.5	5.88 (ddd, 10,5,2)	129.4	5.90 (ddd, 10,5,2)	130.7	5.96 (br d, 10)	79.4		82.4		90.5	3.44 (m)
7							129.7	5.74 (dd, 16,1)	125.6	6.01 (dd, 16,1)	73.7	
8							137.3	5.84 (dd, 16,5)	140.8	6.18 (dd, 16,5)	24.5c	1.13 (s)d
9							68.6	4.33 (qd, 6,5)	68.9	4.37 (qd, 7,5)	26.6c	1.16 (s)d
10							23.8	1.25 (d, 6)	24.0	1.28 (d, 7)	27.9	1.25 (s)
11							74.7	3.60 (d, 10) 3.96 (d, 10)	78.4	3.64 (d, 8) 3.92 (dd, 8,3)		
12							20.2	1.08 (s)	15.6	0.98 (s)		
13							19.5	1.91 (br s)	19.2	1.16 (s)		
1'			105.4	4.81 (d, 8)	105.5	4.74 (d, 8)	104.6	4.15 (d, 8)			105.2	4.34 (d, 8)
2'			76.3	3.38 (dd, 8,9)	76.3	3.33 (dd, 8,9)	75.1	3.15 (dd, 8,9)			75.4	3.25 (dd, 8,9)
3'			78.5	3.54 (t, 9)	78.5	3.52 (t, 9)	78.1	3.32 (t, 9)			78.0	3.37 (t, 9)
4'			72.5	3.43 (dd, 8,9)	72.4	3.42 (t, 9)	71.6	3.27 (t, 9)			71.6	3.31 (t, 9)
5'			78.9	3.49 (m)	78.7	3.48 (m)	78.0	3.21 (m)			78.1	3.30 (m)
6'			63.6	3.75 (dd, 12,6) 3.94 (dd, 12,2)	63.6	3.74 (dd, 12,5) 3.92 (dd, 12,2)	62.7	3.66 (dd, 12,5) 3.84 (dd, 12,2)			62.6	3.65 (dd, 12,5) 3.86 (dd, 12,2)

a) Dissolved in D_2O (δ ppm from TSP). b) Dissolved in CD_3OD (δ ppm from TMS). c,d) Interchangeable in each column.

HR-FAB-MS of **4** afforded a $[\text{M}+\text{Na}]^+$ peak at m/z 425.1788, suggesting **4** to have the molecular formula, $\text{C}_{19}\text{H}_{30}\text{O}_6$. Since a single tertiary, vinyl and secondary methyl signal (δ 1.08 (s), 1.91 (br s), 1.25 (d, $J=6$ Hz)) was observed in addition to those due to the glucose in the ^1H -NMR spectrum, **4** seemed to be a megastigmane glucoside. The ^{13}C -signals at δ 200.9 (s), 127.8 (d) and 167.1 (s) and one olefinic proton signal (H-4, δ 5.90, br s) suggested the presence of a 4-en-3-one, to which one methyl group (H-13, δ 1.91) was attached. A *trans*-disubstituted olefinic linkage was located between C-7 (δ 129.7) and C-8 (δ 137.3) in the side-chain, based on the coupling pattern initiated from the terminal methyl group (H-10, δ 1.25, d, $J=6$ Hz) to H-8 (δ 5.84, dd, $J=16$, 5 Hz), through the proton at the neighboring hydroxymethine proton (H-9, δ 4.33, m).⁵⁾ The tertiary methyl signal (δ_{H} 1.08, δ_{C} 20.2) and the hydroxymethylene signals (δ_{H} 3.60, 3.96 (d, $J=10$ Hz), δ_{C} 74.7) showed correlations with each other via a quaternary carbon at δ 46.2 (C-1) in the heteronuclear multiple bond correlation (HMBC) experiment. Another quaternary carbon signal at δ 79.4 showed 3-bond connectivities from H-2, 4, 8, 11, 12 and 13, respectively. Therefore, the aglycone of **4** was considered to have a planar structure as shown in Chart 1. The β -orientation of the side-chain was determined by application of the CD helicity rule.⁶⁾ Based on the positive CD value ($[\theta] +23900$) at 243 nm, the absolute configuration at C-6 was confirmed to be *R*. The presence of NOEs between H-7 and the 12-methyl group and between H-12 and H-2 β which also showed an NOE to H-7, suggested that the 12-methyl group had a β -orientation (1*R*). The location of the glucosidic linkage was assigned to be at C-11–OH, based on the cross-peak between the anomeric proton and C-11 in the HMBC spectrum.

After hydrolysis with cellulase, **4** afforded the aglycone (**4a**) and glucose, which was confirmed to be in the D-form by the same procedure as for **2** and **3**. In the ^{13}C -NMR spectrum of **4a**, a methylene carbon and a quaternary carbon signal was observed at δ 53.9 and 87.4, respectively, instead of signals at δ 127.8 (d) and 167.1 (s) in **4**. The carbonyl carbon at δ 200.9 in **4** was also shifted to δ 211.2, and **4a** was considered to have an additional linkage between the C-11 hydroxy group and C-5, forming a furanoid ring. The $[\text{M}-\text{H}_2\text{O}]^+$ peak at m/z 222.1255 ($\text{C}_{13}\text{H}_{20}\text{O}_4-\text{H}_2\text{O}$) in the electron impact (EI)-MS also suggested a bicyclic formula for **4a**. The stereochemistry at C-9 was determined to be *R*, based on the results of a modification of Mosher's method.⁷⁾ When **4a** was treated with (*S*)- and (*R*)- α -methoxy- α -trifluoromethylphenyl acetic acid (MTPA) in the presence of dicyclohexylcarbodiimide (DCC) and 4-dimethylaminopyridine (DMAP), 9-(*S*)-MTPA ester (**6**) and 9-(*R*)-MTPA ester (**7**) were obtained, respectively. The $\Delta\delta$ values of $\delta\text{S}-\delta\text{R}$ are given in Chart 1. Compound **4** was, thus, determined to be (1*R*,6*R*,9*R*)-6,9,11-trihydroxy-4-megastigmen-3-one 11-*O*- β -D-glucopyranoside. Recently, a substance having the same planar structure as **4** was reported as 6-hydroxyjunipeionololide from *Juniperus phaeincea*.⁸⁾ Although the ^1H - and ^{13}C -NMR signals showed similar values to those of **4**, final identification was not possible as neither the optical rotation, CD value nor C-9 configuration was determined.

Substance **5** was isolated from the same fraction as **4**, and was suggested to be a monoterpenoid glucoside, $\text{C}_{16}\text{H}_{30}\text{O}_8$, based on a quasimolecular ion peak (m/z : 373.1841, $[\text{M}+\text{Na}]^+$) and the ^1H - and ^{13}C -NMR spectra. The ^1H -NMR spectrum suggested that the aglycone of **5** had three tertiary methyl groups (δ 1.13, 1.16, 1.25), two methylene groups (δ

2.03, 1.54 (m) and δ 1.65, 1.55 (m)) and a terminal methylene group (δ 5.01 (dd, $J=11$, 2 Hz), 5.19 (dd, $J=17$, 2 Hz), 5.91 (dd, $J=17$, 11 Hz)). The remaining three carbons seemed to be oxygenated (δ 73.7 (s), 73.9 (s), 90.5 (d)). Based on the correlations in the HMBC spectrum from the tertiary methyl protons to the carbons bearing hydroxy groups (δ 1.25 $\rightarrow\delta$ 73.9; δ 1.13, 1.16 $\rightarrow\delta$ 73.7, 90.5), as well as the exomethylene protons to the carbon at δ 73.9, the structure of the aglycone was determined to be 3,7-dimethyloct-1-ene-3,6,7-triol. The linkage of the β -D-glucopyranosyl moiety (δ_{H} 4.34, d, $J=8$ Hz) was assigned to be at the 6-OH by the HMBC correlation between the anomeric proton and C-6. Recently, the 3-O-glucoside of the same monoterpenoid was isolated from the fruits of *Cnidium monnieri* CUSSON (Umbelliferae).⁹⁾ In both cases, however, the stereochemistry at C-3 and C-6 was not established.

In order to compare the cyclitols in other Asclepiadaceae plants, the leaves of *T. tanakae* (*T. t.*), *A. curassavica* (*A. c.*) and *A. fruticosa* (*A. f.*) were examined using the same procedure. Conduritol F was obtained from all plant sources examined. In addition, the presence of conduritol F 2-O-glucoside in *T. t.* as well as in *M. tomentosa*,³⁾ 3-O-glucoside in *A. c.*, and 3-O-glucoside and unstable 4-O-glucoside in *C. liukiense* was confirmed. Although no conduritol F glucoside was obtained from *A. f.*, the possibility that the glucoside was hydrolyzed enzymatically during the extraction with 50% acetone solution, cannot be excluded. The behavior of *Parantica sita* with respect to these conduritol F-containing plants is to be described elsewhere.

Experimental

¹H- and ¹³C-NMR spectra were recorded on a JNM-A500 spectrometer in D₂O or CD₃OD. Chemical shifts are given in δ values referred to the internal standard, sodium 3-trimethylsilylpropionate-*d*₄ (TSP) for D₂O, or tetramethylsilane (TMS) for CD₃OD, and the following abbreviations are used: s=singlet, d=doublet, t=triplet, q=quartet, m=multiplet, br=broad. HR-FAB-MS and HR-EI-MS were recorded on a JEOL HX-110 spectrometer. Optical rotations were measured on a JASCO DIP 360 polarimeter. CD spectra were recorded on a JASCO DP 501N in MeOH. GC analysis was carried out by Shimadzu GC17A instrument with a Shimadzu DB-1 column. For silica gel column chromatography and TLC, the following solvent systems were used: CHCl₃-MeOH-H₂O (2:1:0.1–2:1:0.2, solvent 1), EtOAc-MeOH-H₂O (6:1:1.2–4:1:1.2, top layer, solvent 2), CHCl₃-MeOH (20:1, solvent 3). For HPLC (Capcell Pak NH₂ column, UG80 type, 10 mm i.d. \times 250 mm), MeCN-H₂O was used.

Extraction and Isolation Fresh leaves of *Cynanchum liukiense* (2.45 kg) collected in Yaeyama Islands, in September, 1998, were homogenized with cold MeOH, and filtered. The residue was again eluted with MeOH. The homogenate and eluate were combined and concentrated *in vacuo*. The solution was partitioned with CHCl₃ (extract 900 mg) and then with *n*-BuOH (2.96 g). The water layer, after extraction with *n*-BuOH, was concentrated and passed through a charcoal column. The column was eluted with 2 l each of H₂O (Fr. 1), 5% EtOH (Fr. 2), 10–20% EtOH (Fr. 3), 50% EtOH (Fr. 4), and MeOH (Fr. 5). Fraction 1 was chromatographed on a silica gel column with solvent 1 and 2, and then purified on HPLC (90–95% MeCN) to give conduritol F (1, 123 mg) as prisms, mp 132–133 °C, $[\alpha]_{\text{D}}^{28}$ –100.3° ($c=0.66$, H₂O).

3-O- β -D-Glucopyranosyl-conduritol F (2): Fraction 3 was chromatographed on a silica gel column with solvent 1 and then purified on HPLC with 85% MeCN to afford 2 as a solid (6 mg), $[\alpha]_{\text{D}}^{25}$ –30.0° ($c=0.25$, H₂O), FAB-MS m/z : 331.1009 (Calcd for C₁₂H₂₀O₉+Na: 331.1005).

4-O- β -D-Glucopyranosyl-conduritol F (3): Substance 3 was separated from 2 by HPLC and obtained as a solid (10 mg), $[\alpha]_{\text{D}}^{26}$ –4.6° ($c=0.34$, MeOH), FAB-MS m/z : 331.1012 (Calcd for C₁₂H₂₀O₉+Na: 331.1005).

(1R,6R,9R)-6,9,11-Trihydroxy-4,7-megastigmadien-3-one 11-O- β -D-Glucopyranoside (4): Fraction 5 was further purified on a silica gel column with solvent 1, 2, and on HPLC (80–85% MeCN). Finally, 4 (50 mg) was obtained as a solid, $[\alpha]_{\text{D}}^{25}$ +52.4° ($c=1.96$, MeOH), FAB-MS m/z : 425.1788

(Calcd for C₁₉H₃₀O₉+Na: 425.1788), CD $[\theta]$ (nm): +23900 (242) ($c=0.00047$, MeOH). 4 (20 mg) was dissolved in H₂O (1 ml) and shaken with cellulase II (Sigma, 100 mg) for 9 h at 38 °C. The mixture was extracted with *n*-BuOH and the H₂O layer was evaporated *in vacuo*. The BuOH extract was purified on a silica-gel column with solvent 3 to give 4a as a solid, $[\alpha]_{\text{D}}^{25}$ +2.7° ($c=0.30$, MeOH), EI-MS m/z : 222.1255 (Calcd for C₁₃H₂₀O₄-H₂O: 222.1256). A solution of 4a (3 mg) in CH₂Cl₂ (0.3 ml) was treated with (*S*)-MTPA (18 mg) in CH₂Cl₂ (0.2 ml) in the presence of DMAP (12 mg) and DCC (15 mg) and the mixture was allowed to stand for 1 d. The reaction mixture was subjected to silica gel column chromatography directly and eluted with benzene and benzene-acetone (10:1) to give 6 (3 mg). ¹H-NMR (CD₃OD) δ : 0.888 (3H, s, H-12), 1.111 (3H, s, H-13), 1.474 (3H d, $J=7$ Hz, H-10), 2.307, 2.452 (1H each, dd, $J=18$, 3 Hz, H-2), 2.393 (1H, dd, $J=18$, 3 Hz, H-4a), 2.553 (1H, d, $J=18$ Hz, H-4b), 3.625 (1H, d, $J=8$ Hz, H-11a), 3.887 (1H, dd, $J=8$, 3 Hz, H-11b), 5.689 (1H, m, H-9), 6.050 (1H, d, $J=16$ Hz, H-7), 6.110 (1H, dd, $J=16$, 6 Hz, H-8). In the similar procedure, 7 was obtained with (*R*)-MTPA. ¹H-NMR (CD₃OD) δ : 0.914 (3H, s, H-12), 1.149 (3H, s, H-13), 1.416 (3H d, $J=7$ Hz, H-10), 2.337, 2.539 (1H each, dd, $J=18$, 3 Hz, H-2), 2.439 (1H, dd, $J=18$, 3 Hz, H-4a), 2.679 (1H, d, $J=18$ Hz, H-4b), 3.645 (1H, d, $J=8$ Hz, H-11a), 3.911 (1H, dd, $J=8$, 3 Hz, H-11b), 5.679 (1H, m, H-9), 6.175 (1H, dd, $J=16$, 6 Hz, H-8), 6.220 (1H, d, $J=16$ Hz, H-7).

3,7-Dimethyloct-1-ene-3,6,7-triol 6-O- β -D-Glucopyranoside (5): 5 was accompanied by 4 in Fr. 5 and separated from 4 by HPLC (80–85% MeCN). Solid (19 mg), $[\alpha]_{\text{D}}^{28}$ –6.3° ($c=0.55$, MeOH), FAB-MS m/z : 373.1841 (Calcd for C₁₆H₃₀O₈+Na: 373.1839).

GC Analysis of Thiazolidine Derivatives of Glucose from 2–4 and 5 Samples of 2, 3 and 5 (2–3 mg) were hydrolyzed with 1 N HCl (0.5 ml) for 2 h at 95 °C and the aglycone was extracted with *n*-BuOH after dilution with H₂O (3 ml). Following deacidification with IRA-410, the H₂O layer was concentrated *in vacuo*. In the case of 4, the H₂O layer of the enzymatic hydrolysate was examined. All the residues were treated with L-cysteine methyl ester-HCl and pyridine (60 °C, 1 h). The reaction mixture was subjected to GC analysis after trimethylsilylation, column temperature: 250 °C, injection 300 °C, carrier gas: He (30 cm/s), split ratio 1:40. t_{R} : 6.37 (sugars from 2–4 and 5) (authentic D-glucose: 6.37, L-glucose: 6.60).

Isolation of Conduritol F and Conduritol F Glucoside from *Tylophora tanakae*, *Asclepias curassavica* and *A. fruticosa* The fresh leaves were homogenized with MeOH (3.5 kg of *T. t.*, 3.25 kg of *A. c.*). In the case of *A. f.*, the leaves (2.4 kg) were homogenized with 50% acetone. The mixture was filtered, and the filtrate was concentrated *in vacuo*. The concentrated solution was extracted with *n*-BuOH and the H₂O layer was passed through a charcoal column. The column was eluted with H₂O, 25%, 50% EtOH, and MeOH. Conduritol F was obtained from the H₂O effluent (172 mg from *T. t.*, 163 mg from *A. c.*, 190 mg from *A. f.*) and conduritol F glucoside was obtained from the 25% or 50% EtOH eluate (35 mg from *T. t.*, 10 mg from *A. c.*, nothing from *A. f.*).

Acknowledgements We thank Ms. Y. Iwase for NMR and Mr. H. Hanazono for MS operations.

References

- 1) a) Abe F., Yamauchi T., Yaga S., Minato K., *Chem. Pharm. Bull.*, **39**, 1576–1577 (1991); b) Honda K., Hayashi N., Abe F., Yamauchi T., *J. Chem. Ecol.*, **23**, 1703–1713 (1997).
- 2) a) Abe F., Hirokawa M., Yamauchi T., Honda K., Hayashi N., Ishii M., Imagawa S., Iwahana M., *Chem. Pharm. Bull.*, **46**, 767–769 (1998); b) Honda K., Tada A., Hayashi N., Abe F., Yamauchi T., *Experientia*, **51**, 753–756 (1995).
- 3) a) Abe F., Yamauchi T., Honda K., Hayashi N., *Phytochemistry*, **47**, 1297–1301 (1998); b) Honda K., Hayashi N., Abe F., Yamauchi T., The 43rd Ann. Meeting of the Jap. Soc. Appl. Entomol. Zool. at Naha (1999, April), Abst. p 138; Kindl H., Hoffman-Ostenhof O., *Phytochemistry*, **5**, 1091–1102 (1966).
- 4) Hara S., Okabe H., Mihashi K., *Chem. Pharm. Bull.*, **35**, 501–505 (1987).
- 5) Otsuka H., Kao M., Kamada K., Takeda Y., *Chem. Pharm. Bull.*, **43**, 754–759 (1995).
- 6) Oritani T., Yamashita K., *Tetrahedron Lett.*, **1972**, 2521–2524.
- 7) Ohtani I., Kusumi T., Kashman Y., Kakisawa H., *J. Am. Chem. Soc.*, **113**, 4092–4096 (1991).
- 8) Champavier Y., Comte G., Vercauteren J., Allais D. P., Chulia A. J., *Phytochemistry*, **50**, 1219–1223 (1999).
- 9) Kitajima J., Aoki Y., Ishikawa T., Tanaka Y., *Chem. Pharm. Bull.*, **47**, 639–642 (1999).

Antisweet Natural Products. XV.¹⁾ Structures of Jegosaponins A—D from *Styrax japonica* SIEB. et ZUCC.

Kazuko YOSHIKAWA,* Hiromichi HIRAI, Masami TANAKA, and Shigenobu ARIHARA

Faculty of Pharmaceutical Sciences, Tokushima Bunri University, Yamashiro-cho, Tokushima 770-8514, Japan.

Received February 14, 2000; accepted March 9, 2000

From the fresh fruits of *Styrax japonica* SIEB. et ZUCC., four new triterpenoid glycosides, named jegosaponins A—D (1—4), were isolated. Their structures were determined on the basis of spectroscopic data and chemical evidence. Compounds 1—4 are 3-*O*-tetraglycosides of barringtonenol C having an acetyl and a tigloyl or a (2*Z*)-hexenoyl groups at C-21, 22 and 28. The acylated saponins, 1—4, all showed antisweet activity.

Key words *Styrax japonica*; jegosaponin; antisweet substance; Styracaceae; deacyl jegosaponin; barringtonenol C

As part of our studies on naturally occurring antisweet substances, we have reported the isolation and structure determination of the antisweet principles, termed alternosides I—XIX, from the roots of *Gymnema alternifolium* (LOUR.) MERR. (Asclepiadaceae).¹⁾ In continuing this series, we have initiated a chemical study of *Styrax japonica* SIEB. et ZUCC. (Styracaceae), which is a deciduous tree growing in the forests in Japan, Korea, and China. The pericarps are reported to be used as washing soap, cough medicine and as a piscicidal agent.²⁾ Chemical studies of the saponins of the fruit have been performed by Kitagawa *et al.*, and they reported the structures of jegosapogenins and deacyl jegosaponin.³⁾ In this paper, we report the isolation, structural elucidation and antisweet activity of four saponins, named jegosaponins A—D (1—4).

Jegosaponin A (**1**), the main saponin, had the molecular formula C₆₁H₉₆O₂₇ (negative FAB-MS, *m/z* 1259 [M—H][–]) and spectroscopic properties which were characterized the presence of carbonyl functions, a carboxyl group and esters [*v*_{max} 3400 (br), 1730 (br), 1660, 1245; δ_c 172.2 (COOH), 171.1 (C=O), 168.1 (enone)]. Acid hydrolysis of **1** afforded barringtonenol C (**5**)⁴⁾ as the aglycone, besides D-galactose, D-glucose, L-rhamnose, which were confirmed by specific rotation using HPLC with chiral detection.⁵⁾ However, ¹H—¹H shift correlation spectroscopy (COSY), heteronuclear multiple quantum coherence (HMQC) and heteronuclear multiple bond connectivity (HMBC) experiments revealed the presence of glucuronic acid in the sugar units. Therefore, in the ¹H-NMR spectrum, four anomeric protons were observed at δ 6.03 [1H, br s, Rha], 5.97 (1H, d, *J*=7.7 Hz, Gal), 5.63 (1H, d, *J*=7.1 Hz, Glc), and 4.78 (1H, d, *J*=8.0 Hz, GlcA). The configuration of all the sugars in the pyranose form in **1** was completely defined from the chemical shift and the coupling constant of each of the anomeric protons. Accordingly, each galactose, glucose and glucuronic acid moiety was established to have the β configuration, and one rhamnose had the α configuration.⁶⁾ A marked downfield-shift in ¹³C-NMR resonance among the aglycones was observed at δ 90.3 in comparison with that of **5**, indicating that the likely point of glycosidic linkage in the oligosaccharide was at C-3. The sugar attached at C-3 was detected by the nuclear Overhauser effect (NOE) between H-3 at δ 3.29 and H-1 at δ 4.78 of GlcA. Further, the HMBC spectrum showed connectivities between the H-1 signal (δ 5.63) of Glc and the C-2 (δ 79.1) of GlcA, the H-1 signal (δ 5.97) of Gal and the C-3 (δ 81.7)

of GlcA, the H-1 signal (δ 6.03) of Rha and the carbon signal at δ 76.2, which could be assigned to the C-2 of galactose by ¹H—¹H COSY and HMQC. Therefore, prosapogenin was absolutely identified as deacyl jegosaponin (**6**),³⁾ which was afforded by alkaline treatment of **1**, together with acetic acid and tiglic acid. The locations of the acyl groups were determined by spectral comparison of **1** and **5**, and by an HMBC experiment. Thus, acylation shifts were observed at the H-21 (+1.81 ppm), and H-22 (+1.31 ppm) positions (Table 1). The H-21 proton at δ 6.43 showed a correlation with the carbonyl carbon of the tigloyl group at δ 168.1 in HMBC. Therefore, the structure of **1** was established as barringtonenol C 21-*O*-tigloyl-22-*O*-acetyl-3-*O*- α -L-rhamonopyranosyl-(1→2)- β -D-galactopyranosyl-(1→3)-[β -D-glucopyranosyl-(1→2)]- β -D-glucuronopyranoside.

Jegosaponin B (**2**) had the same molecular formula, C₆₁H₉₆O₂₇ (negative FAB-MS, *m/z* 1259 [M—H][–]), as **1**. The carbon signals due to the sugar moieties in **2** are superimposable on those of **1**, indicating that both sugar moieties at C-3 are the same. Indeed, alkaline treatment of **2** gave deacyl jegosaponin (**6**), along with tiglic acid and acetic acid. The locations of the acyl groups were determined in the same way as for **1**: three proton signals shifted by acylation were observed at δ 6.43 (1H, d, *J*=10.0 Hz) which was assigned to H-21, and at δ 4.21, 4.32 (each 1H, d, *J*=11.8 Hz) to H₂-28

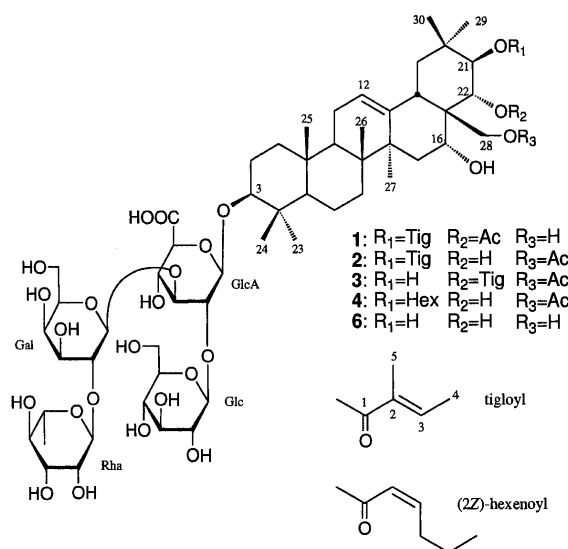


Chart 1

* To whom correspondence should be addressed. e-mail: yosikawa@ph.bunri-u.ac.jp

Table 1. ^1H -NMR Spectral Data for **1**—**4** and **5** (δ ppm in $\text{C}_5\text{D}_5\text{N}$, J in Hz, 600 MHz)

		1 ^{a)}	2	3	4	5 ^{b)}
Aglycon	3	3.29 (dd, 11.5, 4.0)	3.22 (dd, 11.5, 4.4)	3.17 (dd, 11.5, 4.5)	3.19 (dd, 11.5, 4.5)	3.48 (dd, 9.0, 5.5)
	12	5.50 m	5.46 m	5.42 m	5.43 m	5.45 m
	16	4.44 m	4.76 m	4.69 m	4.74 m	5.03 m
	18	3.01 (dd, 13.5, 4.0)	2.86 (dd, 13.0, 4.5)	2.79 (dd, 13.5, 4.0)	2.84 (dd, 13.5, 4.5)	2.80 (dd, 13.0, 4.5)
	21	6.43 (d, 10.2)	6.43 (d, 10.0)	5.00 (d, 9.6)	6.47 (d, 10.0)	4.62 (d, 10.0)
	22	6.10 (d, 10.2)	4.51 (d, 10.0)	5.98 (d, 9.6)	4.48 (d, 10.0)	4.79 (d, 10.0)
	23	1.20 s	1.15 s	1.16 s	1.15 s	1.24 s
	24	1.09 s	1.06 s	1.05 s	1.05 s	1.06 s
	25	0.96 s	0.79 s	0.78 s	0.78 s	0.97 s
	26	0.99 s	0.97 s	0.91 s	0.96 s	0.97 s
	27	1.82 s	1.82 s	1.84 s	1.82 s	1.85 s
	28	3.37, 3.61 (d, 10.9)	4.21, 4.32 (d, 11.8)	4.12 (2H, s)	4.21, 4.32 (d, 11.8)	3.73, 4.03 (d, 10.0)
	29	1.10 s	1.10 s	1.33 s	1.10 s	1.33 s
GlcA	30	1.34 s	1.31 s	1.38 s	1.31 s	1.39 s
	1	4.78 (d, 8.0)	4.85 (d, 7.1)	4.85 (d, 7.1)	4.86 (d, 7.1)	
	2	4.56 (dd, 8.8, 8.0)	4.75 (dd, 8.8, 7.1)	4.75 (dd, 8.8, 7.1)	4.75 (dd, 8.8, 7.1)	
Gal	3	4.63 (dd, 9.1, 8.8)	4.75 (dd, 9.1, 8.8)	4.73 (dd, 9.1, 8.8)	4.74 (dd, 9.1, 8.8)	
	1	5.97 (d, 7.7)	6.21 (d, 7.0)	6.21 (d, 7.4)	6.23 (d, 8.0)	
Rha	2	4.52 (dd, 8.5, 7.7)	4.74 (dd, 8.5, 7.0)	4.73 (dd, 8.5, 7.4)	4.72 (dd, 8.5, 8.0)	
	1	6.03 br s	6.22 br s	6.26 br s	6.26 br s	
Glc	6	1.44 (d, 6.0)	1.40 (d, 6.0)	1.46 (d, 6.3)	1.42 (d, 6.0)	
	1	5.63 (d, 7.1)	5.92 (d, 7.0)	5.93 (d, 7.0)	5.94 (d, 8.0)	
Tig or (2Z)-Hex	2				6.06 (dt, 11.5, 1.4)	
	3	7.11 (q, 7.2)	7.02 (q, 6.0)	6.97 (q, 6.3)	6.14 (dt, 11.5, 7.4)	
	4	1.83 (d, 7.2)	1.60 (d, 6.0)	1.68 (d, 6.3)	2.71 (dq, 1.4, 7.4)	
					2.76 (dq, 1.4, 7.4)	
	5	2.02 s	1.86 s	1.81 s	1.36 (2H, sext, 7.4)	
	6				0.83 (t, 7.4)	
Ac		2.03 s	2.03 s	2.09 s	1.99 s	

a) $\text{C}_5\text{D}_5\text{N}:\text{CD}_3\text{OD}=1:1$. b) 400 MHz.

by a rotating-frame nuclear Overhauser effect spectroscopy (ROESY) experiment. In the HMBC spectrum, H-21 and H₂-28 signals showed long-range correlations with C-1 (δ 168.7) in a tigloyl group and the C-1 (δ 170.9) of an acetyl, respectively. Therefore, the structure of **2** was established as barringtogenol C 21-*O*-tigloyl-28-*O*-acetyl-3-*O*- α -L-rhamonopyranosyl-(1 \rightarrow 2)- β -D-galactopyranosyl-(1 \rightarrow 3)-[β -D-glucopyranosyl-(1 \rightarrow 2)]- β -D-glucuronopyranoside.

Jegosaponin C (**3**) was considered to have the molecular formula, $\text{C}_{61}\text{H}_{96}\text{O}_{27}$, based on a $[\text{M}-\text{H}]^-$ peak at m/z 1259 $[\text{M}-\text{H}]^-$. The NMR spectra suggested that **3** was composed of deacyl jegosaponin (**6**), tiglic acid, and acetic acid as in **1** and **2**. In the HMBC spectrum, long-range correlations were observed between the C-1 (δ 168.2) of a tigloyl unit and δ 5.98 (1H, d, $J=9.6$ Hz) which was assigned to H-22 by a ROESY experiment, and the C-1 (δ 170.8) of an acetyl unit and H₂-28 at δ 4.12 (2H, s). Therefore, the structure of **3** was established as barringtogenol C 22-*O*-tigloyl-28-*O*-acetyl-3-*O*- α -L-rhamonopyranosyl-(1 \rightarrow 2)- β -D-galactopyranosyl-(1 \rightarrow 3)-[β -D-glucopyranosyl-(1 \rightarrow 2)]- β -D-glucuronopyranoside.

Jegosaponin D (**4**) had the molecular formula, $\text{C}_{62}\text{H}_{98}\text{O}_{27}$ (negative FAB-MS, m/z 1273 $[\text{M}-\text{H}]^-$), one methylene greater than **1**—**3**. The ^1H -NMR and ^{13}C -NMR spectra indicated that **4** was composed of deacyl jegosaponin, tiglic acid, and (2Z)-hexenoic acid, which was confirmed by ^1H - ^1H COSY and HMQC. The geometric configuration of the double bond was determined as Z from the $J_{\text{H-H}}$ value (11.5 Hz) and ROESY experiment. A (2Z)-hexenoyl residue has been reported recently in the *Maesa* genus, *M. laxiflora* and *M. japonica*.⁷⁾ ^1H -NMR and ^{13}C -NMR spectral comparisons of **4**

with **2** clearly showed that **4** had acyl units at the C-21 and C-28 positions (Tables 1 and 2). In the HMBC spectrum, long-range correlations were observed between the C-1 of a (2Z)-hexenoyl group at δ 167.0 with H-21 at δ 6.47 and the C-1 of an acetyl group at δ 170.7 with H₂-28 at δ 4.21 and 4.32, respectively. Therefore, **4** was formulated as barringtogenol C 21-*O*-(2Z)-hexenoyl-28-*O*-acetyl-3-*O*- α -L-rhamonopyranosyl-(1 \rightarrow 2)- β -D-galactopyranosyl-(1 \rightarrow 3)-[β -D-glucopyranosyl-(1 \rightarrow 2)]- β -D-glucuronopyranoside.

A 1 mM solution of any of the jegosaponins A—D led to complete suppression of the sensation of sweetness induced by 0.2 M sucrose but did not suppress the sweetness of 0.4 M sucrose. The activity of jegosaponins A—D as half that of gymnemic acids III, IV and VI.⁸⁾

Experimental

Melting points were measured with a Yanagimoto micromelting point apparatus, without correction. Optical rotations were recorded on a JASCO DIP-140 digital polarimeter. IR spectra were measured on a JASCO FT/IR-5300 instrument. NMR spectra were recorded on a Varian UNITY 600 or JEOL GSX-400 spectrometer in $\text{C}_5\text{D}_5\text{N}$ or $\text{C}_5\text{D}_5\text{N}:\text{CD}_3\text{OD}=1:1$ solution using tetramethylsilane (TMS) as an internal standard. NMR experiments included ^1H - ^1H -COSY, HMQC, HMBC, TOCSY (total correlation spectroscopy), and ROESY. Coupling constants (J values) are given in Hertz (Hz). FAB-MS was measured on a JEOL JMS-HX-100 mass spectrometer. Kieselgel 60 (230—400 mesh, Merck) was used for column chromatography, and silica-gel 60F₂₅₄ (Merck) for TLC.

Isolation of Saponins The fresh fruits (1.2 kg) of *Styrax japonica* collected in Tokushima prefecture, Japan, in July 1998, were extracted with 70% EtOH at room temperature for 3 weeks. The ethanolic extract (30 g) was chromatographed on Amberlite XAD-2 with 100% CH_3OH . The CH_3OH elute (20 g) was rapidly subjected to silica gel column chromatography (using increasing concentrations of MeOH in CH_2Cl_2 -MeOH- H_2O as eluent) to give nine fractions (Frs. 1—9). Fr. 5 (8.0 g) was repeatedly sub-

Table 2. ^{13}C -NMR Spectral Data for 1—4 and 5 (δ ppm in $\text{C}_5\text{D}_5\text{N}$, 150 MHz)

		1 ^{a)}	2	3	4	5 ^{b)}
Aglycon	1	39.2	39.0	39.0	38.8	39.2
	2	26.8	26.6	26.7	26.4	28.2
	3	90.3	90.1	89.9	89.8	78.1
	4	40.1	39.8	40.0	39.7	39.4
	5	56.0	55.9	55.9	55.7	55.9
	6	18.9	18.5	18.6	18.4	18.8
	7	33.5	33.3	33.3	33.1	33.3
	8	40.4	40.2	40.3	40.0	40.1
	9	47.2	47.1	47.1	46.9	47.2
	10	37.1	36.9	37.1	36.7	37.3
	11	24.3	24.1	24.2	23.9	23.9
	12	124.7	124.0	124.0	124.0	124.0
	13	142.9	142.9	142.5	142.7	142.9
	14	42.0	41.9	42.0	41.8	42.1
	15	35.0	34.8	35.0	34.7	34.3
	16	68.4	67.9	68.2	67.7	67.9
	17	48.3	47.2	46.5	47.0	47.4
	18	40.4	40.7	41.9	40.6	41.3
	19	47.5	47.5	47.7	47.3	48.3
	20	36.8	36.4	37.0	36.1	36.4
	21	79.7	81.8	76.4	81.1	78.7
	22	74.6	71.4	78.4	70.9	77.3
	23	28.2	28.1	28.2	27.9	28.8
	24	17.1	17.2	17.1	17.0	16.6
	25	16.1	15.8	15.6	15.6	15.9
	26	17.3	16.9	17.3	16.7	17.1
	27	27.9	27.6	27.8	27.4	27.4
	28	63.9	66.7	68.9	66.4	68.4
	29	29.9	29.9	30.4	29.8	30.6
	30	20.6	20.3	19.9	20.1	19.5
Tig or (2Z)-Hex	1	168.1	168.7	168.2	167.0	
	2	129.6	129.9	129.9	121.1	
	3	137.1	136.3	136.3	149.3	
	4	14.7	14.3	14.3	31.2	
	5	12.9	12.6	12.7	22.5	
Ac	6				13.9	
	1	171.1	170.9	170.8	170.7	
	2	21.3	20.9	21.2	20.7	

a) $\text{C}_5\text{D}_5\text{N}$: CD_3OD = 1:1. b) 100 MHz.

jected to HPLC on ODS (70% CH_3OH) to afford jegosaponins A (1, 6.0 g), and B (2, 0.5 g). The residue (70 mg) of Fr. 5 was subjected to preparative HPLC on ODS (70% CH_3OH) to give jegosaponin D (4, 30 mg). Fr. 6 (7.5 g) was subjected to HPLC on ODS (67% CH_3OH) to afford jegosaponins A (1, 6.0 g), and B (2, 0.2 g). The residue (75 mg) of Fr. 6 was further subjected to HPLC on ODS (56% CH_3OH) to afford jegosaponin C (3, 25 mg).

Jegosaponin A (1): Colorless needles, mp 246—248 °C, $[\alpha]_D^{25}$ -24.6° (c = 1.1, MeOH). IR (film) cm^{-1} : 3400 (br), 1730 (br), 1660, 1245, 1160. Negative FAB-MS m/z : 1259 $[\text{M}-\text{H}]^-$. Anal. Calcd for $\text{C}_{61}\text{H}_{96}\text{O}_{27}$: C, 58.08; H, 7.67. Found: C, 58.03; H, 7.70. ^1H -NMR and ^{13}C -NMR: Tables 1—3.

Jegosaponin B (2): Colorless needles, mp 218—220 °C, $[\alpha]_D^{25}$ -8.2° (c = 11.1, MeOH). IR (film) cm^{-1} : 3400 (br), 1730 (br), 1665, 1240, 1160. Negative FAB-MS m/z : 1259 $[\text{M}-\text{H}]^-$. Anal. Calcd for $\text{C}_{61}\text{H}_{96}\text{O}_{27}$: C, 57.26; H, 7.72. Found: C, 57.66; H, 8.02. ^1H -NMR and ^{13}C -NMR: Tables 1—3.

Jegosaponin C (3): Colorless needles, mp 230—232 °C, $[\alpha]_D^{25}$ -26.6° (c = 1.5, MeOH). IR (film) cm^{-1} : 3400 (br), 1730 (br), 1665, 1245, 1165. Negative FAB-MS m/z : 1259 $[\text{M}-\text{H}]^-$. Anal. Calcd for $\text{C}_{61}\text{H}_{96}\text{O}_{27}$: C, 57.26; H, 7.72. Found: C, 57.06; H, 7.96. ^1H -NMR and ^{13}C -NMR: Tables 1—3.

Jegosaponin D (4): Colorless needles, mp 213—215 °C, $[\alpha]_D^{25}$ -12.0° (c = 1.5, MeOH). IR (film) cm^{-1} : 3400 (br), 1735 (br), 1660, 1240, 1160. Negative FAB-MS m/z : 1273 $[\text{M}-\text{H}]^-$. Anal. Calcd for $\text{C}_{62}\text{H}_{98}\text{O}_{27}$: C, 57.57; H, 7.79. Found: C, 58.10; H, 8.09. ^1H -NMR and ^{13}C -NMR: Tables 1—3.

Alkaline Hydrolysis of Jegosaponin A (1) A solution of 1 (40 mg) in MeOH (1.0 ml) was treated dropwise with 28% sodium methoxide (0.3 ml) under N_2 atmosphere. The mixture was stirred for 2 h at room temperature. The reaction mixture was acidified with 1 M HCl, and extracted with CHCl_3 . The CHCl_3 layer afforded acetic acid and tiglic acid confirmed by co-HPLC

Table 3. ^{13}C -NMR Spectral Data of 1—4 (δ ppm in $\text{C}_5\text{D}_5\text{N}$, 150 MHz)

		1 ^{a)}	2	3	4 ^{b)}
GlcA	1	105.8	105.5	105.5	105.4
	2	79.1	79.5	79.5	79.4
	3	81.7	82.6	82.7	82.5
	4	71.9	71.4	71.5	71.2
	5	77.0	77.5	77.7	77.4
	6	172.2	172.4	172.4	172.4
Gal	1	101.2	101.4	101.3	101.3
	2	76.2	76.3	76.4	76.2
	3	76.2	76.1	76.3	76.1
	4	71.6	71.3	71.5	70.9
	5	77.2	77.1	77.2	77.0
	6	62.6	62.2	62.2	61.9
Rha	1	102.3	102.4	102.4	102.4
	2	72.8	72.7	72.8	72.6
	3	72.6	72.7	72.8	72.6
	4	73.9	74.0	74.1	73.9
	5	70.1	69.9	70.0	69.8
	6	18.4	18.3	18.6	18.3
Glc	1	102.8	102.8	102.8	102.6
	2	76.4	76.5	76.5	76.4
	3	78.3	78.2	78.4	78.2
	4	72.8	72.7	72.8	72.6
	5	78.3	78.5	78.6	78.4
	6	63.8	63.7	63.8	63.7

a) $\text{C}_5\text{D}_5\text{N}$: CD_3OD = 1:1. b) 100 MHz.

with an authentic sample. The H_2O layer was passed through an Amberlite XAD-2 column and eluted with MeOH to give prosapogenin (22 mg), which was identified as deacyl jegosaponin (6): Colorless needles, mp 255—257 °C, $[\alpha]_D^{25}$ -20.0° (c = 2.2, MeOH). IR (film) cm^{-1} : 3400 (br), 1730 (br), 1100. $\text{C}_{54}\text{H}_{88}\text{O}_{25}$ (Negative FAB-MS m/z : 1135 $[\text{M}-\text{H}]^-$).

Acid Hydrolysis of Prosapogenin (6) To solution of 6 (15 mg) in MeOH (1.0 ml) was added 5% H_2SO_4 followed by heating at 100 °C for 2 h. The reaction mixture was extracted with EtOAc and the EtOAc layer was purified by HPLC (ODS, 37% CH_3CN) to provide barringtonol C (5, 5.0 mg), mp 266—268 °C, $[\alpha]_D^{25}$ +15.4° (c = 0.5, CHCl_3), $\text{C}_{30}\text{H}_{50}\text{O}_5$ (Negative FAB-MS, m/z 489 $[\text{M}-\text{H}]^-$), which was confirmed by comparison of NMR data (Tables 1 and 2). The aqueous layer was neutralized with Amberlite IRA-35 and evaporated *in vacuo* to dryness. The identification and configuration of the sugar were determined by RI detection (Waters 410) and chiral detection (Shodex OR-1) on HPLC (Shodex RSpak $\text{NH}_2\text{P}-50$ 4D, $\text{CH}_3\text{CN}-\text{H}_2\text{O}-\text{H}_3\text{PO}_4$, 95:5:1, 1 ml/min, 47 °C) by comparison with an authentic sugar (10 mmol D-Gal, D-Glc and L-Rha). The sugar portions gave the following peaks: L-(-)-Rha (t_R 6.40 min), D-(+)-Glc (t_R 20.7 min) and D-(+)-Gal (t_R 24.8 min).

Alkaline Hydrolysis of Jegosaponins B (2)—D (4) A solution of 2—4 (each 5—6 mg) was treated out in the same way as for 1. Each H_2O solution gave deacyl jegosaponin (6), which was confirmed by co-HPLC and co-TLC with an authentic sample.

Bioassay of Antisweet Activity The antisweet activity of 1 mM solutions of 1—4 was tested on three volunteers. Each participant held the test solution in the mouth for 3 min, then spat, rinsed the mouth with distilled water and tasted 0.2 M and 0.4 M sucrose solutions.

References

- 1) a) Yoshikawa K., Ogata H., Arihara S., Chang H.-C., Wang J.-D., *Chem. Pharm. Bull.*, **46**, 1102—1107 (1999); b) Yoshikawa K., Takahashi K., Matsuchika K., Arihara S., Chang H.-C., Wang J.-D., *ibid.*, **47**, 1598—1603 (1999).
- 2) Takahashi H. (ed.), "The Encyclopedia of Trees," Hokuryukan, Tokyo, 1991, pp. 361.
- 3) a) Kitagawa I., Imakura Y., Hayashi T., Yoshioka I., *Chem. Pharm. Bull.*, **22**, 1675—1677 (1974); *idem, ibid.*, **22**, 3009—3010 (1974); b) Kitagawa I., Imakura Y., Hayashi T., Yoshioka I., *ibid.*, **23**, 1520—1531 (1975); c) Kitagawa I., Yoshikawa M., Kobayashi K., Imakura Y., Im K. S., Ikenishi Y., *ibid.*, **28**, 296—300 (1980).
- 4) Barua A. K., Chakrabarti P., *Tetrahedron*, **21**, 381—383 (1965).
- 5) a) Yoshikawa K., Suzuki Y., Tanaka M., Arihara S., Nigam S. K., J.

- Nat. Prod.*, **60**, 1269—1274 (1997); *b*) Yoshikawa K., Satou Y., Tokunaga Y., Tanaka M., Arihara S., Nigam S. K., *ibid.*, **61**, 440—445 (1998).
- 6) Kasai R., Okihara M., Asakawa J., Mizutani K., Tanaka O., *Tetrahedron*, **35**, 1427—1432 (1979).
- 7) *a*) Koike K., Kudo M., Jia Z., Nikaido T., Ide Y., Sakura T., *J. Nat. Prod.*, **62**, 228—232 (1999); *b*) Jiang Z., Gallard J.-F., Adeline M.-T., Dumontet V., Tri M. V., Sévenet T., País M., *ibid.*, **62**, 873—876 (1999).
- 8) Yoshikawa K., Amimoto K., Arihara S., Matsuura K., *Chem. Pharm. Bull.*, **37**, 852—854 (1989).

α,α -gem-Difluorination of α -(Alkylthio)acetophenone Derivatives with *N*-Fluoropyridinium Salts

Sunao TAKEDA,* Yasushi KANEKO, Hiromichi ETO, Minoru TOKIZAWA, Susumu SATO, Kouiti YOSHIDA, Setsuo NAMIKI, and Masaki OGAWA

Central Research Laboratory, SS Pharmaceuticals Co., Ltd., 1143 Nanpeidai, Narita, Chiba 286–8511, Japan.

Received March 21, 2000; accepted April 26, 2000

The α,α -gem-difluorination of 2',4'-difluoro- α -(methylthio)acetophenone (1a) with *N*-fluoropyridinium salts gave 2',4', α,α -tetrafluoro- α -(methylthio)acetophenone (3a). This reaction was accelerated by the addition of zinc chloride, zinc bromide or anhydrous iron(III) chloride, and higher yields than the reaction without additives were obtained. The gem-difluorination reaction using FP-T300 in the presence of zinc bromide was applicable to other α -(alkylthio)acetophenone derivatives (1).

Key words gem-difluorination; *N*-fluoropyridinium; α -(alkylthio)- α,α -difluoroacetophenone; zinc chloride; zinc bromide; iron(III) chloride

The introduction of fluorine atoms into an organic molecule has been widely carried out in the fields of medicinal chemistry, because it causes a dramatic enhancement in biological activity.¹⁾ The change is mainly due to the high electronegativity of the fluorine atom, the strong carbon–fluorine bond and increased lipophilicity.^{1a)} For example, peptides containing difluorostatine or difluorostatone inhibit the hydrolytic action of aspartyl protease renin.²⁾

We have studied a series of antifungal imidazoles³⁾ and triazoles⁴⁾ and found that triazole derivatives containing the $-\text{CF}_2\text{S}(\text{O})_n-$ ($n=0, 1, 2$) moiety had potent antifungal activity against *Candida* and *Aspergillus* species.⁵⁾ These derivatives were synthesized from α -(alkylthio)- α,α -difluoroacetophenones (3).

Although α -(alkylthio)- α,α -difluoroacetophenone analogs have been prepared by the electrolytic fluorination⁶⁾ of α -(phenylthio)acetophenone or oxidative desulfurization–fluorination⁷⁾ of orthothioesters in the literature, the former method is limited to laboratory scale, and the latter lacks wide applicability.

On the other hand, electrophilic fluorinating agents⁸⁾ have been widely used for the introduction of fluorine atoms into an organic compound such as aromatic compounds, 1,3-dicarbonyl compounds, enol silyl ethers and sulfides. However, there are no reports on the α,α -gem-difluorination of α -(alkylthio)acetophenones (1). In this paper, we describe the α,α -gem-difluorination of α -(alkylthio)acetophenone deriva-

Table 1. Physiological and Spectral Data of 1 Derivatives

1	bp (°C/mmHg)	¹ H-NMR (CDCl ₃ , δ)	¹⁹ F-NMR (CDCl ₃ , δ)	IR (cm ⁻¹) (neat)	HR-MS
1a	126/14	2.08 (3H, s), 3.73 (2H, d, $J_{\text{HF}}=2.4$ Hz), 6.86–6.91 (1H, m), 6.97–7.02 (1H, m), 7.98–8.04 (1H, m)	–25.5––25.6 (1F, m), –27.4––27.5 (1F, m)	1677	(M ⁺): Calcd for C ₉ H ₈ F ₂ OS: 202.0264. Found: 202.0249
1b	143/13	1.24 (3H, t, $J=7.3$ Hz), 2.52 (2H, q, $J=7.3$ Hz), 3.78 (2H, d, $J_{\text{HF}}=2.4$ Hz), 6.86–6.91 (1H, m), 6.97–7.01 (1H, m), 7.96–8.02 (1H, m)	–25.5––25.6 (1F, m), –27.4––27.6 (1F, m)	1677	(M ⁺): Calcd for C ₁₀ H ₁₀ F ₂ OS: 216.0420. Found: 216.0427
1c	123/3	0.50–0.54 (2H, m), 0.83–0.88 (2H, m), 1.82–1.88 (1H, m), 3.86 (2H, d, $J_{\text{HF}}=2.4$ Hz), 6.86–6.91 (1H, m), 6.97–7.02 (1H, m), 7.97–8.03 (1H, m)	–25.6––25.7 (1F, m), –27.5––27.6 (1F, m)	1681	(M ⁺): Calcd for C ₁₁ H ₁₀ F ₂ OS: 228.0421. Found: 228.0415
1d	125/5	1.32 (9H, s), 3.88 (2H, d, $J_{\text{HF}}=2.4$ Hz), 6.86–6.91 (1H, m), 6.96–7.01 (1H, m), 7.91–7.97 (1H, m)	–25.7––25.8 (1F, m), –27.9––28.0 (1F, m)	1682	(M ⁺): Calcd for C ₁₂ H ₁₄ F ₂ OS: 244.0734. Found: 244.0752
1e	— ^{a)}	2.37 (1H, br s), 2.73 (2H, t, $J=5.9$ Hz), 3.75 (2H, t, $J=5.9$ Hz), 3.84 (2H, d, $J_{\text{HF}}=2.4$ Hz), 6.87–6.93 (1H, m), 6.98–7.03 (1H, m), 7.98–8.04 (1H, m)	–24.7––24.8 (1F, m), –27.3––27.4 (1F, m)	3423, 1676	(M ⁺ –H ₂ O) ^{b)} : Calcd for C ₁₀ H ₈ F ₂ OS: 214.0264. Found: 214.0258
1f	164/3	2.06 (3H, s), 2.76 (2H, t, $J=6.4$ Hz), 3.84 (2H, d, $J_{\text{HF}}=2.4$ Hz), 4.25 (2H, t, $J=6.4$ Hz), 6.87–6.92 (1H, m), 6.98–7.03 (1H, m), 7.98–8.04 (1H, m)	–24.9––25.0 (1F, m), –27.4––27.5 (1F, m)	1741 1677	(M ⁺): Calcd for C ₁₂ H ₁₂ F ₂ O ₃ S: 274.0476. Found: 274.0470
1g	110/3 ^{b)}	2.14 (3H, s), 3.77 (2H, s), 7.48 (2H, t, $J=7.3$ Hz), 7.58 (1H, dd, $J=7.3, 1.5$ Hz), 7.98 (2H, dd, $J=7.3, 1.5$ Hz)	—	1673	(M ⁺): Calcd for C ₉ H ₁₀ OS: 166.0452. Found: 166.0440
1h	— ^{a)}	2.21 (3H, s), 3.86 (2H, s), 7.43 (1H, dd, $J=8.3, 2.0$ Hz), 7.55 (1H, d, $J=2.0$ Hz), 7.63 (1H, d, $J=8.3$ Hz)	—	1691	(M ⁺): Calcd for C ₉ H ₈ Cl ₂ OS: 233.9673. Found: 233.9669
1i	175/10 ^{c)}	2.14 (3H, s), 3.73 (2H, s), 3.88 (3H, s), 6.95 (2H, d, $J=8.8$ Hz), 7.97 (2H, d, $J=8.8$ Hz)	—	1666	(M ⁺): Calcd for C ₁₀ H ₁₂ O ₃ S: 196.0558. Found: 196.0548
1j	107/5	2.13 (3H, s), 3.77 (2H, s), 7.75 (2H, d, $J=7.8$ Hz), 8.09 (2H, d, $J=7.8$ Hz)	12.6 (3F, s)	1682	(M ⁺): Calcd for C ₁₀ H ₉ F ₃ OS: 234.0326. Found: 234.0350

^{a)} Decomposition was occurred at 210 °C (3 mmHg). ^{b)} lit.⁹⁾ 94–96 °C (0.3 mmHg). ^{c)} lit.¹⁰⁾ 132–136 °C (1 torr). ^{d)} FAB-MS m/z : 233 (MH⁺).

* To whom correspondence should be addressed. e-mail: Sunao.Takeda@ssp.co.jp



FP-T300; R₁ = R₃ = R₅ = CH₃, R₂ = R₄ = H, X = OTf
 FP-T500; R₁ = R₂ = R₃ = R₄ = R₅ = H, X = OTf
 FP-T700; R₁ = R₃ = R₅ = H, R₂ = R₄ = Cl, X = OTf
 MEC-01; R₁ = R₃ = H, R₂ = R₄ = CH₃
 MEC-02; R₁ = R₃ = R₄ = R₅ = H, R₂ = CH₃
 MEC-03; R₁ = R₂ = R₄ = R₅ = H, R₃ = CF₃

Chart 1

tives (**1**) using commercially available *N*-fluoropyridinium salts and the catalytic effect of the additives on this reaction.

Results and Discussion

The α -(alkylthio)acetophenone derivatives (**1**) were prepared from the corresponding phenacyl halides and alkylmercaptans. The hydroxyethyl derivative (**1e**) was acetylated to the acetoxyethyl derivative (**1f**). The physical and spectral data and ¹³C-NMR spectral data of α -(alkylthio)acetophenone derivatives (**1**) are listed in Tables 1 and 2.

The fluorinating reagents (F-reagents) used in this experiment were the FP-T series (FP-T300, FP-T500, FP-T700) and the MEC series (MEC-01, MEC-02, MEC-03) (Chart 1).

Initially, we examined the fluorination of 2',4'-difluoro- α -(methylthio)acetophenone (**1a**) using various F-reagents (Table 3). The reaction with FP-T300 in 1,2-dichloroethane (DCE) at room temperature gave the monofluorinated product, 2',4', α -trifluoro- α -(methylthio)acetophenone (**2**), in good yield (run 1). Whereas that with FP-T300, FP-T500, MEC-01 and MEC-02 in 1,1,2-trichloroethane (TCE) at 105 °C¹¹⁾ afforded a *gem*-difluorinated product, 2',4', α,α -tetrafluoro- α -(methylthio)acetophenone (**3a**), in moderate yield (runs 3, 4, 6, 8, 9). More powerful reagents such as FP-T700 or MEC-03 caused the decomposition of **1a** (run 7) or a low yield of **3a** (run 10), respectively.

The ¹H-, ¹⁹F- and ¹³C-NMR spectra of **2** showed the introduction of one fluorine atom at C α [δ_{H} 6.67 (1H, d, J_{HF} = 49 Hz), δ_{F} -97.2 (1F, d, J_{HF} = 49 Hz) and δ_{C} 95.6 (dd, J_{CF} = 230, 11 Hz)]. The presence of *gem*-difluorine atoms at C α in **3a** was assigned based on the ¹⁹F- [δ_{F} 9.4 (2F, d, J_{FF} = 15 Hz)] and ¹³C-NMR spectra [δ_{C} 123.2 (t, J_{CF} = 289 Hz)] in addition to the absence of a signal due to C α -protons in the ¹H-NMR spectrum.

We next examined the catalytic effect of additives on this difluorination reaction (Table 4). Umemoto and co-workers^{8c)} have reported that zinc chloride or aluminum chloride catalyzes the difluorination of 1,3-dicarbonyl compounds with FP-T300. As a result, we also found that zinc chloride (runs 1, 7), zinc bromide (runs 2, 3, 6, 8) and anhydrous iron(III) chloride (runs 5, 9) were effective catalysts for the difluorination of **1a** with FP-T300 or FP-T500 but not with MEC-01, when higher yields than the reaction without additives were obtained. Other additives (aluminum fluoride, zinc fluoride, zinc iodide, zinc sulfate, tin(IV) chloride, aluminum chloride, boron trifluoride, copper(II) chloride and titanium(IV) chloride) were not fruitful. The best combination of an F-reagent and an additive for the difluorination of **1a** was 3.0 eq of FP-T300 and 0.5 eq of zinc bromide in TCE (run 3).

The combination of FP-T300 and zinc bromide in TCE was applicable to the difluorination reaction of various types of α -(alkylthio)acetophenones (**1b**–**1d**, **1f**–**1j**) (Table 5). Thus, satisfactory results were obtained except in substrates

Table 2. ¹³C-NMR Spectral Data of **1** Derivatives^{a)}

C	1a	1b	1c	1d	1e	1f	1g	1h	1i	1j
ArC=O	190.2 (d, 6)	190.8 (d, 6)	191.5 (d, 3.7)	193.6 (d, 6)	191.2 (d, 6)	190.5 (d, 4)	194.0 (s)	195.3 (s)	192.9 (s)	184.3 (t, 29)
C α	43.6 (d, 7)	41.2 (d, 7)	43.9 (d, 9)	40.1 (d, 7)	41.4 (d, 7)	41.5 (d, 7)	39.0 (s)	42.7 (s)	38.8 (s)	39.0 (s)
C1'	120.4 (d, 11)	120.5 (d, 11)	120.7 (d, 13)	121.1 (d, 13)	120.3 (d, 13)	119.5 (d, 11)	135.1 (s)	132.4 (s)	128.1 (s)	137.8 (s)
C2'	162.4 (dd, 257, 11)	163.3 (dd, 258, 13)	162.4 (dd, 257, 13)	162.3 (dd, 256, 13)	162.9 (dd, 257, 13)	162.5 (dd, 257, 13)	128.7 (s)	135.6 (s)	131.8 (s)	129.1 (s)
C3'	105.5 (t, 26)	104.8 (t, 28)	104.8 (t, 26)	104.8 (t, 28)	104.9 (t, 28)	104.9 (t, 26)	128.6 (s)	130.4 (s)	113.8 (s)	125.7 (d, 4)
C4'	166.1 (dd, 257, 13)	166.1 (dd, 258, 13)	166.0 (dd, 257, 13)	165.9 (dd, 257, 13)	166.2 (dd, 257, 13)	166.2 (dd, 257, 13)	133.3 (s)	137.7 (s)	163.7 (s)	134.5 (q, 31)
C5'	112.5 (dd, 22, 4)	112.5 (dd, 22, 4)	112.4 (dd, 22, 4)	112.4 (dd, 22, 4)	112.6 (dd, 22, 4)	112.6 (dd, 22, 4)	128.6 (s)	127.3 (s)	113.8 (s)	125.7 (d, 4)
C6'	133.4 (dd, 11, 4)	133.4 (dd, 11, 4)	133.3 (dd, 11, 4)	133.3 (dd, 11, 4)	133.4 (dd, 11, 4)	133.4 (dd, 11, 4)	128.7 (s)	131.0 (s)	131.8 (s)	129.1 (s)
C α SC	15.4 (s)	25.8 (s)	12.7 (s)	43.4 (s)	35.2 (s)	30.1 (s)	15.9 (s)	15.7 (s)	15.9 (s)	15.8 (s)
C α SCC	—	14.1 (s)	8.3 (s) × 2	30.8 (s) × 3	60.4 (s)	62.7 (s)	—	—	—	—
OCOCH ₃	—	—	—	—	—	170.8 (s)	—	—	—	—
OCOCH ₃	—	—	—	—	—	20.8 (s)	—	—	—	—
C4'OCH ₃	—	—	—	—	—	—	—	—	55.5 (s)	—
C4'CF ₃	—	—	—	—	—	—	—	—	—	123.5 (q, 274)

a) δ in CDCl₃ (ν_{CF}).

containing acid-sensitive substituents (runs 3 and 4). The physical and spectral data and ^{13}C -NMR spectral data of the gem-difluorinated products (**3**) are listed in Tables 6 and 7.

In summary, the α,α -gem-difluorination of α -(alkylthio) acetophenones (**1**) were found to proceed smoothly by a

combination of FP-T300 and zinc bromide to give the corresponding difluoro derivatives (**3**) in good yields except in the case of compounds with an acid-sensitive function.

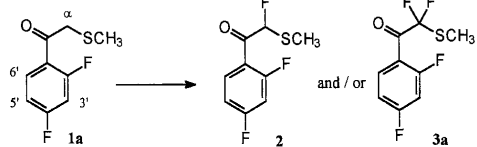
Experimental

IR spectra were measured with a Perkin-Elmer 1600 FT-IR spectrometer. The ^1H - and ^{13}C -NMR spectral data were recorded on a JEOL JNM-EX400 FT-NMR spectrometer in CDCl_3 with tetramethylsilane as the internal standard. The ^{19}F -NMR spectra were measured in CDCl_3 with trifluoroacetic acid as the external standard. The following abbreviations were used: s=singlet, d=doublet, dd=double doublet, t=triplet, q=quartet, m=multiplet, br=broad. FAB-MS or high resolution (HR)-MS were obtained on a JEOL JMS-DX303 or JEOL JMS-AX500 mass spectrometer. TLC was performed on Silica gel 60F₂₅₄ (Merck). Column chromatography was performed on Silica gel 60 (70–230 mesh) (Merck) with hexane–ethyl acetate (10:1) as the eluent. The organic layer was washed with water, brine, dried over magnesium sulfate and evaporated under reduced pressure. The crude product was purified by column chromatography and/or distillation.

Fluorinating Reagent The FP-T series (FP-T300, FP-T500, FP-T700) or the MEC series (MEC-01, MEC-02, MEC-03) was purchased from F-Tech Co., Ltd., or Daikin Industries Co., Ltd., respectively.

Preparation of α -(Methylthio)acetophenones (1a**, **1g**–**1j**): 2',4'-Difluoro- α -(methylthio)acetophenone (**1a**). General Procedure** To a solution of 2',4'-difluorophenacyl chloride (35.00 g, 0.18 mol) in methanol (700 ml) was dropwise added 10% aqueous methylmercaptan sodium salt (151 ml,

Table 3. Fluorination of **1a** with F-Reagents under Various Conditions



Run	F-reagent ^(a)	Solvent	Conditions	Results (yield, %)
1	FP-T300	DCE	r.t., 12 h	2 (91.7)
2	FP-T300	DCE	refl., 3.0 h	2 (17.0) + 3a (31.5)
3	FP-T300	TCE	105 °C, 3.0 h	3a (47.6)
4	FP-T300	AcOBu	105 °C, 4.0 h	3a (42.8)
5	FP-T300	Toluene	105 °C, 4.0 h	Decomposition
6	FP-T500	TCE	105 °C, 1.0 h	3a (47.6)
7	FP-T700	TCE	105 °C, 0.5 h	Decomposition
8	MEC-01	TCE	105 °C, 1.5 h	3a (56.7)
9	MEC-02	TCE	105 °C, 0.5 h	3a (50.7)
10	MEC-03	TCE	105 °C, 5 min	3a (11.9)

a) Three molecular equivalents of an F-reagent were used.

Table 4. Difluorination of **1a** with F-Reagents in the Presence of Additives at 105 °C

Run	F-reagent ^(a)	Solvent	Additive (eq)	Time (h)	Results (yield of 3a , %)
1	FP-T300	TCE	ZnCl ₂ (0.5)	2.5	72.2
2	FP-T300	TCE	ZnBr ₂ (0.2)	2.5	72.8
3	FP-T300	TCE	ZnBr ₂ (0.5)	2.5	82.2
4	FP-T300	TCE	ZnBr ₂ (0.8)	0.5	Decomposition
5	FP-T300	TCE	FeCl ₃ (0.5)	2.5	79.9
6	FP-T300	AcOBu	ZnBr ₂ (0.5)	2.5	62.6
7	FP-T500	TCE	ZnCl ₂ (0.5)	1.0	63.5
8	FP-T500	TCE	ZnBr ₂ (0.5)	1.0	65.2
9	FP-T500	TCE	FeCl ₃ (0.5)	1.0	72.8
10	MEC-01	TCE	ZnBr ₂ (0.5)	1.0	58.1
11	MEC-01	TCE	FeCl ₃ (0.5)	1.0	41.6

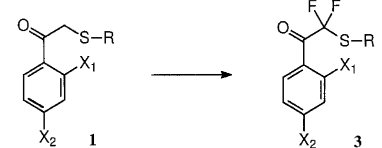
a) Three molecular equivalents of an F-reagent were used.

Table 6. Physiological and Spectral Data of **2** and **3** Derivatives

2 or 3	bp (°C/mmHg)	^1H -NMR (CDCl_3 , δ)	^{19}F -NMR (CDCl_3 , δ)	IR (cm^{-1}) (neat)	HR-MS
2	115/4	2.09 (3H, s), 6.67 (1H, d, $J_{\text{HF}}=49$ Hz), 6.88–6.93 (1H, m), 7.01–7.06 (1H, m), 8.04–8.10 (1H, m)	–23.7––23.8 (1F, m), –25.2––25.3 (1F, m), –97.2 (1F, d, $J_{\text{HF}}=49$ Hz)	1698	(M^+): Calcd for $\text{C}_9\text{H}_6\text{F}_2\text{OS}$: 220.0170. Found: 220.0174
3a	96/5	2.35 (3H, s), 6.91–7.02 (2H, m), 7.95–8.01 (1H, m)	–9.4 (2F, d, $J_{\text{FF}}=15$ Hz), –23.0––23.1 (1F, m), –26.0––26.1 (1F, m)	1713	(M^+): Calcd for $\text{C}_9\text{H}_6\text{F}_4\text{OS}$: 238.0076. Found: 238.0079
3b	105/7	1.37 (3H, t, $J=7.8$ Hz), 2.92 (2H, q, $J=7.8$ Hz), 6.90–7.02 (2H, m), 7.95–8.01 (1H, m)	–6.4 (2F, d, $J_{\text{FF}}=14$ Hz), –23.0––23.1 (1F, m), –26.1––26.2 (1F, m)	1714	(M^+): Calcd for $\text{C}_{10}\text{H}_8\text{F}_4\text{OS}$: 252.0232. Found: 252.0229
3c	115/4	0.71–0.75 (2H, m), 0.99–1.04 (2H, m), 2.06–2.10 (1H, m), 6.91–7.02 (2H, m), 7.96–8.02 (1H, m)	–7.5 (2F, d, $J_{\text{FF}}=12$ Hz), –23.0––23.1 (1F, m), –26.0––26.1 (1F, m)	1713	(M^+): Calcd for $\text{C}_{11}\text{H}_8\text{F}_4\text{OS}$: 264.0232. Found: 264.0206
3f	151/3	2.07 (3H, s), 3.14 (2H, t, $J=6.4$ Hz), 4.31 (2H, t, $J=6.4$ Hz), 6.92–7.03 (2H, m), 7.94–7.99 (1H, m)	–5.4 (2F, d, $J_{\text{FF}}=15$ Hz), –22.4––22.5 (1F, m), –25.5––25.6 (1F, m)	1744, 1712	($\text{M}^+ - \text{AcOH}$) ^b : Calcd for $\text{C}_{10}\text{H}_6\text{F}_4\text{OS}$: 250.0076. Found: 250.0032
3g	87/4	2.36 (3H, s), 7.50 (2H, t, $J=7.8$ Hz), 7.65 (1H, dd, $J=7.8$, 1.5 Hz), 8.14 (2H, dd, $J=7.8$, 1.5 Hz)	–3.3 (2F, s)	1703	(M^+): Calcd for $\text{C}_9\text{H}_6\text{F}_2\text{OS}$: 202.0264. Found: 202.0256
3h	— ^a	2.35 (3H, s), 7.34 (1H, dd, $J=8.3$, 2.0 Hz), 7.53 (1H, d, $J=2.0$ Hz), 7.69 (1H, d, $J=8.3$ Hz)	–10.1 (2F, s)	1723	(M^+): Calcd for $\text{C}_9\text{H}_6\text{Cl}_2\text{F}_2\text{OS}$: 269.9485. Found: 269.9459
3i	140/4	2.36 (3H, s), 3.90 (3H, s), 6.97 (2H, d, $J=8.8$ Hz), 8.14 (2H, d, $J=8.8$ Hz)	–5.2 (2F, s)	1692	(M^+): Calcd for $\text{C}_{10}\text{H}_{10}\text{F}_2\text{O}_2\text{S}$: 232.0369. Found: 232.0359
3j	91/5	2.38 (3H, s), 7.77 (2H, d, $J=8.3$ Hz), 8.25 (2H, d, $J=8.3$ Hz)	12.3 (3F, s), –6.8 (2F, s)	1714	(M^+): Calcd for $\text{C}_{10}\text{H}_7\text{F}_3\text{OS}$: 270.0138. Found: 270.0093

a) Decomposition was occurred at 210 °C/3 mmHg. b) FAB-MS m/z : 311 (MH^+).

Table 5. Difluorination of **1** Derivatives with a Combination of FP-T300 (3.0 eq) and ZnBr₂ (0.5 eq) in TCE at 105 °C



Run	1	X ₁	X ₂	R	Time (h)	Product (3) (yield, %)
1	1b	F	F	CH_2CH_3	2.0	3b (84.3)
2	1c	F	F	Cyclopropyl	2.5	3c (72.3)
3	1d	F	F	<i>tert</i> -Butyl	0.5	Decomposition
4	1f	F	F	$(\text{CH}_2)_2\text{OAc}$	3.0	3f (45.4)
5	1g	H	H	CH_3	1.5	3g (75.9)
6	1h	Cl	Cl	CH_3	1.0	3h (72.3)
7	1i	H	OCH_3	CH_3	1.5	3i (63.9)
8	1j	H	CF_3	CH_3	2.0	3j (60.1)

Table 7. ^{13}C -NMR Spectral Data of **2** and **3** Derivatives^{a)}

C	2	3a	3b	3c	3f	3g	3h	3i	3j
ArC=O	185.5 (dd, 24, 6)	182.6 (t, 31)	183.0 (t, 31)	183.2 (t, 31)	182.8 (t, 31)	185.2 (t, 29)	185.5 (t, 31)	183.7 (t, 28)	184.3 (t, 29)
C α	95.6 (dd, 230, 11)	123.2 (t, 289)	123.6 (t, 291)	123.7 (t, 289)	123.6 (t, 291)	124.4 (t, 289)	122.9 (t, 290)	124.7 (t, 287)	124.0 (t, 287)
C1'	118.6 (d, 11)	117.4 (d, 11)	117.6 (d, 13)	117.6 (d, 11)	117.3 (d, 11)	131.0 (s)	127.7 (s)	123.1 (s)	133.8 (s)
C2'	162.2 (dd, 257, 13)	162.7 (dd, 265, 13)	162.9 (dd, 265, 13)	162.9 (dd, 265, 13)	162.9 (dd, 265, 13)	130.5 (s)	134.5 (s)	133.1 (s)	130.8 (s)
C3'	105.0 (t, 28)	105.5 (t, 26)	105.6 (t, 26)	105.6 (t, 26)	105.6 (t, 26)	128.7 (s)	130.6 (s)	114.0 (s)	125.7 (d, 4)
C4'	166.6 (dd, 259, 13)	166.3 (dd, 259, 13)	166.4 (dd, 259, 13)	166.4 (dd, 259, 13)	166.6 (dd, 259, 13)	134.7 (s)	138.8 (s)	164.8 (s)	135.7 (q, 33)
C5'	113.0 (dd, 22, 4)	111.8 (dd, 22, 4)	111.9 (dd, 22, 4)	111.9 (dd, 22, 4)	112.1 (dd, 4)	128.7 (s)	126.9 (s)	114.0 (s)	125.7 (d, 4)
C6'	133.3 (dd, 9, 4)	133.4 (dd, 11, 4)	133.6 (dd, 11, 4)	133.5 (dd, 11, 4)	133.6 (dd, 11, 4)	130.5 (s)	131.0 (s)	133.1 (s)	130.8 (s)
C α SC	10.9 (s)	10.8 (s)	27.4 (s)	8.6 (s)	27.4 (s)	27.4 (s)	11.2 (s)	10.8 (s)	10.9 (s)
C α SCC	—	—	15.0 (s)	7.6 (s) $\times 2$	63.0 (s)	—	—	—	—
OCOCH ₃	—	—	—	—	170.6 (s)	—	—	—	—
OCOCH ₃	—	—	—	—	20.8 (s)	—	—	—	—
C4'OCH ₃	—	—	—	—	—	—	—	55.6 (s)	—
C4'CF ₃	—	—	—	—	—	—	—	—	123.3 (q, 274)

a) δ in CDCl_3 (ν_{CF}).

0.22 mol) at 0 °C. The mixture was stirred at room temperature for 1.0 h and evaporated under reduced pressure. The residue was poured into water and extracted with chloroform. Distillation gave **1a** as a pale yellow oil (23.90 g, 64.4%).

Preparation of α -(Alkylthio)acetophenones (1b—1e): 2',4'-Difluoro- α -(ethylthio)acetophenone (1b). General Procedure Potassium carbonate (3.92 g, 28.4 mmol) was added to a solution of 2',4'-difluorophenacyl chloride (4.50 g, 23.6 mmol) and ethylmercaptan (1.61 g, 25.9 mmol) in methanol (48 ml) at 0 °C. The mixture was stirred at room temperature for 2.0 h. After filtration, most of the solvent was removed under reduced pressure. The residue was poured into water and extracted with chloroform. Distillation gave **1b** as a pale yellow oil (4.53 g, 88.6%).

α -(β' -Acetoxyethylthio)-2',4'-difluoroacetophenone (1f) Acetic anhydride (0.60 g, 5.9 mmol) was added to a solution of 2',4'-difluoro-2-[(2-hydroxyethyl)thio]acetophenone (**1e**) (1.14 g, 4.9 mmol) in pyridine (10 ml). The mixture was stirred at 50 °C for 3.0 h. The reaction mixture was evaporated under reduced pressure. The residue was poured into water and extracted with ether. Distillation gave **1f** as a pale yellow oil (1.31 g, 97.0%).

2',4', α -Trifluoro- α -(methylthio)acetophenone (2): The Monofluorination of 1a with FP-T300 A solution of **1a** (3.00 g, 14.8 mmol) in DCE (10 ml) was dropwise added to a suspension of FP-T300 (12.80 g, 44.3 mmol) in DCE (100 ml) at room temperature for 10 min. The mixture was stirred at room temperature for 12 h. Column chromatography and distillation gave **2** as a pale yellow oil (3.00 g, 91.7%).

2',4', α , α -Tetrafluoro- α -(methylthio)acetophenone (3a): The gem-Difluorination of 1a with Fluorinating Reagent in the Presence of Zinc Bromide. General Procedure A solution of **1a** (3.00 g, 14.8 mmol) in TCE (10 ml) was dropwise added to a suspension of FP-T300 (12.80 g, 44.3 mmol) and zinc bromide (1.67 g, 7.4 mmol) in TCE (100 ml) at 80 °C¹²⁾ for 10 min. The mixture was stirred at 105 °C for 2.5 h. Column chromatography and distillation gave **3a** as a pale yellow oil (2.90 g, 82.2%).

References and Notes

- a) Kumadaki I., Yuki Gousei Kagaku Kyoukaishi, **42**, 788—793 (1984); b) Filler R., Kobayashi Y., Yagpolskii L. M. (ed.), "Organofluorine Compounds in Medicinal Chemistry and Biomedical Applications," Elsevier, Amsterdam, 1993; c) Banks R. E., Smart B. E., Tatlow J. C. (ed.), "Organofluorine Chemistry, Principles and Commercial Applications," Plenum Press, New York, 1994; d) Hudlicky M., Pavlath A. E. (ed.), "Chemistry of Organic Fluorine Compounds II, A Critical Review," American Chemical Society, Washington, DC, 1995.
- Thaisrivongs S., Pals D. T., Kati W. M., Turner S. R., Thomasco L. M., Watt W., *J. Med. Chem.*, **29**, 2080—2087 (1986).
- Ogawa M., Matsuda H., Eto H., Asaoka T., Kuraishi T., Iwasa A., Nakashima T., Yamaguchi K., *Chem. Pharm. Bull.*, **39**, 2301—2307 (1991).
- a) Japan. Kokai Tokkyo Koho JP 3-223266, 1991 [*Chem. Abstr.*, **115**, 136106q (1991)]; b) Matsumoto M., Asaoka T., Iwasa A., Ikada Y., Yamamoto K., Hirayama F., Abstracts of Papers, The 36th Interscience Conference on Antimicrobial Agents and Chemotherapy, New Orleans, Sep. 1996, pp. 113.
- The report on the antifungal activity of these derivatives is being written now; a) Japan. Kokai Tokkyo Koho JP 9-227531 (1997) [*Chem. Abstr.*, **127**, 121738 (1998)]; b) *ibid.*, JP 10-67757 (1998) [*Chem. Abstr.*, **128**, 88920 (1999)]; c) *ibid.*, JP 11-240871 (1999) [*Chem. Abstr.*, **131**, 73657 (1999)]; d) *ibid.*, JP 11-279160 (1999) [*Chem. Abstr.*, **131**, 129997 (1999)].
- Brigaud T., Laurent E., *Tetrahedron Lett.*, **31**, 2287—2290 (1990).
- Furuta S., Kuroboshi M., Hiyama T., *Bull. Chem. Soc. Jpn.*, **71**, 1939—1951 (1998).
- a) Lal G. S., Pez G. P., Syvret R. G., *Chem. Rev.*, **96**, 1737—1755 (1996); b) Umemoto T., Tomizawa G., *Bull. Chem. Soc. Jpn.*, **59**, 3625—3629 (1986); c) Umemoto T., Fukami S., Tomizawa G., Harasawa K., Kawada K., Tomita K., *J. Am. Chem. Soc.*, **112**, 8563—8575 (1990); d) Umemoto T., Tomizawa G., *J. Org. Chem.*, **60**, 6563—6570 (1995).
- Prelog V., Hahm V., Brauchli H., Beyerman H. C., *Helv. Chim. Acta*, **27**, 1209—1224 (1944).
- Kano S., Yokomatsu T., Ono T., Hibino S., Shibuya S., *Synthesis*, **1978**, 305—307.
- Difluorination of α -(alkylthio)acetophenones (**1**) with F-reagent in TCE at reflux condition occurred vigorously.
- The internal temperature of the reaction mixture rose to ca. 100 °C.

Geranylgeranyl Diphosphate Synthases from *Scoparia dulcis* and *Croton sublyratus*. cDNA Cloning, Functional Expression, and Conversion to a Farnesyl Diphosphate Synthase

Naoe KOJIMA,^a Worapan SITTHITHAWORN,^a
Ekapop VIROONCHATAPAN,^a Dae-Yeon SUH,^a
Naoko IWANAMI,^a Toshimitsu HAYASHI,^a and
Ushio SANKAWA^{*,a,b}

Faculty of Pharmaceutical Sciences, Toyama Medical and
Pharmaceutical University,^a 2630 Sugitani, Toyama 930-0194,
Japan and International Traditional Medicine Research Center,
Toyama International Health Complex,^b Toyama 939-8224, Japan.
Received March 31, 2000; accepted May 9, 2000

cDNAs encoding geranylgeranyl diphosphate synthase (GGPPS) of two diterpene producing plants, *Scoparia dulcis* and *Croton sublyratus*, were isolated using the homology-based polymerase chain reaction method. Both cloned genes showed high amino acid sequence homology (60–70%) to other plant GGPPSs and contained highly conserved aspartate-rich motifs. The obtained clones were functionally expressed in *Escherichia coli* and showed sufficient GGPPS activity to catalyze the condensation of farnesyl diphosphate (FPP) and isopentenyl diphosphate to form geranylgeranyl diphosphate. To investigate the factor determining the product chain length of plant GGPPSs, *S. dulcis* GGPPS mutants in which either the small amino acids at the fourth and fifth positions before the first aspartate-rich motif (FARM) were replaced with aromatic amino acids or in which two additional amino acids in FARM were deleted were constructed. Both mutants behaved like FPPS-like enzymes and almost exclusively produced FPP when dimethylallyl diphosphate was used as a primer substrate, and failed to accept FPP as a primer substrate. These results indicate that both small amino acids at the fourth and fifth positions before FARM and the amino acid insertion in FARM play essential roles in product length determination in plant GGPPSs.

Key words geranylgeranyl diphosphate synthase; farnesyl diphosphate synthase; cDNA cloning; site-directed mutagenesis

Geranylgeranyl diphosphate synthase (GGPPS) supplies the essential acyclic precursor geranylgeranyl diphosphate (GGPP) for the biosynthesis of structurally diverse group of compounds including diterpenes. To date, cDNAs encoding GGPPS have been cloned from various organisms ranging from bacteria to higher eukaryotes. Comparison of the amino acid sequences has revealed that GGPPSs known to date contain five distinct regions with highly similar amino acid levels.¹⁾ Taking advantage of this similarity, a homology-based polymerase chain reaction (PCR) method was applied to obtain GGPPS cDNAs from two different diterpene-producing plants, *Scoparia dulcis* L. (Scrophulariaceae) and *Croton sublyratus* KURZ (Euphorbiaceae). *S. dulcis* is the source of unique tetracyclic diterpenes, scopadulcic acids A and B and scopadulciol,²⁾ whereas *C. sublyratus* accumulates a long-chain diterpene plaunotol³⁾ together with kaurene- and clerodane-type diterpenes.⁴⁾

To clone the genes, degenerate oligonucleotide primers were designed according to the regions in which amino acids

are highly conserved among the known plant GGPPSs. Nested PCR with the same sets of primers successfully amplified the core fragments of GGPPS cDNAs from *S. dulcis* and *C. sublyratus*. Specific amplification of each clone using the rapid amplification of the cDNA end (RACE) method⁵⁾ was carried out to obtain the 5' and 3' termini of the cDNA. The open reading frames (ORFs) of the GGPPS genes from *S. dulcis* and *C. sublyratus* encode proteins of 368 and 351 amino acid residues, respectively. The two clones exhibit 70% amino acid identity to each other. Sequence comparison with other GGPPSs from *Arabidopsis thaliana* L., *Capsicum annuum* L., *Catharanthus roseus* G. DON, and *Sinapis alba* L. revealed a high level of similarity (60–70%) throughout the entire coding regions (Fig. 1). The cloned sequences also contain two conserved aspartate-rich motifs that have been reported to be important in substrate binding and catalysis.^{6,7)} Analysis of the amino acid sequences suggests that the amino terminal parts of GGPPSs cloned from *S. dulcis* and *C. sublyratus* likely encode a transit peptide for chloroplast import. The 50–60 amino terminal residues of the two clones exhibit a low degree of similarity, yet they share common features of plastidial transit peptides in that they are rich in serine, threonine, and small hydrophobic residues but contain few acidic residues.⁸⁾ Previous study of the production of diterpenes in leaf organ cultures of *S. dulcis* revealed that the concentration of diterpenes increased parallel to the differentiation of green leaves.⁹⁾ Furthermore, the labeling pattern of [^{1-¹³C}] glucose incorporated into the diterpenes in shoot cultures¹⁰⁾ demonstrated that they are biosynthesized via a mevalonate-independent pathway that has been shown to function in chloroplast.¹¹⁾ In *C. sublyratus*, an electron microscope study showed that the main diterpene plaunotol accumulated in the leaf.¹²⁾ These data suggest that the biosynthesis of these diterpenes is catalyzed by enzymes present in chloroplasts. As the cloned GGPPSs bear transit peptides for chloroplast imports, they are likely to be involved in the biosyntheses of these diterpenes in chloroplasts.

To confirm that the obtained clones encode GGPPSs, the ORFs were first PCR-amplified with gene-specific 5'- and 3'-flanking primers and subcloned into the *Escherichia coli* expression vector pET32a(+) (Novagen) to give pET-SDG-GPPS and pET-CSGGPPS for the *S. dulcis* and *C. sublyratus* GGPPSs, respectively. The plasmids were then transformed into *E. coli* AD494 (DE3)pLysS cells (Novagen). After isopropyl- β -D-thiogalactopyranoside (IPTG) induction, the crude protein extracts containing heterologously expressed thioredoxin-fusion GGPPS were used to test for enzyme activity according to the method described by Ogura *et al.*¹³⁾ Both pET-SDGGPPS and pET-CSGGPPS transformants exhibited sufficient GGPPS activity to catalyze the condensation of farnesyl diphosphate (FPP) and isopentenyl diphosphate (IPP) to form GGPP, whereas control *E. coli* failed to produce GGPP in noticeable amounts. Specific activities of *S. dulcis* and *C. sublyratus* GGPPSs determined from the radioactivity of GGPP were 71 and 66 pmol/h/mg, respectively, indicating that the obtained clones were catalytically active genes encoding GGPPSs.

Interestingly, in spite of higher amino acid sequence homology, the expression level of pET-SDGGPPS in *E. coli* was apparently higher than that of pET-CSGGPPS judging

* To whom correspondence should be addressed. e-mail: sankawa@toyama-pref-ihc.or.jp

Ara	1MA-SVT-EGSWIVVHHNNHHPSSILTKSRSRSCPITLT-KPTISFRSKRTVSSSSSIVSSSVVTKEDNLR	67
Cap	1M-RMNLVDLWAQOACLVFNOTLSY--KSFNGFMKIPLKNSKINPKLNKRPFSPLTVSAIAT-TKEDERI	66
Cat	1M-RS-N-L-C----HPLKNOLPISFFLSGTIRKPIFSCSRLSIAITK-EOTEESE-SKSK--KEVA-	57
Sin	1MASVTPLGSWV-LL--HHHPSTILTQSRSRSPSLITLKPISLTPKRTVSSSS--SS-LITKEDNN	62
Sco	1M--SLVNPVSTWPNTRSSVFRPKPAINTTHTLPISFLFAGKPI-----SA-VL-----TKEYSH	52
Cro	1M-SVNV-EGSWVHTSSVISQATRSRKSCKPLSFSVSIPLFYRNSKRSVSVVSAIVTKDEETIQEEQNKN	68
Ara	680SEPPSFDMSYII-T--ELVYALDSNPRLREPKHEAHSILAGGRVRVITLACELVGGES	135
Cap	67EAAOTEENFKIYVTEAISTYALDEITVKEPHVHEAHSILAGGRVRVITLACELVGGES	136
Cat	58F--SSSSSDFKAYMIGANSYKALDEAVLYREPHEAHSILAGGRVRVITLACELVGGES	125
Sin	63LK--SSSSSDFMSYIINADSYKALDSNPRLREPKHEAHSILAGGRVRVITLACELVGGES	131
Sco	530T---SSTDFKKYMLEASSYKALDSNPKEPKHEAHSILAGGRVRVITLACELVGGES	119
Cro	69--SSSSLGDFKSYMVQASATKALDEANSLREPKHEAHSILAGGRVRVITLACELVGGES	136
Ara	136TAMPARCAVEMHTMSLIHDDLPCMDNDLRRGKPTNHKVEGEDVAVLAGDALLSESEHLASATSSDV	205
Cap	137NAMAACAVEMHTMSLIHDDLPCMDNDLRRGKPTNHKVEGEDVAVLAGDALLAFEFHIVNSTAG-V-	204
Cat	126VAMPSCAVEMHTMSLIHDDLPCMDNDLRRGKPTNHKVEGEDVAVLAGDALLAFEFHIATATKG-VS	194
Sin	132LAMPARCAVEMHTMSLIHDDLPCMDNDLRRGKPTNHKVEGEDVAVLAGDALLSEFEHLASATSEV-	200
Sco	120TAMPAACTEMHTMSLIHDDLPCMDNDLRRGKPTNHKVEGEDVAVLAGDALLAYSEFLATATEG-VL	188
Cro	137MAMPAACTEMHTMSLIHDDLPCMDNDLRRGKPTNHKVEGENAVLAGDALLAFEFHIAVSTLN-V-	204
Ara	206SPVNVVRAVGEARAGTEGLVAGOVVDSSEGLDNDVGLHKEFTHLHKTALLPASAVALGAVGGGS	275
Cap	205TPSIVGAVALEASTGTEGLVAGOVVDSSEGLDNDVGLHKEFTHVHKTALLLESSVVLGALLGGT	272
Cat	195SE--NINRVVGEARAGTEGLVAGOVVDSSEGLDNDVGLHKEFTHLHKTALLLEGSVVLGAVGGAN	261
Sin	201SPVNVVRAVGEARAGTEGLVAGOVVDSSEGLDNDVGLHKEFTHLHKTALLPASAVALGAVGGGS	270
Sco	189PE--NINRVVGEARAGTEGLVAGOVVDSSEGLDNDVGLHKEFTHLHKTALLLEGSVVLGALLGGN	255
Cro	205SPVNVVRAVGEARAGTEGLVAGOVVDSSEGLDNDVGLHKEFTHLHKTALLLEGSVVLGALLGGT	272
Ara	276DEEIERLRKFARIGLLFOVVDILDVTKSSQELGKTAGKDLIADKLTYPKIMGLEKSRFEAEKLNREAR	345
Cap	273NVEVEKLRKFARIGLLFOVVDILDVTKSSQELGKTAGKDLVADKLTYPKLLGLEKAEKLNREAR	342
Cat	262DEOTSRLKFARIGLLFOVVDILDVTKSSQELGKTAGKDLVADKLTYPKLLGLEKAEKLNREAR	331
Sin	271DEEIERLRKFARIGLLFOVVDILDVTKSSQELGKTAGKDLIADKLTYPKIMGLEKSRFEAEKLNREAR	340
Sco	256DEEVEKLRKFARIGLLFOVVDILDVTKSSQELGKTAGKDLVADKLTYPKLLGLEKAEKLNREAR	325
Cro	273DEEVEKLRKFARIGLLFOVVDILDVTKSSQELGKTAGKDLVADKLTYPKIMGLEKSRFEAEKLNREAR	342
Ara	346DILLGFDSDNVAPLLALANYIAYRN	371
Cap	343DILLGFDSDNVAPLLALANYIAYRN	368
Cat	332DILLGFDSDNVAPLLALANYIAYRN	357
Sin	341DILLGFDSDNVAPLLALANYIAYRN	366
Sco	326DILLGFDSDNVAPLLALANYIAYRN	351
Cro	343DILLGFDSDNVAPLLALANYIAYRN	368

Fig. 1. Alignment of Amino Acid Sequences of GGPP Synthases from Plant Origin

The plants from which GGPP synthases were obtained are indicated in the left column. Abbreviations and Genbank Accession Nos. are: Ara, *Arabidopsis thaliana*, Z99708; Cap, *Capsicum annuum*, X80267; Cat, *Catharanthus roseus*, X92893; Sin, *Sinapis alba*, X98795; and two plants from this work Sco, *Scoparia dulcis*, AB034250; and Cro, *Croton sublyratus*, AB034249. Putative transit peptides are underlined. The broken lines indicate the first and second aspartate-rich motifs (FARM, Asp139-Asp145 in *S. dulcis* and SARM, Asp277-Asp281). Identical amino acid residues are boxed in black and similar residues are shaded in gray. Gaps are inserted to maximize homology.

from SDS-PAGE analysis of the crude extracts (data not shown). Earlier expression studies with *Taxus canadensis* GGPPS in yeasts¹⁴ and spearmint limonene synthase in *E. coli*¹⁵ demonstrated that a higher level of heterologous expression could be achieved upon removal of the transit sequences at the 5'-ends. In line with these studies, GGPPSs from *S. dulcis* and *C. sublyratus* were also expressed as 5'-truncated proteins.

Due to the lack of consensus sequence, the exact locations of the cleavage sites for chloroplast transit peptides could not be determined. Nonetheless, sequence alignment with other plant GGPPSs (Fig. 1) suggested putative cleavage sites to be located in the vicinity of Phe-58 and Phe-75 of *S. dulcis* GGPPS and *C. sublyratus* GGPPS, respectively.^{8,14} Each truncated GGPPS was functionally expressed in *E. coli* by the same methods used for intact proteins. SDS-PAGE analysis showed prominent bands corresponding to the truncated *S. dulcis* GGPPS and truncated *C. sublyratus* GGPPS. As expected, the truncated proteins exhibited sufficient GGPPS activity to catalyze the formation of GGPP with FPP and IPP as substrates. Specific activities of truncated *S. dulcis* and *C. sublyratus* GGPPSs determined from the radioactivity of GGPP were 79 and 74 pmol/h/mg, respectively. The results suggested that for *S. dulcis* GGPPS and *C. sublyratus* GGPPS, the putative signal peptides at the amino terminal regions are not essential for the enzyme activity.

Farnesyl diphosphate synthase (FPPS) is a prenyl enzyme producing FPP (C_{15}) which is one isoprene unit shorter than GGPP (C_{20}). It has been shown that amino acids in the region

around the first aspartate-rich motif (DDXX(X)D, FARM) plays an essential role in determining the product specificity of all FPPSs.¹⁶ Comparison of amino acids around the FARMS of FPPSs and GGPPSs of plant origin revealed two different points. First, amino acids situated at the fourth and fifth positions before FARM in FPPSs are aromatic amino acids, whereas the corresponding residues are non-aromatic amino acids in GGPPSs. Second, FPPSs do not contain any amino acid insertion in FARM, yet GGPPSs contain two additional amino acids. To make mutants producing FPP instead of GGPP as a major product, three GGPPS mutants, mutant YF, mutant PC, and mutant YP, were constructed by site-directed mutagenesis. Due to its higher enzyme activity, *S. dulcis* GGPPS was chosen for this mutagenesis study.

In the mutant YF, the small amino acids Met and Ser were replaced with the aromatic amino acids Tyr and Phe. The mutant PC was also constructed by deleting the two additional amino acids Pro and Cys in FARM. Combination of these two mutants gave the mutant YP. Thus the mutant YP had aromatic amino acids at the fourth and fifth positions before FARM and did not have any amino acid insertion in FARM (Fig. 2A). With dimethylallyl diphosphate (DMAPP) and isopentenyl diphosphate (IPP) as substrates, all these GGPPS mutants produced FPP as the major product along with small amounts of geranyl diphosphate (GPP) (Fig. 2B). On the other hand, the mutants were not able to utilize FPP and therefore no major prenyl compounds could be detected when FPP was used as a primer substrate (Fig. 2C). The radioactivities of GPP, FPP, and GGPP in the reaction of the

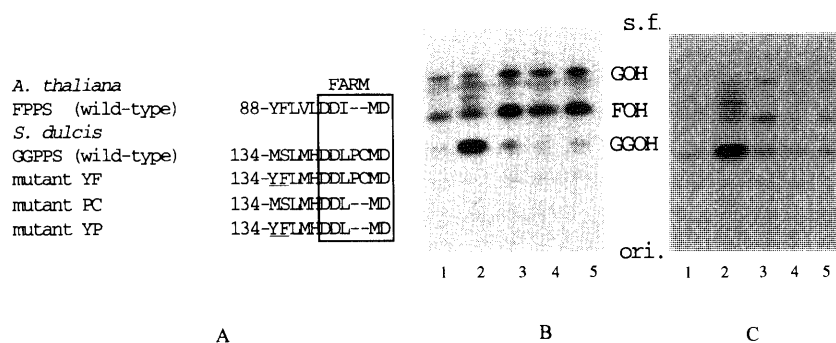


Fig. 2. Amino Acid Sequences around FARMs of Wild-Type and Mutant *S. dulcis* GGPPSs and *A. thaliana* FPPS

Mutated amino acid residues are underlined and FARMs are boxed (A). TLC radiochromatograms of the alcohols obtained by enzymatic hydrolysis of the products produced by the GGPPS mutants. The enzyme activities of the mutants were measured with [$1\text{-}^{14}\text{C}$]IPP and either DMAPP (B) or FPP (C) as the primer substrate and the reaction products were analyzed by reversed-phase LKC-18 TLC. Lane 1, untransformed pET vector; lane 2, wild-type GGPPS; lane 3, mutant YF; lane 4, mutant PC; lane 5, mutant YP. Spots of authentic alcohols: GOH, geraniol; FOH, (all-*E*)-farnesol; GGOH, (all-*E*)-geranylgeraniol. ori., origin; s.f., solvent front.

Table 1. Relative Activity of the Mutated GGPPS to Wild-Type GGPPS Determined from Radioactivities of GPP, FPP, and GGPP

Enzyme	Relative activity (%)		
	GPP	FPP	GGPP
Wild-type	100	100	100
Mutant YF	340	340	7
Mutant PC	200	129	2
Mutant YP	320	278	8

Amounts of GPP, FPP, and GGPP formed in the reaction of wild-type GGPPS were taken as 100%.

mutant YF, mutant PC, and mutant YP based on the specificity of the wild-type GGPPS are shown in Table 1. Relative formation of GPP, FPP, and GGPP fell in the range of 200–340%, 120–340% and 2–8%, respectively. These results clearly demonstrated that either: 1) replacement of small amino acids at the fourth and fifth positions before FARM with aromatic amino acids or 2) deletion of two amino acids in the FARM of *S. dulcis* GGPPS was sufficient to convert a plant GGPPS into a FPPS. A previous mutagenesis study around the FARM region of archaeal bacteria *Sulfolobus acidocaldarius* GGPPS¹⁶⁾ showed that conversion of Thr situated at the fourth position before FARM to Phe was sufficient to allow the GGPPS produce FPP as a major product. Unlike plant GGPPSs, archaeal GGPPS lacks amino acid insertion in FARM. This suggests that plant and archaeal GGPPSs employ different mechanisms to control the chain length of the products. In plant GGPPSs, both small amino acids at the fourth and fifth positions before FARM and the insertion in FARM play essential roles in product length determination. On the other hand, in archaeal GGPPS, having a bulky aromatic amino acid at the fifth and a small amino acid at the fourth position before FARM was essential in chain length

determination. This is the first report of successful conversion of a plant GGPPS into an enzyme producing a shorter prenyl compound by site-directed mutagenesis.

Acknowledgment This work was supported by a Grants-in-Aid for Scientific Research (B) (No. 09044212) from the Ministry of Education, Science, Sports and Culture, Japan.

References and Notes

- Chen A., Kroon P. A., Poulter C. D., *Protein Sci.*, **3**, 600–607 (1994).
- Hayashi T., Kishi M., Kawasaki M., Shimizu M., Suzuki S., Yoshizaki M., Morita N., Tezuka Y., Kikuchi T., Berganza L. H., Ferro E., Basualdo I., *Tetrahedron Lett.*, **28**, 3693–3696 (1987).
- Ogiso A., Kitazawa E., Kurabayashi M., Sato A., Takahashi S., Noguchi H., Kuwano H., Kobayashi S., Mishima H., *Chem. Pharm. Bull.*, **26**, 3117–3123 (1978).
- Kitazawa E., Ogiso A., *Phytochemistry*, **20**, 287–289 (1981) and references cited therein.
- Frohman M. A., Dush M. K., Martin G. R., *Proc. Natl. Acad. Sci. U.S.A.*, **85**, 8998–9002 (1988).
- Song L., Poulter C. D., *Proc. Natl. Acad. Sci. U.S.A.*, **91**, 3044–3048 (1994).
- Tarchis L. C., Proteau P. J., Kellogg B. A., Sacchettini J. C., Poulter C. D., *Proc. Natl. Acad. Sci. U.S.A.*, **93**, 15018–15023 (1996).
- von Heijne G., Steppuhn J., Herrmann G. R., *Eur. J. Biochem.*, **180**, 535–545 (1989).
- Hayashi T., Kasahara K., Sankawa U., *Phytochemistry*, **46**, 517–520 (1997).
- Hayashi T., Asai T., Sankawa U., *Tetrahedron Lett.*, **40**, 8239–8243 (1999).
- Lichtenthaler H. K., Schwender J., Disch A., Rohmer M., *FEBS Lett.*, **400**, 271–274 (1997).
- De-Eknamkul W., personal communication.
- Ogura K., Nishino T., Shinka T., Seto S., *Methods Enzymol.*, **110**, 167–171 (1985).
- Hefner J., Ketchum E. B., Croteau R., *Arch. Biochem. Biophys.*, **360**, 62–74 (1998).
- Williams D. C., McGarvey J. D., Katahira E. J., Croteau R., *Biochemistry*, **37**, 12213–12220 (1998).
- Ohnuma S., Hirooka K., Ohto C., Nishino T., *J. Biol. Chem.*, **272**, 5192–5198 (1997).